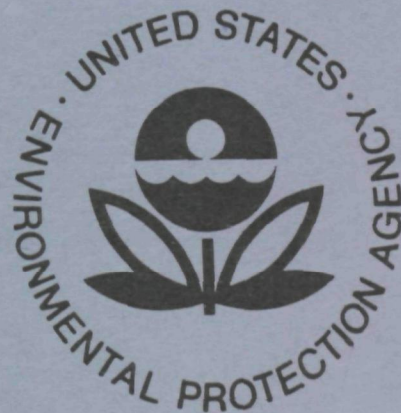


**EPA-600/2-77-016**  
**April 1977**

**Environmental Protection Technology Series**

# **BACKWASH OF GRANULAR FILTERS USED IN WASTEWATER FILTRATION**



**Municipal Environmental Research Laboratory  
Office of Research and Development  
U.S. Environmental Protection Agency  
Cincinnati, Ohio 45268**

## **RESEARCH REPORTING SERIES**

Research reports of the Office of Research and Development, U.S. Environmental Protection Agency, have been grouped into nine series. These nine broad categories were established to facilitate further development and application of environmental technology. Elimination of traditional grouping was consciously planned to foster technology transfer and a maximum interface in related fields. The nine series are:

1. Environmental Health Effects Research
2. Environmental Protection Technology
3. Ecological Research
4. Environmental Monitoring
5. Socioeconomic Environmental Studies
6. *Scientific and Technical Assessment Reports (STAR)*
7. Interagency Energy-Environment Research and Development
8. "Special" Reports
9. Miscellaneous Reports

This report has been assigned to the ENVIRONMENTAL PROTECTION TECHNOLOGY series. This series describes research performed to develop and demonstrate instrumentation, equipment, and methodology to repair or prevent environmental degradation from point and non-point sources of pollution. This work provides the new or improved technology required for the control and treatment of pollution sources to meet environmental quality standards.

EPA-600/2-77-016  
April 1977

BACKWASH OF GRANULAR FILTERS USED IN  
WASTEWATER FILTRATION

by

J. L. Cleasby and E. R. Baumann  
Iowa State University  
Ames, Iowa 50011

Grant No. R802140

Project Officer

S. A. Hannah  
Wastewater Research Division  
Municipal Environmental Research Laboratory  
Cincinnati, Ohio 45268

MUNICIPAL ENVIRONMENTAL RESEARCH LABORATORY  
OFFICE OF RESEARCH AND DEVELOPMENT  
U.S. ENVIRONMENTAL PROTECTION AGENCY  
CINCINNATI, OHIO 45268

## DISCLAIMER

This report has been reviewed by the Municipal Environmental Research Laboratory, U.S. Environmental Protection Agency, and approved for publication. Approval does not signify that the contents necessarily reflect the views and policies of the U.S. Environmental Protection Agency, nor does mention of trade names or commercial products constitute endorsement or recommendation for use.

## FOREWORD

The Environmental Protection Agency was created because of increasing public and government concern about the dangers of pollution to the health and welfare of the American people. Noxious air, foul water, and spoiled land are tragic testimony to the deterioration of our natural environment. The complexity of that environment and the interplay between its components require a concentrated and integrated attack on the problem.

Research and development is that necessary first step in problem solution and it involves defining the problem, measuring its impact, and searching for solutions. The Municipal Environmental Research Laboratory develops new and improved technology and systems for the prevention, treatment, and management of wastewater and solid and hazardous waste pollutant discharges from municipal and community sources, for the preservation and treatment of public drinking water supplies, and to minimize the adverse economic, social, health, and aesthetic effects of pollution. This publication is one of the products of that research; a most vital communications link between the researcher and the user community.

The conventional methods for treatment of municipal wastewaters frequently produce effluents that will not meet local discharge requirements. Granular media filters are being installed to provide tertiary treatment for increased removals of suspended solids and particulate BOD. This report provides valuable information on criteria for selection of media for wastewater filters and design considerations to provide adequate cleaning of the media during backwash.

Francis T. Mayo  
Director  
Municipal Environmental Research  
Laboratory

## ABSTRACT

The use of deep granular filters in waste treatment is of growing importance. The key to long-term operating success of such filters is proper bed design and adequate bed cleaning during backwashing. A number of questions related to adequate backwashing of granular filters were investigated and the study results lead to the following conclusions:

Cleaning granular filters by water backwash alone to fluidize the filter bed is inherently a weak cleaning method because particle collisions do not occur in a fluidized bed and thus abrasion between the filter grains is negligible.

Due to the inherent weakness of water backwashing cited above, auxiliary means of improving filter bed cleaning are essential for wastewater filters. Three auxiliary methods were compared in a wastewater pilot filtration study. The most effective backwash was provided by air scour and water backwash simultaneously at subfluidization velocities. The other two auxiliary methods, surface and subsurface wash and air scour prior to water fluidization wash were about comparable in effectiveness.

The performance of coarse sand, dual-, and triple-media filters was compared, and the backwashing routines appropriate for each media are discussed. A number of investigations concerning the design and backwashing of dual-media filters are also included.

This report was submitted in fulfillment of Grant No. R802140 by Iowa State University under the partial sponsorship of the U.S. Environmental Protection Agency. This report covers a period from September 1, 1971 to May 31, 1976, and work was completed as of December 31, 1975.

## TABLE OF CONTENTS

	<u>Page</u>
ABSTRACT	iv
LIST OF TABLES	vii
LIST OF FIGURES	xi
NOTATIONS, ABBREVIATIONS AND CONVERSION FACTORS	xviii
ACKNOWLEDGMENTS	xxiv
I. INTRODUCTION	1
II. CONCLUSIONS	4
Conclusions Regarding Backwash Effectiveness	4
Conclusions Comparing Filter Performance	5
Conclusions Regarding Expansion, Intermixing, and Dual Media	5
Conclusions Regarding Wastewater Filter Design	7
III. RECOMMENDATIONS	10
IV. BACKWASHING-POTABLE WATER EXPERIENCE	11
V. BACKWASHING WITH FLUIDIZATION AND EXPANSION	16
Some Fluidization Fundamentals	16
Predominance of Hydrodynamic Forces in Cleaning by Water Fluidization Alone	23
VI. OPTIMUM CLEANING BY WATER BACKWASH ALONE	26
Particulate Fluidization and Optimum Turbulence - Evidence from the Literature	26
A New Theory of Optimum Backwashing by Water Fluidization Only	31
Experimental Support for the Optimum Theory	39
VII. WASTEWATER FILTRATION AND BACKWASHING - LITERATURE REVIEW	68
Types of Wastewater Filters and Cleaning Techniques	68
Case Histories	76
VIII. EXPERIMENTAL COMPARISON OF BACKWASH METHODS IN WASTEWATER FILTRATION	89
Pilot-Plant Equipment	89

Chronology of Experiments	91
Equipment Details	91
Analysis of Samples	102
Operation and Results - Phase I Dual-Media	106
Filtration of Alum-Treated Secondary Effluent	
Operation and Results - Phase II Dual-Media	126
Filtration of Secondary Effluent	
Operation and Results - Phase III, IV, and V Single-,	157
Dual-, and Triple-Media Filtration of Secondary	
Effluent	
Operation and Results - Phase VI Coarse Sand Filtration	194
of Secondary Effluent	
IX. EXPANSION AND INTERMIXING OF MULTI-MEDIA FILTERS	204
Introduction	204
Dual-Media and Multi-Media Filtration Literature	205
Backwashing of Granular Filters	207
Bed Expansion Correlations from Fluidization Literature	211
Prediction of Settling Velocities	224
Existing Models for Predicting the Expansion of Fluidized Beds	230
X. EXPANSION AND INTERMIXING EXPERIMENTAL INVESTIGATION	233
Experimental Apparatus	233
Experimental Procedures	239
Illustrative Calculations	242
Results and Analysis - Summary	247
Results - Media Characteristics	247
Fixed Bed Hydraulic Profiles in Dual-Media	256
Filters - Coal and Sand	
Expansion - Flow Rate Observations	271
Intermixing Observations	
IX. EFFECT OF MEDIA INTERMIXING ON DUAL-MEDIA FILTRATION	315
Introduction	315
Objectives and Scope of this Study	315
Experimental Investigation	316
Results	323
Discussion	336
Conclusions	340
XII. ABRASIVE LOSS OF COAL DURING AIR SCOUR	341
Experimental Procedure	341
Results	342
Conclusions	343
XIII. REFERENCES	345
XIV. APPENDIX - Sieve Analyses of Uniform Media	355

# LIST OF TABLES

	<u>Page</u>
Table 1. Analysis of University tap water.	43
Table 2. Experimental design for series 2.	47
Table 3. Backwash procedures for graded sand.	48
Table 4. Effluent quality index and porosity for series 2.	54
Table 5a. Manual backwashing procedure used on full-scale rapid sand filters at Luton [86].	83
Table 5b. Backwashing procedure in full-scale rapid sand filters at Luton in November 1975.	83
Table 6a. Automatic backwashing sequence used on pilot scale Immedium upflow filter at Luton [86].	84
Table 6b. Backwash procedure for full-scale upflow filters at Luton in November 1975.	84
Table 7. Summary of experimental phases for wastewater filtration backwashing study.	92
Table 8. Filter media details for wastewater filtration pilot studies.	99
Table 9. Initial filter head losses during various portions of the study.	113
Table 10. Backwash rates required to achieve 38 to 40% bed expansion.	120
Table 11. Results of analyses during alum treatment (Phase I) for samples from May 17 to July 11, 1973, when both filters were washed by water fluidization only. (All results from composite samples except solids contact influent.)	121
Table 12. Results of analyses during alum treatment series (Phase I) for samples from July 11 to August 20, 1973, when air scour was being used on the south filter. (All results from composite samples except solids contact influent.)	122
Table 13. Suspended solids released from filters in special backwashes after run 78.	125
Table 14. Summary of head loss development during observation runs of Phase II, during direct filtration of secondary effluent.	150

	<u>Page</u>
Table 15. Results of analyses during direct filtration of secondary effluent (Phase II) from August 30 to October 30, 1973. (All composite samples except as noted.)	151
Table 16. Data summary of clean-up operation at the end of Phase II.	153
Table 17. Solids capture per unit head loss results for direct filtration of trickling filter effluent, 1974.	183
Table 18. Summary of analytical test results for Phase III.	185
Table 19. Summary of analytical test results for Phase IV.	186
Table 20. Summary of analytical test results for Phase V.	187
Table 21. Data summary for clean-up operation at the end of the operation period in 1974.	189
Table 22. Action of simultaneous air and water backwash on coarse sand at subfluidization velocities.	197
Table 23. Results of analyses during direct filtration of secondary effluent (Phase VI) from June 24 through August 2, 1975, using coarse sand filters of different depths.	199
Table 24. Mean total head loss during filtration of secondary effluent on coarse sand filters during Phase VI.	200
Table 25. Average initial head loss for three coarse sand filters before and after run 35 in Phase VI when increase of backwash rate was adopted.	200
Table 26. Height that sand is thrown by simultaneous air and water backwash.	202
Table 27. Comparison of $n$ slopes of sea sands (using Jottrand's analysis [69] and Richardson and Zaki's equations).	217
Table 28. Comparison of $n$ slope of crushed coal.	218
Table 29. Size and source of raw graded silica sands and coal studies.	238
Table 30. Sieve analysis of garnet sand media (-14+16).	243

	<u>Page</u>
Table 31. Upflow and/or downflow experimental runs with the various single media in the 6-in. column.	248
Table 32. Upflow and downflow experimental runs with dual-media filters in the 6-in. column.	249
Table 33. Upflow experimental runs with various uniform media and uniform dual media in 2-in. column, 25 °C.	250
Table 34. Average diameter of uniform media by two methods, mean of adjacent sieve sizes and mean equivalent spherical diameter by the count and weigh method [Eq. (40)].	254
Table 35. Summary of the average diameters of the media - $d$ (by several methods).	255
Table 36. Densities of media - $\rho_s$	256
Table 37. Fixed-bed porosities of the three media determined by the two techniques ( $\epsilon_0$ ) and two investigators.	257
Table 38. Settling velocities of uniform garnet and sand media.	258
Table 39. Expansion - flow rate data of run 1, Series A-13 (-14+16 garnet and sand media).	272
Table 40. Summary of minimum fluidization velocities of garnet sand media - $V_{mf}$ .	285
Table 41. Results of the log $V$ vs log $\epsilon$ relationship for garnet sand media.	289
Table 42. Values of Reynold's numbers and Galileo's number for the garnet sand media.	291
Table 43. $V_i$ , $n$ , $\epsilon_{mf}$ to be used in author's expansion models.	292
Table 44. Results of log $V$ vs log $\epsilon$ regression analyses for uniform sized silica sands and coals.	293
Table 45. Predicted values of $m$ , $V_i$ with errors of prediction and maximum error of prediction of expanded bed depth for uniform sands.	295
Table 46. Predicted values of $n$ , $V_i$ with errors of prediction and maximum error of prediction of expanded bed height for uniform coals.	296

	<u>Page</u>
Table 47. Prediction of expanded bed depths for graded sand using models developed for uniform sands and average diameter based on the inverse definition [Eq. (38)].	298
Table 48. Bulk density difference, lb/ cu ft (garnet-silica sand).	307
Table 49. Identification of experimental series.	324
Table 50. Influent and effluent suspended solids data, average and range, for wastewater series.	335
Table 51. Average values of background (bg) turbidity for the treated wastewaters.	336
Table 52. Summary of results comparing filter performance for sharp and mixed interface media.	336
Table 53. Changes in coal bed over a two-week period of air-scour exposure equivalent to about 20 years of normal service.	343

## LIST OF FIGURES

	<u>Page</u>
Fig. 1. Characteristics of fluidized beds.	17
Fig. 2. Fundamental behavior patterns.	19
Fig. 3. Shear forces on an elemental volume of fluid.	33
Fig. 4. Schematic layout of experimental apparatus.	40
Fig. 5. Head loss curves for run 3B, top 6 in. of filter media.	51
Fig. 6. Variation of the ratio of effluent to influent iron with time.	52
Fig. 7. Cumulative differential effluent iron vs time, run 8.	53
Fig. 8. Cumulative effluent quality index vs porosity, series 2, 12-in. depth.	55
Fig. 9. Cumulative effluent quality index vs porosity, series 2, all depths.	56
Fig. 10. Cumulative effluent quality index vs porosity, series 1, 12-in. depth.	56
Fig. 11. Cumulative effluent quality index vs expansion, series 3, 18-in. depth.	57
Fig. 12. Cumulative effluent quality index vs expansion, series 3, all depths.	58
Fig. 13. Backwash water quality vs washwater volume, series 1.	59
Fig. 14. Backwash water quality vs washwater volume, series 1.	60
Fig. 15. Backwash water quality vs washwater volume, series 1.	61
Fig. 16. Terminal backwash water quality vs porosity, series 1.	62
Fig. 17. Backwash water volume vs porosity, series 1.	64
Fig. 18. Iron removable by physical abrasion test vs expansion, runs 20 and 21.	65
Fig. 19. Pilot-scale Immedium filter used at West Hertfordshire, England [142].	71
Fig. 20. Immedium filter arrangements for full-scale installations, open and pressure [13].	72

Fig. 21.	Environmental Elements Corp. (Koppers) full-scale automatic backwash filter (from manufacturer's brochure).	75
Fig. 22.	Pilot-scale "Simater" radial-flow, moving-bed sand filter by Simonacco Ltd. of Carlisle, England [68].	77
Fig. 23.	Schematic representation of pilot-scale filter plant used in experimental investigation.	90
Fig. 24.	Pilot plant solids contact unit.	94
Fig. 25.	Details of filter boxes.	96
Fig. 26.	Abrasion test when filtering secondary effluent treated with alum for phosphorus reduction in Phase I.	112
Fig. 27.	Head loss vs time at various media depths, run 27.	115
Fig. 28.	Head loss vs time at various media depths, run 42.	116
Fig. 29.	Head loss vs time at various media depths, run 59.	117
Fig. 30.	Head loss vs time at various media depths, run 63.	118
Fig. 31.	Head loss vs time at various media depths, run 71.	119
Fig. 32.	Suspended solids concentration of backwash water vs quantity of backwash water used, run 27, second backwash of the south filter immediately following the first application of air scour.	124
Fig. 33.	Standardized abrasion test results (Phase II) during direct filtration of secondary effluent.	136
Fig. 34.	Initial head loss data for north, south, and west filters for entire Phase II study during direct filtration of secondary effluent.	138
Fig. 35.	Frequency plot of initial head loss data, Phase II.	139
Fig. 36.	Chronological head loss development at various media depths, run 2.	141
Fig. 37.	Chronological head loss development at various media depths, run 14.	142
Fig. 38.	Chronological head loss development at various media depths, run 22.	143
Fig. 39.	Chronological head loss development at various media depths, run 29.	144

Fig. 40.	Chronological head loss development at various media depths, run 36.	145
Fig. 41.	Chronological head loss development at various media depths, run 43.	146
Fig. 42.	Chronological head loss development at various media depths, run 54.	147
Fig. 43.	Chronological head loss development at various media depths, run 64.	148
Fig. 44.	Results of special backwash, day no. 242.	164
Fig. 45.	Initial head loss in bottom 16 in. of coarse media filter, observation runs only.	168
Fig. 46.	Standard abrasion test results for Phase III.	170
Fig. 47.	Standard abrasion test results for Phase IV and V.	171
Fig. 48.	Initial head loss data for each filter for entire study.	173
Fig. 49.	Chronological head loss development at various media depths, day no. 155, Phase III.	176
Fig. 50.	Chronological head loss development at various media depths, day no. 183, Phase III.	177
Fig. 51.	Chronological head loss development at various media depths, day no. 239, Phase IV.	178
Fig. 52.	Chronological head loss development at various media depths, day no. 240, Phase V.	179
Fig. 53.	Chronological head loss development at various media depths, day no. 267, Phase V.	180
Fig. 54.	Chronological head loss development at various media depths, day no. 269, Phase V.	181
Fig. 55.	Chronological head loss development at various media depths, day no. 281, Phase V.	182
Fig. 56.	Relationship between superficial velocity - porosity.	212
Fig. 57.	Relationship between $n$ slope and Reynolds number $Re_o$ .	214
Fig. 58.	Schematic layout of 6-in. fluidization column.	234
Fig. 59.	Schematic layout of 2-in. fluidization column.	236

Fig. 60.	Sieve analysis of graded sand media.	251
Fig. 61.	Sieve analysis of graded coal media.	251
Fig. 62.	Sieve analysis of garnet sand media.	252
Fig. 63.	Fixed-bed head loss for graded sand A at 9 gpm/sq ft for various temperatures.	259
Fig. 64.	Fixed-bed head loss for graded sand A at 26.5 °C for various flow rates.	260
Fig. 65.	Head loss for individual graded media in 1-1/2 in. unit filter sections.	262
Fig. 66.	Head loss for individual graded media in 1-1/2 in. unit filter sections.	263
Fig. 67.	Fixed-bed head loss of dual media AA at various temperatures and flow rates.	264
Fig. 68.	Head loss per 1-1/2-in. unit depth in dual media AA and head loss for the two-component media if unmixed.	265
Fig. 69.	Head loss per 1-1/2-in. unit depth in dual media AC and head loss for the two-component media if unmixed.	266
Fig. 70.	Head loss per 1-1/2-in. unit depth in dual media AD and head loss for the two-component media if unmixed.	267
Fig. 71.	Head loss per 1-1/2-in. unit depth in dual media A <sub>2</sub> E and head loss for the two-component media if unmixed.	268
Fig. 72.	Head loss per 1-1/2-in. unit depth in dual media AF and head loss for the two-component media if unmixed.	269
Fig. 73.	Pressure loss - flow rate diagram for garnet sand media (-14+16).	273
Fig. 74.	Pressure loss - flow rate diagram for garnet sand media (M-60-80).	274
Fig. 75.	Expansion - flow rate characteristics (garnet sand, run 1).	275
Fig. 76.	Expansion - flow rate characteristics (garnet sand, run 2).	276
Fig. 77.	Expansion - flow rate characteristics (garnet sand, run 3).	277

Fig. 78.	Expansion - flow rate characteristics (garnet sand, run 4).	278
Fig. 79.	Expansion - flow rate characteristics (garnet sand, run 5).	279
Fig. 80.	Expansion - flow rate characteristics (garnet sand, run 6).	280
Fig. 81.	Expansion - flow rate characteristics (garnet sand, run 7).	281
Fig. 82.	Expansion - flow rate characteristics (garnet sand, run 8).	282
Fig. 83.	Expansion - flow rate characteristics (garnet sand, run 9).	283
Fig. 84.	Expansion - flow rate characteristics (garnet sand, run 10).	284
Fig. 85.	Log plot of $V$ vs $\epsilon$ for garnet sand media (-14+16) (run 1, Series A-13).	286
Fig. 86.	Log plot of $n$ slope vs Reynold's number - $Re_i$ (for garnet sand media, runs 1 through 10, Series A-13 through A-17).	287
Fig. 87.	Log plot of Reynold's number, $Re_i$ , vs Galileo number, $Ga$ (for garnet sand media, runs 1 through 10, Series A-13 through A-17).	290
Fig. 88.	Minimum fluidization velocity, $V_{mf}$ , to achieve 10% bed expansion at 25 °C.	300
Fig. 89.	Effect of temperature on $V_{mf}$ for sand and coal and on absolute viscosity of water.	300
Fig. 90.	Bulk density vs flow rate for garnet sand and silica sands.	302
Fig. 91.	Intermixing of -50+60 garnet sand and -20+25 silica sand.	303
Fig. 92.	Intermixing of -50+60 garnet sand and -30+35 silica sand.	303
Fig. 93.	Intermixing of -50+60 garnet sand and -35+40 silica sand.	304
Fig. 94.	Intermixing of -50+60 garnet sand and -40+45 silica sand.	304

Fig. 95.	Intermixing of silica sand and coal according to the model of Camp et al. [26].	309
Fig. 96.	Bulk density vs flow rate for coal and silica sands (data points not shown on all curves for drafting convenience).	310
Fig. 97.	Expansion vs flow rate of dual media AA and the two-component media at 22 °C.	312
Fig. 98.	Expansion vs flow rate of dual media A <sub>2</sub> C <sub>2</sub> and the two-component media at 22 °C.	314
Fig. 99.	Schematic diagram of apparatus.	317
Fig. 100.	Head loss and filtrate quality vs volume of filtrate, Series IS, run 2, sharp interface, filtration of iron with C <sub>0</sub> = 8.68 to 9.64 mg/l Fe, Avg 9.07 mg/l.	325
Fig. 101.	Head loss and filtrate quality vs volume of filtrate, Series IM, run 11, mixed interface, filtration of iron with C <sub>0</sub> = 9.2 to 9.7 mg/l Fe, Avg 9.42 mg/l.	326
Fig. 102.	Head loss and filtrate quality vs volume of filtrate, Series II S, run 1, sharp interface, filtration of activated sludge effluent with C <sub>0</sub> = 4.5 to 8.5 FTU, Avg 6.16 FTU.	327
Fig. 103.	Head loss and filtrate quality vs volume of filtrate, Series II M, run 1, mixed interface filtration of activated sludge effluent with C <sub>0</sub> = 2.6 to 8.6 FTU, Avg 4.15 FTU.	328
Fig. 104.	Head loss and filtrate quality vs volume of filtrate, Series III S, run 3, sharp interface, filtration of alum coagulated trickling filter effluent C <sub>0</sub> = 3.8 to 10 FTU, Avg 5.21 FTU.	329
Fig. 105.	Head loss and filtrate quality vs volume of filtrate, Series III M, run 5, mixed interface, filtration of alum coagulated trickling filter effluent with C <sub>0</sub> = 1.7 to 6.2 FTU, Avg 2.95 FTU.	330
Fig. 106.	Head loss and filtrate quality vs volume of filtrate, Series IV S, run 3, sharp interface, filtration of trickling filter effluent with C <sub>0</sub> = 4.7 to 8.5 FTU, Avg 6.29 FTU.	331
Fig. 107.	Head loss and filtrate quality vs volume of filtrate, Series IV M, run 3, mixed interface, filtration of trickling filter effluent with C <sub>0</sub> = 12 to 15 FTU, Avg 12.6 FTU.	332

Fig. 108.	Headloss and filtrate quality vs volume of filtrate, Series V S, run 4, sharp interface, filtration of limesoda ash softening precipitate with $C_o = 5.8$ to 6.5 FTU, Avg 6.14 FTU.	333
Fig. 109.	Head loss and filtrate quality vs volume of filtrate, Series V M, run 3, mixed interface, filtration of lime- soda ash softening precipitate with $C_o = 6.8$ to 8.3 FTU, Avg 7.5 FTU.	334
Fig. 110.	Sieve analysis of coal before and after 14 days of continuous air scour.	344

# NOTATION, ABBREVIATIONS AND CONVERSION FACTORS

B	= Camp's backwashing number	-
C	= volume	-
C <sub>o</sub>	= influent concentration	-
C	= effluent concentration	-
C/C <sub>o</sub>	= effluent concentration/influent concentration	-
C <sub>D</sub>	= drag coefficient	-
d	= particle diameter	L
D	= diameter of column or bed	L
d <sub>i</sub>	= diameter of particle in 'i'th layer	L
d <sub>eq</sub>	= equivalent diameter of spherical particle	L
d <sub>60% finer</sub>	= 60% finer of a particle from a probability plot	L
d <sub>inverse</sub>	= $1/\Sigma(W_i/d_i)$ = average diameter of particle by inverse definition	L
d <sub>m</sub>	= $\Sigma W_i d_i$ arithmetic mean diameter	L
F <sub>b</sub>	= buoyant force	ML <sup>-2</sup> T
F <sub>i</sub>	= impelling force	ML <sup>-2</sup> T
g	= acceleration due to gravity	LT <sup>-2</sup>
$G = \frac{dV'}{dz}$	= mean velocity or shear gradient in pores	T <sup>-1</sup>
Ga	= $d^3 \rho (\rho_s - \rho) g / \mu^2$ Galileo number	-
G <sub>f</sub>	= superficial fluid mass velocity, lb(mass)/hr sq ft	ML <sup>-2</sup> T <sup>-1</sup>
G <sub>mf</sub>	= superficial fluid mass velocity at minimum fluidization, lb (mass)/hr sq ft	ML <sup>-2</sup> T <sup>-1</sup>
h or HL	= head loss in flow through granular bed	L
i	= subscript denoting the 'i'th layer of the bed	-

K	= $f(V_s, \psi, d/D_t)$ = constant for a particular fluidized system	$LT^{-1}$
$l$	= height of bed	L
$l_o$	= height of static bed	L
m	= index of fluid regime	-
mf	= subscript denoting condition at minimum fluidization	-
n	= slope of log V vs log $\epsilon$ plot	-
N	= number of particles	-
p	= pressure intensity	$ML^{-1}T^{-2}$
P	= power dissipated	$ML^2T^{-3}$
r	= $d_x/d_y$ ratio of the particle diameters of x and y components	-
R'	= resistance force per unit projected area of the particle	$ML^{-1}T^{-2}$
Re	= $\rho V d/\mu$ = Reynold's number based on the superficial velocity of the fluid above the bed	-
$Re_i$	= Reynold's number based on the velocity $V_i$ intercept at porosity equals one of the log V vs log $\epsilon$ plot	-
$Re_o$	= $\rho V_s d/\mu$ = Reynold's number based on unhindered settling velocity of particle	-
S	= mean shear stress	$ML^{-1}T^{-2}$
t	= time	T
$v_p$	= volume of particle	$L^3$
V	= superficial velocity of the fluid above the bed	$LT^{-1}$
$V_i$	= velocity intercept at a porosity ratio of one of the log V vs $\epsilon$ plot, equal to the settling velocity of a discrete spherical particle ( $V_s$ ) when $d/D$ is negligible	$LT^{-1}$

$V_{mf}$	= minimum fluidization or critical fluid velocity expressed as a superficial velocity	$LT^{-1}$
$V_s$	= unhindered settling velocity of a discrete particle	$LT^{-1}$
$V'$	= $V/\epsilon$ = average fluid velocity within pores of filter	$LT^{-1}$
$W$	= total weight of particles	-
$W_i$	= weight fraction of 'i'th layer	-
$x, y, z,$	= Cartesian coordinates	$L$

#### Greek Symbols

$\alpha$	= $[\mu g K(\rho_s - \rho)]^{1/2}$ = constant for a particular fluidized system in optimum backwashing theory	$ML^{-1}T^{-2}$
$\gamma$	= specific weight of fluid	$ML^{-2}T^{-2}$
$\gamma_b$	= $(\rho_{s_x} - \rho)/(\rho_{s_y} - \rho)$	-
$\gamma_s$	= specific weight of particle	$ML^{-2}T^{-2}$
$\delta$	= $x/d$ = dimensionless spacing of particles in fluidized state	-
$\Delta$	= prefix signifying increment	-
$\epsilon$	= porosity ratio	-
$\epsilon_e$	= porosity ratio of expanded bed	-
$\epsilon_{mf}$	= porosity ratio at minimum fluidization velocity	-
$\epsilon_o$	= porosity ratio of fixed bed	-
$\mu$	= viscosity of fluid in centipoise	$ML^{-1}T^{-1}$
$\nu$	= $\mu/\rho$ = kinematic viscosity	$L^2T^{-1}$
$\rho$	= fluid density	$ML^{-3}$
$\rho_b$	= $(1 - \epsilon)\rho_s + \rho\epsilon$ = bulk density of mixture	$MT^{-3}$
$\rho_s$	= particle density	$ML^{-3}$

= sphericity ratio of the surface area of  
an equivalent volume sphere to the actual  
surface area of the particle

#### Abbreviations

American Society for Testing Materials	ASTM
biochemical oxygen demand	BOD
centimeter	cm
chemical oxygen demand	COD
cubic centimeter	cc
cubic feet	cu ft
cubic feet per minute	cfm
cubic feet per second	cfs
degree(s) celsius	°C
effective size	ES
degree(s) fahrenheit	°F
feet	ft
feet per second	fps
Formazin turbidity units	FTU
gallon(s)	gal.
gallon(s) per minute	gpm
gram(s)	g
horsepower	HP
hour(s)	hr
inch(es)	in.
inches per minute	ipm

inside diameter	ID
Jackson turbidity units	JTU
mercury	Hg
micrometer(s)	$\mu\text{m}$
microliter(s)	$\mu\text{l}$
million gallon(s)	MG
million gallons per day	MGD
milligram(s) per litre	mg/l
milliliter(s)	ml
millimeter(s)	mm
minute(s)	min
nanometer	nm
number	no.
outside diameter	OD
parts per million	ppm
parts per trillion	ppt
percent	%
pound(s)	lb
pounds per square inch, absolute	psia
pounds per square inch, gage	psig
revolutions per minute	rpm
root mean square	rms
second(s)	sec
square centimeter	sq cm
square feet	sq ft
suspended solids	SS

trickling filter	TF
uniformity coefficient	UC
versus	vs
volume	vol
weight	wt

### Conversion Factors

The following factors convert the units used in this report to the more common SI metric unit in popular usage in water engineering practice.

<u>English Unit</u>	x	<u>Multiplier</u>	=	<u>Metric Unit (SI)</u>
cfm(cu ft/min)		1.68		$\text{m}^3/\text{h}$
cfm/sq ft		18.288		$\text{m}^3/\text{m}^2\text{h}$ (i.e., m/h superficial velocity)
ft		0.3048		m
fps (ft/s)		0.3048		m/s
gal		.003785		$\text{m}^3$
gal/sq ft		.0407		$\text{m}^3/\text{m}^2$
gpm (gal/min)		0.2272		$\text{m}^3/\text{h}$
" "		0.0631		1/s
gpm/sq ft		2.442		$\text{m}^3/\text{m}^2\text{h}$ (i.e., m/h superficial velocity)
g/sq ft (gram/sq ft)		10.750		$\text{g}/\text{m}^2$
hp		0.7457		kw
in.		0.0254		m
in./min		1.524		m/h
lb		0.454		kg
lb/cu ft		16		$\text{kg}/\text{m}^3$
lb/hr ft		1.489		$\text{kg}/\text{h m}$
lb/hr sq ft		4.88		$\text{kg}/\text{h m}^2$
mgd (million gal/day)		3785		$\text{m}^3/\text{d}$
psi		6.9		$\text{kN}/\text{m}^2$
sq ft		0.0929		$\text{m}^2$

## ACKNOWLEDGMENTS

The research reported herein was supported by the Engineering Research Institute at Iowa State University, Ames, Iowa, in part through funds made available by research grant No. R802140 (formerly 17030 DKG) from the Office of Research and Monitoring of the U.S. Environmental Protection Agency.

The report incorporates the work of several graduate student theses in sanitary engineering at Iowa State. The students were A. Amirtharajah, R. R. Boss, W. J. Carvalho, J. C. Lorence, A. M. Malik, G. A. Rice, G. D. Sejkora, E. W. Stangl, and C. F. Woods. Their contribution is gratefully acknowledged. The report was compiled by the principal investigator, John L. Cleasby. The assistance of Oliver Hao in the statistical analysis of the data is also acknowledged.

## I. INTRODUCTION

The use of deep granular filters in wastewater treatment is of growing importance. Filters are an essential unit operation in many tertiary wastewater treatment flow schemes and in all physical-chemical wastewater treatment flow schemes.

The deep granular filter used in wastewater treatment is subjected to more severe operating conditions than it faced in potable water treatment. The wastewater filter receives heavier and more variable influent suspended-solids loads, and the solids tend to stick more tenaciously to the filter media.

The key to long-term operating success of deep granular filters is proper bed design and adequate bed cleaning during backwashing. Due to the heavier burden received by such filters, a coarser media at the entering surface is essential to achieve reasonable filter run length. Dual- and triple- (multi-) media are commonly being used to achieve the coarser surface media in the United States. Coarser coal sizes are advocated to encourage better penetration of suspended solids (and thus longer filter runs), preventing the ready transfer of prior experience from the water filtration field to wastewater filtration. Other approaches, such as deep beds of coarse sand backwashed without bed expansion and shallow beds of fine sand backwashed automatically at frequent intervals are also being used.

The research conducted on this grant was designed to answer a number of important questions related to the design and operation of wastewater filters. In general, the original questions proposed for study were how to select the appropriate media sizes in dual- and triple-media filters, how to predict the minimum and optimum backwash flow rate for the media selected, and how to demonstrate the value of air scour or surface wash as auxiliaries to water backwashing.

Recent developments have added even greater importance to the project, as discussed in the following paragraphs.

The importance of wastewater filters is emphasized by the requirement of secondary treatment as the minimum acceptable treatment and by the recent EPA definition of secondary treatment which requires an effluent quality of 30 mg/l BOD<sub>5</sub> and 30 mg/l suspended solids, both for 30 consecutive day averages. Many existing municipal plants cannot meet the 30 BOD, 30 suspended solids goal, especially trickling filter plants during winter seasons. Tertiary filtration of such effluents appears to be one of the most attractive alternatives for upgrading such plants to meet the new standards. This attractiveness exists because the technology is well known from

long use in potable water treatment, and because the operating costs and energy requirements are low.

Tertiary wastewater filtration is also attractive for plants which must meet more stringent effluent standards. In some locations, effluent BOD<sub>5</sub> and suspended solids limits of 5 mg/l each have been established. Direct filtration of a good secondary effluent will come close to meeting this goal. Chemical coagulation prior to filtration will be needed in most cases.

Thus, it appears that a growing number of tertiary filtration plants will be installed in the next few years. It is vitally important that tertiary filters be designed and built so they do not fail to meet the desired standards over their service life. A vital element of proper design is the provision of adequate backwashing facilities.

The growing interest in wastewater filtration is evidenced by a growing number of equipment companies marketing such equipment. Some of these companies know very little about filtration, especially wastewater filtration. The interest is also evidenced by requests from EPA regional offices for Technology Transfer Seminars on upgrading secondary plants by tertiary filtration.

During the third year of the current project, the crucial importance of the backwashing provisions for tertiary wastewater filters was demonstrated and is reported herein. Water fluidization alone as a means of backwashing was found to be totally inadequate to maintain the filter media in acceptable condition. Both the use of an air-scour auxiliary before the water backwash and the use of a surface wash auxiliary before and during the water backwash made substantial improvement in the cleaning effectiveness. However, some evidence of inadequate backwash remained, even with these auxiliary cleaning schemes.

#### Specific Aims

The specific aims of the project from the original research proposal are repeated here for reference, with modifications as adopted in the continuation proposals.

- A-1 To attempt to extend the successful prediction model of Amirtharajah for sand expansion to anthracite coal and garnet sand filter media. If unsuccessful, attempt to develop a satisfactory model.
- B-1 To test the validity of the equal bulk density approach to prediction of degree of intermixing of two filter media of different size and specific gravity.

- C-1 To evaluate the hydraulic behavior of dual- and multi-media beds with different degrees of interfacial intermixing and develop a tentative bed design approach.
- C-2 To compare the filtering efficiency of a partially intermixed filter bed with the same media without intermixing. Also, to compare the ease of backwashing of the two types of filter bed.
- C-3 To compare the effectiveness of backwash at various rates providing different degrees of expansion, and to attempt to verify or refute the theoretical optimum expected at porosities of 0.65 to 0.70. Backwash effectiveness will be measured first by the bed cleanliness resulting from the wash and later by the quality of the water in the next filter run.
- C-4 To compare the effectiveness of a programmed backwash covering a range of wash rates with a constant rate backwash, and to recommend an optimum water backwashing procedure. This objective was dropped in the second year continuation proposal.
- C-5 To compare the effectiveness of various air-water backwashing schemes with the optimum water wash procedure alone. This objective was expanded to include surface wash auxiliary in the second year of the study.
- C-6 To reaffirm or revise the tentative design of dual- and multi-media filters suggested in (C-1).

Additional objectives were added in the third year continuation proposal as follows:

- C-7 To determine if coarse, single-media, sand filters can be cleaned successfully by using air and water simultaneously, with the water backwash rates well below minimum fluidization velocity for the media.
- C-8 To evaluate the acceptability of filter designs which permit backwashing with various qualities of backwash water, including the feed water (secondary effluent).

The original objectives were heavily oriented to dual- and triple-media filters because that is the common approach in the United States. During the conduct of the project over a four-year time period, it became evident that other types of granular filters may have merit, and some new objectives were added dealing with the deep-bed coarse sand filter. No work has been included in this study on proprietary filters such as the ABW filter, the Hydroclear filter, the Immedium upflow filter, etc. The absence of such work should not be taken as either a favorable or unfavorable view toward such filters. Rather, their omission from the study only reflects that limited objectives had to be selected to fit within the scope of the project.

## II. CONCLUSIONS

A four-year study of wastewater filtration and filter backwashing is reported herein. Various granular media filters were studied including those using single-, dual-, and triple-media. Various methods of backwashing were compared including: (1) water fluidization only, (2) air scour followed by water fluidization, (3) surface wash and subsurface wash before and during water fluidization backwash, and (4) simultaneous air scour and subfluidization water backwash.

### Conclusions Regarding Backwash Effectiveness

1. The cleaning of granular media filters by water backwash alone to fluidize the filter bed is an inherently weak cleaning method because particle collisions do not occur in a fluidized bed and thus abrasion between the filter grains is negligible.
2. The cleaning which results in a water fluidized bed is due to the hydrodynamic shear at the water-media grain interfaces. A simple mathematical model was developed to calculate the porosity of maximum hydrodynamic shear in a fluidized bed. Maximum hydrodynamic shear in a fluidized bed occurs at a porosity of 0.68 to 0.71 for sand sizes normally used in filtration. Optimum cleaning of the filter media at this porosity was demonstrated experimentally.
3. When backwashing by water fluidization alone, a slight economy in total washwater used is achieved by expanding the bed to the optimum porosity outlined in conclusion 2 above. Lower wash rates (anywhere above the rate for minimum fluidization) will result in nearly the same terminal washwater turbidity, but proportionately longer backwash times will be required. Therefore no economy of water use is achieved by use of low backwash rates.
4. The weakness of water fluidization backwash alone was clearly demonstrated during wastewater filtration studies where a dual-media filter which was washed by water fluidization alone developed serious dirty filter problems such as floating mud balls, agglomerates at the walls, and media surface cracks. These problems were observed when filtering either secondary effluent or secondary effluent which had been treated with alum for phosphorous reduction.
5. The heavy mud ball and agglomerate accumulations caused higher initial head losses and shorter filtration cycles. They may also cause poorer filtrate quality in some cases, although such detriment was not demonstrated in this study.

6. Simultaneous air scour and subfluidization backwash of coarse sand filters proved to be the most effective method of backwash. However, this method should not be used for finer filter media such as the coals and sands of the typical sizes used in dual- and triple-media filters because loss of media will occur during backwash overflow. The choice of the simultaneous air and water flow rates must be appropriate for the size of sand being used, and should result in some circulation of the sand for effective backwashing.
7. The other two methods of improving backwashing, namely air scour followed by water fluidization backwash, and surface (and subsurface) wash before and during water fluidization backwash, proved to be comparable methods of backwash which can be applied to single-, dual- and triple-media filters. These two methods did not completely eliminate all dirty filter problems, but both auxiliaries reduced the problems to acceptable levels so that filter performance was not impaired.

#### Conclusions Comparing Filter Performance

8. In a comparison of a coarse sand filter (2 to 3.6-mm sand, 46 in. deep)\* with a dual-media filter (1 to 2-mm coal, 15 in. deep; 0.5 to 0.8-mm sand, 9 in. deep) and a triple-media filter (same as dual except for the addition of 3 in. of 0.27 to 0.54-mm garnet sand) while filtering secondary effluent, the coarse sand filter produced a filtrate slightly poorer in quality, but produced substantially more filtrate to a common terminal head loss. The performance of the dual- and triple-media filters was comparable.
9. In a comparison of three coarse media sand filters (2.5 to 3.7-mm sand) of different depths (24, 47, 60 in.) while filtering secondary effluent, there was no apparent difference in filtrate quality or in rate of head loss development.

#### Conclusions Regarding Expansion,

##### Intermixing, and Dual Media

10. Methods for prediction of filter bed expansion are desirable for rational design of filters and filter backwashing provisions. Existing models for prediction of filter bed expansion are not adequate for the three filter media in prominent use today: coal, silica sand, and garnet sand. New unified

---

\* This report contains common English units since part of the data are derived from progress reports prepared before the requirement for reporting in metric units. Metric equivalents will be found on page xxvi

empirical models for prediction of bed expansion for all three common media are presented.

11. The expansion prediction models provide acceptable prediction accuracy for garnet and silica sand, but the coal model is not sufficiently accurate without further refinement. Some measure of sphericity for coal seems essential to improvement of the model. In the expansion models, prediction is made from measurable properties of the media and the fluid including media density, fixed bed porosity, sieve analysis, fluid density and fluid viscosity. The models permit calculation of expanded bed porosity, bulk density, and bed depth as a function of backwash flow rate.
12. Complete fluidization of the filter bed during backwashing is common practice in the United States. Data are presented for the minimum fluidization velocity of all three media of various common sizes. The data will be useful in selecting minimum backwash rates for specific media and water temperatures.
13. The prediction of intermixing tendency between different filter media in use today is important to rational design of dual and triple media filters. Lack of such capability may lead to filters with the media excessively intermixed, or with the fine media located on the top of the filter bed where it is not wanted. Two existing models for prediction of intermixing between media of different size and specific gravity were tested against experimental data. Both were found to be lacking in sensitivity.
14. The degree of intermixing is a function of the backwash flow rate and the manner in which the backwash valve is shut off at the end of the filter backwash.
15. There is an intermixing tendency between garnet sand and silica sand, and between silica sand and coal; intermixing in both tends to increase at higher backwash rates. This is because the bulk density of the heavier media, in each case, decreases more rapidly than that of the lighter media as flow rate is increased.
16. Under some circumstances, the smaller but higher specific gravity media can be on the bottom of the bed at lower backwash rates but move to the top of the bed at higher backwash rates. Recommended guidelines for differences in bulk density and ratios of diameter between garnet and silica sand to prevent this occurrence are presented.

17. Rapid shut off of the backwash valve tends to trap the different media in the general position associated with the maximum backwash rate. Very slow closing over several minutes would be required for restratification of the bed in new positions associated with lower backwash flow rates.
18. Intermixing at the interface of typical dual-media filters comprised of coal and silica sand decreases the permeability of the lower coal layers and increases the permeability of the upper sand layers. Thus, the intermixed zone has pore diameter, permeability, and fixed-bed hydraulic gradient values during flow which lie between the values for those parameters for the individual media. This tends in the desired direction of providing coarse to fine filtration.
19. The degree of intermixing at the interface of coal and silica sand filters is determined more by the amount and size of the finer sands present than by the coal.
20. Interfacial intermixing of dual-media filters does not in itself affect filter performance as measured by both head loss development and effluent quality.
21. Intermixing at the interface of dual-media filters is an unavoidable phenomenon which results when United States anthracite coal (sp gr about 1.7) and sand are used and the sizes are selected to achieve coarse to fine filter media in the direction of flow.
22. The possible abrasive loss of anthracite coal media due to air scour was evaluated in a speedup test to simulate the total period of abrasive exposure which the coal might experience in a 20-year life. The abrasive loss was found to be negligible.

#### Conclusions Regarding Wastewater Filter Design

23. The use of some form of air-scour auxiliary or some form of surface wash auxiliary is essential to the satisfactory functioning of wastewater filters comprised of deep beds (2 to 5 ft) of granular material which are backwashed after several feet of head loss development. The auxiliary and the backwash routine must be appropriate to the filter media. For example, subfluidization wash is limited to single-media filters because stratification is not essential (or even desired) for such filters. Fluidization capability is essential for dual- or triple-media filters to permit restratification of the layers in their desired positions at the end of the backwash. Air scour and water backwash simultaneously during overflow is primarily useful on coarse sand filters because finer media

will be lost due to the violence of the combined air and water action. However, the simultaneous use of air and water can be useful on dual- and triple-media prior to the onset of backwash overflow.

The above conclusion is not intended to apply to all types of wastewater filters such as the various proprietary filters with their special backwashing provisions. Such filters and provisions were not studied in this research.

24. The use of graded gravel to support the filter media without special provisions to prevent gravel upset is not recommended where the simultaneous flow of air scour and backwash water can pass through the gravel by intention, or by accident, due to the danger of moving the gravel and thus upsetting the desired size stratification of the gravel.
25. Media-retaining underdrain strainers with openings of less than 1 mm are not recommended for wastewater filters due to the danger of progressive clogging.
26. The filter influent feedwater (e.g., secondary effluent) is not recommended as a backwash water source because of the danger of progressive clogging of underdrain strainers and/or gravel. The advantages of using feedwater do not justify the risks that result therefrom.
27. Air scour is compatible with dual- or triple-media filters from the standpoint of minimal abrasive loss of the coal media. However, the backwash routine must be concluded with a period of fluidization and bed expansion to restratify the media layers after the air scour.
28. The coal and sand sizes for dual-media filters should be selected to encourage some intermixing at the interface to achieve improved filtrate quality. However, to prevent some of the fine sand from reaching the top surface of the coal, the fines should be skimmed from the sand after installation of the sand in the filter and hydraulic grading by backwashing. This skimming is a desirable construction specification even though it may be inconvenient in the construction scheduling.
29. In the filtration of secondary effluent, a coarser surface filter media is favored to achieve longer filter run length and greater solids capture per unit of head loss development. Substantial difference was observed when comparing a stratified dual-media filter having a coal size of 1 to 2-mm with an unstratified coarse sand filter of 2 to 3.6-mm sand. The 1 to 2-mm coal gave much shorter run length. As coarser coal sizes are considered, backwash rates required for fluidization may

become excessive (uneconomical), and the advantage of subfluidization backwash becomes increasingly attractive. However, the choice of subfluidization backwash dictates the use of a single-media filter and an air-scour auxiliary rather than a surface-subsurface wash auxiliary.

30. The use of coarser filter media is also favored by the desire to eliminate supporting gravel and fine slot strainers in the underdrain design.

### III. RECOMMENDATIONS

The objectives of this research project have been largely fulfilled. Some require additional work, and, as is the usual case, the research conducted has led to the knowledge of additional work needed. The following recommendations for additional work are offered:

1. The work reported herein on the stability of double reverse graded gravel as a media support should be repeated using filtered water as a backwash source.
2. The work reported herein on prediction of the expansion of coal filter media should be refined to improve its accuracy, perhaps by incorporation of a sphericity measure in the expansion model.
3. The problem of media loss when backwashing with air and water simultaneously during overflow should be studied in a systematic manner which includes the study of the prominent media materials and sizes as well as a range of air and water flow rates.
4. A comprehensive field investigation of existing full-scale wastewater filters should be made to see if the backwash routines in use are maintaining the filters in good condition. The study should include the prominent proprietary filters currently in use because of the unusual backwash routines employed in some of these filters.

#### IV. BACKWASHING-POTABLE WATER EXPERIENCE

Rapid filters are washed to restore their capacity when the effluent quality becomes unacceptable, or when the pressure drop through the filter reaches a predetermined value. For gravity filters, the terminal head loss selected is usually the actual head available; thus operation beyond this time results in an inability to maintain the desired filtration rate. In some cases, filters are backwashed on a regular time cycle based on experience with the two criteria above, or at more frequent intervals dictated by past maintenance problems created by excessively long filter runs. Filter runs in different plants may vary from 12 hr to several days, one day being considered an acceptable average value.

The filter is usually washed by reversing the flow of water through the filter. In typical United States practice today (1975), the rate is adequate to lift the grains of filter medium into suspension, that is, the rising water causes expansion of the filter medium. The deposited material is thus flushed up through the expanded bed and to waste through the washwater gutters.

If the backwash is not effective, dirty filter problems such as filter cracks and mud balls may occur. Inadequate cleaning leaves a thin layer of compressible dirt or floc around each grain of the medium. As pressure drop across the filter medium increases during the subsequent filter run, the grains are squeezed together and cracks form in the surface of the medium, usually along the walls first.

The heavier deposits of solids near the surface of the media break into pieces during the backwash. These pieces, called mud balls, may not disintegrate during the backwash. If small enough and of low enough density, they float on the surface of the fluidized media. If larger or heavier they may sink into the filter, to the bottom, or to the sand-coal interface in dual media filters. Ultimately they must be broken up or removed from the filter or they reduce filtration effectiveness or cause shorter filter runs by dissipating available head loss.

Early sand filters of the late nineteenth century in the United States were provided with low washwater rates, 8 to 15 in. rise per minute (in./min), which did not expand the bed, or expanded it only slightly. Auxiliary methods of agitation were provided in an attempt to clean a filter. These methods included mechanical rakes that stirred the sand as they rotated in the filter sand and air agitation systems in which air was introduced into the bottom of the sand bed before or during the water backwash. Neither method was completely successful, due to inadequate washwater rates.

United States potable water practice has abandoned these methods in favor of a high velocity backwash (commonly 24 to 30 in./min for 5 to 10 min duration). This wash rate results in about 15 to 30% expansion of the sands currently specified, depending upon water temperature, media gradation, and specific gravity. Early work [62] on the high velocity wash indicated that with the fine sands then in use, 50% sand expansion gave the best washing results. However, the trend to the use of coarser sands results in excessively high wash rates if 50% expansion is to be achieved, so it is seldom attempted in present practice.

The high velocity wash commonly employed in the United States did not solve all problems with dirty filters, and it has created problems with the shifting of finer supporting gravel layers when they are used. The provision of a surface wash system which introduces high velocity water jets before and during the backwash has largely solved the problem of dirty filter medium for potable water filters, but has not solved the problem of shifting gravel.

Evidence of the benefits of surface wash led to its wide adoption for potable water filters in the United States [60,10]. Surface wash is introduced at pressures of 45 to 75 psig through orifices on a fixed piping grid or on a rotating arm, located 1 to 2 in. above the fixed bed. Surface wash flow rates are about 1 in./min for the rotary type, and 3 to 6 in./min for the fixed nozzle type [3]. The desired operating sequence involves draining the filter to the wash trough level or below, applying the surface wash flow with no concurrent backwash flow for 1 to 2 min to break up surface layers on top of the media, then continuing the surface wash with concurrent backwash flow for several minutes until the backwash water begins to clear up. The concurrent application may be at two rates, a low rate to barely immerse the surface wash jets in the media followed by a period with normal bed expansion. The surface wash is then terminated and water fluidization backwash alone follows for 1 to 2 min to stratify the bed, which is only important in dual-media filters.

British and European continental backwashing practice continues to use low rate backwash with little or no bed expansion assisted by air scour. This continued use has sparked a renewed interest in and use of such practice in the United States since about 1965.

The interest in air scour has also been stimulated by the problem of shifting gravel and the more difficult backwashing of wastewater filters. There is also interest in the use of underdrains with fine strainers that do not require supporting gravel, a system which was abandoned in the early twentieth century due to clogging and corrosion problems.

Air scour consists of the distribution of air over the entire filter area at the bottom of the filter media so that it flows upward

through the media. It is used in a number of fashions to improve the effectiveness of backwashing, and/or to permit the use of lower backwash water flow rates. The air may be used prior to the water backwash or concurrently with the water backwash. When used concurrently during backwash overflow, there is legitimate concern over potential loss of filter media to the overflow due to the violent agitation created by the air scour. When air is used alone, the water level is lowered a few inches below the overflow level to prevent loss of filter media during the air scour.

Air scour may be introduced to the filter through a pipe system which is completely separate from the backwash water system, or it may be through the use of a common system of nozzles (strainers) which distribute both the air and water, either sequentially or simultaneously. In either method of distribution, if the air is introduced below graded gravel supporting the filter media, there is concern over the movement of the finer gravel by the air, or especially by air and water used concurrently, by intention or accident. This concern has led to the use in some filters of media-retaining strainers which eliminate the need for graded support gravel in the filter. However, these strainers may clog with time, causing decreased backwash flow capability or, possibly, structural failure of the underdrain system.

In view of the concerns expressed above and the renewed interest in air scour in the United States, a summary of European air-scour practice is appropriate because it has been used there since the beginning of rapid filtration.

British potable water practice has included the use of air scour for many years. Air scour is used alone first, followed by water backwash. Plastic strainer nozzles with 3-mm slots are commonly used in the underdrains and are generally covered by layers of graded gravel to support the media. Single-media sand filters have been the most common, but dual-media filters are becoming more common since about 1970. In the single-media sand filters, the wash rate is only intended to reach minimum fluidization velocity with only 1 to 2% expansion of the bed. The sand grain size used in Britain for potable water filtration is about the same size as in the United States, although they specify the range of size of the sand (e.g., 0.5 to 1 mm, meaning that the sand would pass a 1-mm sieve and be retained on a 0.5-mm sieve) rather than the effective size. In the backwash operation, the air scour is intended to loosen the dirt and is followed by the water backwash to flush away the dirt. Air is introduced through the gravel at rates of 1 to 1.5 scfm/sq ft, sometimes up to 2 scfm/sq ft, followed by water at 8 to 12 in./min [118]. The upper rate is common in current practice. These British water rates of flow are substantially lower than the United States practice and are not sufficient for bed expansion. The apparent success of such low rates must, therefore, be attributed to the prior air scour and the use of single media

which do not require restratification. Problems with gravel movement have occurred but only in a few cases [65]. The absence of such problems must be attributed to the low water and air flow rates which are presumably not sufficient to move the fine gravel, and the fact that air and water are not used simultaneously. Problems with clogged strainers have been controlled by using strainers with 3-mm slots after prior clogging problems were experienced using strainers with 0.5-mm slots.

In the British practice, the water level is lowered to 1 to 2 in. (5.75 cm) above the fixed bed surface, a little below the edge of the washwater overflow which is located about 4 in. (10 to 15 cm) above the surface of the sand. Then air is applied through mushroom type strainers that are used both for air and water distribution. The air scour is applied for 3 to 5 min and then is shut off. Backwash water is then injected immediately through the same nozzles.

The backwashing practice on the European continent as described below is obtained from four sources [61,37,70,108] and therefore probably does not reflect the diversity of the continental practice. The sources describe several points about continental practice which differ substantially from both United States and British practice.

- a. Deeper beds of coarser sand are used and the backwash of these sands is at low rates, with little or no expansion of the bed (<10%)
- b. Backwash is with air and water simultaneously at low water rates followed by water alone to flush the solids out of the bed and to the overflow. The air rate is 2 to 4 cfm/sq ft and the water rate is 10 in./min for the smaller sand sizes (1 to 2-mm size range); for the coarser sizes such as 2 to 3 mm or 2 to 4 mm, the rates are 6 to 8 cfm/sq ft air and 10 to 12 in./min water. In fact, the use of air and water simultaneously is considered absolutely essential because air alone compacts the bed and causes solids to be pushed deeper into the bed between the rising columns of air bubbles. The potential danger of media loss is acknowledged if the simultaneous air-water backwash is continued during overflow. It is suggested that if loss is observed that the backwash water rate be reduced during the simultaneous air-water backwash [37]. Mud balls are unknown in Europe using this type of bed design and backwash system.
- c. Supporting gravel is sometimes used but it is of the double reverse graded gravel arrangement, i.e., coarse to fine to coarse in gradation [108]. Otherwise, media-retaining strainers are used but the dangers of clogging and underdrain failure are acknowledged [61].

The renewed use of air scour in the United States has been patterned more after the British practice of using air scour alone first, followed by water backwash. United States air rates have been typically 3 to 5 scfm/sq ft and the subsequent water wash is above fluidization velocity to expand and restratify the dual-media bed, typically 24 to 36 in./min. The filters are usually equipped with media-retaining underdrain strainers without graded gravel support for the media. Because of the fine sand media used in potable water filters (0.5 mm effective size), the strainer openings are very small (0.25 to 0.5 mm), and strainer clogging problems and some underdrain failures have occurred therefrom. Because of these problems, a reconsideration of the United States air-scour design practice may be appropriate.

## V. BACKWASHING WITH FLUIDIZATION AND EXPANSION

In view of the common practice in the United States of backwashing at high velocity with expansion and fluidization of the filter bed, studies were conducted on this method of backwashing. Extensive literature reviews have been completed of both the chemical engineering fluidization literature and the sanitary engineering backwashing literature [4,5,28,80]. That literature will not be repeated in total in this Final Report, but appropriate portions are included to support the stated conclusions.

### Some Fluidization Fundamentals

The phenomenon of fluidization can best be visualized by passing a fluid (gas or liquid) upward through a bed of solid particles in which it encounters a resistance to flow and a resultant pressure drop  $\Delta p$ . As the flow rate  $V$  is increased there is a linear relationship between  $\Delta p$  and  $V$ . As  $V$  is further increased a point is reached at which the pressure drop is sufficient to bear the weight of the solid particles. Any further increase in flow rate causes the bed to expand and accommodate the increased flow while maintaining the pressure drop  $\Delta p$  effectively the same. The fluidized bed thus formed closely resembles that of a liquid [50]. The feature which distinguishes the fluidized bed from other processes (fixed bed, filtration, etc.) is the motion of the particles within the bed. The characteristics of an ideal fluidized bed and the distortions due to real conditions are indicated in Fig. 1.

Within the last two decades a flowering of thought has occurred in the field of fluidization, fertilized by the necessity of its use in the catalytic cracking of heavy hydrocarbons into petroleum products. This has given rise to five books in English [35,76,91,144,145], six symposia, and countless papers in the literature. The above books and the reviews of recent work by Coulson and Richardson [33] and Botterill [15,16] form excellent general references for this study.

### Point of Incipient Fluidization or Minimum Fluidizing Velocity - $V_{mf}$

This is the fluid velocity required for the onset of fluidization. It could be defined exactly as point A in Fig. 1 for an ideal fluidized bed. For a real graded bed it is defined by some as the intersection of the two linear sections of the curve [35,76] while alternate definitions are presented by others [110].

The bed is completely fluidized when the friction drag or pressure drop across the bed is just enough to support the weight of the filter media [35]. Mathematically, this relationship is given by

$$h\rho g = l(\rho_s - \rho)g(1 - \epsilon) \quad (1)$$

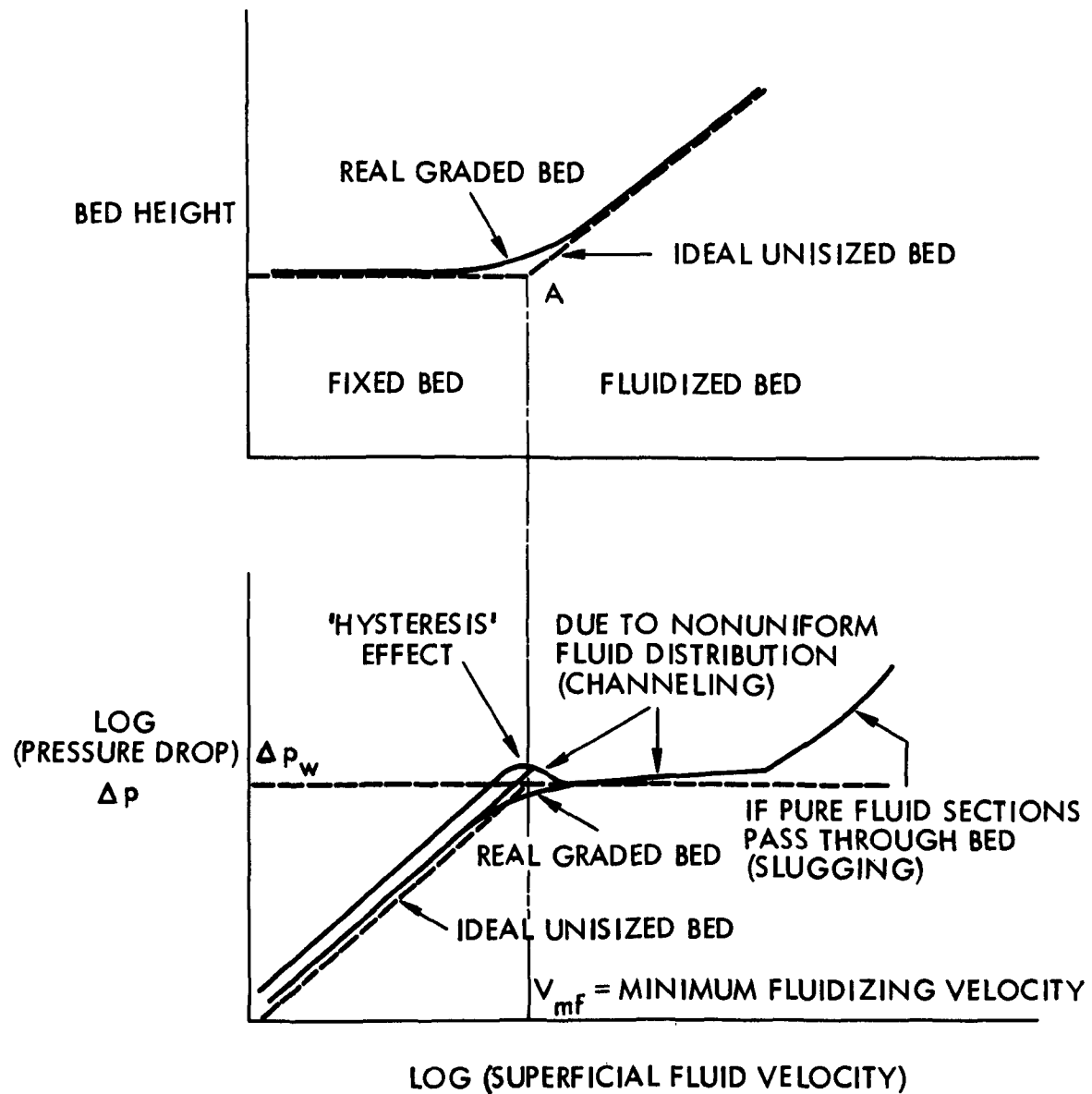


Fig. 1. Characteristics of fluidized beds.

where

$h$  = pressure drop across the fluidized bed  
 $\ell$  = height of expanded bed  
 $\epsilon$  = porosity of expanded bed  
 $g$  = acceleration due to gravity  
 $\rho_s$  = particle mass density, and  
 $\rho$  = fluid mass density.

The simplest bed expansion can be worked out by considering a bed which is fluidized from initial porosity  $\epsilon_0$  at height  $\ell_0$  to a porosity  $\epsilon$  and a height  $\ell$ . Since the volume of solids within the bed remains constant, then for a bed of constant cross section we have

$$\ell_0(1 - \epsilon_0) = \ell(1 - \epsilon). \quad (2)$$

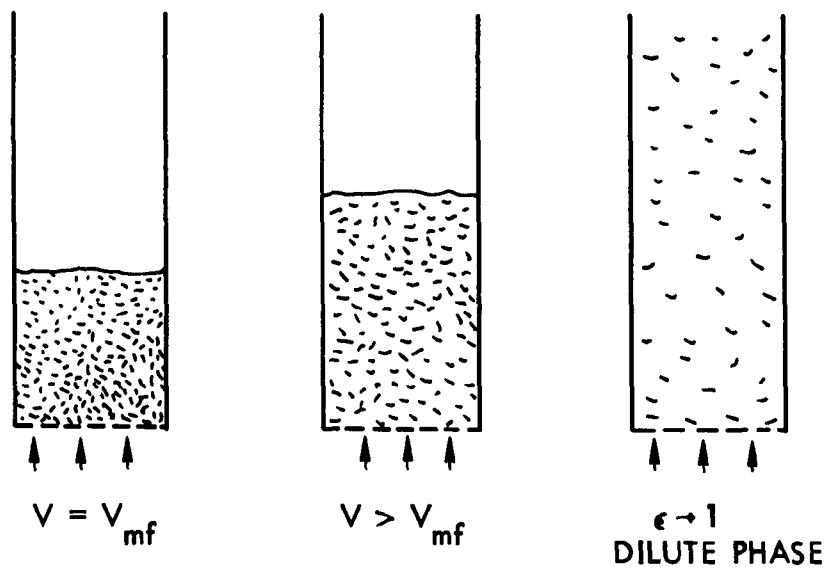
#### Particulate or Homogeneous Fluidization

In most liquid fluidized beds there is a uniform increase of bed height for velocities greater than  $V_{mf}$ , and the liquid passes smoothly and appears uniformly distributed within the interstices of the solid particles as shown in Fig. 2. This type of fluidization with a uniform distribution of particles was termed "particulate" by Wilhelm and Kwauk [141]. The condition of a filter bed while being washed by water is particulate.

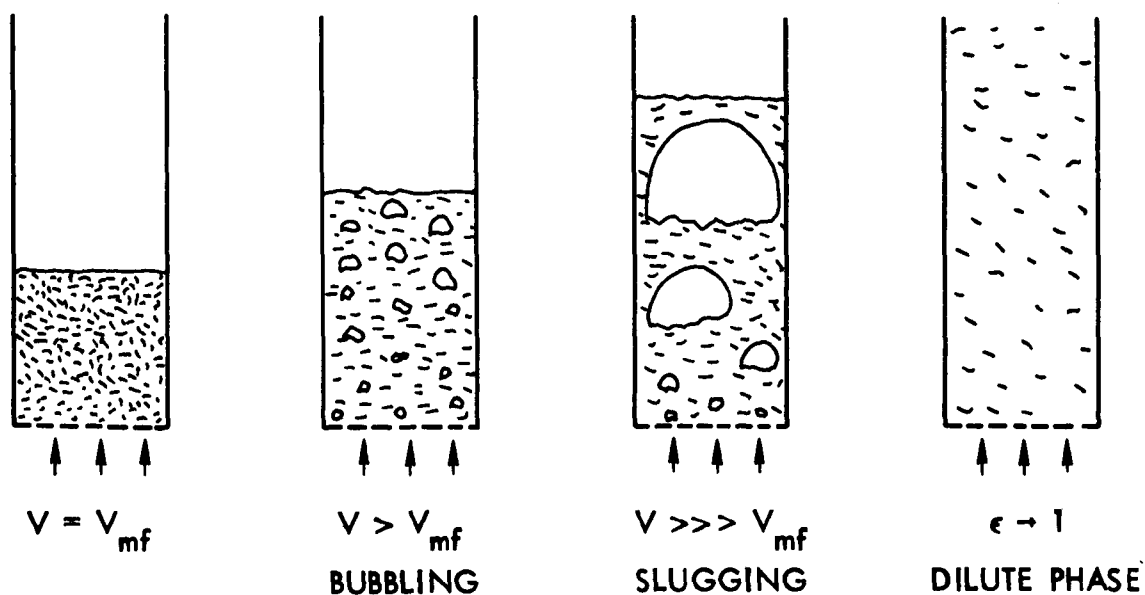
#### Aggregative or Nonhomogeneous Fluidization

For most gas-fluidized systems, part of the gas breaks through the bed in the form of bubbles which are considered shaped as a spherical cap or a sphere with a collection of solid particles at the bottom as shown in Fig. 2. The two-phase theory of aggregative fluidization postulates that all gas in excess of minimum fluidization passes through the bed as bubbles. The bubbles increase in size as they pass through the bed and burst at the surface of the fluidized bed with a light scattering of the surface solid particles and those carried by the bubbles. This is termed "aggregative" fluidization. At higher rates of gas flow, the frontal diameters of the bubbles build to the diameter of the containing apparatus, and a condition of the bed called "slugging" is developed. It cannot be overemphasized that all discussion in this review referring to aggregative fluidization is a description of a two-phase system, composed of solids and gas. Air scouring in backwashing of filters is a three-phase system containing the media, water, and air, as will be discussed later.

In recent years it has been shown theoretically [7,57,66] as well as experimentally [35,57,98,113] that both particulate and aggregative fluidization are the ends of a continually changing spectrum of an intrinsically unstable system. There are bubbles of liquid in a particulately fluidized bed, but their magnitude is of the order of the



**PARTICULATE FLUIDIZATION  
(MOST LIQUID SYSTEMS)**



**AGGREGATIVE FLUIDIZATION  
(MOST GAS SYSTEMS)**

Fig. 2. Fundamental behavior patterns.

solid particles; hence, they are not discernible for a bed of small height. However, their effects are noticeable in beds of large depth or when the ratio of the density of solid to liquid increases [66]. Thus steel or lead balls fluidized in water behave aggregatively while hollow resin or FCC catalysts fluidized by air behave particulate.

It should be noted that an aggregatively fluidized condition cannot be maintained at large average porosities of the bed due to an inadequacy of available solid material to form the shells of the bubbles. Thus a reappearance of homogeneous fluidization can be expected at very high mean bed voidages. Several workers have presented relationships for predicting whether particulate or aggregative fluidization will occur [35,104,141,145].

### Channeling

Channeling [76,145] is a condition in which the fluidizing medium passes through a bed of particles along a preferred path. Channeling can occur in both particulate and aggregatively fluidized beds but is more common and pronounced in gas-fluidized beds. In an aggregatively gas-fluidized bed, channeling can be described as follows.

The majority of the gas passes through in the form of bubbles randomly distributed throughout the bed. When these bubbles are not randomly distributed but tend to rise through the bed along a preferred path, then the bed is approaching a channeling condition. Once this trouble has started, it will lead to a greater and greater degree of channeling. Two typical cases of channeling have been mentioned, "through channeling," when the flow paths extend through the entire bed, and "intermediate channeling," when only a portion of the bed is subject to irregularity. The design of the gas inlet device at the bottom of the bed has an important effect on channeling. Channeling is also affected by the characteristics of the solid phase such as size, shape, and density. It is more pronounced for finer particles which tend to agglomerate. Channeling tendencies are always smaller with porous plate distributors than with multi-orifice distributors.

### Spouting

Spouting [12,76] is a technique for agitating a bed of particles too coarse to fluidize well. It is in a sense a combination of a dilute fluidized phase in the form of a rising spout surrounded by a downward moving fixed bed of solids. Becker [12] observed that there is a maximum bed depth above which spouting cannot occur. He observed that the minimum spouting velocity, expressed as a superficial velocity, required to fluidize the maximum spoutable bed depth is identical with the minimum superficial gas velocity causing onset of aggregative fluidization for the same fluid and solid system. The author differentiated between real spouting and pseudospouting. According to

him, pseudospouting is a case in which an internal channel is formed under any condition. Pseudospouting is described as a feeble form of agitation. It is nothing more than an empty vent containing essentially no rising solids and owing its stability to the bridging tendencies of the particles. In real spouting, agitation is caused by an intense, continuous jet of gas piercing a quiescent bed and yielding its energy to generate a well defined stream of particles, the spout, whose upward motion is balanced by the downward motion of the surrounding annulus.

### Gas-Liquid Fluidization

Some research workers [39,89,119] have studied the use of gas-liquid fluidized beds. In gas-liquid fluidization, the liquid flows upwards through a bed of solid particles which is fluidized by the flowing liquid, while the gaseous phase moves as discrete bubbles through the liquid fluidized bed. Gas-liquid-particle operations, also called three-phase systems, are of comparatively complicated physical nature. Three phases are present, the flow patterns are extremely complex, and exact mathematical models of the fluid flows and mass transport in these operations probably cannot be developed at the present time. Description of these systems will be based upon simplified concepts. These processes are, however, distinguished by their high rate for various purposes (e.g., heat transfer), good phase contact, and wide ranges over which the process can be varied.

For air scouring to be identical to aggregative fluidization, the water from the filter must be completely drained and sufficient air supplied to fluidize the sand bed. The rate of air supply required to fluidize a sand bed of average size (0.8 mm) would be 80-100 cfm/sq ft [4] as compared to the 3 to 5 cfm/sq ft commonly used for air scour in backwashing. It is clear that a true case of aggregative fluidization is not possible in a normal air-scour operation in filtration. But there are similarities between three-phase fluidization and aggregative fluidization. Three-phase fluidization in filter backwashing exists when air is applied to a bed which is fluidized with water. A three-phase system of backwashing rapid sand filters such as this is discussed by Camp [26] and Simmonds [112]. Note that there is a danger of loss of filter media in this operation unless the air scour is stopped before the water level overflows into the wash troughs. The more common method of air scouring is a special case of a three-phase system where the water level is lowered to just above the top surface of the sand and then the bed is air scoured at the rate of 3 to 5 cfm/sq ft without the concurrent upward flow of water and without fluidization of the bed.

It has been observed [89,119] that an increase of the gas flow rate often causes a decrease of bed expansion for three-phase fluidization, whereas bed expansion increases as the flow rate of the fluid medium is increased for two-phase fluidization. It was reported [89] that this reduction in bed height or porosity is more marked in beds of

small particles than in beds of large particles. A contraction of 48% has been observed in a highly expanded bed of 0.28-mm ballotini. The reduction in bed height was explained by the hypothesis that a portion of the liquid moved upward in the wakes of the gas bubbles at a velocity much higher than the average liquid velocity. The liquid velocity in the rest of the bed was consequently reduced below the average liquid velocity, and the expansion of the bed is reduced correspondingly. This reduction in bed height is more than the gas volume present at any instant, thus causing a net reduction of total bed volume.

Rigby et al. [101] have investigated bubble properties in three-phase systems. They showed that gas bubbles have a greater tendency to rise in the center of the bed than near the walls. This tendency was observed even when bubbling at the base of the column was quite uniform. As result of this tendency, these authors concluded that the most favorable gas distributor may not be one which distributes gas evenly over the bed cross section, as has generally been assumed, but one which introduces relatively more gas near the walls to counteract the natural tendency for bubbles to rise in the center of the bed.

Ostergaard [90] measured the rate of growth of gas bubbles formed in a liquid-fluidized bed at a single orifice of 3.00-mm diameter for gas flow rates varying from 9 to 63 cc/sec. The experiments were carried out with tap water, atmospheric air, and sand particles having an average equivalent diameter of 0.64 mm. The equivalent diameter was defined as the diameter of a sphere with the same average particle volume. The bubble frequency at the orifice was measured by an electrical resistance probe connected to an oscilloscope. The bubble frequency at the bed surface was calculated from cinephotographs. The measured rate of coalescence was markedly dependent on bed porosity, having a relatively high value near the point of incipient fluidization and decreasing with increasing liquid velocity and bed porosity. This is in general agreement with the results of Rigby et al. [101], as is the observation that the main change in bubble frequency occurs within a relatively short distance from the orifice. The rate of coalescence did not vary significantly with gas flow rate. Observations of bubbles emerging through the bed surface show that bubble shape is markedly dependent on liquid velocity. A bed near incipient fluidization is characterized by a high viscosity, and an emerging bubble is of nearly spherical shape, whereas a fluidized bed of high porosity is characterized by a viscosity not very much higher than that of water, so that an emerging bubble is of spherical cap shape. The author [90] also observed that no individual bubbles were observed at the orifice at zero liquid velocity. This was probably due to the formation of gas channels in the fixed bed.

### Predominance of Hydrodynamic Forces in Cleaning by Water Fluidization Alone

The basic hydrodynamic behavior of a fluidized bed is frequently forgotten in trying to explain the removal of impurities from the grain of a filter sand during backwashing. Fair and Geyer [45] mention that "substances adhering to the filter grains are dislodged ... by the rubbing together of the suspended grains." Babbitt et al. [8] state that the "purpose of such expansion is to cause the sand grains to rub against one another."

From purely theoretical grounds the suspension of particles in a rising stream of fluid is expected to require a field of flow around each particle, thus negating the concept of a number of particles rubbing together when fluidized. Considerable direct evidence [105,106,135] as well as most correlations [4,76,91] are based on the assumption that the particles are uniformly distributed within the beds. Thus, experimental verification of these correlations implies that the assumption of uniform distribution is reasonably valid. Further qualitative support of the above assumption is the fact that particle attrition [145] is negligibly small in fluidized beds and also the fact that however well filters are backwashed, sand growth by layers of deposited material frequently occurs in significant amounts. Johnson and Cleasby noted a growth from 0.43 mm to 0.65 mm in 14 years at the Ames plant [67].

The most significant work which removed the above from the realm of postulates to that of fact is Rowe's studies of "Drag Forces in Hydraulic Models of Fluidized Beds I, II" [105,106]. He showed in a fundamental study that the drag forces on spheres arranged in regular arrays is extremely sensitive to the separation between the particles. The required modification to the drag coefficient for a single particle  $C_p$ , due to neighboring particles, was effectively to multiply it by  $[1 + (0.68/\delta)]$ , where  $\delta = x/d$ , the dimensionless spacing of the particles based on the particle diameter,  $d$ , and the clear distance between particles,  $x$ . Particles in rhombohedral packing were found to be subjected to a drag about 70 times greater than that on an isolated particle for the same superficial velocity of the fluid [106]. The value of the drag coefficient given by the above expression when  $\delta = 0.01$  is 69 and was considered to refer to the maximum condition [105].

Rowe's studies showed that small local changes of particle concentration were unstable because they required a very large change in the velocity distribution. A local decrease in particle concentration of 3% required the velocities to be doubled. It can be seen that as  $\delta \rightarrow 0$ , the drag coefficient  $\rightarrow \infty$ ; however, the expression does not apply for  $\delta = 0$ . The studies indicate the existence of lateral repulsive hydrodynamic forces between particles; these became extremely large as the spacing between particles was reduced. Thus physical contacts between particles in fluidized beds were extremely limited, and the particles

were uniformly distributed in the fluid field. Rowe clearly indicates that his development does not eliminate the existence of particle contacts and concentration effects, but only shows that they cannot persist and that their effect is negligible. Adler and Happel [1] have also indicated that solid-solid frictional effects in the low porosity range of fluidized beds where they should be most significant were inconsequential.

In a study of the stability of particulate fluidization, Jackson developed general equations of motion for a fluidized assembly of identical particles [66]. In discussing the equations of motion, he neglected terms due to the direct interaction by collision and justified it in two ways. First, if collisions between particles were of comparable importance to drag forces then the number of particles per unit volume would be expected to decrease with height above the bed support, in the same way as the pressure of the atmosphere decreases with height above the earth's surface. Second, a posteriori justification was provided by the fact that the equations of motion obtained by neglecting collisions gave a good qualitative account of the main phenomena of fluidization.

Murray [85] summarized Jackson's arguments and also gave some of the other reasons for the fact that negligible particle collisions occur in fluidized beds. He stated that

Collision forces, which are a form of particle pressure, are also small, since, if such a term were important it would probably increase with  $n_p$  ( $n_p$  = number density of the particles). This would result in a gradation in  $n_p$  from the surface into the bed from zero to a finite value, this is not observed. The surface appears to be a discontinuity. Furthermore, observation of particle flow round a bubble by X-ray techniques seems to show little or no contact interference between neighboring particles. Also, if collisions were frequent, the noise would be noticeable, which is not the case.

Though Murray was chiefly concerned with aggregative fluidization, it is a well known fact [4,35,85,145] that the fluidized section of the bed outside the bubbles is very similar to a particulate fluidized bed at minimum fluidization. The hydrodynamical behavior of the continuous phase is hence similar to that of a particulate fluidized bed.

In a recent two-dimensional study (which may not effectively extrapolate to three dimensions) using a monolayer of fluidized particles, Volpicelli et al. [135] indicated the presence of inhomogeneities in particle distribution within the bed. They presented photographic stills from their motion picture study of the fluidized beds. A study of these photographs by the author of this report showed that particle contacts are rare, which confirms Rowe's studies. Their

studies must be interpreted with caution since they used steel balls and water as one of their systems; this system will exhibit marked aggregative tendencies. This study also indicated that particle flow patterns switch from a circulation regime to a regime of quasirandom motion as the voidage increases. This characteristic, confirmed by other workers too, has important implications in the development of criteria for backwashing at optimum rates.

In a recent Russian theoretical study, on the pseudoturbulent diffusion of particles in homogeneous suspensions using tensor analysis, turbulence equations were developed for a two-phase system by Buevich and Markov [20]. In a discussion on the collisional dissipation of energy the authors stated that particles undergoing collision have step changes in velocity which will always be small for dilute suspensions. They also said that the collisions of particles suspended in a liquid are characteristically very gradual, and there are no step-wise changes in the particle velocities. The latter is due to significant increases in the pressure in the liquid layer between the particles as they approach each other and to the need for "squeezing out" this layer before direct contact of the particles occurs. An analogous effect also occurred as particles approach a solid wall and in lubrication processes, when the lubricating liquid in the gap between bearing and slider played the part of this liquid layer. Hence, they concluded that any model of energy dissipation based on elastic collisions will be in error by at least an order of magnitude.

Ruckenstein [107] developed a physical model for a homogeneous (particulate) fluidized bed, using the equation of motion of one particle which is part of an ensemble of particles in interaction with a fluid. The equation is established by neglecting the interaction by collision of the particles of the ensemble.

All the above evidence in the fluidization literature pinpoints one single fact: the effect of collisional interactions between particles in the fluidized state is comparatively insignificant. This fact, now becoming more and more accepted in the sanitary engineering literature [4,6,26,132], indicates that the age-old argument whether abrasions between particles or the hydrodynamic shear forces are the predominant cleaning mechanism, should finally be laid to rest. This conclusion is also one of the basic assumptions of the theory of optimum backwashing developed in this chapter.

## VI. OPTIMUM CLEANING BY WATER BACKWASH ALONE

### Particulate Fluidization and Optimum Turbulence - Evidence From the Literature

Analyzing a filter being backwashed, qualitatively, will indicate that at minimum fluidization individual particles have no motion and that frequently the fluid motion is streamline, and hence cleaning of the media will be negligible; at the other extreme overexpansion of the bed will also reduce the cleaning action due to large separations between particles. This macroscopic analysis indicates that somewhere between the two extremes lies an optimum condition which we seek.

The review of the literature quoted in this section indicates a striking phenomenon discovered in particulate fluidization research: the existence of a maximum value for most turbulence parameters at a porosity of 0.65 to 0.70. This was the fact that originally led Amirtharajah toward inferring that the elusive condition of optimum backwash would probably be centered around this porosity [4]. This section summarizes his theoretical and experimental proof of this hypothesis [5].

Considerable evidence was collated in a previous section to show that particle abrasions or collision are inconsequential in a fluidized bed. This fact leads immediately to the deduction of two very important hypotheses: (1) the present United States mode of cleaning filters by fluidization has an intrinsic weakness in the process itself, and (2) the most that can be achieved from the process is to backwash at flow rates which will produce the maximum turbulence and the maximum shear in the fluid-particle field, for this is the principal mode of cleaning. The first weakness is being remedied by the use of backwash auxiliaries such as air scour or surface washers. The second problem is far more tractable both theoretically as well as experimentally with the systems we have at present and the knowledge we have in fluidization.

Hanratty, Latinen and Wilhelm [56] were the first to use Taylor's turbulence equations to describe the diffusion of a tracer dye in particulate fluidized beds. They established the mixing parameters - eddy diffusivity and the scales and intensities of turbulence. The experimental studies were made in a 5.40-cm Lucite tube, by admitting methylene blue dye from a central location to the bed of fluidized particles. Four different systems consisting of glass spheres of diameter 0.47, 0.93, and 3 mm, as well as silica spheres of 1.84 mm were used for the solids in the bed. In all runs except two, a constant expanded bed height of 20.3 cm was maintained, and the porosity was adjusted by changing the amount of solids in the bed. Two types of sampling traverses - radial and centerline - were used to measure the spreading of the dye.

The results indicated that the theoretical equations of Taylor's theory of turbulence were applicable for diffusion in a particularly fluidized bed. A minimum Peclet number, i.e., maximum eddy diffusivity, was found for all particle sizes and corresponded to a porosity of 0.70. This maximum eddy diffusivity was directly related to the maximum in the length scale of turbulence, which also occurred at this porosity. The intensity of turbulence increased continuously for all porosities. For the bed of 3-mm spheres the maximum scale of turbulence was approximately 4 mm.

Hanratty et al. did not attempt to provide a quantitative explanation for the minimum Peclet number at the porosity of 0.70. Qualitatively explaining the observed phenomenon in terms of the random-walk model they stated

Mixing in a packed bed was found to be explainable in terms of a random-walk model, and it is suggested that a dense fluidized bed retains elements of this mechanism. The distance a fluid element must side step in order to pass around a particle decreases as the bed is expanded. Eventually, at a fraction void of 0.70, a fluid element may begin to flow past solid particles without the necessity at each level of flowing laterally in order to evade a particle. Beyond the critical fraction void, in dilute beds, the turbulence is particle generated, and the eddy diffusivity is a direct function of particle population, leading to an increase in the Peclet number as the velocity is increased.

Cairns and Prausnitz [21,22] studied macroscopic mixing and longitudinal mixing in solid liquid fluidized beds. The studies in longitudinal mixing were made by determining the electrical conductance break-through curves using very small electrical conductivity probes with a step-function input of salt-solution tracer. The principal advantage of the conductivity method is that it enables continuous monitoring, and hence the tracing, of transient velocities in the system. Longitudinal eddy diffusivities were determined for 1.3- and 3.0-mm lead spheres and 3.2-mm glass spheres in 2- and 4-in. diameter beds at a distance of five bed diameters from the injection point.

The analysis of the data was based on a statistical model developed by H. A. Einstein in connection with the motion of pebbles in a water stream. The model gives an easy and rapid method of determining the Peclet groups from the experimental data. The longitudinal eddy diffusivities were determined for various solids-to-column-diameter ratios, various radial positions and various void fractions. The results were consistent with the fact that the fluidized bed was considered as a transition between a packed bed and an open tube. It was found that the ratio of longitudinal to radial eddy diffusivity was approximately 20 to 30. Thus, the rate of longitudinal mass transfer was very much greater than the radial transfer.

In all cases a maximum of the longitudinal eddy diffusivity occurred at a porosity of 0.65 to 0.70. This maximum was much more pronounced for the lead sphere system than for the glass sphere system. On defining the Peclet group in terms of the diameter of the solids in the system, a minimum Peclet number occurred at a porosity of 0.7 in all cases. However, for the glass sphere system an asymptotic minimum value was reached for all porosities greater than or equal to a porosity of 0.7. The authors concluded that the eddy diffusivity was strongly affected by the density and concentration of particles in fluidized beds and a maximum in the mixing properties occurred at a fraction voids of 0.7.

In the study reported later the authors investigated macroscopic mixing [22] with a similar experimental setup. They measured the frequency distribution of fluctuations and the correlation coefficients at two points separated by a known distance. From the mixing data, radial eddy diffusivities, scales of turbulence, and intensities of turbulence were measured.

Since mixing-length theory suggested that the mixing process in fluidized beds was analogous to molecular diffusion, a similar analytical model for a steady-state system in cylindrical coordinates was used for analysis of the data. The results showed that the scale of turbulence maximized at a porosity of 0.70. A plot of the Peclet number indicated a minimum corresponding to this same porosity. Detailed visual records of the behavior of the solids and the fluid were also noted. The most active particle motion was found to occur in the range of  $\epsilon = 0.70$ ; the motion of the particles changed from a circulation pattern to that of random motion. This change in flow pattern was also noted by Volpicelli et al. [135], as recorded before, in their studies of a monolayer of particles in the vertical plane.

Lemlich and Caldas [75] studied the heat transfer characteristics from the wall to the fluid within a particulate fluidized bed. They used a bed of glass spheres fluidized by water and found that the heat transfer coefficient maximized at a transition between two regimes of flow. The lower regime indicated limited axial mixing, while considerable mixing was evident in the temperature profiles at the higher rates of flow. The maximum heat transfer coefficient occurred at porosities of 0.66 and 0.81 for solid particles having diameters of 0.50 and 0.29 mm, respectively.

Handley et al. [55] studied the mechanics of fluid and particles in a particulate fluidized bed using unusual experimental techniques. They obtained a transparent solid-liquid system using soda glass (density = 2.50, refractive index = 1.52) and methyl benzoate (density = 1.08; refractive index = 1.52). An opaque white glass tracer particle having the same properties as the transparent soda glass was used, and the motion of this particle was studied by cine photography. A similar technique was used in Ulug's studies of flow visualization [132].

Fifty histograms of displacement vectors measured from projected stills showed a mean zero solids velocity and showed that standard deviations were independent of radial or vertical positions in the bed. The mean zero solids velocity means that a single particle over a sufficient length of time does not have a velocity, which is to be expected because solids in a fluidized bed do not have a finite velocity over a long period. Thus, particle motion was random, and homogeneous although isotropic conditions were not obtained. They then applied Taylor's random-walk statistical analysis [49,125,126] to the motion of the particles as well as the fluid regimes. The results showed that the root mean square (rms) of the turbulent fluid velocity, passed through a maximum at some voidage between 0.44 and 0.75; the extrapolated graph indicated a value near 0.70. The rms of the turbulent particle velocity similarly passed through a maximum at a voidage between 0.44 and 0.75. Using fluid dynamic pressure measurements (made with a pitot meter), they also found that the vertical turbulent fluid velocity component passed through a maximum at  $\epsilon = 0.68$  to 0.70. Unfortunately, due to the experimental limitation requiring transparency, the authors did not investigate sufficient systems expanded to porosities less than 0.65.

In one of the pioneering studies in fluidization, McCune and Wilhelm [81] determined mass transfer characteristics by measuring the partial dissolution of spherical and flake-shaped naphthalene particles in a fluidizing stream of water. They found that the mass transfer characteristics for 1/8-in. pellets maximized around a porosity of 0.70 to 0.75.

In a recent study, Galloway and Sage [51], using an instrumented copper sphere within a packed bed of spheres, studied the local thermal transfer from the instrumented sphere. Using the data of McCune and Wilhelm [81] and Rowe [105,106], they established a boundary layer model based on the behavior of thermal and material transfer from single spheres and cylinders in turbulent fluid streams. The studies showed that a maximum mass transfer occurred at fraction voids of 0.70 for fixed beds. Extending the use of the model for fluidized beds with literature data, they showed that the maximum mass transfer correlated with the maximum turbulence at the expanded porosity of 0.70.

Except for the qualitative observation of changing flow fields, the researchers have not sought to explain why this maximum occurred at this porosity. Probably the answer to this lies in Jackson's studies [66]. Jackson probed the fundamental mechanics of the fluidized bed and concluded that particulate and aggregative fluidization were both mechanistically unstable systems. The instability manifested itself as traveling waves of increasing amplitude. His theory predicted that disturbances similar to those of bubbles in aggregative systems would also develop in particulate fluidized beds. However, for particulate systems these disturbances are of the same order of magnitude as the size of the solids in the system and do not develop to a noticeable extent, except in very deep beds. The visual observations of Cairns and Prausnitz [22] previously described were mentioned by Jackson as

evidence for the results he deduced from his stability study. As additional evidence he referred to the papers by Slis et al. [115] and Kramers et al. [73].

Kramers, who was a coauthor of both papers [73,115], studied in the second paper [73] the longitudinal dispersion of liquid in a fluidized bed. The study used an experimental setup similar to that used by Cairns and Prausnitz [21], except that Kramers et al. used very deep beds (12 and 6 m) and fluidized glass spheres of diameters 0.50 and 1.0 mm [73]. In order to avoid any external influences they took great care to eliminate as far as possible all visible systematic eddies. In fact the tubes used for the bed were purchased as a single piece and had no connections or protuberances.

The results indicated [73] a hump in the longitudinal diffusivity at a porosity of 0.7 for the 0.50-mm particles. However, at porosities greater than 0.75, the value of the diffusivity continued to increase. For the 1.0-mm system the hump at the porosity of 0.7 was barely perceptible. Analyzing these results in terms of the reported maxima of Cairns and Prausnitz's studies [21,22], the authors concluded that the eddy diffusivity was composed of two parts. One part was supposed to be due to the eddies produced by individual particles, and this contribution passed through a maximum at the porosity  $\epsilon \approx 0.70$ . The other part, which strongly increased at higher values of porosity, was thought to be connected with the presence of local porosity fluctuations which were seen to travel upwards through the bed.

All the above studies have considered a solid phase and a pure fluidizing liquid. In order for the above results to be directly applicable to backwashing, it is necessary to assess whether the presence of a number of small floc particles in the liquid phase will affect the turbulence parameters. Precisely this question, the effects of solids on turbulence in a fluid, was studied by Kada and Hanratty [71]. Using the same technique as that used by Hanratty et al. [56] to study turbulent diffusion in fluidized beds, mentioned previously in this report, Kada and Hanratty studied the effect of solids concentrations of 0.13 to 2.5% by volume on the turbulent dispersion characteristics of a pure fluid. They found that one of the chief variables affecting the system was the slip velocity, which was the difference between the particle and fluid velocities in the direction of flow. For the systems studied the slip velocity was equal to that of the free fall velocity. It was found that glass particles having diameters of 0.10 and 0.38 mm and concentrations of 1.5 and 1.7% by volume had no effect at all on the turbulent dispersion characteristics of the fluid. One of the principal conclusions of the study was that for systems with small slip velocities the effect of solid concentrations up to 1.5% had no effect at all on the dispersion characteristics. This study provides the final argument for applying the results of the studies reviewed in this chapter to the backwashing of filters.

The evidence recorded above is impressive, since several studies have confirmed the central result. The impressiveness lies in the fact that totally different experimental techniques used to study different, but hydrodynamically related characteristics, namely, scales of turbulence, eddy diffusivities, Peclet numbers, particle and fluid motions, mass transfer and heat transfer effects, all yielded the surprising fact of maximization at a porosity of approximately 0.65 to 0.70. The very few studies which have sought to explain the reason for this maximization of the turbulence parameters indicate that the diffusivity is probably due to two factors: the eddies associated with the particles and the porosity fluctuations which travel up the bed.

The essential conclusions of the preceding literature review can be summarized as follows:

1. Considerable evidence exists in the fluidization literature that particle collisions in the fluidized state are of negligible consequence compared to the hydrodynamic effects. This fact is also being realized in the sanitary engineering field and as a corollary it implies that the use of water fluidization alone to clean a filter is inherently unsatisfactory, and various auxiliary scour systems can be used to overcome this weakness.
2. The fluidization literature abounds with evidence that the fluid and particle fields in particulate fluidization can be described by the statistical turbulence theories, even though the actual fluid velocities are not in the turbulent regime. It has been found that most turbulence parameters have a maximum at an expanded porosity of 0.65 to 0.70. It is hence hypothesized that, within the constraint that fluidization is not an excellent process for cleaning, the best cleaning that can be achieved is by expanding the bed to these porosities.
3. Only qualitative and semiquantitative attempts have been made to unravel the reasons for the optimum in the turbulence parameters. These have been based on the assumption that dispersion is caused by (a) eddies around individual particles and (b) the movement of porosity fluctuations through the bed.

The theory developed for optimum backwashing in the next section of this chapter is entirely new and original; however, it draws sustenance principally from the conclusions and results reported and summarized in this literature review.

#### A New Theory of Optimum Backwashing by Water Fluidization Only

It has been shown in the previous sections that filter cleaning during backwash is due to the turbulence of the fluidized bed and

hydrodynamic shear forces. The voluminous fluidization literature quoted has shown that turbulent diffusion is maximized at the porosity of 0.65 to 0.70. Some mathematical theories have sought to identify this maximum with the eddies around particles and with the fluctuations in porosity which travel up the fluidized bed.

The following new theory shows that hydrodynamic shear forces in a fluidized bed reach a maximum at this porosity of 0.65 to 0.70 for most systems considered. Even if the turbulence parameters cannot be directly related to the shear forces at the present time, on the basis of the discussion in the previous section the cleaning in a backwashed filter bed necessarily reaches an optimum with the maximum shear. Since shear and turbulence parameters are inseparably related it should be possible as a future extension of the theory to obtain an analytical model which will relate the maximum in the hydrodynamic shear to the maxima in the turbulence parameters. This is also predicated on the fact that the actual fluid velocities in a fluidized bed are in the transitional regime and that only the interaction with the solids produces a system having behavior similar to that of a turbulent field.

Consider a one-dimensional analysis of the motion of an elemental volume of fluid as in Fig. 3. Let  $p$  be pressure intensity,  $S$  shear stress,  $V'$  velocity, and  $\Delta x$ ,  $\Delta y$ , and  $\Delta z$  the dimensions of the cube.

The work done by shearing stresses is irreversible and is dissipated as heat. This loss in energy corresponds to what is frequently called head loss or friction loss in fluid flow problems.

Let the power dissipated by the torque composed of the shear forces due to  $S$ , be  $P_1$ ,

$$P_1 = \text{torque} \times \text{angular velocity}$$

$$= (S\Delta x\Delta y)\Delta z \times \frac{\left(\frac{dV'}{dz} \Delta z\right)}{\Delta z}$$

$$= S \frac{dV'}{dz} \Delta x\Delta y\Delta z .$$

By definition

$$S = \mu \frac{dV'}{dz} \quad \text{where } \mu \text{ is absolute viscosity.}$$

Therefore,

$$P_1 = \mu \left(\frac{dV'}{dz}\right)^2 \Delta x\Delta y\Delta z. \quad (3)$$

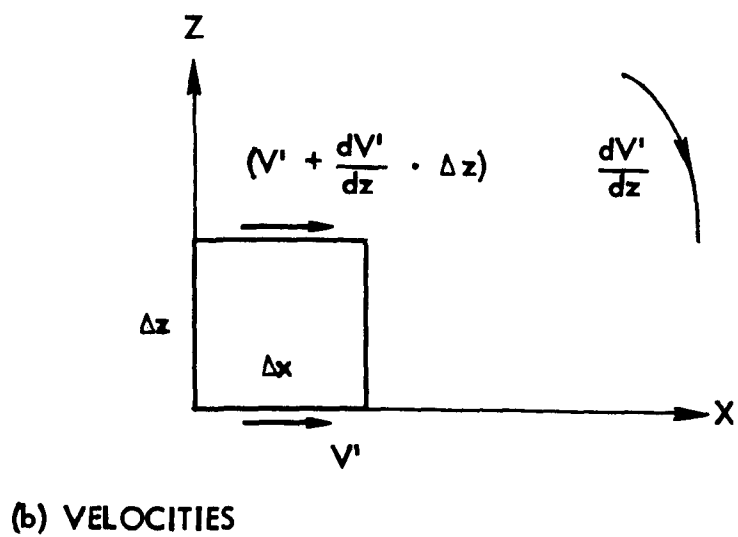
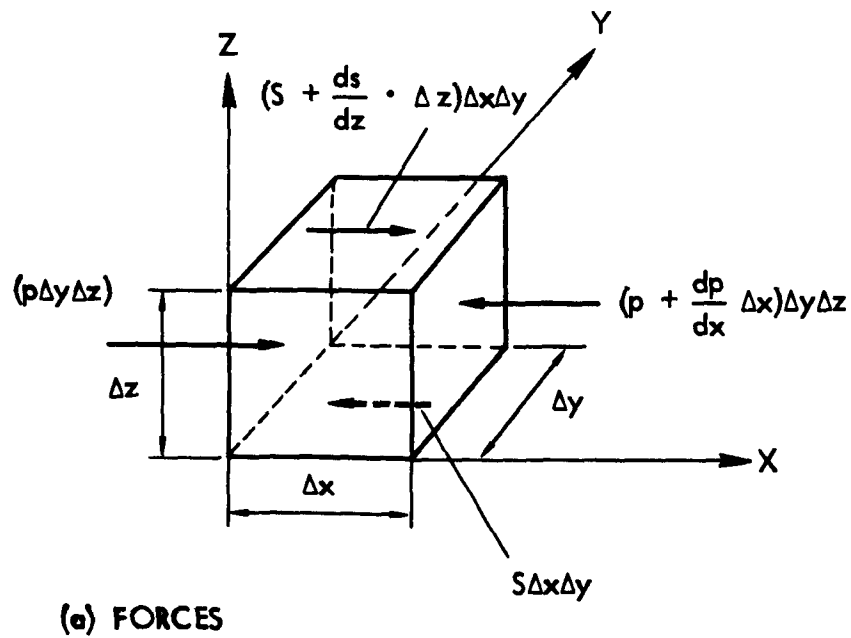


Fig. 3. Shear forces on an elemental volume of fluid.

Let the hydraulic gradient in the  $z$  direction or the head loss per unit length be  $(dh/dz)$ .

Hence the power dissipated by the element of height  $\Delta z$  and area of cross section  $\Delta x \Delta y$ , moving with a velocity  $V'$ , and having mass density  $\rho$  is

$$P_2 = \left(\frac{dh}{dz}\right) \Delta z \cdot \Delta x \Delta y \rho g \cdot V' \quad (4)$$

Since the power dissipated by the shear forces corresponds to the head loss, Eqs. (3) and (4) give

$$\mu \left(\frac{dV'}{dz}\right)^2 \Delta x \Delta y \Delta z = \left(\frac{dh}{dz}\right) \Delta x \Delta y \Delta z \rho g V',$$

that is,

$$\left(\frac{dV'}{dz}\right) = \left[ \frac{g V' \rho}{\mu} \left(\frac{dh}{dz}\right) \right]^{\frac{1}{2}}. \quad (5)$$

Now,  $[(dh/dz) \rho g V']$  is the power dissipated per unit volume, say  $P/C$ , and  $G$  is the velocity or shear gradient defined as  $(dV'/dz)$ ; hence Eq. (5) reduces to

$$G = \left( \frac{P}{\mu C} \right)^{\frac{1}{2}} \quad (6)$$

Equation (6) is the familiar form of Eq. (5), originally derived by Camp and Stein [27] as the general power dissipation function in a three-dimensional treatment. The derivation of Eq. (6) in condensed form is also presented in Fair, Geyer, and Okun [46].

For a fluidized bed with a superficial velocity  $V$ , where  $V' = V/\epsilon$ , the hydraulic gradient  $(dh/dz) = i$ , and  $\mu/\rho$  is kinematic viscosity ( $\nu$ ), Eq. (5) becomes

$$G = \left( \frac{g i V}{\nu \epsilon} \right)^{\frac{1}{2}}. \quad (7)$$

Equation (7) has previously been presented by Camp [25] for calculating the shear forces during filtration and backwashing.

Equation (5) will now be put in the form most useful for the following development of the theory of optimum backwashing:

$$S = \mu \frac{dV'}{dz} = \left[ \mu g \rho \frac{V}{\epsilon} \left(\frac{dh}{dz}\right) \right]^{\frac{1}{2}}$$

that is,

$$S = \left[ \mu g \rho \frac{V}{\epsilon} \left( \frac{dh}{dz} \right) \right]^{\frac{1}{2}} \quad (8)$$

where

$S$  = shear intensity

$V$  = superficial fluid velocity

$\left( \frac{dh}{dz} \right)$  = head loss gradient.

An important property of fluidized beds arises from the fact that particles suspended in a fluid require that the frictional drag of the fluid exactly counterbalance the pull of gravity. In effect, this leads to the requirement that the head loss across a fluidized bed must equal the buoyant weight of the particles [Eq. (1)]. Two of the earliest researchers to report this well known property were Fair and Hatch [47]. In differential form this result is

$$dh \rho g = dz(\rho_s - \rho)g(1 - \epsilon)$$

that is

$$\left( \frac{dh}{dz} \right) = \frac{(\rho_s - \rho)}{\rho} (1 - \epsilon) \quad (9)$$

Equations (8) and (9) above and Eq. (10) below, form the principal equations of the optimum backwashing theory.

Richardson and Zaki's equation, modified by Amirtharajah and Cleasby [6] for graded and irregular particle systems, is

$$V = K \epsilon^n \quad (10)$$

where

$K = f(V_s, \psi, d/D_t)$  = constant for a particular system

$\psi$  = sphericity

$d$  = particle diameter

$D_t$  = diameter of tube or bed

$V_s$  = unhindered subsiding velocity of the particle

$n$  = expansion coefficient in Richardson and Zaki's equation (presented below).

The coefficient  $n$  is a function of the flow regime and the dimensions of the apparatus but is constant for a particular system. For the flow regimes of interest under filter backwashing conditions,

$$n = \left( 4 \cdot 45 + 18 \frac{d}{D_t} \right) Re_o^{-0.1} \text{ for } 1 < Re_o < 200 \quad (11)$$

where

$$Re_o = \frac{\rho V_s d}{\mu} = \text{Reynolds number based on unhindered subsiding velocity.}$$

It should be pointed out that Eq. (11) was developed from fluidization studies of spherical particles and is not directly applicable to nonspherical particles as Amirtharajah and Cleasby had presumed [6]. Nevertheless,  $K$  and  $n$  are constants for a particular filter media.

Substituting Eqs. (9) and (10) in Eq. (8) gives

$$\begin{aligned} S &= \left[ \mu g \rho \cdot \frac{K \epsilon^n}{\epsilon} \cdot \frac{(\rho_s - \rho)}{\rho} (1 - \epsilon) \right]^{\frac{1}{2}} \\ &= \left[ \mu g K (\rho_s - \rho) (\epsilon^{n-1} - \epsilon^n) \right]^{\frac{1}{2}} \end{aligned}$$

that is,

$$S = \alpha (\epsilon^{n-1} - \epsilon^n)^{\frac{1}{2}} \quad (12)$$

where

$$\alpha = \left[ \mu g K (\rho_s - \rho) \right]^{\frac{1}{2}} = \text{constant for a particular system.}$$

The above equation is the basic equation of the writer's theory. It is a relation between the shear stress and the porosity in a fluidized bed.

Let us analyze this function by classical optimization techniques to determine the stationary points of the function as the porosity  $\epsilon$  changes.

The simplest analysis is to consider the function  $S^2$ :

$$S^2 = \alpha^2 (\epsilon^{n-1} - \epsilon^n).$$

Differentiating with respect to  $\epsilon$  by treating  $S^2$  as an implicit function, we have

$$\begin{aligned} 2S \frac{dS}{d\epsilon} &= \alpha^2 [(n-1)\epsilon^{n-2} - n\epsilon^{n-1}] \\ &= \alpha^2 \epsilon^{n-2} [(n-1) - n\epsilon]. \end{aligned} \quad (13)$$

For stationary points,  $dS/d\epsilon = 0$ . Since  $\alpha^2 \epsilon^{n-2}$  cannot be zero, then

$$(n-1) - n\epsilon = 0;$$

therefore,

$$\epsilon = \frac{(n-1)}{n}. \quad (14)$$

Hence the maximum or minimum value of  $S$  is given by the value of  $S$  when  $\epsilon = (n-1)/n$ .

Differentiating Eq. (13) again, we have

$$2S \frac{d^2 S}{d\epsilon^2} + 2 \left( \frac{dS}{d\epsilon} \right)^2 = \alpha^2 \epsilon^{n-3} [(n-1)(n-2) - n(n-1)\epsilon].$$

When  $\epsilon = (n-1)/n$ ,  $dS/d\epsilon = 0$ ; therefore,

$$\begin{aligned} 2S \frac{d^2 S}{d\epsilon^2} &= \alpha^2 \left( \frac{n-1}{n} \right)^{n-3} (n-1) [(n-2) - (n-1)] \\ &= \alpha^2 \left( \frac{n-1}{n} \right)^{n-3} (n-1) [-1]. \end{aligned}$$

Since  $S \neq 0$  and  $n > 1$ ,

$$\frac{d^2 S}{d\epsilon^2} < 0 \text{ when } \epsilon = \frac{(n-1)}{n}.$$

Thus the stationary point is a maximum. Alternatively, the following simpler analysis gives the same result.

Consider the sign of  $dS/d\epsilon$  as it passes through the stationary point. From Eq. (13),

$$\frac{dS}{d\epsilon} > 0, \text{ for } \epsilon < \frac{(n - 1)}{n}$$

$$\frac{dS}{d\epsilon} < 0, \text{ for } \epsilon > \frac{(n - 1)}{n}$$

Hence the stationary point is a maximum.

For a typical filter sand with an effective size of 0.45 mm and a uniformity coefficient of 1.47,  $n$  for the top 3 in. of the graded sand is 3.54 at 25 °C. For a uniform sand of 0.66-mm size,  $n = 3.2$  at the same temperature by Eq. (11).

For the graded sand, maximum shear stress  $S$  occurs at

$$\epsilon = \frac{(n - 1)}{n} = \frac{(3.54 - 1)}{3.54} = 0.72.$$

For the uniform sand,

$$\epsilon = \frac{2.2}{3.2} = 0.69$$

Thus, a maximum shear stress  $S$  occurs in a fluidized bed at the porosity  $\epsilon = (n - 1)/n$ , which corresponds to porosities of 0.69 to 0.72 for real sand systems. This is the main result of the optimum backwashing theory.

The above result, derived entirely from the theory, indicates that optimum cleaning of the filter by maximum hydrodynamic shear forces occurs at the porosity of about 0.70. This theory, in combination with the literature cited in fluidization, which reviewed several experimental studies indicating an optimum diffusion at the porosity 0.65 to 0.70, provides an excellent theoretical framework for experimentally studying optimum backwashing. Detailed experimental studies which provide confirmation of this theory are presented in the next section of this report.

The above theory is developed from three equations which are valid for all types of flow regimes in fluidization. Camp and Stein's equation is valid for viscous as well as turbulent flows since it only equates the energy dissipated by shear to the head loss. The constant head loss equation is valid for all fluidized beds, and Amirtharajah and Cleasby's equation is a modified form of a power function of porosity which is valid for all shapes and sizes of particles. Hence the theory developed is applicable for all particulate fluidized systems in all regimes of flow.

As a fitting closure to the above theory, it is necessary to anticipate the results that can be derived by applying this theory to backwashing in practice. The theory predicts an optimum in cleaning at a porosity of 0.70. Consider a uniform sand bed of depth  $\ell_0$  with a fixed bed porosity of 0.43. For the porosity to be 0.70 in the expanded state of depth  $\ell$ ,

$$\ell (1 - 0.70) = \ell_0 (1 - 0.43);$$

therefore,

$$\ell = 1.9 \ell_0 .$$

Hence the expansion required is about 90%. This can rarely be achieved in practice. However, for a graded system the particle diameters at the top of the bed are a fraction of the diameters in the deeper sections. Thus an expansion much smaller than 100% will cause the porosities to be 0.70 in the top layers. Since these layers are the ones that remove most of the suspended matter in filtration, it can be rationally expected that optimum cleaning of the top layers will produce the best cleaning for the system. Expansions higher than that producing the porosity of 0.70 in the top layers will tend to increase the porosities of the layers on top but will simultaneously cause the lower layers to reach the optimum porosity of 0.70, hence we would expect only a negligibly small decrease in the optimum cleaning. This would cause a nearly asymptotic curve of optimum cleaning to be produced for graded systems.

#### Experimental Support for the Optimum Theory

##### Experimental Apparatus

A schematic layout of the experimental apparatus is shown in Fig. 4. The arrows in Fig. 4 trace the path of water from the tap supply to the outlet drain for filter F3 during a filtration run. The main pilot plant consisted of the university tap water supply (hot and cold) blended in a thermostatically controlled mixing valve A (Lawler Automatic Controls, Inc., Mt. Vernon, New York). The blended water passed through a centrifugal pump B, used as an in-line booster. After being metered in the flowmeter C, the water passed through a dual outlet; one end of this outlet fed the supply water to the mixing tank D, while the other end provided the backwash water supply. Each of these outlets was used singly, and the pump B was only used during high rates of backwash since the normal tap pressure was sufficient for most uses.

The influent to the filters was mixed in tank D with the chemicals being added from constant head capillary feeders. The influent water was pumped from the mixing tank by a centrifugal pump E, which was driven by a variable speed DC motor. This enabled influent control

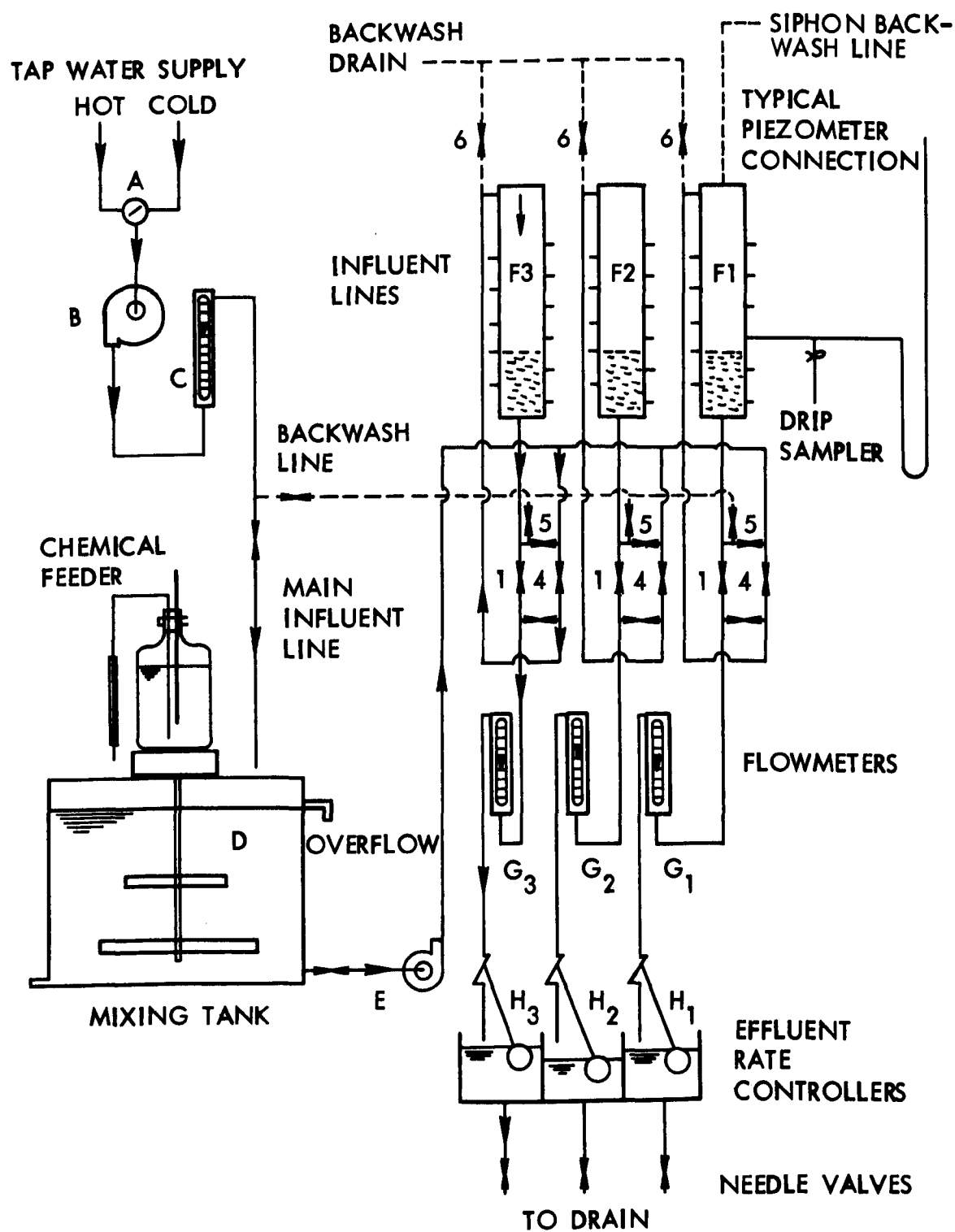


Fig. 4. Schematic layout of experimental apparatus.

to be achieved. The main influent line trifurcated to the filters via the filter valve system. The effluent from each of the filters F1, F2, and F3 passed through its own flowmeter and then discharged freely into a float operated effluent rate controller. Eleven piezometer connections enabled the head losses to be determined at every 3-in. depth of the filter. The expanded height of the filters was determined by a scale placed along the side of the filter.

For backwashing the filters, blended tap water was used and metered in flowmeter C. The backwash line passed via the valve system and discharged in a drain.

The filters consisted of 6-in. inner diameter, 1/2-in. thick plexiglass tubes 4 ft 5 in. deep with a 3-in. high calming section at the bottom. The water was fed through 59 orifices of 1/16-in. diameter in a 1-in. thick underdrain plexiglass plate. Sets of orifices were staggered from one another so as to provide a uniform matrix of orifices on the entire plate. The calming section was filled with 1/2-in. diameter glass marbles. Two pressure gauges, one attached to the center of the calming section and the other to the cover plate of the filter, were provided to serve as safety gauges to warn of dangerous pressures.

The solid particles composing the bed were supported on two stainless steel meshes (No. 50 over No. 10) placed above the 1-in. plexiglass plate with the orifices. Sixteen pressure taps were located on two rows on diametrically opposite sides of the filter to permit observation.

A mixing tank 3-ft high and 3 ft 6 in. in diameter equipped with a slow speed paddle was used to provide the necessary detention time for completion of the iron precipitation reaction. Allowing 6 in. of freeboard, this 180-gal. tank provided a 30-min theoretical detention time at a pumping rate of 6 gpm.

A 1.5-in. outlet diameter, self-priming centrifugal pump (Teel Self-Priming Centrifugal Pump, Model 1P746, Dayton Electric Manufacturing Co., Chicago, Illinois) was used to pump the influent water from the mixing tank to the filters. The pump was driven by a 2 by 3.5-in. pulley drive from a 1/3-HP DC motor equipped with a variable speed control. (Westinghouse Hi-Torque Speed Control with DC Motor, Westinghouse Electric Corporation, Springfield, Massachusetts). This system enabled the influent pumping rate to be increased simultaneously on all three filters by a gradual increase in the speed of the centrifugal pump. Thus influent control was achieved; any changes in flow-rate affected all three filters to the identical extent.

The total flow to the mixing tank during filtration and the total backwash rates were metered by a rotameter C which had a range up to 13 gpm.

The effluent from each filter passed through a rotameter suitable for water flow measurement from 0.2 to 2.0 gpm. These flowmeters,  $G_1$ ,  $G_2$ , and  $G_3$ , were calibrated by determining the time to fill a liter-measuring cylinder.

The effluent from each filter passed via each flowmeter into a float-operated, rate-of-flow controller. The controller maintained a constant rate of filtration by holding a constant head on a needle valve outlet. As the head loss through the filter increased during a run the float valve gradually opened to maintain a constant filtration rate. These rate-of-flow controllers functioned remarkably well.

Granular filter sand (Fine sand, from Northern Gravel Co., Muscatine, Iowa) was used for this study. The original sand had an effective size of 0.455 mm, a uniformity coefficient of 1.52, a specific gravity of 2.648 and a porosity of 0.412. The graded sand used in the latter stages of the study was this original sand. The uniform sand used in the earlier stages of this study was prepared by sieving in a Gilman set of United States Standard sieves on a mechanical shaker for 10 min. The uniform sand used was that sand, 100% of which passed sieve no. 30 and was retained on sieve no. 35. This sand had an arithmetic mean size of 0.548 mm or a geometric mean size of 0.545 mm on the basis of the adjacent sieve openings. Special precautions were taken to insure that the sand was identical in all three filters.

#### Laboratory Analytical Procedures

The influent suspension was prepared by dripping a stock solution of ferrous sulphate ( $\text{FeSO}_4 \cdot 7\text{H}_2\text{O}$ ) from a constant head capillary feeder to the mixing tank, into which a metered quantity of water (4.5 gpm) was added continuously. This flow rate was sufficient to apply to the three filters at 7 gpm/sq ft, and allowed a continuous bleed from the bottom of the mixing tank as well as continuous overflow. The stock solution had an iron concentration of approximately 0.2 M in an acid solution of strength 0.1 N to prevent precipitation in the bottle.

Table 1 gives a typical analysis of the University tap water used in the studies. This is a hard well water of high alkalinity and total dissolved solids and of relatively constant quality. When ferrous sulphate in acid solution was added to this water a yellowish brown precipitate formed. A sample of the suspension from the influent to the filters, after the normal detention in the mixing tank, was filtered through a 0.45- $\mu\text{m}$  millipore filter, and the filtrate was analyzed for any dissolved iron. It was found that within the accuracy of the equipment used no dissolved iron was detectable. This indicated that the precipitation was complete in the mixing tank. It should be noted that no aeration or addition of air was required for the formation of the precipitate. All the runs were made without the addition of any air except that which occurred at the water surface of the tank which was open to the atmosphere.

Table 1. Analysis of University tap water.

Characteristic of water	Concentration, mg/l
Total dissolved solids	680
Total hardness as $\text{CaCO}_3$	365
Calcium hardness as $\text{CaCO}_3$	254
Magnesium hardness as $\text{CaCO}_3$	111
Total alkalinity as $\text{CaCO}_3$	270
Calcium as $\text{Ca}^{++}$	102
Magnesium as $\text{Mg}^{++}$	27
Bicarbonate as $\text{HCO}_3^-$	330
Chlorides as $\text{Cl}^-$	17.5
Sulphates as $\text{SO}_4^{--}$	160
Fluorides as $\text{F}^-$	0.9
Manganese as $\text{Mn}^{++}$	0.0
Iron as $\text{Fe}^{++}$	0.03

The actual nature of the precipitate formed by addition of ferrous sulphate to high alkalinity water has been the subject of considerable controversy during the last decade [30,52,114]. It has been supposed by various workers that the precipitate could be ferric hydroxide, ferrous carbonate, or a combined precipitate of both. It is suggested as a future project that wet chemical analyses be performed on the precipitate to identify its character more definitely.

The main series of experiments consisted of 18 runs, 12 made on uniform sand filters and 6 on graded sand filters. The influent and effluent qualities were evaluated on the basis of iron content. During these 18 runs nearly 5400 analyses for iron were made; thus a simple and accurate method of analysis was required.

During the initial series (run 1 to run 6) the standard method in the water supply field, namely the 1, 10-phenanthroline method was chosen [117]. The procedure was considerably simplified by using the patented single-powder formulation (Hach Chemical Company, Ames, Iowa - FerroVer) which dissolves and reduces the iron without any heating. Since very few interfering ions were present the results were unaffected by such interferences. The developed color was observed at 510 nm on a Beckman Model B spectrophotometer and the iron content read on a calibration curve.

The above procedure for measuring the effluent iron had the following weaknesses: (1) The procedure for measuring the quantity of reagent using a scoop had possible errors from analysis to analysis; (2) the transmittances of the final effluent at the 12-in. depth was too high; (3) the molar absorptivity of phenanthroline limited the possible accuracy of small changes in iron concentration.

In order to alleviate these weaknesses the following modified procedure was used in all the runs after run 6, and it improved the accuracy of the analyses considerably. A new patented reagent (Hach Chemical Company, Ames, Iowa), disodium salt of 3-(2-pyridyl)-5,6-bis(4-phenyl sulfonic acid)-1,2,4 triazine, hereafter called FerroZine, having a molar absorptivity of 27,900 was used. This compound reacts with divalent iron to form a stable magenta complex species which is very soluble in water and may be used for the spectrophotometric determination of iron. The absorption spectrum of the complex has a sharp peak at a wavelength of 560 nm and is uniform in development over the pH range from 4 to 10. Further details of interference studies and statistical data on multiple laboratory studies of FerroZine can be seen in Stookey [120].

The above reagent as a single-solution formulation, FerroZine Solution 1 (Hach Chemical Company, Ames, Iowa), can be added directly to iron hydroxides or carbonates for reduction and dissolution. The procedure for analysis was to add 0.5 ml of FerroZine Solution 1 to 25 ml of water and read the transmittance on a spectrophotometer after allowing 5 min for development of color.

In order to obtain increased accuracy of the transmittance readings on the spectrophotometer, a dual standard procedure, based on the method of ultimate precision as described in Ewing [44] was used. This precision calibration method nullified all the stated weaknesses of the FerroVer method considerably and increased the accuracy of the effluent quality analyses in the second and third series of runs.

During the runs, the influent suspension was sampled every half hour. These samples had iron concentrations of 7 mg/l, and hence they had to be diluted for obtaining readings within the range of the calibration curves.

All the samples of influent and effluent were collected every half hour. Also, the initial effluent quality was analyzed at frequencies of nearly a minute during the first 10 min of a run to study the initial degradation and improvement of effluent quality. These samples were also analyzed by the FerroZine test.

While backwashing the filters after a dirtying run, samples of the backwash water were collected periodically. These samples had considerable amounts of suspended iron floc, some as high as 800 mg/l. These samples were also analyzed using the phenanthroline procedure, the samples being diluted to obtain reasonable readings on the spectrophotometer.

During the course of the research project it was realized that additional evidence of the effectiveness of backwash could be obtained by analyzing the amount of iron left as a coating on the sand after the wash. Not only would this provide comparative evidence for studying

various expansions, but it would also prove beyond any shadow of a doubt that abrasion in the fluidized bed was negligible. This of course, was already anticipated from theory and other experimental results quoted in the earlier chapters.

It was decided to evaluate two methods of washing the sand: (1) a physical wash and (2) a chemical acid wash. The physical wash procedure was selected as outlined below.

The filter was fluidized, and a long-handled scoop was used to remove a sample of sand from the top layers of the fluidized bed. Each sample of sand weighed approximately 25 g. This sand was washed from the scoop into a 250-ml beaker using exactly 100 ml of distilled water. The beaker had already been weighed, empty and dry. It was now weighed containing the sand, the water drawn by the scoop and the distilled water. A 1.25-in. magnet was placed in the beaker with the sand and water, and the sand was washed by the magnetic stirrer for 10 min at a fixed speed. It was found that the distilled water turned quite dark and cloudy and that considerable amounts of iron had been removed from the sand by abrasion between sand particles as well as by abrasion with the magnet. The supernatant iron suspension was stirred by the tip of a pipette and 25 ml were withdrawn and delivered into a 500-ml volumetric flask. Distilled water was added to make up to 500 ml and this diluted solution (1:20) was analyzed for iron concentration using the Ferro-Zinc standard calibration technique.

The beakers containing the sand and the iron suspension (approximately 75 ml) were placed in an oven. The water in the beakers was evaporated, and the beakers containing the dry sand were cooled to room temperature and weighed again.

From the above readings the amount of iron removed from the sand in mg/g can be determined from the following formula:

$$\text{Iron removed (mg/g)} = [\text{Conc. of iron in diluted solution (mg/l)}] \times \frac{[\text{Dilution Factor}] \times [\text{Weight of water (g)}]}{1000 \times [\text{Weight of sand (g)}]} \quad (15)$$

Note that the weight of water in grams is assumed to represent the volume of water in milliliters, and it is the total water in the beaker including whatever water is drawn with the sand from the fluidized bed. This formula gives the iron removed from the sand quite accurately.

The above was the procedure used in all the analyses run on samples of the graded sand during the third series, runs 20 to 25. At the

end of each sand analysis, and prior to the beginning of the subsequent run, the withdrawn samples of sand were returned to their respective filters. Thus, the sand in all the runs was identical and no sand losses were allowed to develop.

#### Chronology and General Descriptions of Filter Runs

Twenty-five filter runs, of which 18 were dual runs, were made. The dual runs consisted of a dirtying run designated A, the backwash of A, and a filtration run designated B. In the following, a reference to a run means the complete dual run. Runs A and B are designated as such. The first 12 runs (series 1: 1A, 1B to 6A, 6B; series 2: 7A, 7B to 12A, 12B) were made on filters with 12-in. depth uniform sands of 0.548-mm mean size. The runs in series 1 and 2 were made at 7 gpm/sq ft, and each run (A or B) lasted for approximately 5 hr. Runs A or B had to be terminated due to the fact that the head losses developed were nearly 8 to 9 ft, and this was the maximum differential height that could be measured on the piezometer boards.

The reagent used for iron analysis in series 1 was FerroVer. In the first series of runs, the dirtying runs A were made on the first day, and the backwash and the filtration runs B were made on the following day. Since it was possible that some physical and chemical changes could have occurred in the solids removed, due to overnight standing, and also because in actual treatment plants backwashing is performed soon after a filter is removed from service, the two runs A and B, and the backwash of runs A in series 2 were made on the same day. Each dual run including backwash required about 15 hr. and two experimenters were required to work continuously to take the readings and make the analyses of iron. In run 1 the samples of water at depths other than the full depth of 12 in. were collected by a single experimenter and kept for about two to three days before all the analyses were completed. It was found that iron in suspension tended to be deposited on the sides of the plastic sampling bottles and that the effluent quality at 9-in. depth of the filter measured on a later date was better than the effluent quality measured at the 12-in. depth on the day the run was made. These results were invalid and were not used in the analyses. All iron analyses from run 2 onward were made within a couple of hours after sampling, and rational readings were obtained. This could only be accomplished because two experimenters worked. The reagent used for series 2 and 3 was Ferro-Zine.

The last six dual runs (run 20A, 20B through run 25A, 25B) were made on 18-in. depth graded sands with an effective size of 0.45 mm and a uniformity coefficient of 1.47. This set of runs was called series 3. These runs were made using identical procedures to those of series 2. However, in addition to ferrous sulphate, a nonionic polyelectrolyte (Dow Chemical Company, Midland, Michigan - Separan) was also added to the influent suspension to obtain a concentration of 0.10 mg/l of

polyelectrolyte in the feed to the filters. The polyelectrolyte was added in the hope of magnifying the differences of backwashing at different expansions.

The parameters used to study the effectiveness of backwash in all three series were (1) initial effluent quality, (2) head loss increase, (3) cumulative effluent quality in the run following backwash, (4) the backwash water quality during backwash, and (5) the backwash water volume.

For series 3 the additional parameter based on the iron which is physically removable from samples of the backwashed sand was also used. The variation of each of these parameters with porosity was studied at six different porosities, 0.55, 0.60, 0.65, 0.70, 0.75, and 0.78, on each of the filters. The expansions needed to obtain these porosities for the uniform sand were approximately 33, 50, 70, 100, 140, and 190% respectively. Since each run was made on a bank of three filters and each series consisted of six runs, the effective number of points for each series was 18. The experiment was designed such that each filter was studied at the six different porosities during a series. Thus by considering all 18 readings of a series of six runs, the small variations between filters and the small variations from run to run were averaged out. Table 2 illustrates the format of the experimental design for series 2, and how the backwash at the different expansions was studied for the three filters F1, F2, and F3. A similar format was used for series 1.

Table 2. Experimental design for series 2.

Run number	Porosity during backwash					
	0.55	0.60	0.65	0.70	0.75	0.78
	Filter number					
7		F1		F2		F3
8	F2		F1		F3	
9	F1			F3		F2
10	F3	F2			F1	
11			F3	F1	F2	
12		F3	F2			F1

For the series 3, the format of runs 7 and 8, as shown in Table 2 for series 2, was repeated three times. This procedure was adopted to enable a particular run to be studied with the backwash expansions of 30, 50, and 75% or 15, 40, and 60%. This format avoided two adjacent expansions such as 40 and 50% being studied in a single run, and the differences for purposes of comparison were enhanced. This was thought advantageous because of the anticipated smaller differences in effectiveness of backwash at different porosities for graded

systems. The cause for the anticipated smaller differences in backwash for graded systems has been discussed previously.

The expansions needed to obtain porosities of 0.58 to 0.82 in the top layers of the graded sand ranged from 15 to 75%, and these were much less than the expansions required for the uniform sand. All backwashing expansions were controlled on the basis of the expanded heights of the fluidized bed during backwash.

In order to reproduce identical conditions with a clean filter at the beginning of each dual run, the following standardized procedure was used for all runs. The filter was expanded to the anticipated optimum at a porosity of 0.70 and washed for 15 min. During the runs 1 to 10 the filters were washed twice before each run began, once at the completion of the previous run and again immediately preceding the start of a run. However, from run 11 onwards, in order to achieve identical conditions to those in a treatment plant, the solids removed in run B of the preceding run were not washed until the following run A. Immediately before the dirtying run A, the filter was expanded to the anticipated optimum at a porosity of 0.70 and washed for 15 min.

In the case of series 1 and 2 the time of backwash was the same for all expansions; for the graded sand studies of series 3, however, the operation was modified slightly. In series 3, the backwash at different expansions was done for different times, so that the same volume of washwater, approximately 36 gal., was used during the total sequence of washing (i.e., valve opening, washing, and valve closing). Also, while the bed was fluidized, one experimenter collected two samples of the backwashed sand at different times. The samples were collected after approximately 10 and 21 gal. of washwater had been used for backwash. A resume of the backwash sequences and sand collection times for the graded sand at different expansions is presented in Table 3.

Table 3. Backwash procedures for graded sand.

Expansion, %	Porosity in top 3 in.	Wash sequence			Sand collection times	
		Valve opening, min	Wash time, min	Valve closure, min	Sample 1, min	Sample 2, min
15	0.58	1.0	10.5	2.0	4.5	9.0
30	0.67	1.0	6.5	2.0	3.0	6.0
40	0.70	1.0	5.0	2.0	2.75	5.0
50	0.74	1.0	4.0	2.0	2.5	4.5
60	0.77	1.0	3.25	2.0	2.0	3.75
75	0.82	1.0	2.75	2.0	2.0	3.5

The observations made during the course of a run can be grouped into two categories, (1) data for analysis and (2) data for quality control. For series 1 and 2 the following readings were taken as data for analysis.

During runs A:

- a. The initial effluent quality for each of the three filters at intervals of 1 min each for the first 10 min of a run.
- b. Piezometer readings at depths of 0, 3, 6, and 9 in. for each of the three filters at frequencies of one-half hour.
- c. The effluent quality at the total depth of 12 in. for each of the three filters at every half hour. The samples were collected at the outlets flowing into the effluent rate controller chambers.
- d. The effluent quality at intermediate depths of 3, 6, and 9 in. for each of the three filters at intervals of every hour beginning with the first sampling at 0.5 hr after the run began. These samples were collected from the continuous drip samplers.

During backwash:

- e. The heights of the expanded bed.
- f. The backwash flow rate.
- g. The piezometer readings at every 3-in. depth of the expanded bed.
- h. The temperature of the washwater.
- i. The backwash water quality from each filter at times of 0.5, 1.0, 2.0, 3.0, 4.0 and 5.0 min during the washing time of 5 min.

During runs B:

Similar readings to those taken during runs A, and indicated above by a, b, c, and d were taken.

For purposes of maintaining identical conditions from run to run, the following data were taken for purposes of quality control, during runs A and B.

- j. Influent iron concentration for one of three filters at frequencies of one-half hour.
- k. The flow rate through the three filters was monitored and adjusted if necessary every half hour. Adjustments were only required during the latter halves of runs A or B.

1. The room temperature and the water temperature were monitored every half hour. Any small changes of water temperature were adjusted.

A similar set of readings were taken during series 3 for the graded sand, subject to the following modifications.

- a. In order to obtain the peak of the initial effluent quality curve, the samples of water were collected at 0.5, 1.0, 1.5, 2.0, 3.0, 4.0, 5.0, 6.0, 8.0, and 10.0 min, respectively.
- b. Since the depth of sand was 18 in., piezometer readings were taken at 0, 3, 6, 9, 12, and 15 in.
- c. The effluent quality was measured at the total depth of 18 in.
- d. The effluent quality at intermediate depths was measured at 3, 6, and 12 in.

The sampling for backwash water quality from each filter was variable depending on the duration of the washing sequences as shown in Table 3. However, the sample collection times were preplanned so that seven samples were collected from each filter at times corresponding to usage of equal volumes of washwater.

In order to evaluate the degree of segregation and the distribution of particle sizes in layers of the fluidized bed, the following experiment was made on the graded sand. The graded sand bed was fluidized to 50% expansion and allowed to stabilize for nearly one half hour and then approximately 3-in. layers of the fluidized bed were siphoned off. These sections of sand were then oven dried and cooled. The total dry volumes were measured, and then representative samples from each layer for purposes of sieving were obtained by repeatedly reducing the total volume of each layer in a two-way splitting sampler to about 500 g. Using the balance sand from each layer after selecting the 500 g, bed porosities of each layer were measured by procedures described elsewhere [4]. From the measured volumes and the expanded heights of the same layers, the porosity of each layer when the total bed expansion was 50% was also calculated.

For purposes of quality control and to check the general form of the curves, the following curves were plotted for most of the runs: (1) head loss against time and (2) ratio of effluent to influent concentration against time (i.e.,  $C/C_0$  vs  $t$ ). Some typical results are shown in Figs. 5 and 6. From the head loss curves it can be seen that the behavior is reasonably linear for the uniform sand. The ratio of effluent to influent curves indicate that even after backwash at various expansions the variation from filter to filter is very small. Thus, for using the effluent quality as a parameter to indicate the effectiveness of wash needs a cumulative effluent quality curve as described by Johnson and Cleasby [67].

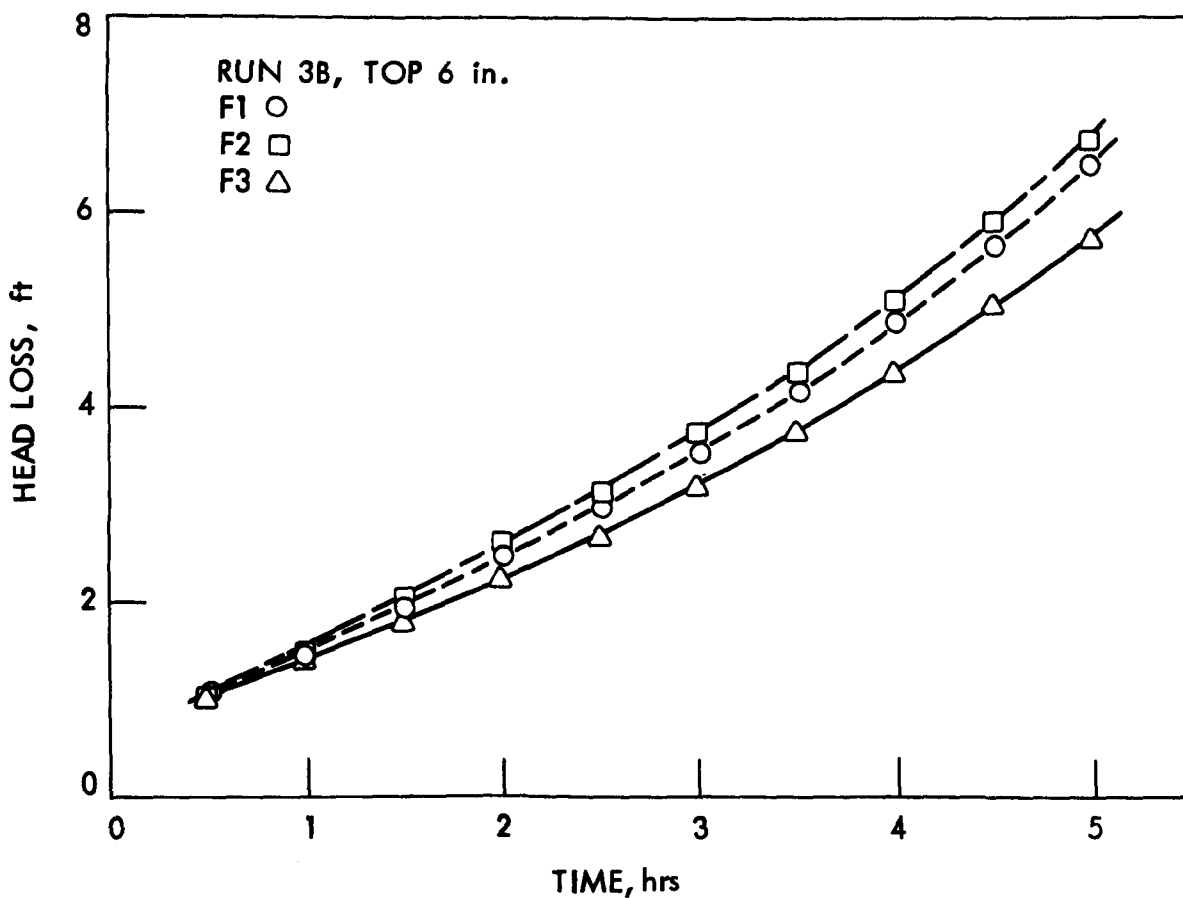


Fig. 5. Head loss curves for run 3B, top 6 in. of filter media.

### Results

The results in this section indicate the variation of the following parameters with the porosity provided during the controlled backwash following the dirtying run: (1) effluent quality at various depths, (2) head loss increases, (3) backwash water quality, (4) backwash water volumes, and (5) sand wash analysis.

Cumulative effluent quality and porosity. Figure 7 shows typical plots of the cumulative differential iron of the effluent with time (run 8, series 2). The ordinate is the accumulated difference between the iron in observation run B and dirtying run A for the effluent from the full depth of the filter. If the ordinate is negative, the cumulative iron in run A was greater than that in run B, or mathematically  $\sum_{\text{time}} \text{Iron (B-A)} < 0$ . In each run all three filters

were dirtied under identical conditions, as explained in the previous chapter. The filters were then backwashed at different expansions, and the quality was studied in the following run. Study of these figures towards the end of the run will indicate which filter

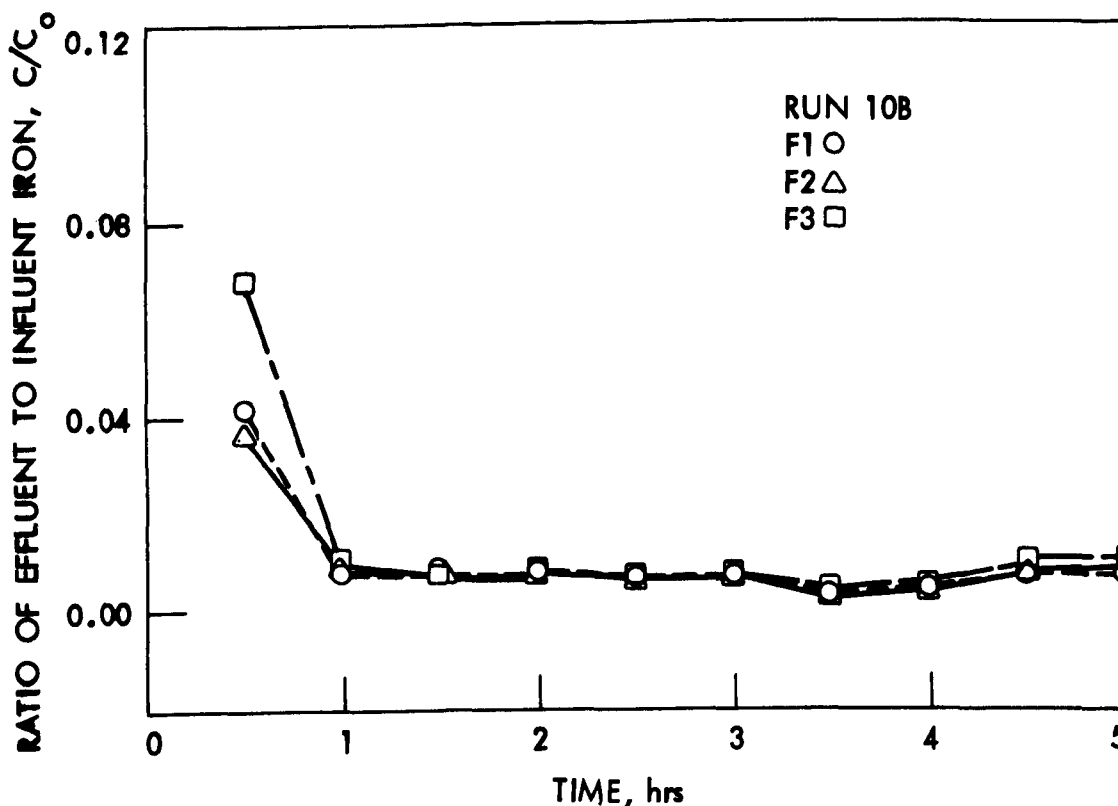


Fig. 6. Variation of the ratio of effluent to influent iron with time.

performed the best in a particular run. The filter with the smallest positive, or the most negative iron produced the filtrate of the best quality in the filtration run compared to the dirtying run.

An index called the effluent quality index was defined to comparatively grade the filters in each run. In each run the filter producing the best cumulative differential effluent quality was given an index value of 3, the next best quality was given an index value 2, and the worst quality was given an index 1. If two filters performed almost identically in a run then the two effluent quality index grades were divided between the two corresponding filters.

The values of the index for all the runs from 7 to 12 and the corresponding porosities in each case are shown in Table 4.

Originally, it was thought that the differential cumulative iron could be summed from run to run to give the basis for comparison. In practice it was found that even with the best possible experimental controls it was impossible to reproduce identical dirtying runs in the series, due to the inevitable fluctuations in flow rate and iron concentrations. However, within a single run, such changes occurred on all three filters simultaneously, and comparisons within filters

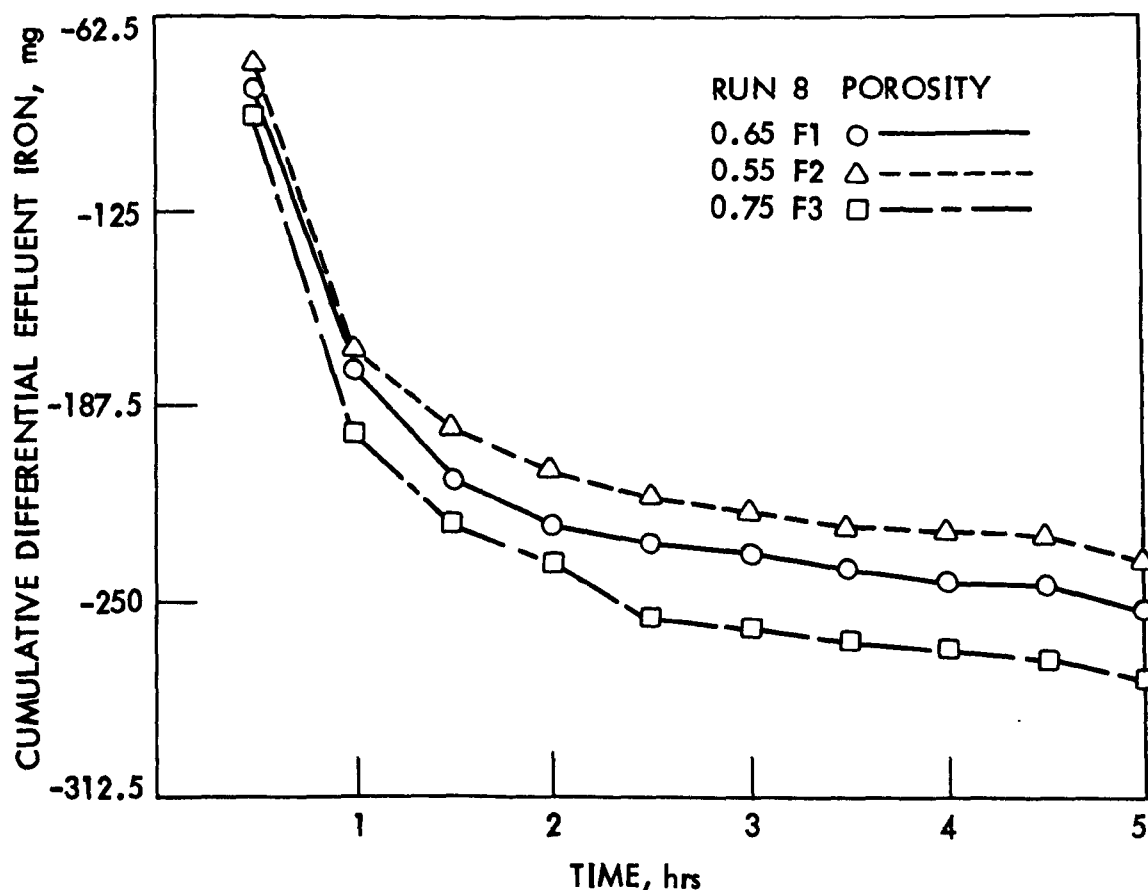


Fig. 7. Cumulative differential effluent iron vs time, run 8.

during a run were the best possible means of study. Using the above artificial effluent quality index and repeating the runs so that each filter was subjected to all the expanded porosities during backwash, differences due to variations in the sands of the filters were averaged and hence eliminated. Thus the index provides the best means of comparison of backwashing effectiveness between different expansions.

The variation of the cumulative effluent quality index (i.e., summing the index for all runs) with porosity for runs 7 to 12 shown in Table 4 is plotted graphically in Fig. 8. The results show a maximum in the cumulative effluent quality index at a porosity of 0.65 to 0.70. The maximum indicates that the best effluent quality in the run following backwash is produced by backwashing the dirty filter at the expanded porosity of 0.65 to 0.70.

The same type of analysis was done for the effluent qualities measured at depths of 3, 6, and 9 in. during series 2. The variations of the cumulative effluent quality index with porosity for all the depths of 3, 6, 9, and 12 in. are shown in Fig. 9.

Table 4. Effluent quality index and porosity for series 2.

Run number	Expanded porosity					
	0.55	0.60	0.65	0.70	0.75	0.78
	Backwashing index					
7		2		3 <sup>a</sup>		1
8	1		2		3	
9	1			3		2
10	2	1			3	
11			3	2	1	
12		2	3			1
Cumulative effluent quality index	4	5	8	8	7	4

<sup>a</sup>The best performance in effluent quality was given in index 3, the next best 2, and the worst 1.

The results for runs 1 to 6 for the 12-in. depth are presented graphically in Fig. 10. The results at other depths were not analyzed due to the fact that the readings of effluent iron in run 1 were invalid due to storage of the samples for too long a period before analysis, as already mentioned under experimental observations. Since a complete set of readings is required for an unbiased analysis at all porosities, the results for series 1 could not be analyzed for the intermediate depths.

The results of the variation of the cumulative effluent quality index with expansion for the graded sand for the full depth of 18 in. and for all depths of 3, 6, 12, and 18 in. are shown in Figs. 11 and 12. Also marked on figures are the experimentally determined porosities of the top 3 in. of the graded sand bed while in the fluidized state.

All the results of series 1, 2, and 3 shown in Figs. 8 to 12 indicate quite clearly that in every case the best effluent quality in the run following backwash is obtained by expanding the bed to porosities of 0.65 to 0.70 during backwashing.

Initial effluent quality and porosity. A technique similar to above was used to study the variation of initial effluent quality with porosity during the preceding backwash. The cumulative initial effluent index was given a value of 3, 2, or 1, depending on the cumulative differential iron between runs B and A during the first 10 min of a run. The method was identical to that used to evaluate the

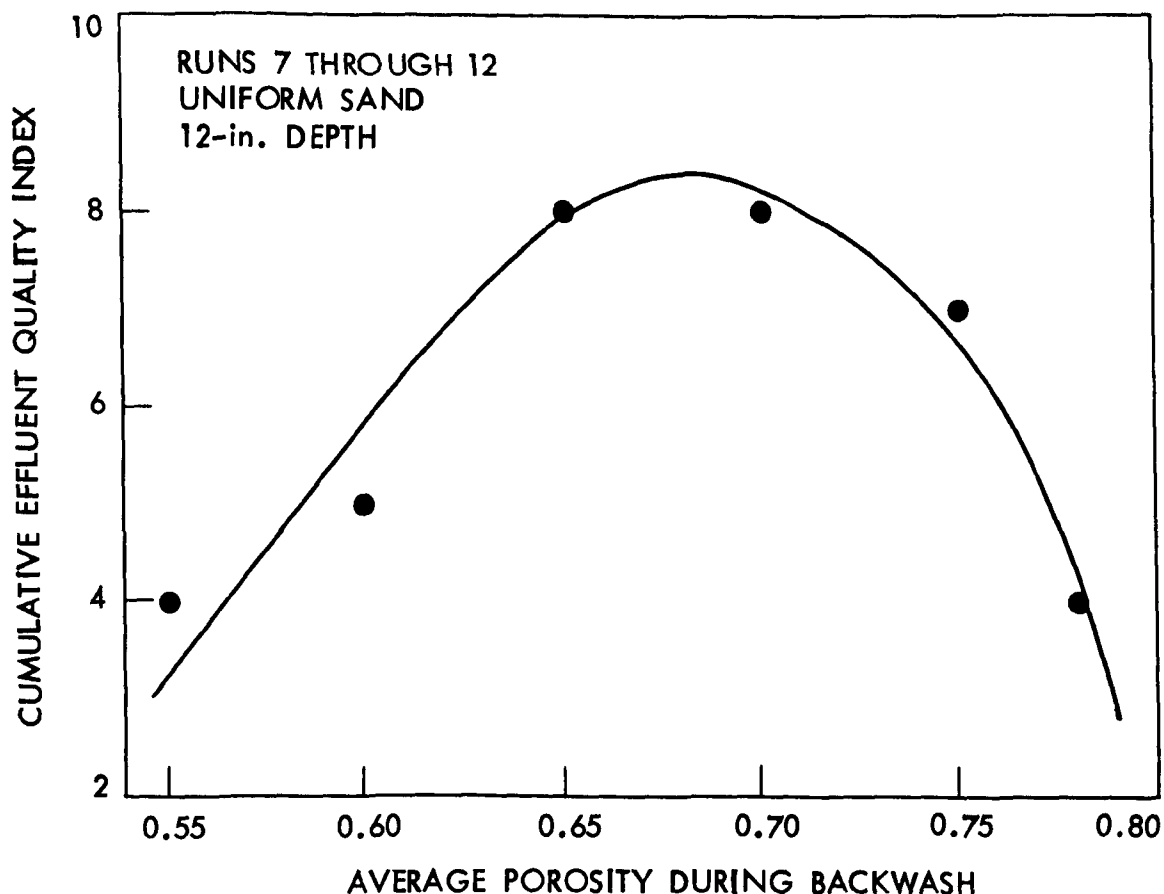


Fig. 8. Cumulative effluent quality index vs porosity, series 2, 12-in. depth.

effluent quality as already described. The results indicate no relationship between the initial effluent quality in the run following backwash and the porosity of the expanded bed during backwashing. It was felt that the initial effluent quality was not dependent on the backwash expansion but was a function of the rate of closure of the backwash valve.

Head loss increases and porosity. A study was also made on the effect of backwash on the head losses in the run following backwash. Again comparison was made between filters based on the difference of head loss in run B over that of the dirtying run A. The results were not conclusive and are not presented here.

Backwash water quality and porosity. The parameter which provided data that was the most consistent in all the runs was the backwash water quality. It enabled comparisons between different backwash porosities to be made on the basis of usage of equal quantities of washwater, even though the actual washwater used in the series 1 and 2 was dependent on the constant wash duration of 5 min. For series 3

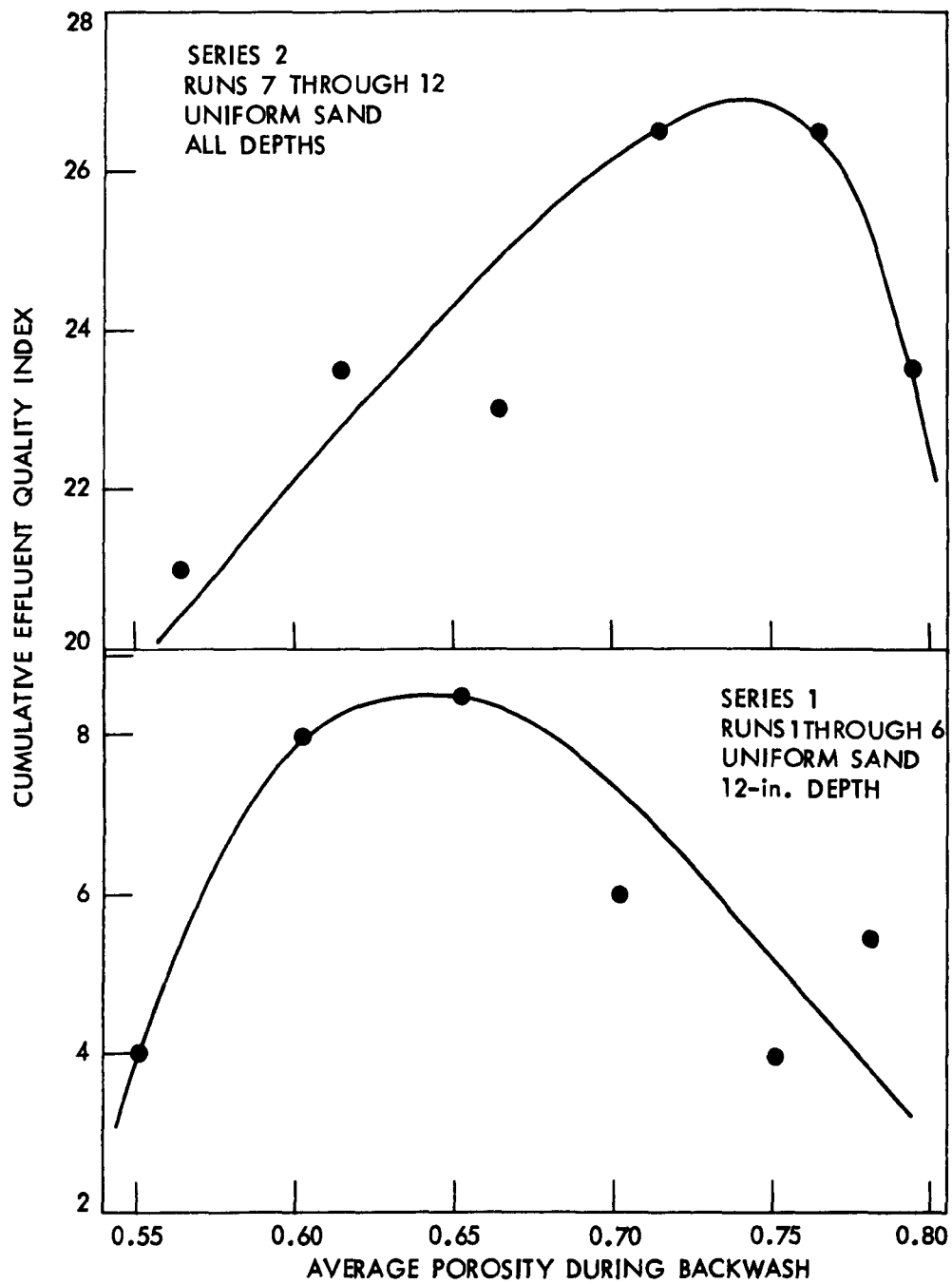


Fig. 9. Cumulative effluent quality index vs porosity, series 2, all depths. (above)

Fig. 10. Cumulative effluent quality index vs porosity, series 1, 12-in. depth. (below)

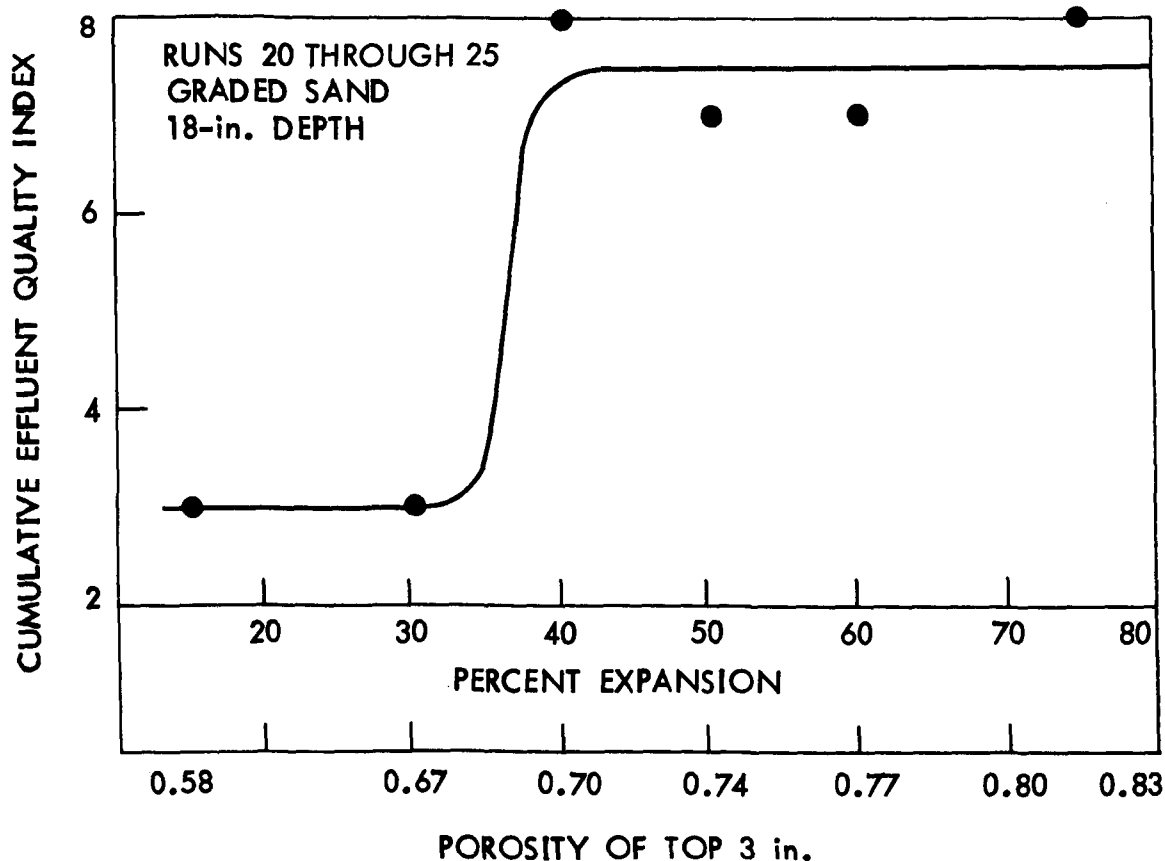


Fig. 11. Cumulative effluent quality index vs expansion, series 3, 18-in. depth.

the total volume of washwater used for the different expansions was maintained the same for all the runs by varying the durations of wash.

Figures 13 and 14 illustrate the backwash water quality for series 1 in terms of the iron concentration in mg/l in samples of washwater as a function of the total volume of washwater used up to the time of sample collection. Using the time of collection of samples and the flow rate during that particular wash the total washwater used was calculated and plotted as the abscissae. The plotted points are from different filters and different runs but are grouped together to indicate the variation of backwash water quality with porosity. The apparent scatter in the points towards the end of the backwash is due to the graphs being plotted on logarithmic coordinates. The logarithmic coordinates were necessary to show the variations in backwash water quality which range from 1000 to 0.2 mg/l. However, for purposes of analysis the most relevant sections of these primary curves shown in Figs. 13 and 14 are the lower curved portions before the curves reach asymptotic values. Magnified curves of these sections

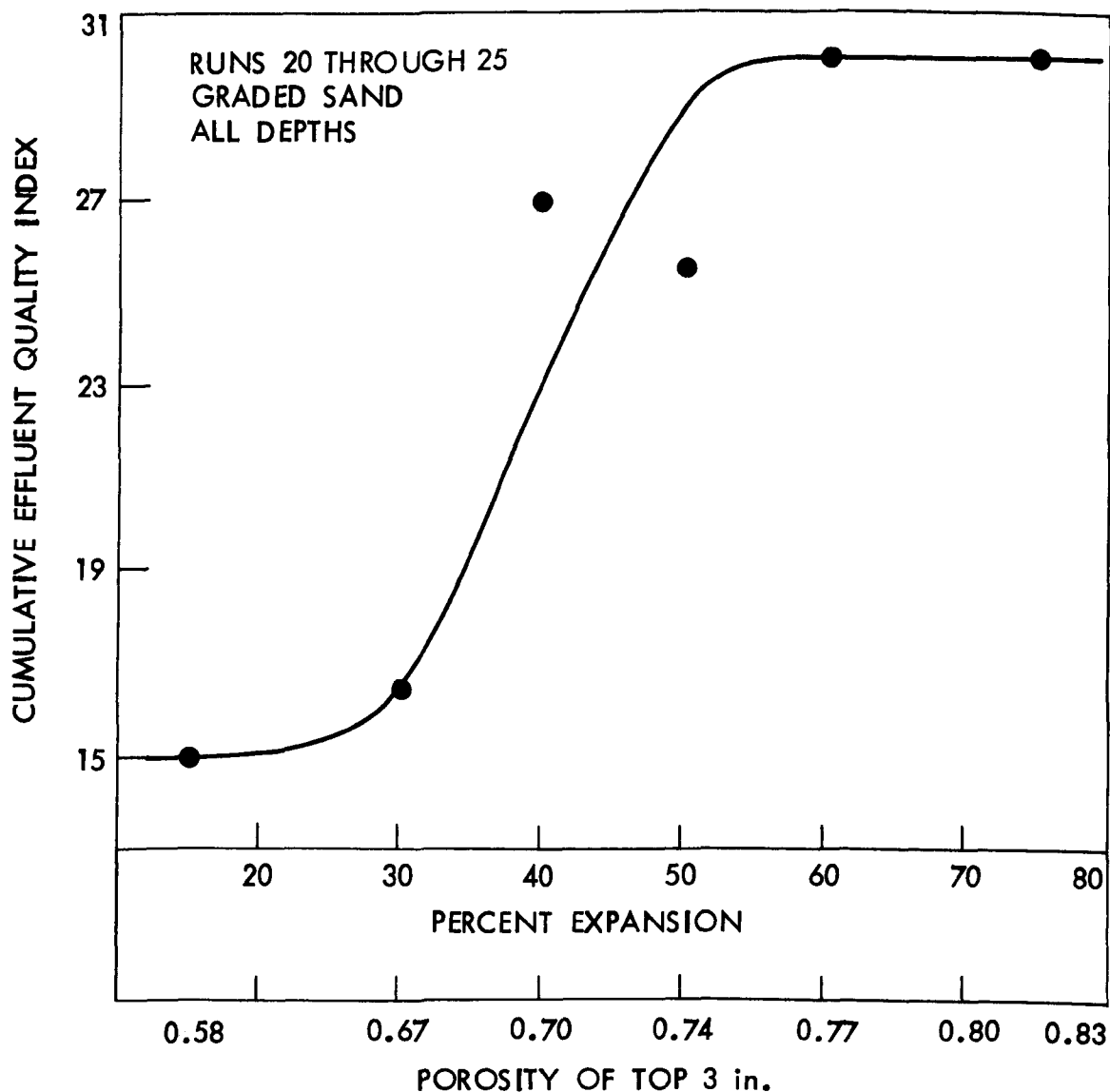


Fig. 12. Cumulative effluent quality index vs expansion, series 3, all depths.

for series 1 are shown in Fig. 15 in arithmetic coordinates. The lines drawn are smoothed curves through the means of the values from the three filters. The curves represent the mean variations of backwash water quality with volume of washwater at the different porosities.

The smoothed curves of Fig. 15 were used to prepare secondary curves showing the variations of final backwash water quality with porosity for constant volumes of total washwater (Fig. 16). The points plotted are the intersections of ordinates at washwater volumes of 20 and 25 gal., respectively, with the smoothed curves drawn in Fig. 15.

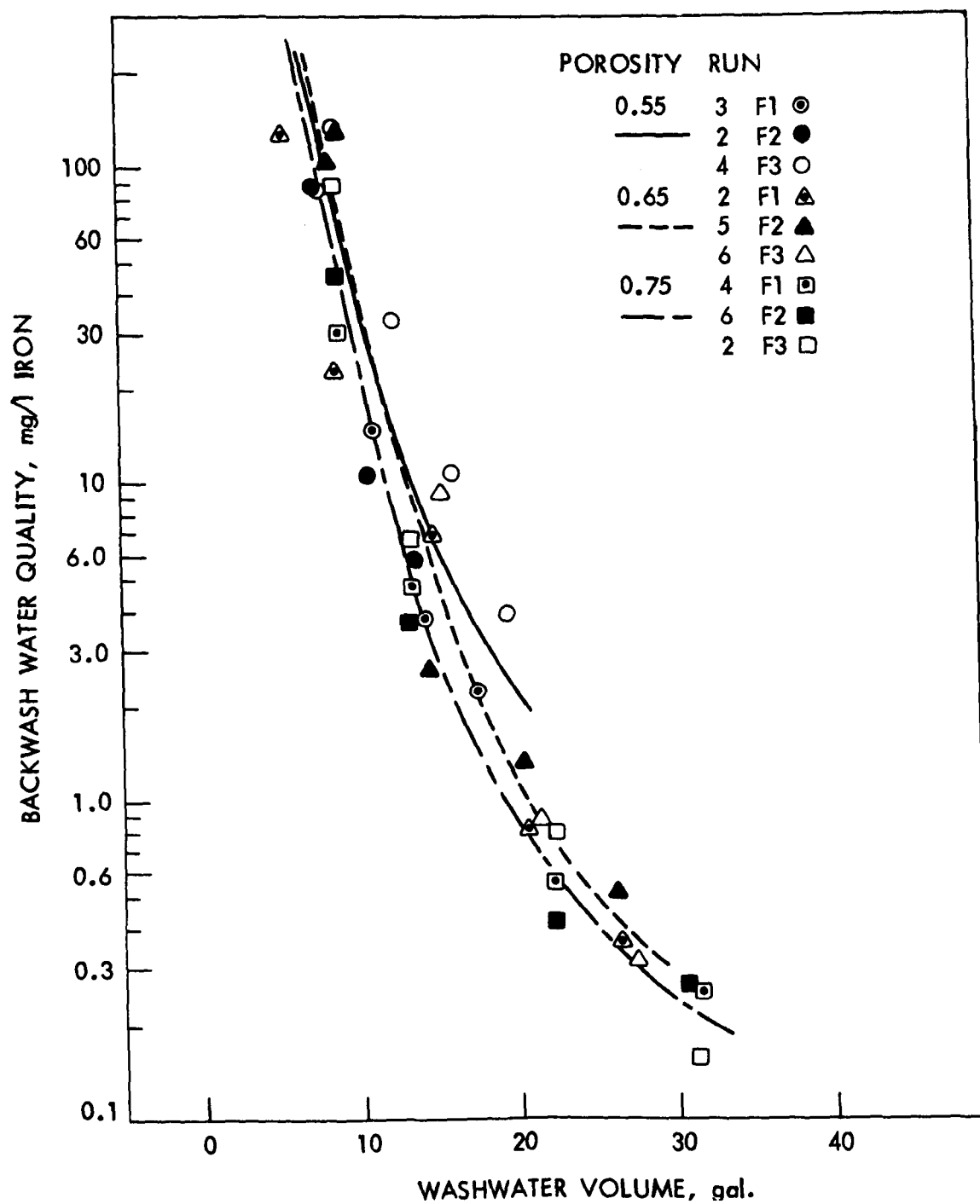


Fig. 13. Backwash water quality vs washwater volume, series 1.

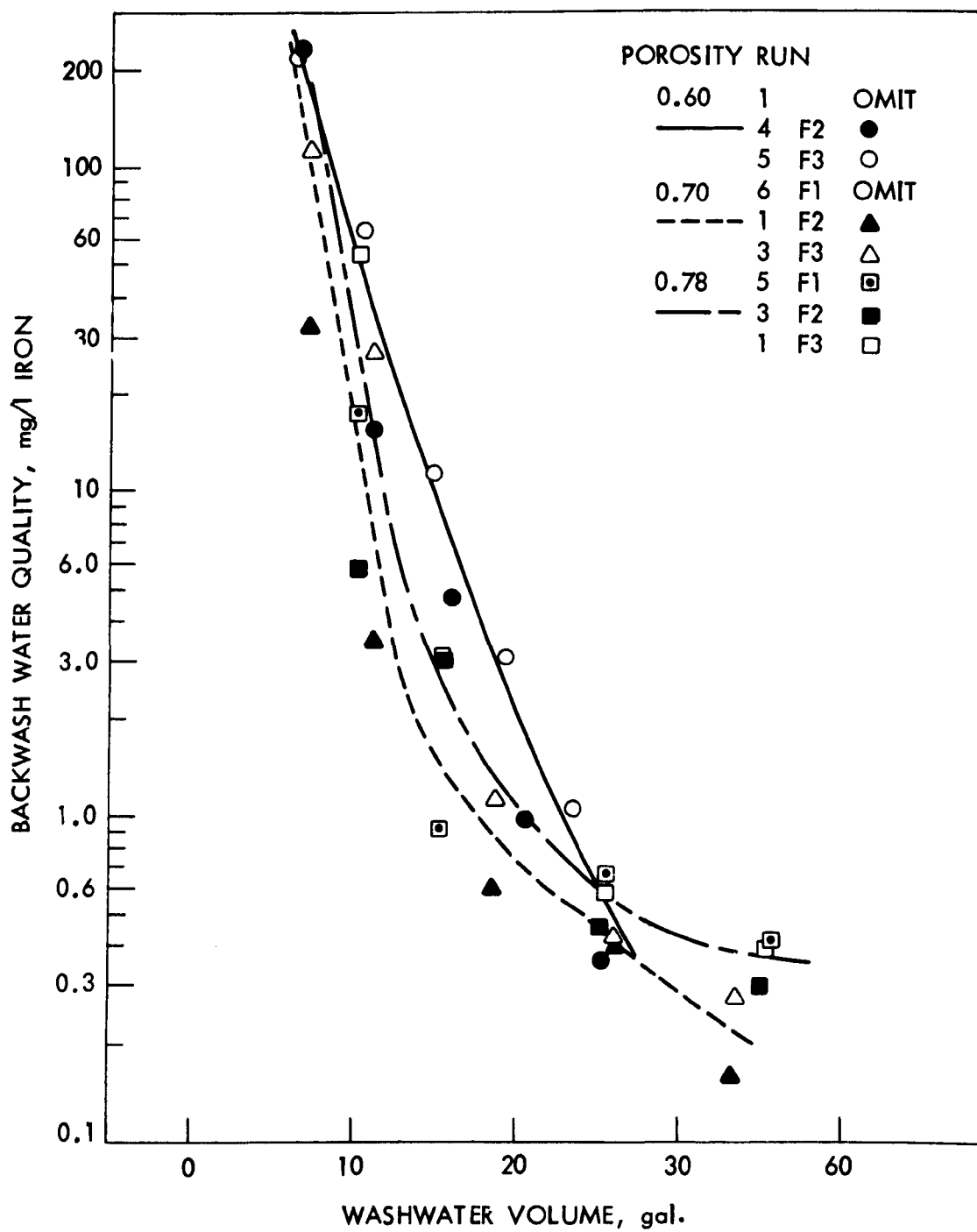


Fig. 14. Backwash water quality vs washwater volume, series 1.

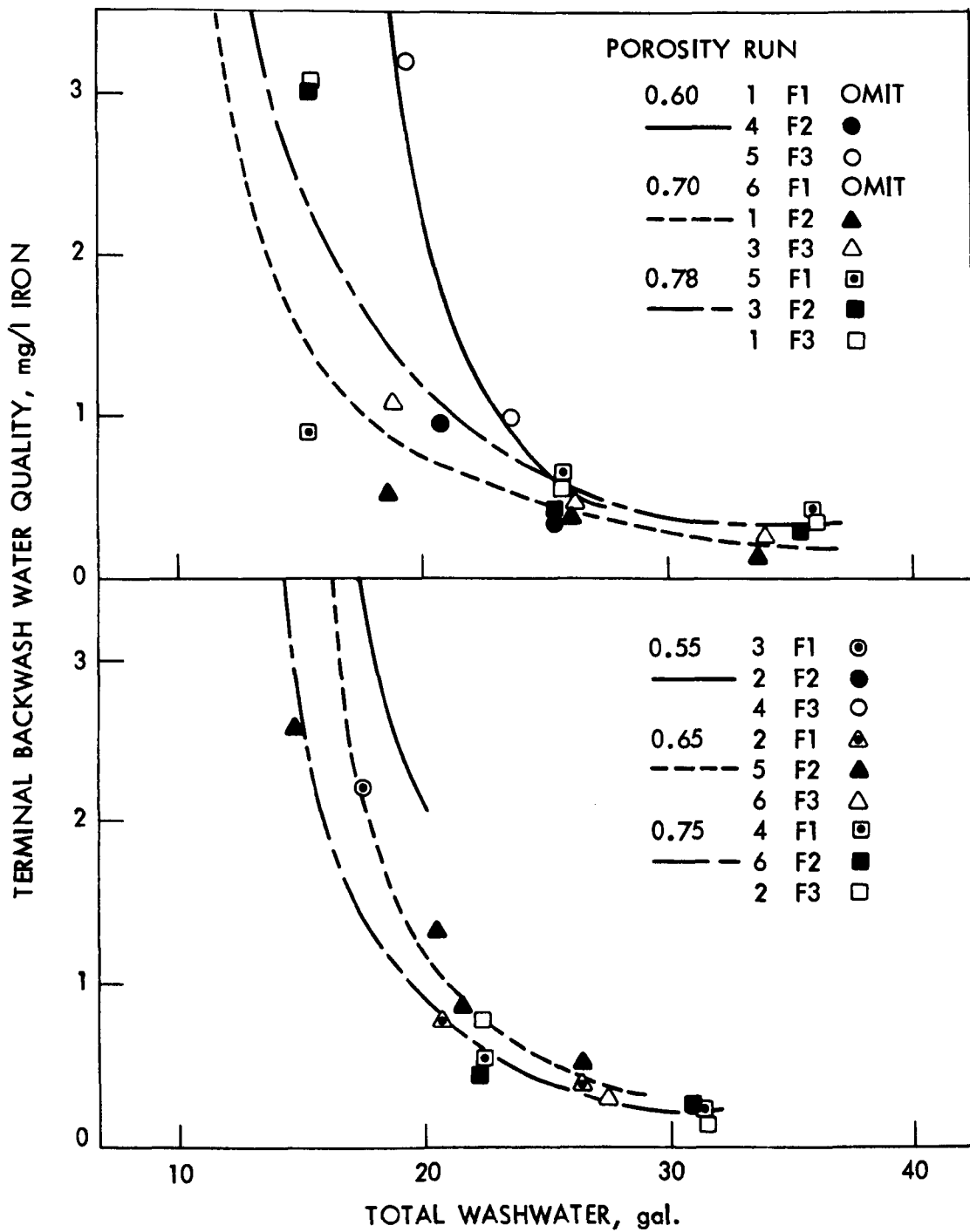


Fig. 15. Backwash water quality vs washwater volume, series 1.

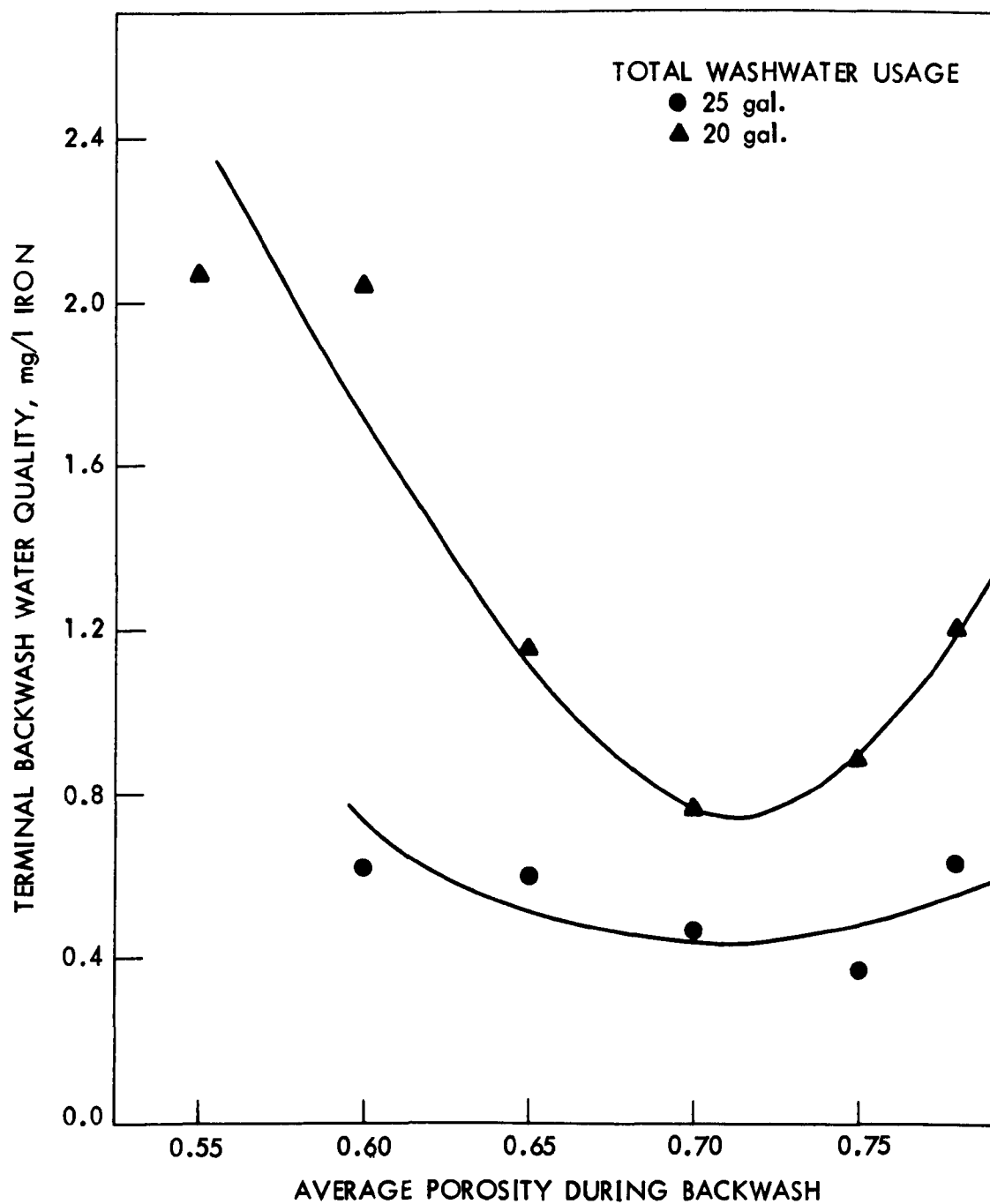


Fig. 16. Terminal backwash water quality vs porosity, series 1.

The results show once again that the best terminal backwash water quality is achieved by backwash at the porosity of 0.70. This has resulted from analyses which consider backwashing to different expansions, but using a constant total volume of washwater. The results indicate that most effective backwash is achieved by expansion to porosities around 0.70.

An alternative graph, also derived from Fig. 15 by considering the different volumes of washwater needed at the different expanded porosities to achieve a given terminal backwash water quality, is shown in Fig. 17. A family of curves for terminal backwash water qualities of 0.75, 1.00, and 1.50 mg/l of iron is shown. These graphs show again that the minimum quantity of washwater necessary to obtain a given terminal backwash water quality occurs at the porosity of 0.70.

The above analyses should be restricted to the lower sections of the curves when the quality changes become small, since only in these sections are the results meaningful. Identically, similar graphs resulted in all the experiments of series 2 for the uniform sand and of series 3 for the graded sand. In every graph a minimum in the total washwater volume usage or the terminal washwater quality occurred around the anticipated porosity range of 0.65 to 0.70. Thus both of these parameters have provided still further evidence of the optimum theory developed in a previous chapter.

Physical sandwash and porosity. As already recorded, an extra parameter to evaluate the effectiveness of backwash was proposed based on the amount of iron removable from the sand by a physical wash. The washing procedure was simple abrasion using a magnetic stirrer under standard conditions. Considerable amounts of iron were removable from the sand by this method, providing final evidence for the fact that negligible collisions and abrasions between particles occur in a fluidized bed. If there were considerable abrasion in the fluidized state, it should not be possible to remove these large amounts of iron by a physical wash.

The iron removable from the graded sand in mg/g as a function of expansion is shown in Fig. 18. The points plotted are for the first two runs on the graded sand - runs 20 and 21. These runs were the initial runs made on the new graded sand after it had been subjected to one unnumbered run for purposes of coating the new sand with at least a small layer of the iron floc. Though similar measurements were made for all the runs of series 3, it was found that the results of runs 22 to 25 were subject to considerable error due to the following cause. In series 3, the influent suspension contained 7 mg/l iron and 0.10 mg/l of a nonionic polyelectrolyte. As series 3 progressed from run to run, mudballs started building up due to the added polyelectrolyte. These were about 0.5 to 2.0 mm in size and consisted entirely of globules of the precipitated iron without any sand within them. They floated on top of the sand layer during fluidization, and every time the sample of sand was drawn for analysis

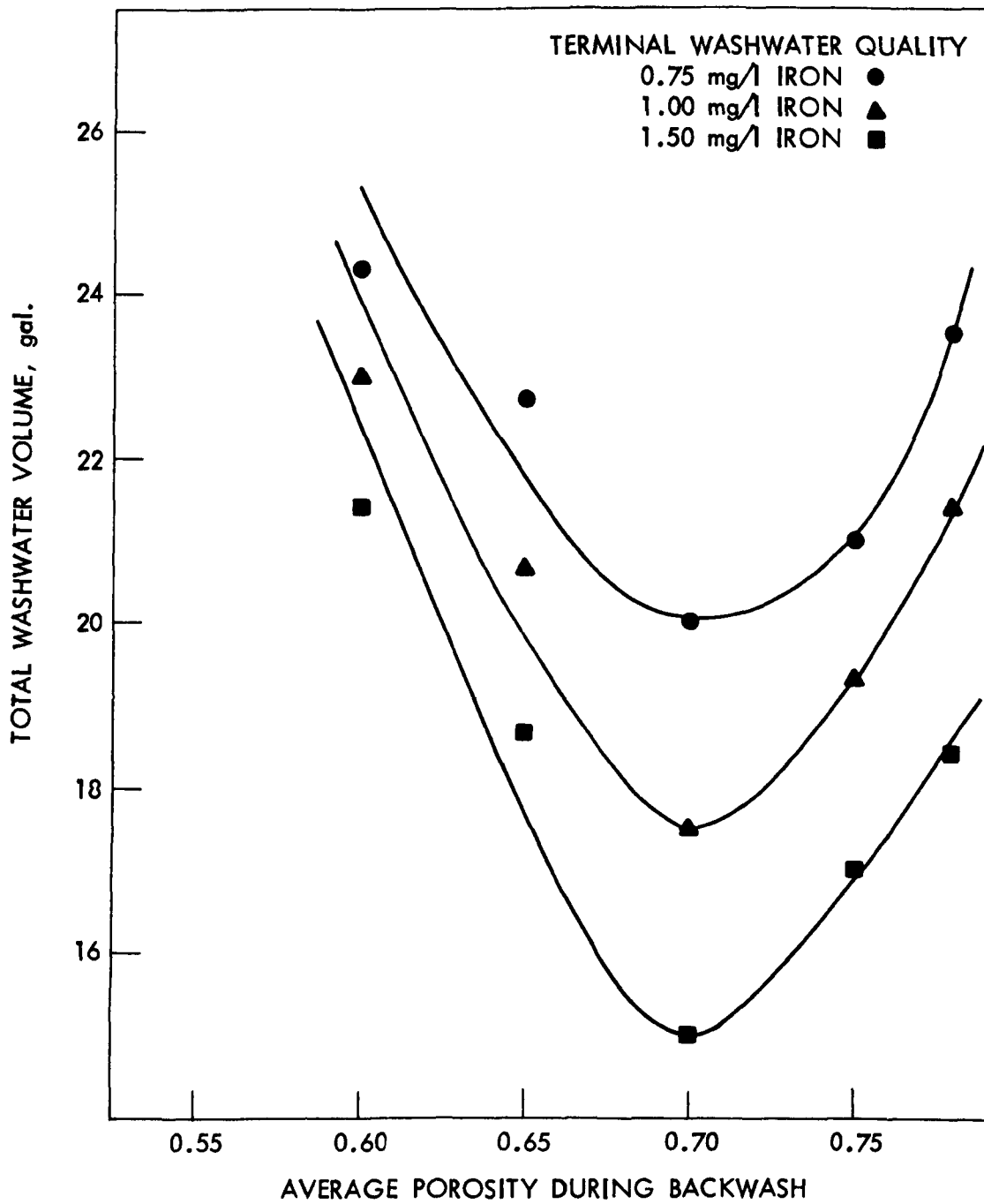


Fig. 17. Backwash water volume vs porosity, series 1.

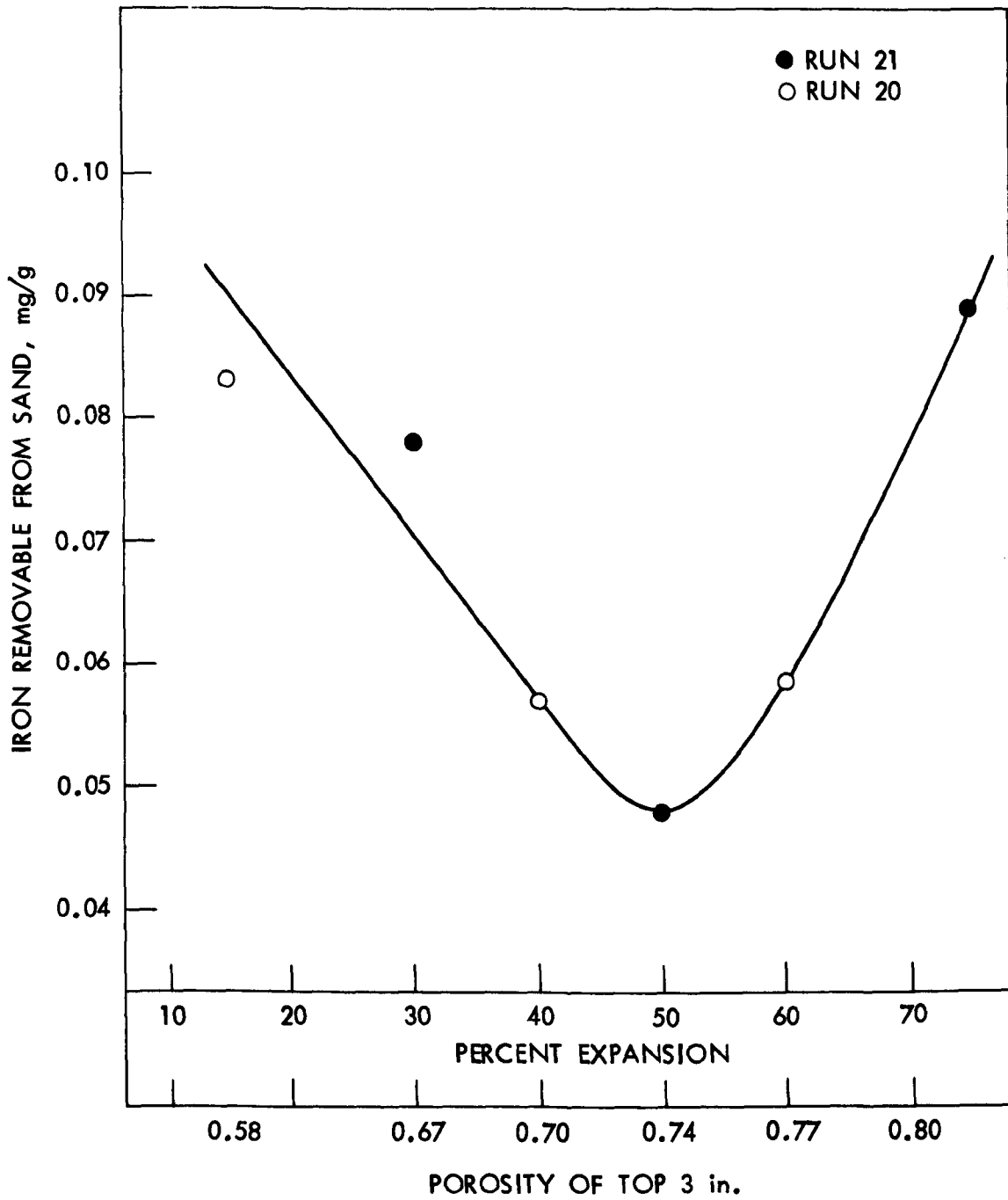


Fig. 18. Iron removable by physical abrasion test vs expansion, runs 20 and 21.

considerable amounts of these mud balls or globules were drawn with the sand sample and caused the iron removable readings to be erratic from run to run. We found that as the series of runs progressed the mud balls became bigger and bigger, causing larger and larger errors. Even though a modified larger expansion wash, nearly 100%, was used for a few minutes during the standard cleaning at the start of each run, removing substantial amounts of the mud balls was still not possible.

For the above reason the physical abrasion test results of runs 22 to 25 were invalid and are not presented. However, in runs 20 and 21 the mud balls were still few in number and small in size and did not substantially affect the readings.

The results shown in Fig. 18 reconfirm the fact indicated in the other sections that an expansion of about 40 to 50% produces the cleanest sand in the graded filter. These expansions cause porosities of about 0.70 to 0.74 in the top 3-in. layer of the expanded bed of graded sand.

Analysis. The results presented in the preceding pages prove beyond little doubt that an optimum backwash occurs in a system expanded to achieve a porosity of approximately 0.65 to 0.70 in the layers containing the most amounts of suspended matter. In the case of a uniform sand bed an expansion to a porosity of 0.70 is equivalent to nearly 90% expansion of its height. For a theoretical uniform sand consisting of identical particle sizes this expansion is an exact and fixed condition. However, in filtration practice uniform sand beds are never used, nor is it feasible to provide for 100% expansions because of the unreasonably large backwash flows required. We are fortunate that both these limitations are simultaneously removed by use of a graded sand. A 40% expansion of a typical graded filter sand can be shown to cause the porosity of the top 3-in. layer to reach a value of 0.70, and use of three different parameters has shown that the optimum backwash for the graded system occurs at expansions of about 40 to 45%. These values of expansion can be obtained in practice.

A few points need to be made regarding this optimum of 40 to 50% for graded systems and the results reported in the sanitary engineering literature. The fact that effective backwash requires an expansion of about 50% for graded systems has been a well known rule of thumb in filtration design and practice. This rule developed originally from the work of Hulbert and Herring [62] in 1929.

Several workers have suggested during the last decade that expansions of 20 to 25% may be sufficient for effective backwash [10,26,67,132]. None of these papers, however, provide fundamental considerations or experimental results which are valid to draw this conclusion. Baylis [10] suggested the figure without any experimental work. Camp et al. [26] reported this expansion as suitable for all filters on the basis

that serious problems did not occur in the operation of the Billerica water treatment plant. But note that the Billerica plant had multi-media filters, and expansions of 20 to 25% easily give porosities of about 0.70 in the top coal layer. This can be seen in the results reported by these workers themselves. This, in fact, is additional evidence for the hypothesis of this report.

Thus, careful analysis indicates that the results reported in the literature [26,62] are consistent with the theory and experimental work of this report. Also, remember that effective backwashing does not necessarily mean optimum backwashing, and due to the rather flat nature of the shear stress maximum it is possible to backwash filters effectively even though the optimum condition is not obtained. In case one may be tempted to run away with the idea that a lower expansion may result in a saving of washwater, Fig. 17 needs to be remembered. It clearly shows that backwashing at lower expansions than the optimum necessarily results in the usage of larger amounts of washwater to achieve a given bed cleanliness.

A concluding summary. The results summarized and the analyses presented in this section give a complete picture of optimum backwashing by water fluidization alone. The experimental results are entirely consistent with the theory of optimum backwash developed in a previous section and provide excellent confirmation of the theoretical results. Optimum backwash has been shown to simultaneously provide these advantages: (1) a better effluent in the following run, (2) a minimum usage of washwater, and (3) a minimum growth of the coatings on the sand. This plurality of advantages should considerably improve the performance of most filtration plants, if optimum backwashing is put into operation.

## VII. WASTEWATER FILTRATION AND BACKWASHING — LITERATURE REVIEW

Filtration has been used in the United States as a liquid and solids separation process for wastewater since 1883, but was not widely implemented over the years because settling and biological treatment processes were considered adequate for the needs of the times. However, with stringent federal and state effluent standards presently reflecting the demands of the citizenry for more complete treatment of wastes, filtration is becoming increasingly popular. Similar requirements for better waste treatment were necessary in Britain nearly 25 years ago, so the majority of what has been accomplished in wastewater filtration and backwashing progress since 1949 has been the result of British research, development, and experience.

Experience with filters used in water treatment has demonstrated the need for effective media cleaning techniques. A similar need exists with respect to wastewater filtration, but the problem is greatly compounded because of the variable characteristics of sewage. Often sticky and gelatinous, the solids removed by the media are much more resistant to cleaning procedures than those normally encountered in water treatment.

The following literature review summarizing wastewater filtration and backwashing experience is a summary of a more comprehensive review prepared by Rice [99].

A diverse array of designs is available for wastewater filtration, varying in flow configuration, bed depth, media type and gradation, and performance. Cleaning methods, however, generally rely on the application of water or air and water to remove entrapped solids from the bed (chemicals such as chlorine occasionally are used as cleaning aids). The purpose of this section of the review is to review in a general way the wastewater filter designs and cleaning techniques.

### Types of Wastewater Filters and Cleaning Techniques

#### Conventional Rapid Sand Filtration

Because of their use for years in filtering water for potable use, it is not surprising that rapid sand filters were among the first to be used in wastewater filtration. Bed depths of 6 to 36 in. have been reported [13,41,87,121,136] for full-scale applications, but current practice favors depths of 24 in. or greater. The gradation of sand used in the installations varies widely with location, but research and operating experience have demonstrated that the relatively fine sand, approximately 0.5 mm, used in water treatment is unsuitable for wastewater filtration because of rapid head loss buildup and consequently shorter filter runs. Considerable pilot scale research has shown that 1 to 2-mm media size will produce good effluent quality and allow reasonable filter runs [59,68,129].

Design of these facilities closely parallels that employed for years in waterworks, the filters placed in rectangular concrete boxes equipped with perforated block, nozzle type, or header and lateral underdrain systems [41,87,136].

Backwash water is usually drawn from a filtered wastewater storage tank although unfiltered water is occasionally used. In either case the washwater is pumped through the bed in an upward direction, carrying the accumulated solids upward to washwater collection troughs. Washwater is ordinarily applied at a rate sufficient to expand the sand bed 10 to 20% during fluidization, usually at rates from 15 to 25 gpm/sq ft.

In Britain, air is almost universally used in wastewater filtration plants as a media scouring aid prior to or in the course of introducing the washwater. The air agitates the media and helps to break up agglomerations within the bed, thus allowing the water backwash to more easily remove the entrapped solids. Although installed less frequently, rotary surface washers have been used for the similar function [87,88]. No reports of backwashing studies testing the effectiveness of either of these two scouring techniques were discovered, and since wastewater filtration plants in the United States are rare, little direct evidence exists as to which method best cleans the media. Indications from scattered passages in filter performance reports are that omission of either air scour or rotary surface wash has led to difficulties [59,68,118].

#### Dual- and Triple-Media Filters

Dual- and triple-media filters are being used to provide filtration from coarse to fine media size in the direction of flow, and thus to achieve longer filter cycles without detriment to filtrate quality [38,59].

The most common type of dual-media filter is an anthracite and sand design although other combinations such as activated carbon and sand, resin beds and sand, and resin beds and anthracite have been reported [82]. Studies [59,127,128] appear to conflict somewhat on the degree to which solids penetration and efficient bed utilization occur in a dual-media filter. Bed depth, flow rate, media sizing, and the nature of the filter influent (activated sludge versus trickling filter effluent) appear to be variables influencing both the penetration and degree of removal in a dual-media filter [38].

As with any granular media filter, efficient backwashing is essential to prevent deterioration of the filter bed condition, which results in filter cracks, mud balls, high initial head losses and reduced filter runs or poorer filtrate quality. Backwashing techniques commonly used for dual-media filters are essentially the same as those described for rapid sand filters. Air scour prior to backwashing is common practice and is introduced through the nozzle underdrain

systems common with this type of filter [58]. The use of a series of air-scour and rest cycles, referred to as pulsed air scour, has been recommended as a means of improving the efficiency of media agitation [58,86]. Initially the air will follow the path of least resistance and may completely skirt agglomerations in the bed if continued. By pulsing the air and allowing the media to resettle, areas of the bed resistant to break up are continually lifted and dropped, resulting in better separation of the entrapped solids from the filter media.

Triple-media filters are the result of a logical extension of the principles outlined for dual-media filters. The most frequently used design incorporates anthracite, sand, and garnet, which are substances having approximate specific gravities of 1.7, 2.65, and 4.2, respectively. Gradation from coarse to fine follows, obviously, the same sequence, and it is claimed that the filter is less susceptible to shock from rapid fluctuations in suspended solids concentration [111]. It has also been suggested that triple-media filters are superior to deep-bed filters using a single coarse media [111], but reliable pilot-scale studies have not demonstrated superiority in effluent quality or process reliability [68].

Promoters of the triple-media filter have expressed concern about the use of air scour in this and other filters [111]. Disadvantages of air scour are listed as increased downtime, possible media loss or bed upset, and complication of the backwash cycle. The use of rotary surface washers is recommended as an alternative. Others have suggested that air scour is perhaps the only practical method for cleaning deep bed filters like the dual- and triple-media units [38,86], and that increased scouring efficiency is possible with air. Filtered water is, in any case, generally used as washwater and is applied at a rate of about 15 gpm/sq ft.

The use of triple-media filters for waste treatment is growing in popularity in the United States, with over 50 installations in operation to date. Most designs have favored bed depths of 36 to 42 in. and hydraulic loading rates of 5 to 6 gpm/sq ft. Pressure filters are normally used for treating secondary effluent from plants with flows of less than 5 mgd and gravity filters for treatment works with flows in excess of this figure [43].

#### Immedium Upflow Filter

Although relatively unknown in the United States, the Immedium filter was invented in 1961 by a Dutchman named Pieter Smit and was subsequently developed by the Bobby Corporation in Britain [9,13]. It is a deep-bed, high rate, upflow filter using a patented grid placed several inches below the top of the bed to prevent the expansion of the media during filtration. Typical arrangements for both pilot- and full-scale Immedium filters are presented in Figs. 19 and 20. The grid is the key to the success of the design and consists of a series of parallel bars at 4 to 6-in. centers which normally provides

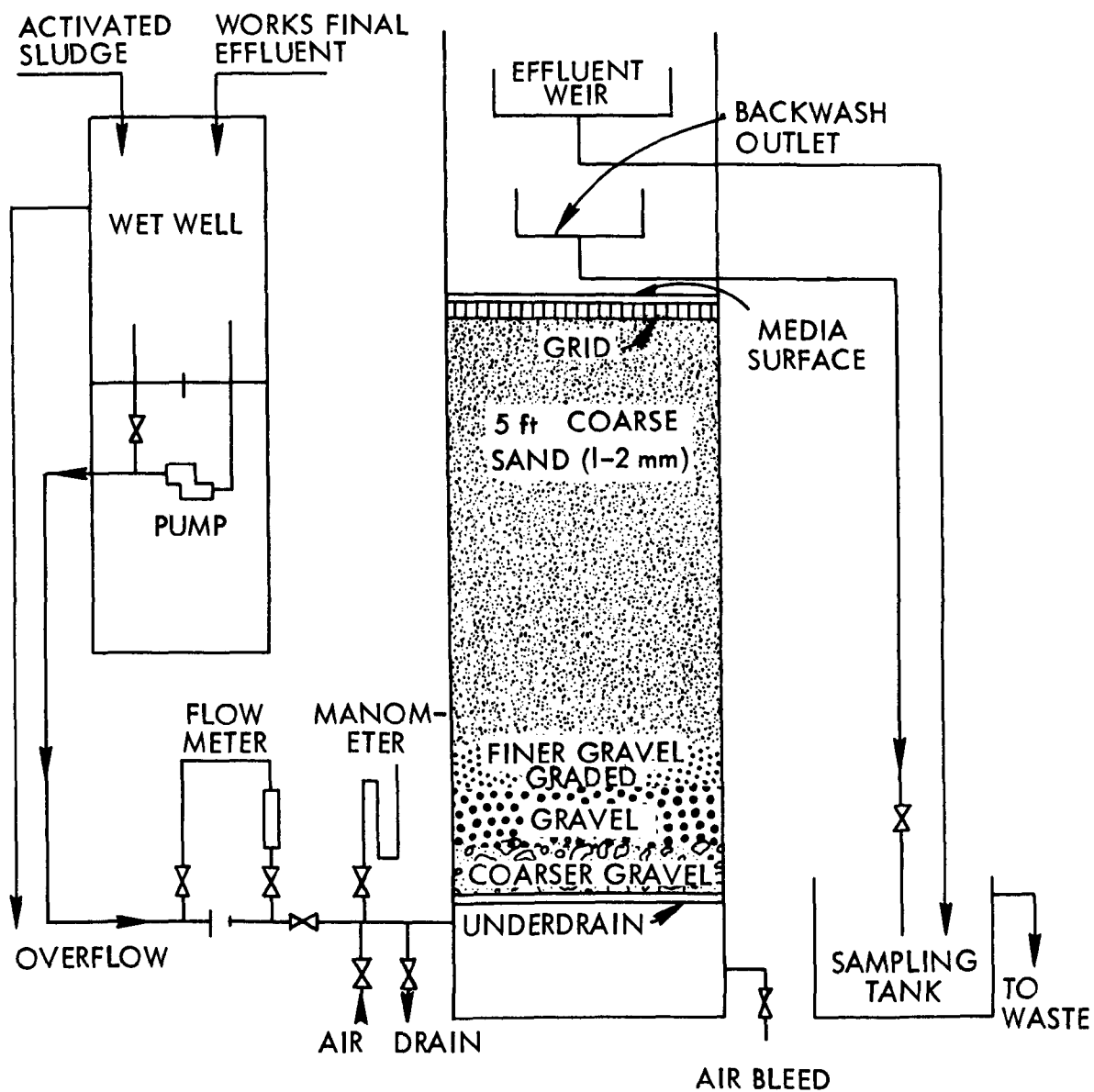


Fig. 19. Pilot-scale Immedium filter used at West Hertfordshire, England [142].

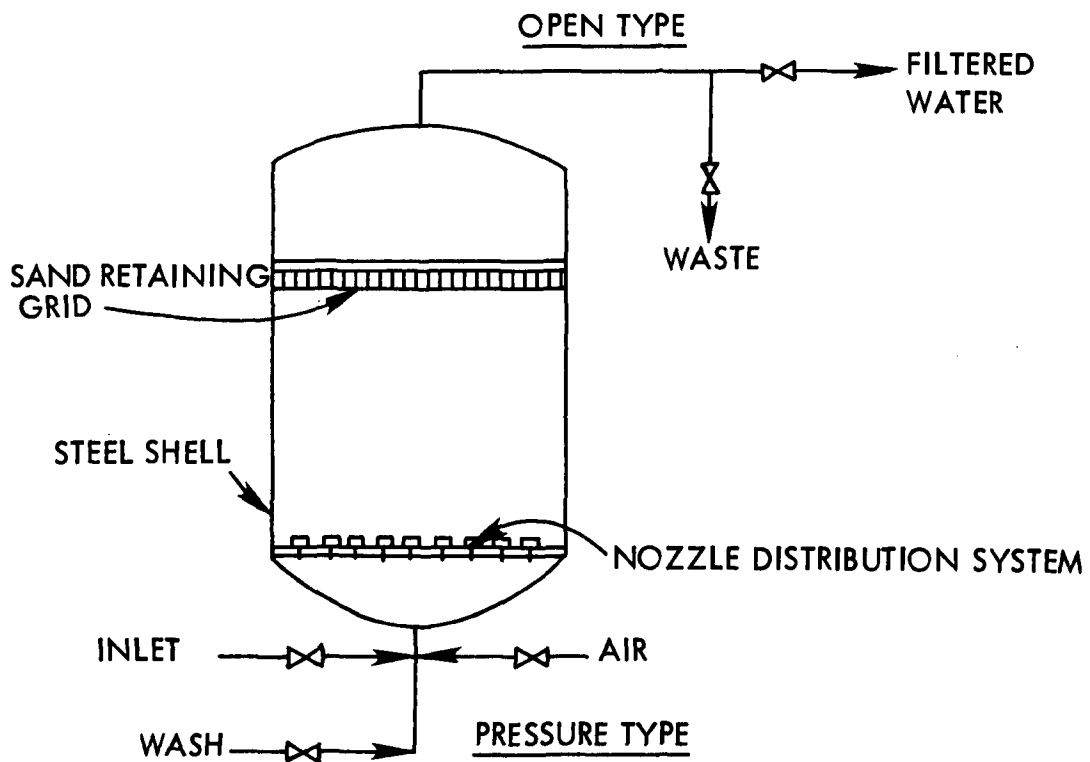
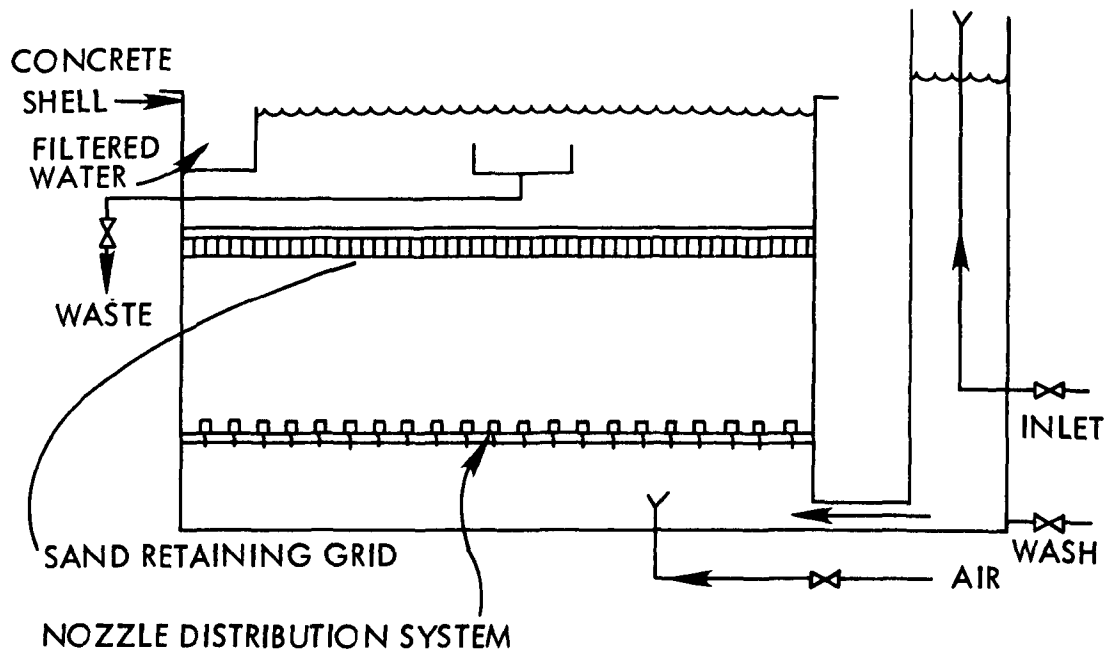


Fig. 20. Immediate filter arrangements for full-scale installations, open and pressure [13].

openings 100 to 150 times the size of the smallest particle contained in the bed [13,58]. During the course of filtration the sand forms compression arches in the vicinity of the grid which resist the tendency to lift or fluidize the bed, even at rates up to 6 gpm/sq ft and at pressure drops equivalent to 20 ft of water.

Intense interest in the Immedium upflow filter in Great Britain has resulted in at least five independent studies [68,83,86,131,142], which are discussed in more detail later. Typical media gradations and depths, in the direction of flow through the filter, are 4 in. of 10 to 15-mm gravel, 10 in. of 2 to 3-mm gravel and 60 in. of 1 to 2-mm sand, and the filter can be operated in a pressure or open type housing as shown in Fig. 20 [9,13,58].

Backwashing is usually initiated when the head loss reaches 6 ft and is preceded by draining the water above the filter to a level just above the media surface and air scouring the filter at a rate of 5 cfm/sq ft. The air serves also to break up the sand compression arches at the grid, and the backwash water is then turned on to expand the bed before the arches can reform. Since backwash water is applied at 16 gpm/sq ft in the same direction as the influent, the latter is conveniently used as washwater in most instances. Expansions of 2% [9] to 20% [13] have been reported as common during backwashing, but it is the writer's opinion that the former value is more accurate for 1.0 to 2.0-mm sand fluidized at 16 gpm/sq ft.

The first reported full-scale Immedium filter plant became operational in 1969 at the East Hyde Works in Luton, England following a series of pilot-scale studies. As a result of the pilot-scale studies, the backwashing procedure was modified to provide a series of alternating high and low rate air scours and washwater applications, both of which have been automated [9,82].

#### Deep-Bed, Coarse Sand Filters

The use of deep-bed filters with a single media of coarse sand has been developed in Germany. According to Jung and Savage [70] its use is widespread in potable water treatment, with over 200 existing installations. They are also being promoted for wastewater treatment with media depths of 4 to 6 ft and media sizes of 1 to 2, 2 to 3, and 3 to 6 mm for wastewater filtration [108]. Sand is very uniform, with a uniformity coefficient of 1.25 or less. Backwash is first, with air and water simultaneously followed by water alone. The backwash rate is 6 gpm/sq ft during the simultaneous air-water phase and 8 gpm/sq ft during the water only phase. Air-scour rates are 6 scfm/sq ft for the 2 to 3-mm and 3 to 6-mm sand and 3 scfm/sq ft for the 1 to 2-mm sand. Adequate freeboard to overflow level (20 to 30% of bed depth) is required to prevent media loss with the finer sand. Backwash is for extended periods of 15 to 20 min so that total washwater used per backwash is not reduced compared to higher rates used in United States dual-media filters.

The backwash described above is well below fluidization velocity for the media of the sizes indicated. Thus, the mechanism of cleaning comes into question. Jung and Savage [70] describe the air and water delivery systems and the presumed action in some detail. Air is distributed evenly by a pipe network. Water is delivered by a no (very low) head loss precast block underdrain floor. The rising columns of air act as airlift pumps to ensure uniform water distribution. The localization of the air columns causes the velocities of air and water flow to vary from zero to quadruple the mean and results in vigorous pulsating washing action.

Quantitative studies demonstrating the effectiveness of this backwashing system were not found.

#### Automatic Backwash Filters

In order to backwash any of the wastewater filtration systems previously discussed, it is required that they first be removed from service. However, the automatic backwash (ABW) filter, as manufactured by the Environmental Elements Corp. (formerly the Hardinge Division) of Koppers Company, Inc., allows both filtration and backwashing to occur in the same bed. A full-scale version of this system, similar to that shown in Fig. 21, is now in operation at Chicago, Illinois, and is filtering chemically treated secondary effluent in two 12-in. deep sand beds having a total surface area of 1329 sq ft. The filter beds consist of a series of 8-in. wide, contiguous compartments separated by steel plates which run perpendicular to the long axis of the filter. A carriage assembly traveling on rails mounted on the filter box walls suspends a cleaning hood above the compartmented bed for the full width of the filter [116].

Backwashing is accomplished by centering the cleaning hood over a given compartment, thus isolating it and allowing the rest of the bed to continue filtration. A port on the side of the isolated compartment is opened to the moving backwash supply pump and shoe, and the washwater is pumped into the compartment underdrain and up through the sand. Another pump mounted on the cleaning hood withdraws the spent washwater and discharges it to waste. The time required to completely wash all the compartments in one of the 53.2 by 12.5 ft beds at the Chicago installations is 57 min [116].

The principal investigator recently (1975) visited this Chicago installation at Hanover Park after it had been in service about seven years. During that period the filters had been used for direct filtration of a prechlorinated secondary effluent from an activated sludge plant which was sometimes coagulated prior to filtration. The plant superintendent, Mr. Robert A. Ziols reported satisfaction with the filters and no particular problems related to inadequate backwash. The automatic backwash occurs about nine times per day. They have routinely replaced about 1 in. of filter sand each year. Inspection of the media at such times had not revealed typical dirty

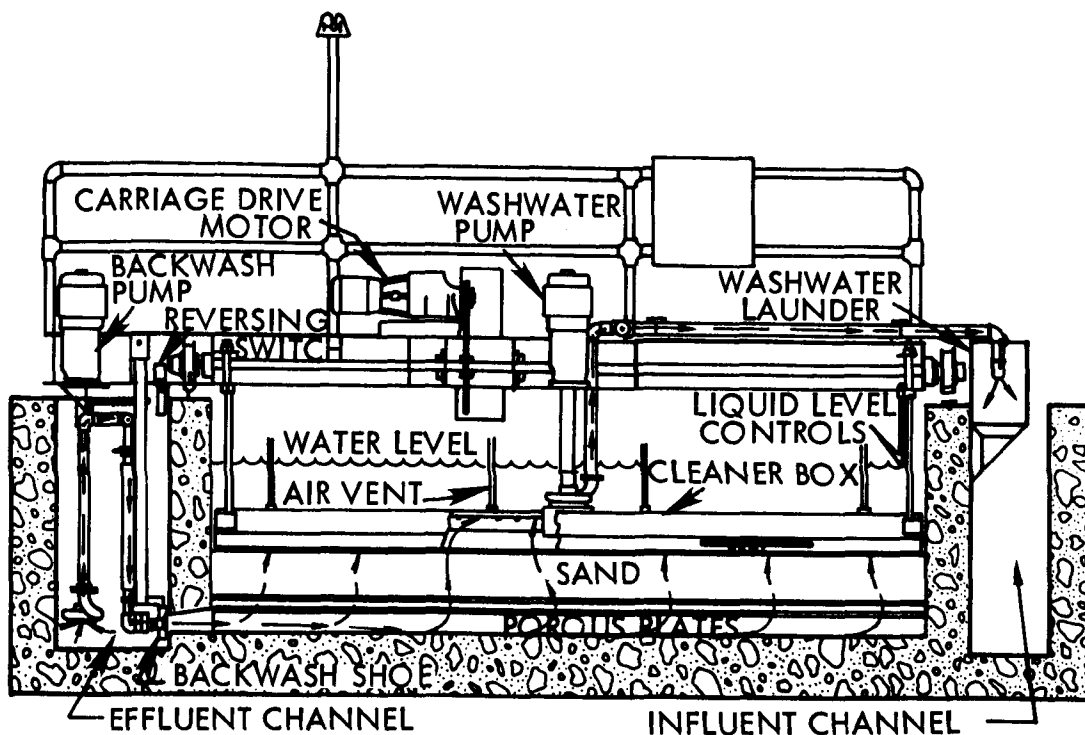


Fig. 21. Environmental Elements Corp. (Koppers) full-scale automatic backwash filter (from manufacturer's brochure).

filter problems such as mud balls and filter cracks. An expansion of the plant will include additional filters of the same type. The manufacturer now uses sand with an effective size of 0.6 to 0.65 mm for wastewater filters and reports 25 wastewater installations between 1966 and 1974.

#### Moving-Bed, Continuously Cleaned Filters

In the next few years wastewater filtration practice may encompass the use of moving-bed filters which are at present in the research and development phase. One filter of this type is basically a vertical, upflow unit in which provisions have been made to continuously remove a small portion of the bottom-most sand, the media making first contact with the influent. The sand is then cleaned and lifted to the top of the filter where it is redeposited. In this manner the flow through the filter contacts progressively cleaner media as it travels through the bed, and the dirtiest portion of the media is constantly being drawn off and cleaned. Preliminary results indicate that raw water quality has little effect upon performance for flow rates comparable to conventional upflow and downflow units [58].

A variation of the moving-bed filter known as the Simater filter is being manufactured by Simonacco Limited of Carlisle, England, and was tested in a pilot-scale study in Derby, England [68]. Figure 22 shows the basic arrangement of the unit, which differs from the previously described filter in that the unit distributes the influent radially from the center of the bed (A and B). Vertical perforated pipe laterals whose orifices are covered with filter cloth are spaced around the outer circumference of the filter housing to collect the effluent, which is then discharged through lines D and E. Dirty media is withdrawn in line F and air lifted to the top of the filter where it is discharged into the upper chamber, G. During the lifting processes the solids are removed from the media by the scrubbing action so that the sand falling to the top of the filter has been cleaned. The solids are then withdrawn from the upper chamber at point G [68].

### Case Histories

The following case histories will present the backwashing procedures and their effectiveness as reported in various wastewater filtration studies from the literature. In many of these papers, substantial filter performance data are also presented but will not be repeated in this backwashing report. The performance data have also been summarized by Rice [99].

#### Early Practice According to Streander

Perhaps one of the unsung pioneers of wastewater filtration was Philip B. Streander, a New York City consulting engineer whose interest in sewage filtration began in the late 1920's. In a solitary article published in 1935 [121] and a subsequent series of three articles published in 1940, Streander [122,123,124] outlined the state-of-the-art of sewage filtration in this country and abroad.

Streander proposed a mechanically cleaned downflow filter [121] of silica sand or crushed anthracite graded to 0.59 to 0.84-mm particle size. Filtration rates of 2 gpm/sq ft were recommended, and cleaning was accomplished by a moving, full-width cleaning head. The head was equipped with two rows of hollow rake teeth, positioned to break up the surface and subsurface portions of a 6 to 18-in. deep filter bed. The teeth were equipped with orifices through which high pressure washwater was pumped, causing an expansion of the media directly under the cleaning heads equivalent to a rise rate of 16 in./min. Solids entrapped by the media were released and carried above the expanded bed to an upper zone where they were withdrawn in the spent washwater by a pump mounted on top of the hood.

Although it was thought that the combined mechanical and hydraulic action would be sufficient to thoroughly clean the filter, performance in actual installations proved otherwise. It was discovered that the cleaning method was highly efficient in the upper part of

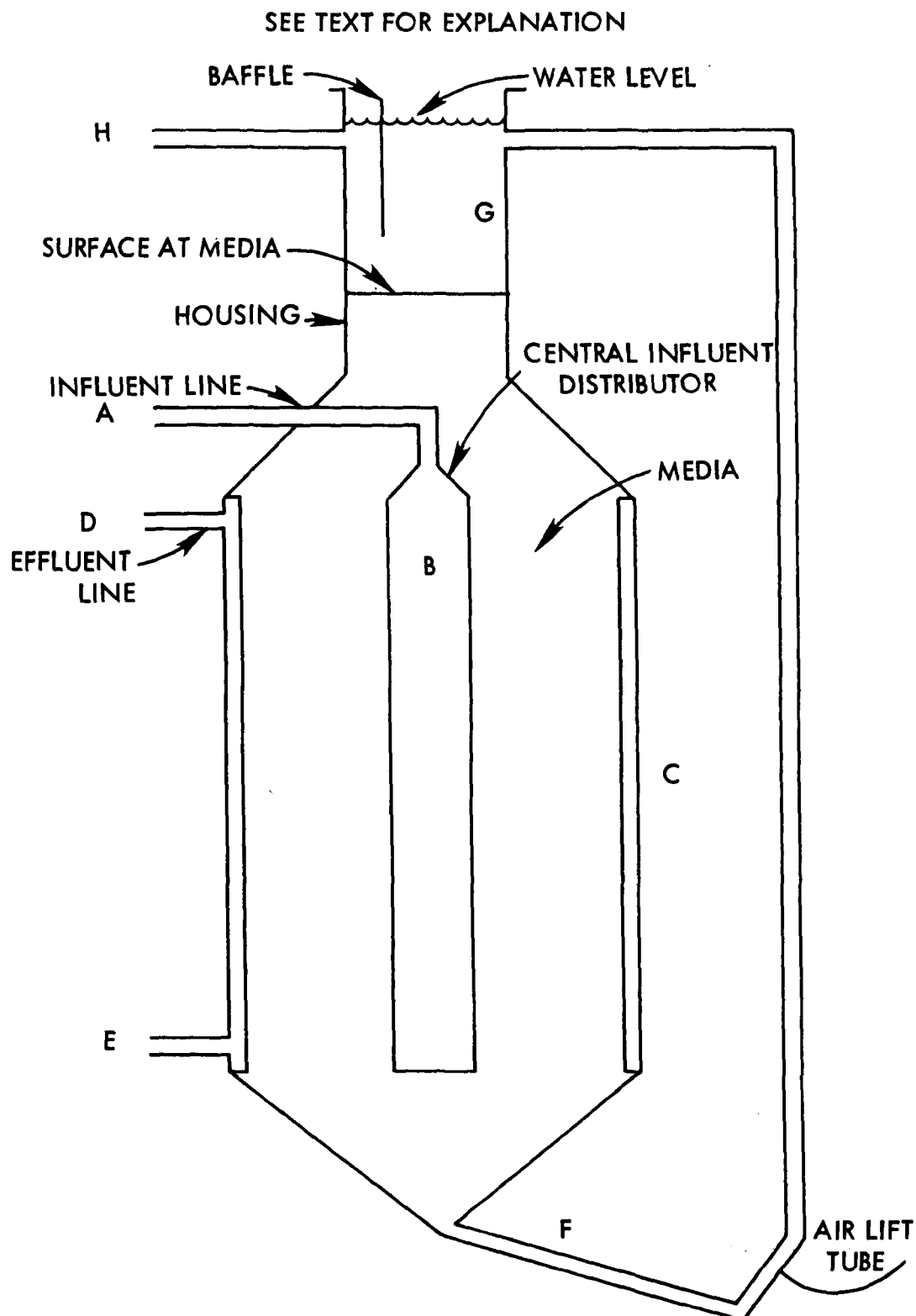


Fig. 22. Pilot-scale "Simater" radial-flow, moving-bed sand filter by Simonacco Ltd. of Carlisle, England [68].

the bed but could not effectively clean the media directly above the supporting screen. As a result bacterial slimes developed which adversely affected the capacity and efficiency of the filter [122].

Much of Streander's thinking was directed along the lines of shallow-bed silica sand filters employing mechanical cleaning devices. He felt these designs had definite merit as a secondary treatment system for the removal of solids escaping the primary settling process. Because of the automatic backwash feature, installations of this equipment for direct filtration of primary effluent had consistently removed 50% of the incoming suspended solids regardless of solids concentration or filter hydraulic loading (apparently 2 gpm/sq ft was maximum) [124]. Streander recommended bed depths of 6 to 12 in. and hydraulic loadings less than or equal to 2 gpm/sq ft.

Although a proponent of shallow-bed, mechanically cleaned filters, Streander was also aware of the potential of backwash type, deep granular filters in sewage treatment. He reported on the full-scale installation of such a plant in Wuppertal, Germany, a city of about 410,000 people at that time [122]. As a result of extensive pilot-scale studies of filtration rate, sand size, and bed depth, the designers of the Wuppertal plant chose a 1.0 to 2.0 mm sand placed to a depth of 28 in. over a 4-in. layer of coarse and fine gravel. Ten filter beds were provided, each 26 ft 3 in. by 123 ft long, giving a combined filtering area of 32,280 sq ft for a flow rate of 24 mgd. At the relatively low hydraulic loading rate of 0.5 gpm/sq ft and filtering primary effluent, suspended solids removals averaged only 40%. Streander felt that the low efficiency was the direct result of a poor backwashing procedure which did not thoroughly clean the filter. Basically the backwash sequence consisted of air scour of unspecified rate and duration followed by a low rate backwash of 6 to 8 in./min (vertical superficial velocity). Streander speculated that the air agitation loosened the heavier trapped solids, but the low wash rate could not effectively carry these away nor remove the finer, more tenaciously bound solids.

Regardless of the depth of bed employed, Streander realized the need for proper sand size selection and the dependence of such upon the nature of the influent solids, the concentration of the solids, and the availability of washwater [122]. He stressed that media selection should be carefully considered to prevent premature clogging and to promote distribution of the suspended solids removal throughout the filter bed. Furthermore, he recognized the necessity of adequate media cleaning techniques with respect to proper filter operation.

Streander predicted the increased use of filtration as an effluent polishing application for treating activated sludge and trickling filter plant effluents. Placed after final settling tanks, filters could, he believed, be used to remove the lighter, less settleable solids, thus permitting a smaller clarifier or overloading of an

existing unit. The following quote [124] summarizes his views on the potential of wastewater filtration:

It is the writer's belief that this matter of dollars and cents value of effluent strainers has only begun to be realized, and that the future will find these worthy adjuncts to treatment plants coming into widespread use as an economy feature as well as being producers of more even and dependable quality of plant effluent.

### British Studies

Luton. British wastewater treatment literature abounds with references to the Luton Corporation Works filtration plant and to experimental filtration studies conducted there. In 1949, prior to the installation of filtration facilities, initial studies were begun by Pettet et al. [92,93] using pilot-scale equipment. Treatment at that time consisted of primary settling, activated sludge and trickling filters in series, and final settling. The investigations were conducted using two pilot-scale pressure filters operating at a hydraulic loading of 2 gpm/sq ft, which filtered plant effluent over an 11-month period. Filter housings consisted of vertical, cast iron cylinders 3 ft high and 2 ft in diameter capped with a flanged dome and seated with a flanged cone. The overall bed depth in each filter was 24 in.; however, one was equipped with sand graded 0.85 to 1.7 mm and the other with 10 in. of 2.1 to 6.0-mm anthracite under 14 in. of 0.85 to 2.1-mm anthracite.

Backwashing was scheduled on a 24-hr interval and was applied at a rate of 14 gpm/sq ft using filter effluent. Spent washwater, comprising approximately 3% (300 gal.) of the throughput, was discharged through a valve in each housing and returned to the treatment plant settling tank. To assist in the breakup of the clogged bed, each filter housing was equipped with a handwheel-operated rake whose teeth extended 1 ft below the media surface. As the study progressed, daily head loss increased from 4.5 to 30 ft because of inefficient cleaning. An examination of the filter interior revealed that the filter walls and sand were covered with gelatinous coatings of 1/2 in. and 1/4 in., respectively. Sodium hypochlorite solutions were applied in varying doses and for several contact times, the most successful combination being 0.05% sodium hypochlorite as chlorine with a 2-hr contact time. After this cleanup procedure, no additional chlorination was required.

Immediately following the conclusion of the first Luton study, Pettet et al. [92,93] began a second pilot-scale study at a nearby trickling filter plant, the Finham Works in Coventry. Again, separate sand and anthracite filters were investigated except that they were now gravity operated. One 12-in. diameter housing contained 24 in. of sand graded 1.0 to 2.0 mm and the other contained 3-in. of 2.6 to 6.0-mm anthracite supporting 24 in. of coal graded 1.0 to 2.0 mm.

Backwashing requirements were approximately 2% of the filter throughput, and each bed was air scoured prior to introducing the washwater.

During the latter four months of the Finham study the terminal head loss of the sand filter approached 8 ft on occasion where it normally did not exceed 2 ft. This problem was reduced by using approximately three times the normal washwater volume during the backwashing following every third run. At no time was chlorination required to control gelatinous accumulations within the filters. Based upon the data available from both studies Pettet concluded that air scour was worthy of additional study as a backwashing aid.

Upon completion of the Finham study, Pettet et al. [93,94] returned to the Luton Corporation Works to conduct additional experiments with pressure and gravity filtration. Equipment for the pressure filter study were the same as previously described for Luton. Media type, depth, and gradation were changed several times during the study. Initially one filter contained 24 in. of 0.35 to 1.7-mm sand and the other, 24 in. of 1 to 2-mm anthracite. These two filters were operated at rates varying from 1.2 to 4.0 gpm/sq ft over a seven-month period. Backwashing of each filter was conducted on a 24-hour basis and was preceded by three minutes of air scour at 18.3 scfm (5.8 scfm/sq ft). Washwater was drawn from the filter effluent tank and pumped at rates of 14 gpm/sq ft and 8 to 10 gpm/sq ft for the sand and coal filters, respectively. Total washwater volume was approximately 2 to 3% of throughput. Throughout the comparison of sand and coal filters, no appreciable differences in effluent quality were observed, but effluents from each deteriorated markedly after six months of operation. An inspection of the media in both filters revealed that the individual particles were heavily coated with a biological slime which was believed to be the source of the problem. Pettet et al. [93,94] considered this the result of inadequate air scour, so the media was chlorinated and, subsequently, the air-scour time was increased to 10 to 15 min. The effluent quality of both filters was restored to previous levels and the increased air scour appeared to maintain the cleanliness of the media so that no additional chlorination was required.

The next phase of the study was directed at determining the effect of depth on effluent quality. The old media in each filter was replaced with a single size range (0.85 to 2.06 mm) of hand-graded sand placed in one filter to a depth of 24 in. and in the second to a depth of 42 in. It was thought that the deeper bed would prevent solids breakthrough at higher hydraulic loadings, but it was discovered that the shallow bed reached terminal head loss before exhibiting breakthrough. The filters were operated for two months at hydraulic loadings up to 5.7 gpm/sq ft, but no appreciable differences in effluent quality were observed below loadings of 4.6 gpm/sq ft and only slight improvement by the deep filter at rates above this figure. Backwash requirements for the shallow sand bed were the same as those for the sand bed of the preceding phase: 14 gpm/sq ft and 2 to 3% of the

filtered volume. For proper cleaning of the deeper bed, however, the wash rate had to be increased to 20 gpm/sq ft, and the total volume of washwater used also increased [93,94]. Each was air scoured at an unspecified rate and duration prior to the water backwash.

Based upon the data collected by Pettet et al. [92,93,94] in the extensive experimental studies previously discussed, six rectangular rapid sand filters were installed at Luton in 1951 [41,42]. Each filter was operated at a hydraulic loading of 4 gpm/sq ft, which was maintained by a rate controller on the filter effluent line. The media in each filter consisted of 36 in. of sand graded so that 90% of the grains were within the 0.85 to 1.67-mm size range. Water backwashing was preceded by air scour at a rate of 1 scfm/sq ft for an unspecified duration. Washwater was then pumped at a rate of 14 gpm/sq ft from a filtered water storage tank, each filter normally requiring a washwater volume equal to 2-1/2% of its throughput. Spent washwater (approximately 15,000 gal. per filter backwash) was collected in a second storage tank and fed back gradually to the head of the plant. The filters ordinarily exhibited an initial head loss of 1 to 1.5 ft following backwashing and were allowed to attain a head of 8 to 9 ft before cleaning was again initiated. Under average conditions the filters required backwashing twice daily [41,42,86,94].

In 1954 the filter plant capacity was increased by 50% with the addition of three more units, which corresponded to a simultaneous 50% expansion of the activated sludge treatment units. The new filters were essentially the same as the original units although the sand was apparently graded somewhat finer.

Data gathered over the years since the installation of the units has shown that the rapid sand filters generally performed well although they were susceptible to effluent deterioration from poor backwashing or shock loads of sewage containing high suspended solids concentration [86]. It had also been observed that media was being lost as a result of slime coatings which decreased the effective particle density and, thus the grains were more easily carried away with the spent washwater. Backwashing procedures were changed to those as presented in Table 5. Because of these difficulties and of more stringent effluent standards recently imposed upon the Luton plant, a new study was initiated.

The objectives of the investigation were to directly compare a pilot-scale Immedium upflow filter with one of the existing rapid sand filters and to determine the best means of backwashing each. The results of the study demonstrated the superiority of the upflow unit for the following reasons [86]:

1. Suspended solids removals were consistently better even at flow rates 50% higher.

2. Greater utilization of the bed for solids removal resulted in longer runs and greater throughput.
3. High influent suspended solids concentrations did not cause severe upsets and were readily handled at slightly reduced loadings (3.4 gpm/sq ft).
4. Backwash can be conducted readily with filter influent.
5. Reduced capital costs resulting from elimination of high filter walls (no static head requirements).
6. Less down time for backwashing.

Backwashing procedures are summarized in Tables 5A and 6A, which are copied from the original references. The pulsating air scour is reportedly very effective in breaking up the agglomerated media of the upflow filter following a run. Apparently, the agitation is quite severe, and the disturbance travels upward through the bed in a wave-like motion.

A visit to the Luton works in November, 1975, revealed the following developments. Sand in the rapid sand filter after backwashing had heavy organic slimes surrounding the sand grains, but no mud balls were visible. The slimes in the upper sand layers after backwashing caused about 12% dry weight loss when a sample was ignited in a standard loss in ignition solids test. The backwash procedure had been changed to that shown in Table 5B incorporating a pulsed air scour. Sand loss was still a problem, and periodically sand is added to maintain desired sand depth. The dirty sand did not appear to affect the filtrate quality. Run lengths were only about 7 hr due to high influent suspended solids (about 35 mg/l) coming from overloaded final settling tanks.

The upflow filters have also experienced sand loss, which at times has completely exposed the hold down grid. During high flows, this has resulted in uplifting of the bed and breakthrough of solids at head losses of greater than 6 ft. The backwash procedure had been modified in 1975 as shown in Table 6B to attempt to improve backwash effectiveness. The change included an increase in the high rate wash from 15 to 19 gpm/sq ft. The condition of the deep media was not observed due to difficulty of sampling.

Immedium filter studies. The favorable results obtained at Luton sparked interest in the Immedium upflow filter as a wastewater filter and spawned three additional studies over the next four to five years. The first of these studies was conducted by Woods et al. [142] using a pilot-scale unit at the West Hertfordshire Works and activated sludge plant effluent. Details of media sizing and bed depth were not presented; however, the pilot Immedium filter was described as a

Table 5A. Manual backwashing procedure used on full-scale rapid sand filters at Luton [86].<sup>a</sup>

Minutes after stoppage of inflow	Description of operations
0	Inflow stopped. Drain down commenced and, if possible, continued to completely drain down the water through the filter sand into the effluent channel.
15	Backwash outlet valve opened to remove any water remaining above the level of the backwash weir.
20	High-rate air scour and slow-rate backwash commenced together.
30	Air scour stopped. High-rate backwash commenced.
40	High-rate backwash stopped. Normal inflow commenced.

<sup>a</sup> Filtered water used for backwashing, water and air rates were not specified.

Table 5B. Backwashing procedure in full-scale rapid sand filters at Luton in November 1975.

Minutes after inflow stoppage	Operation
0-28	Drain down to bottom of sand level.
28-32	Low-rate air and water backwash simultaneously to a water level 9 cm above the fixed bed surface. Air at 1.23 cfm/sq ft and water at 2.1 gpm/sq ft
32-41	Intermittant air scour. Air on at 1.23 cfm/sq ft for 45 sec and off for 45 sec, and cycle repeated for 9 min
41-49	High-rate backwash at 13.7 gpm/sq ft

Table 6A. Automatic backwashing sequence used on pilot-scale Immedium upflow filter at Luton [86].<sup>a</sup>

Minutes after initiation of backwash cycle	Description of operations
0	Backwash cycle initiated by pressure switch. Inflow stopped. Drain down commenced.
5	Drain down completed. High rate air scour (4.8 cfm/sq ft) and slow-rate backwash (2.4 gpm/sq ft) commenced together.
9	Slow rate backwash stopped by electrode 9 in. above sand level. Pulsating air-scour commenced (3.3 cfm/sq ft for 45 sec alternating with 0.5 cfm/sq ft for 45 sec).
19	Pulsating air scour stopped. High-rate backwash (15 gpm/sq ft) for 30 sec, then dropped to slow rate backwash for 10 sec, then increased to high-rate backwash. (This pulsing of the backwash rates ensures that any entrapped air bubbles rise up out of the sand bed.)
26	High rate backwash stopped. Normal inflow commenced.

<sup>a</sup>Feed water used for backwashing.

Table 6B. Backwash procedure for full-scale upflow filters at Luton in November 1975.

Minutes after inflow stoppage	Operation
0-27	Drain down to bottom of sand.
27-31	Air and water wash together to a level 9 cm above sand surface. Air at 2.85 cfm/sq ft and water at 2.5 gpm/sq ft
31-37	Intermittent air scour at 2.14 cfm/sq ft, 45 sec on, 45 sec off for 6 min
37-47	High rate backwash at 19 gpm/sq ft

typical unit, which would mean that it consisted of a 1-ft layer of gravel topped by 5 ft of 1 to 2-mm sand.

Operational advantages of the unit were: excellent ability to handle hydraulic shock loads, high suspended solids and biochemical oxygen demand (BOD) efficiency at higher flow rates per unit area, and ease of backwashing. The latter item was accomplished by draining down the filter to the media surface and air scouring at unspecified rate, then applying filter influent at a rate sufficient to break the compression arches in the bed and fluidize the media. This backwashing procedure was a departure from that recommended by Boby and Alpe [13] because the backwash water was introduced after the air scour. No leaves, paper, or fat was observed lodged in the base of the filter, which is the point of initial contact with the influent and backwash water [142]. The backwash water removed 1.33 lb of entrapped solids per square foot of filter area and required an average 1056 gal. for each wash.

At approximately the same time, Truesdale and Birkbeck [131] were conducting a similar Immedium filter study at another activated sludge plant in Letchworth. Their pilot-scale apparatus consisted of a 2.5-ft diameter housing containing a 1-ft layer of graded support gravel and 5 ft of 1 to 2-mm sand. The media-restraining grid consisted of a series of parallel bars at 4-in. centers located 2 in. below the sand surface. When the head loss reached a predetermined value, cleaning was initiated with an air scour at unspecified rate followed by backwash with filter influent at 14 gpm/sq ft for 15 min. The total volume of washwater used averaged 5.7% of the throughput.

Michaelson [83] conducted a third study on upflow filtration using trickling filter effluent from the plant at Ashton-Under-Lyne. Few details about the backwash were presented except that backwash was on a daily basis and used 1.25% of the throughput.

Derby. An extensive, pilot-scale investigation of wastewater filtration was begun in 1966 by Joslin and Greene [68] using trickling filter effluent from the treatment works at Derby. During the next two years, seven separate filters using three different flow configurations were studied:

1. A 24-in. deep downflow sand filter with media graded 1.2 to 2.4 mm.
2. A 36-in. deep downflow sand filter with media graded 1.2 to 2.4 mm.
3. A 24-in. deep downflow sand filter with media graded 1.2 to 1.7 mm.

4. A 24-in. deep triple-media downflow filter consisting of anthracite, sand, and garnet graded 1.4 to 2.4 mm, 1.2 to 1.4 mm, and 0.71 to 0.85 mm, respectively.
5. A 24-in. deep upflow sand filter graded 0.71 to 2.40 mm.
6. An Immedium upflow sand filter with 26 in. of graded gravel and 48 in. of 1 to 2-mm sand.
7. A radial flow, moving bed sand filter containing 0.5 to 1.0-mm sand.

Joslin and Greene demonstrated that with respect to filtration of Derby effluent, flow direction was insignificant in comparison to proper media depth and gradation. This was in direct contrast to several other studies where the Immedium upflow filter had demonstrated superiority to conventional downflow sand filters [83,131,142]. Although flow configuration appeared to play no role in improved suspended solids removal, increased bed depth did improve removal, as evidenced by the superior efficiency of both the Immedium upflow (4-ft depth) and deep-bed rapid sand filters (3-ft depth). Head loss development was less rapid in the filters containing 1 to 2-mm graded sand than those, such as the triple-media filter, containing finer particles. Because of the subsequently longer filter runs and the ability to meet desired effluent standards at high loading rates, the overall conclusion of the study was that deep-bed filters of coarse 1 to 2-mm sand were most suitable for a full-scale application.

Backwashing experiences with the filters at the Derby installation were interesting and were reported in some detail. An inadequate air supply precluded the use of air scour prior to applying washwater to the media, so an attempt was made to compensate for this deficiency by backwashing at higher rates. Difficulties were encountered in all the units, however, with mud ball and agglomerate formations which resisted breakup by the water (only) backwash. This problem was partially relieved by draining the water level to within 1 in. of the surface and then directing a jet of water onto the surface of the filter prior to backwashing. Mud balls which escaped breakup by the jet tended to settle deeper in the filter. Difficulties were also encountered at the start of each backwash because the filter media tended to rise as a plug upon initial application of the washwater and caused fluctuation on the backwash rate indicator.

Minworth. Activated sludge effluent from the Minworth treatment plant was used as filter influent in an investigation conducted by Tebbutt [129]. Three pilot-scale filters were assembled. Total bed depth in each filter was 24 in., with the first filter containing 0.5 to 1.0-mm sand, the second filter containing 1.0 to 2.5-mm anthracite, and the third containing half 0.5 to 1.0-mm sand and half 1.0 to 2.5 mm anthracite. Flow rates to each filter were varied from 1.7 to

10.3 gpm/sq ft, and no substantial drop in efficiency with increasing rate was observed.

A second series of in-plant tests was also conducted using 24-in. bed depths, the three filters having one of the following specifications: 1.0 to 2.5-mm anthracite, 1.2 to 2.4-mm sand, 2.4 to 4.7-mm sand. Flow rates applied to the filters were the same as for the first in-plant series.

Backwashing details provided in the text of the article by Tebbutt are scanty, but no air scour was used, and difficulties were encountered with the media rising as a "plug" at the start of the wash, a problem also reported by Joslin and Greene [68]. Filter beds containing anthracite were most pronounced in exhibiting this problem, while the sand beds were generally easier to maintain. Coarse sand (1.2 to 2.4 mm) was not expanded but did clean readily. Tebbutt felt that the rising plug problem could be eliminated in a full-scale plant with the use of air scour and that this would place the anthracite media in an operating advantage since the Minworth studies showed less washwater was required for anthracite filters in spite of the plugging.

#### South African Studies

Ancor. In 1947 Vosloo [136] reported the results of an investigation in which a pilot-scale pressure filter was used to treat the effluent from the Ancor waste disposal plant. Although the nature of the treatment of the Ancor plant was not described by Vosloo, Huang [59] described it as having secondary treatment. A reasonable assumption, considering the climate and other installations in the area [87], is that the plant consisted of primary settling, trickling filters, and final clarifiers.

The pilot filter was contained in a 2-ft diameter steel casing having a height of 4.5 ft. The filter media consisted of a 24-in. layer of graded 0.5-mm sand and 5 in. of 0.8 to 1.7-mm sand, both layers of which were supported by 7 in. of graded gravel. Flow configuration was downward, and effluent from the filter was collected by nozzle mounted in a steel plate false bottom. In a manner similar to the arrangement on the early Luton pressure filters [92], the housing for the Ancor filter was equipped with a handwheel-operated rake to break up the media surface during backwashing. Unfortunately, no other details about backwashing effectiveness or backwashing problems were presented.

Pretoria. Since 1954 full scale gravity filters have been used at the Pretoria Purification Works to remove suspended solids from a 3 mgd flow at the trickling filter plant [87]. The five filters are each 13.5 ft in diameter and can develop a maximum head of 9 ft. Air-scour capability for backwashing has been provided on the four filter beds equipped with a steel plate false bottom containing 1-in.

diameter nozzles at 6-in. centers [72,88]. Compressed air is introduced below the false bottom of these filters by a 1-1/2-in. diameter, T-shaped head and is distributed through the nozzles to the media. The remaining filter is equipped with a United States-manufactured carborundum block false bottom and rotary surface washers. Each filter contains sand media graded to 0.55 to 0.85 mm for 21 in. and 0.85 to 3.2 mm for 6 in., and those equipped with the steel plate (nozzle) underdrain have been provided with a 12-in. layer of support gravel.

Designed for a maximum rate of 3 gpm/sq ft, the filters have been operated at an average rate of 2.6 gpm/sq ft to a terminal head loss of 6.5 ft [72]. During an average 8 to 10-hr run, the filters consistently reduced the influent suspended solids level of 22 mg/l from the treatment works to less than 5 mg/l [102]. Backwash pumps were sized to provide a maximum rate of 45.6 gpm/sq ft, which is sufficient to expand the sand 50%; however, a rate of 25.7 gpm/sq ft has been found to be adequate [111]. Washwater volume normally comprised 192,000 gal. or approximately 9.5% of the treated flow. Interestingly, Nicolle [87] has reported that the filter equipped with rotary surface washers had slightly longer runs and appeared quite clean compared to the filters equipped with air scour. Several comments by Nicolle [87,88] with respect to design and operation of the filters are important:

1. Filter influent at Pretoria is chlorinated at a dosage 4.7 mg/l to control biological growths and deposits and is considered highly beneficial.
2. The filters have demonstrated a distinct susceptibility to hydraulic shock caused by stopping, starting, or altering the application rate and have required backwashing soon thereafter.
3. The use of a circular shape for wastewater filter housings should be avoided because of increased space requirements and difficulty in altering washwater trough placement.

## VIII. EXPERIMENTAL COMPARISON OF BACKWASH METHODS IN WASTEWATER FILTRATION

### Pilot-Plant Equipment

#### The Ames Plant

Experimental work comparing different backwashing methods was conducted at the Ames Water Pollution Control Plant using a pilot-scale filter plant designed and built for this study. The Ames treatment plant facility employs biological treatment via three standard rate trickling filters. The plant was completed in 1951 and at the time of this study (1973-75) was somewhat overloaded. Raw sewage enters the plant through a comminutor pit and then is lifted to an aerated grit removal chamber. Effluent from the grit chamber is then passed through four rectangular primary sedimentation tanks which provide about 2 hr detention time at a flow rate of 4 mgd. The primary tank effluent is then applied to the trickling filters by rotary distributors and thence to three circular final settling tanks. Although chlorination facilities have been provided, they have never been used because of hydraulic difficulties in discharging from the tank to the Skunk River. Therefore after final clarification, the flow is collected and discharged to the Skunk River.

Primary sludge and scum are collected and directed to an anaerobic digester. Final sludge is drawn off from each of the tanks and mixed with raw sewage at the head of the plant.

Serving both the University and the city, the plant treats sewage which is primarily domestic in nature and not subject to unusual load or strength variations from large industrial water users. Variations are observed in sewage strength, however, during the regular school year and the summer vacation, when the university population fluctuates widely. Furthermore, the sewage collection system is quite susceptible to infiltration and inflow, and high flows of dilute sewage are not unusual during wet weather.

#### General Arrangement

The pilot plant was arranged as shown in Fig. 23 for the influent, flow-splitting method of rate control. In this arrangement the influent to each of the three filters was provided by throttling the supply pump discharge and then splitting the pump discharge equally into thirds. Outlet lines from the filter housings were connected to a single effluent line which was placed at an elevation above the surface of the media in the filters and defined the low static water level in the filter boxes. As head loss developed in the filters during the course of a run, the water level above the media surface continued to rise until it reached an elevation equal to the

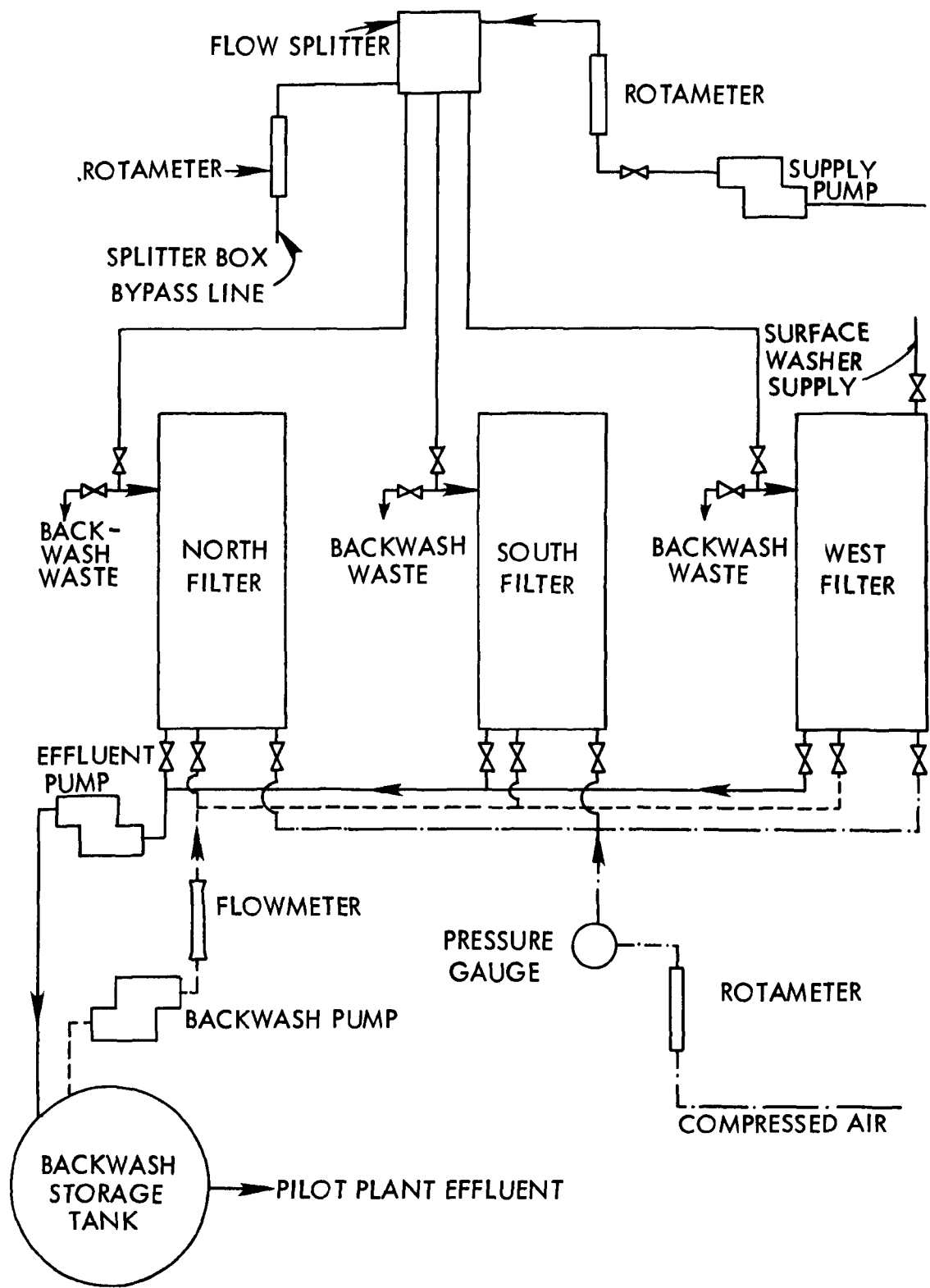


Fig. 23. Schematic representation of pilot-scale filter plant used in experimental investigation.

height of the bypass line in the influent flow-splitting device. This latter elevation defined the high static water level, or terminal head loss, which was available in the pilot plant. When filter head loss reached the terminal stage, part of the influent was bypassed automatically, and the filter ceased to operate at a constant and equal rate and thereafter declined in rate until it was backwashed.

### Chronology of Experiments

The experimental work with the pilot plant was conducted in several phases in which different filter media and or backwashing techniques were used. The phases are summarized in Table 7. In addition to the differences shown in the table, there was also a difference in source of backwash water. During Phases I and II the filtered effluent was used as the backwash supply by passing it through the backwash storage tank of Fig. 23. In Phases III through VI, the unfiltered secondary effluent was used as a backwash source.

### Equipment Details

The west filter was completed during the middle of Phase I. Since a complete set of data were not collected for that filter on Phase I, the data for that filter in Phase I are not presented herein.

### Flow Splitting

Two different flow splitters were used. During the first half of Phase I, a standard 1-in. pipe tee was used. Globe valves on either branch were used to adjust the split. This arrangement was easy to construct and functioned reasonably well. During the last part of Phase I, it was desired to split the flow three ways so that the West filter could be used. This was accomplished by use of an influent splitter box which was used for all subsequent Phases. The splitter box consisted of two fabricated steel boxes, or halves, that fit on top of each other. The influent flow was split equally to the three filters by identical orifices located in the bottom of the upper box. A float valve on the influent pipe was used to maintain a constant water level on the orifices in the upper box. Discharge from each of the three orifices dropped through an air gap into one of the inlet lines to the filters which were connected to the bottom of the lower box. When one or more of the filters reached terminal head loss, water would back up in the lower box and overflow to waste. The filter inlets and overflow line were arranged so that the other filters continued to function without interruption or change in flow rate. This arrangement allowed completely independent operation between the three filters. Several sets of identical orifices were available which could be inserted in the flow-splitter box to achieve various desired filtration rates. The actual filtration rate to each filter was measured with a rotameter on the overflow line. The flow to any

Table 7. Summary of experimental phases for wastewater filtration backwashing study.

Phase	Period	Filter Influent	Media			Backwash		
			N <sup>a</sup>	S <sup>a</sup>	W <sup>a</sup>	N	S	W
I	5/17/73- 8/21/73	Alum treated sec. effl.	Identical dual media			Water only	Air scour type 1 <sup>b</sup>	Fixed surface wash
II	8/28/73- 10/20/73	Secondary effl.	Same			"	"	Rotary surface wash
III, IV and V	5/16/74- 11/2/74	Secondary effl.	Dual media	Coarse sand media	Mixed (tri) media	Air scour type 2 <sup>b</sup>	Air and water together type 3 <sup>b</sup>	Surface and subsurface wash
VI	6/4/75- 8/4/75	Secondary effl.	Identical coarse sand			Identical air and water type 3 <sup>b</sup>		

<sup>a</sup>N, S, W refer to the north, south, and west filters, respectively.

<sup>b</sup>Type 1 air scour means air first followed by water with full-bed fluidization and expansion.

Type 2 air scour means air and water together briefly during the rising water level followed by water only with full-bed fluidization and expansion.

Type 3 air scour means air and water together during most of the backwash while overflow was occurring. Used only for coarse sand media which was not fluidized or expanded during the backwash.

filter was purposely bypassed to the rotameter to measure the rate whenever desired.

#### Alum Treatment Equipment

During Phase I, the settled secondary effluent was pumped to an upflow solids contact unit where it was treated with alum for phosphate precipitation and settled before filtration. Figure 24 shows the upflow solids contact unit. This unit was mounted in a truck and formerly served as part of a mobile water purification plant for the United States Army. The conical shaped settling and reaction tank is referred to as an erdlator. It had a volume of approximately 530 gal.

Raw water was pumped through a pair of nozzles into two troughs. This aerated the water just before it overflowed into a vertical, cylindrical, center column in the erdlator. Alum solution was added in one of these troughs. The center well contained an agitator that mixed the alum solution with the raw water and provided some flocculation. Rapid mixing was not provided. After flowing downward through the center column, the water moved upward to a collection trough.

The flocculant precipitate comprised of  $\text{AlPO}_4$  and  $\text{Al}(\text{OH})_3$  separated in a floc blanket where the upward water velocity became equal to the hindered settling velocity of the floc. The blanket of floc provided an environment that aided the reactions with the alum and encouraged flocculation or the agglomeration of smaller floc particles into larger ones. Either sedimentation or enmeshment in the floc blanket removed much of the material suspended in the erdlator influent. The surface of the floc blanket was easily observed through the clear water above. The blanket itself appeared to be fairly thick, but its lower surface could not be observed.

The clear water above the floc blanket was collected in a circular trough. Orifices on both sides near the top of the trough provided for even collection of water. From the collection trough the water flowed to a clear well.

As the floc in the erdlator formed and as sewage particles were enmeshed in it, a considerable volume of sludge was created. A slot in the side of the erdlator drew the sludge from the top of the blanket into a sludge concentrator tank. The clear supernatant from the concentrator was drawn off into the clear well and the concentrated sludge was drawn to waste by a positive displacement pump.

A dual head, diaphragm type, positive displacement pump was used to feed the alum solution. The pump drew from two 150-liter containers where the alum was prepared.

Water was drawn from the clear well by a self-priming centrifugal pump. A rotameter and a globe valve in the pump discharge line

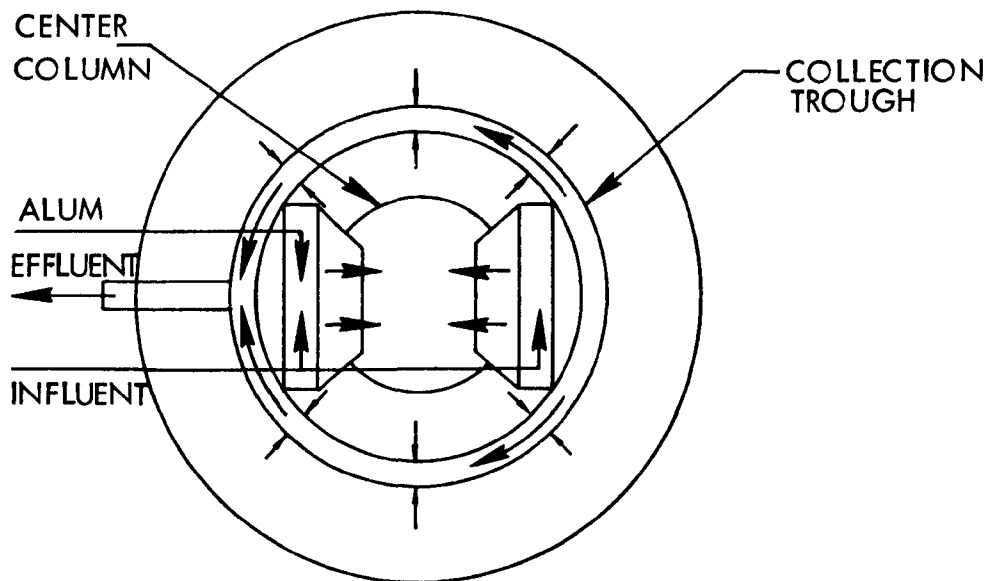
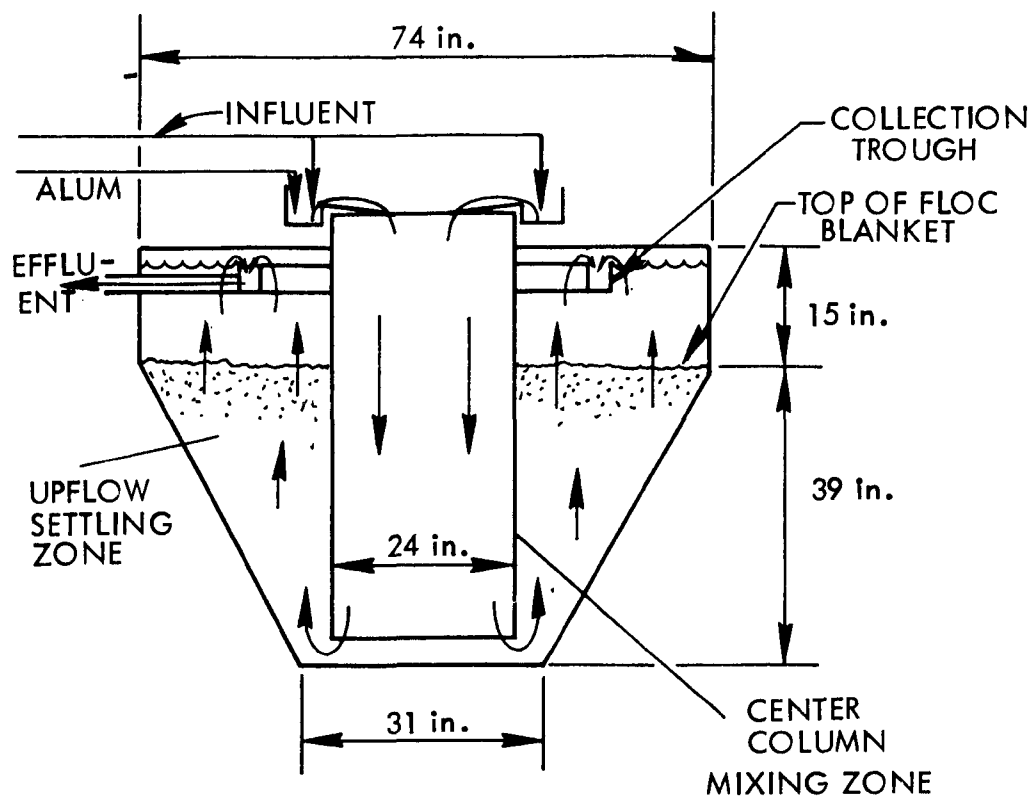


Fig. 24. Pilot plant solids contact unit.

enabled quick flow measurement and adjustment. The pump then discharged to the flow splitter.

### Filters

Housing details. Each of the three filter housings used in this experimental investigation was fabricated from 3/16-in. steel plate and was equipped with a 1/2-in. thick plexiglass front for viewing the interior during the backwashing cycle. Vent pipes were installed on each housing to permit the filters to operate by gravity for this study, although each unit can be completely sealed for pressure filter operation. The interior horizontal cross sectional area of each filter was 2.25 sq ft, and other pertinent interior dimensions are shown in Fig. 25. Access to the interior of the housing was provided by a top mounted, 6-in. diameter, hand hole. At the beginning of Phase VI, all three filter housings were extended in height to 10 ft so that deeper media could be used.

Located near the top of each housing was a 1-1/2 by 4-in. inverted bell mouth which distributed the influent during the course of a filter run and collected the washwater during the backwash cycle.

Each filter housing was equipped with an underdrain system consisting of a steel plate false bottom and five General Filter Company media-retaining strainers (or nozzles). During a normal run the nozzles collected the filtrate and directed it to the plenum below the false bottom where the effluent lines carried it to the backwash storage tank. When cleaning was required, water and air (if used) entered the plenum and were distributed uniformly to the media through the nozzles. The media-retaining nozzles had openings of 0.4 mm during Phases I and II. There was evidence of partial clogging of these fine openings by the end of Phase II. Therefore, nozzles with 1-mm slots were installed at the beginning of Phase III and graded gravel was needed for the north and west filters to prevent loss of filter media. A nozzle clogging incident occurred during Phase III which required termination of that phase. During rebuilding of the two filters, new nozzles with 4.5-mm slots were installed. The incident will be described later in the results section. Nozzles with 4.5-mm slots were used in all three filters in Phase VI.

Head loss development in the filters was monitored by seven piezometers attached to taps located vertically along one side of the filter housing. The taps were located at 4-in. centers starting just above the underdrain plate. Each tap consisted of a 3-in. length of 1/4-in. copper tubing soldered to 1/4-in. brass fittings which could be threaded directly into the side of the housing. The interior end of the tap extended slightly into the media and was covered by a fine stainless steel mesh. The exterior end of each tap was connected to a length of 1/4-in. clear plastic tubing which was then mounted to a piezometer board. Thus, using the false bottom as a datum, the pressure at several points within the filter media was determined by

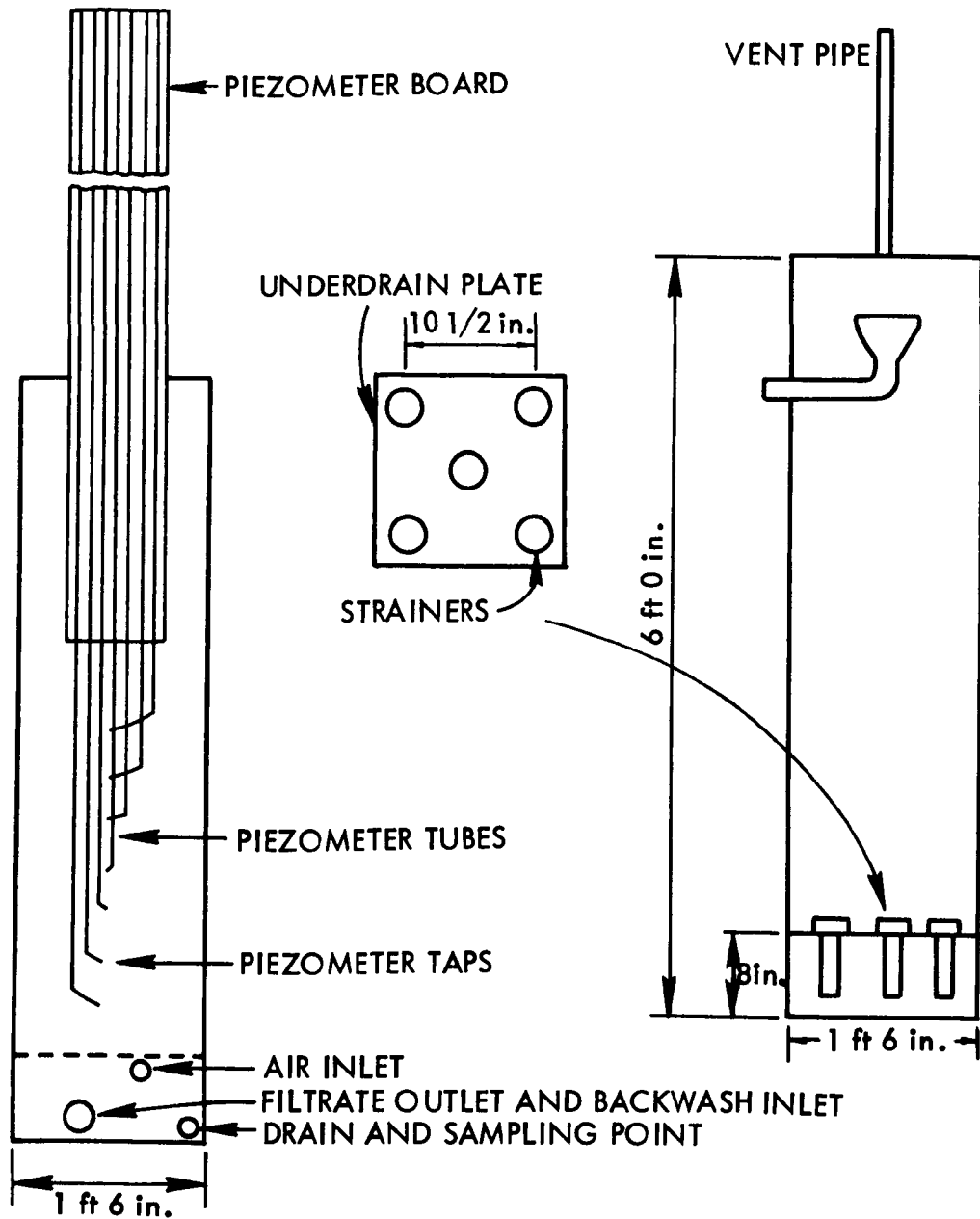


Fig. 25. Details of filter boxes.

observing the water level in each of the clear plastic tubes. Different piezometer tap positions were used in the various phases depending upon the depth of media in service.

Surface washer. The west filter was chosen for installation of a rotating surface washer consisting of an inverted lawn sprinkler which threaded into a coupling on the back plate of the filter housing. Water was supplied to the surface washer from a yard hydrant supplied by the treatment plant non-potable well water system. Hydrant line pressure was usually 60 to 70 psig and surface washer operating pressure generally was from 40 to 45 psig.

After about 30 filter runs in Phase II using the improvised rotary surface washer, a two-armed model incorporating two nozzles was installed. The new rotating surface washer more closely resembled systems in actual use and produced strong, highly directional jets. The two arms of the surface washer consisted of 1/2-in. diameter brass nipples, were each 6-in. long, and were positioned 180° apart in a horizontal plane. One 1/8-in. diameter nozzle (Leopold Corporation) was placed on a 45° elbow at the end of each arm and positioned toward the media surface at an angle of 15° to the horizontal.

This system was used essentially as described for the remainder of Phase II except for a slight shortening of the rotating arms to better direct the end nozzles to the media. At the beginning of Phase III, a subsurface washer was added to the west filter, and a booster pump was added to the surface wash supply line, which increased the operating pressure to about 80 psig. Both nozzles were positioned down at a 15° angle to the horizontal for the surface washer while the subsurface washer had one nozzle pointed up and one down at the same angle. Two 1/2-in. pipes in the filter supported the washers. At the start of Series IV, both surface washers were modified. Both washer arms were changed to 1/4-in. nipples approximately 5 in. in length. A 1/4-in., 90° elbow was attached to the end of each arm, and a Leopold nozzle was fastened on the end of each elbow. Both nozzles of the surface washer were pointed down at a 15° angle. The subsurface washer had rubber capped nozzles, one up and one down, both at a 15° angle. The vertical position of the washers was changed to coincide more closely with the coal-sand interface for the subsurface washer, and the surface of the coal for the surface washer.

At the beginning of Phase VI, the surface and subsurface washer were removed from the west filter.

Filter media. The filter media was obtained from several sources and in several sizes for the various phases as summarized in Table 8. In Phase I and II, it was desired that the dual media be as identical as possible in each of the filters. To achieve this objective the following precautions were used at the beginning of each phase when placing new media in the filters. The total volume of a particular

media layer required for the desired finished depth plus a 3-in. skimming depth was determined, and the required number of bags were poured onto a concrete slab. After the media had been thoroughly mixed, it was split and placed in each housing. Next the media was backwashed at a rate of about 15 to 20 gpm/sq ft for 15 min to allow the fine particles to work their way to the surface. Finally, with the backwash rate reduced to the point that the coal was just fluidized, the top 3-in. layer was removed from the housing with a siphon. The sand layer in Phase I was not skimmed in this fashion.

After the layer had been placed and skimmed, a core sample of the layer was taken from each filter and subjected to a sieve analysis, the results of which are presented in Table 8.

A similar procedure was used in Phase III and IV to ensure that the coal and sand of the dual- and triple-media filters were identical. The only difference was that the skimming depth of each layer was 1/2 in., in accordance with the suppliers recommendation. The coarse sand of the south filter was not skimmed in this fashion since it was too coarse to fluidize with backwash rates that were available, and also because fluidization was not to be practiced in the routine backwash operation of that filter. The splitting precautions without skimming were also used in Phase VI.

Gravel support. No gravel support layers were used in the filters during Phases I and II, when media retaining underdrain strainers were used. However, the clogging problems encountered in the strainers led to the use of larger openings in the strainers in Phases III through VI and necessitated the use of gravel support in some cases. It was desired to test the stability of a double reverse graded gravel during air scour to determine if gravel movement could be avoided, and to compare that behavior with a conventional graded support gravel. Therefore, at the beginning of Phase III, a double reverse graded gravel support system was installed in the dual-media filter and a regular graded gravel system in the mixed-media filter. Originally, the double reverse graded system was accidentally installed upside down, and the gravel started to mound immediately. The gravel was then installed properly in the following manner:

	<u>Size (in.)</u>	<u>Thickness (in.)</u>
Top	1/2 x 3/4	3
	1/4 x 1/2	1.5
	1/4 x 1/8	1.5
	1/8 x #10	2
	1/4 x 1/8	3

Later, when the filter was rebuilt at the beginning of Phase IV, the underdrain gravel was modified to accommodate strainers with larger

Table 8. Filter media details for wastewater filtration pilot studies.

Phase	Filter	Media type	Layer Details		Size Information <sup>a</sup>			Specific gravity	Supplier
			Type	Thickness in.	Effective size, mm	Uniformity coeff.	90% finer, mm		
I	N and S	Dual	Coal	11.8 <sup>a</sup>	0.94	1.31	1.4	1.67	Carbonite Filter Corp. Delana, Pa.
			Sand	12	0.38	1.50	0.73	2.65	Northern Gravel Co. Muscatine, Ia.
II	N, S, and W	Dual	Coal	12 <sup>a</sup>	0.92	1.52	1.5	1.67	Carbonite Filter Corp.
			Sand	12 <sup>a</sup>	0.38	1.50	0.73	2.65	Northern Gravel Co.
III	N	Dual	Coal	15 <sup>a</sup>	1.03	1.57	2.03	1.7	Neptune Microfloc Corp. Corvallis, Or.
			Sand	9 <sup>a</sup>	0.49	1.41	0.82	2.65	Neptune Microfloc Corp.
	W	Triple	Coal	(Same as N filter)					
			Sand	(Same as N filter)					
			Garnet	3 <sup>a</sup>	0.27	1.55	0.54	4.2	Neptune Microfloc Corp.
	S	Coarse sand	Sand	46	2.0	1.52	3.6		CX Products Corp. Brady, Tx.
IV & V	N and W	Same as Phase III except new media installed and coal depth changed to 17 in.							
VI	N	Coarse sand	Sand	24)					CX Products Corp.
				)					
	W		"	47)	2.5	1.28	3.7		"
				)					
	S	"	"	60)					"

<sup>a</sup>Depth and size after placement, stratification by backwashing and skimming fines from the surface of the layer with a siphon. Coarse sand was not skimmed.

(4.5-mm) slots. The support system used for the rest of the study was:

	<u>Size (in.)</u>	<u>Thickness (in.)</u>
Top	3/4 x 1/2	3
	1/4 x 1/2	1.5
	1/4 x #10	5
	1/2 x 1/4	1.5
	3/4 x 1/2	1.5

The mixed-media filter employed a normally graded support system. The original system and the rebuilt one are the following:

	<u>Original</u>	<u>Rebuilt</u>
Top	3 in. of Coarse Garnet	3 in. of Coarse Garnet (-12+16 mesh)
	2 in. of 1/8 x #10	3 in. of 1/4 x #10
	2 in. of 1/4 x 1/8	2 in. of 1/2 x 1/4
	2 in. of 1/4 x 1/2	2 in. of 3/4 x 1/2
Bottom	3 in. of 3/4 x 1/2	

As will be reported later, the double reverse graded gravel was not stable in Phases III through V, so a similar but revised support was used in Phase VI in the north filter. The gradations in that support were:

	<u>Size (in.)</u>	<u>Thickness (in.)</u>
Top	1/2 x 3/4	4
	1/4 x 1/2	2
	1/4 x #10	2
	1/4 x 1/2	2
Bottom	1/2 x 3/4	2

#### Backwash Supply

A centrifugal pump mounted on the backwash tank pumped washwater to the filters in Phases I and II. The flow rate of the backwash water was measured by a type of Venturi meter. This meter was fabricated by replacing a portion of the 1-1/2-in. diameter backwash line with a section of 1-in. diameter pipe using two reducing fittings. Pressure taps on the 1-1/2-in. and 1-in. pipes were connected to opposite legs of a mercury filled manometer. The meter was calibrated volumetrically by measuring the rate at which water rose in the filters for

different manometer readings. In Phases III through VI, the filter influent supply pump was used also for backwashing with unfiltered secondary effluent. An additional pump discharge connection was made from the pump to the same Venturi meter described above.

### Air Supply

A Speedair belt driven, dual piston compressor supplied compressed air for the air scour sequence. A pressure switch automatically started the compressor when the pressure in the storage tank fell below 40 psig. A Fisher Model 95L pressure reducer, reduced the storage pressure to an operating line pressure of about 8 psig. The amount of air flow was regulated by adjusting a globe valve and reading the percent of full flow through a Brooks rotameter. The manufacturer's calibration of the rotameter at standard conditions was accepted, but was corrected to the operating temperature and pressure of the air supply at the rotameter. Near the end of the research, an approximate calibration was achieved by noting the time for a given pressure drop on the air storage tank while the air was being used at a constant rate and the compressor was shut off. Appropriate calculations assuming the ideal gas law was applicable verified the manufacturer's calibration.

### Samplers

In Phase I, composite samplers were used to collect samples of effluent from both filters and the erdlator (Surveyor Sampler, N-Con Systems Co., Inc., New Rochelle, N. Y.). During Phase II, the same three samplers were used on the three filter effluents. A fourth sampler was obtained late in Phase II which was then always used on the filter influent (the Ames plant secondary effluent). Up until that time, the secondary effluent samples were either grab samples or composite samples collected manually by the Ames plant operators.

Each sampler consisted of an electric motor driven positive displacement pump actuated by a timing mechanism. The sampler contained two arms on a timing face, one of which set the pump running time and one of which could be set to activate the pump from 3 to 20 times per hour. To ensure that a fresh sample was obtained each time the pump was running, the waste line on the discharge side of the pump was 1/2-in. diameter while the sample line was 1/4-in. diameter. This meant that there was a delay before the filtrate was pumped to the sample container, thus allowing the system to first flush itself through the waste line. Vents were provided in both the waste and sample lines to prevent siphoning into or out of the polyethylene collection containers, which were kept refrigerated in an ordinary domestic refrigerator to preserve the sample during the compositing period. The compositing period for each phase was somewhat different and will be described later in the presentation of the results.

To evaluate the effectiveness of the various backwashing techniques, core samples of the media were taken periodically following the normal backwash cycle for a particular filter. The core sampler was constructed of a 4-ft length of 1-1/2-in. diameter copper tubing fitted with a shear gate at one end. With the gate fully open, the sampler was lowered to the desired depth in the media, at which time the gate was closed and the sample removed. Because it is well known that the majority of solids removal takes place in the upper layers of a deep bed granular filter, the penetration of the core sampler was restricted to approximately the top 12 in. of the filter media. Sometimes, the backwash water was turned on slightly, not enough to fluidize or expand the bed, but to ease the entrance of the sampler. After removal of the core, the backwash water was turned on at the normal rate for about 1.5 min to even out the surface of the media.

### Analysis of Samples

The analysis of samples was the same during all phases of the study except for the media abrasion test. The procedures are summarized in the following paragraphs.

#### Filter Media

Sieve analysis. A set of United States standard sieves was used to determine the media size. Samples were dried and then split with a riffle type sample splitter until approximately 300 g of media were obtained. The media samples were hand shaken through the sieves until 1 min of additional hand shaking changed the weight of media retained on any sieve by less than 1% of the weight on that sieve. The weights of sieves empty and with media were measured and recorded to the nearest 0.05 g.

Media density and specific gravity. The density of the media was determined by a water displacement technique with a 100-ml pycnometer. The procedure is presented in more detail with illustrative calculations in a later chapter.

Media abrasion. The media abrasion procedures changed several times during the research. However, in all cases, the purpose of the test was the same: to determine the relative amount of dirt or suspended solids remaining on the media after the normal backwash procedure for the filter.

The procedure in Phase I was as follows. Samples were reduced in size by dividing them in half with a riffle type sample splitter. Then each half was divided twice again so that two samples, each one-eighth of the original sample, were obtained. The abrasion test was then performed in duplicate. When samples were taken and split, a portion of the dirt attached to the media was undoubtedly loosened. Therefore, as the samples of sand and coal were split, the liquid

portions were also split and the dirt present included in the calculation of dirt removed from the media.

After the sample was split, it was placed in an 800-ml beaker and stirred at 200 rpm for 10 min with a 2-in. diameter, three-bladed propeller (Cole Parmer Constant Speed and Torque Control Unit) immersed in the media. After stirring, the dirt was rinsed into a graduated cylinder. Care was taken so that no sand or coal was transferred with the dirt. The media was swirled and rinsed repeatedly with distilled water and the dirty rinse water decanted into the graduate cylinder, until the rinse water was clear. The total amount of water used to wash the media was recorded. Suspended solids concentration of the wash water was determined on triplicate samples according to Standard Methods [117] by filtering an aliquot through Whatman GF/C glass fiber filter paper. The media samples were then dried overnight at 103 °C and weighed. The dirt removed was calculated by the following formula and results expressed as mg of suspended solids removed per gram of filter media.

$$\frac{(\text{SS of washwater, mg/l})(\text{Volume of washwater, l})}{(\text{Weight of filter media, g})}$$
$$= \frac{\text{mg SS removed}}{\text{g media}}$$

A different abrasion test procedure was used in Phases II and III through V. The main differences were the deletion of the splitting of the sample on the riffle type splitter (since that was not considered very suitable for a sample containing water) and the extension of the period of abrasion to 30 min (because the media was dirtier in the direct filtration of secondary effluent). A motor driven support stand was added to rotate the beaker in the direction opposite that of the propeller. The other details of the procedure are as follows:

The entire core sample and any water collected with it was put in a 2000-ml beaker and placed on the revolving stand (Driven by a Gerald H. Keller Co. variable speed direct current motor). The sample was stirred for 30 min with a 2-in. diameter, three-blade propeller rotating at 200 rpm. The propeller and the stand, revolving in opposite directions, were positioned so the propeller would traverse through the media in a circle, abrading all the sample. After mixing, the supernatant was poured into a 6000-ml flask. The media was rinsed repeatedly with distilled water and the dirty rinse water decanted into the 6000-ml flask until the rinse was clear. The total amount of washwater in the 6000-ml flask was then recorded. The remainder of the procedure was unchanged from that in Phase I.

The final modification of the abrasion test procedure was adopted at the beginning of Phase IV due to concern that the 30-min abrasion was causing excessive abrasion of the coal itself, and not merely of the

solids adhering to the coal. The abrasion period was reduced to 5 min. The details were as follows:

As before, the core sample was placed in a 2000-ml beaker, but this time distilled water was added to bring the level up to an easily read mark. The sample was then mixed in the same way as previously mentioned but only for 5 min. The coal or sand was allowed to settle for 5 sec before a 100-ml sample of the supernatant was pipetted off and transferred to a 1000-ml volumetric flask. The flask was then filled to the mark (10:1 dilution), and the suspended solids test previously mentioned was run on this suspension. If the media was very dirty, a higher dilution factor was used to speed up the filtering step in the suspended solids test. The media was dried and weighed as before. The abrasion test result was then figured as follows:

$$\text{Abrasion Test Result (mg/g)} = \frac{(\text{Avg SS})(\text{Dilution factor})(\text{Supernatant Vol})}{(\text{Weight media})}$$

Even though the abrasion test procedure for Phases IV and V was shorter and less complex, it still provided the data needed to evaluate the relative effectiveness of the backwashing procedures. Naturally, the absolute values obtained were lower due to the shorter abrasion period.

Abrasion tests were not conducted during Phase VI.

#### Water Quality Analyses

During the various experimental phases, extensive testing of filter influent and effluent samples were performed to see if the backwashing methods being used had any affect on filter performance.

Observation filter runs in which detailed observations were recorded and composite samples were collected were made at regular intervals. During these "observation runs," grab samples of filter influent and effluent were collected for immediate turbidity measurement in the field. Composite samples were collected over the observation run and transported to the laboratory for further analysis. Most of the analyses were conducted there by personnel of the Analytical Services Laboratory of the Engineering Research Institute. Suspended solids analyses were done by project personnel in Phases I, II, and VI, and by the laboratory personnel during Phases III through V.

A typical composite sample was subjected to several analyses: five-day biochemical oxygen demand (BOD), soluble BOD, suspended solids (SS), total organic carbon (TOC), soluble organic carbon (SOC), and ammonia (NH<sub>3</sub>). Periodic composite samples were also analyzed for the following: nitrite (NO<sub>2</sub>), nitrate (NO<sub>3</sub>), total Kjeldahl nitrogen, total phosphate, and orthophosphate. Soluble BOD and SOC were not

analyzed in Phases I and II. The analytical procedures were as follows.

Suspended solids. Suspended solids tests were conducted on filter influent samples, filter effluent samples, and abrasion test washwater aliquots in accordance with Standard Methods [117]. Disposable aluminum weighing tins and Whatman GF/C glass fiber filtering discs were placed in a 103 °C oven for 15 min to drive off moisture and then cooled and weighed to 0.1-mg precision. The filter discs were then placed on a Millipore filter holder which was connected to a Millipore vacuum pump. Under a steady vacuum of 15 in. of mercury, the following sample amounts were filtered through the discs:

1. Filter influent, 100 ml or 250 ml depending upon the level of SS
2. Filter effluent, 500 ml
3. Abrasion test washwater, 25 ml

After filtration had been completed, the discs and weighing tins were returned to the oven and dried overnight at 103 °C. Finally, the discs and tins were cooled and reweighed, and the subsequent gain in weight was divided by the volume filtered to yield the suspended solids concentration in mg/l.

Turbidity. Turbidity measurements were made using a Hach Model 2100 turbidimeter during Phase I and a Hach Model 2100 A during the remainder of the studies. Both turbidimeters have four ranges graduated in Formazin turbidity units (FTU). Formazin standards provided by the manufacturer were used to properly calibrate the instrument in each range. For the purpose of this study, only the 0 to 1, 0 to 10, and 0 to 100 FTU ranges were required. Glass cells were rinsed with distilled water before each use, and care was taken to dry the outside of each cell before inserting it into the instrument.

TOC and SOC. Total organic carbon (TOC) and soluble organic carbon (SOC) determinations were conducted on a Beckman Model 1R315 carbon analyzer using the tentative procedure outlined in Standard Methods [117]. Fifty-milliliter portions from the filter influent and effluent samples were transferred to small polyethylene bottles, treated with several drops of concentrated H<sub>2</sub>SO<sub>4</sub>, and then refrigerated until analysis. The depressed pH, as well as the refrigeration, retarded bacterial decomposition of the organic carbon present.

At the time of analysis, the containers were purged with nitrogen to eliminate carbonate and bicarbonate interferences (in conjunction with the acidification step). Samples of 25 µl size were analyzed in triplicate by comparison with acetic acid standards. Soluble organic carbon samples were filtered through Whatman GF/C glass fiber paper prior to analysis. The carbon analyzer was down for repairs for extended periods during the course of these measurements and the

acidified samples were held under refrigeration for long periods while repairs were made. This is a questionable procedure and thus the TOC and SOC results reported herein are not considered to be of uniform reliability.

BOD. Determinations of BOD and soluble BOD were conducted using a dilution technique as outlined in Standard Methods [117]. A container of primary effluent from the Ames Water Pollution Control Plant was supplied with each new set of samples for use in seeding the dilutions. Because of a misunderstanding between the laboratory and the research personnel, nitrification was not suppressed in the BOD analyses in Phases I and II. Nitrification was suppressed thereafter using "N-serve" from Hach Chemical Company. Soluble BOD samples were filtered through Whatman GF/C glass filter paper prior to analysis.

Other analyses. Procedures for the remaining three analyses were automated using a Technicon Autoanalyzer. Total Kjeldahl nitrogen, which included both organic and ammonia nitrogen, was conducted as described in Standard Methods [117]. The test differs from the classic Kjeldahl determination of organic nitrogen only in that ammonia is not removed from the sample before digestion and distillation. For use on the autoanalyzer a colorimetric technique using the tentative phenate method was employed for the final nitrogen measuring step of the procedure.

Both phosphate determinations were also conducted in accordance with procedures described in Standard Methods [117]. Orthophosphates were measured using the tentative ascorbic acid procedure, which involved a colorimetric determination preceded by filtration of the sample. The digestion step of the total phosphate analysis was modified by using both perchloric and sulfuric acids in the presence of a selenium acid catalyst to convert the various phosphate forms to orthophosphate. A colorimetric determination using the vanadomolybdo-phosphoric acid method was employed for final phosphate measurement in the autoanalyzer.

### Operation and Results - Phase I

#### Dual-Media Filtration of Alum-Treated

#### Secondary Effluent

Phase I was a comparison of two backwashing methods during the filtration of alum-treated secondary effluent. The alum treatment was to reduce the phosphorous level of the secondary effluent to about 1 mg/l phosphorous. Both filters were equipped with dual media. One was washed by water fluidization only. The other was washed with air scour followed by water fluidization, hereinafter referred to as air-scour auxiliary.

## Operation - Phase I

A filter run started with a backwashed filter and ended when the filter had operated for a cycle and had then been backwashed and was ready for service again. Filter runs were numbered consecutively starting with number 1. Since both filters were backwashed at the same time, and placed in service simultaneously, a particular run number refers to both filters.

The first filter run of Phase I started on May 17, 1973, and the last one using alum-treated water ended on August 21. The filters were operated continuously during this period except during equipment failures and when major maintenance work was needed. The filters did not operate for a total of about 1-1/2 weeks.

Solids contact unit. Commercial grade, granular alum (approximately  $\text{Al}_2(\text{SO}_4)_3 \cdot 14 \text{H}_2\text{O}$ , approximate molecular weight 600) was mixed at the rate of 37.8 g/l of water. This solution was fed to the erdlator to achieve an alum dosage of 200 mg/l when the erdlator was operating at 10 gpm. For runs 1 through 45, the first 7-1/2 weeks of operation, the erdlator operated at approximately 10 gpm, but for runs 46 through 57, the next 3-1/2 weeks, it was operated at 12 gpm and therefore the alum dosage was only 167 mg/l. For the last three weeks, after run 57, the erdlator was operated at approximately 15 gpm, and the alum feed was increased so that the dosage was 200 mg/l. The detention time in the upflow portion of the erdlator was 53 min at 10 gpm and 35 min at 15 gpm. The detention time in the center mixing column was 11 min at 10 gpm and 7 min at 15 gpm. The surface loading was 0.37 gpm/sq ft at 10 gpm and 0.56 gpm/sq ft at 15 gpm based on the area outside of the center column. Sludge was wasted at a rate of about 1 gpm.

The use of alum was discontinued after run 73, 13-1/2 weeks of operation. For another week, or eight filter runs, the trickling filter effluent flowed through the erdlator without any chemical treatment.

Filters. The filtration rates averaged 2 gpm/sq ft for runs 1 through 45 and for runs 59 and on. The filters were operated at 1.6 gpm/sq ft for runs 46 through 57.

After about 12 weeks, run number 65 for the south filter and run number 66 for the north filter, a layer of fine sand was skimmed from the top of the coal. This layer was removed to see what effect it was having on the development of head loss in the filters.

Backwash. A combination of time and head loss was used to determine when the filters were backwashed. If one of the filters approached the maximum available head loss of 7 ft, both filters were backwashed. Frequently the filters were backwashed after 24 hr of service even though neither filter was near the maximum head loss.

For runs 1 through 26, air scour was not used on either the north or the south filter. The backwash for run 27 consisted first of the normal water fluidization backwash. Samples of filter media were taken for the abrasion tests. Then the south filter was air scoured. Following the air scour, a second normal water backwash was conducted and waste washwater samples were collected at various intervals of time during the backwash. Another sample of media from the south filter was then taken. From run 27 to the end of Phase I (run 78), the north filter received water backwash only, while the south filter received air scour followed by water backwash.

After run 78, the very end of Phase I, a series of special backwashes was used in an effort to restore the filter media to a clean condition. After the normal backwash, the following procedures were used on both filters in the order given.

1. A normal air scour followed by a normal water backwash.
2. Simultaneous air and water backwash (as the water rose from the media to near the overflow) followed by a normal water backwash.
3. Step 1 repeated.
4. Step 2 repeated.
5. Step 2 repeated.

During each step samples of waste backwash water were composited for later analysis.

The normal water backwash procedure at any time was the same for both filters. For runs 1 through 28 a constant rate of 20 gpm/sq ft for 5 min was used. For runs 29 through 63, both filters were backwashed for 5 min at rates that expanded the beds 38 to 40%. The backwash rates to achieve these expansions changed from one backwash to another and varied between the two filters. Rates from 18 to 23.8 gpm/sq ft were required. After run 63, a constant backwash rate of 18.6 gpm/sq ft was adopted, again for a 5 min duration. Filter bed expansion then varied from 25 to 38%. When air scour was used, it consisted of 9 scfm [scfm (standard cubic foot per minute at 14.7 psi and 70 °F)] or 4 scfm/sq ft of air for 5 min.

The backwash procedure included the following details. The flow to both filters was stopped. Then effluent valves were closed, the valves to the composite samplers were closed, and the backwash waste drain valve was opened. If air scour was to be used, the effluent valve on that filter was left open until the water level had drained at least 1 ft below the backwash water outlet. This was to prevent loss of media due to the violent agitation caused by the air scour. After the air scour was terminated, the water wash was started at a very low rate until all of the trapped air had escaped. This usually

took 1 to 2 min. The filter was then backwashed with water. The backwash water inlet valve was gradually opened over a 20-sec period. The water backwash continued for 5 min, and then the inlet was closed over a 10-sec period. It was closed in as nearly as possible the same manner each time.

After both filters were backwashed, flow was started through them simultaneously. Piezometer readings and turbidity measurements were taken about 15 min later. This allowed time for head loss and flow to reach an equilibrium with each other. Also any backwash water left in the filter was flushed out by then.

Because the primary purpose of this study was to evaluate backwashing techniques, careful notes were recorded during the backwashing of each filter after every run. Bed expansion, backwash rate, air-scour rate (where applicable), surface washer line pressure, water temperature, and media heights before and after backwashing were noted for each filter. Comments concerning the condition of the bed before, during, and after cleaning were also recorded. The comments were particularly important because they contained information with respect to surface cake formation, cracks in the media, mud ball or agglomerate formations, and other unusual qualitative observations.

Maintenance. Periodic maintenance was required in various parts of the pilot plant to ensure proper operation and collection of meaningful data. Because the sewage being filtered was a rich source of nutrients and the pilot plant was constantly exposed to the sun, algal growths flourished if not properly controlled. To prevent algal growths from occurring in piezometer tubes and composite sampler lines, a 10 to 20-ml dose of 5% NaOCl (household bleach) was introduced to each line on a once weekly basis. After allowing a 15 to 20 min contact time, the lines were drained and thoroughly flushed.

Because the filter housings had plexiglass fronts, some means of controlling algal growths within the filter housing was necessary. To retard algal accumulations, therefore, removable 1/4-in. plywood covers were constructed to fit over the glass front of each filter housing and prevent the passage of sunlight.

Although the covers were effective in preventing algal growths within the filters, they could not prevent the accumulation of biological solids on the inside face of the plexiglass fronts. If left unattended, such growths became thick enough to prevent one from viewing the media. It was necessary to scrape the growths from the glass at least once a week using a rubber squeegee lowered into the 6-in. handhole in the top of each filter housing.

A particularly troublesome and persistent problem encountered was the clogging of the piezometer taps. This was probably caused by an accumulation of biological solids on the fine steel mesh soldered over

the internal end of each 1/4-in. copper tube. It was found that one could generally free the tap by fitting a filled water bottle, with stem removed, over the end of the tap and applying hand pressure. If this was unsuccessful, a length of 1/4-in. tubing was fitted to the tap and connected to the well hydrant.

Biological solids coated the surface of the influent rotameter tube and float. Solids accumulating on the float increased its drag, causing it to rise higher in the tube and give erroneously high readings. Daily cleaning was required to enable the meter to function properly, and this proved particularly inconvenient because of the construction of the rotameter. Therefore, at the end of Phase II the rotameter was removed from the flow scheme, and flows were monitored only after the flow splitter, as shown in Fig. 23, for all remaining phases of the study.

### Results - Phase I

Various parameters were used to compare the backwash effectiveness between the two filters. The most direct measurement was the abrasion test, which revealed the relative amount of solids left on the media after a backwash. Visual observations of the filter media through the transparent filter wall also directly indicated the effectiveness of the backwash. Indirect measures included the initial head loss of the filter media after backwash, the head loss development patterns and the filtrate quality. Excessively dirty filter media or the presence of agglomerates and mud balls should result in higher initial head losses, more rapid head loss development, shorter filter runs and potentially poorer filtrate quality. In addition, dirty filter media will alter the backwash rate required to achieve a particular degree of expansion. Coatings should reduce the effective density of the grains and reduce the required wash rate. Agglomerates will cause erratic behavior because portions of the bed may not fluidize above the agglomerates, and because part of the media is held in the agglomerate and is not free to be fluidized.

The observations related to these measures of backwash effectiveness are presented in the following paragraphs.

Visual observations. Small mud balls that appeared to be mixtures of sand, coal, and alum floc began forming during the first few filter runs. The mud balls started out on the surface of the coal. By the end of the sixth filter run and backwash, the mud balls had grown from 1/16 in. in diameter until 1/4 to 3/4-in. balls covered over 90% of the filter bed surface. Before run 10 some of the mud balls were up to 1-1/2 in. in diameter and had sunk into the coal layer. By the end of run 14 almost all of the mud balls had sunk into the coal and very few remained on the surface. A layer of fine sand had worked its way to the surface of the coal, presumably due to reduction of hydraulic subsiding velocity of the sand by the coatings which had developed on the sand grains.

Just before the air scour was used (run 27), both filters had large numbers of mud balls up to 3 in. in diameter at the sand-coal interface. The first use of air scour dramatically reduced the number of mud balls in the south filter, and the largest one left was 3/4 in. in diameter instead of 3 in. After the backwash for run 29, three backwashes after the first air scour, only one mud ball was observed in the south filter, while numerous mud balls up to 2 in. in diameter remained in the north filter. The layer of fine sand had also disappeared from the surface of the south filter.

Starting with the backwash for run 51, a layer of fine sand was once again noticed over the coal in the south filter. Also, a portion of the media near the plexiglass front did not easily fluidize in the water wash. However, only a few small mud balls were seen in the coal from then until the end of Phase I.

The north filter developed a heavy layer of fine sand over the coal. As the head loss increased during filter runs, large cracks up to 3/4-in. wide and several inches deep formed at the media surface. While most of the cracks extended along the filter walls, some smaller ones appeared toward the center of the media surface. The south filter had developed some cracks at the media surface, but they were much smaller and occurred less frequently than those in the north filter. After the fine sand was skimmed from above the coal, the cracks at the media surface stopped forming. However, another layer of fine sand soon worked its way to the top of the coal and the cracks at the surface of the north filter reappeared.

The sand used in the filters was somewhat small and undoubtedly contributed to the difficulties encountered in keeping the filter media clean and to the migration of fine sand to the surface. The use of a larger sand would have been better. Also, it should be recalled that for this experimental Phase I, the sand was not skimmed to remove fines, which may have contributed to the sand migration problem.

Abrasion tests. Figure 26 shows the amount of suspended solids released from the core samples of filter media as indicated by the abrasion test results. Two values are shown for the south filter at run 27 because the normal water fluidization backwash was followed by an air-scour assisted backwash as previously described. A core sample was taken after each backwash. The abrasion test results started out at about 4 mg/g and increased to 22 mg/g. The use of air scour greatly reduced the abrasion test results in the south filter where values dropped from over 11 mg/g at run 27 to less than 2 mg/g at run 34. After run 45, the abrasion test results for the south filter started to increase. The lines shown in Fig. 26 are least square fits using all of the values for the north filter and the values from runs 45 through 72 for the south filter.

The benefit of the air-scour auxiliary in cleaning the filter is clearly evident from the abrasion test data. However, the gradual

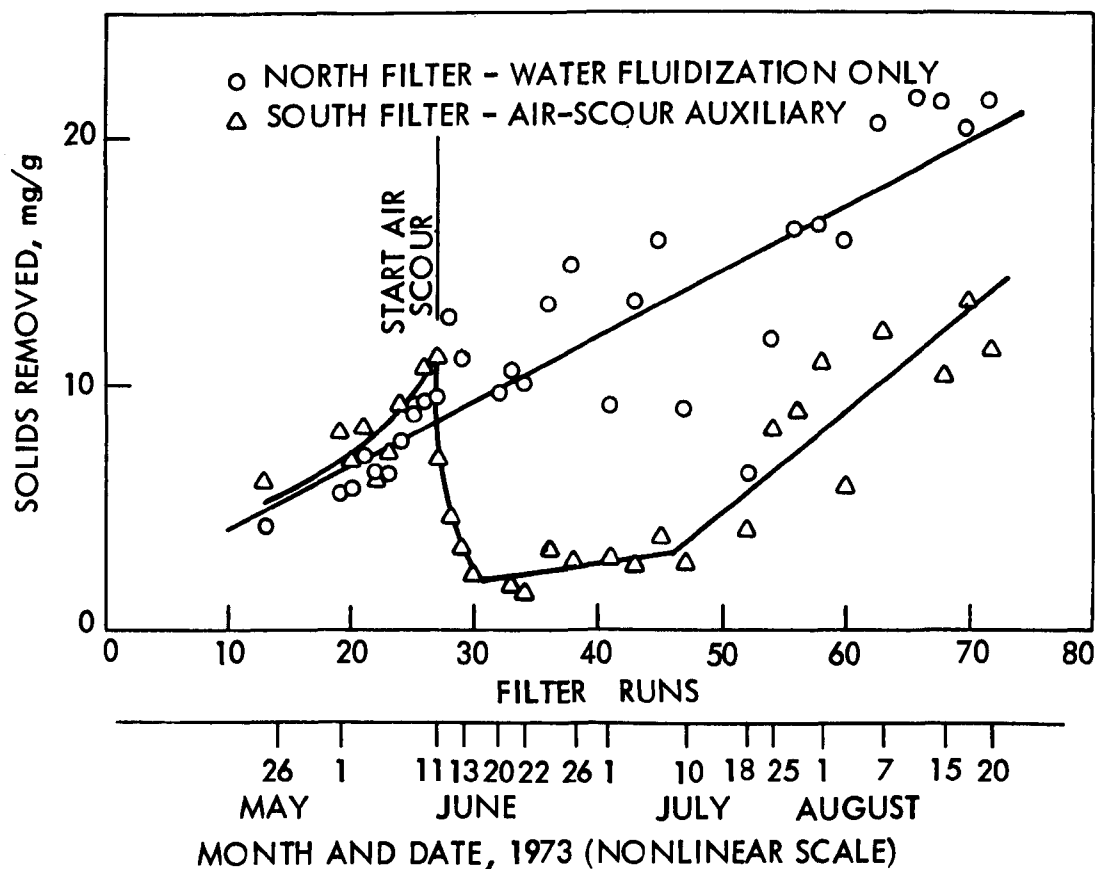


Fig. 26. Abrasion test when filtering secondary effluent treated with alum for phosphorus reduction in Phase I.

deterioration evident toward the end of Phase I indicates that even the air-scour auxiliary as used in this phase was not totally effective in keeping the media clean.

Initial head loss. As mud balls form, the volume of void space in the filter is reduced. This results in greater water velocities between the grains of filter media and therefore greater initial head losses. Therefore, an increase in initial head loss would indicate the accumulation of mud balls in a filter.

At the beginning of Phase I when both filters were clean, the initial head loss was 0.44 ft for both filters. Table 9 summarizes the means and standard deviations of the initial head losses for various periods of filter operation in Phase I. During the 3-1/2 weeks at the beginning of the project, the values of initial head loss progressively increased. In the week immediately preceding the start of air scour in the south filter (filter runs 22 through 27), the average initial head loss was 0.82 ft for the north filter and 0.80 ft for the south filter. The difference between the filters was negligible.

Table 9. Initial filter head losses during various portions of the study (ft of water).

Runs		N filter, water fluidization only	S filter, air-scour auxiliary
22-27	Mean	0.82	0.80
	Std. dev.	0.096	0.105
28-45	Mean	0.64	0.44
	Std. dev.	0.141	0.036
46-57 <sup>a</sup>	Mean	0.55	0.37
	Std. dev.	0.057	0.061
58-65	Mean	0.72	0.52
	Std. dev.	0.144	0.114
68-73	Mean	0.54	0.41
	Std. dev.	0.062	0.029

<sup>a</sup> During this period the flow rate was only 1.6 gpm/sq ft instead of 2 gpm/sq ft as for the other periods.

After the south filter was backwashed using air as auxiliary agitation, the initial head loss on the following filter run dropped nearly to that observed at the very beginning of the project. In the next 3-1/2 weeks, the initial head loss for runs 28 through 45 averaged 0.64 ft for the north filter and 0.44 ft for the south filter. From the eleventh week of operation through the twelfth week of operation the initial head losses for both filters increased. For these eight runs, 58 through 65, the north filter averaged 0.72 ft and the south filter averaged 0.52 ft. By this time a quantity of fine sand had worked its way to the top of the coal layer. It was felt that this fine sand was adversely affecting the head loss characteristics of the filters, therefore, it was skimmed out of the filters. Not surprisingly, the initial head losses for both filters decreased. For the next six runs, 68 through 73, the north filter averaged 0.54 ft and the south filter averaged 0.41 ft of initial head loss. The initial head losses in the filters after skimming out the fine sand should not necessarily be the same as the initial head losses at the beginning of the experimental work because the media characteristics were changed somewhat by the skimming operation.

The initial head loss data above supports the visual and abrasion test observations. The benefit of the air-scour auxiliary compared to water fluidization only is clearly demonstrated. However, a slight deterioration is evident in the south filter, even with the air-scour auxiliary.

Head loss development. Before the use of air scour was started, the head loss in each filter was similar with respect to time and to

depth in the filter. Figure 27 shows typical head loss versus time curves for various intervals of media depth, measured from zero depth at the top surface of the media.

After air scour was begun on the south filter, it developed head loss at a slower rate than the north filter. Figure 28 is a typical example. During the two weeks following the beginning of the air scour (runs 28 through 44), the filters were generally backwashed before they reached 4 ft of head loss. Later they were operated to higher head losses. Starting with run 45, terminal head losses for both filters were about equal, with the south filter frequently having a slightly greater head loss. This was particularly true when higher head losses were reached. Figures 29 and 30 are typical examples. After run 65, 8-1/2 weeks after air scour was started, the layer of fine sand that had worked its way into the coal was removed from the filters. Figure 31 shows a typical curve of head loss versus time after the fine sand was removed.

The effect of the air-scour auxiliary on head loss patterns is clouded by the variable extent of surface cracks in the filters. If surface cracks were absent and mud balls were present, the dirtiest filter should have the highest rate of head loss development. A higher rate of head loss development for the dirtier north filter was not consistently observed in this Phase. This anomaly is explained as follows.

During the first four weeks after air scour was started, the filter runs were generally terminated when the head loss reached only 3 or 4 ft. It was then observed that, at greater head losses, the head loss in the south filter would approach and even surpass that in the north filter. This was attributed to the fact that the north filter experienced more extensive surface cracking during the filter runs. These cracks allowed the surface to be bypassed and solids removal to take place in deeper layers of the filter. The head losses shown in Figures 29 and 30 clearly indicate that most of the removal in the south filter took place in the top 4 in. of the media, while in the north filter the removal took place over the upper 8 in. This indicates that the greater head loss in the south filter on some occasions was not due to accumulated dirt, but was rather due to the fact that the dirtier media in the north filter resulted in more extensive surface crack formation.

Backwash rates required. For runs 31 through 63, both filters were backwashed to a constant expansion of 38 to 40% and the backwash rate needed to achieve this was recorded. For runs 31 through 49 the north filter required an average of 19.4 gpm/sq ft, and the south filter required an average of 22.2 gpm/sq ft. For runs 51 through 61 the required backwash rates were 19.7 gpm/sq ft for the north filter and 20.0 gpm/sq ft for the south filter. Table 10 lists the means and standard deviations of the backwash rates of the filters for the

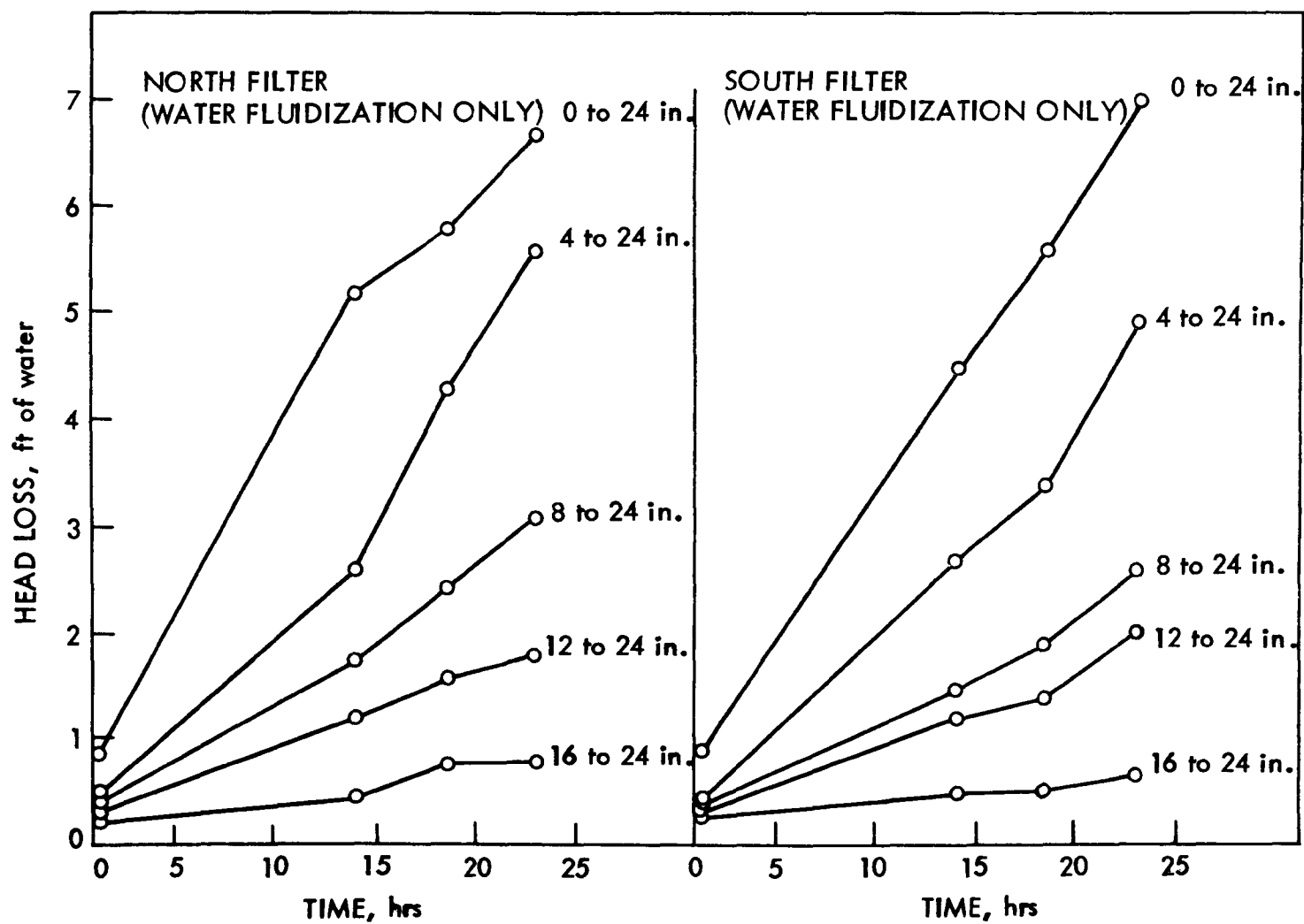


Fig. 27. Head loss vs time at various media depths, run 27.

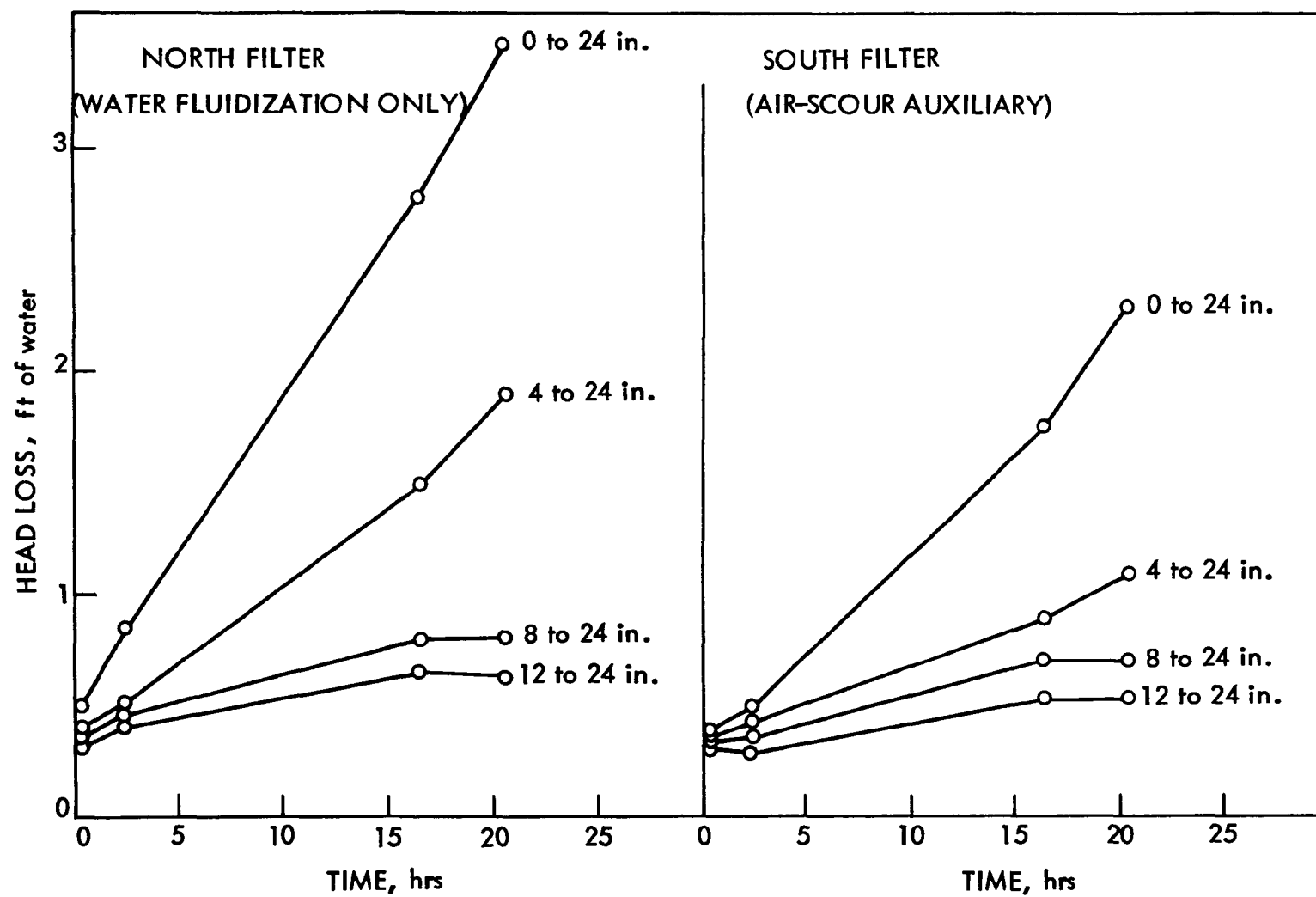


Fig. 28. Head loss vs time at various media depths, run 42.

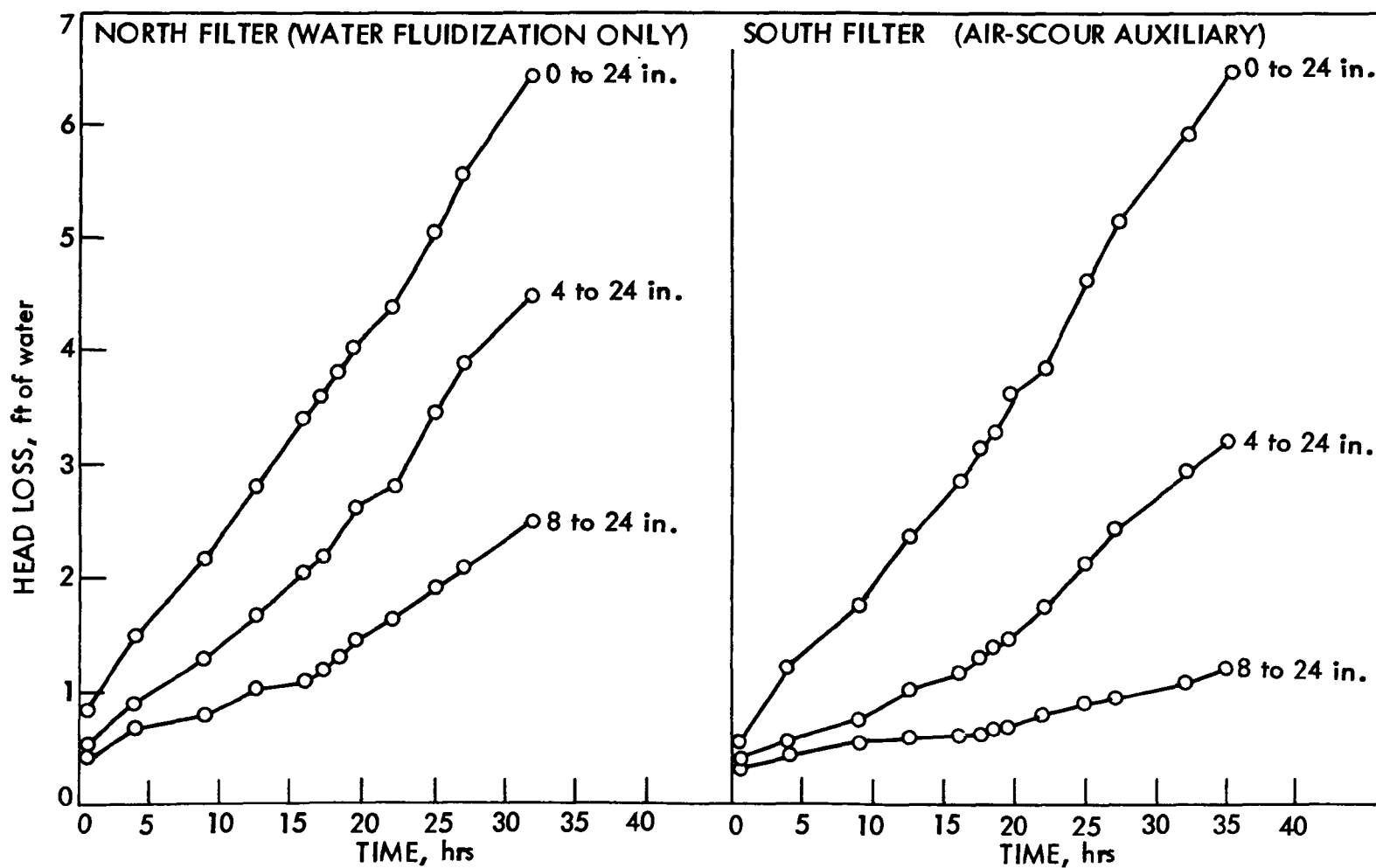


Fig. 29. Head loss vs time at various media depths, run 59.

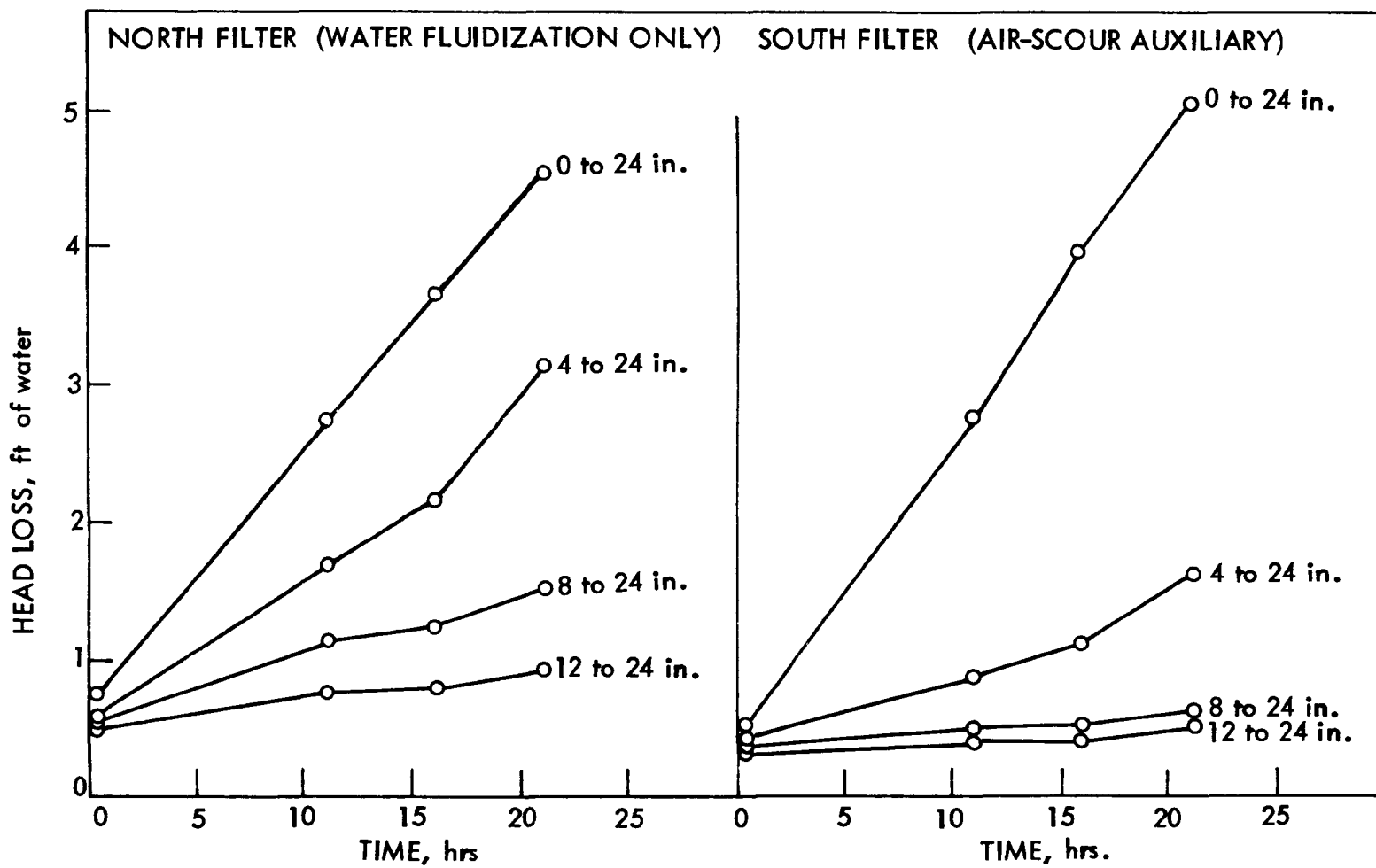


Fig. 30. Head loss vs time at various media depths, run 63.

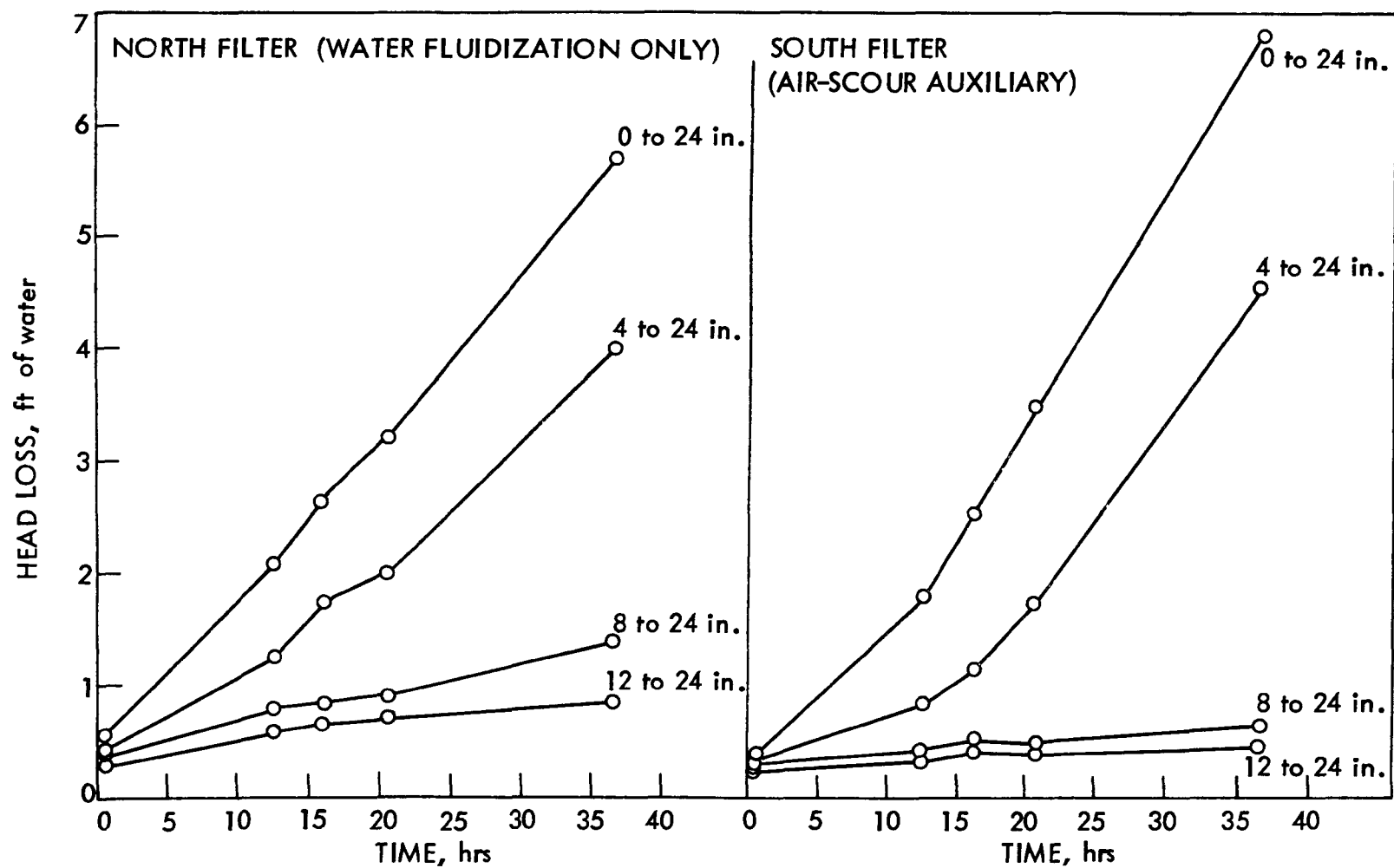


Fig. 31. Head loss vs time at various media depths, run 71.

Table 10. Backwash rates required to achieve 38 to 40% bed expansion (gpm/sq ft).

Runs		N filter, water fluidization only	S filter, air-scour auxiliary
31-49	Mean	19.4	22.2
	Std. dev.	0.88	0.80
50-61	Mean	19.7	20.0
	Std. dev.	1.85	1.07

two periods. The backwash temperature averaged 22.9 °C for runs 31 through 49 and 23.1 °C for runs 50 through 61.

The data presented support the other observations concerning the cleanliness of the filter media. Shortly after initiation of air scour, the media of the south filter was cleaner and thus had a higher average density than the north filter. The higher density required a higher backwash rate to achieve a given expansion. Later, as coatings developed on the air-scoured media, the average density decreased and the required backwash rate decreased. Thus, the results of Table 10 are in harmony with the abrasion test results and initial head loss results. All three tests demonstrate the superiority of air-scour auxiliary over water fluidization alone, but all three also indicate some deterioration of the air-scoured filter towards the end of Phase I.

Water quality. The means and standard deviations of the various water quality parameters are given in Tables 11 and 12. Results for each parameter were divided into two periods. The first period (Table 11) covers the initial 3-1/2 weeks of filter operation when both filters were backwashed by water fluidization only. The second period (Table 12) covers the remaining 8-1/2 weeks of filter operation when the south filter received air-scour auxiliary. Except for turbidity, the values for the solids contact unit influent may not be used to calculate actual removals through the treatment process. Samples of influent to the solids contact unit were grab samples, while the other samples were composited over approximately one day. All of the turbidity measurements were made on grab samples taken at approximately the same times for each point in the treatment process.

From the data on filter effluent quality, no apparent differences are evident between the two filters. One would expect the dirtier filter to yield poorer filtrate due to surface cracks permitting deeper penetration of solids, and due to higher interstitial velocities caused by mud balls and agglomerates. The absence of detriment to filtrate quality in this work must be attributed to the fine grain size of the media, the low filtration rates and the low terminal head

Table 11. Results of analyses during alum treatment (Phase I) for samples from May 17 to July 11, 1973, when both filters were washed by water fluidization only. (All results from composite samples except solids contact influent.)

	Solids contact influent	Filter influent	Filter effluent	
			N filter, water fluidization only	S filter, air-scour auxiliary
Avg suspended solids (mg/l)	51.1	11.90	1.18	1.12
$\sigma^a$ (N = 16)	40.5	8.74	1.24	0.88
Avg turbidity (FTU) <sup>b</sup>	10.0	2.86	0.77	0.77
$\sigma^a$ (N = 55)	3.4	1.68	0.67	0.71
Avg BOD <sub>5</sub> <sup>c</sup> (mg/l)	31.4	10.05	3.12	4.14
$\sigma^a$ (N = 13)	7.2	6.38	2.21	2.21
Avg TOC (mg/l)	19.7	8.19	5.69	6.43
$\sigma^a$ (N = 15)	9.0	1.58	1.60	2.34
Avg total PO <sub>4</sub> (mg/l)	12.1	4.18	1.55	1.43
$\sigma^a$ (N = 8)	2.2	4.00	1.47	1.45
Avg ortho PO <sub>4</sub> (mg/l)	12.0	1.31	0.94	0.87
$\sigma^a$ (N = 10)	1.6	1.07	1.04	0.86
Avg total Kjeldahl N (mg/l)	4.6	4.86	5.26	5.26
$\sigma^a$ (N = 13)	2.8	1.84	2.50	2.56

<sup>a</sup> $\sigma$  = standard deviation; N = number of observations averaged.

<sup>b</sup>Units = formazin units in accord with Standard Methods procedure.

<sup>c</sup>Nitrification not suppressed in BOD test.

Table 12. Results of analyses during alum treatment series (Phase I) for samples from July 11 to August 20, 1973, when air scour was being used on the south filter. (All results from composite samples except solids contact influent.)

	Solids contact influent	Filter influent	Filter effluent	
			N filter, water fluidization only	S filter, air-scour auxiliary
Avg suspended solids (mg/l)	25.4	10.32	1.17	1.37
$\sigma^a$ (N = 41)	15.3	5.68	0.90	0.74
Avg turbidity (FTU) <sup>b</sup>	10.9	2.35	0.69	0.67
$\sigma$ (N = 207)	7.4	1.23	0.67	0.44
Avg BOD <sub>5</sub> <sup>c</sup> (mg/l)	38.6	10.80	4.80	5.29
$\sigma$ (N = 14)	17.5	5.43	2.70	3.17
Avg TOC (mg/l)	14.0	7.59	6.90	7.01
$\sigma$ (N = 50)	8.3	2.77	2.20	2.20
Avg total PO <sub>4</sub> (mg/l)	19.3	3.91	2.62	2.33
$\sigma$ (N = 16)	3.6	1.91	1.51	1.44
Avg ortho PO <sub>4</sub> (mg/l)	18.7	2.39	1.28	1.24
$\sigma$ (N = 6)	3.03	2.36	1.28	1.22
Avg total Kjeldahl N (mg/l)	4.9	4.93	5.60	5.41
$\sigma$ (N = 20)	3.4	2.44	2.47	2.38

<sup>a</sup>  $\sigma$  = standard deviation; N = number of observations averaged.

<sup>b</sup> Units = formazin units in accord with Standard Methods procedure.

<sup>c</sup> Nitrification not suppressed in BOD test.

losses. Had one or more of these filtration variables been increased, the detriment may have occurred.

Statistical comparisons to determine differences in the effect of backwashing on filter performance efficiency between the filters are not reported since a proper statistical base did not exist in this experimental study. Since the filter media was not returned to exactly the same condition following each backwash, the individual runs on a filter cannot be considered independent, which is a fundamental assumption in statistical theory. Because it was desired to determine the cumulative effects of the various backwashing methods over a period of continuous operation of the filters, it was not practical to thoroughly restore the media after each filter run, and it was equally impractical to replace it. The minimum effort alternative for the application of statistical comparisons would be to run at least two separate eight-week studies using identical media, switching the backwashing techniques on each housing, and replacing or completely restoring the media at the end of each eight-week series. Time and expense considerations precluded the additional study, so no base exists for making statistical inferences.

Clean up operations at the end of Phase I. The results of the suspended solids concentrations versus quantity of backwash water for the first backwash following the use of air scour (run 27) are shown in Fig. 32. Since a normal backwash using only water fluidization immediately preceded this backwash, the area under the curve represents the additional suspended solids released by the first air scour. The suspended solids removed by the air scour was 109.6 g per sq ft of filter area. If the suspended solids are assumed to come from a 12-in. layer of coal and a 1-in. thick layer of sand, 4.13 mg suspended solids were removed per gram of filter media.

The amounts of suspended solids released from the filter media in the final cleanup operations after run 78 are shown in Table 13. Based on the same amount of filter media as was assumed before, 13.3 and 3.2 mg of suspended solids were released per gram of media for the north and south filters respectively. All mud balls were broken up during the cleanup operation. The series of cleanup steps was continued until the media appeared to be in new condition and the last step appeared to release very few additional solids. The substantial difference in total suspended solids released clearly shows that the south filter which had routinely been washed with air-scour auxiliary was in much cleaner condition than the north filter. It should be borne in mind that this final cleanup operation came after a week of filtering uncoagulated trickling filter effluent at the end of the alum treatment series.

#### Summary and Conclusions - Phase I

The objectives of this phase were to evaluate the effectiveness of filter cleaning by water fluidization backwash alone as compared to

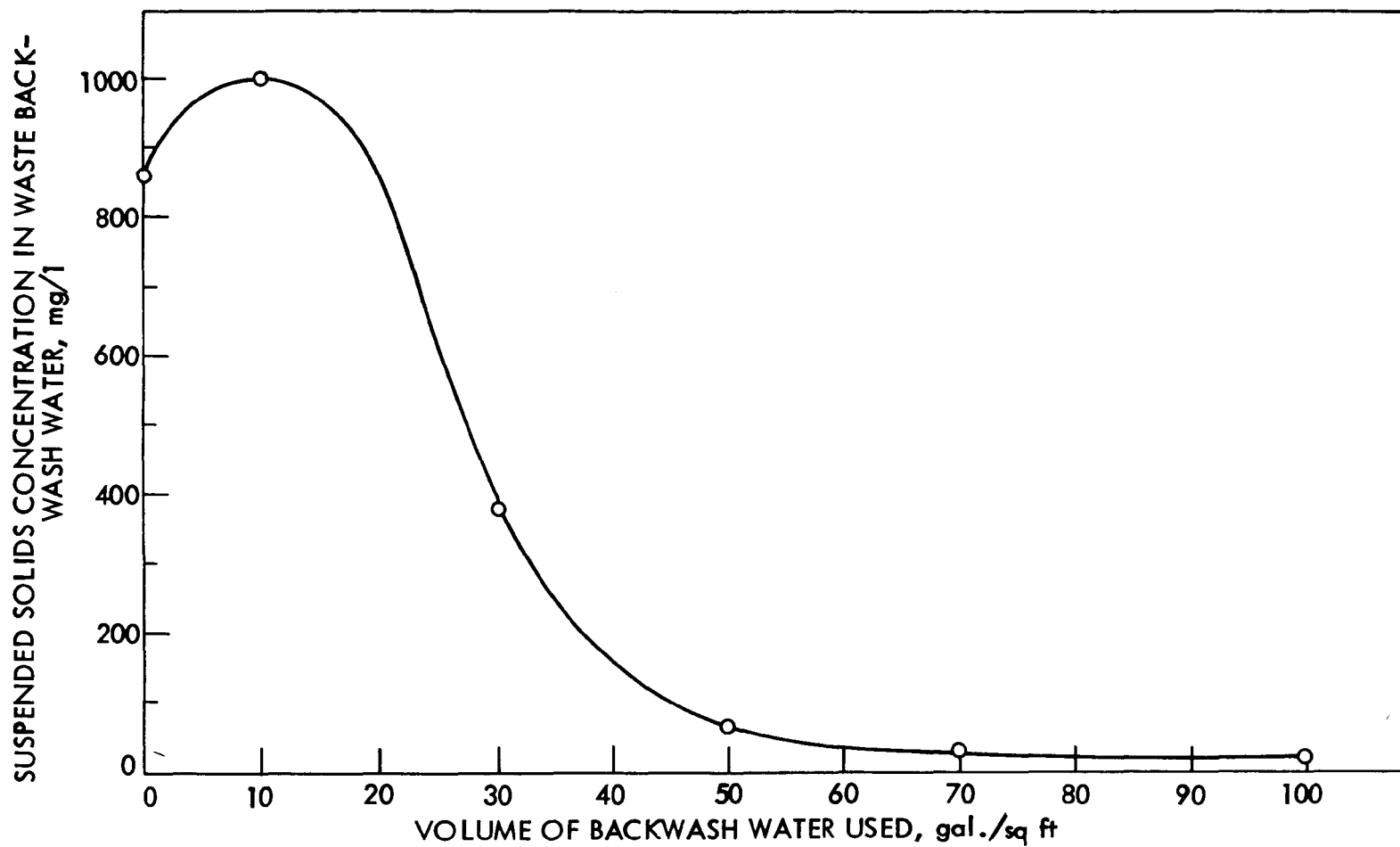


Fig. 32. Suspended solids concentration of backwash water vs quantity of backwash water used, run 27, second backwash of the south filter immediately following the first application of air scour.

Table 13. Suspended solids released from filters in special backwashes after run 78.

Backwash used	g of SS removed/sq ft of filter area	
	North filter	South filter
Air followed by water	87	37.3
Air and water combination	144	28.2
Air followed by water	57.5	— <sup>a</sup>
Air and water combination	47	14.4
Air and water combination	<u>28.2<sup>b</sup></u>	<u>8.5</u>
Total	393.7	88.4

<sup>a</sup> Step omitted.

<sup>b</sup> Backwash conducted but no suspended solids value obtained therefore, the value indicated is based on the comparison of turbidity with the other samples.

air scour followed by water fluidization backwash, and to compare the performance and operation of filters backwashed by these methods when filtering wastewater. For this study two dual-media filters were used following alum treatment of domestic wastewater for phosphate removal. One filter used air scour followed by water backwash, while the other used water fluidization backwash alone.

The media in the filter backwashed with water only became very dirty, while the media in the filter with air scour during backwash was much cleaner. However, toward the end of the project, the media in the air-scoured filter also showed some deterioration. Few mud balls were observed in the air-scoured filter while numerous, large mud balls were observed in the other filter. When operated at only 3 to 4 ft of head loss the filter backwashed with water only had greater head losses than the filter with air scour. When operated to greater head losses this was not true due to the formation of surface cracks in the filter receiving water backwash alone. Little difference in effluent quality was observed between the two filters.

The study of the filtration of domestic wastewater which had been subjected to secondary treatment and subsequent alum treatment for phosphate reduction leads to the following conclusions concerning backwashing:

1. Filter media were kept cleaner by air scour than by water fluidization backwash alone as evidenced by the results of visual

observations, media abrasion tests, initial head losses, backwash flow requirements, and the final cleanup operation.

2. Some minor deterioration of the condition of the media of the air-scoured filter was evident toward the end of this experimental phase as evidenced by the results of the media abrasion test, initial head losses and backwash flow requirements.
3. Air scour prevented the formation of mud balls, while water backwash alone did not.
4. The two methods of cleaning resulted in little difference in effluent quality. The use of a coarser filter media, a higher filtration rate, or higher terminal head loss may have demonstrated that a cleaner media would give better filtrate quality.
5. The sand used in the experimental filters was smaller than desirable (0.38-mm effective size) and was not skimmed of fines on placement. This contributed to backwashing difficulty and sand migration to the surface of the coal of the dual-media filters.

#### Operation and Results - Phase II

##### Dual-Media Filtration of Secondary Effluent

Phase II was a comparison of three methods of backwashing during the direct filtration of secondary effluent at the Ames, Iowa, trickling filter plant. All three filters were equipped with dual media. One was washed by water fluidization only. The second was washed by air scour followed by water fluidization, hereinafter referred to as air-scour auxiliary. The third was washed with a rotary surface wash auxiliary which operated before and during the water fluidization backwash.

Prior to commencing Phase II, the west filter with surface wash auxiliary was installed and new filter media was installed in all three filters. This was done to ensure that Phase II would not be influenced by any carry-over effects from Phase I.

#### Operation - Phase II

The secondary effluent of the Ames trickling filter plant was pumped directly to the influent splitter box and thus became the filter influent as illustrated in Fig. 23.

Filters. Because it was desired to observe the effects of continuous operation on filter efficiency, the pilot plant was operated without major interruptions from August 28 to October 30, 1973. The entire series of runs was designated Phase II, with individual runs being numbered consecutively from 1 to 64. Normal procedure dictated one

observation run per week at which time the head loss development, influent and effluent turbidities, and flow temperature were monitored, and composite samples were collected. During the remaining runs of a given week, only initial readings immediately following backwashing were recorded. The backwashing observations outlined in Phase I were recorded for each backwash.

When the series was begun it was hoped to be able to operate the filters at a loading rate of 2 gpm/sq ft. Piping losses and solids accumulations in the lines gradually reduced this figure as operating time increased to 1.6 gpm/sq ft near the end of Phase II. Even though the rate declined gradually, the flow split to the three filters was equal, so that valid comparisons between the filters are possible.

Backwashing. Ordinarily one would backwash filters when the head loss had reached some maximum permissible value or on a time cycle prior to attainment of the maximum permissible head loss. Neither of these procedures was deemed practical during Phase II because the runs were quite short and too much operational time would be required. Typically, the filters required approximately 10 to 12 hr to attain maximum head loss (point of incipient bypass in the splitter box). Furthermore, divergence in run lengths was expected to become more pronounced as operation time increased. Therefore, a schedule was adopted whereby the filters were backwashed and placed in service each morning as a group. This meant that by late evening the filters had begun to bypass through the lower half of the splitter box and that by the next morning nearly all of the influent was being bypassed.

Although each of the filters was backwashed using a different technique, all three filters required similar initial preparations as described previously in the Phase I operational discussion.

A nominal water fluidization backwash rate of 20 gpm/sq ft was selected for use on all three filters, this value being an upper limit for normal backwashing of filters used in water treatment. The rate was easily obtained during the first 20 runs, but after that the attainable rate decreased, presumably due to solids accumulations in the backwash lines and partially clogged underdrain strainers. From run 21 on the rates varied from 18.5 to 20 gpm/sq ft, with a preponderance of values in the 19.0 to 19.5 gpm/sq ft range. Attempts to clean the distribution nozzles were not made because to do so would have required all media to be removed from the filter housing.

Backwashing of the north filter consisted of a water fluidization (only) backwash at the 20 gpm/sq ft rate for a duration of 5 min and was not preceded by air scour or surface wash. Bed expansion during fluidization varied from a low of 8.3% to a high of 37.5%, with an average value of 25.6%. The slightly reduced backwash rates had no noticeable influence on bed expansion, which appeared to be

more a function of bed condition, i.e., number of mud balls and agglomerates.

The south filter was subjected to air scouring at a rate of 3.72 scfm/sq ft for 5 min prior to the water (only) backwash. Before the air line valve to the filter was opened, the filter was drained down through the effluent line until the water level was 6 in. below the backwash water collection trough. This prevented the loss of media out the backwash waste line. By run 36 this procedure had proved unsatisfactory because a surface coating formed on the anthracite which made draining the water above the filter nearly impossible. More importantly, the filter itself was draining below the surface cake, causing a negative head condition in the interior of the media. This caused air to be drawn in through the piezometer tubes, which air bound the filter and impaired the air-scour agitation. To combat these difficulties in subsequent backwashes, the procedure was altered by first "bumping" the bed with a short, low volume application of air. This practice broke the surface layer of the media sufficiently to allow proper draining without negative head development, after which the air scour could proceed in the normal fashion.

Upon completion of the air scour, the air line valve was closed and the backwash line valve opened to a rate of 20 gpm/sq ft for a total duration of 5 min. Expansion for the south filter ranged from 25.5 to 42.6%, with an average value of 34.0%.

The west filter backwashing procedure was initiated with a 2-min solo operation of the rotating surface washer. Next the 20 gpm/sq ft water backwash rate was applied to the filter and was operated in combination with the surface washer for a total of 3 min. Finally, the surface washer was shut off and the water (only) backwash was continued at the initial rate for an additional 2 min so that both the surface wash and water backwash were operated for 5 min each. Expansion of the west filter during the water fluidization (only) phase ranged from 25% to 50%, with an average value of 37.4%.

Sampling procedures and data collection. The frequency of observation runs in Phase II was less than in Phase I to reduce budget expenditures. Observation runs in Phase II were conducted once weekly and consisted of a careful monitoring of performance parameters throughout the duration of the run. Flow rates, influent and effluent turbidities, flow temperatures, and head loss development were monitored at 1 to 2-hr intervals. Prior to the beginning of each observation run the normal maintenance, described in a later section, was performed to ensure the collection of meaningful data. The automatic composite samplers were also turned on and checked before placing the discharge lines into refrigerated sample receivers. At the conclusion of each observation run, core samples were collected for the abrasion tests and influent and effluent composite samples collected for laboratory analyses.

In all cases the filter effluent samples were composited for the duration of the filter observation run. However, for the first six observational runs (2, 14, 22, 29, 36, 43) the composite samplers were left on for the entire 24-hr period even though the filters began to bypass after about 12 hr. Because it was thought that this procedure may have generated misleading data, the routine was changed for the last two observation runs so that each composite sampler was shut off when the filter first started to bypass.

Filter influent samples were not composited for the majority of the runs because filter performance was not considered a prime objective of the research, and because adapting the available sampler to the pilot plant posed some difficulties which were not solved until later in Phase II. A grab sample was taken at the conclusion of each observation run for numbers 14, 22, 29, 36, 43. Admittedly, this was a weak procedure, even for a parameter of secondary importance, but the influent data were, fortunately, later obtained from the log sheets of the Ames Water Pollution Control Plant (composite samples). For the final two observational runs the filter influent was automatically composited, and the sampler was shut off after the last filter began to bypass. The influent was also composited during the first observation run (run 2), which occurred while the influent was still being pumped through the erdlator of the mobile water purification unit used in Phase I. This practice was discontinued after run 3 of Phase II. Although the influent was composited over the entire 24-hr period during observation run 2, no unusual differences were noted between the sample analyses of this run and the last two runs.

Other details of sampling, data collection, and maintenance were identical with Phase I.

## Results - Phase II

Visual observations. Although the condition of the media varied substantially among the three filters, certain characteristics were common to all three. One common trait, the accumulation of mud balls and agglomerates, was a problem encountered in varying degrees throughout the study. Because of the downflow configuration of the filters and the relatively small particle size of the anthracite, the majority of the suspended solids removal took place in the uppermost 4 to 6 in. on the anthracite layer. As each run progressed, the solids in the influent filled the interstices of this upper layer and simultaneously compressed the layer into a tightly packed mat as the head loss across the layer increased.

Because of the biological nature of the influent solids and the adsorptive properties of the anthracite, the particles of media in the matted layer were bound tenaciously together, forming a plug at the surface which required violent agitation for its complete disintegration. Since this was not always accomplished by a given backwash technique or within a given backwash cycle, the matted layer was more

often split into fragments which descended to the sand-coal interface during fluidization and were then designated as mud balls as they floated at the interface of the fluidized bed. Those fragments which affixed themselves to the sides of the filter housing were designated as agglomerates. Nomenclature aside, all fragments observed during fluidization were spawned from the matted layer as a direct result of the overall ineffectiveness of the backwash technique being used.

When present in sufficient concentrations, the mud balls and agglomerates caused similar types of problems, in varying degrees of severity, in all three filters. If not broken up by the preceding backwash cycle, these accumulations shortened filter runs by increasing the initial head loss and reducing interstitial volume of the bed available for subsequent solids removal. During the backwash cycles, the mud balls and agglomerates prevented uniform distribution of water or air and forced them to form high velocity jets or streams. Because of this channeling effect, areas of poor fluidization developed above the fragments which reduced the effectiveness of the wash and created conditions favorable for the formation of additional mud balls.

Not once in the course of this study were mud balls observed to have originated in the sand layer of any of the filters. All were composed originally of anthracite and solids trapped during the course of the filter run, and were formed as previously described. Sand was observed in some of the mud balls and agglomerates, but this was caused by the jets of water which tended to lift the sand high into the coal layer where it became trapped.

Surface layers of solids on the very top of the media were observed frequently on all the filters just prior to backwashing.

Surface cracking was observed in all three filters but was most pronounced and sustained in the north filter. Cracks in the north filter were generally 1/4-in. wide, 3 to 7-in. long, and usually appeared to result from the media pulling away from the filter walls as the bed compressed. More severe cracking in the north filter was observed on three occasions when the cracks were from 1/4 to 1/2-in. wide and extended the full 18-in. width of the filter. Surface cracks in the south filter were less severe and less frequent than those in the north filter. Slight cracking, usually 1/16-in. wide and 1 to 2-in. long, was noticed, but only about one-third as often as in the north filter. The west filter was essentially free of surface cracks throughout the study.

Dead spaces were observed at the bottom center of the sand layer in each filter. The sand in this location, between two outside adjacent underdrain distribution strainers, did not fluidize during the backwash. No difficulties were encountered as a result of this.

Visual observations - north filter. Because of the relative ineffectiveness of the water fluidization (only) backwash, the accumulation of mud balls and agglomerates in the north filter was rapid and sustained. During the backwashing cycle of the first five filter runs, the mud balls observed ranged in size from about 2 to 6 in. in diameter and appeared in number of about 10 to 20. By the end of the fifteenth run, however, the size and concentration of the mud balls and agglomerates had increased to the extent that fluidization and stratification during backwashing did little more than shuffle and shift the mud balls slightly. Actual cleaning of the media was virtually halted. From run 16 until the completion of the study, mud balls and agglomerates consistently composed 50 to 70% of the volume of the anthracite layer visible at the window of the filter. Typical comments as recorded in the data book are presented below for runs 17 and 50, respectively.

Heavy surface coating. No cracking. 4-in. penetration into bed. Large mud ball at start 18 in. x 8 in. (almost entire coal layer). Smaller mudballing also present. Bed poorly stratified.

1/4-in. cracks, length of glass, heavy surface coating. Intermixing and agglomerates 70-80% of bed. Fluidization poor, huge agglomerates - 24 in. x 6 in. x 8 in., and 6-12 in. diameter - causing jets and intermixing. Large agglomerate is only 3 in. from bottom of filter. Bed essentially intermixed - agglomerates did not break.

Occasionally the concentration of mud balls and agglomerates was even higher although this higher level (80 to 90%) was not sustained for any length of time. The complete clogging of the media was probably prevented in part by anaerobic decomposition within the large masses in the filter. The distinct odor of hydrogen sulfide was detected frequently while backwashing the filter and lent some qualitative support to this possibility.

On 10 occasions (runs 14, 17, 21, 39, 49, 51, 53, 56, 60, and 62), the weakness of water (only) backwashing technique as applied to sewage filters was dramatically demonstrated. When the backwash water was applied to the media, the entire matted layer, a block 18-in. square and 4 to 6-in. deep, rose as a plug in the filter housing. Three times (run 14, 49, 62) the water backwash failed to break the layer (even slightly), and it settled as one large mass to the sand-coal interface. In the remaining instances the matted layer was broken into large chunks which formed mud balls or agglomerates.

Although the high concentration of mud balls and agglomerates in the north filter had no apparent effect upon the quality of the filtrate,

it did cause the most severe instances of high initial head loss and shortened runs. Initial head loss readings averaged nearly 1 ft greater than those observed for the other two filters, and filter runs were noticeably shorter as will be shown later. The large, solid masses often covered one-half to two-thirds of the bed width and caused the backwash water to channel and to lift sand high into the anthracite layer where it became trapped. Dead areas occurred above the mud ball layers and the unequal distribution of backwash water left the media mounded and piled after the backwash. Fluidization of free media was poor, and stratification of the coal and sand layers became virtually non-attainable. Frequently, large gaps and holes were left around the mud balls and agglomerates after the wash which failed to fill in with filter media.

Visual observations - south filter. The media of this filter underwent a series of significant changes throughout the course of this investigation. Through run 5 the build up of mud balls and agglomerates in the bed had been minimal, roughly a half dozen mud balls were observed during each backwash ranging in size from 1 to 2 in. in diameter. During this initial period the 5-min air scour appeared to be thoroughly breaking up the matted layer and intermixing the sand and coal layers. Air-scour agitation was most pronounced during the first minute, during which time layers intermixed. The bed quickly subsided to a steady, pulsing action, primarily at the surface, for the remainder of the scour.

Starting with run 6, however, much larger mud balls and agglomerates began to appear during the backwash. While the bed was being fluidized these large chunks settled to the sand-coal interface and channeled the backwash water to the sides of the housing. As it had in the north filter, the channeling action caused sand to be carried and trapped in the upper anthracite layer. Additionally, the effectiveness of the air scour had decreased markedly, and the air appeared to agitate only the top 1 to 2 in. of the anthracite. The air-scour agitation was carefully observed during the backwash following run 10. The air was channeled readily through the media instead of being uniformly dispersed, and the bed as a whole exhibited a gelatinous or cohesive character. By the end of the air scour the agitation had usually begun to be most effective, eroding a small portion of the bed and piling it on the surface. Even more perplexing, the media fluidized and stratified fairly well following the seemingly ineffective scour.

Compared to results obtained from Phase I on alum-treated, secondary effluents, the air-scour agitation results were quite poor. Initially this was attributed to the much higher solids loading on the filter, but a slight procedural change in the backwash cycle of run 36 proved otherwise. Until this particular run, the procedure had been to lower the water level 6 in. below the washwater trough to prevent media loss. Because of the highly clogged nature of the upper anthracite layer, this was a relatively slow process, so the procedure was

altered for run 37. During this backwash cycle the water level was not lowered below the overflow weir, and the air was applied at the standard rate. The results were surprising because the air scour suddenly regained its past effectiveness. The matted surface layer was effectively broken up as was a very large 4 by 18-in. agglomerate at the interface. Furthermore, the sand and coal thoroughly intermixed during the air scour and then stratified excellently during fluidization of the bed.

A subsequent investigation revealed the reason for the poor air agitation during the previous 26 backwashes of the south filter. Both the surface coal and the matted anthracite layer severely restricted the ability of the bed to drain the water above, as evidenced by the long period required to do so. This caused the water within the media below the matted layer to drain faster than the water above could pass through the mat. Therefore, a negative head condition occurred in the filter which, in turn, drew air into the bed through the piezometer taps. The entrained air tended to bind the filter media, causing it to appear gelatinous and to resist break up by the air agitation.

A simple procedural alteration was incorporated in the south filter backwashing sequence for subsequent runs. Before draining the media, the bed was subjected to a short, low volume application of air to break up the compressed surface layer. This allowed the filter to drain freely without inducing negative head and air binding of the media.

Immediately following the procedural change, the condition of the bed improved with respect to mud ball and agglomerate concentration. However, smaller 2 to 3-in. diameter mud balls began to accumulate and cause backwash water distribution problems during runs 39 and 40, although these were quickly dispersed and reduced in number by run 41. The next 20 runs were characterized by relatively few mud balls, but were hampered by an inability of the air agitation to completely disintegrate the upper clogged layer in the anthracite. Typically, the air scour broke the left and right one-third portions of the mat, but left the middle fragment which settled to the sand-coal interface. This may be the result of poor air distribution by the filter underdrain systems with strainers on about 7-in. centers. These fragments varied in length from 6 to 12 in. and in depth from 2 to 3 in., and interfered with proper fluidization and stratification of the media. Usually the agglomerate was broken up during the next backwash cycle, but was immediately replaced by another. The backwashing entry for run 54 typified this period of operation.

Minor surface cracking present. Air scour does not break up mat. At media interface mud balls sinking into sand. Approx. 1/3 of bed is not washing. Bed frees during wash and media is well stratified.

For the remaining four runs, the above trend disappeared, and the air scour appeared very effective in breaking the mat. Several small mud balls were observed but caused no serious problems with backwash distribution, intermixing, or fluidization and stratification.

Visual observations - west filter. Except for the first two runs of the study, the west filter was equipped with a rotating surface washer as described previously in detail. For the first two runs the bed was subjected to surface wash from a fixed nozzle washer. For the next 29 consecutive runs a rotating jet washer was used which consisted of an inverted, three-armed lawn sprinkler. Finally, a two-armed, two-nozzled, rotary washer was installed using nozzle jets similar to those in actual surface washers.

Backwashes following runs 1 and 2 were characterized by one or two large agglomerates (6 by 5 in. and 12 by 3 in.) accompanied by a host of smaller 2 to 3-in. diameter mud balls. The fixed nozzle washer was breaking the mat into chunks which remained fairly well intact for the rest of the wash. When first used following run 3, the make-shift surface washer appeared to do an excellent job in breaking up the matted layer leaving only three, 2 to 3-in. diameter mud balls visible in the bed. The very next backwash revealed a highly plugged surface layer which effectively resisted break up by the surface washer. When the bed was fluidized, the matted anthracite layer rose as a plug with cross section equal to that of the housing and a depth of about 8 in. Below this plug approximately five 2-in. diameter mud balls floated at the interface of the sand and coal layers. Eventually the plug broke up into large agglomerates which sank to the interface.

The condition of the bed stabilized during the next 10 backwashes to one of several small mud balls, 3 in. in diameter or less, plus one or two large agglomerates at the interface, sized approximately 8 by 2 in. to 6 by 2 in. After a brief period of almost no mud balls or agglomerates, this pattern was consistently observed from run 17 to run 32. Although these accumulations caused some channeling of backwash water and intermixing of media, the media continued, generally, to fluidize and stratify quite well, as evidenced by this entry for run 30:

7-in. penetration into bed. Heavy surface coating. Mud balls in bed larger than in south filter. 4-in. dia., 2-in. dia., three 3-in. dia., 8 in. x 2 in. Bed is generally well stratified.

Preceding the backwash for run 32, the third surface washer was installed. Although the action of the newly installed washer did not appear particularly violent, the condition of the bed continued to improve for the next three runs. Then the familiar pattern of several large agglomerates accompanied by approximately six small mud balls

returned with the backwash following run 36. Except for a brief period from run 46 to 49, during which the bed was relatively free of mud balls and agglomerates, this trend continued for the balance of the phase and is exemplified by the entry for run 43:

No visible cracks, cannot see surface coating (blocked by support). No appreciable inter-mixing. Bed is well stratified. One 5 in. x 1 in. agglomerate visible at sand-coal interface. Surface washer working, violent swirling in area of washer when bed fluidized. Several large mud balls observed: 3 in. x 12 in. x 12 in., 6 in. x 6 in. x 3 in., (2) 2-in. dia., (2) 1-in. dia.

Regardless of the washer used, therefore, the condition of the bed remained relatively constant throughout the study - not good but not exceptionally poor as in the north filter. Several periods of significantly improved condition of the media were observed, but were also short-lived. Fluidization and stratification of the media were not severely hindered except when the accumulations became heavily concentrated, which was also infrequent. Surprisingly, the action of the surface washer was most effective after the bed had been fluidized and the rotating arm was turning through the fragments of the mat, and not when it was attempting to break up the surface of the static layer.

Abrasion tests. The abrasion tests were considered of prime importance in evaluating the effectiveness of the various backwashing techniques because they directly indicate the condition of the filter media. As previously described, the abrasion test contained a step in its procedure in which the core sample was subjected to a vigorous 30-min mechanical mixing. Obviously, the mixing action tended to break up some of the anthracite sample, so a background level was determined for the test by subjecting an unused sample of anthracite (out-of-bag) to the procedure. The test was run twice on the same sample of clean anthracite and yielded values of 0.61 mg/g and 0.22 mg/g, respectively. The latter value was accepted as the background level because the former was influenced by coal dust which initially adhered to the media.

The results of the abrasion tests are displayed graphically in Fig. 33. Unquestionably, the most striking trend is that exhibited by the north filter. Except for a slight dip after run 20, the abrasion test values for this filter climbed steadily throughout the filter run series. The rapid and sustained build up of solids on the north filter media, as evidenced by these tests, is a direct result of the ineffectiveness of the water fluidization (only) backwashing technique which was used to clean the filter. The test results are also quite in line with visual observations of the north filter, which

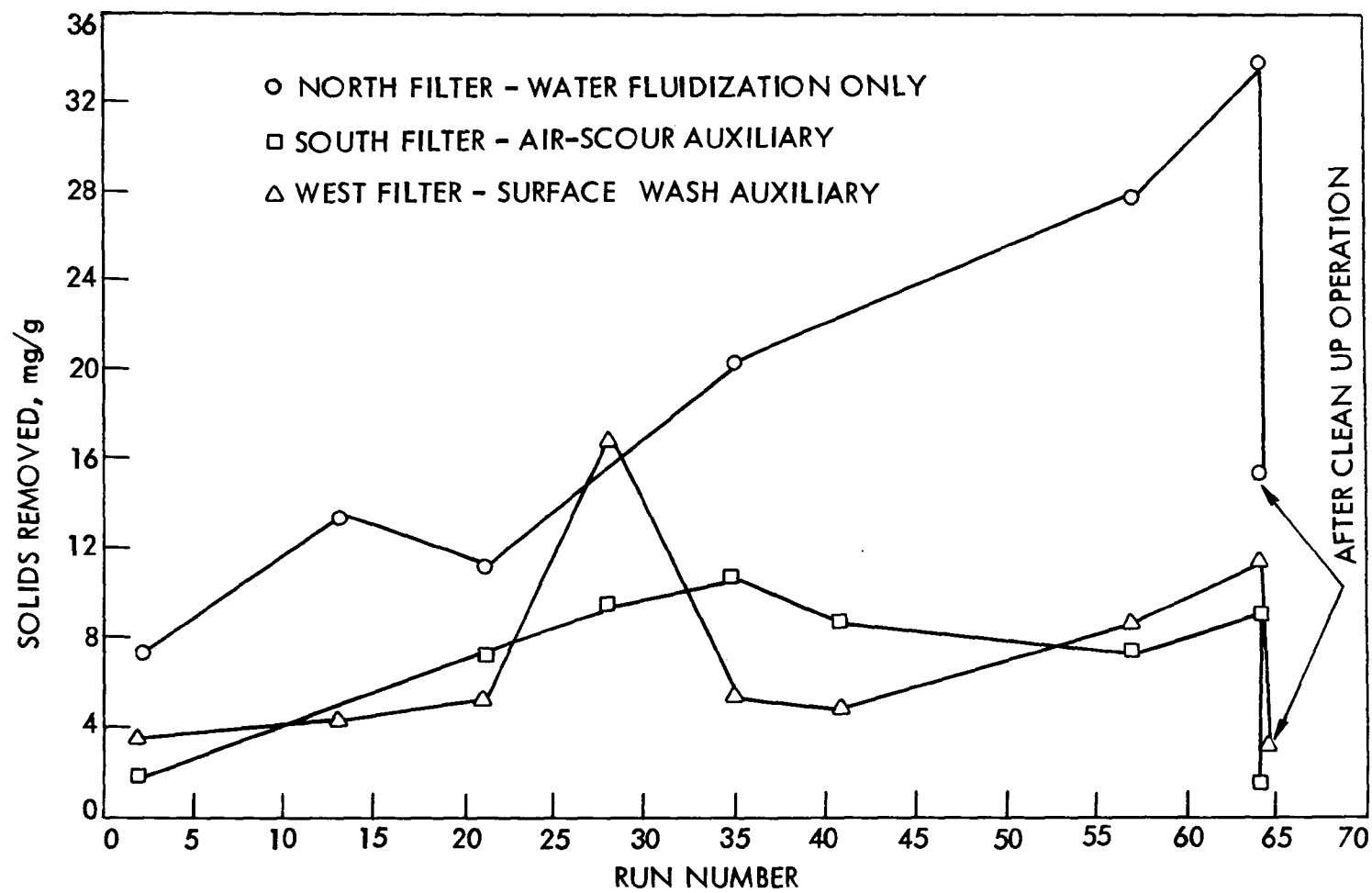


Fig. 33. Standardized abrasion test results (Phase II) during direct filtration of secondary effluent.

qualitatively labeled it as the bed in worst physical condition as described previously.

The lower of the two values plotted for each filter at run 64 was the abrasion test result at the conclusion of a clean up operation which will be described in more detail later. Interestingly, the north filter was still in worse condition (in terms of solids remaining on the media) at the end of its extensive clean up procedure than the other two filters were before the start of their clean up operations.

The abrasion test data is certainly less definitive with respect to differences in condition of the media between the south and west filters. The graphs for these two filters cross each other four times, although each displays an average upward trend. The west filter exhibited a sharp peak at run 28, but immediately dropped with the next test. This point is viewed with suspicion and is thought to be in error, although nothing in the test record indicated an error.

Unfortunately, conclusions about differences in the cleanliness of the media in the south and west filters are not warranted based upon the available abrasion test data. It is apparent that the filters should have been operated for a longer period of time to establish definite trends; however, this was impossible because of the onset of winter.

Initial head loss. Initial head loss readings were recorded at the start of each run for each filter. The procedure was standardized by allowing 15 min after opening the filter influent valve before taking readings on the piezometer tubes. The initial head loss, as plotted for each filter in Fig. 34, represents the total loss in head through the filter media after 15 min of operation.

By rearranging the data for each filter without regard to time and plotting the percent of observations exceeding a given head loss value on normal probability paper, one obtains three curves as shown in Fig. 35.

Clearly, the north filter exhibits substantially higher initial head losses than either the south or west filters. One would expect such results since throughout the filter run series, the accumulation of mud balls and agglomerates was most rapid and sustained in the north filter. Because of the ineffectiveness of the water fluidization (only) backwashes, many of these masses were not broken up during the backwash and remained in the bed at the start of the next run. Since much of the bed remained plugged by these solid masses, the filter influent was forced to find paths around them, causing increased flow velocity through the cleaner portions of the bed and proportionately increased initial head loss through the filter.

Substantial differences in initial head losses between the west and south filters were not apparent. Although the west filter data

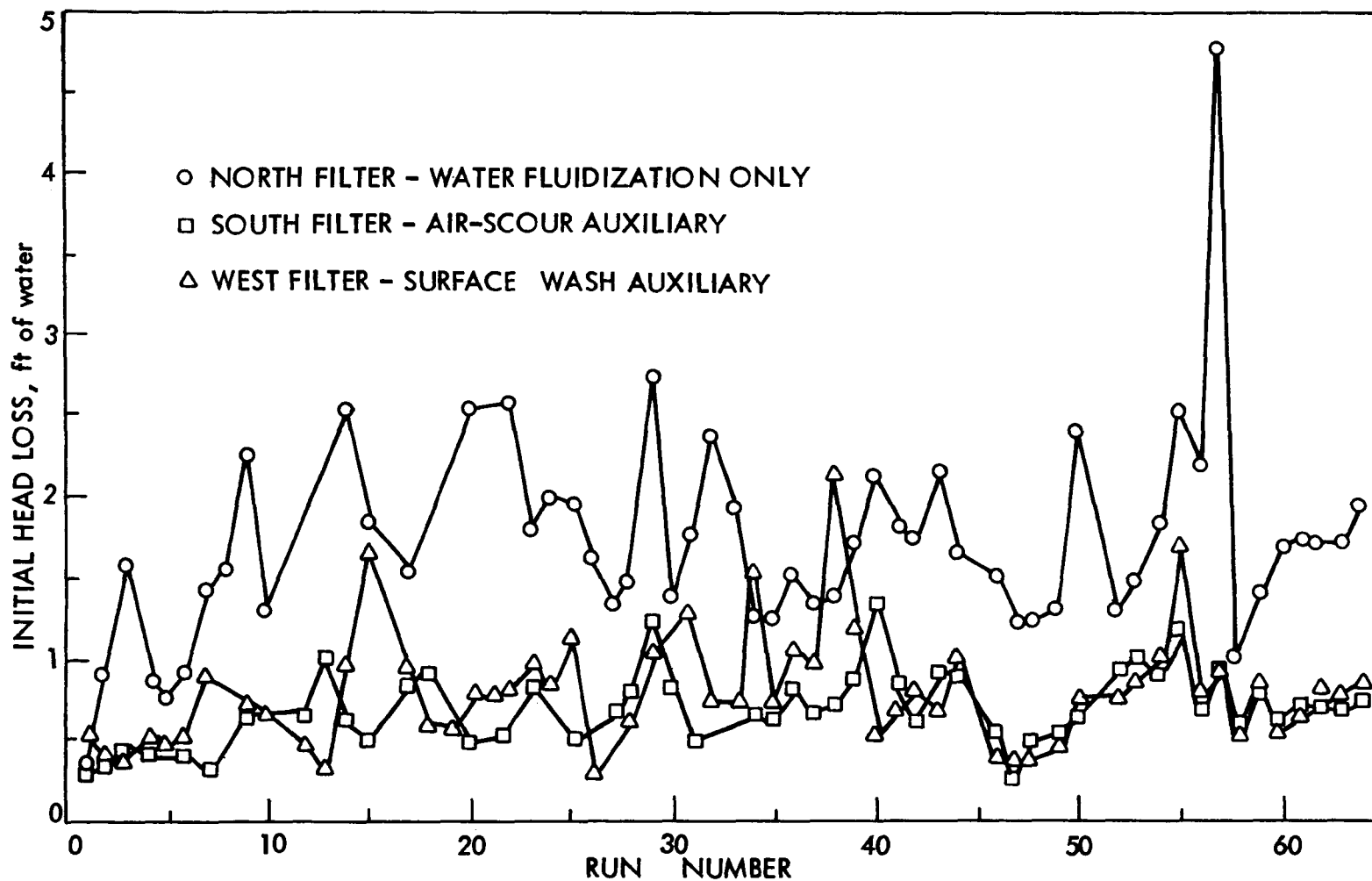


Fig. 34. Initial head loss data for north, south, and west filters for entire Phase II study during direct filtration of secondary effluent.

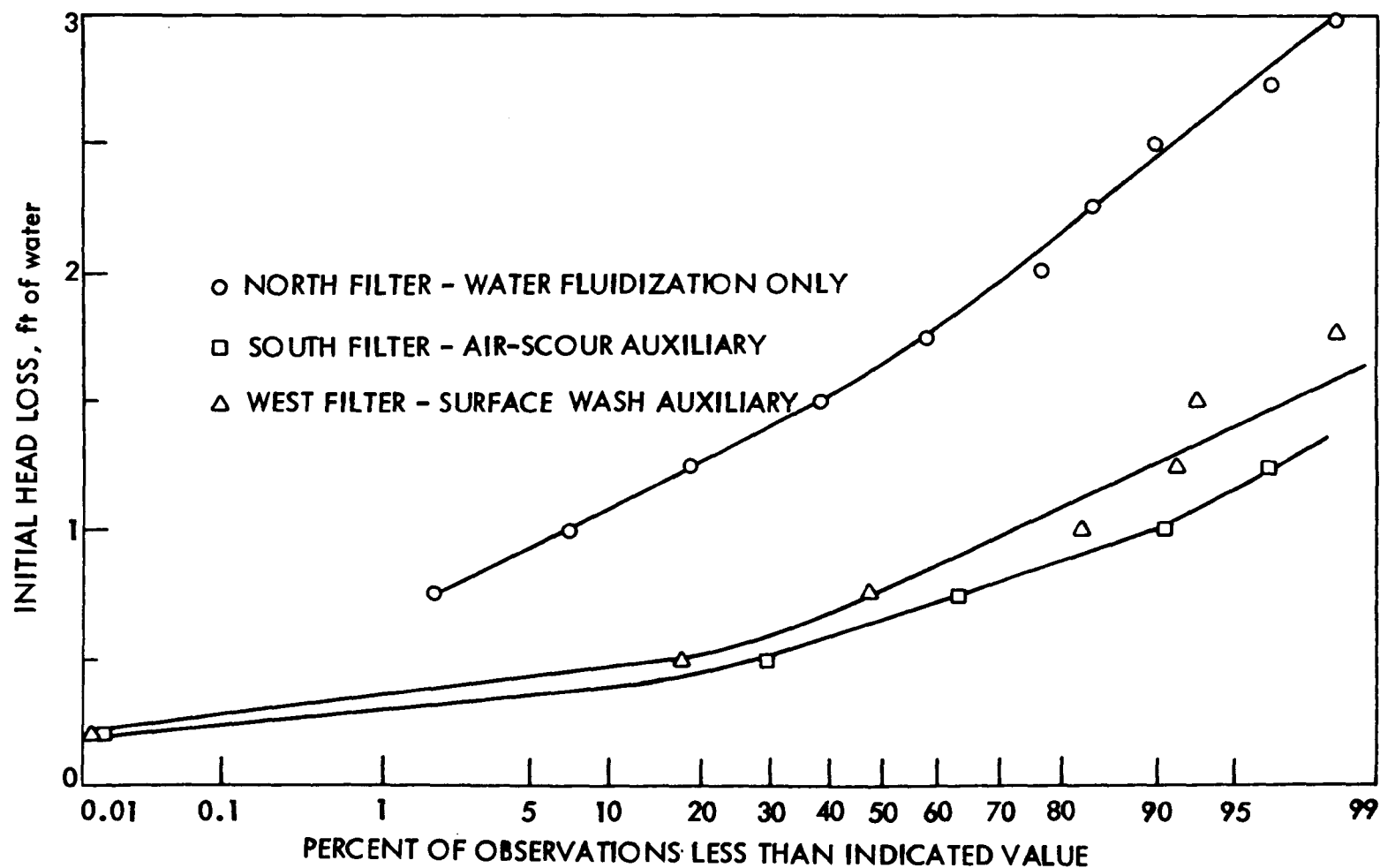


Fig. 35. Frequency plot of initial head loss data, Phase II.

plotted slightly higher in Fig. 35 and had nearly twice as many observations above 1 ft, the differences were not appreciable. For the majority of the runs the initial head loss values were quite close and followed similar trends.

A typical pattern developed for all three filters wherein the initial head loss exhibited a cyclic trend. Although, there was no quantitative means of correlating initial head loss data with the visual observations of the backwashing procedures, the latter demonstrated a similar trend. Mud balls and agglomerate accumulations appeared to attain a maximum concentration, decrease somewhat, and then resume their build up. This trend was most noticeable in the north and west filters, but was also observed in the south filter to a lesser extent. It seems reasonable, although admittedly speculative, that the cyclic trend of initial head loss was paralleling the cyclic solids build ups in the filters.

Head loss development. Studies by Cleasby and Baumann [31] have revealed that surface layers which form on sand filters used in water treatment cause a characteristic exponential shape to the head loss versus time curve. The accelerated head loss development with time was attributed to the surface layer or "cake" because the layers act as filters themselves. Once established, the layers remove more influent suspended solids and increasingly compress during the course of a run, so that by the time terminal head loss is attained, the layers form dense mats which are resistant to cleaning.

As described earlier in the section on media appearance, layers of organic matter on the filter surface were frequently observed prior to backwashing the filters in Phase II. One might reasonably expect an exponential shape for the total head loss curve, although the data as plotted in Figs. 36 through 43 exhibited no such tendency. The nearly straightline development of head loss by the filters could have been indicative of solids removal occurring much deeper in the bed, particularly since penetration of solids was consistently visible 4 to 6 in. below the surface in all filters. However, this does not seem plausible since surface layers were observed; therefore, it seems as though some other phenomenon was acting to alter the shape of the curve.

An explanation of the linear head loss development may be hypothesized by observing the head loss development in the 4-in. layer of media directly below the surface and by noting that surface cracking was observed primarily in the north and south filters throughout the study, as described earlier. During the course of a run, the bed depth was consistently compressed from 1.0 to 1.5 in. in each filter, which was likely the result of the effect of compressible coating on the media due to inefficient backwashing. The compression can cause the media surface to crack and to pull away from the sides of the filter housing walls or to break, as in a beam failure, over the protruding piezometer tap. When surface cracks open up as the filter

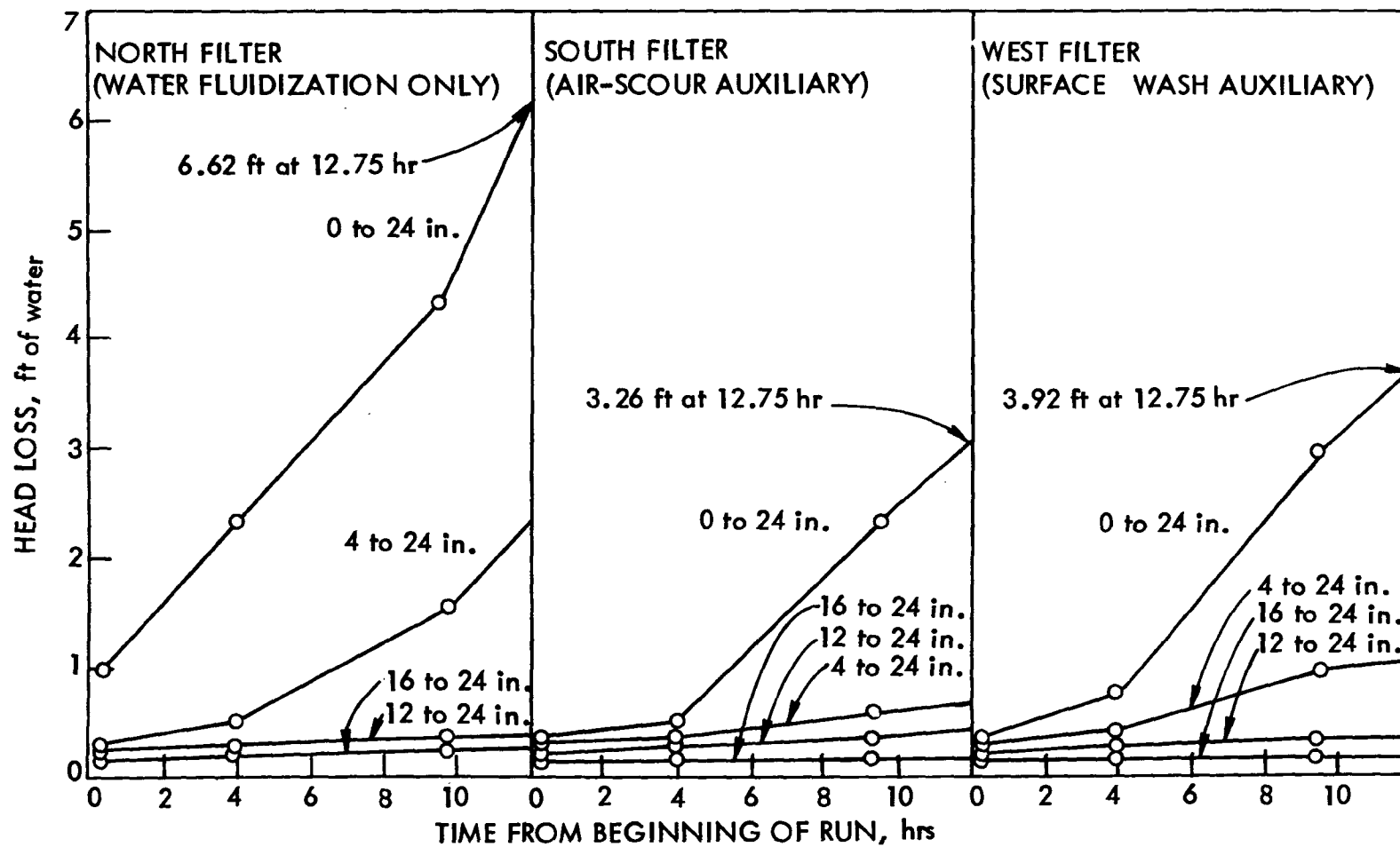


Fig. 36. Chronological head loss development at various media depths, run 2.

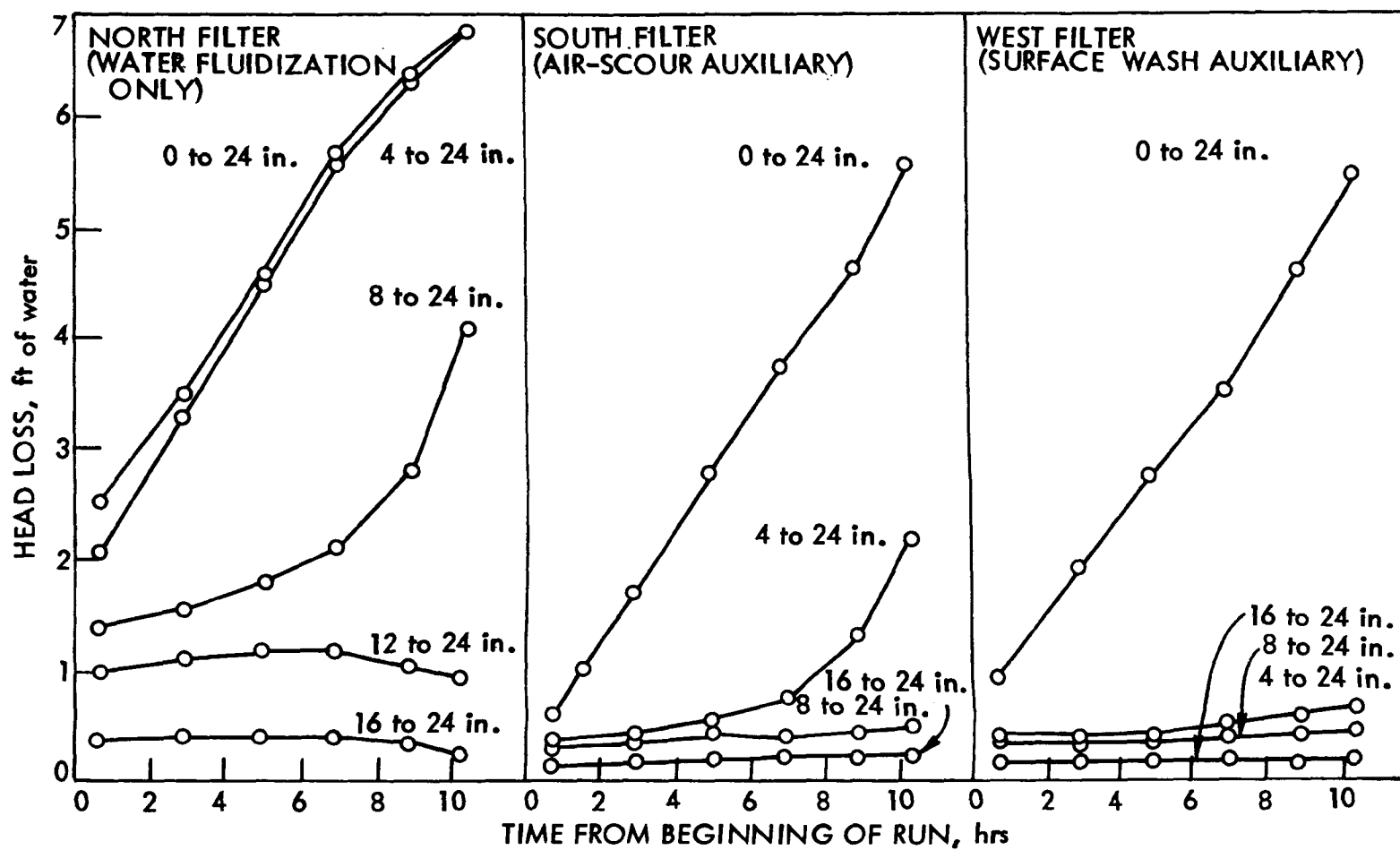


Fig. 37. Chronological head loss development at various media depths, run 14.

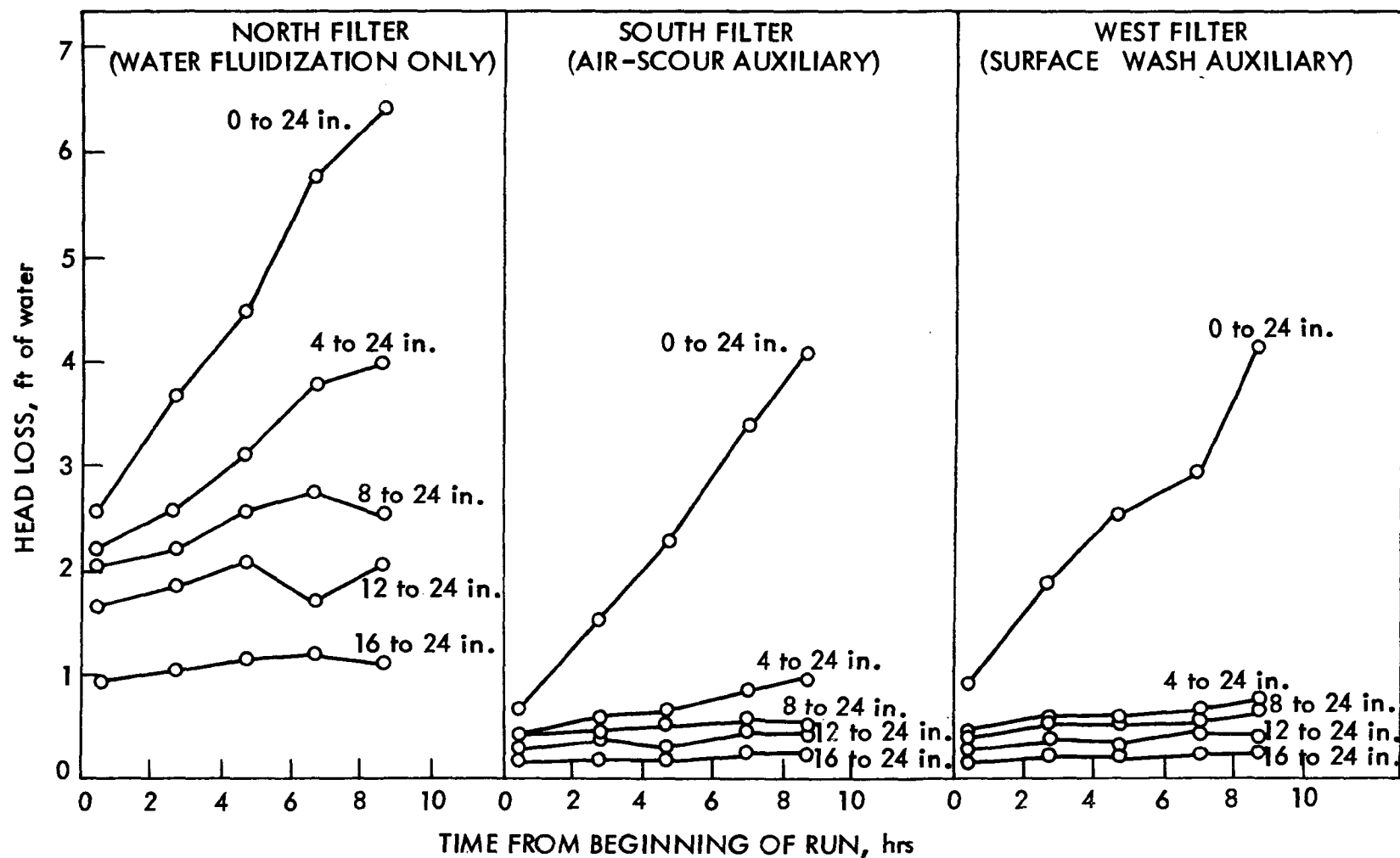


Fig. 38. Chronological head loss development at various media depths, run 22.

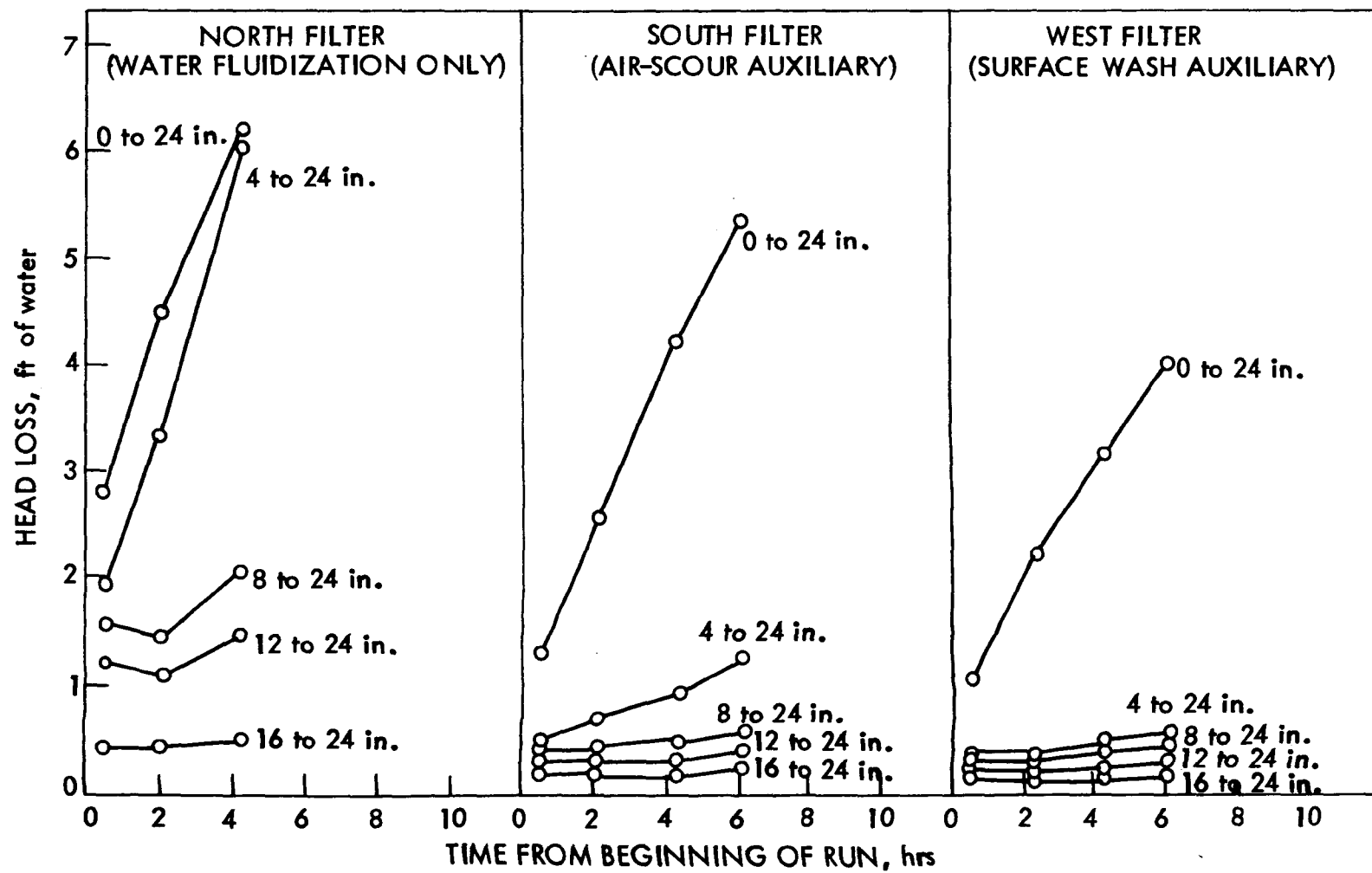


Fig. 39. Chronological head loss development at various media depths, run 29.

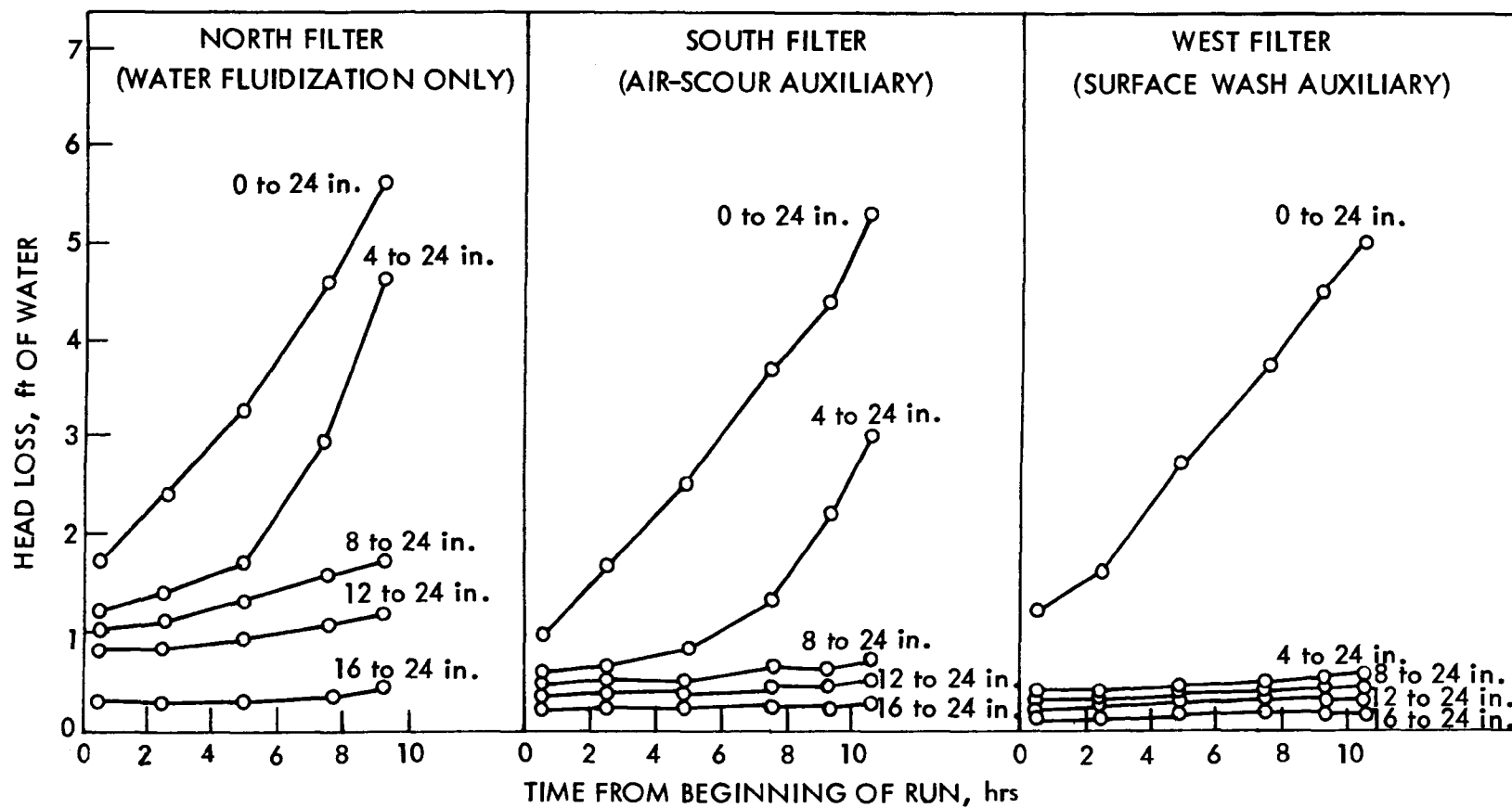


Fig. 40. Chronological head loss development at various media depths, run 36.

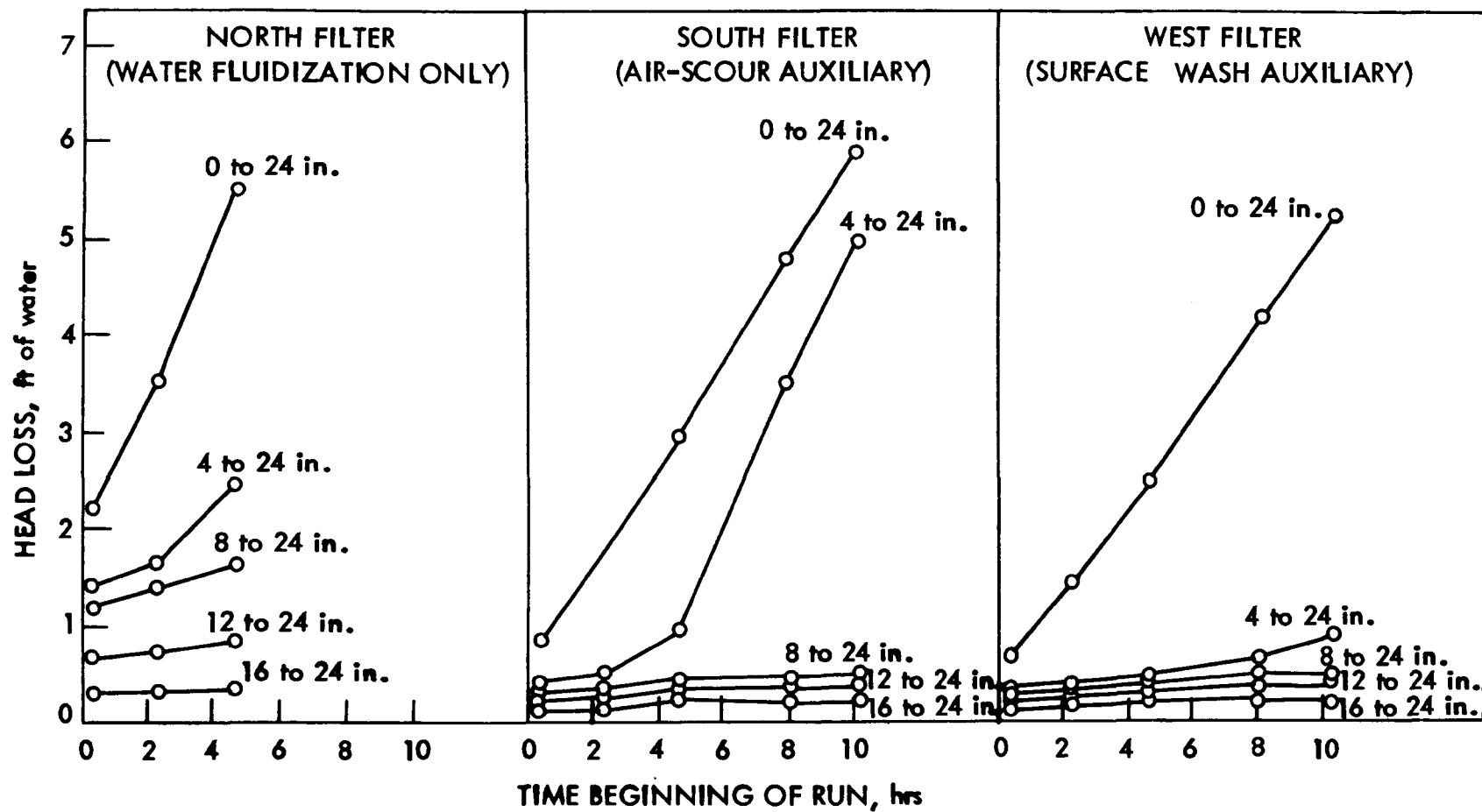


Fig. 41. Chronological head loss development at various media depths, run 43.

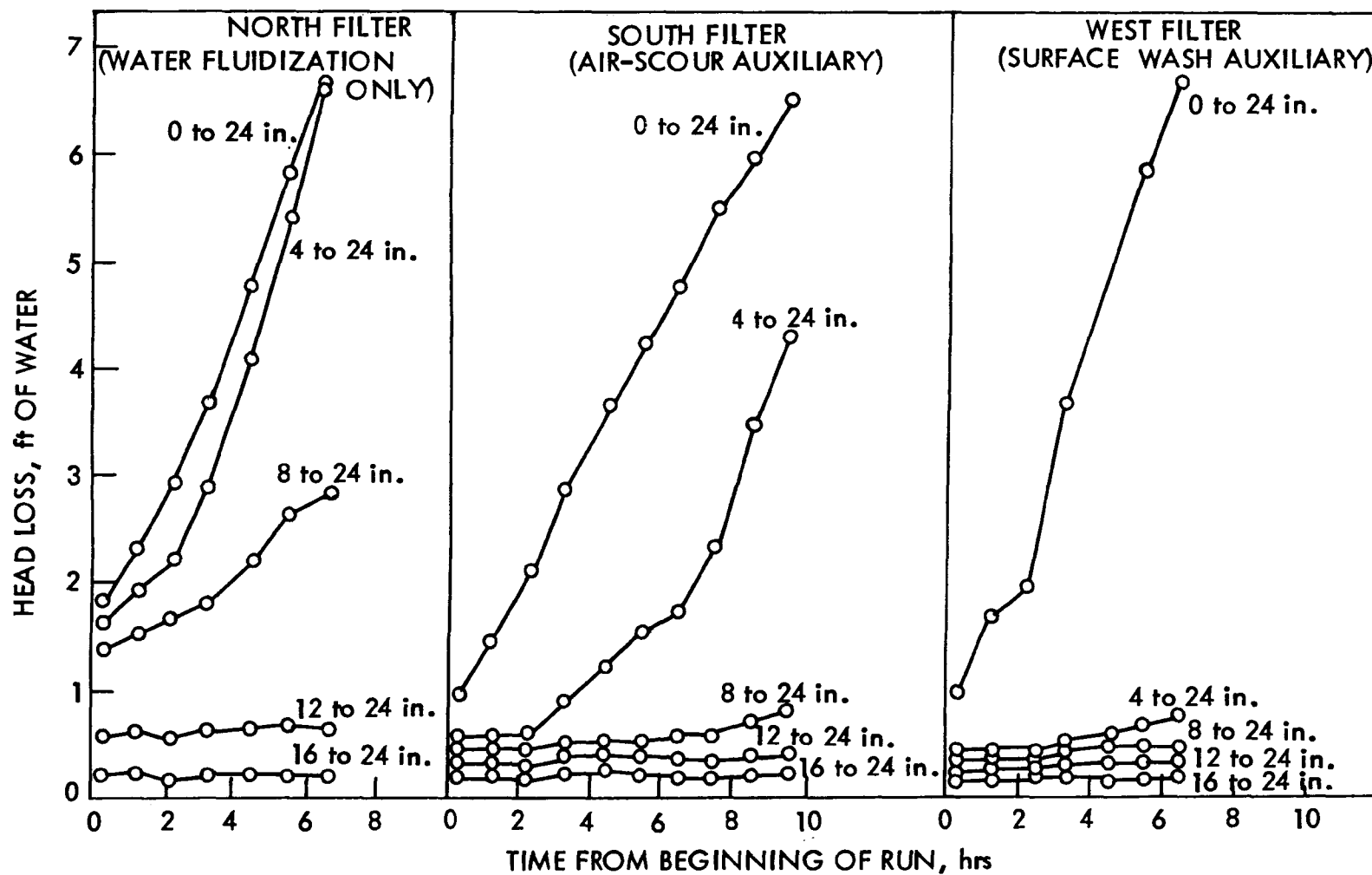


Fig. 42. Chronological head loss development at various media depths, run 54.

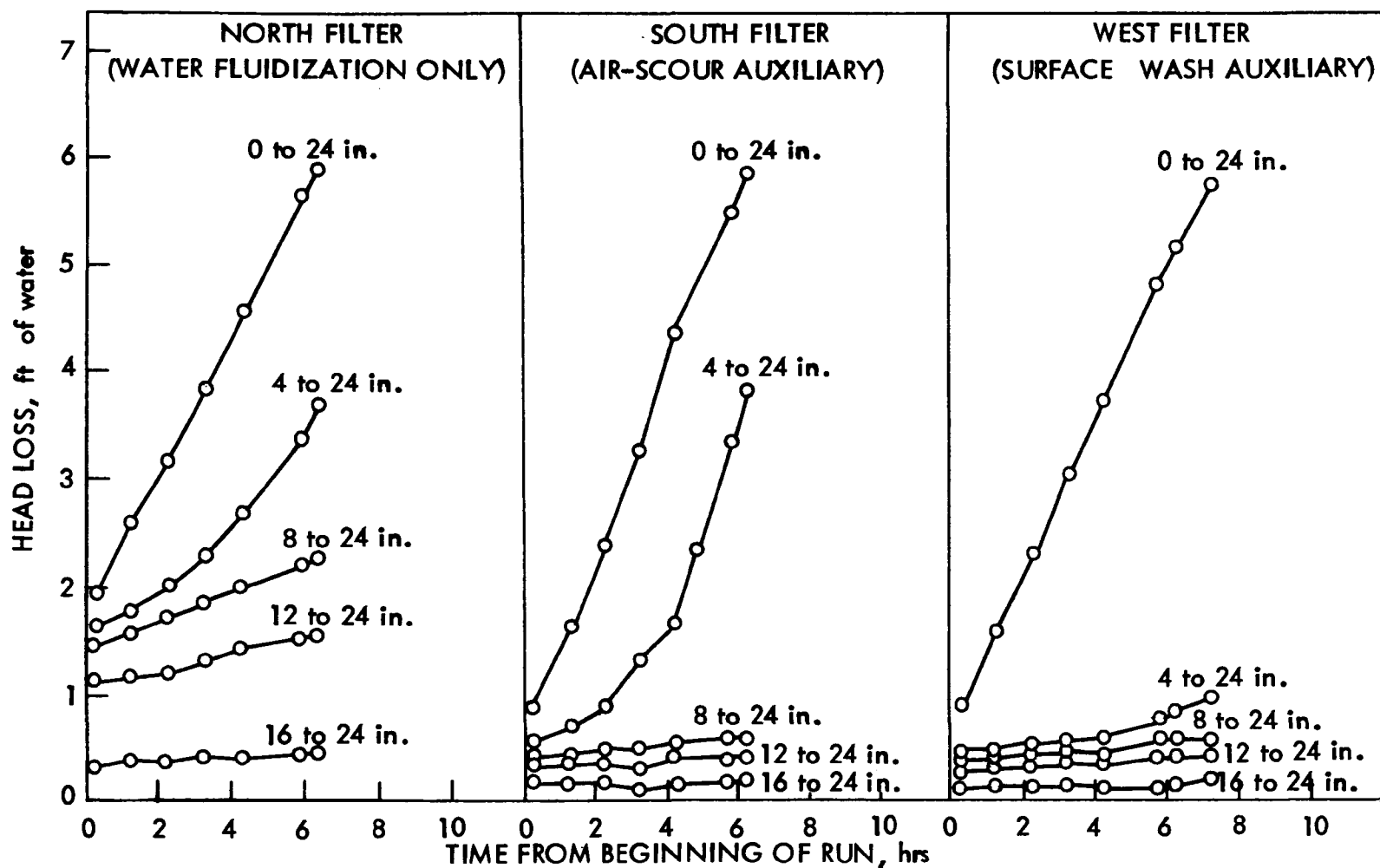


Fig. 43. Chronological head loss development at various media depths, run 64.

run progresses (as they did in this study) they may preclude the formation of an exponential total head loss pattern since the influent is being introduced deeper into the bed through the cracks. The net effect would be to increase the head loss in the media layer directly below the surface layer, which was frequently observed in the north and south filters.

In some cases, a crack must have formed by beam failure over the first protruding piezometer tap at 4-in. depth, which caused the head loss curve at that depth (4 to 24 in.) to converge on the curve for the piezometer above the media (0 to 24 in.). This is evident on several of the curves for the north filter, which had the most extensive surface cracking.

Table 14 illustrates the initial total head loss and the time required to reach 3 ft and 4 ft of total head loss for each filter. It is apparent that the initial head loss was higher for the north filter, which reduced the head available for solids accumulation during the filter run. Consequently, the average run length for the north filter was reduced compared to the other filters. Differences between the south and west filters are not great or consistent, so conclusions are not warranted.

Water quality. The means and standard deviations of the various water quality parameters are given in Table 15. No statistical comparison between the filters was attempted for the reasons explained in Phase I. There is no apparent difference between the filters, even though the condition of the north filter was substantially poorer than that of the other two filters.

As the result of sampling difficulties, composited samples of the influent were not made for the majority of the observation runs. Therefore, reporting removal efficiencies on the basis of influent grab samples was not considered meaningful or proper. Fortunately, the Ames Water Pollution Control Plant personnel had conducted suspended solids and BOD determinations on composited samples collected over a period corresponding closely to the observation runs of this study; these are included in Table 15.

At roughly 2-hr intervals during the observation runs, grab samples were collected from the effluent of each of the filters and from the influent, and turbidity determinations were made. These values were treated as a hand-sampled composite, averaged for each run, and reported in Table 15.

Filter clean up operations. At the conclusion of the regular filter run series in Phase II, special cleanup operations were conducted on each of the three filters. The purpose of these operations was to determine if the media in each filter could be restored to its original state by a series of consecutive backwashes using varied techniques. Core samples were taken at the beginning and at the end of

Table 14. Summary of head loss development during observation runs of Phase II, during direct filtration of secondary effluent.

Run	Initial head loss <sup>a</sup> , ft			Time to 3 ft head loss <sup>a</sup> , hr			Time to 4 ft head loss <sup>a</sup> , hr		
	N	S	W	N	S	W	N	S	W
2	1.00	0.33	0.38	5.8	11.8	9.6	8.4	15.6 <sup>b</sup>	12.8
14	2.53	0.62	0.96	1.8	5.2	5.4	3.8	7.4	7.8
22	2.58	0.54	0.79	1.5	6.3	7.2	3.6	8.8	8.8
29	2.77	1.31	1.05	0.6	2.6	4.0	1.6	4.0	6.0
36	1.55	0.81	1.09	4.2	6.0	5.6	6.4	8.3	8.2
43	2.19	0.89	0.63	1.6	4.8	5.8	3.0	6.8	7.8
57	4.76	0.95	0.95	2.4	3.5	2.9	3.6	5.2	3.6
64	<u>1.95</u>	<u>0.84</u>	<u>0.88</u>	<u>2.0</u>	<u>3.0</u>	<u>3.2</u>	<u>3.6</u>	<u>4.0</u>	<u>4.6</u>
Avg	2.42	0.79	0.84	2.5	5.4	5.5	4.2	7.5	7.5

<sup>a</sup>Total head loss across the filter media in each case.

<sup>b</sup>Extrapolated value.

Table 15. Results of analyses during direct filtration of secondary effluent (Phase II) from August 30 to October 30, 1973. (All composite samples except as noted.)

	Filter influent	Filter effluent <sup>a</sup>		
		N filter, water fluidization only	S filter, air-scour auxiliary	W filter, surface wash auxiliary
Suspended solids (mg/l)	30.5 <sup>c</sup>	4.05	3.63	4.10
σ (N = 8)	7.6	2.80	1.58	1.6
Turbidity (FTU)	17.4	4.84	4.69	4.61
σ (N = 9)	2.2	1.33	1.42	1.36
BOD <sub>5</sub> (mg/l) <sup>b</sup>	40.1 <sup>c</sup>	12.1	14.2	12.7
σ (N = 8)	15.4	3.1	4.9	4.6
TOC (mg/l)	17.4 <sup>d</sup>	12.7	12.0	14.2
σ (N = 7)	4.1	2.8	2.9	5.3
Total PO <sub>4</sub> (mg/l)	20.6 <sup>d</sup>	23.9	24.6	24.4
σ (N = 8)	3.9	4.5	3.3	3.7
Ortho PO <sub>4</sub> (mg/l)	19.3 <sup>d</sup>	22.7	22.8	22.5
σ (N = 8)	3.3	3.7	2.4	2.5
Total Kjehldahl nitrogen (mg/l as N)	12.7 <sup>d</sup>	15.4	15.5	15.1
σ (N = 8)	4.4	2.6	2.6	2.6

<sup>a</sup> Average filtration rate 1.8 gpm/sq ft

<sup>b</sup> Nitrification not suppressed in BOD test except in the samples run by Ames WPC Laboratory.

<sup>c</sup> Two of the observations are from grab samples, and two from composites run by Ames WPC Laboratory.

<sup>d</sup> Four of the observations are from composite samples, the remainder from grab samples.

the clean up procedure to evaluate the overall effectiveness of the operations. Additionally, samples of the backwash wastewater were taken at 30-sec intervals and composited throughout each step of the three clean up procedures. The results of these procedures are summarized in Table 16 and discussed in detail below.

Initial head loss readings, abrasion test results and visual observations all indicated the media of the north filter to be in the worst condition of the three filters. A visual check just prior to the start of the clean up operation, further confirmed the poor condition of the north filter. The media had a heavy surface layer, and 1/4 to 1/2-in. wide cracks of varying lengths were visible at the surface. The sand and coal layers had become highly intermixed as the result of poor fluidization and poor stratification in previous backwashes. Finally, two 6-in. diameter agglomerates were clearly visible.

To initiate the clean up procedure for the north filter, the media was subjected to a normal water fluidization (only) backwash. At the beginning of the fluidization of the media, the top 6-in. layer of anthracite rose as a plug and then settled to the sand-coal interface. The backwash was successful only in breaking up this layer into large chunks and could not effect further breakdown. A core sample was taken at this stage, and the abrasion test results indicated a high value of 33.7 mg/g. This initial step was necessary to place the media in the state in which it would normally be at the conclusion of its standard backwashing procedure and, therefore, to establish a starting point for the evaluation of subsequent and varied backwashes.

The second step in the procedure consisted of a subfluidization backwash with simultaneous air scouring, the only introduction of air to this media since the beginning of the Phase II. Prior to the backwash, the water level in the filter was drained to the media surface. Air was then applied at 3.72 scfm/sq ft and water at 11 gpm/sq ft, until the water level reached an elevation 6 in. below the washwater trough. At this point the air was shut off and the water rate increased to 20 gpm/sq ft, which fluidized the media by itself. The combination air and water wash seemed to produce substantial agitation in the media and effectively disintegrated many of the mud balls in the media. However, many mud balls were still present during the 5-min water (only) backwash which immediately followed, and one large, 5-in. mud ball was observed deep in the sand layer near the conclusion of the wash.

The third clean up step was essentially a repeat of the previous step, and it continued to improve the condition of the media. During the combined air and water wash, the water rate was reduced slightly to 10 gpm/sq ft, but the agitation of the media was quite good. The combined action was particularly effective because the media exhibited no tendency to "pack" after 30 sec to 1 min of operation, as it did when using air scour alone as on the south filter during the

Table 16. Data summary of clean up operation at end of Phase II.

Steps	Brief description of cleanup procedure - see text	Solids released (g/sq ft)	Media abrasion (mg/g)
<u>North Filter</u>			
1.	Normal water (only) backwash.		33.7
2.	Air and water combination (water at subfluidization rate) as water rose from 1 in. above media to 6 in. below trough. Follow with water (only) backwash.	314	
3.	Repeat Step 2 with a reduced wash rate during air and water combination.	163	
4.	Repeat Step 3 except continue air scour after combination air and water. Follow with water (only) backwash.	205	
5.	Air and water combination, water above fluidization. Follow with water (only) backwash.	84	
6.	Repeat Step 5, but leave air on 3 min. after air water combination. Follow with water backwash.	67	15.3
Total		833	= (35.1 mg/g) <sup>a</sup>
<u>South Filter</u>			
1.	Normal air (only) followed by water (only) sequence.		9.0
2.	Combination air and water with water just at fluidization rate. Follow with air (only) (2 min.) and then water (only).	100	
3.	Repeat Step 2.	42	
4.	Repeat Step 2.	17	1.9
Total		161	= (6.8 mg/g) <sup>a</sup>
<u>West Filter</u>			
1.	Water (only) backwash.		11.3
2.	Subsurface wash and water wash simultaneously.	52	
3.	Repeat Step 1 without drawdown of water above media.	18	
4.	Repeat Step 2.	12	
5.	Air and water combination, follow by 2 min. air (only), and finally 3.5 min. water (only) backwash.	120	
6.	Repeat Step 5, except for 5 min. water (only) backwash.	26	2.9
Total		228	= (9.6 mg/g) <sup>a</sup>

<sup>a</sup>Based on 12 in. coal media involved in filtration and weight of coal media of 23,742 g/sq ft.

series. Layer stratification was more pronounced during the water fluidization backwash which followed, and the number of mud balls was further reduced. However, some mud balls persisted at the sand-coal interface, and one large, 5-in. diameter agglomerate was observed near the end of the water (only) backwash.

The fourth cleaning procedure consisted of the previously described air and water combination followed by air (only) for 2 min at the same rate and concluded with water backwash at 20 gpm/sq ft. Careful observation during the combined action revealed that violent agitation took place mainly in the upper 18 in. of the bed while the lower 12 in. became fairly packed with little movement. As expected, the agitation during the air (only) scour was fairly good for the first minute until the bed packed, but overall agitation appeared much less effective than the combined action. One large, 6-in. diameter mud ball and several smaller ones were observed at the conclusion of the water backwash.

The final two steps in the north filter clean up operation were essentially the same and differed from the fourth step only in that the water rate used during the combined air-water scour was increased to 14 gpm/sq ft. However, this change in rate caused the media to be fluidized and improved the media agitation by extending the action throughout the bed. By the end of the water backwash of the fifth step, the remaining agglomerates had disappeared, although two "clusters" of four to six 1-in. diameter mud balls persisted and were not broken up even at the conclusion of the final step. In each of the last two steps, the air (only) scour produced the now typical result: good action during the first minute but little movement after 1 min because of intermixing and packing of sand and coal layers.

Throughout the regular filter run series, the south filter was cleaned using a 5-min air-scour auxiliary at 3.72 scfm/sq ft followed by a 5-min water fluidization backwash at 20 gpm/sq ft. This procedure was used to initiate the cleanup operations on the south filter. The media was not in nearly as poor condition as the north filter, but during the last 30 sec of the water wash, six 3 to 4-in. diameter mud balls were observed. At the conclusion of the initial step, a core sample was taken and subjected to an abrasion test. The test results indicated the media to be approximately four times cleaner than the north filter at the same stage. The clean up procedure consisted of an air and water combination wash with the media slightly fluidized (14 gpm/sq ft), an air (only) scour for 2 min at 3.72 scfm/sq ft, and a water (only) backwash at 18 gpm/sq ft. Expanded bed depth remained constant at 32-1/2 in. for the remaining three steps, and fluidization and stratification were consistently good. As the clean up continued, the number of mud balls observed during the water backwashes diminished. At the conclusion of the fourth and final step, only one small mud ball was observed, and the physical appearance of the bed was excellent. A final core sample taken at

this time was analyzed in the laboratory and was found to verify the visual observations: the abrasion test value was determined as 1.88 mg/g which indicated the bed was in very good condition.

As one will recall from an earlier discussion, the west filter had been equipped with a rotating surface washer which operated both independent of and in conjunction with the water backwash during the backwash sequence of the filter series. The routine wash was not used to begin the west filter clean up operation; instead, a water (only) backwash rate of 19.5 gpm/sq ft for 5 min was used. The surface washer had been modified prior to the start of the wash, and while the media was fluidized, the rotating washer was pushed to the fluidized interface of the sand and coal layers for use in subsequent steps. At the conclusion of the water wash, a core sample was taken, and a subsequent abrasion test resulted in a value of 11.26 mg/g, very close to that of the south filter.

Steps 2, 3, and 4 were combination rotating subsurface wash, water backwash, with the former operating for 3, 4, and 3 minutes, respectively. The rotating washer had been lowered into the bed to see if it could effectively break up the mud balls which accumulated at the sand-coal interface. By the end of the second step no mud balls were seen even though several large (4 to 8-in. diameter) mud balls had been observed at the start of step 2. Only three small mud balls, approximately 1 in. in diameter, were seen during the third step, and none at all were observed during the fourth step -- the last combination subsurface wash, water backwash used in the cleanup. The rotating subsurface washer, therefore, appeared to do an excellent job of breaking up the large agglomerates and mud balls in the media.

At the conclusion of the fourth step, however, there were signs that the media was not thoroughly clean even though the mud balls had been eliminated. Dirt remained floating on the surface of the coal after step 4, and the anthracite itself had a grayish cast, as though it were still coated. This seemed an excellent opportunity to change the backwash procedure for step 5 to include the use of air scour and see if it could further clean the coal layer.

The procedure for step 5 was, therefore, changed to provide combination air and water wash with the water wash rate set at 12.5 gpm/sq ft to fluidize the media as the water rose from the media to near the overflow. This was to be followed by 2 min of air (only) scour at 3.72 scfm/sq ft and, lastly, by 5 min of water (only) backwash at 20 gpm/sq ft. Prior to step 5 the composited backwash waste water had shown a decline in suspended solids concentration equivalent to a dirt released value of 12 g/sq ft after step 4. The composited sample for step 5, however, indicated a nearly ten-fold increase in the dirt released value to 120 g/sq ft. These results seemed, at first glance, even more significant because a dwindling supply of backwash water limited the actual water (only) backwash to 3-1/2 min.

Step 6 in the west filter clean up was identical to step 5, although the water (only) wash was extended 5 min after building up the backwash supply. It was noted that, again, the composited backwash waste sample had a suspended solids concentration twice that of step 4. During this final step of the west filter cleanup, no mud balls were observed, all floating material had disappeared from the surface, and the anthracite regained its rich, black lustre. An abrasion test of a core sample taken after this step was completed yielded a value of 2.19 mg/g, which further confirmed the clean condition of the bed.

The results from steps 5 and 6 initially appeared to demonstrate the superiority of the air and water combination wash over the rotary surface wash backwash auxiliary. However, as noted in step 4, much dirt was visibly released from the media which was not carried out during the water (only) backwash, and large solids were also noted adhering to the sides of the filter housing. At the conclusion of step 6 the floating material had disappeared entirely, and some of the wall solids had also been removed. Therefore, one can state confidently that the air and water combination backwashes (steps 5 and 6) were definitely more effective in loosening solids from the filter housing, and in disintegrating solids so they could be transported out of the filter during the water (only) backwash, but one cannot state categorically that it was more efficient in releasing dirt from the media.

The data presented in Table 16 clearly demonstrate the benefit of both auxiliaries in maintaining the filter media in cleaner condition. However, it is not possible to choose which auxiliary is better from the data. The fact that the air and water used simultaneously were able to release substantial additional solids from the south and west filters, which had been routinely washed with air-scour and surface wash auxiliaries, respectively, implies the superiority of air and water together as a backwash method. One should be careful about jumping to such a conclusion, however, since the research of Phase II was not designed to prove that point. To prove the superiority of air and water together over the other two backwash auxiliaries, it would be necessary to conduct an entire research phase in which the three methods of backwash auxiliary were compared in parallel.

#### Summary and Conclusions - Phase II

The objectives of the experimental investigations in Phase II were to determine the effectiveness of three different backwashing techniques on dual-media filters and to compare the performance of the three filters while filtering secondary effluent. The backwashing techniques used were as follows:

1. North filter, backwash by water fluidization alone.

2. South filter, two-phase sequence consisting of air (only) scour followed by water fluidization backwash (i.e., air-scour auxiliary).
3. West filter, three-phase sequence consisting of surface wash (only), surface wash and water backwash, and water fluidization backwash.

The experimental data were collected over a nine-week interval at the Ames, Iowa, trickling filter plant using pilot-scale equipment. The following are the conclusions of the phase:

1. None of the three methods of backwashing was able to keep the filter bed completely free of mud balls and agglomerates.
2. Based upon higher initial head losses, steadily increasing solid accumulation observed in abrasion test results, visual observations of the media condition, and results of the clean up operation, the north filter was clearly in the worst condition of the three beds. Therefore, water fluidization (only) backwashing is ineffective in maintaining the filter media in good condition, and some means of auxiliary cleaning is required.
3. On the basis of the items mentioned in conclusion 2, no conclusive differences were observed between the south and west filter in the effectiveness of their cleaning techniques, air-scour auxiliary and surface wash auxiliary, respectively.
4. No apparent differences were observed in the effluent qualities among the three filters, particularly in the primary removal efficiency parameters BOD, suspended solids, and turbidity. This indicates bed condition played little part in removal efficiency in this study; however, this may have been due to the choice of a fine filter media, low filtration rate or low terminal head loss in this research.
5. The use of some form of air-scour auxiliary or some form of surface wash auxiliary is essential to the satisfactory functioning of wastewater filters. The methods used in this research did not completely eliminate all dirty filter problems, but both auxiliaries reduced the problems to acceptable levels so that filter function did not seem to be impaired.

Operation and Results - Phases III, IV and V  
Single-, Dual-, and Triple-Media Filtration  
of Secondary Effluent

Phases III through V were prompted by the deficiencies in water fluidization backwashing demonstrated in Phase I and II, even when assisted by air-scour or surface wash auxiliary. These phases were

also prompted by the implied superiority of simultaneous air and water backwash revealed in the cleanup operations at the end of Phase I and II. There were other questions raised by Phase II which needed evaluation so Phases III through V were designed to try to answer those questions.

During Phases III through V, the north filter was equipped with dual media. The backwash included three steps, including air scour alone, air and water simultaneously for a very brief period without overflow, and finally, water fluidization backwash alone. Coarser underdrain strainer openings were used which required the use of gravel below the media. A double reverse graded gravel was used to resist movement by the simultaneous air and water backwash action.

The south filter was equipped with a deeper bed of coarse sand (6 to 10 mesh, 2 to 3.36-mm sieve range) and was washed at subfluidization rates with air and water simultaneously during overflow for a rather extended period, followed by a brief period of subfluidization water backwash.

The west filter was equipped with triple media (i.e., commercially obtained "mixed-media" from the Neptune Microfloc Corporation). The media was underlain by a graded gravel, and the water fluidization backwash was assisted by a surface and subsurface washer. The subsurface washer was added in this phase because of the problem of mud balls sinking to the coal-sand interface and floating there out of reach of the normal surface washer.

The details of media sizes and depths, gravel gradation, and underdrain strainers have been presented previously. Details of the backwash are presented in the following pages.

#### Operation - Phases III through V

The first filtration run of the testing period was on May 16, 1974, and operation continued daily, except when the equipment malfunctioned, to the cleanup operations on November 2, 1974. The five-month period was divided into three phases coinciding with changes in media and sampling technique. The first runs were designated as Phase III, a continuation of the notation started the previous year, and were continued to July 18, 1974, when Phase IV began. Due to an incident of clogging of the underdrain strainers (to be described in detail later) and the rebuilding of two of the filters, Phase IV was started here to signify these changes. It continued to August 27, 1974, or to the start of Phase V. New sampling containers were purchased and a more careful sample bottle washing procedure was used starting on this date, so a phase change was felt to be appropriate. Each particular day of filtration was designated as a run. Phase III ran from run 1 to run 50; a new run sequence was started at Phase IV but not at Phase V, so from July 18 to November 2, 1974, a single sequence of runs was used (run 1 to run 99). Rather than report the

results by phase and run number, which is misleading for Phase V since a new run number sequence was not started, the actual number of the day of the year the run was performed will be used to designate the occurrence. For example, Phase III began on May 16 or calendar day no. 136 and the cleanup operations were November 2 or day no. 306. This notation will be used to discuss the results of Phases III through V. Another reason for this choice of notation was the method used to figure averages and to plot data points over the entire testing period. It was simpler to have the abscissa as one continuing sequence rather than as various run and phase numbers.

The flow rate for Phase III was 2.1 gpm/sq ft. The flow rate varied slightly between runs in Phase III but was evenly split between filters in any particular run. At the start of Phase IV and continuing through Phase V, the flow rate was changed to 3.2 gpm/sq ft (7.8 m/hr), a 50% increase. Here again the flow rate between runs was slightly variable. The flow rate for the runs discussed will be presented individually in a later section.

Backwashing. One objective of this study was to compare the effectiveness of three different backwashing procedures. One backwashing procedure was assigned to each filter for the length of the study, and it was not changed although minor changes in duration of the various backwash operations were adjusted as they seemed necessary. Although each filter was backwashed by a different technique, they all were prepared for backwashing by the same series of steps as was used in prior phases.

The dual-media filter was designated for an air-scour cycle and a fluidized waterwash. After some initial experimenting in the first few runs, the following backwash procedure was decided upon for the dual-media filter.

- Step 1. Drain water from above the media to within 1 in. of the surface.
2. Add air at 3 scfm/sq ft (standard cubic ft/min of air at 70 °F and 1 atmosphere pressure) and water at 13 gpm/sq ft in combination until 6 in. below overflow trough.
3. Shut air off and continue water alone wash at 23 gpm/sq ft for 5 min.

There were a few days where the air wash rate was 4 scfm/sq ft, but the above procedure was run as indicated for approximately 2-1/2 weeks. At that point, the water alone wash rate was cut to 21.5 gpm/sq ft, and that change was continued to run 38 (day 183) of Phase III. The following backwashing procedure was the one used from run 38 to the end of the Phase V.

Step 1. Drain down as before.

2. Apply air scour alone at 3 scfm/sq ft for 2 min.
3. Add water at 13 gpm/sq ft in addition to the air until the water is 6 in. below the overflow.
4. Shut off air and continue water at 21.5 gpm/sq ft for 5 min.

The only minor change to the above procedure came at run 32, Phase IV (day no. 232), when the time of the air scour was increased to 5 min and continued to the end of the study.

The mixed-media filter was equipped with a surface and subsurface auxiliary washer. The backwash technique for this filter began by starting the surface washer and continuing it for 2 min. The surface washer was left on, and then the backwash water was started at 15 gpm/sq ft, fluidizing the bed, and followed by the starting of the subsurface washer. The subsurface washer failed to spin at all until the bed became fluidized. After 3 min, the surface and subsurface washers were stopped, thus providing 5 min and 3 min total operating time, respectively. The water alone backwash continued for 4 min to end the cycle. Throughout the first 16 runs of Phase III, the water only backwash lasted for only 2 min, and the water rate used during surface and subsurface washer cycle varied from 13 to 15 gpm/sq ft. However, by run 17, the backwash cycle first mentioned was established and used until run 30 of Phase III. There had been some trouble getting the surface washer to break up the surface mat. The washer was just a little too high to fully agitate the surface of the media. Beginning with run 30 (day 173), a very small amount of backwash water was added during the first 2 min to provide a slight expansion of the bed, enabling the surface washer to do a more effective job.

The coarse sand filter was backwashed with air scour and water simultaneously at washwater rates far below fluidization for the media. The backwashing sequence involved only two steps. The first step applied an air-water combination wash at rates of 7 scfm/sq ft and 9.7 gpm/sq ft, respectively, for 15 min. The second step was a waterwash only cycle at the same rate for 5 min to expel as much air as possible from the media.

Sampling procedures and data collection. Sampling procedures and data collection were similar to those described for Phases I and II, with the following exceptions. An influent composite sampler was in operation during Phases III through V in addition to the effluent samplers which had been in service during prior phases.

Observation runs were conducted two times per week during Phases III through V. As before, an observation run consisted of carefully monitoring and recording of the performance parameters throughout the duration of the run. In most cases, all three filters were observed

up to the point when the head loss reached the splitter box elevation and the filter began bypassing. The run lengths for the dual- and mixed-media filters were much shorter than for the coarse sand media. Therefore, during observation runs, filters were backwashed whenever they reached terminal head loss and put back in service so they would operate at constant rate for the same total amount of operating time as the coarse sand filter. Detailed observations were not continued for these two filters after the first backwashing, but the composite samplers were continued in operation (except during backwashing) to obtain a sample from each filter over the same time period.

### Results - Phases III through V

Visual observations - dual-media filter. The dual-media filter (north filter) showed good backwashing in the first stages of the study. The filter had been in operation five days, day no. 144, before the first mud ball appeared, 6 by 1 in. The small mud balls grew over the next week until the air-water combination wash failed to disperse the surface mat. Since the air-water wash could be run just until the backwash water was near the overflow trough, the bed received approximately 1 min of the combination wash. When the surface mat was thick and highly compacted, this was not enough time to completely break up the mat. However, the air-water wash did provide excellent agitation throughout the entire bed when being applied. The coal and sand were completely mixed after only the short time the combination wash was applied. Complete fluidization was then required to restratify the filter media. With the clean filter media in the first part of this study, the fluidization and stratification was easily accomplished. However, as the size and population of the mud balls increased, jetting action occurred along with dead areas in the bed. Sometimes sand remained mixed with the coal in various areas above excessive mud ball deposits. A typical comment recorded in the data book over the next month of operation was 5 to 6 mud balls, 2 to 3 in. in diameter, excellent air-water wash agitation followed by complete fluidization and restratification. After over a month of operation, two successive days of observations indicated no mud balls present in the dual-media filter. However, the backwash for day no. 177 failed to break up an 8 by 3-in. agglomerate. The agglomeration sunk to the interface, channeling the backwash water around it and producing a "dead" space above it. The following backwashes had similar results with the formation of an increasing number of mud balls and less effective backwashing. Water channeling became common, and cracking was evident 1-1/2 in. into the bed. During the next few days, the top 2 to 3-1/2 in. of media became heavily packed with solids, which made the air-water combination almost totally ineffective. The bed was in extremely poor condition on day no. 181, with numerous dead areas and layers of previous surface mats resting in the coal. On day no. 183 the backwashing procedure was modified in an attempt to improve the condition of the bed.

The new procedure added a step which applied air only. The complete backwashing technique was now 2 min of air scour, air-water wash to just under overflow, and, finally, 5 min of waterwash only. This modification immediately improved the condition of the bed. Since the coal was not so agglomerated now, the air-water wash efficiency was improved as well. It was noted that the action of the air scour alone was most effective during the first 30 sec of application; after that the scouring action was confined to only the top 2 to 3 in. of media. The condition of the bed improved, as indicated by the decreasing number and size of mud balls and agglomerates until on day no. 188, the comment recorded was, "...a few mud balls present but not to any great extent." It would seem the addition of the air-scour cycle improved the bed condition of the dual-media filter. It was at this time, trouble developed with the strainers, and the filter was rebuilt, signaling the commencement of Phase IV.

After the filter was rebuilt, the same backwashing procedure was still used. The first week showed no problems or mud ball formation, rather complete mixing during the combination wash, good fluidization, and very distinct restratification. Small mud balls (2 to 3 in. in diameter) were observed the following week until during the third week of operation large pieces of the surface mat (2 by 6 in.) were observed falling into the bed. Day no. 221 and 222 note large mud balls (3 by 4 in. and 4 by 5 in.) falling to the interface. Typically, along with these large agglomerations, several smaller (1/2 to 1 in.) were noted as well.

On day no. 232, a special backwashing sequence was performed to try and rid the dual-media filter of its high surface layer head loss. The first step of the special backwash was simply the routine backwash procedure combined with turbidity measurements of the dirty washwater collected at 30-sec intervals. After completion of step 1, it was noted there was a considerable amount of gray organic matter on the surface of the filter along with some 2 by 3-in. mud balls 8 in. below the surface. Step 2 of the special backwash was: (a) 5 min of air alone, (b) air-water wash for approximately 30 sec as the water rose to the overflow trough, and (c) 5 min of water alone, all at the same rates as previously used. Six small (1 by 2 in.) mud balls were observed following Step 2. Following this day, the routine backwashing sequence was changed to that of Step 2.

On day no. 235 it was noted that the top 8 in. of fluidized coal were individual grains covered with a hairy, stringy slime. When fluidization was stopped, this 8 in. of media was compacted into the top 2 to 3 in. of media, causing excessive initial head loss. Special observations were made on day no. 241 which described the stringers made of organic matter, 1/16 to 1/8-in. long, and fuzz-like in appearance. A special backwash was conducted on day no. 242 to attempt to correct this problem.

The special backwash consisted mainly of simultaneous air-water wash at low rates for an extended period of time. The media was subjected to 1.5 scfm/sq ft of air and 7.5 gpm/sq ft of water for 21 min. The media that was carried out of the filter was collected in a garbage pail to be replaced later. Samples of the waste backwash water were collected every minute. Figure 44 presents the suspended solids and turbidity for the samples versus the time they were taken. The stringy growths were reduced but not eliminated. The initial head loss for the two days prior to this experiment was 1.19 ft and 1.28 ft, while after this day it was 0.86 ft.

The hairy growths were still a problem five days later, so another special backwash was conducted. The lost media was again collected and returned, and the bed was then restratified. No samples were taken, but these observations were made. The stringy attachments did not appear as long or thick as before; however, the initial head loss following the experiment was 1.38 ft. No positive changes were seen in the condition of the dual-media filter, so chlorination was tried. The filter was drained down to within 1 in. of the surface and 200 ml of household bleach (5.25% sodium hypochlorite by weight) was added, stirred in by air scour, and let set for 10 hr before backwashing. No immediate results were seen. It was at about this time, day no. 255, that a similar stringy coating was noted on the mixed-media filter but in a much milder concentration. This condition was recorded for only a few days for that filter, and day no. 269 was the last day the stringy attachments were mentioned on either of the two filters.

Following the disappearance of the stringy attachments, the operation of the dual-media filter was rather routine to the end of the testing period. The air scour alone provided good mixing and bed agitation for the first minute, then the air passed upward through the bed in a channelized manner, causing little action, except as the air bubbles came out of the bed surface, which violently mixed the top inch of media. The air-water wash accomplished excellent mixing, but the average duration was only 30 sec. Typical mud ball observations were 4 to 5 in number and 1 to 3 in. in size. Every few days the surface mat would be extremely thick, causing pieces of it to tumble down to the sand-coal interface where they would disintegrate or reduce in size.

Visual observations - mixed-media filter. As previously stated, the mixed-media filter was equipped with a surface and subsurface washer. The main observation which relates to mud ball formation and bed condition was to note if the washers were working properly. Following one day of operation, the surface washer turned freely with a 30 psig line pressure. The subsurface washer did not turn, but the jet action of the washer nozzles lifted coal layers within the bed. The next week of operation caused excessive mud ball formation, still without the turning of the subsurface washer. On day no. 146, a booster pump was installed on the water supply to the surface and

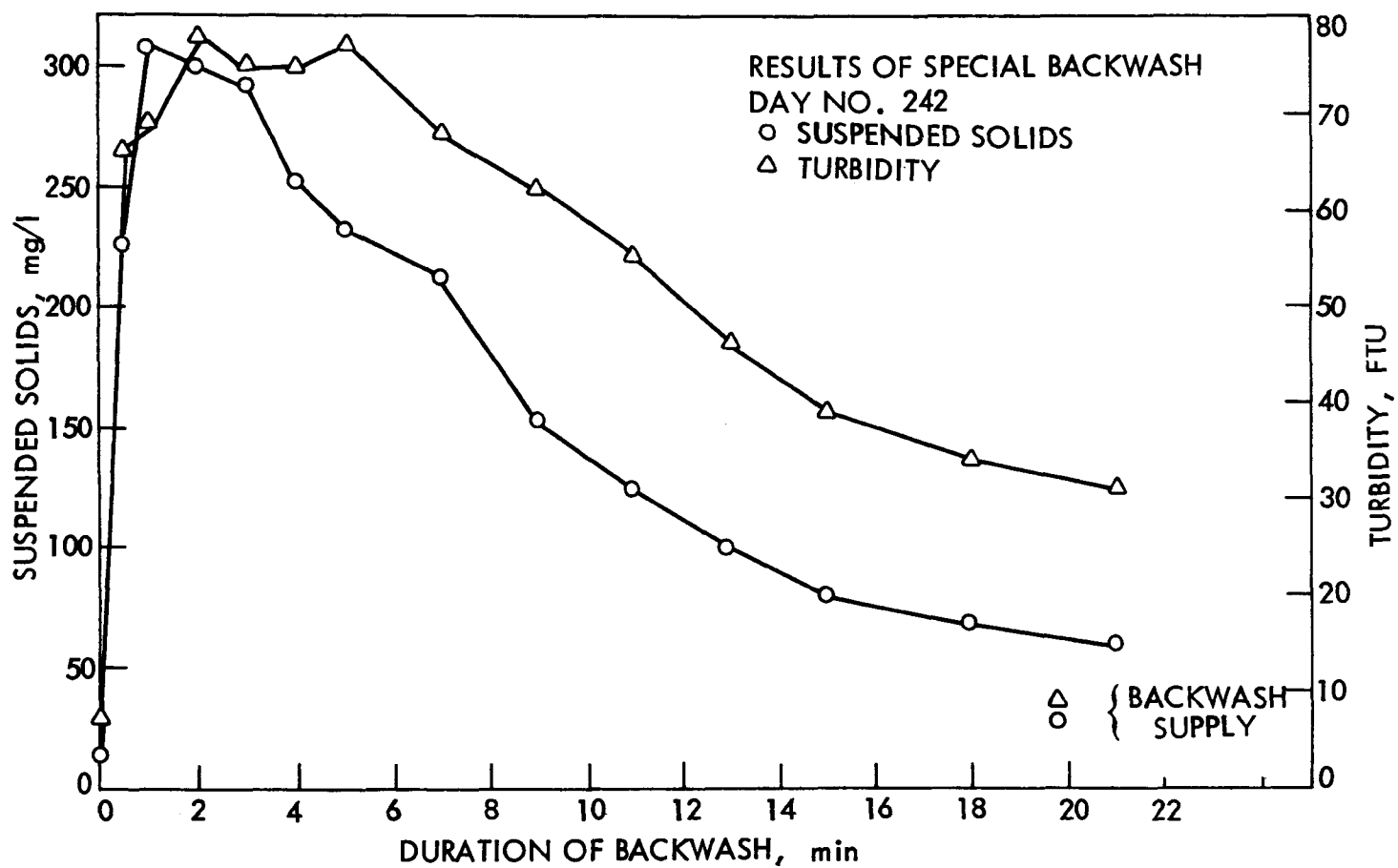


Fig. 44. Results of special backwash, day no. 242.

subsurface washer line to increase the line pressure and possibly free the "hung-up" washers; the line pressure was increased to 60 to 80 psig. This did not solve the problem, and the following day a large 3 by 4-in. agglomerate and 10 to 12 small, 1-in. mud balls were observed. These mud balls fell to the interface and were still not broken up because the subsurface washer was below the interface. Finally, the rubber caps on the subsurface washer were removed and the washer rotated by hand, freeing the washer so that it worked properly for the next two weeks of operation.

The action of the surface washer was described in detail for several observations. The washer violently mixed the top 3 to 4 in. of the coal. Ineffective action was noted in the corners of the filter housing, as could be expected with a rotary washer in a square housing.

Sometimes the surface cake was broken up by this mixing action, while at other times it simply broke into smaller pieces which, upon fluidization, fell into the bed. Also during this same period, considerable amounts of fine silica and garnet sand were observed working their way into the coal layer. The condition of the bed gradually deteriorated until channeling of the backwash water was common and numerous mud balls, 4 to 6 of 2 to 3 in. in diameter, were observed.

On day no. 173, a backwashing procedure change was made to increase the effectiveness of the surface washer. During the surface washer only cycle, a small amount of backwash water was now added to expand the bed so the surface washer was submerged in the top 1 to 2 in. of media. At the low rate of application, the backwash had trouble raising the thick, heavy surface mat to the surface washer, so the ineffective wash was still present at times. The surface washer worked best when the bed was completely fluidized, but since several large mud balls (5 by 2 in., 4 by 2 in., 10 by 2 in.) were observed on day no. 180, complete cleaning of the bed was still not accomplished. Shallow cracks were observed at the top of filter media. Solids penetration into the bed in general was 2 to 4 in. The lower 12 in. of the coal contained silica and garnet sand and was highly agglomerated on day no. 191, just before the filter was rebuilt. Mud balls and agglomerates were so dense that complete fluidization and stratification was not attainable.

The media depths were changed during the rebuilding so the washers were relocated to better coincide with the interface and surface. Also, modifications of the washers themselves were made, with changes in the washer arms and nozzles.

The line pressure was commonly 60 to 80 psig after the modifications, which helped break up mud balls and surface mats in the first few runs. Typically, both the surface and subsurface washers worked well at times if all the water was channeled through each one separately. However, both washers would not turn at the same time unless almost

all of the water went through the subsurface washer; this condition required a very delicate balance and was not reproducible from day to day. The bed remained in good condition for the first two weeks; no mud balls were observed on day no. 210 and 211. Both the washers worked fine in the following days, and on day no. 216, pieces of the surface mat that were not destroyed by the surface washer, fell and were broken up by the subsurface washer. One or two mud balls of 1 to 2 in. in size were typically observed during this period of operation.

For the next several weeks of operation, the equipment worked fine, and a very few small mud balls were observed. Smaller mud balls (less than 1 in. in diameter) were seen floating between the washers, too small to fall down and be broken by the subsurface washer. No cracks were observed, and penetration of solids was estimated at between 4 and 5 in. The media was reported to be very clean for day no. 235, 244, and 247. Both the fluidization and stratification were easily accomplished with the clean, almost mud ball-free media. It was at this time, day no. 256, that the stringy attachments similar to those observed on the dual-media filter were noticed.

A special observation was performed on day no. 241 to document in detail the operational characteristics of the washers. When the surface washer was on by itself, the line pressure was about 70 psig with the washer rotating at approximately 80 rpm. A steady-state revolution condition was hard to maintain when both washers were operating; 27 rpm was typical for both. The subsurface washer alone operated at 75 psig and 27 rpm. The surface washer provided violent agitation to the top 6 in. of media when it was immersed in the fluidized bed, but the water fluidization (only) cycle provided very little action. On day no. 263 trouble with the subsurface washer was noted; only 20 rpm was observed. The surface washer revolved at 100 rpm but was throttled down to 60 rpm for the backwash.

The first night in October, day no. 274, was extremely cold, causing the surface washer booster pump to freeze and split. A used pump was installed, but the washers turned at a slower rate thereafter, and it was feared dirt particles in the replacement pump plugged a portion of the washer nozzles. Because the surface washer turned much slower now and sometimes not at all, mud balls began to develop in the bed. Four to five, 2-in. and 10 to 12 less than 1-in. mud balls were common. In the remaining month of operation several days of no washers rotating or only one of the two washers rotating were noted. The bed condition quickly showed signs of the loss of the auxiliary washers. Finally, on day no. 293, a length of pipe was used to manually reach into the filter and turn the washers. The surface washer was freed quickly, but the subsurface washer failed to turn at all. In the process of trying to free the subsurface washer, the bed was fluidized and stirred for approximately 30 min, breaking up all the

mud balls present. The subsurface washer failed to turn again for the remainder of the study.

Visual observations - coarse sand filter. As previously stated, the coarse sand filter was backwashed for a longer period at wash rates below minimum fluidization velocity. The backwashes were all very similar and rather "dull" as compared to the other two filters. No mud balls were formed, fluidization did not occur, and extensive descriptions of the backwash sequence were not warranted. Very simple, short data notes completely described all the action taking place. The first backwashes provided only 5 min of air-water wash followed by 3 min of water only. The dirt could be seen moving upward and out of the bed. The typical backwash pulsed the top 6 to 8 in. of the bed. Pronounced air channeling causing jetting which mounded the top couple of inches of media and produced an uneven surface for the rest of the study was noted. The mounds moved about during successive backwashes. Early in the study, the air-water wash was changed to 15 min in duration and the waterwash to 5 min. Nine days into Phase III, the bed began to show signs of dirt accumulation.

Dark grey areas were starting throughout the bed except in the top 4 in., which retained their original appearance. The pulsing action was noted in the top 12 to 18 in. as streaks of dirt were seen on the plexiglass window being carried away. The bed cleaned up nicely after each wash, particularly the top 18 in. On day no. 157, darker areas appearing in the bed were reported. A 2 to 3-in. vertical strip along both edges of the window in the corners of the filter box was covered with this matter. The dark patches at the window also started to develop at the two-thirds depth and below. On day no. 165, the dark areas shifted to the lower parts of the filter, covering the bottom 15 in. of media. Penetration of solids into the filter was recorded between 12 and 15 in. on day no. 185. The filter condition remained very constant for the remaining four months of the testing period. The bed cleaned very well with the pulsating action except for the bottom 15 in. of the filter, scattered areas of anaerobic deposits which shifted position as the filter runs progressed, and areas along the corners of the filter box.

A special investigation was conducted to determine if the bottom 15 in. of media showed any progressive increase in initial head loss due to its dirty condition. Figure 45 shows the head loss in the bottom 16 in. of the coarse sand filter. As can readily be seen, no distinct pattern was indicated. The head loss increased when the 50% rate increase was made at the start of Series IV. No definite conclusions can be drawn about this dark 15 in. in the bottom of the filter. A possible explanation could be simply a wall effect in conjunction with the strainers which were located at about 4 in. from the window and 10.5 in. apart. They created a dead space near the walls and between the strainers which received ineffective washing.

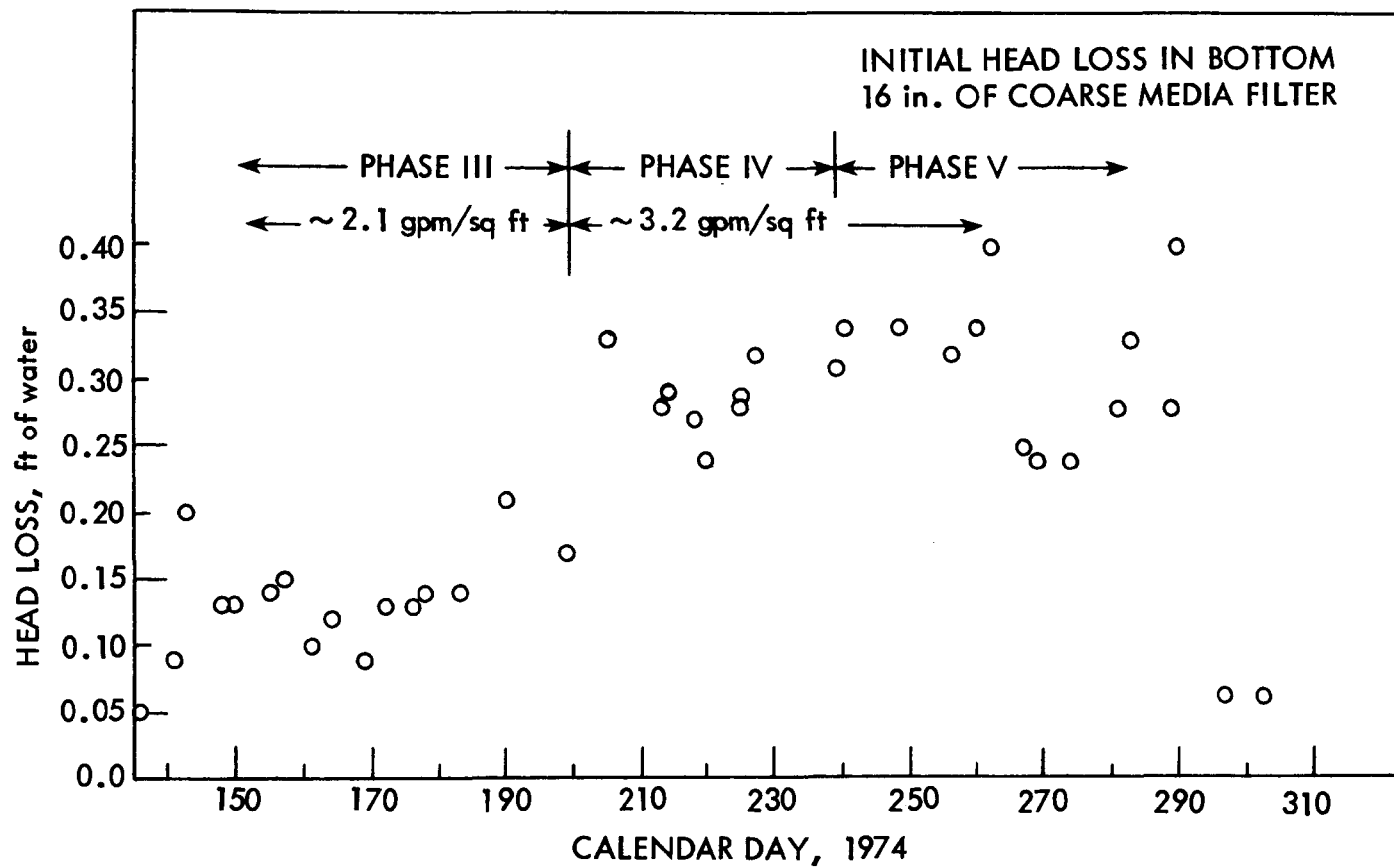


Fig. 45. Initial head loss in bottom 16 in. of coarse media filter, observation runs only.

The visual observation and operation of the coarse sand filter was very routine. However, very late in the study, the left and lower half of the bed became dirtier. By the growth of the dark areas it was obvious the left strainer near the window was partially or fully plugged. The study was terminated due to cold weather without any further changes.

Abrasion tests. The abrasion test was also used in Phases III through V as a direct measure of backwashing effectiveness. The results of the abrasion tests for the entire test period cannot be compared because two different tests were performed. As previously described, Phase III employed a complex, rather long abrasion test procedure while Phases IV and V used a short modified version of the same basic test. For that reason, the abrasion test results for Phase III are presented in Fig. 46 and the results for Phases IV and V in Fig. 47.

An abrasion test was performed on the clean filter media to obtain a control or background level to see if the media itself was being abraded. An unused sample of both the anthracite coal and coarse sand was subjected to the longer abrasion test used for Phase III. First, however, the coal was mixed for 45 min with the abrasion propeller and then flushed with water until the rinse water remained clear. The sand sample was subjected to only the rinsing water before testing. The mixing and rinsing of the filter media prior to the abrasion test was to remove any dust remaining on the media from shipment. The coal and sand samples were then subjected to the abrasion test procedure. The results for the new media using the Phase III procedure were 1.38 mg/g for coal and 0.94 mg/g for sand. Several days later, the same media sampler were again subjected to the abrasion test procedure, yielding 3.17 mg/g and 0.39 mg/g for the coal and sand, respectively. It was this high value, 3.17 mg/g, for the coal that prompted the change of the abrasion test procedure in Phase IV. Too much abrasion of the coal itself was taking place during the 30-min mixing period of the Phase III test procedure. Since the abrasion testing procedure was modified at the start of Phase IV, a new standardization was necessary. Here again, an unused (out-of-bag) sample of both the coal and sand was mixed and flushed as before. The abrasion test results using the new procedure were 0.04 mg/g for coal and 0.018 mg/g for sand.

Despite the fact that the testing procedure was modified during the testing period, the same pattern can be seen for all three series. The abrasion test results for Phase III, Fig. 46, shows the coarse sand filter always had cleaner media than the other two filters. Also, except for the very first and last values, the mixed-media filter was cleaner than the dual-media filter. Furthermore, the graph shows an erratic buildup of solids for the dual-media filter. The coarse sand and mixed-media filters show a rather level result, except that there is some erratic behavior in the mixed-media filter in the latter days of the series. Based on the abrasion test results of

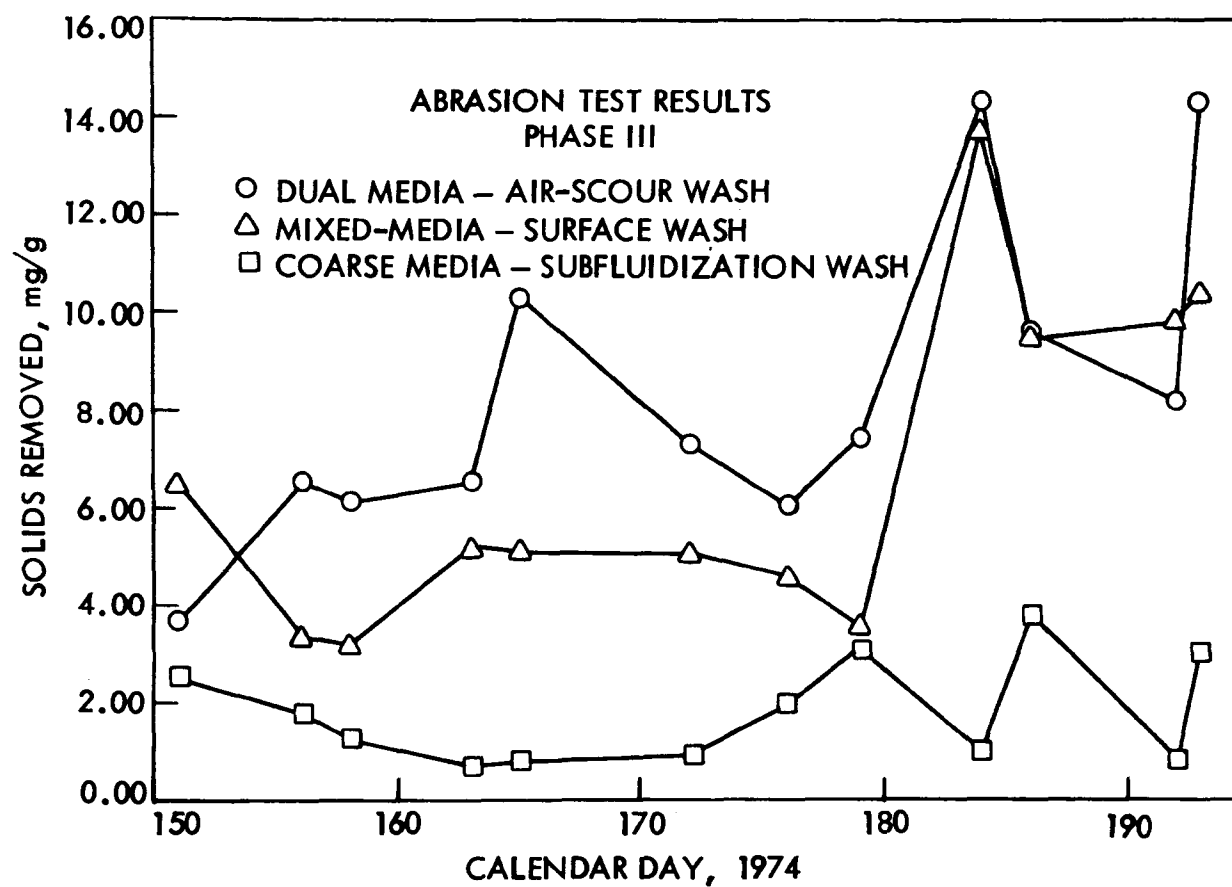


Fig. 46. Standard abrasion test results for Phase III.

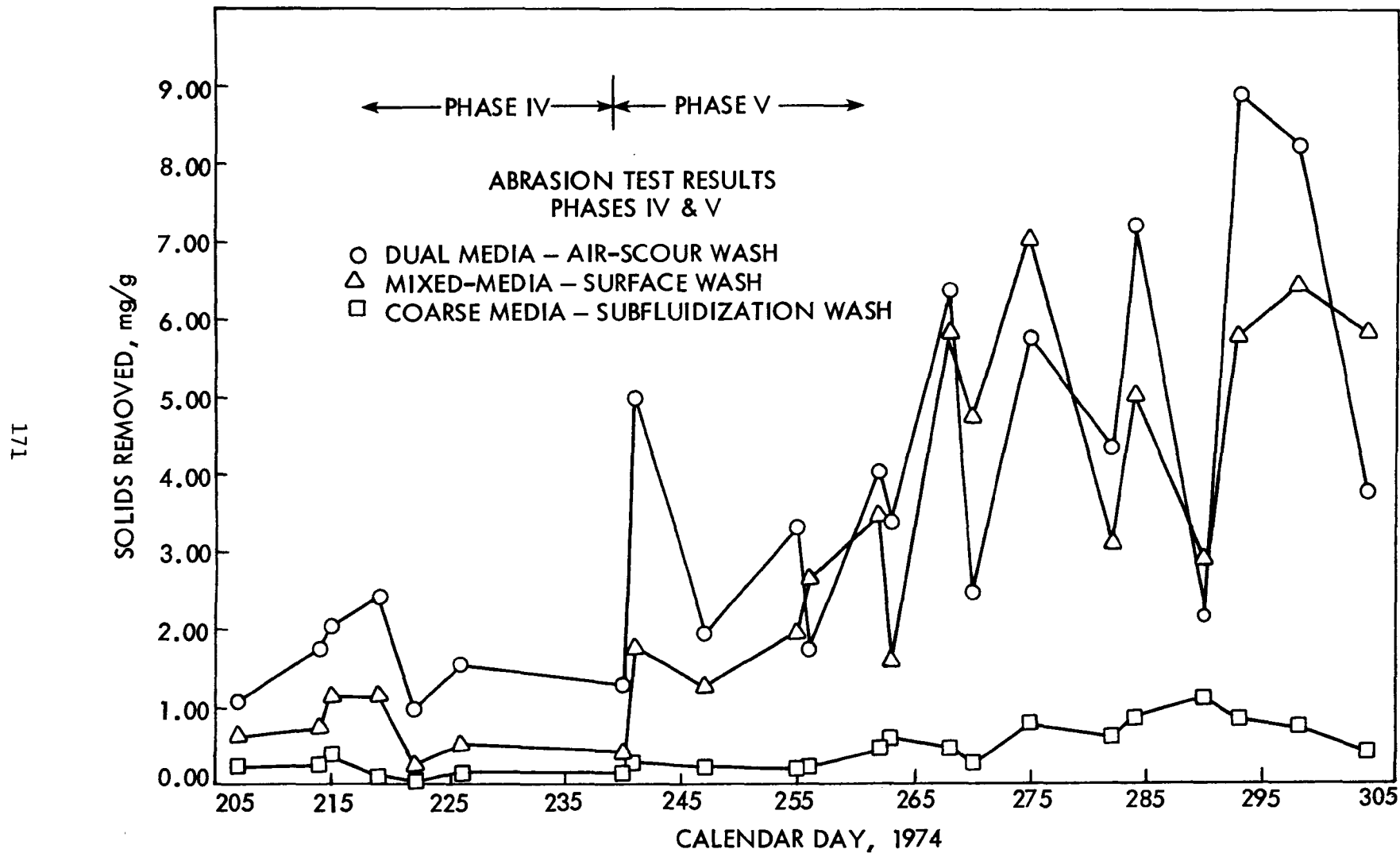


Fig. 47. Standard abrasion test results for Phases IV and V.

Phase III, the simultaneous air and water wash of the coarse sand below fluidization velocities maintains the filter media in cleaner condition than the air scour and water wash for the dual-media filter and the auxiliary surface wash of the mixed-media filter. Also, it would appear the auxiliary surface wash used on the mixed-media filter resulted in better backwashing than the air scour and water wash as used on the dual-media filter up to day no. 180 of the series, and thereafter they were comparable.

The results for Phases IV and V are shown in Fig. 47. The same basic patterns similar to Phase III exist here as well. The simultaneous air and water wash of the coarse sand below fluidization velocities was superior during the entire period of Phases IV and V. During the first half of operating period, up to about day no. 252, the auxiliary surface wash filter maintained a cleaner filter bed than the air scour, fluidized water wash method of backwashing. After that day, the test results vary a great deal. No pattern exists between the dual- and mixed-media filters as before. The only constant aspect of behavior during this period was in the coarse sand filter where very little, if any, buildup of solids is shown by the test results. However, the other two filters and corresponding method of backwashing show a gradual buildup of solids on the media. Some operational difficulties were experienced throughout this period with the surface and subsurface washers, especially after day no. 274. They either turned very slowly or failed to turn at all at times. This might explain the erratic results for the filter using surface and subsurface washers. No explanation can be given to qualify the results for the air-scour, water wash except to say it was caused by the simple failure of the backwashing method to maintain the media in clean condition. The effectiveness of the combined air-water scour on the dual-media filter was no doubt hampered by brief time of application, approximately 30 sec due to the short rise distance from the media to the overflow trough. One can conclude from the abrasion test results that the simultaneous air and water wash below fluidization velocities is the superior backwashing technique. Also, when working properly, the surface and subsurface washer backwashing auxiliary and the air-scour auxiliary as used in the dual-media filter are roughly equivalent in effectiveness, with a possible edge in favor of the former.

Initial head loss. The initial head loss readings throughout the testing period were also recorded in an attempt to evaluate the effectiveness of the three backwashing techniques. The initial head losses were monitored for each day of filter operation. All the readings were standardized by allowing 15 min of filtration before reading the piezometer tubes; later in the testing period they were read after the head loss readings had stabilized, which ordinarily took less than 15 min. Figure 48 graphically displays the initial head loss readings of all the filter observation days and several additional data points for non-observation runs around periods of interest.

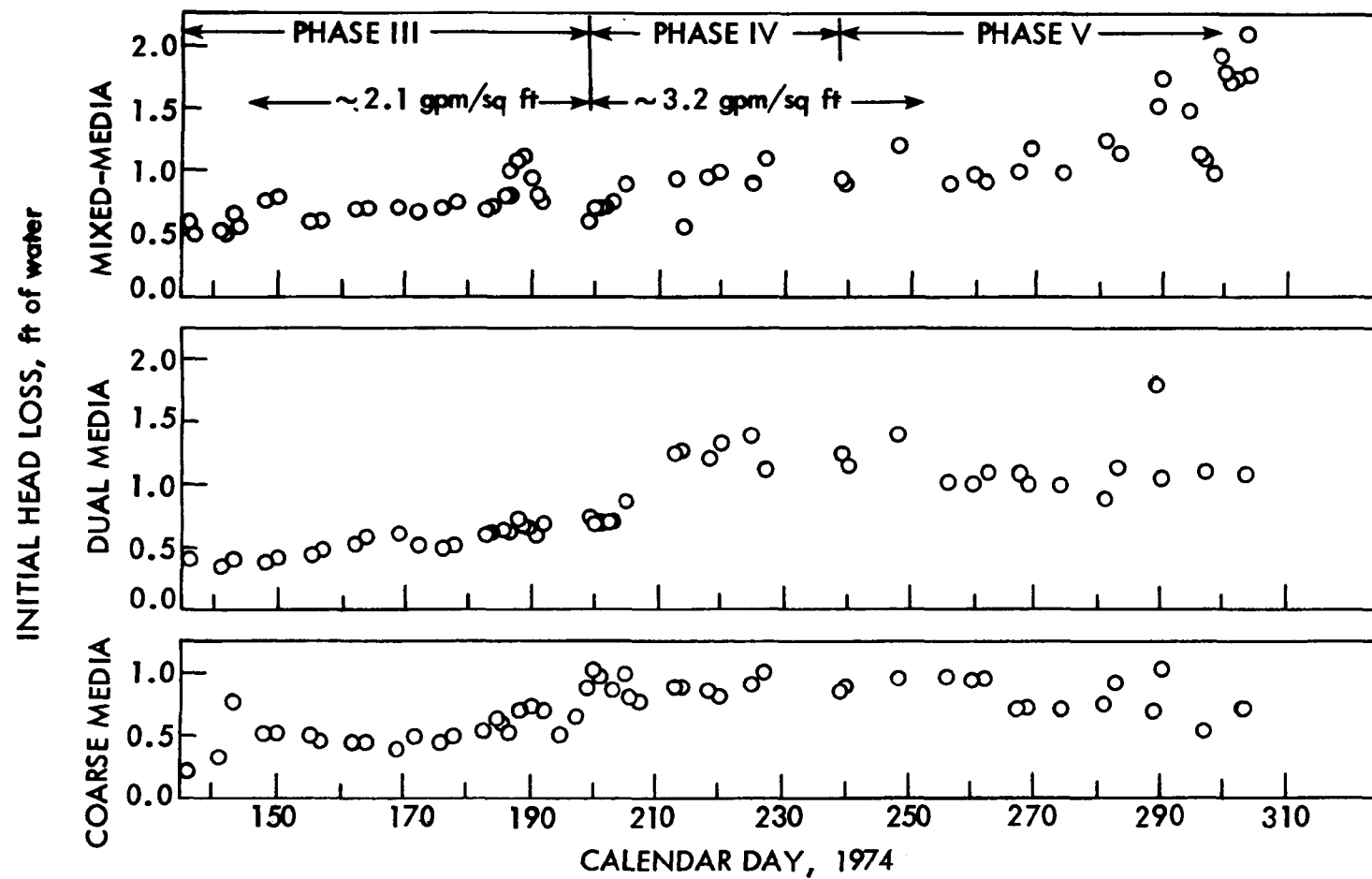


Fig. 48. Initial head loss data for each filter for entire study.

Before one can attempt to evaluate Fig. 48, the reader must be aware of several points. There were several changes between Phase III and the rest of the study. First of all, the media depths and piezometer locations were changed for the dual- and mixed-media filters. Therefore, the points representing the initial head loss in Phase III are not under the exact same conditions as Phases IV and V. For the dual-media filter, the initial head loss represents the head loss across the entire bed, 27 in. that is, from the top of the filter, including 15 in. of coal, 9 in. of sand, and 3 in. of supporting gravel. For the mixed-media filter, the values represent the head loss across the filter bed from 3 in. into the bed to 27 in. into the bed. Inadvertently, there was no piezometer tap above the media bed, so the head loss in the top 3 in. (approximately) of coal was excluded from the measurement. Therefore, the total head loss presented corresponds to the head loss across the 12 in. of coal, 9 in. of sand, and 3 in. of garnet sand below and excludes the head loss in the first 3 in. of coal at the top of the bed. Therefore, valid conclusions or trends can not be made for the mixed-media filter in Phase III. The initial head loss for the coarse sand filter is the head loss across the entire 46 in. of media; there was no change of media or piezometer tap location for this filter throughout the length of the testing period. At the start of Phase IV, new bed depths and piezometer taps were established in the dual- and mixed-media filters. The initial head loss for the dual- and mixed-media filter now corresponds to the head loss across the total bed depth. The media used in Phase III was discarded and new media of the same gradation was installed. Also, the filtration rate was changed from approximately 2.1 gpm/sq ft for Phase III to approximately 3.2 gpm/sq ft for Phases IV and V. Because of these changes, and because of the scatter of the measured values, it is difficult to draw firm conclusions from the initial head loss data.

Several observations can be made of Fig. 48. As stated earlier, an increase in initial head loss is indicative of mud balls and agglomerates due to poor backwashing. During Phases IV and V, when valid trends can be identified because there were no changes in experimental routine, the mixed-media filter with auxiliary surface and sub-surface wash exhibits a more pronounced upward trend, especially at the end of the testing period, than the other two filters. The dual-media filter with air scour and water wash and the coarse sand filter washed below fluidization velocities show little if any buildup in initial head loss. The surface and subsurface wash equipment of the mixed-media filter experienced operational difficulties in the latter stages of Phase V as already discussed. Since the water fluidization backwash alone could not maintain the bed in clean condition, the initial head loss increased. On day no. 293, the filter bed was fluidized and the surface and subsurface washers were turned manually by reaching down into the bed with a length of pipe. The bed was fluidized approximately 30 min, and the washers were turned around 50 times with the washer supply turned on, in an effort to free the washer. In the process, the stirring action broke up all the mud

balls and agglomerates within the bed. This cleaning of the bed corresponds to the drop in initial head loss for the next few days. Since the washers were not freed, the buildup of mud balls returned shortly and continued to the end of the testing period, and the higher values of initial head loss returned. Thus, the rising initial head loss in the mixed-media filter at the end of the study must be attributed to the non-functioning of the surface and subsurface wash auxiliary.

Head loss development. Some typical head loss curves during Phases III through V are presented in Figs. 49 to 55. Only a limited number are presented because they are all very similar in general appearance. The curves show the head loss across various depths of media within the filter bed (with zero depth at the top surface of the media). The initial bed depth of each filter was measured before each run and was used to determine the actual depths of media covering the piezometer taps. Since the initial bed depths varied throughout the study, the depths of media reported on the head loss curves varied as well. All the depths were measured to the nearest 1/4 in. and then rounded to the closest 0.1 in. for presentation. Attention is again called to the inadvertent omission of a piezometer tap above the media in Phase III for the mixed-media filter as is evident from the top head loss curves for that filter during Phase III.

A casual review of the curves shows the marked advantage of the coarse sand filter in terms of run length. Since all three filters were operated at identical filtration rates, production would be directly proportional to the run length. A comparison between the filters with regard to head loss performance can be made in a number of ways, e.g., run length to a given head loss, volume of production per unit increase head loss, or solids capture per unit increase in head loss. The latter method was selected because it can be used to compare filtration studies conducted at different times and on various types of influents and is sometimes used to predict head loss development in filter design [133]. The influent and effluent suspended solids concentrations, run length, flow rate, and the initial and terminal head loss are the operational data needed to calculate a solids capture by the following equation:

$$\text{Solids capture value} \quad \frac{(\text{SS}_{\text{infl}} - \text{SS}_{\text{effl}})(\text{Run length})(\text{Flow rate/unit area})}{(\text{ft}^2/\text{ft of HL})} = \frac{(\text{Head loss increase})}{(\text{Head loss increase})}$$

Table 17 presents average solids capture values for all the observation runs reaching a total head loss of at least 4 ft. Phase IV is omitted from the table because of uncertainty about the suspended solids analysis results and will be discussed later. As would be expected from the head loss curves which have been presented, the coarse sand filter has a higher solids capture value for both series. The average solids capture values for the dual- and mixed-media filters are a factor of two or three times smaller than the coarse sand

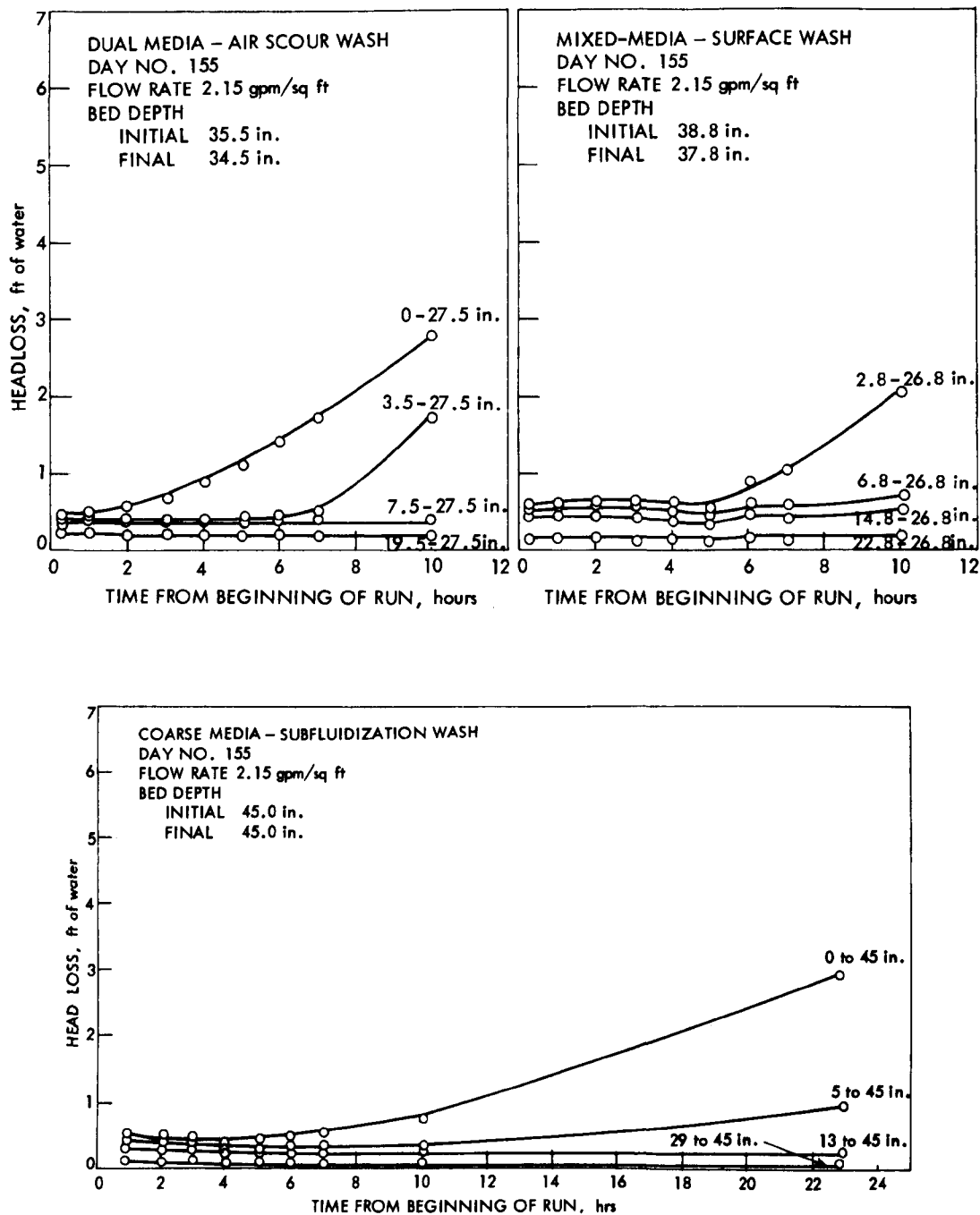


Fig. 49. Chronological head loss development at various media depths, day no. 155, Phase III.

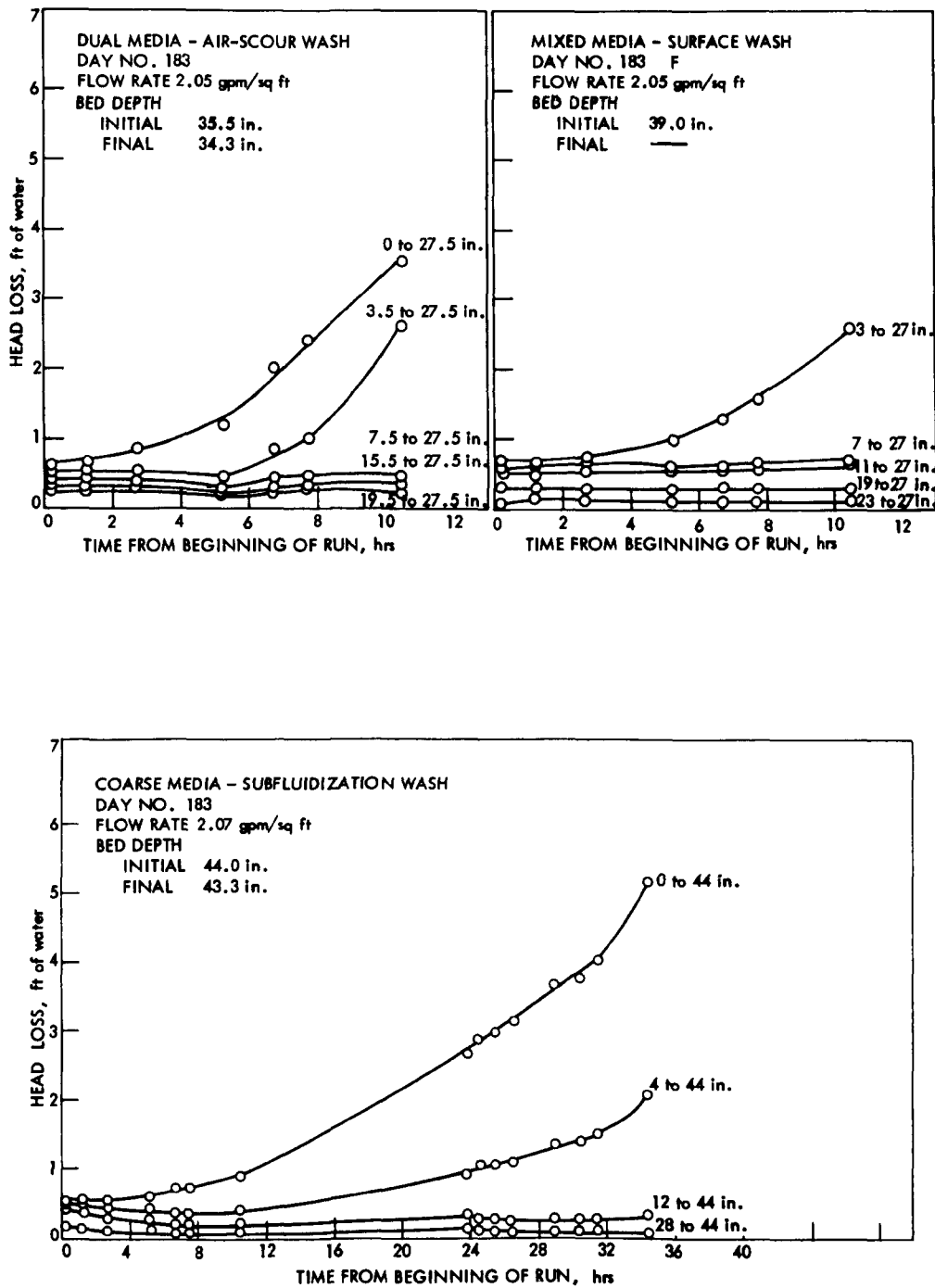


Fig. 50. Chronological head loss development at various media depths, day no. 183, Phase III.

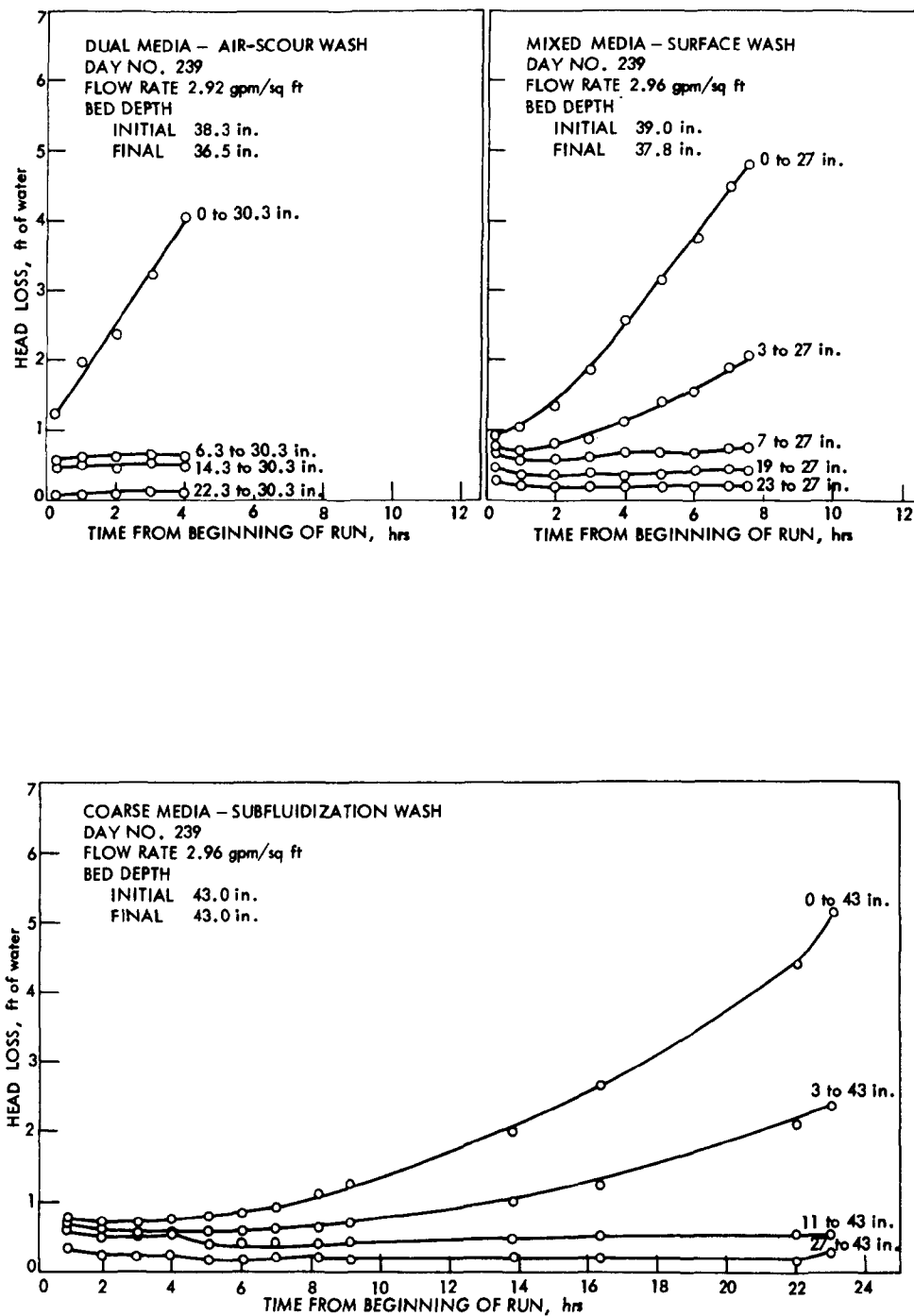


Fig. 51. Chronological head loss development at various media depths, day no. 239, Phase IV.

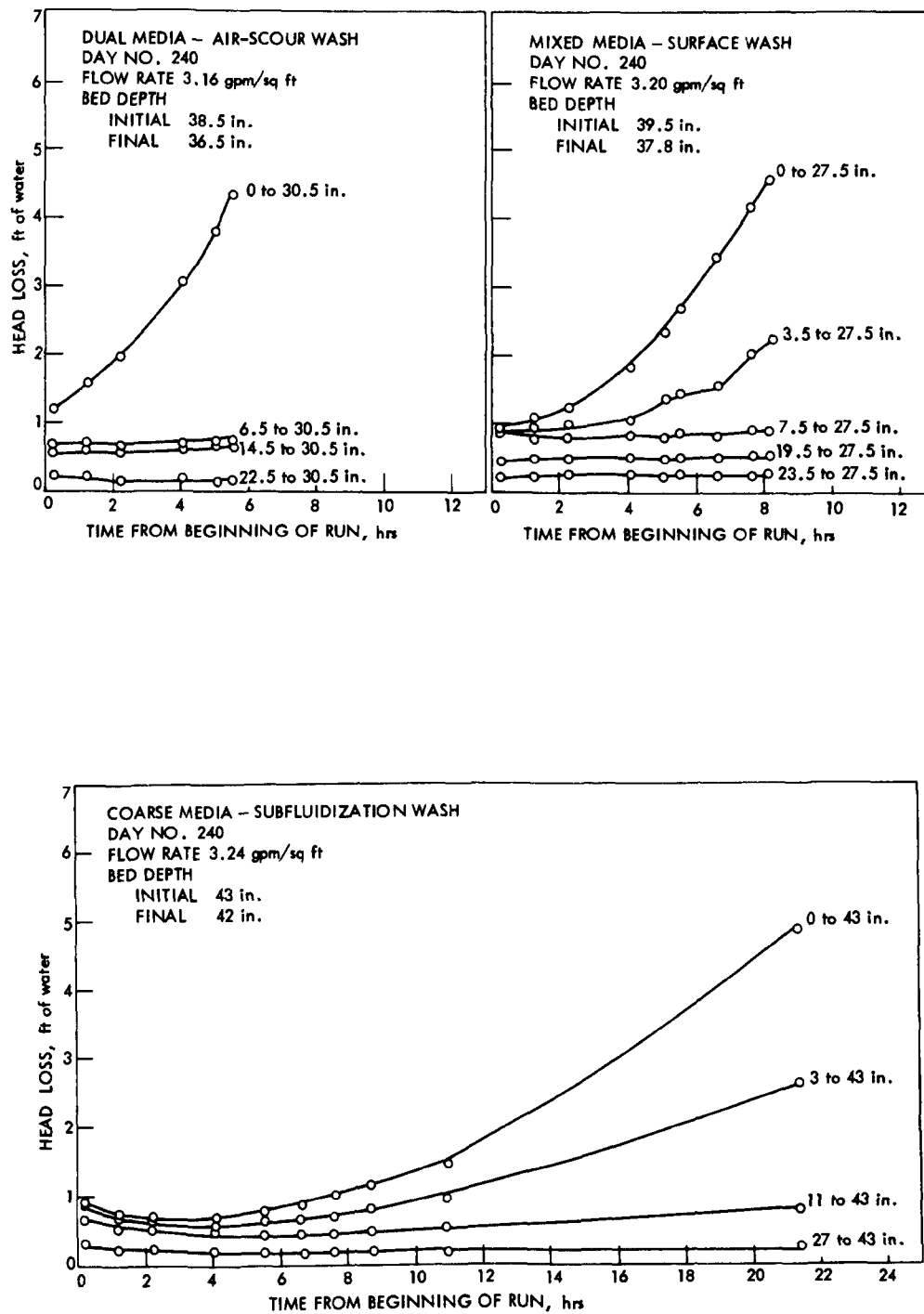


Fig. 52. Chronological head loss development at various media depths, day no. 240, Phase V.

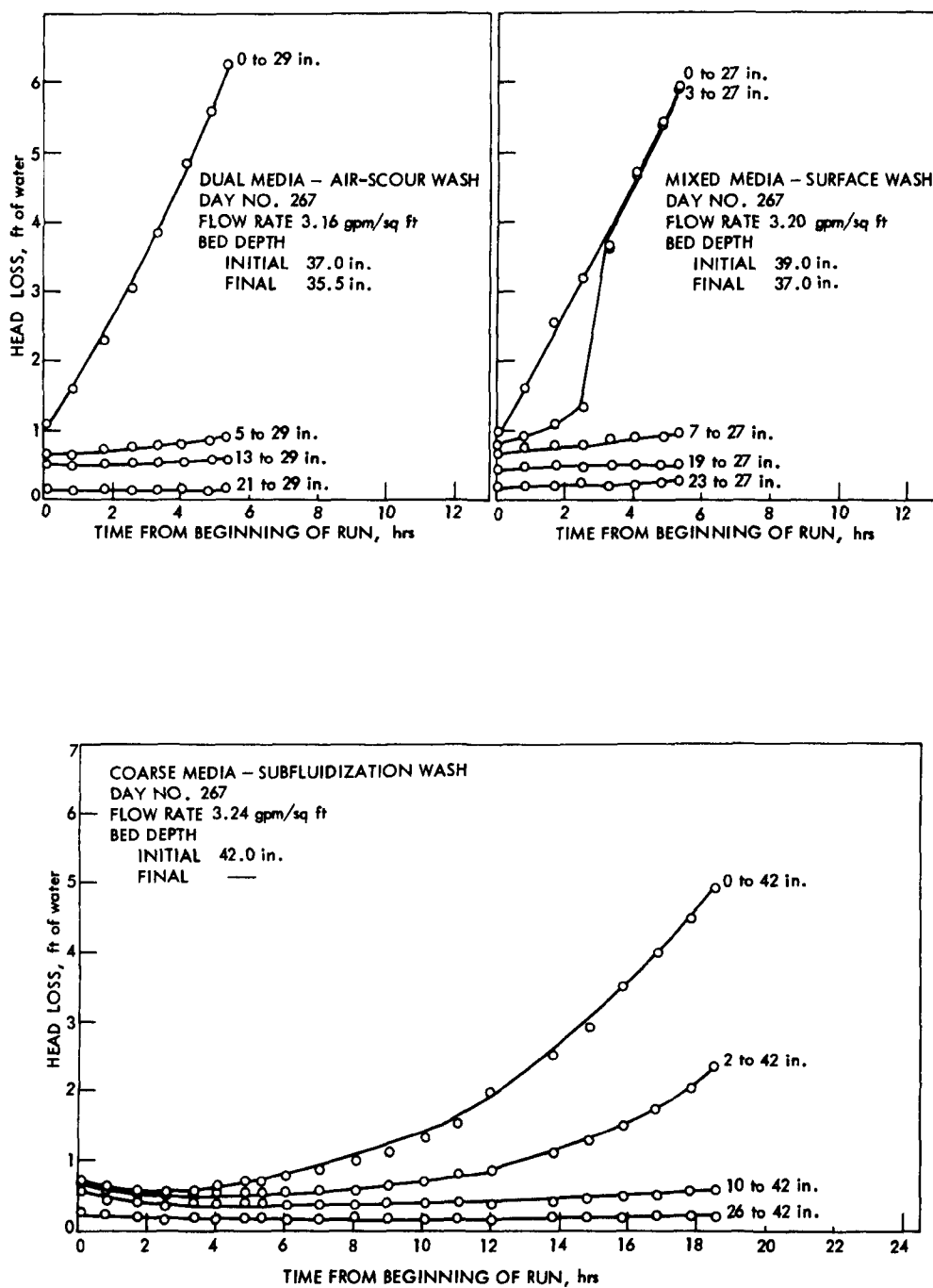


Fig. 53. Chronological head loss development at various media depths, day no. 267, Phase V.

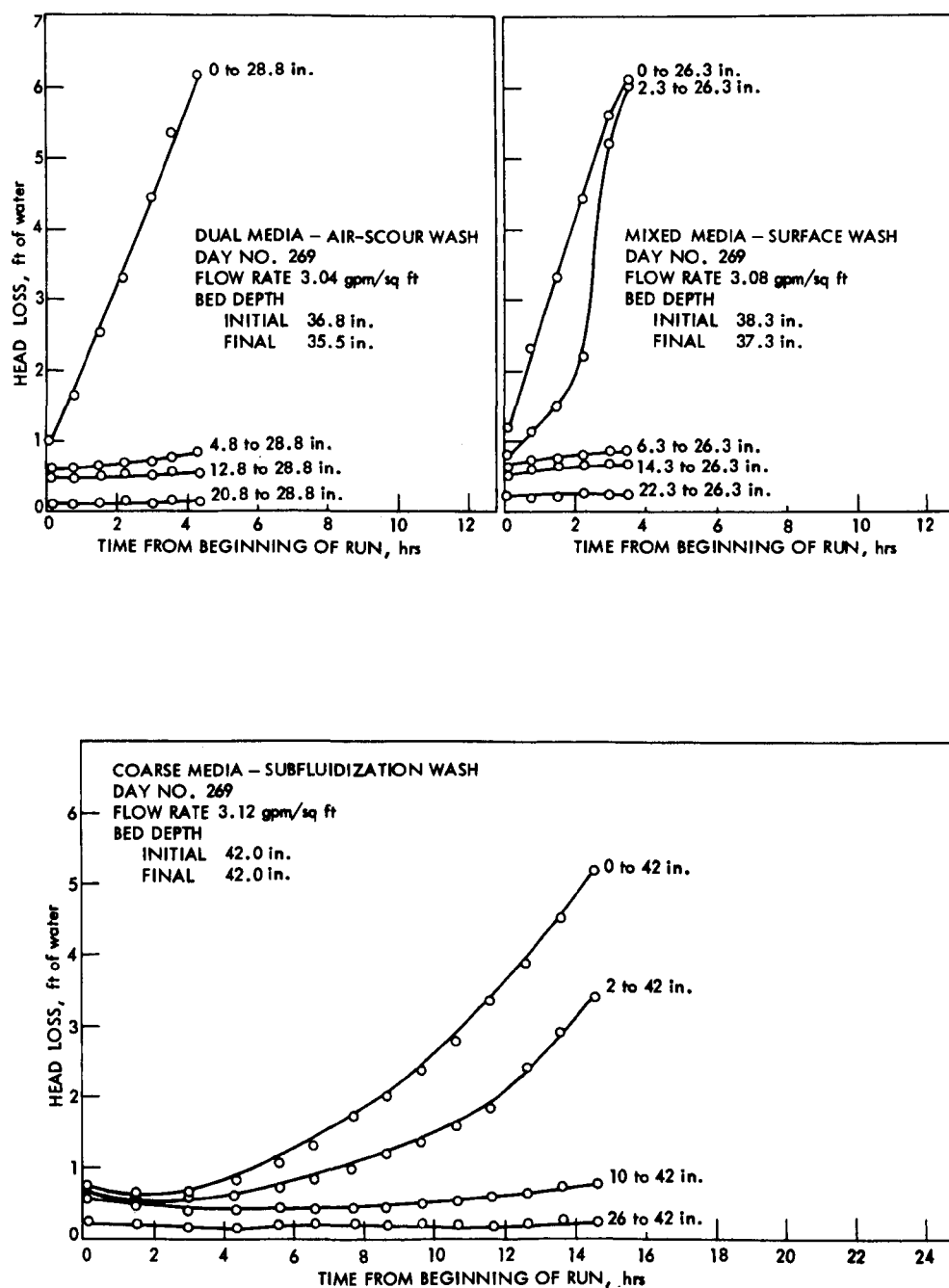


Fig. 54. Chronological head loss development at various media depths, day no. 269, Phase V.

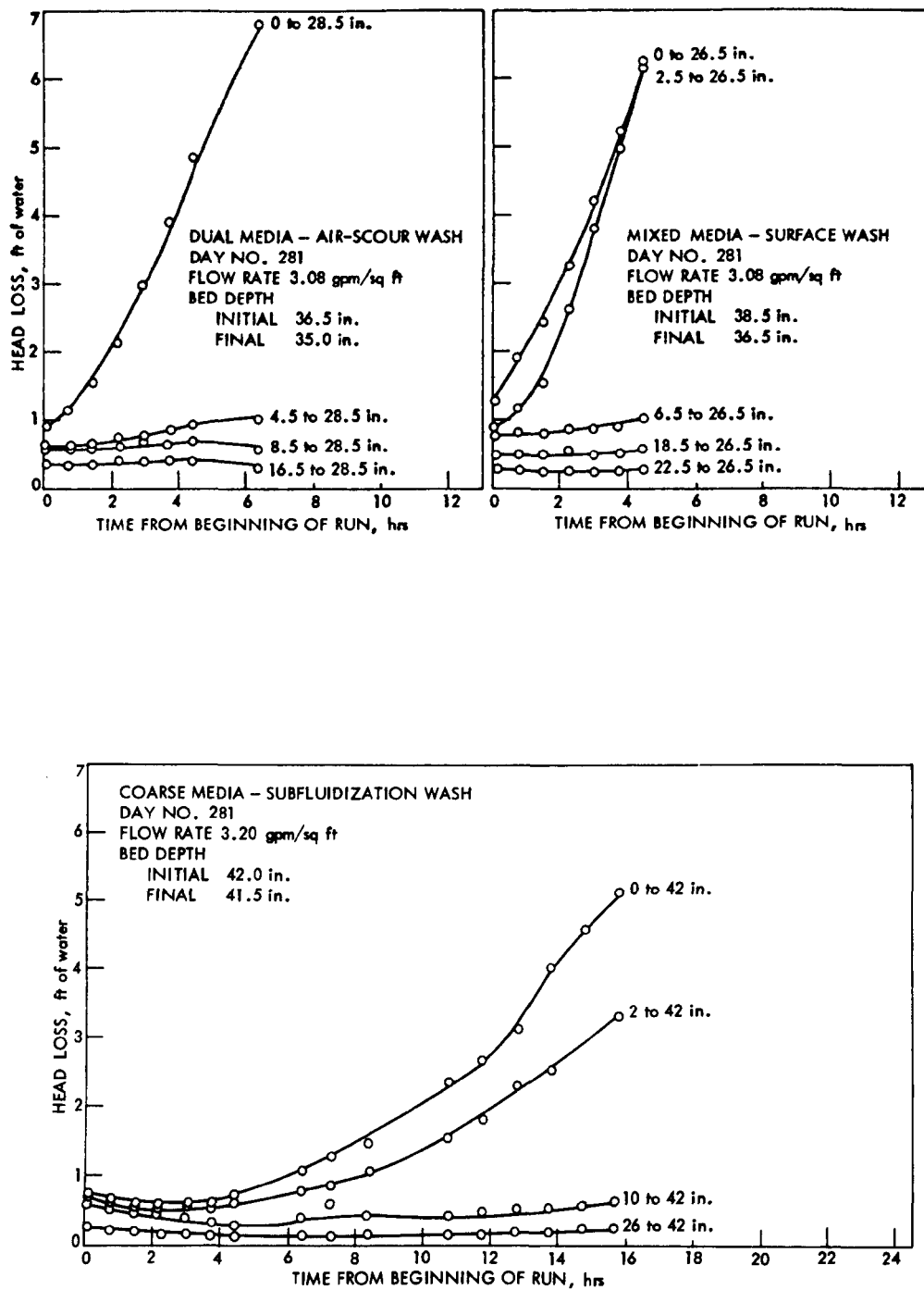


Fig. 55. Chronological head loss development at various media depths, day no. 281, Phase V.

Table 17. Solids capture per unit head loss results for direct filtration of trickling filter effluent, 1974.

	Solids capture value <sup>a</sup>		
	Dual media	Mixed media	Coarse sand
Phase III	0.081	- <sup>b</sup>	0.156
Phase V	0.042	0.038	0.140

<sup>a</sup> lb SS captured/sq ft/ft head loss increase.

<sup>b</sup> Omitted because no piezometer in operation above the media surface during Series III.

filter. This higher value for the coarse sand filter indicates a slower rate of head loss development and longer run lengths than for the dual- and mixed-media filters. The dual- and mixed-media filters were approximately the same in Series V, indicating similar head loss development patterns. Therefore, no conclusion about backwashing effectiveness between these two filters is warranted from the head loss development patterns.

The shape of the head loss curves also is an interesting finding. Most of the curves for the dual- and mixed-media filters show a steep, straight increase (i.e., day no. 269) or an exponential curve (i.e., day no. 240). The exponential curve is indicative of partial surface filtration of compressible solids. The straightline head loss curve found in this study is believed to be caused partly by surface filtration as well, but bed compression and surface cracking clouded the results as discussed in the Phase I results. However, the head loss curves for the coarse sand filter develop at a much slower rate.

An interesting result is shown in Fig. 52 on the head loss curve for the coarse sand filter on day no. 240. The initial head losses were recorded, but as the filtration run progressed the head loss or resistance decreased gradually then increased gradually. This pattern of decrease followed by increase is present in every single head loss curve for the coarse sand filter. One possible explanation for this strange behavior is the following. After the air and water wash is finished, a water only wash is applied to flush out the dirt particles within and above the media and to force out the air remaining in the bed. It was observed that even after this water wash there were a large number of air bubbles still remaining in the bed. The bubbles take up volume, which reduces the available space for water passage, thereby increasing the actual flow rate and initial head loss. It is hypothesized that throughout the filtration run the air is dissolving into the wastewater (which is generally below the

saturation level in oxygen) while the head loss is increasing due to the accumulation of solids. At the beginning of the run the air is dissolving at a faster rate than head loss buildup which would provide an increased filtration area and a lower head loss value. This occurs up to a point where the oxygen is completely dissolved or the rate of dirt accumulation is greater so the head loss development curve would then have an increasing pattern.

Water quality. The means and standard deviations of the various water quality parameters are given in Tables 18 through 20 for Phases III through V. The analytical tests were performed on composite samples of the influent and effluents taken throughout each observation run. Turbidity measurements were taken approximately every two hours for the entire length of the filtration run. All of the values for a particular run were averaged to arrive at one number representing a turbidity value for each observation run. The first six tests reported in the tables, that is, BOD, soluble BOD, suspended solids, TOC, SOC, and turbidity, represent parameters commonly used to measure the removal efficiency of the filters. For these parameters, the average lab test result value, which appears in Tables 18, 19 and 20, was calculated omitting partial data. If the analytical results for any particular observation run were missing a parameter, i.e., BOD, TOC, etc., for one or more filters, then all the other data for that parameter, and run, partial data, were excluded in averaging the lab test results. The remaining parameter averages, that is,  $\text{NH}_4$ ,  $\text{NO}_3$ ,  $\text{NO}_2$ , ORG N,  $\text{OPO}_4$ , and  $\text{TPO}_4$ , were calculated including all the data obtained from the lab tests.

The same sampling containers were used for Phases III and IV. During Phase IV, the lab results seemed erratic, so new sample containers were purchased and more rigorous washing of sample containers was commenced at the beginning with the start of Phase V. It was believed that the old sample containers were not being adequately washed during Phase IV, so the conclusions drawn about filter performance will be based on Phases III and V.

Excluding Phase IV, the coarse sand filter effluent proved to be of slightly, but consistently, poorer quality than the dual- or mixed-media filter effluent. When comparing the dual- and mixed-media filters, no such pattern existed. Comparing just these two filters, virtually half of all the effluent quality tests were low for each filter. Also, because of the small sample number and the large standard deviation, one would be hesitant to declare that even the coarse sand filter produced the poorest effluent quality. The effluent quality data between the filters are close, yet so variable, that no firm conclusions can be drawn concerning performance differences.

Filter bed compression. An additional observation made throughout the study was the amount of compression experienced throughout the filter run. Excessive compression is indicative of dirty filter media caused by inefficient backwashing procedures. When dirt

Table 18. Summary of analytical test results for Phase III.

	Influent	Filter effluent		
		Dual media	Mixed media	Coarse sand
BOD <sub>5</sub> (mg/l) N = 13 <sup>a</sup>	14.61 $\sigma=6.00^b$	3.73 $\sigma=1.72$	4.11 $\sigma=2.03$	4.73 $\sigma=2.56$
Soluble BOD <sub>5</sub> (mg/l) N = 10	3.88 $\sigma=1.79$	1.97 $\sigma=0.96$	2.20 $\sigma=0.99$	2.34 $\sigma=1.11$
Suspended solids (mg/l) N = 14	37.49 $\sigma=12.03$	6.84 $\sigma=3.23$	6.31 $\sigma=3.87$	7.92 $\sigma=5.80$
TOC (mg/l as C) N = 12	12.51 $\sigma=4.53$	8.06 $\sigma=2.24$	8.19 $\sigma=1.87$	7.07 $\sigma=1.88$
SOC (mg/l as C) N = 12	7.54 $\sigma=1.67$	6.97 $\sigma=1.43$	7.21 $\sigma=1.40$	7.44 $\sigma=2.01$
Turbidity (FTU) N = 16	16.38 $\sigma=4.31$	2.38 $\sigma=0.97$	2.20 $\sigma=0.56$	2.89 $\sigma=1.10$
Ammonia (mg/l as N)	4.62 $\sigma=1.77$ N=17	4.48 $\sigma=1.74$ N=17	4.35 $\sigma=1.59$ N=14	4.26 $\sigma=1.99$ N=17
Nitrate (mg/l as N)	5.53 $\sigma=1.21$ N=14	5.92 $\sigma=1.50$ N=14	5.70 $\sigma=1.55$ N=13	5.17 $\sigma=1.41$ N=14
Nitrite (mg/l as N)	0.43 $\sigma=0.11$ N=12	0.68 $\sigma=0.33$ N=12	0.74 $\sigma=0.39$ N=12	0.65 $\sigma=0.34$ N=12
Organic nitrogen (mg/l as N)	0.70 $\sigma=0.42$ N=2	2.30 $\sigma=1.98$ N=2	2.90 $\sigma=2.26$ N=2	4.65 $\sigma=5.16$ N=2
Orthophosphate (mg/l as PO <sub>4</sub> )	10.99 $\sigma=2.79$ N=13	10.18 $\sigma=3.06$ N=13	10.43 $\sigma=3.34$ N=13	10.03 $\sigma=2.88$ N=13
Total phosphate (mg/l as PO <sub>4</sub> )	12.17 $\sigma=3.53$ N=6	9.27 $\sigma=2.92$ N=5	10.60 $\sigma=3.82$ N=6	10.49 $\sigma=3.03$ N=6

<sup>a</sup>N = number of observation runs averaged.<sup>b</sup> $\sigma$  = standard deviation.

Table 19. Summary of analytical test results for Phase IV.

	Influent	Filter effluent		
		Dual media	Mixed media	Coarse sand
BOD <sub>5</sub> (mg/l) N = 8 <sup>a</sup>	17.04 $\sigma=4.21^b$	6.57 $\sigma=5.68$	4.46 $\sigma=2.86$	5.98 $\sigma=2.17$
Soluble BOD (mg/l) N = 8	4.71 $\sigma=1.92$	3.56 $\sigma=2.73$	2.39 $\sigma=0.97$	3.10 $\sigma=1.13$
Suspended solids (mg/l) N = 8	36.41 $\sigma=9.22$	4.34 $\sigma=3.57$	3.11 $\sigma=2.01$	3.96 $\sigma=1.39$
TOC (mg/l) N = 8	11.84 $\sigma=3.86$	7.59 $\sigma=3.82$	8.41 $\sigma=4.05$	9.38 $\sigma=4.17$
SOC (mg/l) N = 8	8.35 $\sigma=3.70$	6.79 $\sigma=2.86$	7.19 $\sigma=3.51$	8.58 $\sigma=4.07$
Turbidity (FTU) N = 8	13.68 $\sigma=3.95$	3.24 $\sigma=2.58$	3.32 $\sigma=2.45$	3.54 $\sigma=1.71$
Ammonia (mg/l as N)	9.41 $\sigma=2.96$ N=8	7.96 $\sigma=3.37$ N=8	8.21 $\sigma=2.61$ N=8	8.79 $\sigma=2.76$ N=8
Nitrate (mg/l as N)	5.71 $\sigma=2.17$ N=3	5.64 $\sigma=1.58$ N=3	6.33 $\sigma=2.30$ N=3	5.07 $\sigma=0.79$ N=3
Nitrite (mg/l as N)	0.46 $\sigma=0.23$ N=3	0.45 $\sigma=0.19$ N=3	0.78 $\sigma=0.59$ N=3	0.28 $\sigma=0.12$ N=3
Organic nitrogen (mg/l as N)	5.87 $\sigma=0.0$ N=1	6.09 $\sigma=0.0$ N=1	5.75 $\sigma=0.0$ N=1	5.58 $\sigma=0.0$ N=1
Orthophosphate (mg/l as PO <sub>4</sub> )	16.16 $\sigma=1.77$ N=3	14.18 $\sigma=1.80$ N=3	15.70 $\sigma=3.09$ N=3	17.50 $\sigma=2.14$ N=3
Total phosphate (mg/l as PO <sub>4</sub> )	18.59 $\sigma=2.56$ N=3	16.58 $\sigma=1.38$ N=3	17.00 $\sigma=3.14$ N=4	18.73 $\sigma=2.46$ N=4

<sup>a</sup> N = number of observation runs averaged.

<sup>b</sup>  $\sigma$  = standard deviation.

Table 20. Summary of analytical test results for Phase V.

	Influent	Filter equipment		
		Dual media	Mixed media	Coarse sand
BOD <sub>5</sub> (mg/l) N = 15 <sup>a</sup>	30.38 <sub>b</sub> $\sigma=14.52$	12.68 $\sigma=6.88$	12.99 $\sigma=6.82$	14.46 $\sigma=6.56$
Soluble BOD <sub>5</sub> (mg/l) N = 15	9.67 $\sigma=3.76$	7.21 $\sigma=3.72$	7.27 $\sigma=3.61$	7.78 $\sigma=3.57$
Suspended solids (mg/l) N=14	34.08 $\sigma=16.87$	7.05 $\sigma=4.27$	6.82 $\sigma=3.10$	9.46 $\sigma=4.53$
TOC (mg/l) N = 10	19.86 $\sigma=8.03$	12.02 $\sigma=4.16$	12.77 $\sigma=3.20$	12.99 $\sigma=3.96$
SOC (mg/l) N = 10	13.41 $\sigma=3.22$	12.00 $\sigma=3.98$	11.83 $\sigma=2.60$	12.98 $\sigma=3.47$
Turbidity (FTU) N = 15	17.60 $\sigma=6.18$	4.80 $\sigma=2.28$	6.78 $\sigma=3.01$	4.66 $\sigma=2.12$
Ammonia (mg/l as N)	21.08 $\sigma=5.30$ N=15	20.00 $\sigma=6.24$ N=15	19.79 $\sigma=5.76$ N=15	20.69 $\sigma=5.47$ N=15
Nitrate (mg/l as N)	3.09 $\sigma=1.77$ N=6	2.84 $\sigma=2.05$ N=6	2.25 $\sigma=1.78$ N=6	2.65 $\sigma=1.27$ N=6
Nitrite (mg/l as N)	0.48 $\sigma=0.24$ N=6	0.52 $\sigma=0.24$ N=6	0.46 $\sigma=0.28$ N=6	0.44 $\sigma=0.15$ N=6
Organic nitrogen (mg/l as N)	2.13 $\sigma=1.28$ N=2	2.17 $\sigma=1.95$ N=2	2.49 $\sigma=1.51$ N=2	1.81 $\sigma=0.65$ N=2
Orthophosphate (mg/l as PO <sub>4</sub> )	24.61 $\sigma=4.17$ N=5	24.67 $\sigma=6.09$ N=5	25.04 $\sigma=5.05$ N=5	25.62 $\sigma=5.14$ N=5
Total phosphate (mg/l as PO <sub>4</sub> )	23.41 $\sigma=0.69$ N=4	20.66 $\sigma=3.10$ N=4	21.31 $\sigma=2.69$ N=4	23.39 $\sigma=0.75$ N=4

<sup>a</sup> N = number of observation runs averaged.<sup>b</sup>  $\sigma$  = standard deviation.

adheres to the filter media, the actual grains do not contact each other but rest upon the dirt layers that surround the grains. As head loss develops during filtration and thus applies a load to the filter bed, these dirt layers compress, which results in a noticeable compression of the entire bed. Clean media show no compression during filtration since the grains touch one another and no compressible layers exist. The head loss developments curves (Figs. 49 through 55) indicate the initial and final depth of the entire filter bed. As can readily be seen, the dual and mixed filters have approximately 1-in. compression in the early stages of the study progressing up to 2-in. compression in Phase V. The coarse sand filter shows no compression at all early in the study, with minor compression later. The recorded compression of the coarse sand filter is less reliable because an uneven surface results from the combined air and water wash below fluidization velocity. Thus, the depths recorded are average depths by visual estimation and subject to greater uncertainty. These observations of compression reinforce the conclusion previously established that the coarse sand filter was cleaner than the other two filters. The dual- and mixed-media filters exhibited roughly comparable degrees of compression, indicating both were in somewhat dirty condition.

Filter cleanup operations. After 170 days or over five months of testing, the three filters were removed from normal service and subjected to clean up operations. All three filters were first subjected to a normal backwashing sequence. This was followed by a new backwashing technique to see if more dirt could be removed from the media. Samples of the dirty backwash water were collected and composited during the new backwash routine. The total solids of the three composite samples were then determined.

The cleanup operation consisted of a prolonged air-water combination wash below fluidization velocities. The water wash rate was 8 gpm/sq ft and the air wash rate was 4 scfm/sq ft. The dual-media filter was the first filter subjected to this new sequence. The filter overflow was collected in a 30-gal. garbage pail to catch the media being washed into the overflow weir. The dirty washwater samples were collected at the weir overflow in the filter. For the first 2 min of backwashing, when samples were taken every 30 sec, approximately 20 ml of sample was composited. After the first 2 min, samples were taken every minute, approximately 40 ml of sample was composited for each collection. This was continued for 13 min until the washwater was quite clear in appearance leaving the filter. Turbidity measurements were attempted on all the samples, but the water was so dirty it was doubtful the readings were within the capabilities of the instrument, and they are therefore not reported. The total solids of three aliquot samples of the washwater composite was measured. The average result of the three aliquot samples for the dual-media filter was 1019 mg/l. The underdrain plate was also removed to see if any sand was evident from leakage through the disturbed gravel. None was evident.

The mixed-media filter was treated to the same cleanup procedure as the dual-media filter. The dirt released in the first few minutes was phenomenal. The water was literally black with solids and described as much dirtier than the dual-media filter. The media quickly worked its way about 6 in. into the gravel. The bed was completely mixed in a few seconds, and as the wash progressed the garnet became more evident throughout the bed. Samples were taken and composited in the same manner as in the dual-media filter but continued for 20 min because it took longer for the washwater to clear up. The 30-sec sample was diluted 10 to 1 and still recorded a 60 FTU turbidity reading, indicating a 600 FTU condition. However, since the turbidity readings were so doubtful, the remaining samples were not measured. The total solids of the washwater composite for the mixed-media filter was 1415 mg/l.

The same backwashing procedure and sampling technique was performed on the coarse media filter except that the air rate was increased to the usual level for that filter (7 scfm/sq ft). The backwash was very similar to those seen throughout the study for that filter and was continued for only 10 min. The discharge water was very clear throughout the wash compared to the dual- and mixed-media filters. The total solids for the coarse media filter was only 616 mg/l. Finally, all three filters were drained and air blown through them in hopes the media could be left through the winter without breaking the plexiglass window. No damage was noted the following spring. Table 21 presents a summary of the data obtained during the filter cleanup operation. As indicated by the visual observations, the

Table 21. Data summary for cleanup operation at the end of the operating period in 1974.

	Duration of special backwash procedure, min	Total solids of composite samples of backwash water, mg/l	Total dirt released, g/sq ft
Dual media	15	1,019	1,041
Mixed media	20	1,415	1,928
Coarse sand	10	616	419

mixed-media filter released the greatest total amount of dirt during the cleanup operation, indicating it was in the dirtiest condition prior to the cleanup. The difference between the filters would have been more dramatically evident if suspended solids analyses had been measured rather than the total solids which were measured inadvertently. The total solids values include soluble inorganic solids estimated at about 300 to 400 mg/l which have nothing to do with the dirt released in the cleanup operation. Nevertheless, the cleanup operation results do show a marked advantage for the simultaneous air

and water backwash of the coarse sand compared to the other two filters. The results also show an advantage of the air-scour auxiliary for the dual-media filter compared to the surface and subsurface auxiliary of the mixed-media filter. This is partly due to release of solids from the gravel layers, and from the inside walls of the mixed-media filter upon the first application of air-water wash, as was also noted in Phase II.

Other backwash design investigations. A number of other observations were made in Phases III through V to try to answer some important design questions related to backwashing. Due to strainer clogging problems in Phases I and II, strainers with coarser slots were used in Phases III through V. These strainers necessitated the use of gravel in the underdrains with the potential problem of gravel movement, especially when air and water backwash were used simultaneously. Unfiltered secondary effluent was used for backwashing. The advantage of this arrangement is that recycled backwash water does not increase the hydraulic load to the filters. The disadvantages are the increased hazard of strainer clogging and the potential effects of the dirtier backwash water on the underdrain gravel. The details of these investigations follow.

Filter influent "feedwater" was used as a backwash supply for all three filters in Phases III through V. That supply was the normal secondary effluent in this case. Two problems arose as a result of this backwash supply.

The first problem arose after 51 days of operation when there was a slight increase in the underdrain pressure for the dual-media filter. Two days later, it exceeded 15 psig (the gage limit) when normally it was approximately 3.5 psig. Only 75% of the backwash rate previously used could be attained even when the control valve was wide open. The next day there was a popping noise, and water streamed upward along one side of the filter during the backwash cycle. Originally, it was thought a nozzle had failed, but closer examination showed a gasket around the underdrain plate had failed.

The media was removed and the nozzles examined. A 1/4-in. thick ring of coal was found around the inside of the nozzle slits. The backplate for the underdrain plenum was removed, and more coal and sand was found. Although no failure had occurred in the mixed-media filter, a similar increase in underdrain pressure led to the same work on that filter. Coal and sand were found there as well. The same modifications and cleanup were performed on that filter also. The coarse sand filter had no evidence of strainer plugging at the time of this incident. The low wash rates were believed to be the reason for this. Late in the Phase V, however, some plugging of one strainer was evident at the window, as reported before.

It was believed that some media had been washed out of the filter and pumped back into the underdrain. Since the influent pump and backwash

waste discharge meet in the same collection box, this was a believable explanation. An apparatus was installed which carried the backwash waste discharge out of the collection box, and no similar problems occurred.

The second problem observed was the accumulation of substantial black solids in the supporting gravel layers of the dual- and multi-media filters and in the bottom 15 in. of the coarse sand filter. It is not possible to attribute the solids solely to the backwash water or to the filtered water reaching those depths. Nevertheless, the gravel layers were very dirty and gravel movement did occur as described in more detail in the following paragraphs.

A double reverse graded gravel underdrain (coarse to fine to coarse) was used in the dual-media filter as previously described to avoid movement from the combined air and water backwash. As previously stated, the double reverse graded underdrain was installed upside down, and the backwashing with air and water simultaneously caused almost immediate mounding of the fine gravel. Excessive mounding required attention, so the media was removed and the gravel was placed correctly in the filter two weeks later. No shifting or mounding of the gravel was noted immediately following or for the next six weeks following the change until a strainer clogging incident completely disrupted the bed. Even larger strainer openings were used in the filter rebuilding (4.5 mm), so a revised gravel support was used to accommodate the larger slots as previously described. No gravel mounding or shifting was observed during the next three weeks. However, some temporary cracks (horizontal, 1/2 by 6 in.) were noticed in the finest gravel layer during backwashing throughout these weeks. At about that time, some of the fine middle gravel escaped to the top of the coarser gravel above. The details of the escape were not observed or recorded, but it may have happened in a single wash, and further progressive escape did not seem to occur. The escaped fine gravel first appeared on the sides, but later it was observed to have moved to the center as well. During backwashing the fine gravel was carried up into the silica sand by jets, and some gravel remained there after fluidization had ceased.

Since the gravel escape and mounding came so suddenly, one would suspect that the desired water wash rate was exceeded during the combination air-water wash cycle. The control valve was a 1/4-turn plug valve, and the flow rate was difficult to control precisely. The data book had no evidence of this, however, and no quick jumps or explosions in the gravel were noted.

Nevertheless, the potential hazard of gravel movement was demonstrated, and the opening of horizontal cracks in the fine gravel during backwashing was recorded. Such cracks in a large filter could result in an upset to the gravel layers. The accumulation of solids in the gravel no doubt contributed to the pressure drop across the

fine gravel during backwashing, and thus to the formation of the cracks.

A conventional graded gravel was used in the mixed-media filter. It proved to be unstable, even though washed with water only at normal backwash rates reported as follows.

Within 20 days, the top fine gravel of the regular graded support gravel was intermixing with the coarse support garnet layer. The migration of the gravel upward and the coarse garnet downward was very pronounced two days later. The coarse garnet progressively worked through 6 in. of gravel while the fine gravel broke through the coarse garnet layer and began mixing with the silica sand. The fine garnet layer between the silica sand and the coarse garnet layer had already mixed up into the silica sand in the first filter wash and effectively disappeared from view. Finally, on day no. 168, after 32 days of operation, the coarse garnet and the top fine gravel were "totally mixed" and mounding. The mounding and shifting caused channeling, leading to more mounding up to the point when the filter was rebuilt due to the strainer clogging incident.

In the very first backwash after rebuilding, coarse garnet migrated into the gravel base until just eight days later mounding of the fine gravel and extensive mixing of the coarse garnet and gravel was noted. Once again, the gravel mounded on the sides as before causing jetting action. On day no. 234 the coarse garnet had worked to within 3 in. of the false bottom. The same reports of coarse garnet and fine gravel migration were recorded to the end of the study. Unlike the double reverse graded gravel, the underdrain problems encountered with the regular gravel were well documented and occurred gradually.

One can draw several wastewater filter design conclusions from the foregoing observations. First, there are inherent dangers in the use of feedwater for backwashing which must be recognized. For example, if gravel is used in the underdrain, and if the backwash water should accidentally contain an unusually high concentration of suspended solids, these solids may be partially removed in the fine gravel. This could result in sufficient pressure drop across the gravel layer to lift the gravel and cause an upset of the gravel.

Second, the double reverse graded gravel design used in the research did not prove adequately stable to resist movement when backwashed with air and feedwater simultaneously. The solids in the backwash water may have contributed to the instability, and the research should be repeated using filtered water for a backwash supply.

Third, the conventional graded gravel support was unstable when washed with feedwater alone. This observation reiterates the weakness of the conventional design reported by prior workers [10,11].

Therefore, the use of underdrain strainers without supporting gravel is a desirable design arrangement, but the use of fine slots of less than 1 mm should be avoided, and feedwater should not be used as a backwash. The advantages of using feedwater do not justify the risks which result therefrom.

#### Summary and Conclusions - Phases III through V

The objectives of the experimental investigations of these phases were to compare the effectiveness of three backwashing techniques on three different types of filters while filtering secondary effluent, and to look at the problems of underdrain strainers and supporting gravel when backwashed with unfiltered secondary effluent. The filters and backwashing techniques were as follows:

1. A dual-media filter backwashed with air scour followed by water fluidization backwash. The filter media was supported on a double reverse graded gravel.
2. A mixed (triple) media backwashed with a surface and subsurface wash auxiliary before and during water fluidization backwash. The filter media was supported on a conventionally graded gravel.
3. A coarse sand media with a deeper bed backwashed with air scour and water simultaneously at subfluidization velocity. This filter was supported directly on the underdrain strainers without the use of gravel.

The experimental data were collected over a five-month period of continuous operation of the filters at the Ames, Iowa, trickling filter plant, using pilot-scale equipment. All three filters were backwashed with unfiltered secondary effluent (i.e., feedwater) throughout the course of the study. The following conclusions resulted from the study.

1. Of the three backwash methods, simultaneous air scour and subfluidization water backwash of the coarse sand media proved to maintain the cleanest filter media based on the abrasion test results, bed compression data, visual observations, and a terminal cleanup operation.
2. The use of air scour and subfluidization water backwash simultaneously on coarse sand media was able to keep the filter bed completely free of mud balls, but there were dirty regions in the bottom 15 in. of the filter and along the vertical corners of the bed. These dirty regions did not impair the functioning of the filter, and those in the corners would be inconsequential in full-scale filters.

3. The surface and subsurface backwash auxiliary in the mixed-media filter and the air-scour auxiliary in the dual-media filter provided equivalent backwashing effectiveness. Both filters experienced mud ball problems and other indications of dirty filter media. Comparing these two methods alone, the air-scoured filter was cleaner based on terminal cleanup observations, whereas the filter with surface and subsurface auxiliary was cleaner based on visual observations of the media and slightly lower abrasion test results.
4. Both the double reverse graded gravel support and the conventional graded gravel proved unstable as used in this research. The work should be repeated using filtered water as a backwash supply before deciding on the suitability of the use of gravel in wastewater filters.
5. Feedwater is not recommended as a backwash water source because of the danger of clogging underdrain strainers and/or gravel. The advantages of using feedwater do not justify the risks which result therefrom.
6. The underdrain orifice or strainer system should have sufficiently large openings so that solids in the backwash water do not cause progressive clogging problems. Media-retaining strainers with slots less than 1 mm are not recommended. This recommendation dictates the use of a sufficiently coarse filter media or supporting gravel to prevent loss of media to the underdrains.
7. Comparing the three filters of this study, the coarse sand filter produced a filtrate slightly poorer in quality than that produced by the dual- and mixed-media filters but provided substantially more filtrate to a common terminal head loss. These differences can not be attributed to the backwashing methods used, but rather to the differences in the filter media.

#### Operation and Results - Phase VI

##### Coarse Sand Filtration of Secondary Effluent

This final research phase was devoted to further studies of coarse sand filters backwashed with air and water simultaneously at subfluidization velocity. The favorable results with one filter of this type in Phases III through V prompted this final phase to answer some additional questions about such filters. It was concluded in Phases III through V that this type of filter and backwashing routine resulted in a cleaner filter bed than the dual- and multi-media beds which were studied. However, there was a layer of dirty sand observed in the bottom of the filter about 15 in. deep. It was also observed that the filtrate was slightly poorer from the coarse sand filter than from the dual- and multi-media filters.

Therefore, Phase VI was conducted to determine (1) the effect of depth of media on the extent of the dirty zone at the bottom of the filter and (2) the effect of depth of media on the filtrate quality.

To study these questions, the three pilot filters were equipped with new filter media of slightly coarser size, with depths of 24, 47, and 60 in. The shallowest filter media was supported on a double reverse graded gravel of revised design to gain further experience on the stability of the gravel when backwashed with air and water simultaneously. The three filters were operated for two months in 1975 filtering secondary effluent at the Ames, Iowa, trickling filter plant. The secondary effluent was used for backwashing throughout Phase VI.

#### Operation - Phase VI

Operating routine and sampling details were identical with Phases III through V. The filters were backwashed every 24 hr. Observation runs were conducted twice each week, with detailed observations recorded and composite samples collected for chemical analysis. Details of media size, gravel gradations, and underdrain strainers have been described previously in the equipment section.

Backwashing. The backwashing routine for the first 35 runs of Phase VI included the simultaneous use of air at 7 scfm/sq ft and water at 8 gpm/sq ft for 15 min followed by water alone at 8 gpm/sq ft for 3 min. This was a slightly lower water flow rate than used in Phases III through V and was selected because this is the normal recommendation of one filter manufacturer who promotes this type of filter in the United States (Dravo Corporation). It was visually evident from the start that the three filters were not as clean after backwashing in Phase VI as the single coarse sand filter had been in Phases III through V. Therefore, beginning with run 36 of Phase VI, the backwash flow rate was increased to 15 gpm/sq ft during both the combination air-water wash and the water wash (alone) which followed. The period of combination wash was reduced to 10 min to maintain the total water usage for each backwash approximately unchanged. This routine continued to the end of Phase VI at run 51.

#### Results - Phase VI

The results of Phase VI will not be presented in as much detail as were prior phases because the objectives were more limited.

Visual observations. The condition of the filter media was observed during and after each backwash. Prior to run 35 (lower rate of water backwash) the condition of the three filters was roughly comparable. The descriptions of the media as reviewed through the plastic window after the backwashes had been completed are characterized by the following comments. The top 6 to 18 in. of the media appeared clean except for dirty strips along the vertical corners of the filters. These strips varied in width from 2 to 5 in. Below the clean area of

the media, the sand was progressively dirtier toward the bottom of the filter. At times, the clean region was not continuous with, for example, a 6-in. clean area at the surface and another similar area a bit deeper, separated by a horizontal dirty region in the bed. Small black anaerobic strips and spots were generally evident but changed position with time in the dirtier regions of the bed. No mud balls were observed on the surface or anywhere within the bed.

The air-water backwash action was described as a feeble pulsing of the top 10 to 15 in. of the bed, which was most noticeable in the first couple of minutes of the air-water backwash.

Due to the relatively dirty condition of the bed reported above, the water backwash rate was increased beginning with run 35, as previously described. The condition of the media improved immediately and continued in a steady good condition for the remainder of the study. The descriptions of the media for all three filters at the completion of each backwash are similar. The media was consistently clean to within 12 to 15 in. of the filter bottom except for dirty strips along the vertical corners of the filter. These strips varied from 0 to 2 in. in width. The bottom 12 in. was quite dirty except for two clean penetrations immediately above the two underdrain strainers closest to the window. One or both of these penetrations would reach nearly to the strainer level at the bottom.

The north filter with supporting gravel was slightly different. The gravel remained dirty for its full 12-in. depth. The clean penetrations above the strainers would reach the gravel surface, but a dirty region between them would reach 6 in. above the gravel.

Small black anaerobic regions were occasionally reported in the dirty strips in the vertical corners of the filter. They were seldom observed in the bottom 12-in. dirty region of any of the three filters.

The air-water backwash action was described as a good pulsing action throughout the bed except for the bottom 12 in. and in the vertical corners. These regions remained dirty as a result.

In view of the marked difference observed before and after run 35, when the rate change was made, some detailed observations of the media movement were made at the end of Phase VI. The water rate was increased stepwise from 8 to 20 gpm/sq ft. The media action was carefully recorded.

The general behavior was an increase in the vigor and extent of pulsing as the water rate was increased. In addition, and more importantly, it was noted that a circulation of the sand occurred and that the rate and the circulation increased with the water flow rate. Apparently, the rising air and water moved sand up in the center of the bed, because the sand was observed to move down slowly at the

window. The observed details at different rates are summarized in Table 22.

Table 22. Action of simultaneous air and water backwash on coarse sand at subfluidization velocities.<sup>a</sup> (Air rate = 8 scfm/sq ft for all observations.)

Water rate, gpm/sq ft	Action of media
8	Slight pulsing on right side in top 3 ft. No downward circulation patterns.
10	A bit more vigorous pulsing in a little wider zone on right side in the top 4 ft of the bed. No downward circulation patterns.
12	Pulsing full width of bed in top 1 ft, in left side of top 3 ft and in right side of top 4.5 ft. Very slow downward media circulation in the center at about 0.5 in/min.
15	Pulsing about same as at 12 gpm/sq ft. Downward circulation of media over entire width (except for 2-in. wide strips at corners) at a rate of 2 to 3 in./min. Movement downward continues to 18 in. from the bottom.
20	Similar but faster action with downward circulation of media at 4 to 10 in./min., the lower rate observed where the rising pulsations are more pronounced.

<sup>a</sup>As observed in a 1.5 by 1.5 ft filter with 5 ft of sand and 2.5 to 3.7-mm size, water temp = 21°C. No fluidization of the bed was observed at any of the flow rates in the table.

It is believed that this circulation of media is essential for good cleaning because it moves the media periodically through regions of intense upward pulsing and movement in which the better cleaning action occurs.

At the completion of the observations reported in Table 22, the sand was removed from the filters, with special attention to the conditions in the bottom dirty region of the bed. It was noted that circular zones of clean media were found directly above the five strainers in the dirty region of the bed. In the north filter with gravel support, the above pattern was noted from about 3 to 10 in. above the gravel. In the west filter, without gravel, it was noted about 12 in.

from the bottom of the filter. No details were reported for the south filter. It was difficult to tell the upper extent of the zone because part of the sand fell out of the filter spontaneously when the back plate of the filter box was removed to facilitate removal of the sand.

It was also noted that some filter sand had escaped into the under-drain plenum in the west and south filters, which were not equipped with gravel. About two pounds was reported in the west filter. This observation is not surprising since these filters had strainers with 4.5-mm slots, and the media was 2.5 to 3.7 mm in size range. In fact, it is surprising that more media did not move downward through the strainers. The use of the 4.5-mm strainer for this sand was an oversight; it should not have been used.

Underdrain gravel stability. The double reverse graded gravel in the north filter again proved to be not completely stable. On about 40% of the backwashes, a horizontal crack was observed to open in the finest gravel layer at the beginning of the air-water backwash. The thickness of the crack varied from 1/8 to 3/4 in. and the length from a few inches to the full width of the filter. It generally contracted as the wash proceeded.

The gravel did not upset in Phase VI as it had in Phase IV, but the potential for upset remains evident in these observations. Therefore, the prior conclusions drawn from Phases III through V about the use of gravel in filters washed with air and feedwater simultaneously remain unchanged.

Water quality. Fewer water quality parameters were measured in Phase VI than in previous phases due to budget limitations. The means and standard deviations for the analyses of the composite samples are reported in Table 23. There was no apparent difference between the performance of the three filters of different depth. There appears to be a very slight advantage in the 60-in. depth as measured by suspended solids and turbidity, but it would be impossible to prove it statistically.

By comparing the values of each run using a ranked analysis, some reinforcement of that conclusion is obtained. In this analysis, the rank of 1 is assigned to the lowest value, the rank of 2 to the middle value, and the rank of 3 to the highest value for a particular filter run. Comparing the turbidity values in this fashion, the 60-in. deep filter had seven lowest, three middle, and one highest value for a total score of 16. The 24-in. filter had a total score of 22, and the 47-in. filter a total score of 28. The 24-in. filter was supported on 12 in. of gravel in a rather dirty condition, which may have contributed to the filtration and resulted in its exceeding the performance of the 47-in. filter. Using a ranked analysis in the manner above also placed the 60-in. filter in first position in suspended solids removed and BOD<sub>5</sub> removed.

Table 23. Results of analyses during direct filtration of secondary effluent (Phase VI) from June 24 through August 2, 1975, using course sand filters of different depths.

	Filter influent	Filter effluent <sup>a</sup>		
		N filter, 24-in. depth <sup>b</sup>	W filter, 47-in. depth	S filter, 60-in. depth
Suspended solids (mg/l)	31.3	5.9	6.4	5.7
$\sigma$ (N = 11) <sup>c</sup>	9.7	2.1	2.3	1.8
Turbidity (FTU)	12.6	3.30	3.38	3.14
$\sigma$ (N = 11)	3.14	1.21	1.14	1.14
BOD <sub>5</sub> (mg/l)	15.6	6.5	7.1	6.6
$\sigma$ (N = 11)	4.7	2.8	2.5	2.5
Soluble BOD <sub>5</sub> (mg/l)	5.3	3.9	4.0	3.8
$\sigma$ (N = 11)	1.7	1.3	1.3	1.3

<sup>a</sup>Filtration rate 3.0 gpm/sq ft.

<sup>b</sup>Filtrate from 24 in. of sand and 12 in. of supporting gravel.

<sup>c</sup> $\sigma$  = standard deviation, N = number of observations.

Looking at the mean values in Table 23, one must conclude, however, that there was little gained by using the deeper media. In the filtration of secondary effluent, one would need to use alternate approaches to reach a higher quality filtrate, either chemical pre-treatment or a finer filter media. Deeper media should prolong the period of acceptable filtrate if higher filtration rates and/or terminal head losses had been used. In this work, however, deterioration of the effluent at the end of the filter run was not observed on any of the filters.

Head loss patterns and initial head loss. The shape of the head loss development curves in Phase VI were very similar to those observed for the coarse sand filter in Phases III through V. Therefore, no additional curves are presented for Phase VI. Furthermore, there was no apparent difference between the curves for the three filters of different depth in Phase VI, except for a different initial head loss. As expected, the initial head loss was higher for the deepest filter since they were all operated at the same filtration rate.

An analysis of the head loss developed to a common time for each observation run is summarized in Table 24. A total of 11 observation runs are included, the same 11 runs for which water quality data were

Table 24. Mean total head loss during filtration of secondary effluent on coarse sand filters during Phase VI.

	N filter, 24 in. sand <sup>a</sup>	W filter, 47 in. sand	S filter, 60 in. sand
Mean total head loss <sup>b</sup> , ft	4.49	4.35	4.54
$\sigma$	0.48	0.55	0.49

<sup>a</sup>Head loss includes 12 in. supporting gravel.

<sup>b</sup>Head loss for an average run length of 16.18 hours ( $\sigma = 1.89$  hours).

presented in Table 23. It is apparent that very little difference in head loss was observed between the three filters. This would be expected since they have the same media size and the suspended solids removed was nearly the same for three filters, as shown previously.

The initial head loss for the three filters was different due to the different depths of media. One observation of interest is the change in initial head loss that occurred when the backwash flow rate was increased after run 35. The average initial head loss values for a few filter runs before and after the change in backwash rate are presented in Table 25.

Table 25. Average initial head loss for three coarse sand filters before and after run 35 in Phase VI, when increase of backwash rate was adopted.

Period	N filter, 24 in. sand <sup>a</sup>	W-filter, 47 in. sand	S filter, 60 in. sand
Runs 26-34 (inclusive)	0.84 <sup>b</sup> $\sigma=0.07$	0.89 $\sigma=0.04$	1.15 $\sigma=0.09$
Runs 36-42 (inclusive)	0.45 $\sigma=0.03$	0.55 $\sigma=0.00$	0.69 $\sigma=0.03$
Runs 43-47 (inclusive)	0.64 $\sigma=0.04$	0.64 $\sigma=0.07$	0.82 $\sigma=0.05$

<sup>a</sup>Head loss includes 12 in. of supporting gravel.

<sup>b</sup>All values in feet.

It is clearly evident from Table 25 that a marked reduction in initial head loss occurred at the higher backwash rate. This indicates that the bed was somewhat dirty before the change and that the new backwash routine achieved a cleaner bed.

There was again some deterioration indicated by the initial head loss in the later runs of Phase VI, but the series was not continued long enough to see if that trend continued.

It would be desirable to compare these initial head loss data with values for the clean media at the beginning of Phase VI. Unfortunately, the operating routine used prior to Run 26 was not such as to obtain reliable initial head loss data. This weakness did not influence the head loss data for the bulk of each run, only the initial value recorded.

The mean removal of suspended solids, the mean run length and increase in head loss (total head loss - initial) and the filtration rate were used to calculate the solids capture value as explained in the Phase III through V discussion. The average value for all these filters in Phase VI is 0.16 lb SS captured/sq ft/ft of head loss increase. This value compares favorably with the value obtained in Phases III and V in Table 17.

Media loss in air-water backwashing. The primary advantages of coarse sand filters washed with air and water are (1) more effective backwash and (2) lower headloss development, and thus longer filter runs. The primary danger of this type of filter and backwash is the potential loss of media which can occur during overflow due to the violence of the air-water action.

Some preliminary observations on this question were made in the laboratory using a 5.5-in. diameter filter column of transparent plastic construction. Sands of two sizes were observed in the column while being washed with air and water simultaneously at various rates. The sand depth was 24 in. The height to which the sand grains were thrown by the backwash was observed visually. This was admittedly difficult to judge because of the presence of the air bubbles and the violence of the motion.

The results of the observation are summarized in Table 26 for the two sand sizes. The data are admittedly very limited and should be repeated covering a broader range of flow rates and media sizes. They are presented here for the record, merely to call attention to the danger of media loss, and the need for adequate distance from the media to the overflow in the filter design.

No loss of sand was observed during the two months of observation of the three filters in Phase VI. No loss was expected because of the large distance which existed from bed surface to overflow, a minimum of 3 ft in the filter with 5 ft of media.

Table 26. Height that sand is thrown by simultaneous air and water backwash.

Water rate, gpm/sq ft	Air rate, scfm/sq ft	Height sand thrown above bed surface, in.	
		1 to 2-mm sand, in.	2 to 3.6-mm sand, in.
2	4	11-12	nil
2	8	12-13	nil
4	4	11-12	5-6
4	8	13-14	5-6
6	4	15-16	5-6
6	8	16-17	5-6

Some small loss of media appeared to have occurred in prior Phases III through V on the single course sand filter then in use. During five months of operation, the recorded depths of filter media decreased 2 to 3 in. The uneven surface of the sand made the surface depth measurement difficult, and thus the loss reported above is only approximate. The distance from bed surface to overflow in Phases III through V was only about 12 in. In view of this reported loss, a distance of more than 12 in. should be provided with 2 to 3.6-mm sand to prevent loss.

#### Summary and Conclusions - Phase VI

The objectives of the experimental investigation of Phase VI were to observe the effect of depth of media on the backwashing effectiveness of deep coarse sand filters washed with air and water simultaneously and to observe the effect of depth on filtrate quality. Three pilot filters were operated in parallel while filtering secondary effluent at the Ames, Iowa, trickling filter plant. The filters were equipped with 24 in., 47 in., and 60 in. of coarse sand in a size range of 2.5 to 3.7 mm. Double reverse graded gravel was used to support the sand in the filter with 24 in. of sand. All three filters were backwashed with secondary effluent (i.e., feedwater) throughout the two-month period of operation.

The following conclusions have resulted from the investigations in Phase VI:

1. A backwash routine including simultaneous use of air at 7 scfm/sq ft and water at 8 gpm/sq ft for 15 min was not effective in keeping the filter sand in clean condition.
2. A backwash routine including the simultaneous use of air at 7 scfm/sq ft and water at 15 gpm/sq ft for 10 min was effective in keeping the filter sand in clean condition except for about

a 12-in. layer at the bottom of the filters. The extent of this dirty layer at the bottom was independent of the depth of media and probably is a function of the underdrain strainer type and spacing.

3. In backwashing of coarse sand filters with air and water simultaneously, the rates of flow of air and water should be selected to ensure that a modest circulation of the sand occurs in the filter, upward above the underdrain strainers and downward between the strainers.
4. The filtrate quality produced by the three filters of different depth was nearly the same when filtering secondary effluent. Thus, one cannot achieve much improvement in filtrate quality with such filters and feedwater merely by increasing the depth of media.
5. The double reverse graded gravel backwashed with feedwater proved somewhat unstable again in Phase VI, and the prior conclusions about the suitability of feedwater and gravel are thus unchanged as a result of the Phase VI experiments.
6. The principal advantages of coarse sand filters washed with air and water simultaneously were again demonstrated in this phase, namely, lower head loss development and thus greater solids capture per unit head loss development, and better backwash effectiveness. The principal hazard in this backwash arrangement is the potential loss of filter media during backwash overflow due to the violence of the air-water action. Adequate freeboard must be provided and the rates of air and water flow must be selected to ensure no loss of media.

## IX. EXPANSION AND INTERMIXING OF MULTI-MEDIA FILTERS

### Introduction

Granular filters are widely used for water treatment and are gaining importance for tertiary treatment of wastewater because of the recent higher effluent quality standards. In a conventional single-media rapid sand filter, the sand particles are hydraulically graded during backwashing, resulting in the finest particles being in the upper layer. This stratification remains after backwashing. In a stratified filter bed, the pore openings between the particles vary directly with the particle size. Because of this, most of the material removed by the filter during filtration is at or near the surface of the filter. An ideal filter would have this stratification reversed so that the pore size would be the largest in the top layer and steadily decrease in size to the bottom layer of the filter. The recent development of multi-media filters with media of anthracite coal, silica sand, and garnet sand approach this ideal pore size arrangement. The densities of these three media vary with the anthracite coal having the lowest density, the garnet sand the highest density, and the silica sand between the two extremes. The average particle sizes of the anthracite coal, silica sand, and garnet sands are selected to decrease in that respective order. With proper selection of particle sizes, the filter will stratify with the anthracite coal on the top, the garnet sand on the bottom, and the silica sand in the middle. Although the pore size may increase with depth within each individual media, the overall effect will be a decrease in pore size of the filter with increasing depth. This decrease in overall pore size with increased depth will greatly increase the penetration of filterable solids into the filter bed, thereby increasing utilization of the filter bed and extending the filter run length, hopefully without detriment to the filtrate quality.

With the addition of anthracite coal and garnet sand in dual and multi-media filters, new problems have arisen. What degree of expansion of the individual media will provide optimum cleaning during backwashing? Is there an optimum degree of intermixing at the interface of the individual media? Can the degree of intermixing of the media be predicted and controlled through selection of backwashing rate and media size?

The specific aims of this research are fourfold:

1. to evaluate the effectiveness of existing expansion models for predicting the expansion of garnet sand, silica sand, and coal, and to suggest new or modified models if necessary,
2. to test the validity and sensitivity of two available models for the prediction of intermixing between silica and garnet sands, and between coal and silica sands,

3. to observe the fixed-bed hydraulic profiles of various coal and sand filters selected to produce different amounts of intermixing in order to study the effect of the intermixing on the permeability of the intermixed zone of the filter, and
4. to observe the effect of interfacial intermixing on the performance of dual-media filters.

### Dual-Media and Multi-Media Filtration Literature

#### Media Design Characteristics

Baylis et al. [3] gave these typical dual-media design characteristics. Sand medium usually has an effective size (ES) of 0.40 to 0.55 mm and a uniformity coefficient (UC) of 1.3 to 1.7. The sand medium should be clean and well graded and have a specific gravity greater than 2.65. The depth of the sand bed is normally 6 to 12 in. The top 1/2 in. or more of sand is usually removed after hydraulic grading to prevent the head loss at the surface from being excessive. Similarly, the anthracite coal layer usually has an effective size of 0.8 to 1.2 mm, a uniformity coefficient of 1.3 to 1.7, a specific gravity greater than 1.5, and a hardness factor on the MOH scale between 2.0 and 3.5. The coal medium should be clean and free of all thin or scaly pieces, often prevalent in smaller sized coal particles. Depth of the coal medium is partially dependent on the uniformity coefficient.

According to Camp [24], the top layer of anthracite coal has interstitial spaces approximately 20% greater in volume than those of the top sand layer. The larger void capacity of coal absorbed more solids per volume of filter medium. As a consequence, Camp [24] successfully used filtration rates up to 6 gpm/sq ft and achieved longer filtration runs. Walker [137] suggested a dual-media filter is best designed by first choosing a favorable coal size for filtering the influent water. The sand size should be chosen to complement the coal size.

Baylis et al. [3] considered that the coal layer should contain the bulk of the filtering capacity. The sand layer was then used to further polish the water after it had passed the coal layer. Coal particles should not be present at the bottom of the sand layer since larger pore spaces occur around the coal particles. These large pore spaces lessen the effectiveness of the sand layer as a good filter.

#### Observed Intermixing in Dual-Media Filters

Conley [32] found that the intermixing of coal and sand avoided the rapid buildup of head loss at the interface, while acceptable water quality was still achieved. Camp [23] disagreed with Conley [32] by recommending a non-intermixed filter and suggesting that the good water quality results obtained by Conley were due to excellent

chemical control. According to Camp [23], removal of suspended solids was more efficient if the fine sand was not intermixed with the coarse anthracite coal.

Later, Robeck and Kreissl [103] studied the effect of intermixing in coal and sand filters at Erie, Pennsylvania. They considered intermixing beneficial for increasing the run length. They demonstrated that run lengths increased with increasing size of the surface coal. This was achieved by removing the coal finer than 1.0 mm from the source medium.

The amount of intermixing at the interface was studied by using hydraulic profiles of three different graded-media filters. The dual-media filter contained 18 in. of 1.14-mm ES coal and 6 in. of 0.43-mm ES sand, while the two, single-media filters contained 24 in. of 0.75-mm ES coal and 24-in. of 0.43-mm ES sand, respectively. The coal and sand media were unskimmed, and both created a large head loss at the surface. Limited data concerning the hydraulic profiles through the three filter beds were presented for downflow with clean water. Cumulative head losses were 1.83 ft for the unskimmed coal, 4.75 ft for the unskimmed sand, and 2.50 ft for the dual-media filter at 14.5 gpm/sq ft. The intermixing zone depth could be determined since the hydraulic profiles gave evidence that the head loss per unit depth gradually increased from the coal to sand layer through a 6-in. bed depth. Robeck and Kreissl [103] also showed that permeability in the upper sand layer can be controlled by varying either media to produce different amounts of intermixing or by varying the backwashing shutdown procedure. An instantaneous shutdown shifted the level of maximum head loss upwards 2 in. from the level of maximum head loss for the slow shutdown. In addition, the instantaneous shutdown gave a greater maximum head loss. Thus, the instantaneous shutdown gave less available capacity.

Brosman and Malina [19] studied intermixing of dual-media filters made from 18 in. of 0.43-mm ES silica sand having a UC of 1.32 and a specific gravity of 2.64; and 6 in. of 1.00-mm ES anthracite coal having a UC of 1.40 and a specific gravity of 1.77. Four of the many conclusions were: (1) intermixing gave more uniform bed porosity with depth; (2) increased intermixing decreased head loss at the interface; (3) increased initial downflow head loss accompanied increased backwash rate and shorter backwash valve closure time for intermixed filters; and (4) greater size ratios of anthracite to sand gave greater intermixing. The intermixing zone was defined as the filter length which has, within each infinitesimal section, quantities of media equalling at least 20% of the dry weight of each medium. Intermixing was not considered to have occurred if the intermixing zone was less than 5% of the total bed height since flow patterns and bed instabilities probably caused any observed intermixing.

Brosman and Malina [19], in studying filter performance, concluded that intermixing in dual-media filters resulted in longer filter

runs, more uniform head loss with depth, and better filtrate quality. However, in the opinion of the authors of the present report, this conclusion may not be valid because the initial cumulative head losses in the various dual-media filters were unequal; thus valid comparisons of filter performance were impossible.

### Backwashing of Granular Filters

Since the advent of the rapid sand filters around the turn of the century, the study of hydraulics of the filtration process has progressed. The prediction of the expansion of granular filters during backwashing usually was approached from an extension of filtration hydraulics.

This extension of the fixed-bed hydraulics to a fluidized bed is subject to challenge from a theoretical viewpoint. In filtration or fixed-bed conditions, the particles are not free to move about; while in the fluidized state, they are suspended in the fluid and free to move about with little if any contact with other particles for two-phase, liquid-solid fluidization. However, expansion of the filter media is seldom greater than 50%. Because of this relatively low degree of expansion, the extension of the fixed-bed hydraulics to the fluidized bed has provided models that provide results which are agreeable with the experimental results [24,29,46].

Recently, Amirtharajah [5] has shown that the optimum porosity for effective cleaning of silica sand by water backwash is approximately 70%. Expansion required to achieve this porosity would be dependent upon the initial porosity ratio of the bed and the expansion-flow rate characteristics of the graded media. For a graded bed of silica sand, the required expansion would be approximately 45% to expand the top layer of the bed, where most of the filtered solids are retained, to a porosity of about 70%.

### Flow through a Fixed Bed

Many of the sanitary engineering models for prediction of bed expansion and some of the expressions for determining the minimum fluidization velocity of granular beds are based in part on equations describing flow through a fixed granular bed. Fair, Geyer, and Okun [46] present the classical Kozeny equation for head loss through a granular bed for laminar flow as,

$$\frac{h}{l} = k \cdot \frac{\mu}{\rho g} \cdot \frac{(1 - \epsilon)^2}{\epsilon^3} \cdot \left(\frac{6}{\psi d}\right)^2 \cdot v \quad (17)$$

where:

$h$  = loss of head

$l$  = depth of bed

$k$  = Kozeny's constant

$g$  = acceleration due to gravity

$\mu$  = viscosity of the fluid

$\rho$  = mass density of the fluid

$V$  = superficial velocity of the fluid above the bed

$\epsilon$  = porosity

$d$  = particle diameter = diameter of equivalent volume spheres

$\psi$  = sphericity - defined as the ratio of the surface of an equivalent volume sphere to the actual surface area of the particle.

From Coulson and Richardson [33 (p. 7)], Carmen modified the Kozeny equation to apply to transitional and turbulent flow. This equation is commonly called the Kozeny-Carmen equation,

$$\frac{h}{l} = \frac{R_1}{\rho(V')^2} \cdot \frac{(1 - \epsilon)}{\epsilon^3} \cdot \frac{6}{d} \cdot \frac{V^2}{g} \quad (18)$$

where:

$R_1$  = drag force per unit area of particle surface in the direction of flow motion

$V'$  =  $\frac{V}{\epsilon}$  = velocity of the fluid in the pore openings

$$\frac{R_1}{\rho(V')^2} = 5 \text{Re}_1^{-1} + 0.4 \text{Re}_1^{-0.1}$$

and

$\text{Re}_1$  = modified Reynold's number =  $[V\rho/(1 - \epsilon)\mu][d/6]$  which uses specific surface ( $d/6$ ) for the diameter term.

Another equation that describes head loss through fixed granular beds in the laminar, transitional, and turbulent ranges was developed by Ergun [23,40] (Clark, Viessman, and Hammer [29, p. 368] incorrectly called Eq. (19) the Carmen-Kozeny equation).

$$\frac{h}{L} = f_1 \cdot \left(\frac{1}{d}\right) \cdot \frac{(1 - \epsilon)}{\epsilon^3} \cdot \frac{v^2}{g} \quad (19)$$

where:

$$f_1 = \text{dimensionless friction factor} = 150 \frac{(1 - \epsilon)}{Re} + 1.75$$

and

$$Re = \text{Reynold's number} = \frac{\rho V d}{\mu}.$$

### Sanitary Engineering Bed Expansion Models

In sanitary engineering practice, three different approaches used for predicting expansion are of particular interest.

Two of the approaches are given by Fair, Geyer, and Okun [46, Sect. 27, p. 19].

The Kozeny equation [Eq. (17)] and the constant head loss equation [Eq. (1)] can be equated and solved for the porosity terms resulting in,

$$\frac{\epsilon_{e_i}^3}{(1 - \epsilon_{e_i})} = k_e \cdot \frac{\mu}{g(\rho_s - \rho)} \cdot v \cdot \left(\frac{6}{\psi d_i}\right)^2 \quad (20)$$

where:

$k_e$  = Kozeny's constant which assumes a value at about 4 for a fluidized bed of low expansion.

Subscript 'i' denotes the 'i'th layer of the bed.

The ratio of the expanded height,  $l_{e_i}$ , to the unexpanded height,  $l_{o_i}$ , is from Eq. (2),

$$\frac{l_{e_i}}{l_{o_i}} = \frac{(1 - \epsilon_{o_i})}{(1 - \epsilon_{e_i})}$$

and the total expanded bed height  $L_e$  is

$$L_e = \sum \ell_{e_i} = \sum_{i=1}^n \ell_{o_i} \frac{(1 - \epsilon_{o_i})}{(1 - \epsilon_{e_i})} \quad (21)$$

Alternatively, they presented the experimental correlation,

$$\frac{V}{V_s} = \epsilon^{5.0} \quad (22)$$

where:

$V_s$  = unhindered settling velocity of a particle.

The porosity of individual layers can be determined for a given backwashing flow rate, and the total expansion of the bed can then be determined from Eq. (21).

The third approach to filter backwashing was developed by Camp [24]. Working with the Kozeny equation [Eq. (17)], the constant head loss equation [Eq. (1)], and a modified form of the Darcy-Weisbach formula, he developed a dimensionless backwashing number,  $B$ , which is a constant for a given layer of a granular filter,

$$B = \frac{\mu^2}{g(\rho_s - \rho)\rho d^3} = \frac{2\epsilon^2}{f \cdot Re_c^2 \cdot \sqrt{\epsilon(1 - \epsilon)}} \quad (23)$$

where:

$f$  = Darcy-Weisbach friction factor

$Re_c$  = Camp's modified Reynold's number =  $\frac{Vd\rho}{\mu\sqrt{\epsilon(1 - \epsilon)}}$ .

A log-log plot of  $Re_c$  vs  $B$  produces a family of curves in which each curve represents a different porosity.

The porosity of an expanded layer of the bed at a selected backwashing rate is determined by trial and error as follows. A trial porosity is selected, and  $Re_c$  and  $B$  are calculated. The intersection of the  $Re_c$  abscissa and the  $B$  ordinate on the family of curves is observed to see if it falls on the curve representing that selected porosity. If not, a new porosity is selected and the process repeated. The expanded bed height is then calculated from Eq. (21).

Tesarik's discussion [130] of Camp's paper was critical of the grouping of terms for Camp's modified Reynold's number. Tesarik redefined the Reynold's number in a more conventional way,

$$Re = \frac{V \rho d}{\mu}$$

where:

Re = Reynold's number based on the superficial velocity (V) of the fluid above the bed.

Tesarik continued his discussion by showing that the expansion of a granular filter is adequately described by Richardson and Zaki's [100] expression of  $V/V_i = \epsilon^n$  (as presented below) and presented results of his own work.

#### Bed Expansion Correlations from Fluidization Literature

Fluidization, although a relatively young field, gained most of its importance in the early 1940's with the use of fluidized beds in the catalytic cracking of petroleum. Since that period, extensive studies of the fluidization process have been published. The work of Amirtharajah [4-6] is a collection of many of the different aspects of fluidization that pertain to backwashing of granular filters in sanitary engineering.

#### Richardson and Zaki's Correlations

Richardson and Zaki [100] determined that the ratio of superficial velocity above the bed (V) to the settling velocity of a discrete particle ( $V_s$ ) is a function of the Reynold's number ( $Re_o$ ) based on the settling velocity of a discrete particle, porosity ( $\epsilon$ ), and the ratio of particle diameter to the tube diameter,

$$\frac{V}{V_s} = f \left[ \frac{dV_s \rho}{\mu}, \epsilon, \frac{d}{D} \right] \quad (24)$$

where:

$\frac{d}{D}$  = ratio of the particle diameter to column diameter.

Under laminar and turbulent conditions, the ratio  $V/V_s$  is independent of

$$\frac{dV_s \rho}{\mu}.$$

They presented their data graphically by plotting  $\log V$  vs  $\log \epsilon$  (Fig. 56). Above minimum fluidization, the data plotted as a straight line with  $n$  representing the slope of the line and  $V_i$  the intercept of the line at a porosity of 1.0, the mathematical expression for the line is

$$\log V = \log V_i + n \log \epsilon \quad (25)$$

or

$$\frac{V}{V_i} = \epsilon^n .$$

They also observed empirically that  $V_s$ , for spherical particles, and  $V_i$  could be related by the expression

$$\log V_s = \log V_i + \frac{d}{D}, \text{ or } \frac{V_s}{V_i} = 10^{d/D} \quad (26)$$

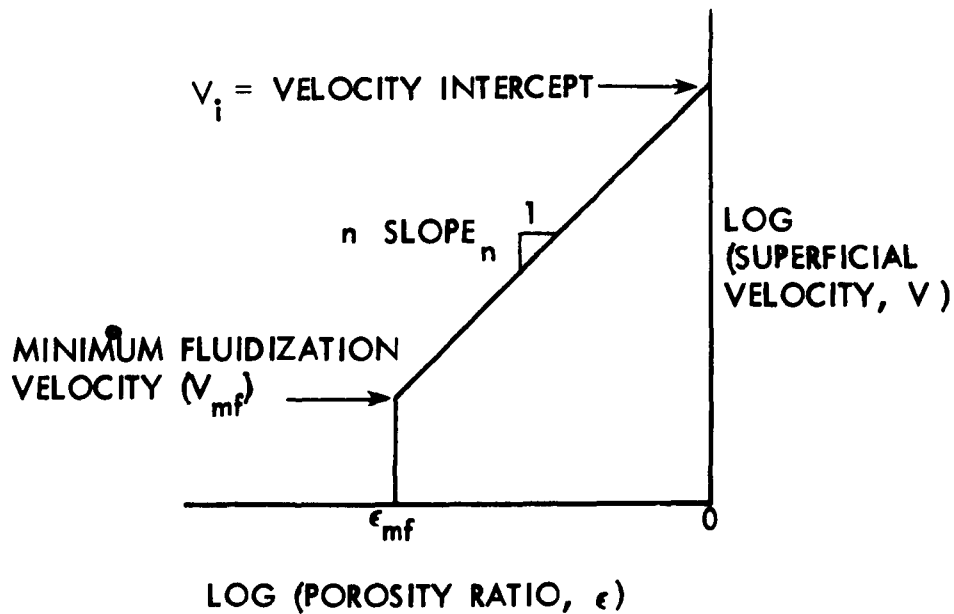


Fig. 56. Relationship between superficial velocity - porosity.

combining Eqs. (25) and (26),

$$\frac{V}{V_s} = \frac{\epsilon^n}{10^{d/D}} \quad \text{for spherical particles only.} \quad (27)$$

Replacing  $V_i$  for  $V_s$  in Eq. (24) and from Eq. (25),  $\epsilon^n$  is shown to be

$$\epsilon^n = \frac{V}{V_i} \quad \text{for all particle shapes.} \quad (28)$$

Therefore,  $n$  slope is independent of  $\epsilon$  and dependent upon the Reynold's number of a free settling particle ( $Re_o$ ) and the ratio of particle diameter to column diameter. They developed the following empirical equations for  $n$  slope for spherical particles,

for

$$0.2 < Re_o < 1$$

$$n = (4.35 + 17.5 \frac{d}{D}) Re_o^{-0.03} \quad (29)$$

for

$$1 < Re_o < 200$$

$$n = (4.45 + 18 \frac{d}{D}) Re_o^{-0.1} \quad (30)$$

for

$$200 < Re_o < 500$$

$$n = 4.45 Re_o^{-0.1} \quad (31)$$

The above equations are for the transitional range of flow. Where the inertia forces are negligible (laminar regime), the results were correlated by

$$n = 4.65 + 19.5 \frac{d}{D} \quad (32)$$

and where the viscous forces are negligible (turbulent regime)

$$n = 2.39. \quad (33)$$

The change in  $n$  slope for the three different flow regimes is shown graphically in Fig. 57. In Richardson and Zaki's work, they studied

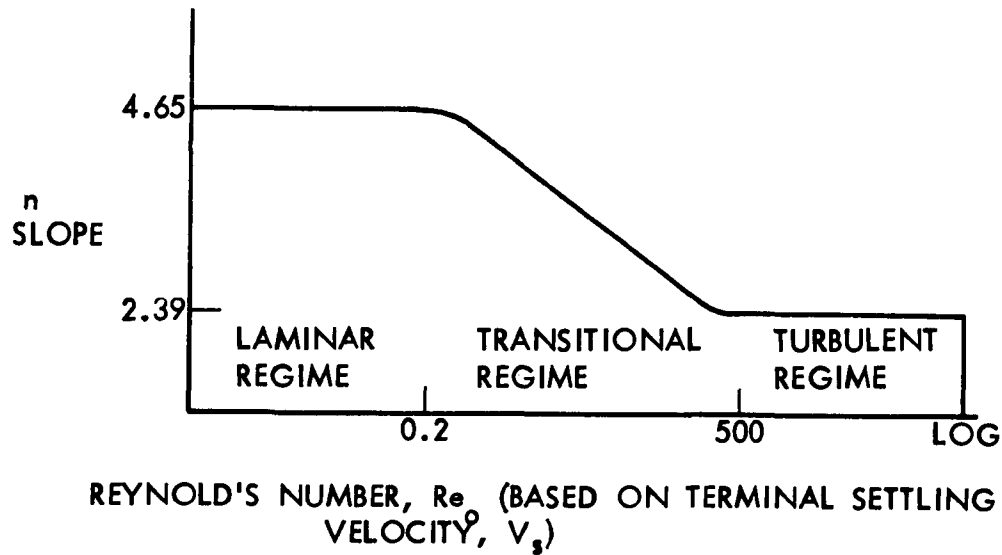


Fig. 57. Relationship between  $n$  slope and Reynold's number,  $Re_o$ .

liquid-solid fluidization and sedimentation of spherical particles of uniform size greater than 100 microns in diameter with a density range of 1.06 to 10.6, in all three flow regimes.

They had excellent correlations between calculated  $V_s$  and observed  $V_i$  as  $d/D \rightarrow 0$ , supporting the validity of Eq. (26), for spherical particles.

#### Wen and Yu's Correlations

Another expansion correlation was proposed by Wen and Yu [138]. From force considerations, they showed that porosity is a function of the following equation,

$$f(\epsilon) = \frac{F_g - F_b}{F_{ks}} \quad (34)$$

where:

$$F_g = \text{gravitational force} = \frac{\pi d^3 \rho_s g}{6g_c}$$

$$F_b = \text{buoyancy force} = \frac{\pi d^3 \rho g}{6g_c}$$

$$F_{ks} = \text{drag force on a discrete particle}$$

$$g_c = \text{Newton's law conversion factor.}$$

For the evaluation of  $F_{ks}$ , they used Schiller and Naumann's equation,

$$F_{ks} = \frac{\pi d^2 \rho V^2}{g_c} \left( 3 \text{Re}^{-1} + 0.45 \text{Re}^{-0.313} \right) \quad (35)$$

which is valid for Reynold's number from 0.001 to 1000.

Using data from their own work as well as from the literature they found,  $f(\epsilon) = \epsilon^{-4.7}$ . Combining Eqs. (34) and (35), the following form of the equation was developed,

$$\epsilon^{4.7} Ga = 18 \text{Re} + 2.70 \text{Re}^{1.687} \quad (36)$$

where:

$$Ga = \frac{d^3 \rho (\rho_s - \rho) g}{\mu^2} = \text{Galileo number (dimensionless)}.$$

#### Effect of Particle Shape on Expansion Correlations

The effect of particle shape on the expansion correlations has not been studied extensively.

Richardson and Zaki's [100] work with nonspherical particles of regular shape (cylinder, cubes, plates) was in the turbulent range only. They tried two different shape factors, sphericity ( $\psi$ ) and volumetric shape factor ( $K$ ).

The  $K$  factor correlated best for the evaluation of the  $n$  slope. The equation for  $n$  slope in the turbulent range was

$$n = 2.7 K^{0.16} \quad (37)$$

where:

$$K = \frac{\pi}{6} \frac{d_s^3}{d_p^3} = \text{volumetric shape factor}$$

$d_s$  = diameter of sphere of equivalent volume of particle

$d_p$  = diameter of a circle of same area as the projected profile of a particle when lying in its most stable position.

Lewis and Bowerman [79] reported that the expansion of nonspherical particles could be correlated by using a modified porosity ratio for

the nonspherical particles. The modification is obtained by multiplying the porosity ratio ( $\epsilon$ ) by the sphericity ( $\psi$ ) of the particles ( $\psi\epsilon$ ).

Whitmore [139,140], working with nonspherical particles, found that the  $n$  slope of the rough particles was higher than Richardson and Zaki's  $n$  slope for spherical particles in the laminar range. Whitmore stated that this higher  $n$  slope increased as particle size decreased. He presumed that this increase was because a rough particle settling in a fluid has a layer of attached fluid that smoothes off the irregular outline of the particle. This trapped liquid gives the particle a larger effective diameter and a lower density.

Jottrand [69] fluidized uniform crushed sands with water in the laminar range. His plot of  $\log V$  vs  $\log \epsilon$  resulted in a series of parallel straight lines with an  $n$  slope of 5.60. From the experimental investigation, he found that the fluidization velocity of given particles at a given expanded porosity closely approximated the hindered settling velocity of the fluidized bed after the liquid flow was cut off. In subsequent experiments, he attempted to replace the fluidization experiments by a more simple measure of the rate of hindered settling of particles after good agitation. The results of the hindered settling at a given concentration of particles after good agitation was found to be about 45% greater than velocities observed by the first technique for the same particle concentration.

Wilhelm and Kwauk [141] did extensive research on fluidization with water and air. The particles ranged in size from 5 to 0.3 mm and in density from 1.125 to 10.792. Their raw data of flow rate, pressure drop, and porosity is completely reported. Of particular interest is their work with sea sand, which was described as prismatic with rounded edges. Jottrand [69] extended the analysis of Wilhelm and Kwauk's sea sand data with a  $\log V$  vs  $\log \epsilon$  plot. The results of the analysis of the sea sands are given in Table 27.

The authors of the present report calculated the  $n$  slopes for the sea sands using Richardson and Zaki's equation [Eq. (30)], and these values are included in Table 27. The  $n$  slopes calculated from Eq. (30) are somewhat lower than the  $n$  slopes from the  $\log V$  vs  $\log \epsilon$  plots for the nonspherical particles as reported by Jottrand.

Carvalho [28], working with crushed anthracite coal of uniform sizes, plotted  $\log V$  vs  $\log \epsilon$  and determined the  $V_i$  intercept and the  $n$  slope. He also experimentally determined the discrete settling velocity,  $V_s$ , for the various uniform sized coal particles (Table 28). The  $V_s$  determined experimentally was approximately 25% lower than the  $V_i$  intercept (Table 28). He attributed this discrepancy to the shape of the crushed particles. Carvalho did not compare the  $n$  slopes from the  $\log V$  vs  $\log \epsilon$  with the  $n$  slopes calculated from Richardson and Zaki's equation [Eq. (30)].

Table 27. Comparison of  $n$  slopes of sea sands (using Jottrand's analysis [69] and Richardson and Zaki's equations).

Sand	Density, g/cc	Diameter, mm	$Re_i^a$	Jottrand $n$ slope from log $V$ vs log $\epsilon$ plot	$n$ slope from Eq. (30) <sup>b</sup>
1	2.639	0.373	21	3.45	3.28
2	2.639	0.556	45.5	3.15	3.04
3	2.639	1.000	122	2.95	2.76

<sup>a</sup> Reynold's number based on the velocity intercept at porosity ratio of one from the log plot of  $V$  vs  $\epsilon$ .

<sup>b</sup> Assuming that  $Re_i = Re_o$  and neglecting the  $d/D$  term.

Values of  $Re_i$  from Carvalho's reported  $V_i$  and subsequent determinations of  $n$  from Eq. (30) were calculated by the writers. The results are also presented in Table 28.

From the preceding literature, two significant points can be made:

1. The  $n$  slopes for fluidized beds of nonspherical particles are greater than the  $n$  slopes of fluidized beds of equivalent sized spherical particles.
2. The experimentally determined discrete settling velocity of a nonspherical particle of a bed does not equal the velocity intercept at porosity equal to unity of the log  $V$  vs log  $\epsilon$  plot.

#### Effect of Particle Size Distribution on Expansion Correlations

The media used for filtration does not consist of one-size particles but of a range of particle sizes. The narrowest size range of media that can be prepared conveniently and results in the largest to smallest particle diameter ratio of about 1.2 is the media that is retained between two adjacent sieves. Although there is no limit to the widest range of particle size, for multi-media filters the widest diameter ratio suggested for any of the individual media comprising the bed is about 2.5 [34].

Various investigators have used different methods of determining the representative particle diameter for expansion correlations:

Table 28. Comparison of  $n$  slope of crushed coal.

Run <sup>a</sup>	Average size, mm	Temp, °C	$V_s$ experimentally observed fps	$V_i$ $\frac{\text{fps}}{n}$		$Re_i^b$ based on $V_i$	$n$ from $Re_i^{b,c}$ and Eq. (30)
				From log V vs log $\epsilon$ plot			
I	1.3	16.0	0.194	0.265	4.20	95.2	2.82
II	1.1	16.0	0.171	0.255	4.70	77.7	2.88
III	0.9	12.5	0.139	0.176	4.70	40.3	3.07
IV <sup>d</sup>	1.1	16.0	0.172	0.203	4.15	61.9	2.95
V	1.3	16.0	0.208	0.278	3.70	100.0	2.80
VI	1.1	16.0	0.182	0.232	4.00	70.6	2.89
VII	0.9	16.0	0.165	0.222	4.35	55.5	2.98
VIII <sup>e</sup>	1.1	16.0	0.185	0.220	3.80	67.0	2.92

<sup>a</sup>Runs I to IV coal density = 1.35 g/cc, Runs V to VIII coal density = 1.65 g/cc.

<sup>b</sup>Values determined by the writers.

<sup>c</sup>Assuming  $Re_i = Re_o$  and neglecting the  $d/D$  term.

<sup>d</sup>Run IV the media for this run was comprised of equal volumes of media from Runs I to III.

<sup>e</sup>Run VIII the media for this run was comprised of equal volumes of media from Runs V to VII.

1. In sanitary engineering practice [24,29,46], the particle diameter is described as the arithmetic mean of adjacent sieve sizes. Expansion correlations are made by summing the expansion of individual layers of filter media comprising a graded media bed.
2. Amirtharajah [4,6], using data from the sieve analyses of graded sands, plotted the percent passing by weight on a probability scale against sieve size and used the diameter corresponding to 60% passing by weight in his expansion correlations. One sand investigated was not normally distributed about the mean size

and did not plot as a straight line when plotted in this manner. This sand was analyzed as two separate components.

Wen and Yu [138] determined the effective diameter of two-component mixtures by an inverse relationship,

$$d_{\text{inverse}} = \frac{1}{\sum_{i=1}^n \frac{W_i}{d_i}} \quad (38)$$

where:

$W_i$  = weight fraction of 'i'th layer

$d_i$  = mean diameter of weight fraction of 'i'th layer.

Van Heerden et al. [134], with gas fluidization of fine particles in the laminar range, also used the inverse definition of particle diameter. He compared the  $d_{\text{inverse}}$ ,  $d_{\text{arithmetic mean}}$ , and  $d_{\text{geometric mean}}$  with minimum fluidization velocity studies and found that the  $d_{\text{inverse}}$  gave the best correlation. The arithmetic average gave higher diameter values and the geometric average gave lower values than the  $d_{\text{inverse}}$  diameter.

Leva et al. [77,78] used the arithmetic mean diameter ( $d_m$ ),

$$d_m = \sum W_i d_i \quad (39)$$

for two-, three-, and four-component mixtures in the development of an equation for minimum fluidization velocity.

Another method of particle size determination used by some authors [24,28,46] is the equivalent diameter of a spherical particle,

$$d_{\text{eq}} = \left[ \frac{6W}{N\pi\gamma_s} \right]^{1/3} \quad (40)$$

where:

$\gamma_s$  = particle specific weight

$W$  = total weight of  $N$  particles

$N$  = number of particles.

Fair, Geyer, and Okun [46] point out that when determining particle size by sieve analysis, the mean or 50% size is determined by weight,

but the average diameter as determined by number is more closely represented by the 10% finer size on a weight basis.

### Particle Segregation or Stratification

Particle stratification resulting from backwashing is very apparent in rapid sand filters. For equal density particles with varying diameters, different workers have reported rather widely different ratios above which stratification would occur. These ratios have ranged from 1:1.3 [138] up to 1:4 [96].

Pruden [96,97] did significant work to explain particle segregation in particulate fluidization on a rational basis. He presumed that the driving force towards segregation of two different groups of particles is the difference in bulk density between the groups. His definition of bulk density ( $\rho_b$ ) is,

$$\rho_b = (1 - \epsilon)\rho_s + \rho\epsilon = (1 - \epsilon)(\rho_s - \rho) + \rho. \quad (41)$$

The bulk density difference between the large particles x and the small particles y is then,

$$\rho_{b_x} - \rho_{b_y} = (1 - \epsilon_x)(\rho_{s_x} - \rho) - (1 - \epsilon_y)(\rho_{s_y} - \rho). \quad (42)$$

Pruden used Richardson and Zaki's correlations for velocity and porosity [Eq. (27)] and a theoretical equation for the settling velocity of a single particle which is applicable in all ranges of flow,

$$V_s = \frac{C_D(\rho_s - \rho)^{1/m} \cdot g^{1/m} \cdot d^{(3-m)/n}}{\rho^{(m-1)/2} \cdot \mu^{(2-m)}} \quad (43)$$

where:

$C_D$  = drag coefficient (function of  $Re_o$ )

$m$  = index of fluid regime ( $m = 1$  in Stoke's regime,  $m = 2$  in Newton's regime,  $m = 1.4$  in transitional regime for a straight line approximation)

$n$  = slope of the  $\log V$  vs  $\log \epsilon$  plot.

Combining Eqs. (42) and (43), Pruden developed the following equation for bulk density difference,

$$\rho_{b_x} - \rho_{b_y} = (\rho_{s_x} - \rho) \left[ 1 - \frac{1}{\gamma_b} - \epsilon_x \left\{ 1 - r^{(3-m)/mn} \cdot \frac{10^{(d_y - d_x)/nD}}{\gamma_b^{(mn-1)/mn}} \right\} \right] \quad (44)$$

where:

$$\gamma_b = \frac{(\rho_{s_x} - \rho)}{(\rho_{s_y} - \rho)}$$

$$r = \frac{d_x}{d_y} \text{ ratio of particle diameters.}$$

The assumptions of the above equation are that  $m_x = m_y = m$ ,  $n_x = n_y = n$ , and drag coefficients are approximately equal. He tested the validity of the above equation experimentally by evaluating  $m$ ,  $n$ , and  $\epsilon$  from fluidization of the separate components.

He hypothesized that when the bulk density difference is equal to zero, the components should be completely mixed. A positive or negative value would mean that stratification would occur. He experimented with equal density and low diameter ratio components and concluded that Eq. (44) does give the correct trend of component stratification, but that a limiting bulk density difference for stratification would depend upon properties of the particles. He proposed the following modification to the bulk density difference: a reduced bulk density,  $\beta$ ,

$$\beta = \frac{(\rho_{b_x} - \rho_{b_y})}{\rho_{s_x} - \rho} \quad (45)$$

where:

$0 \leq \beta \leq 0.01$  mixing was observed

$0.01 < \beta \leq 0.04$  partial segregation occurred

$\beta > 0.04$  segregation with an interface occurred.

Amirtharajah [4], in discussing Eq. (44), stated that a separate determination of  $\rho_{b_x}$  and  $\rho_{b_y}$ , by evaluating the  $\epsilon$  for each component from Eq. (25) and solving for the bulk density difference in Eq. (42), would eliminate the uncertainty of some of the assumptions.

Le Clair's thesis [74] of two-component fluidization is a complementary study to Pruden's particle size segregation. Le Clair observed that when some two-component mixtures  $x$  and  $y$ , such that  $\rho_{s_x} > \rho_{s_y}$  and  $d_x < d_y$ , were fluidized at low flow rates, the  $x$

component was below the y component. At an increased flow rate, both components were intermixed. At still a higher flow rate, a reversal of the components occurred, resulting in the small size, dense material above the larger size, less dense material.

He explained that this phenomena could be attributed to the change of the individual bulk densities of the two components as flow rate changes. At low fluidization rates, the x component had a greater bulk density than the y component, and at increased flow rates, the bulk densities were equal. With still higher flow rates, the x-component bulk density was less than the y-component bulk density. Various densities and sizes of media can be selected which should display this behavior. The selection would depend upon the expansion-flow rate characteristics of the individual components.

The porosity at which the particles are completely mixed is called the inversion porosity ( $\epsilon_I$ ) and is approximated by,

$$\epsilon_I = \frac{1 - \gamma_b}{\gamma_b^{1/mn} \cdot r^{(3-m)/mn} - \gamma_b} \quad (46)$$

which is derived from Eq. (44) at zero bulk density difference.

Le Clair pointed out the following intermixing problems which are of particular interest.

1. Equation (46) will give only an approximate value for  $\epsilon_I$  and corresponding velocity because of all of the assumptions made for the development of Eq. (44).
2. Data collected for the individual components will not predict the  $\epsilon_I$  precisely because even for a narrow size range, the individual component data will give the average porosity of the component, not point porosities within the component.
3. The completely mixed state of two components is reached at a lower velocity than predicted by the individual component data. This he attributed to particle size distribution. The small particles, sized by sieving, have a greater variation in size and subsequently greater range in bulk density than the larger particles, also sized by sieving. This difference in change of bulk densities would cause the completely mixed state to be achieved at a lower flow rate than predicted from the individual component data.
4. Inversion of the components would be observed for fluidization in the laminar range but not in the transitional or turbulent

ranges because of turbulence, particle circulation, and macroscopic mixing which would destroy the bulk density gradients.

5. The expanded height of a two-component mixture is closely approximated by the sum of the expanded heights of the two individual components whether the mixtures are segregated or completely mixed.

Another somewhat similar approach to intermixing is given by Camp et al. [26]. They proposed that the driving force for intermixing is the relationship between the particle density of the lighter material and the bulk density of the more dense particles and water.

The equation used to calculate intermixing tendency was developed by considering the forces acting upon the grains. The buoyant force ( $F_b$ ) on a grain in a fluidized bed is equal to the weight of the mixture displaced,

$$F_b = v_p g \rho_b \quad (47)$$

where:

$v_p$  = the volume of mixture displaced

$\rho_b$  = bulk mass density of the mixture.

The impelling force ( $F_i$ ) acting on a floating particle in the mixture is its weight downward and the upward drag force of the wash-water past the particle. The drag term presented assumes spherical shaped particles.

$$F_i = \underbrace{v_p g \rho_s}_{\text{weight term}} - \underbrace{C_D \frac{3}{2d} v_p \frac{\rho}{2} \left(\frac{v}{\epsilon_e}\right)^2}_{\text{drag term}} \quad (48)$$

where:

$C_D$  = drag coefficient of the particle, a function of Reynold's number and particle shape.

Equating  $F_b$  and  $F_i$  leads to the following:

$$\rho_b = \rho_s - C_D \frac{3}{2d} \frac{\rho}{2g} \left(\frac{v}{\epsilon_e}\right)^2 \quad (49)$$

As applied to a dual-media filter, if  $\rho_b$  of the lower heavier layer is greater than the right-hand terms for the upper lighter layer, normal separation of the two media will result. If the reverse is true, intermixing can be expected. Camp et al. presented very little experimental evidence in support of the model presented above.

However, using this approach, they concluded that at common back-washing flow rates of multi-media filters, the silica sand particles (1.00 to 0.595 mm) will fall into and mix with the garnet sand (0.500 to 0.354 mm), but that the coal (1.41 to 1.00 mm) will be stratified above the silica sand. The writers observe, however, that the coarse end of the coal is finer than that commonly used in practice.

Brosman and Malina, in discussion of the Camp paper [26], stated that intermixing for multi-media filters was more correctly described by the bulk density approach described by Le Clair [74]. However, in their closing discussion of the paper, Camp et al. vigorously defended their model.

### Prediction of Settling Velocities

The solution of the Richardson and Zaki expansion correlation,  $V/V_i = \epsilon^n$ , requires the velocity intercept of the  $\log V - \log \epsilon$  plot and the Reynold's number, corresponding to the settling velocity ( $V_s$ ) for the determination of the  $n$  slope. Two different approaches can be used to find  $V_i$ : (1) the direct determination from experimental observation or from tables or graphs found in the literature, or (2) an indirect method of using the minimum fluidization velocity and a ratio of settling to minimum fluidization velocities.

### Settling Velocities

Most textbooks in which there is a discussion of settling or sedimentation give a method of calculating the settling velocity of a discrete spherical particle. The settling velocity is solved by a direct solution in the laminar or turbulent range. In the transitional range, the calculation consists of a trial and error solution which simultaneously satisfies the settling velocity equation, the drag equation, and empirical correlations of the drag coefficient vs Reynold's number. In the transitional range, which is of most interest, there is considerable variation from the equations or graphs presented for the evaluation of drag coefficient of non-spherical particles. Graphical methods of solving for settling velocity of nonspherical particles suffer from the same weakness.

One particular method of solving for the settling velocity of a discrete particle involves the Galileo number ( $Ga$ ), a term which occurs frequently in the fluidization literature [17,33,53,69,76,95,100,141]. The development for the Galileo number is as follows. The resistance force per unit projected area of the particle when equilibrium is established for a settling particle can be expressed as,

$$R' \frac{1}{4} \pi d^2 = \frac{1}{6} \pi d^3 (\rho_s - \rho) g$$

or,

$$R' = \frac{2}{3} dg(\rho_s - \rho)$$

where:

$R'$  = resistance force per unit projected area of the particle.  
Dividing both sides by  $\rho V_s^2$  and multiplying both by  $Re_o^2$   
yields,

$$\begin{aligned} \frac{R'}{\rho V_s^2} Re_o^2 &= \frac{2}{3} \frac{d^3}{\mu} \rho (\rho_s - \rho) g \\ &= \frac{2}{3} Ga. \end{aligned}$$

The Galileo number is a dimensionless term that is independent of velocity and the product of Reynold's number squared and drag force. Interesting to note is that  $Ga$  is equivalent to Camp's dimensionless backwashing number  $B$ , presented previously.

Coulson and Richardson [33] present a table and a graph relating  $Re_o$  to  $Ga$ . They also present a table for a correction factor to be applied to the  $Re_o$  for nonspherical particles.

#### Minimum Fluidization Velocities and Ratios of Settling and Minimum Fluidization Velocities

Most of the formulas for predicting  $V_{mf}$  are developments from the Kozeny equation [Eq. (17)] and the constant head loss equation [Eq. (1)]. Leva [76] and Leva et al. [77,78] developed the following by equating a modified Kozeny equation and the constant head loss equation. This equation incorporates a Reynold's number relationship for  $\epsilon_{mf}$  and  $\psi$ ,

$$G_{mf} = \frac{688 d^{1.82} [\gamma(\gamma_s - \gamma)]^{0.94}}{\mu^{0.88}} \quad (50)$$

where:

$G_{mf}$  = superficial fluid mass velocity at minimum fluidization in lb (mass)/hr sq ft

$d$  = diameter of particle in inches

$\gamma, \gamma_s$  = fluid and particle specific weights in lb/cu ft

$\mu$  = viscosity in centipoise

valid for  $Re_{mf} < 10$ . For  $Re_{mf} > 10$ , Leva presents a graphical correction to be applied to  $G_{mf}$ .

Upon expressing  $G_{mf}$  as a superficial velocity ( $V_{mf}$ ), as done by Amirtharajah [6], the equation becomes,

$$V_{mf} = 0.00381 \frac{d^{1.82} [\gamma(\gamma_s - \gamma)]^{0.94}}{\mu^{0.88}} \quad (51)$$

where:

$V_{mf}$  = minimum fluidization in gpm/sq ft

$d$  = particle diameter in mm

$\mu$  = viscosity in centipoise.

Again, valid for  $Re_{mf} < 10$ .

Zabrodsky [144] gives a multiplication correction factor for the velocity for  $Re_{mf} > 10$ ,

$$k_{mf} = 1.775 Re_{mf}^{-0.272} \quad (52)$$

for  $10 < Re_{mf} < 300$ .

Wen and Yu [138], starting with Ergun's equation [Eq. (19)], developed the following,

$$Re_{mf} = \sqrt{(33.7)^2 + 0.0408 Ga} - 33.7. \quad (53)$$

They used their own work plus the work of many others to develop this equation which is valid for gas and liquid fluidization with a  $Re_{mf}$  range of 0.001 to 4000.

Frantz [48], using gas-solid fluidization, made over 400 experiments with eight different media and extensive analysis of the data determined that for the solution of the critical fluid mass velocity, ( $G_{mf}$ ), the theoretical coefficients and exponents give better results than Leva's empirical correlations [Eq. (50)] and that further refinement of the coefficients and exponents from the theoretical values was not recommended for extrapolation outside the range of his experiments. The theoretical equation for fluid mass velocity is,

$$G_{mf} = 4.45 \times 10^5 \frac{d^2 \gamma(\gamma_s - \gamma)}{\mu} \quad (54)$$

where:

$G_{mf}$  = fluid mass velocity in lb (mass)/hr sq ft

$d$  = particle diameter in ft

$\gamma, \gamma_s$  = fluid and solid specific weights, respectively,  
in lb/cu ft

$\mu$  = viscosity in lb/hr ft

The relationship of free settling velocity and minimum fluidization velocity has been presented by relating the ratio of  $Re_o/Re_{mf}$  to the log Ga by several investigators [17,53,95]. Galileo number is a constant for given particle and fluid properties.  $Re_{mf}$  and  $Re_o$  were calculated from various empirical equations. The results of the various correlations of the ratio of  $Re_o/Re_{mf}$  vs Ga are presented graphically in the respective papers.

The above correlations could be used in the solution of the terminal settling velocity by calculating Ga from the physical properties of the fluid and the particle, and the  $Re_o/Re_{mf}$  ratio can be read from the above correlations.  $Re_{mf}$  can be determined from Eq. (50), (53), or (54), or the appropriate equations in the following discussion.  $Re_o$  can then be calculated from  $Re_{mf}$  and the  $Re_o/Re_{mf}$  ratio.

A brief discussion of the individual papers follows. Pinchbeck and Popper [95] worked with gas-solid fluidization and plotted  $Re_o/Re_{mf}$  vs log  $1/Ga$ .  $Re_o$  was evaluated from,

$$Re_o = -6 + \sqrt{36 + \frac{2}{3} Ga}. \quad (55)$$

Van Heerden's equation for  $Re_{mf}$  [Eq. (56)] was chosen over Leva's equation [Eq. (50)] because the former equation fit their data better,

$$Re_{mf} = 0.00123 (1 - \epsilon_{mf}) Ga. \quad (56)$$

They assumed that  $\epsilon_{mf}$  was a constant of 0.406, as proposed by Van Heerden et al. [134] for a bed of spheres of homogeneous diameter. Hence, the constant  $(1 - \epsilon_{mf})$  would be 0.594 in the above equation. Pinchbeck and Popper's [95] correlations of  $Re_o/Re_{mf}$  and Ga, using limited experimental data, could be termed as fair.

Bourgeois and Grenier [17] used Ergun's equation [Eq. (19)] and the constant head loss equation [Eq. (1)] to develop the following equation for  $Re_{mf}$ ,

$$Re_{mf} = 42.86(1 - \epsilon_{mf}) \left[ \left( 1 + 3.11 \times 10^{-4} Ga \cdot \frac{\epsilon_{mf}^3}{(1 - \epsilon_{mf})^2} \right)^{0.5} - 1 \right]. \quad (57)$$

They also assumed  $\epsilon_{mf}$  as a constant 0.406, but pointed out the effects of a change in porosity from this assumed value and simplified Eq. (57) further. The terminal settling velocity was evaluated from an empirical plot of  $Re_o$  vs  $Ga$ .

They also found a substantial difference of experimental results between air and water fluidization and analyzed them separately. They developed the following analytical expressions for the  $Re_o/Re_{mf}$  vs  $Ga$  correlation for water fluidization,

$$1. \quad 50 < Ga < 2 \times 10^4$$

$$\frac{Re_o}{Re_{mf}} = 132.8 - 47.1 \log Ga + 4.6 (\log Ga)^2 \quad (58)$$

$$20 < \frac{Re_o}{Re_{mf}} < 60$$

$$2. \quad 2 \times 10^4 < Ga < 10^6$$

$$\frac{Re_o}{Re_{mf}} = 26.0 - 2.7 \log Ga \quad (59)$$

$$9 < \frac{Re_o}{Re_{mf}} < 20$$

$$3. \quad 10^6 < Ga$$

$$\frac{Re_o}{Re_{mf}} = 9.0 \quad (60)$$

Godard and Richardson [53] related  $Re_{mf}$  with  $Ga$ . Starting with the Kozeny-Carmen equation [Eq. (18)] and the constant head loss equation [Eq. (1)], they developed,

$$Ga = 180 Re_{mf} \cdot \frac{(1 - \epsilon_{mf})}{\epsilon_{mf}^3} + 2.88 Re_{mf}^2 \cdot \frac{(1 - \epsilon_{mf})^{0.1}}{\epsilon_{mf}^3} \quad (61)$$

They also used Ergun's equation [Eq. (19)] and the constant head loss equation to develop,

$$Ga = 150 Re_{mf} \cdot \frac{(1 - \epsilon_{mf})}{\epsilon_{mf}^3} + 1.75 Re_{mf}^2 \cdot \frac{1}{\epsilon_{mf}^3} \quad (62)$$

They related  $Ga$  to the Reynold's number based on the free falling velocity by the following equations:

$$Ga = 18 Re_o \quad Ga < 3.6 \quad (63)$$

$$Ga = 18 Re_o + 2.7 Re_o^{1.687} \quad 3.6 < Ga < 10^5 \quad (64)$$

$$Ga = \frac{1}{3} Re_o^2 \quad Ga > 10^5 \quad (65)$$

Equations (63), (64), and (65) were obtained for the laminar, transitional, and turbulent range, respectively. Equation (64) is obtained from Schiller and Naumann's equation, previously discussed.

They also illustrated the effects of  $\epsilon_{mf}$  on the  $Re_o/Re_{mf}$  ratio. The higher the  $\epsilon_{mf}$ , the lower the  $Re_o/Re_{mf}$  ratio for a given  $Ga$ . The curves of  $Re_o/Re_{mf}$  vs  $\log Ga$  are quite sensitive to changes of  $\epsilon_{mf}$  at low values of  $Ga$  corresponding to the laminar range. However, this sensitivity diminishes as  $Ga$  increases and is almost negligible at high values of  $Ga > 10^5$  (turbulent range).

The  $Re_o/Re_{mf}$  ratio reported in the preceding papers varied from 40 to 110 in the laminar range of flow, where the  $\epsilon_{mf}$  effects on the ratio is most pronounced, down to 7 to 12 in the turbulent range of flow.

Godard and Richardson [53] extended the use of the ratio of  $Re_o/Re_{mf}$  to the determination of the  $n$  slope.

Equation (27) can be rearranged to the following form of

$$n = \frac{\log \frac{V}{V_s}}{\log \epsilon} = \frac{\log \frac{Re_{mf}}{Re_o}}{\log \epsilon_{mf}} \quad (66)$$

(if  $d/D$  is negligible). Using this relationship, it was possible to replace  $Re_o/Re_{mf}$  with  $n$  slope in their correlations with  $Ga$  and to present a series of curves of  $n$  slope vs  $Ga$  for different values of  $\epsilon_{mf}$ . The values of the  $n$  slope were somewhat higher than corresponding experimental values from the literature. They attributed the high values of  $n$  slope to the phenomena that at minimum fluidization the particles become free to orientate in a manner to offer least resistance to flow, but the Ergun and the Kozeny-Carmen equations do not reflect this change and, therefore, give higher values of  $Re_{mf}$ , which then give higher  $n$  slopes from Eq. (66).

### Existing Models for Predicting the Expansion of Fluidized Beds

#### Amirtharajah's Model

Amirtharajah's [4,5] method for predicting bed expansion was a modification of the method proposed by Leva [76]. Amirtharajah's procedure was,

1. Experimentally determine  $\epsilon_{mf}$  and  $\rho_s$ .
2. From a probability plot of the sieve analysis, determine the 60% finer size ( $d_{60\% \text{ finer}}$ ).
3. Calculate  $V_{mf}$  from Leva's equation [Eq. (51)]; if  $Re_{mf} > 10$  apply Zabrodsky's correction factor,  $k_{mf}$ , [Eq. (52)] to  $V_{mf}$ .
4. Use the relationship,

$$V_s = V_{mf} \sqrt{71.3}$$

to determine  $V_s$ . The above expression is based on the empirical relationship of drag force on an isolated spherical particle to drag force on the same spherical particle in a fixed bed,

$$\frac{C_{D \text{ particle isolated}}}{C_{D \text{ particle in bed}}} = 71.3. \quad (67)$$

This ratio was proposed by Rowe [105] and Rowe and Henwood [106] and validated by Davies and Richardson [36]. Amirtharajah also assumed that drag forces are proportional to the square of the velocities; thus he used the square root of the drag force ratio in the above expression.

5. The  $n$  slope can then be determined by the use of Richardson and Zaki's equations [Eqs. (29) through (33)] where Reynold's number is based on  $V_s$ .

6. Using a modified form of Eq. (27),

$$V = k\epsilon^n \quad (68)$$

and inserting  $V_{mf}$  for  $V$ ,  $\epsilon_{mf}$  for  $\epsilon$ , and  $n$  into the equation, the value  $k$  can be determined. The  $k$  value has the same units as a velocity term.

7. The  $\epsilon$  of the expanded bed can then be determined for any superficial velocity,  $V$ , by reapplying Eq. (68) with the values of  $k$  and  $n$  slope previously calculated.

8. The expanded bed height is then found from Eq. (2).

Step 4 of this model is incorrect. The ratio of drag forces used by Amirtharajah (71.3) is valid for rhombohedral packing of spheres and can thus be reasonably applied to the bed at the onset of fluidization. However, from fundamental hydrodynamics, the drag force is proportional to  $V^1$  in laminar range,  $V^2$  in turbulent range, and between  $V^1$  and  $V^2$  over the transitional range. Thus, Amirtharajah's use of drag force being proportional to  $V^2$  is the source of his error and is a misinterpretation of Rowe's paper [105]. This error was somewhat self-corrected in Amirtharajah's subsequent steps. For Amirtharajah's fine sand A, his reported value of  $Ga$  was equal to 5810 [4, p. 109]. The ratio of  $Re_o/Re_{mf}$  or  $V_s/V_{mf}$  for this  $Ga$  should be approximately 20 from the literature [19,53,95] rather than  $\sqrt{71.3}$  as used by Amirtharajah. This would mean that the  $V_s$  and the  $Re_o$  Amirtharajah used for determination of the  $n$  slope from Eq. (30), neglecting  $d/D$ , would be lower by a factor of  $20/\sqrt{71.3} \approx 2.5$ . The correct  $n$  slope would, therefore, be larger by a factor of approximately,

$$\frac{n_{\text{Amirtharajah}}}{n_{\text{correct}}} = \frac{4.45(Re_o)^{-0.1}}{4.45(Re_o \times 2.5)^{-0.1}} = (2.5)^{0.1} = 1.09.$$

In his step 6,  $\epsilon_{mf}$ ,  $V_{mf}$ , and  $n$  slope were used to calculate a  $k$  value. Theoretically, for spherical particles, this  $k$  value should approximate  $V_s$ . In his thesis [4, p. 113], the  $V_s$  calculated from  $V_s/V_{mf} = \sqrt{71.3}$  and the  $k$  value from subsequent calculations were 75.1 gpm/sq ft and 140.7 gpm/sq ft, respectively. The ratio of these values is  $140.7/75.1 \approx 2$ , which is approximately the factor which the  $V_s/V_{mf}$  or  $Re_o/Re_{mf}$  ratio was assumed to be off. Thus, Amirtharajah used an  $n$  slope which was slightly high, which led to an erroneous  $k$  value. Thus, his expansion model was somewhat self-correcting and gave good results when compared with his experimental data.

### Leva's Model

Leva's method of predicting bed expansion is as follows:

1. Experimentally determine  $\epsilon_{mf}$  and  $\rho_s$ .
2. From the sieve analysis, define the diameter by the inverse definition [Eq. (38)].
3. Determine the minimum fluidization mass flow rate,  $G_{mf}$ , from Eq. (50).
4. Determine the fluid mass flow rate,  $G_f$ , at the superficial fluidization velocity of interest.
5. From this  $G_f$ , determine the Reynold's number using  $V_f$  corresponding to  $G_f$ , and from Richardson and Zaki's equations (Eqs. (29) through (33)] determine  $n$  slope.
6. Calculate  $V_i$  from the previously determined  $V_{mf}$ ,  $\epsilon_{mf}$ ,  $n$  slope, and Richardson and Zaki's Eq. (28),  $V_i = V_{mf} / (\epsilon_{mf})^n$ .
7. Repeat the above calculation using  $V_i$ ,  $n$  slope, and  $V$  to solve for the expanded  $\epsilon$  at  $G_f$ .
8. The expanded height can be determined by Eq. (2).

Amirtharajah [4,5] pointed out a significant error in Leva's model. Leva uses the Reynold's number based on the superficial flow rate of the expanded bed to determine the  $n$  slope. This is incorrect. Richardson and Zaki's  $n$  slopes should be determined from the Reynold's number based on  $V_i$  at  $\epsilon$  of 1.0. For spherical particles, this would be the point where  $V_s = V_i$ .

### Wen and Yu's Method

Wen and Yu's [138] method of predicting the expansion is very straightforward. The expanded porosity can be determined by the fluid and particle properties and Eq. (36),

$$\epsilon^{4.7} Ga = 18 Re + 2.70 Re^{1.687}.$$

The expanded height of the bed can then be calculated from Eq. (2),

$$L = \frac{l_o(1 - \epsilon_o)}{(1 - \epsilon)}$$

$l_o$  and  $\epsilon_o$  having been previously determined.

## X. EXPANSION AND INTERMIXING EXPERIMENTAL INVESTIGATION

### Experimental Apparatus

#### General Layout of 6-in. Fluidization Column

A schematic layout of the 6-in. fluidization apparatus is shown in Fig. 58. This apparatus was used in the expansion vs flow rate observations of garnet sand, silica sand, and anthracite coal for purposes of developing expansion prediction models. It was also used in observations of intermixing of silica sand and coal and the hydraulic gradients which exist in these intermixed beds.

The source of water (hot and cold) was the university tap water supply. Two sets of water taps were used, A and B. The high flow rates were metered by flowmeter  $F_1$ . The lower flow rates were passed through a thermostatically controlled mixing valve, C, then through flowmeters  $F_2$  and  $F_3$  and to the fluidization column, D. The water temperature was measured by a thermometer placed within the expansion column.

The fluidizing column consisted of 6-in. inner diameter, 1/2-in. thick plexiglass tube 4 ft 5 in. deep with a 3-in. high calming section at the bottom. The water was fed through 59 orifices of 1/16-in. diameter in a 1-in. thick underdrain plexiglass plate. Sets of orifices were staggered from one another so as to provide a uniform matrix of orifices on the entire plate. The calming section was filled with 1/2-in. diameter glass marbles.

The solid particles composing the bed were supported on two stainless steel meshes (No. 50 over No. 10) placed above the 1-in. plexiglass plate with the orifices. Pressure taps were located on the column to permit observation of pressure drop along the depth of the bed.

The first pressure tap was placed in the bottom flange of the column and projected to within 1/4 in. above the stainless steel screens. The second pressure tap was placed in the column wall 3 in. above the screens and directly above the first pressure tap. The rest of the pressure taps were at 3-in. intervals up the column in the garnet sand experiments. An identical column with pressure taps at 1.5-in. intervals was used on the silica sand and coal experiments. The pressure taps were constructed of 1/4-in. copper tubes. The inner opening of the pressure taps was covered by a 50-mesh or 100-mesh stainless steel screen soldered in place. The first pressure tap protruded 1-1/2 in. into the column. The remainder of the pressure taps protruded 1/2 in. into the column.

The above pressure taps were connected by plastic tubing to glass piezometers mounted on boards.

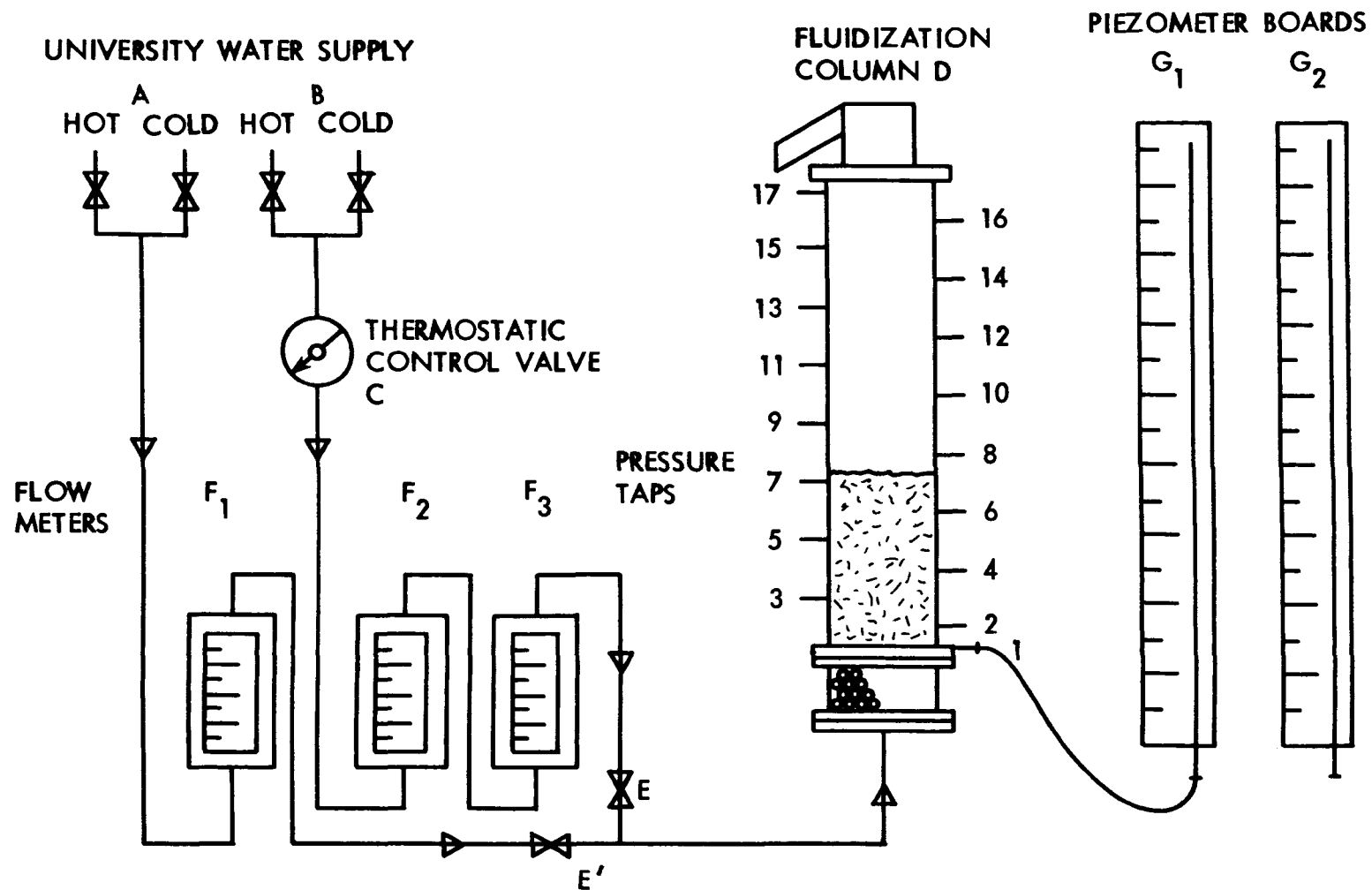


Fig. 58. Schematic layout of 6-in. fluidization column.

### General Layout of 2-in. Fluidization Column

A schematic layout of the intermixing column is shown in Fig. 59. This column was used in expansion vs flow rate observations for uniform sizes of silica sand, garnet sand, and coal. It was also used in observation of intermixing tendency between dual media comprised of uniform sizes of either garnet and silica sand or silica sand and coal.

The source of water (hot and cold) was the water taps, B, discussed in connection with Fig. 58. The mixing valve and flowmeter  $F_3$  were also used with the 6-in. column experiments. Flowmeter  $F_4$  was connected in series to flowmeter  $F_3$ . Between the two flowmeters was a 1/4-in. needle valve and a 1/4-in. quick shutoff valve.

The column consisted of the calming section, the fluidizing chamber, and an overflow structure. The fluidizing chamber was made of a 2-in. inside diameter plexiglass column 68-3/4 in. in height with 3/4-in. plexiglass flanges on each end. The inlet to the calming section was by a 3/8-in. opening. The height of the calming section was 2-1/4 in., with an inside diameter of 2 in. The lower 1-1/2 in. were filled with glass beads 6 mm in diameter. A stainless steel screen of 50 mesh was placed in the bottom of this section to prevent loss of the glass beads. The remaining volume of the calming section was filled with 2-mm lead beads. Between the calming section and the fluidizing chamber, a 100-mesh stainless steel screen was placed.

The overflow structure was an 11-1/4-in. extension of the fluidizing chamber. The top of this structure was perpendicular to the column axes, and the water flowed radially out of the column. This water was collected by a circular trough and drained to the floor drain.

### Flowmeters

Four flowmeters were used during the collection of data. They were the rotameter type and, for the purpose of this research, were designated as  $F_1$ ,  $F_2$ ,  $F_3$ , and  $F_4$ . The range of flows and scale of the flowmeters are as follows:

<u>Flowmeter</u>	<u>Range</u>	<u>Scale</u>
$F_1$	0 to 24 gpm	in % of 24 gpm
$F_2$	0 to 11.5 gpm	in gpm
$F_3$	0 to 2 gpm	in gpm
$F_4$	0 to 0.6 gpm	in % of 0.6 gpm

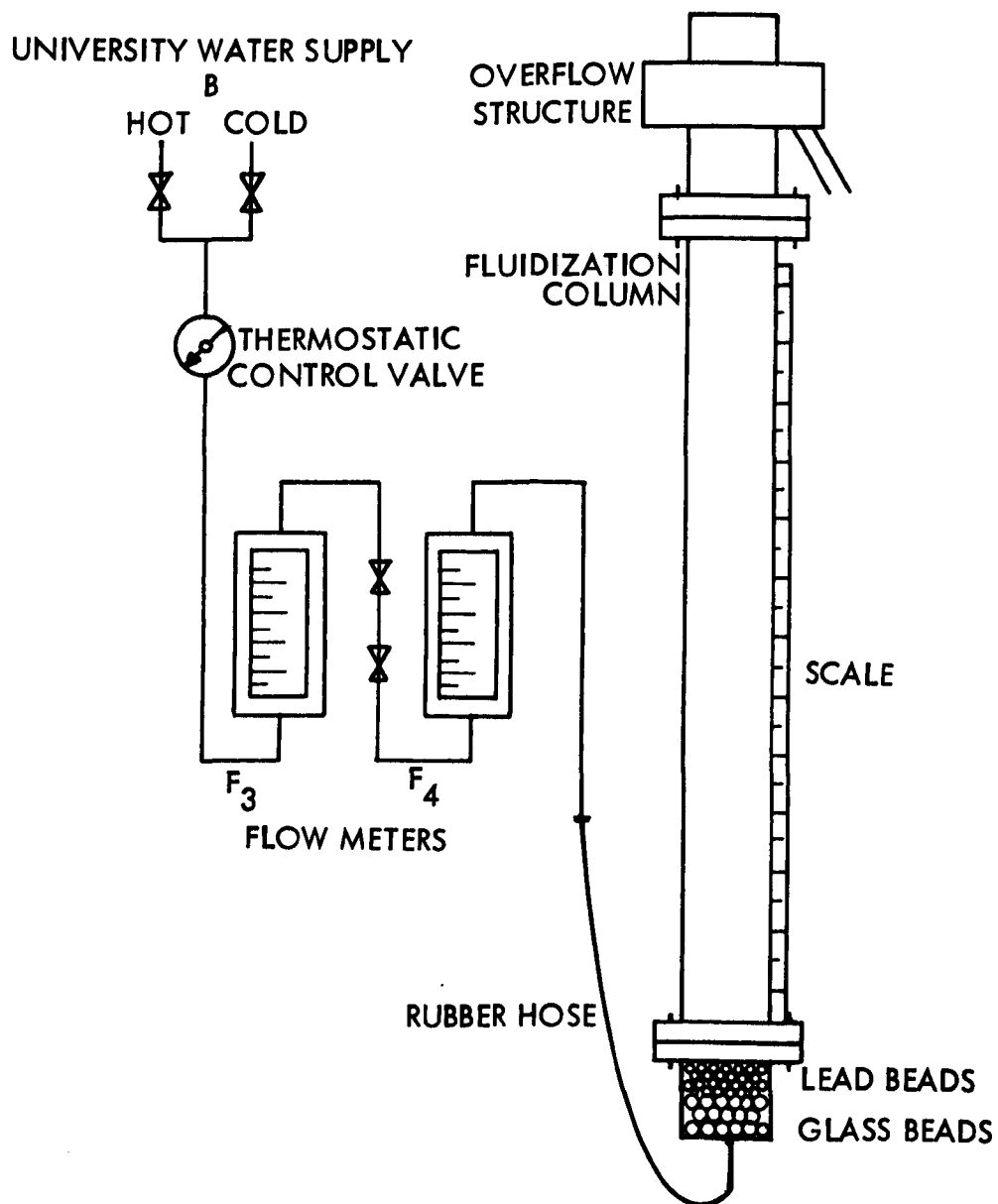


Fig. 59. Schematic layout of 2-in. fluidization column.

Flowmeters  $F_1$ ,  $F_2$ , and  $F_3$  were calibrated at the two temperatures used by a weighting technique. A least squares fit was used in determining the calibration equation for the flowmeters. These equations are as follows:

<u>Flowmeter</u>	<u>Temperature, °C</u>	<u>Actual flow, gpm</u>
$F_1$	16.5	$= 0.038 + 1.007 (\text{meter reading}) \times 24$
	25.0	$= 0.113 + 1.003 (\text{meter reading}) \times 24$
$F_2$	17.0	$= 0.169 + 1.032 (\text{meter reading})$
	25.0	$= 0.197 + 1.027 (\text{meter reading})$
$F_3$	17.0	$= - 0.067 + 0.994 (\text{meter reading})$
	25.0	$= - 0.069 + 1.026 (\text{meter reading})$

The flowmeter reading of meter  $F_4$  was checked using a volumetric technique. The results of this calibration were judged acceptably close so that the flowmeter reading was accepted to be the actual flowrate.

#### Sieves

United States Standard sieves were used in determining the gradation of the sands and also to separate uniform sizes from wider size ranges received from the suppliers of the garnet sand, silica sand, and coal.

#### Filter Media

Two different types of sands, garnet and silica, and crushed anthracite coal were used in this research. The garnet sands are obtained from alluvial deposits which are crushed to requirements and sieved to desired specifications. The individual particles are very angular and vary widely in shape. The recommended sizes of garnet sand for wastewater filtration range from passing United States Standard Sieve No. 20 to that retained on No. 80 [34].

Five different garnet media (Idaho Garnet Abrasive Company, Kellogg, Idaho) were studied in the garnet expansion experiments. They were: (1) uniform sized (-14+16) (uniform sizes are defined as passing (-) and retained United States Standard sieves) separated from manufacturers rating size M-16, (2) uniform sized -25+30 separated from manufacturers rating size M-36, (3) uniform sized -50+60 separated from manufacturers rating size M-60-80, (4) graded sized, as received, manufacturers size M-60-80 and, (5) graded size, as received, manufacturers rating size M-36.

For the garnet-silica sand intermixing experiments, a single uniform garnet sand was fluidized in successive experiments with various uniform silica sands. The garnet sand was the uniform -50+60 used in the expansion experiments. The silica sand used in this series of experiments were uniform sizes of -20+25, -30+35, -35+40, and -40+45 separated from manufacturers (Northern Gravel Co., Muscatine, Iowa) rating fine sand. The graded silica sands and anthracite coals used in the 6-in. column experiments are presented in Table 29.

Table 29. Size and source of raw graded silica sands and coals studied.

Type	Designation	Effective size, mm	Uniformity coefficients	Source
Graded sand	A	0.54	1.41	1
Graded sand	C	0.72	1.42	1
Graded coal	A	0.89	1.53	2
Graded coal	B	0.98	1.43	2
Graded coal	C	1.08	1.53	3
Graded coal	D	1.30	1.47	4
Graded coal	E	1.46	1.38	4
Graded coal	F	1.92	1.72	3

1. Silica Sand, Northern Gravel Co., Muscatine, Iowa.
2. Philterkol No. 1 Special Anthracite, Reading Anthracite Coal Company, Locust Summit, Pennsylvania.
3. Carbonite #B, Carbonite Filter Corp., Delano, Pennsylvania.
4. Shamokin Coal Company, Shamokin, Pennsylvania.

Uniform silica sands and coals were used in the 2-in. column to observe expansion, bulk density, and intermixing behavior as a function of flow rate. These uniform media were prepared by sieving the above graded media and included the following sizes: -10+12 and -12+14 mesh from Sand C; -14+16, -16+18, -18+20, -20+25, -30+35, -35+40, and -40+45 mesh from Sand A; -4+7, -7+8, -8+10 and -10+12 mesh from Coal F; and -10+12, -12+14, -14+16, -16+18, -18+20, -20+25, and -25+30 mesh from Coal A.

## Experimental Procedures

### Separation Sieving for Uniform Media

The two sands and the coal that were used were sieved into uniform sizes by using a stack of appropriate sieves and a Combs Gyratory machine (Great Western Mfg. Co., Combs Gyratory Sifting Machine, Leavenworth, Kansas). The sieving time was 5 min for sand and 8 min for coal, and the total load to the sieves was 300 to 350 g for sand and 200 to 250 g for coal. The sands and coals of each uniform size were sieved a second time using the same procedure as in the first separation sieving to improve the uniformity.

### Average Particle Size Determination

Sieve analysis. The ASTM Standard Method for Sieve or Screen Analysis of Fine and Coarse Aggregates [2, p. 93] states the following criteria for sieve analysis:

The sample of aggregate to be tested for sieve analysis shall be thoroughly mixed and reduced by use of a sample splitter or by quartering - to an amount suitable for testing.

... not more than 1% by weight of the residue on any individual sieve will pass that sieve performed as follows: Hold the individual sieve, provided with a snug-fitting pan and cover, in a slightly inclined position in one hand. Strike the side of the sieve sharply and with an upward motion against the heel of the other hand at a rate of about 150 times/min, turn the sieve about 1/6 of a revolution at intervals of about 25 strokes.

The criteria of not more than 1% passing in an additional minute of hand sieving was not met by using the sieving machine. Because of this, machine sieving was abandoned for the sieve analysis procedure, and a modified method of hand sieving was adopted. This method followed the above ASTM Standard Methods describing hand sieving except that the sieving time was extended to 3 min. It is recognized that the hand sieving technique would also have been better for the separation sieving previously described. However, hand sieving was not practical for that step due to the large quantities of media that were separated.

Equivalent diameter of a sphere. The particle size of the three uniform garnets was also determined by counting and then weighing particles and calculating the equivalent diameter of a spherical particle of the same weight and density. The equivalent diameter of a spherical particle is given by Eq. (40),

$$d_{eq.} = \left( \frac{6w}{N\pi\gamma_s} \right)^{1/3}.$$

### Density

The densities of the silica and garnet sands were determined by the water displacement technique using a 50-ml pycnometer bottle. The sand samples were dried at 110 °C for 2-1/2 hr as a preliminary procedure prior to the test and were submerged for 1 hr before final weighings.

The same water displacement method was used for the coal because the filter coal media during actual operating conditions would be similarly submerged in water. The samples were dried at 110 °C for 2-1/2 hr as a preliminary procedure prior to the test and were submerged for 24 hr before final weighings to allow the water to penetrate the pore spaces.

### Porosity

Two methods of porosity determination were used. The first was a water displacement and simulated fluidization technique, hereafter referred to as the graduate cylinder technique. Two 1000-ml graduate cylinders were used. In one cylinder, sand with a dry volume between 200 and 400 ml was measured. In the other cylinder, exactly 500 ml of water was placed. The known volume of sand was poured slowly into the cylinder that contained the 500 ml of water. The total volume of the sand and water and the apparent volume of the sand were measured. The next step was to simulate fluidization of the particles. But before this was done, enough water was added to completely fill the cylinder. There were two reasons for adding the additional water: (1) to prevent the trapping of air in the settled bed and (2) to prevent some of the particles from sticking to the sides of the cylinder and rubber stopper. With a rubber stopper placed tightly in the open end of the cylinder, the cylinder was rapidly inverted a number of times then quickly set down and the particles allowed to settle. The apparent volume of sand was then measured. In this method, it was assumed that the particles would settle in their least dense volume and represent the same porosity as that at minimum fluidization velocity. Three sets of measurements were made for each garnet-sand media.

The second method used for porosity determination of a media in a fixed-bed condition in the column will be hereafter referred to as the column technique. The volume of media was found from the weight of the media placed in the fluidizing column and the specific weight of the media. The total volume of the media and entrapped fluid was determined from the column diameter and the bed height of the media after the bed was fluidized, expanded, and slowly contracted. The column technique was used as a check of the graduate cylinder technique for the garnet sand and was the only method used for porosity determinations of the silica sand and coal.

### Settling Velocities

The settling velocities of discrete particles were experimentally determined for representative samples of the three uniform size garnet sands. A 5-in. diameter plexiglass column, 56 in. in height, was used for this experiment. The column was filled to the top with water. The particles that were placed in the water, rolled gently between two fingers to completely remove any air attached to the particle, and then released. They then fell through 16 in. of water to come to dynamic equilibrium before a stopwatch was started. The particles then fell through a 30-in. timed interval. The average settling velocity of each uniform garnet-sand media was determined at two different water temperatures of 16 to 17 °C and 25 °C. The water temperature was adjusted when it deviated more than 0.5 °C from the temperature desired.

### Expansion - Flow Rate Experiments

Expansion experiments were made in both the 6-in. column and the 2-in. column previously described. The total bed was fluidized to about 50% expansion and allowed to contract slowly. Starting with a fixed bed, the flow rate was incrementally increased to a maximum expansion. Readings were taken of flow rate, temperature, bed height, and (for the 6-in. column) the piezometer tubes.

Readings were not made until the water temperature was constant, the influent temperature matched the effluent temperature, the water pressure was steady, and the bed height was stabilized. Visual observations of bed behavior, such as portions of the bed which were fluidized, and any circulation patterns were also noted.

Upon fluidization of the first garnet sample, run 1 (Series A-13), it was noticed that the top 1/2 to 1 in. of the bed consisted of a lighter colored material than the rest of the bed, which was the purple color characteristic of the garnet sand. The bed was completely fluidized and then contracted slowly. The light-colored greyish material was then siphoned off the top of the bed. Removal of this light-colored, less-dense material was done before any expansion data were taken for garnet gradations.

### Bulk Density and Intermixing of Uniform Sized Media

A full range of uniform-sized media of each type (coal, silica sand, and garnet sand) were fluidized in the 2-in. column for purposes of determining expansion vs flow rate. From these data, bulk density could be calculated at all flow rates. Some of the uniform media were then observed in dual-media beds comprised of silica sand and coal or garnet sand to determine their intermixing behavior. The procedure for the garnet sand-silica sand experiments is presented here as an example. Essentially the same procedures were used for the coal and silica sand observations.

One uniform size garnet sand -50+60 and uniform size ranges of silica sand -20+25, -30+35, -35+40, and -45+50 were used. The garnet was split down to approximately  $1000 \pm 40$  g samples by the use of a sample splitter. The samples were then adjusted by the removal or addition of garnet to  $1000.0 \text{ g} \pm 0.1$ .

The silica sand was separated into uniform sizes as described previously, washed, and dried. Then the sieve analyses were made. The uniform silica sand samples were then weighed with a precision of  $\pm 0.1$  g.

One of the 1000-g garnet sand samples and all of the uniform silica sand samples were individually fluidized in the intermixing column. The samples were completely fluidized and slowly contracted to a fixed bed at zero upward flow. Then the flow rate was incrementally increased. Readings of temperature, bed height, and flow rate were recorded during the expansion. Visual observations of the portions of the bed fluidized and the circulation patterns were also recorded.

After each of the individual silica sand media was fluidized and observed as described in the above paragraph, a 1000.0-g garnet sand sample was poured into the intermixing column on top of the silica sand. The dual media was then expanded 60 to 70% and very slowly allowed to contract to a fixed bed with no flow. Bed height, relative location of each media, and qualitative concentration of each media were noted. Expansion of the bed was started and incrementally increased to a height of about 60 in. (200%). The previously mentioned bed height, qualitative location and concentration of the individual media, temperature, and visual observations of circulation patterns were recorded at several flow rates.

### Illustrative Calculations

The illustrative calculations presented are for the uniform garnet sand -14+16 which had been separated in accordance with the separation sieving technique previously described.

### Sieve Analysis

The results of three sieve analyses are shown in Table 30. The results of using the mechanical sieving machine and hand sieving are shown. Sample 1 was sieved for 5 min on the Gyratory sieving machine. Samples 2 and 3 were hand sieved for 3 min. Samples 1a and 3a are the percentage of the material retained on an individual sieve which passes that sieve in one additional minute of hand sieving. The percentage that passed the No. 14 sieve in the additional minute of hand sieving is highly distorted because the amount that was retained in the initial sieving was very small. The percentage that passed the No. 16 sieve in the additional minute of hand sieving is slightly higher than the ASTM recommended value of 1% passing an individual sieve in one additional minute of hand sieving, but comparison of the mechanical and

Table 30. Sieve analysis of garnet sand media (-14+16).

Sample no.		1	1a	2	3	3a		
Sieved load, g		148.99		145.92	154.15			
Sieving procedure		Machine	Hand	Hand	Hand	Hand		
Sieving time, min		5	1	3	3	1		
Sieve no.	Sieve opening, mm	% retained	% passing <sup>a</sup>	% retained	% retained	% passing <sup>a</sup>	% retained mean of 2 and 3	% passing mean of 2 and 3 <sup>b</sup>
14	1.41	16.72	23.20	0.17	0.31	16.66	0.24	99.76
16	1.19	81.32	11.54	88.10	87.35	2.38	87.72	12.04
18	1.00	1.85	0.08	11.69	12.30	0.00	12.00	0.04
Pan	—	0.11	—	0.04	0.04	—	0.04	0.00

<sup>a</sup>Percent passing in one additional minute of hand sieving expressed as percentage of original amount retained on that individual sieve.

<sup>b</sup>One hundred minus mean percent retained.

hand sieving methods shows the improvement of the hand sieving method over the mechanical sieving method. The results of sample 1 are representative of the results obtained by mechanical sieve analysis of other samples for sieving times of up to ten minutes. The increase in mechanical sieving time was found to improve the sieve analysis only slightly. Because the results of hand sieving method conform quite closely to the recommended standards of ASTM, as previously stated, the hand sieving method was adopted, and all sieve analyses reported herein are by the 3-min hand sieving technique.

#### Average Particle Size Determination

From sieve analysis. The average sizes are determined by the inverse definition Eq. (38) and by the arithmetic mean definition Eq. (39) as follows:

Sieve no.	Sieve opening, mm	Mean opening between sieves ( $d_i$ ), mm	Weight fraction ( $W_i$ )	$W_i/d_i$	$W_i d_i$
12	1.68	1.55	0.24	0.16	0.37
14	1.41	1.30	87.72	67.48	114.04
16	1.19	1.09	12.00	11.01	13.08
18	1.00	0.92	0.04	0.04	0.04
Pan	0.841				

$$\Sigma \frac{W_i}{d_i} = 78.69$$

$$\Sigma W_i d_i = 127.53$$

Therefore, changing of the weight from percent to a fraction, the diameter as defined by the inverse definition Eq. (38) is,

$$d_{\text{inverse}} = \frac{1}{\Sigma \frac{W_i}{d_i}} = \frac{1}{0.7869} = 1.271 \text{ mm.}$$

and as defined by the arithmetic mean average from Eq. (39) is,

$$d_{\text{m}} = \Sigma W_i d_i = 1.275 \text{ mm}$$

Note: the difference in the two definitions of diameter is small for a uniform media but is greater as the variation in size of media increases as will be shown in the results section of this report.

Equivalent diameter of a sphere.

<u>Sample</u>	<u>1</u>	<u>2</u>
Number of particles	110	110
Weight of particles	0.5798	0.5968
Density of solid, g/cc	4.140	4.140

Equivalent diameter of a spherical particle of the same volume is given by Eq. (40),

$$d_{eq} = \left[ \frac{6(0.5798)}{110 \pi 4.15} \right]^{1/3} \qquad \qquad \left[ \frac{6(0.5968)}{110 \pi 4.15} \right]^{1/3}$$

$$d_{eq}(\text{mm}) = \qquad 1.343 \qquad \qquad 1.356$$

$$\text{avg } d_{eq}(\text{mm}) = \qquad 1.349$$

Density

1. Weight of dry pycnometer	= 25.9310 g
2. Weight of pycnometer full of water	= 125.4432 g
3. Weight of pycnometer with inside wet	= 26.1743 g
4. Weight of pycnometer inside wet + garnet sand	= 45.7310 g
5. Weight of pycnometer + garnet sand + water to fill	= 140.2815 g
6. Temperature of water	= 24 °C
7. Therefore, weight of sand = 4 - 3	= 19.5567 g
8. Weight of water to fill pycnometer = 2 - 1	= 99.5122 g
9. Weight of extra water to fill pycnometer over the sand = 5 - 1 - 7	= 94.7938 g
10. Weight of equivalent volume of water = 8 - 9	= 4.7184 g

11. Therefore, specific gravity of garnet sand at 24 °C = 7/10  
= 4.1448
12. Density of water at 24 °C = 0.99707 g/ml
13. Density of garnet sand = (11) (12) = 4.133 g/ml

### Porosity

Graduate cylinder technique. The following three samples are from the garnet sand -14+16,

	<u>i</u>	<u>ii</u>	<u>iii</u>
1. Dry volume of sand (ml)	340	390	170
2. Volume of water (ml)	500	500	500
3. Total volume of sand + water (ml)	695	740	610
4. Volume of sand after simulating fluidization (ml)	360	440	200
5. Porosity $[4 - (3-2)]/4$	0.458	0.455	0.450

Average of row 5 = 0.454

### Column technique.

Dry weight of -14+16 garnet sand removed from column, lb	= 31.5
Fixed bed height, ft	= 1.138
Cross-sectional area of column, sq ft	= 0.196
Total volume of water and garnet sand, cu ft	= 0.2235
Specific weight of garnet sand, lb/cu ft	= 257.9
Volume of garnet sand removed from column, cu ft	= 0.1221
Fixed bed porosity = $(0.2235 - 0.1221)/0.2235$	= 0.453

### Settling Velocities

Number of particles dropped	= 100
Distance of timed fall, ft	= 2.5
Temperature of water	= 16.5 °C

Observed settling time of single particles, sec

3.3	3.5	3.5	4.1	3.1	2.9	3.9	3.4	3.4	4.2
4.9	2.9	3.2	3.2	3.0	3.0	3.2	3.1	4.2	3.6
3.4	3.6	4.4	3.0	2.9	4.1	3.3	5.4	3.1	3.2
2.8	3.0	2.9	3.0	3.0	3.4	3.0	3.9	3.1	3.2
3.8	2.7	2.6	3.1	4.2	3.5	3.1	4.0	3.2	4.8
4.4	4.3	4.0	3.5	4.3	3.7	3.1	2.9	3.4	3.1
3.4	3.7	3.1	4.4	4.3	3.6	3.5	3.2	4.1	2.8
3.9	3.1	3.1	3.4	3.7	3.0	3.2	3.7	3.8	3.7
3.6	4.0	3.2	3.0	3.5	4.0	3.8	4.2	5.1	3.5
3.4	3.9	3.7	3.6	3.8	4.4	4.3	4.0	3.9	3.2

Mean time of fall = 3.56 sec

Standard deviation = 0.5534 sec

Mean velocity = 0.703 fps = 315 gpm/sq ft

Expansion - Flow Rate and Intermixing

Illustrative calculations for the expansion-flow rate and intermixing data will be presented along with the presentation and analysis of the data.

Results and Analysis - Summary

The main series of experimental runs for the study have been summarized in Tables 31-32. Table 31 lists the downflow and/or upflow runs in the large column for various single media. Table 32 describes the upflow and downflow runs in the large column for various dual-media filters. Table 33 gives the upflow runs in the small column for uniform single- and dual-media filters.

Results - Media Characteristics

Sieve Analyses

The results of the sieve analyses for the various media studied are presented in Figs. 60, 61 and 62. Effective size and uniformity

Table 31. Upflow and/or downflow experimental runs with the various single media in the 6-in. column.

Series	Media <sup>a</sup>	Description		Initial depth, in.	Downflow		Upflow
		ES mm	UC		Rate, gpm/sq ft	Temp, °C	Temp, °C
A-1	Coal A	0.89	1.53	12.75	7,8,9	18,22,26,30	18,22,26,30
A-2	Coal UCA	1.38	1.12	6.38	4,8	18,26	22
A-3	Coal B	0.98	1.43	12.75	4,8	18,26	22
A-4	Coal C	1.08	1.53	12.25	4,8	18	22
A-5	Coal C <sub>2</sub>	1.16	1.49	11.12	4,8	18	22
A-6	Coal D	1.30	1.47	11.20	4,8	18	22
A-7	Coal E	1.46	1.38	8.00	4,8	18	22
A-8	Coal F	1.92	1.72	6.63	4,8	18	22
A-9	Sand A	0.54	1.41	12.40	4,7,8,9	18,22,26,30	18,22,26,30
A-10	Sand A <sub>2</sub>	0.60	1.28	9.75	4,8	18	22
A-11	Sand C	0.72	1.42	12.38	4,8	18	22
A-12	Sand C <sub>2</sub>	0.75	1.43	11.38	4,8	18	22
A-13	Garnet -14+16	1.20	1.08	12.65	—	—	16,25
A-14	Garnet -25+30	0.60	1.07	12.35	—	—	16,25
A-15	Garnet -50+60	0.25	1.10	12.50	—	—	17,25
A-16	Garnet M-60-80	0.17	1.71	14.80	—	—	17,25
A-17	Garnet M-36	0.47	1.43	15.45	—	—	17,25

<sup>a</sup>Subscript 2 signifies media remaining after hydraulic grading and skimming 10% of the fines from the raw media of same letter designation.

Table 32. Upflow and downflow experimental runs with dual-media filters in the 6-in. column.

Series	Dual media <sup>a</sup>	Depth, in.			Downflow		Upflow
		Sand	Coal	Total	Rate, gpm/sq ft	Temp, °C	Temp, °C
B-1	AA	A = 11.25	A = 12.75	23.50	4,8	18,26	22
B-2	AB	A = 6.26	B = 12.63	18.50	4,8	18,26	22
B-3	AC	A = 10.75	C = 12.25	21.75	4,8	18	22
B-4	AD	A = 13.25	D = 12.25	24.75	4,8	18	22
B-5	A <sub>2</sub> E	A <sub>2</sub> = 12.00	E = 9.00	20.50	4,8	18	22
B-6	AF	A = 6.25	F = 6.50	12.00	4,8	18	22
B-7	A <sub>2</sub> A <sub>2</sub>	A <sub>2</sub> = 12.00	A <sub>2</sub> = 11.00	22.75	4,8	18	22
B-8	AUCA	A = 6.25	UCA = 6.25	12.00	4,8	18,26	22
B-9	A <sub>2</sub> C <sub>2</sub>	A <sub>2</sub> = 9.75	C <sub>2</sub> = 11.12	20.00	4,8	18	22
B-10	A <sub>2</sub> F <sub>2</sub>	A <sub>2</sub> = 6.63	F <sub>2</sub> = 7.88	12.90	4,8	18	22
B-11	A <sub>2</sub> F <sub>2</sub>	A <sub>2</sub> = 6.63	F <sub>2</sub> = 16.00	20.00	4,8	18	22
B-12	A <sub>2</sub> F <sub>2</sub>	A <sub>2</sub> = 6.63	F <sub>2</sub> = 23.75	27.75	4,8	18	22
B-13	CF	C = 12.25	F = 12.00	22.50	4,8	18	22
B-14	C <sub>2</sub> F <sub>2</sub>	C <sub>2</sub> = 11.25	F <sub>2</sub> = 10.87	20.38	4,8	18	22

<sup>a</sup>Described by the letter designation for the component sand and coal, respectively, from Table 31.

Table 33. Upflow experimental runs with various uniform single media and uniform dual media in 2-in. column, 25 °C.

Series	Uniform media description	Depth, in.
C-1	Sand A (-10+12)	12.20
	Sand A (-12+14)	12.65
	Sand A (-14+16)	11.90
	Sand A (-16+18)	11.25
	Sand A (-18+20)	11.90
	Sand A (-20+25)	12.00
	Sand A (-25+30)	12.85
	Sand A (-30+35)	11.75
	Sand A (-35+40)	11.65
	Sand A (-40+45)	10.20
C-2	Coal F (-4+7)	12.60
	Coal F (-7+8)	11.95
	Coal F (-8+10)	4.85
	Coal F (-10+12)	13.15
C-3	Coal A (-10+12)	12.05
	Coal A (-12+14)	11.60
	Coal A (-14+16)	11.50
	Coal A (-16+18)	11.20
	Coal A (-18+20)	10.90
	Coal A (-20+25)	10.65
	Coal A (-25+30)	12.50
C-4	Coal F (-4+7), 5.9 in. and Sand A (-40+45), 6.6 in.	10.0
	Coal F (-4+7), 6.7 in. and Sand A (-35+40), 5.5 in.	10.5
	Coal F (-4+7), 5.8 in. and Sand A (-30+35), 6.0 in.	10.0
	Coal F (-4+7), 5.7 in. and Sand A (-25+30), 6.3 in.	10.3
	Coal F (-4+7), 5.5 in. and Sand A (-20+25), 5.5 in.	9.5
	Coal F (-4+7), 5.4 in. and Sand A (-18+20), 5.8 in.	10.3
D-1	Garnet (-50+60)	11.40
	Sand A (-20+25)	12.75
	Sand A (-30+35)	
	Sand A (-35+40)	13.85
	Sand A (-40+45)	9.80
	Sand A (-20+25), 12.75 and Garnet (-50+60), 11.40	23.9
	Sand A (-30+35), <sup>a</sup> and Garnet (-50+60), 11.40	22.25
	Sand A (-35+40), 13.85 and Garnet (-50+60), 11.40	25.10
	Sand A (-40+45), 9.80 and Garnet (-50+60), 11.40	20.80

<sup>a</sup>Not recorded.

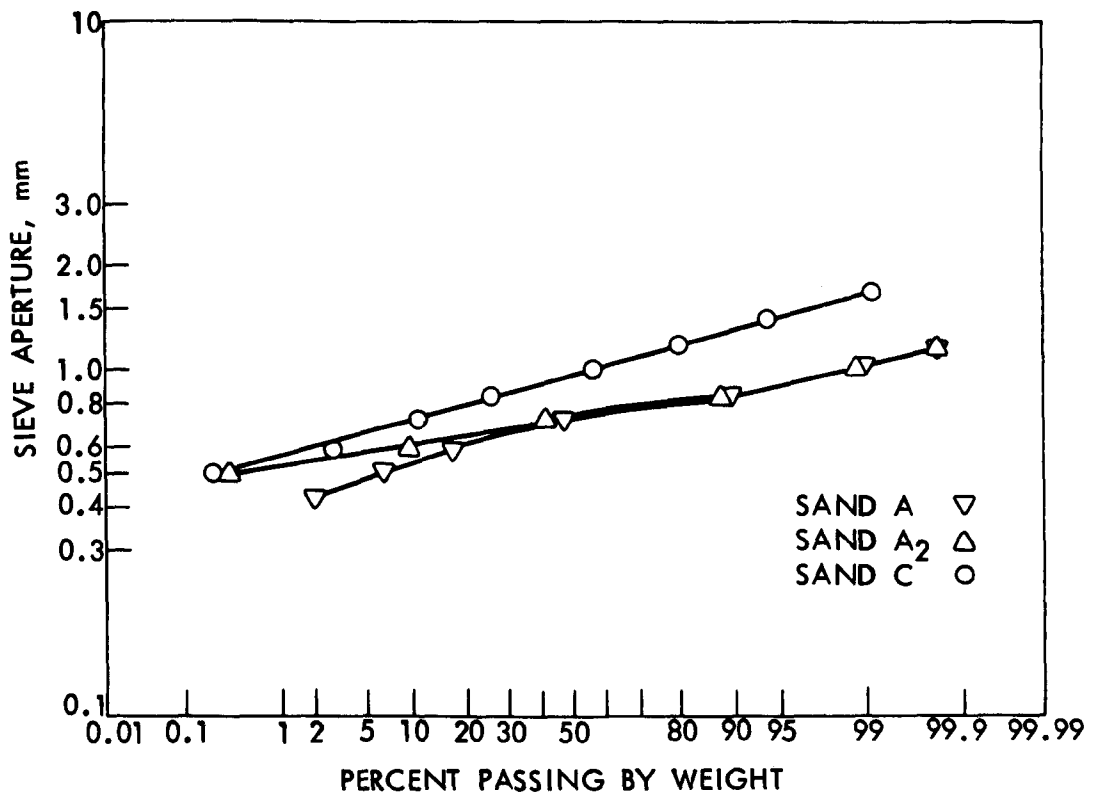


Fig. 60. Sieve analysis of graded sand media.

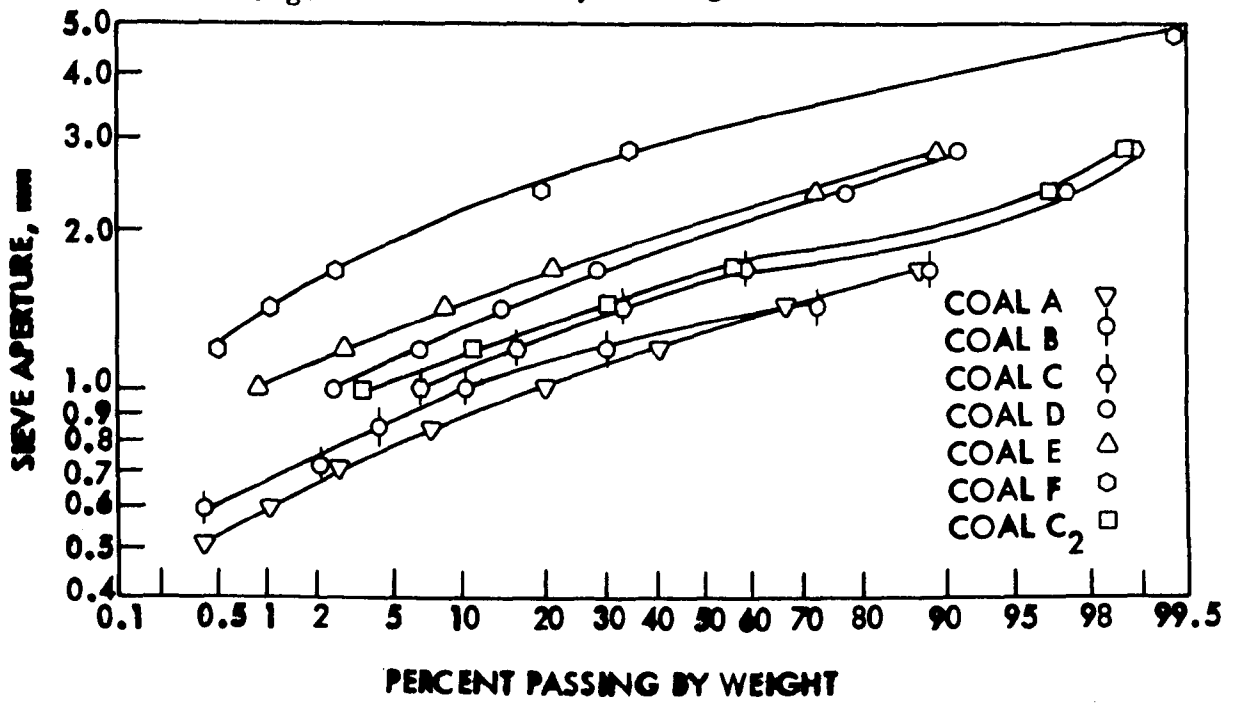


Fig. 61. Sieve analysis of graded coal media.

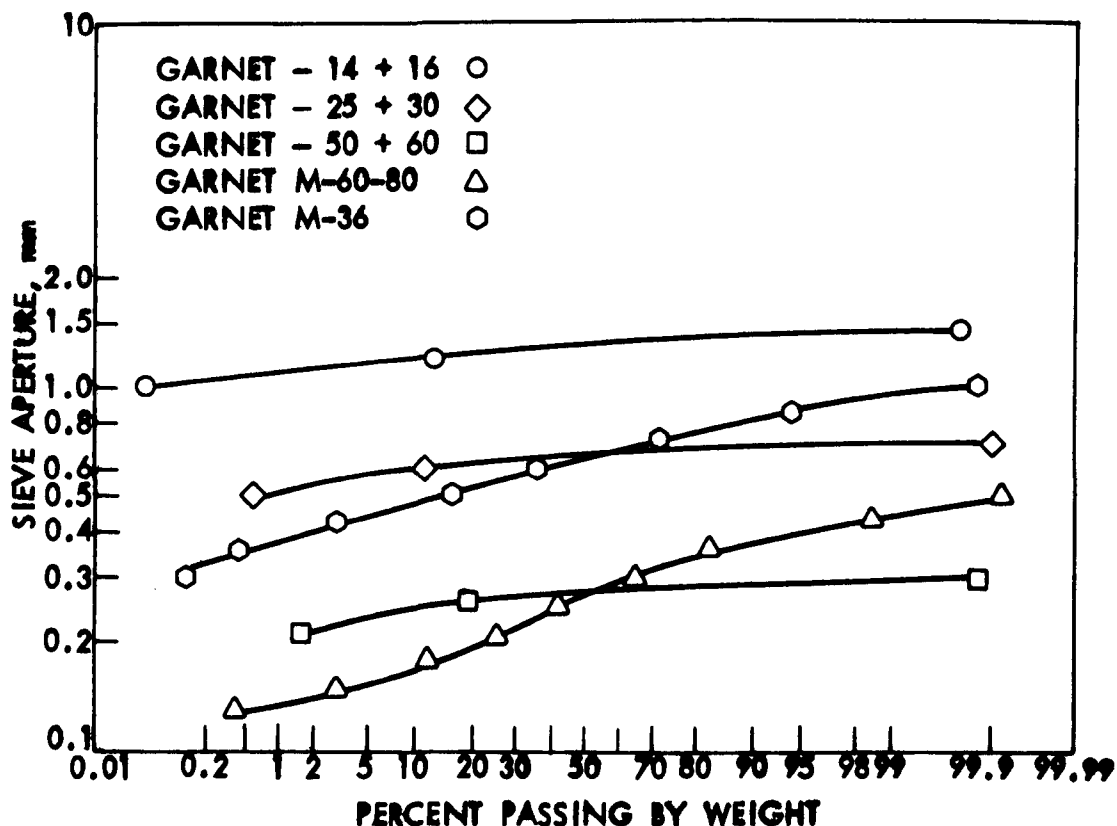


Fig. 62. Sieve analysis of garnet sand media.

coefficients for the graded sands and coals have been presented previously in Table 29.

In two cases, 10% of a medium was removed by skimming the uppermost layer of the filter bed through the use of a siphoning hose after the medium had been stratified by backwashing. Unskimmed graded media were alphabetically designated, for example, Sand A, whereas skimmed media were additionally labelled with a subscript, for example, Sand A<sub>2</sub>. Figures 60 and 61 demonstrate that a slightly larger effective size and a smaller uniformity coefficient resulted from skimming as the finest media particles were removed.

The graded media, as shown in Figs. 60, 61, and 62, followed a near log-normal distribution.

The results of the sieve analyses of the uniform silica sands and uniform coals are presented in Appendix A. The results indicate that at least 70% (generally greater than 80%) of the total sample was retained between the adjacent sieves indicated in the size designation (e.g., -20+25).

### Average Particle Size Determinations

The average sizes of the particles for the uniform media were determined from the sieve analysis presented previously and the equivalent diameter of a spherical particle. The data for the equivalent diameter of a spherical particle is presented in Table 34. A summary of the results for the average particle size for the various methods is presented in Table 35. The table includes average diameter by the arithmetic mean defined by Eq. (39), the inverse diameter defined by Eq. (38), the diameter of the 60% finer size from the sieve analyses plotted in Figs. 60, 61, and 62, and the equivalent diameter of a spherical particle by Eq. (40).

It is apparent from Table 34 that the equivalent spherical diameter of the various media is larger than the mean of adjacent sieve size for the uniform media. This is to be expected because of the non-sphericity of the media.

Table 35 indicates that the inverse definition for the graded media gave a somewhat lower average diameter than the arithmetic mean diameter. The diameter corresponding to the 60% finer size was closer to the arithmetic mean diameter.

### Densities

The results of the density determinations for the garnet sand, silica sands, and coal are given in Table 36. Several replicates are reported for the garnet sand to illustrate the precision of the analysis.

The garnet sand used for density determinations was from the uniform -14+16 and -25+30 sizes (Table 36). The density of the -25+30 garnet was somewhat lower than that of the -14+16 garnet sand. The pycnometer bottles were shaken vigorously to remove air attached to the particles and allowed to cool to room temperature. Therefore, it was assumed that the inclusion of air or the temperature effects on the density of water were not the source of the difference. The probable source of difference was that the -25+30 garnet contained a small amount of the less-dense, grayish-colored material that was assumed to be removed. The difference was quite small; therefore, the average of all six determinations was used in all necessary calculations involving garnet sand media.

### Porosities

The fixed-bed porosities for the media used in the experiments were determined two ways: (1) the graduate cylinder technique and (2) the column technique (using both the 2-in. and 6-in. diameter fluidization columns). The results for the porosity determinations by the graduate cylinder technique and by the column technique are given in Table 37. In some cases, data were collected by both investigators (Woods [143], Boss [14]). Both values are reported to indicate the spread between measurements made by different investigators.

Table 34. Average diameter of uniform media by two methods, mean of adjacent sieve sizes and mean equivalent spherical diameter by the count and weigh method [Eq. (40)].

Uniform media mesh range	Particles		Mean of adjacent sieve sizes, mm (1)	Mean equivalent spherical diameter, mm (2)	(2)/(1)
	Number counted	Weight, g			
Sand A (-10+12)	100	1.0754	1.840	1.98	1.08
Sand A (-12+14)	100	0.5752	1.545	1.61	1.04
Sand A (-14+16)	100	0.3532	1.300	1.36	1.04
Sand A (-16+18)	100	0.2190	1.095	1.16	1.06
Sand A (-18+20)	100	0.1514	0.920	1.02	1.11
Sand A (-20+25)	100	0.0434	0.775	0.78	1.07
Sand A (-25+30)	100	0.0406	0.650	0.66	1.02
Sand A (-30+35)	100	0.0231	0.545	0.55	1.01
Sand A (-35+40)	100	0.0174	0.460	0.46	1.00
Sand A (-40+45)	100	0.0095	0.385	0.41	1.06
				Sand mean	1.05
Coal F (+4)	100	12.8546	—	5.22	—
Coal F (-4+7)	100	3.5898	3.790	3.40	0.90
Coal F (-7+8)	100	1.8299	2.595	2.72	1.05
Coal F (-8+10)	100	1.3413	2.180	2.46	1.13
Coal F (-10+12)	100	0.8490	1.840	2.10	1.14
Coal A (-12+14)	100	0.3410	1.545	1.57	1.02
Coal A (-14+16)	100	0.3040	1.300	1.51	1.16
Coal A (-16+18)	100	0.1331	1.095	1.15	1.05
Coal A (-18+20)	100	0.0791	0.920	0.92	1.00
				Coal mean	1.08
Garnet (-14+16)	110	0.5798	1.300	1.347	1.036
Garnet (-14+16)	110	0.5968	—	1.360	1.046
Garnet (-25+30)	110	0.0729	0.650	0.675	1.039
Garnet (-25+30)	110	0.0685	—	0.661	1.017
Garnet (-50+60)	98	0.0042	0.273	0.270	0.989
Garnet (-50+60)	91	0.0042	—	0.277	1.015
				Garnet mean	1.024

### Settling Velocities

The experimentally determined settling velocities for the three different uniform garnet sand media at the two different temperatures are given in Table 38. The mean time, the standard deviation, and mean velocity of the time measurements are included in Table 38.

A comparison of these experimental values of  $V_s$  with the velocity intercept ( $V_i$ ) at a porosity equal to one on the  $\log V$  vs  $\log c$  plots

Table 35. Summary of the average diameters of the media - d (by several methods).

Size	$d_m$ , mm	$d_{inverse}$ , mm	$d_{60\% \text{ finer}}$ , mm
Sand A	0.711	0.685	0.74
Sand C	1.008	0.946	1.03
Coal A	1.285	1.205	1.35
Coal B	1.305	1.246	1.35
Coal C	1.572	1.480	1.65
Coal D	1.988	1.800	1.90
Coal E	2.094	1.912	2.00
Coal F	3.228	2.941	3.30
Garnet (-14+16)	1.275	1.271	1.27
Garnet (-25+30)	0.639	0.637	0.635
Garnet (-50+60)	0.265	0.263	0.267
Garnet (M-60-80)	0.272	0.249	0.29
Garnet (M-36)	0.642	0.615	0.67
Source:	Eq. (39)	Eq. (38)	Figs. 60, 61, and 62

presented later in Table 41 shows that the experimental  $V_s$  was substantially lower than the  $V_i$ .

These results are consistent with the findings of Carvalho for crushed coal [28] previously discussed and can be attributed to the nonspherical shape of the particles.

Table 36. Densities of media -  $\rho_s$ .

Media	Density of sample, g/ml			Density, g/ml
	1	2	3	
Garnet sand (-14+16)	4.1337	4.1384	4.1359	
Garnet sand (-25+30)	4.1228	4.1243	4.1201	Avg 4.13
Silica sand A				2.65
Silica sand C				2.65
Coal A				1.70
Coal B				1.70
Coal C				1.71
Coal D				1.72
Coal E				1.74
Coal F				1.73

The average settling velocities for the -25+30 and -50+60 garnet sands were slightly faster at 17 °C than at 25 °C, contrary to expectations. However, the differences are not statistically significant.

#### Fixed Bed Hydraulic Profiles in Dual-Media Filters -

##### Coal and Sand

##### Downflow Observations of Single-Media Filters

To observe the effect of various degrees of intermixing on the permeability of dual-media filters, head loss vs depth was observed for the individual graded sand and graded coal media. These hydraulic

Table 37. Fixed-bed porosities of the three media determined by the two techniques ( $\epsilon_o$ ) and two investigators.

Media	Porosities			Investigator
	Graduate cylinder technique	Column technique (2 in.)	Column technique (6 in.)	
Sand A (-10+12)		0.440		Boss [14]
Sand A (-12+14)		0.442		Boss [14]
Sand A (-14+16)		0.443		Boss [14]
Sand A (-16+18)		0.448		Boss [14]
Sand A (-18+20)		0.440		Boss [14]
Sand A (-20+25)		0.439		Woods [143]
Sand A (-20+25)		0.436		Boss [14]
Sand A (-25+30)		0.444		Boss [14]
Sand A (-30+35)		0.451		Woods [143]
Sand A (-30+35)		0.441		Boss [14]
Sand A (-35+40)		0.456		Woods [143]
Sand A (-35+40)		0.458		Boss [14]
Sand A (-40+45)		0.457		Boss [14]
Sand A (-40+45)		0.452		Woods [143]
Garnet sand (-14+16)	0.454		0.453	Woods [143]
Garnet sand (-25+30)	0.504		0.505	Woods [143]
Garnet sand (-50+60)	0.550	0.554	0.580	Woods [143]
Garnet sand (M-60-80)	0.557		0.536	Woods [143]
Garnet sand (M-36)	0.508		0.495	Woods [143]
Coal F (-4+7)		0.554		Boss [14]
Coal F (-7+8)		0.560		Boss [14]
Coal F (-8+10)		0.573		Boss [14]
Coal F (-10+12)		0.573		Boss [14]
Coal A (-10+12)		0.551		Boss [14]
Coal A (-12+14)		0.555		Boss [14]
Coal A (-14+16)		0.552		Boss [14]
Coal A (-16+18)		0.554		Boss [14]
Coal A (-18+20)		0.554		Boss [14]
Coal A (-20+25)		0.558		Boss [14]
Coal A (-25+30)		0.572		Boss [14]

profiles for graded media of 6 to 12-in. depth were studied in the 6-in. fluidization column. The hydraulic profiles of the media were then to be compared to the hydraulic profiles of the corresponding dual-media filters, comprised of the same components, to observe the effects of intermixing.

Table 38. Settling velocities of uniform garnet sand media.

	Garnet sand media					
	-14+16		-25+30		-50+60	
Temperature, °C	16.5	25.0	17.0	25.0	17.0	25.0
Number of particles observed	100	100	100	100	60	60
Mean time, <sup>a</sup> sec	3.56	3.55	6.92	7.00	17.86	18.53
Standard deviation, sec	0.553	0.615	0.993	0.991	2.953	3.151
Mean velocity, fps	0.703	0.703	0.362	0.357	0.140	0.135

<sup>a</sup>Distance of timed free fall = 2.5 ft.

Several variables affecting head loss in a filter are correlated in Eq. (17) and are evident in Figs. 63 and 64. The variables have previously been studied and correlated in equations by several investigators. However, the figures are included here to help the reader visualize the nature of the raw downflow data collected.

A fluid temperature of 18 °C, the lowest consistently attained temperature with the laboratory water system, and an 8 gpm/sq ft flow rate were chosen for the downflow measurements. At high filtration rates, the head losses were more substantial and could thus be measured with greater relative precision. Thus, the high flow rate of 8 gpm/sq ft was chosen for the experiments.

Given the same flow rate and temperature, the difference in cumulative head losses between two plotted points in Figs. 63 or 64 is the difference in pressure between two adjacent piezometers on the large column. From this pressure difference, the experimental values of head loss per 1-1/2-in. depth were taken to plot the hydraulic profile. Bed depth vs the head loss per 1-1/2-in. depth was then plotted in Figs. 65 and 66 to provide downflow hydraulic gradient profiles of all graded media used. Analysis of Figs. 65 and 66 demonstrates that the top sand layer had a head loss of 0.35 ft, while the bottom coal layers had a head loss of 0.01 to 0.04 ft. Since precision of piezo-

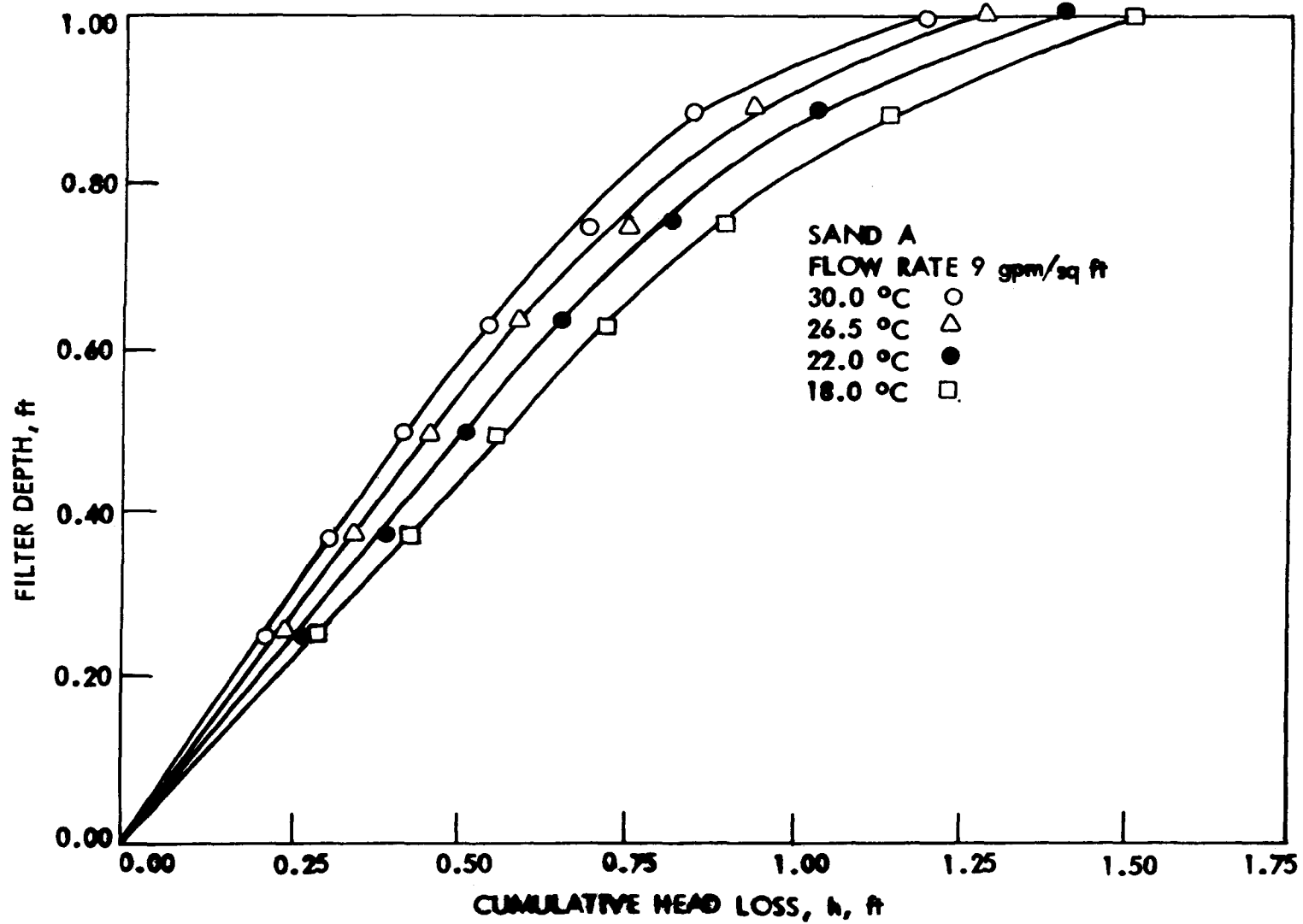


Fig. 63. Fixed-bed head loss for graded sand A at 9 gpm/sq ft for various temperatures.

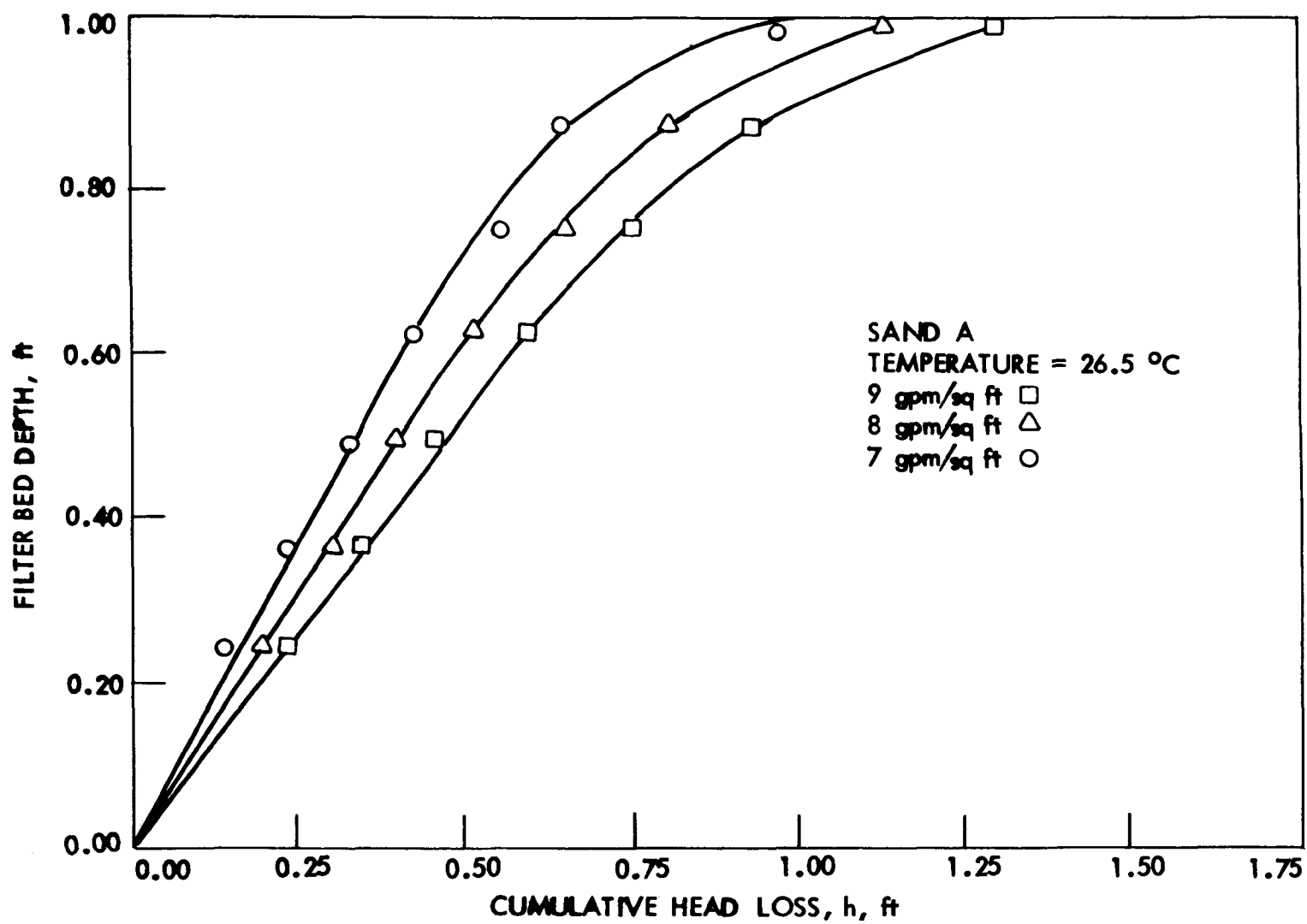


Fig. 64. Fixed-bed head loss for graded sand A at 26.5 °C for various flow rates.

meter readings was limited to 0.01 ft, the small head losses between adjacent piezometers resulted in larger relative errors in the coal head loss readings.

Study of Fig. 65, the hydraulic profile of the basic sand, reveals that a great head loss change occurs in the top half of the filter bed depth. Head loss throughout the graded coal media filter, as shown in the hydraulic profile, Fig. 66, remained fairly constant with depth. The surface head loss in the graded coal media filter was only slightly larger than that of the lower layer. Therefore, skimming of the sand media is expected to have more impact on filter performance than skimming of the coal media.

#### Downflow Observations of Dual-Media Filters

To determine the effect of intermixing on the fixed-bed hydraulic profiles of dual-media filters is one of three specific aims of this research, and Figs. 67 through 72 illustrate typical related experimental findings. Figure 67 is a typical example of cumulative head loss vs bed height for dual media AA. The gradual bend of the plotted lines in Fig. 67 exemplifies the effect of modest intermixing on head loss.

Since pressure readings could only be made to the nearest 0.01 ft, some of the data points were relatively inaccurate. Such points on figures such as Fig. 67 were adjusted by drawing the best fitting, curved line for the cumulative head loss. Values from this curved line were then chosen at 1-1/2-in. increments of the filter bed. These values were used to plot the solid-line hydraulic profile of the dual-media filters, as in Figs. 68 through 72. The adjusted points did not vary by more than  $\pm 0.02$  ft from the original experimental points.

Figures 68-72 also provide combined, individual hydraulic profiles of the dual-media filter components. These dashed-line hydraulic profiles show the head loss which would result at the interface if intermixing did not occur. To obtain these theoretical profiles, the hydraulic profiles for the appropriate sand and coal from Figs. 65 and 66 were combined. Coal was plotted above sand, and the two hydraulic profiles were connected with a horizontal line. The horizontal connecting line was plotted at the bed height corresponding to the sand depth indicated in Table 32. Thus, the hydraulic profiles of a hypothetical nonintermixed filter and actual intermixed filter are shown in Figs. 68 through 72. In Figs. 69 and 72, where the sand or coal depth was not the same as in Figs. 65 and 66, the gradient curve for the sand and coal was compressed vertically to fit the experimental sand depth. The actual observed location of the intermixing zone is shown in Figs. 68 through 72. The upper limit of the intermixing zone corresponds to the lowest filter level where only coal particles were evident, and the lower limit corresponds to the

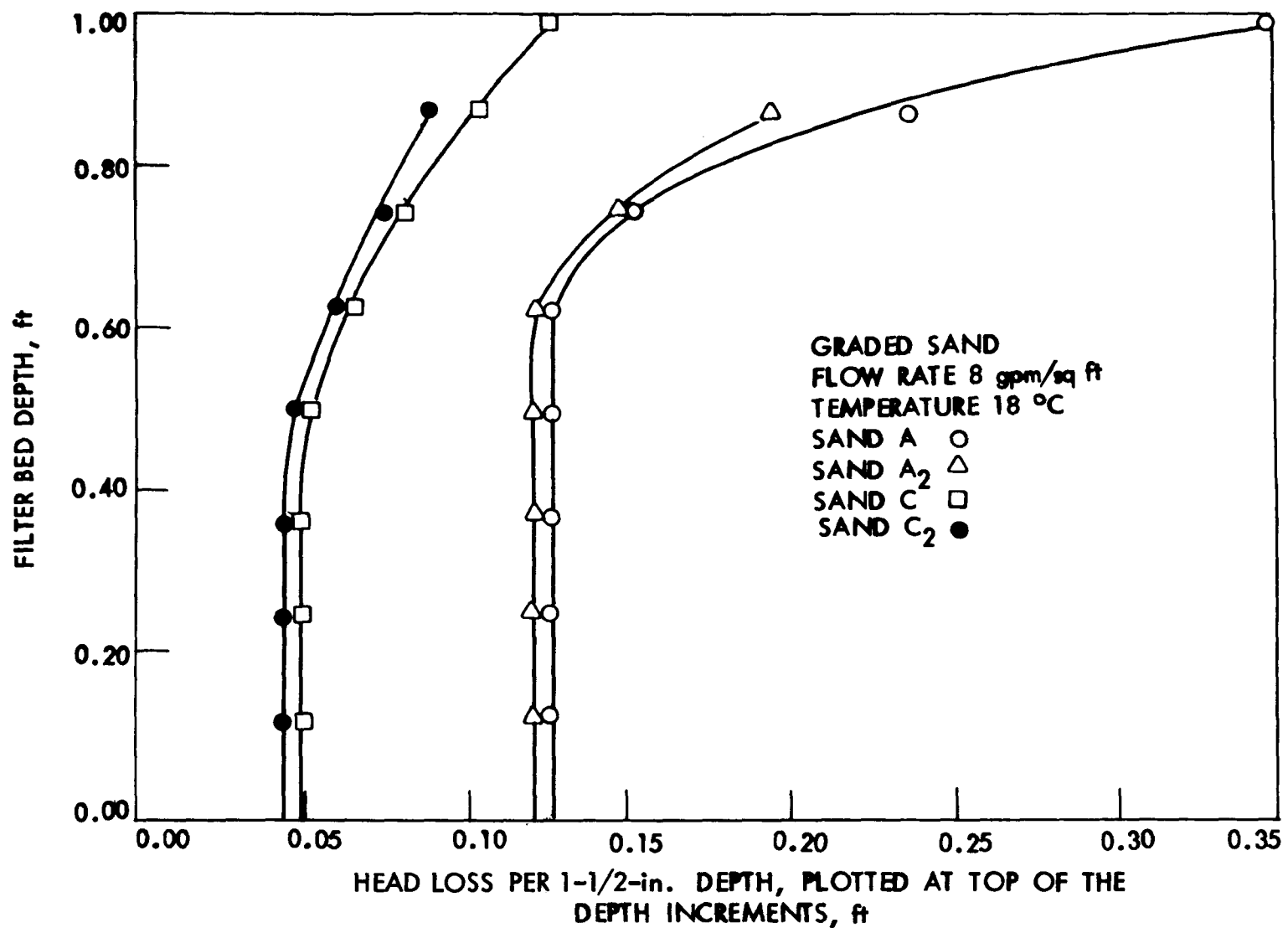


Fig. 65. Head loss for individual graded media in 1-1/2-in. unit filter sections.

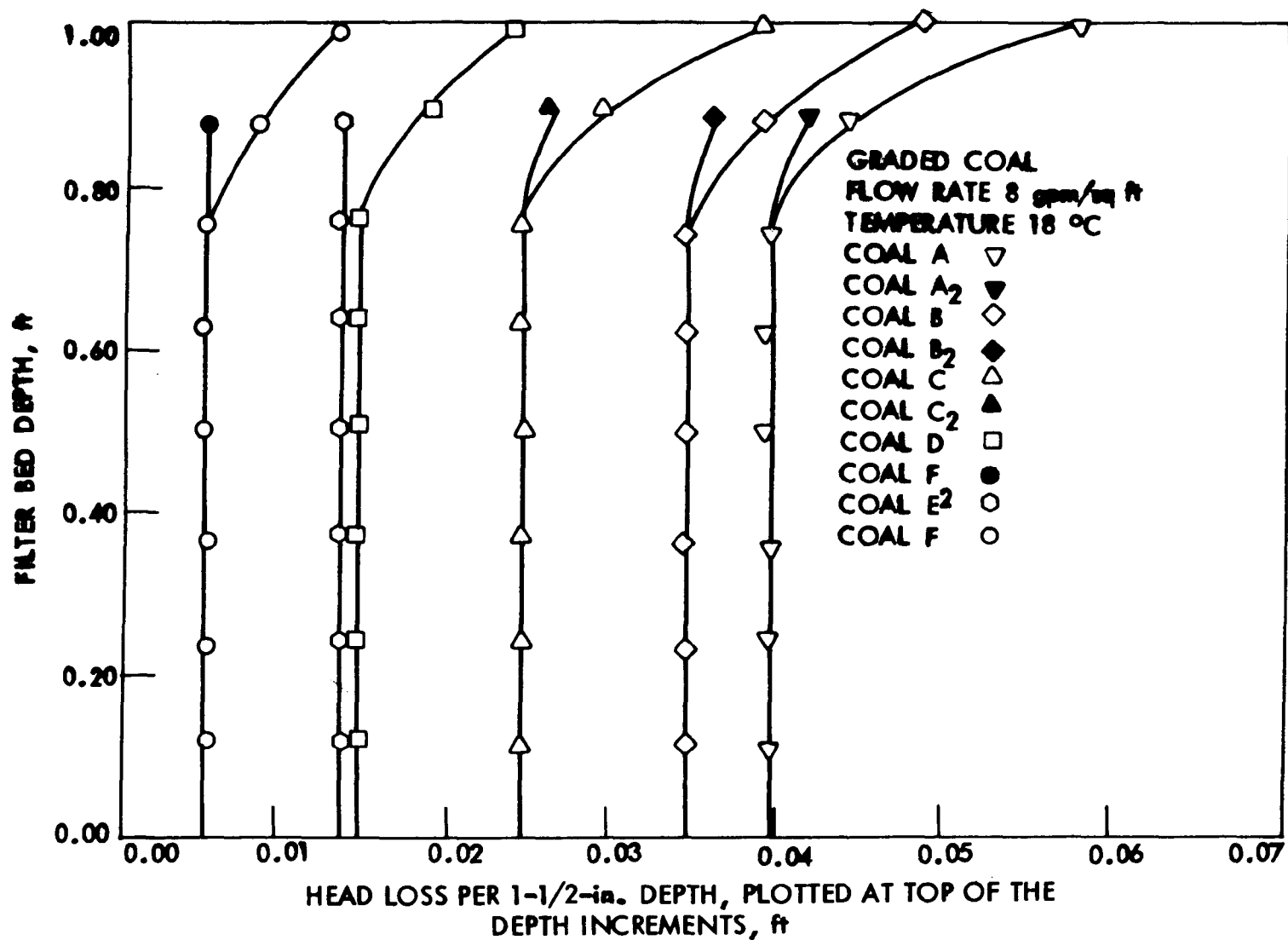


Fig. 66. Head loss for individual graded media in 1-1/2-in. unit filter sections.

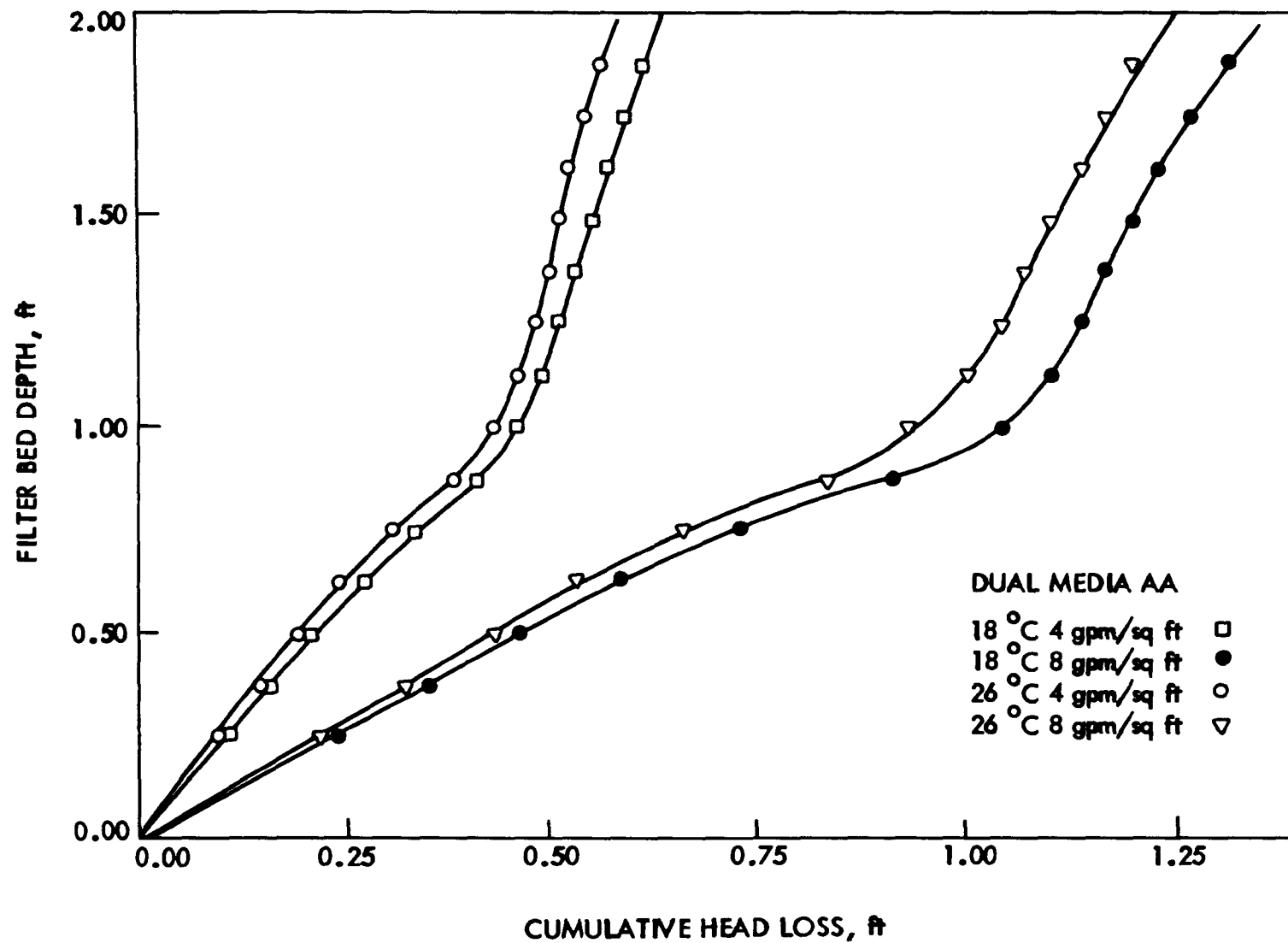


Fig. 67. Fixed-bed head loss of dual media AA at various temperatures and flow rates.

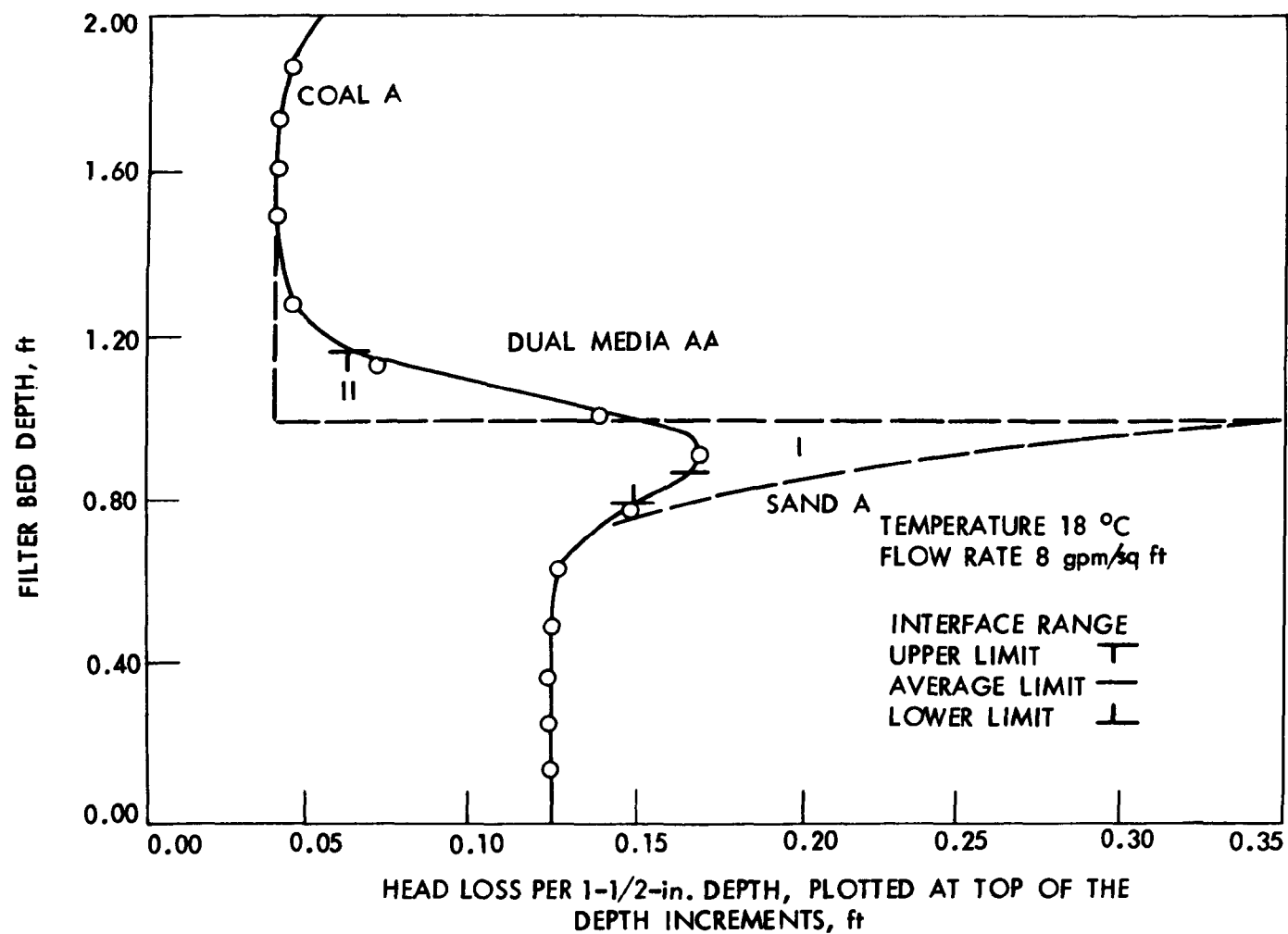


Fig. 68. Head loss per 1-1/2-in. unit depth in dual media AA and head loss for the two-component media if unmixed.

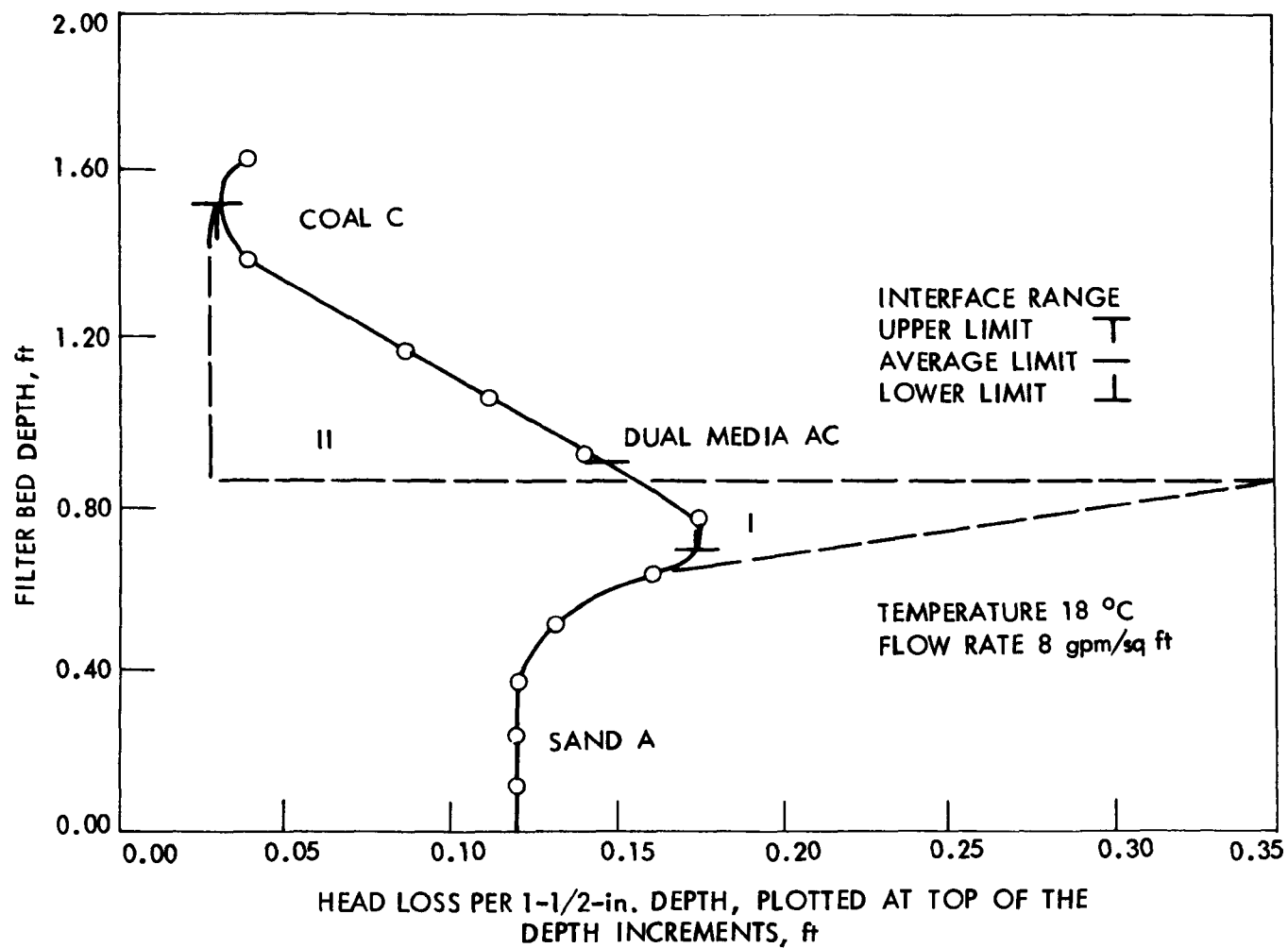


Fig. 69. Head loss per 1-1/2-in. unit depth in dual media AC and head loss for the two-component media if unmixed.

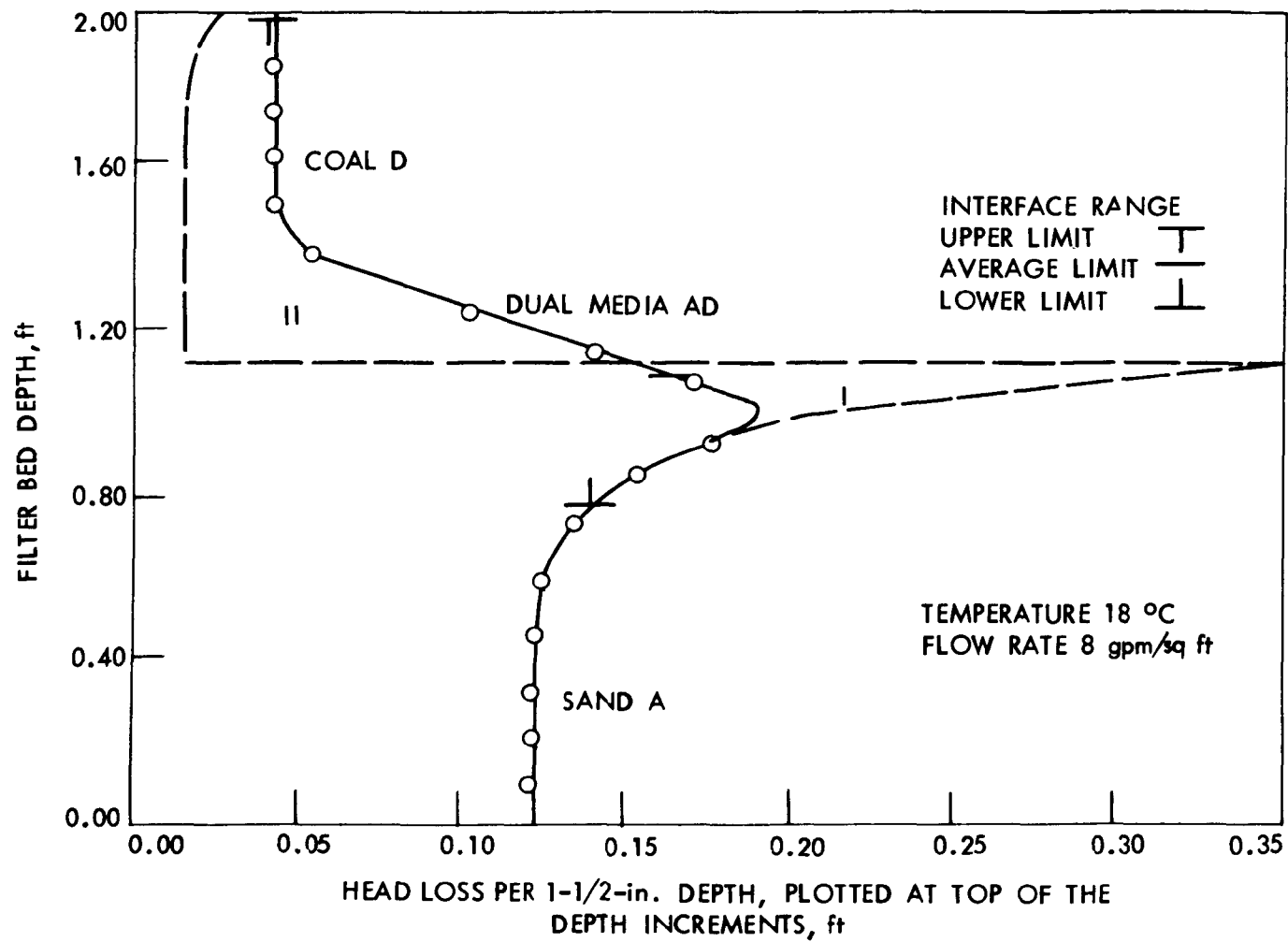


Fig. 70. Head loss per 1-1/2-in. unit depth in dual media AD and head loss for the two-component media if unmixed.

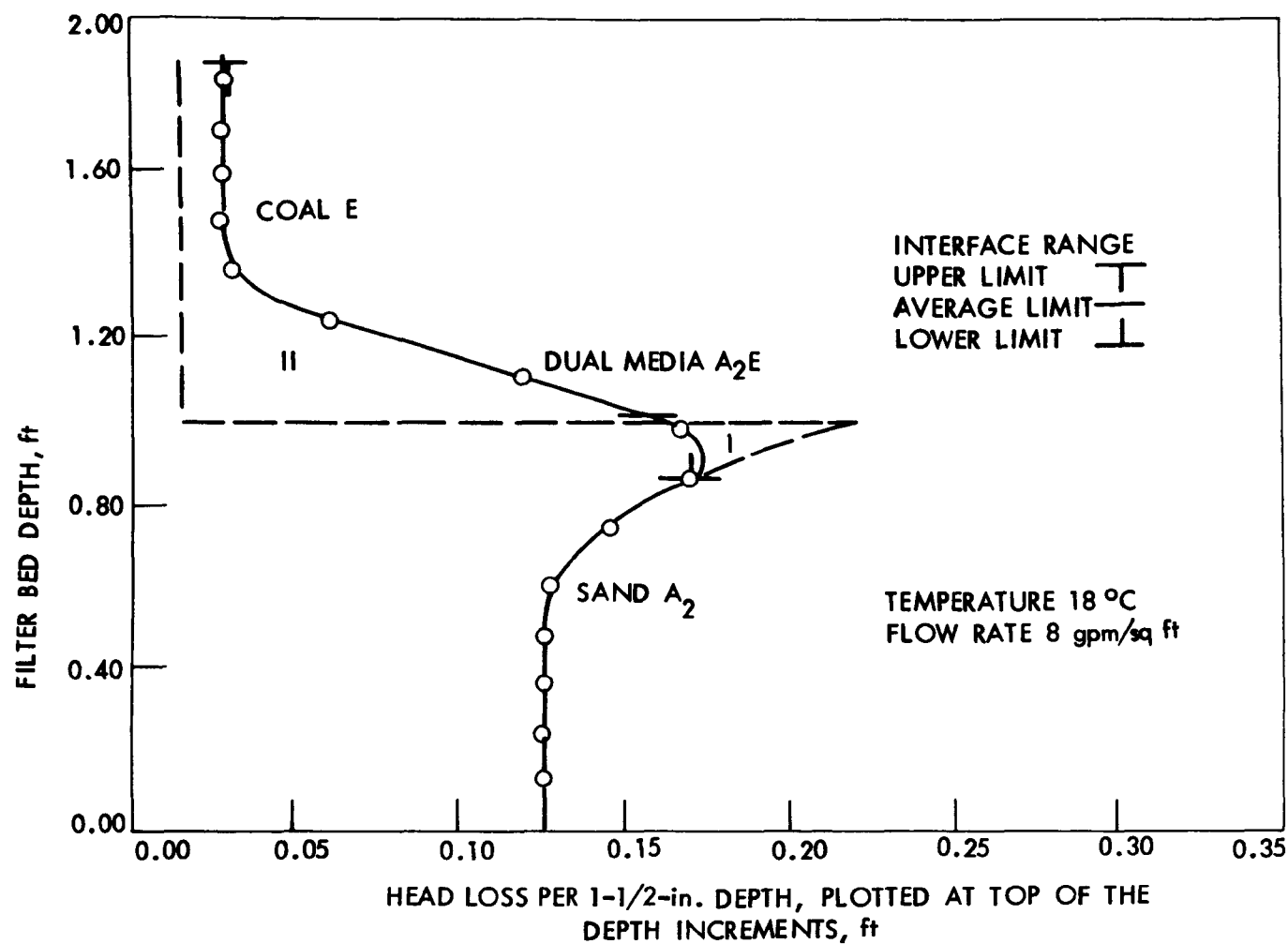


Fig. 71. Head loss per 1-1/2-in. unit depth in dual media A<sub>2</sub>E and head loss for the two-component media if unmixed.

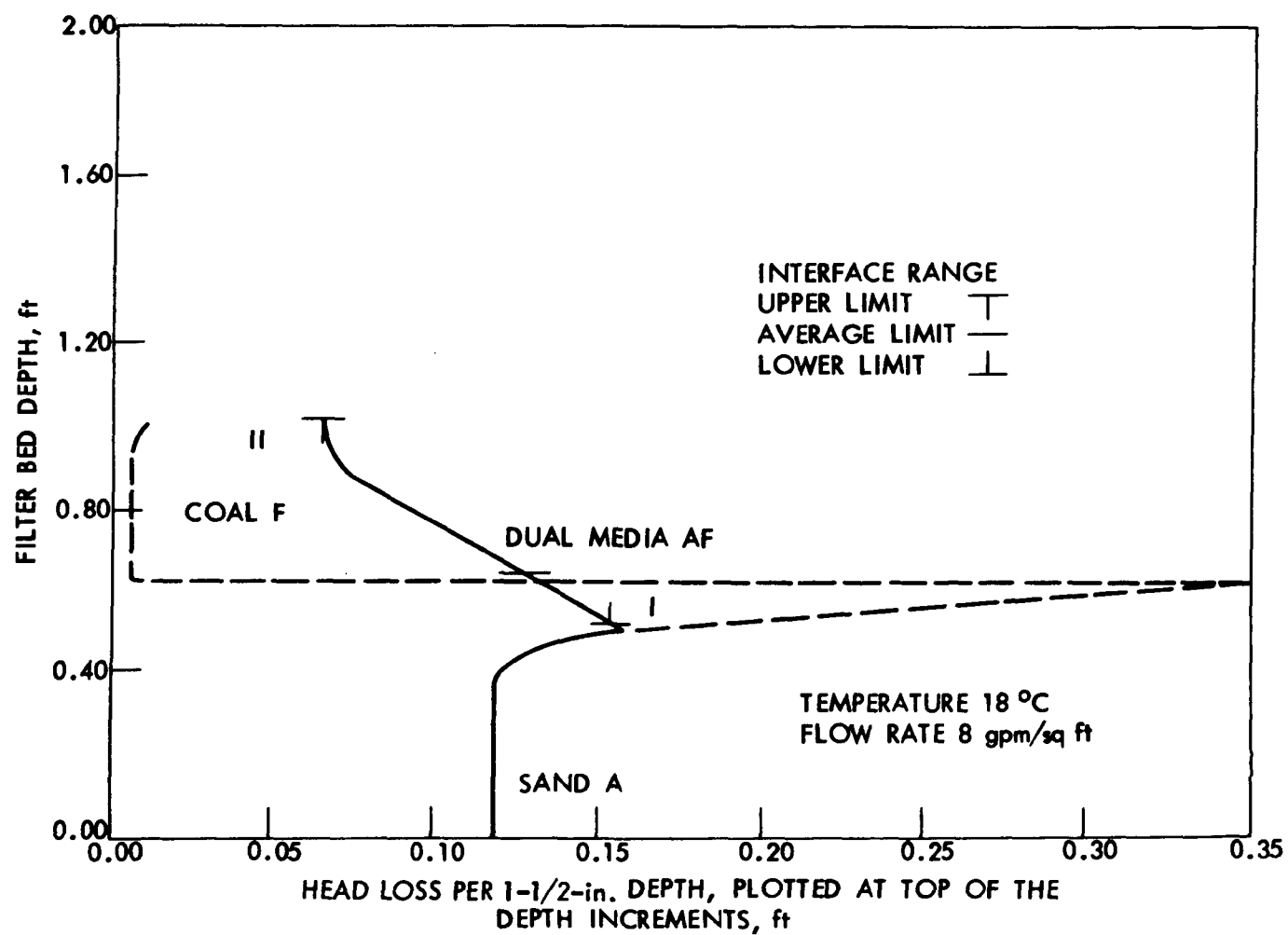


Fig. 72. Head loss per 1-1/2-in. unit depth in dual media AF and head loss for the two-component media if unmixed.

highest filter level where only sand particles were evident. The average interface was judged as the filter level at which the coal and sand particles are approximately equal in number. Of course, these intermixing zone distinctions are based on visual observations and are subject to errors in judgment.

Figure 68 shows a typical example of head loss reduction at the interface, which results when intermixing occurs. Without intermixing, the head loss gradient in the sand layer at the interface, as shown in Figure 68, would be expected to be 0.35 ft. Intermixing of the coal and sand reduced this head loss gradient to 0.17 ft, a 50% reduction in the head loss. This reduction was attributed to intermixing, because the zone of intermixing was visually observed to occur whenever the experimental hydraulic profile differed from the individual component hydraulic profiles. As the very fine sand mixed up into the coarser coal layer, a redistribution of the hydraulic profile was observed, causing a greater head loss in the coarser coal layer, with a correspondingly decreased head loss in the sand layer. The enclosed areas of Figs. 68 through 72, which illustrate this decrease in head loss, labelled I, in the sand layer and increase in head loss, labelled II, in the coal layer, are approximately equal in area, except in cases where excessive intermixing occurred.

The installation of various graded coal media with the same graded sand medium, as illustrated in Figs. 68 through 70, did not significantly change the 0.17-ft maximum head loss at the interface. Therefore, the graded sand medium was deemed as controlling the interface head loss, regardless of the coal media involved in the intermixing process. The effect of using increasingly coarser coals with the same sand is also evident in Figs. 70 through 72. The portion of bed showing intermixing increases with the coarser coals. The general effect of intermixing in Figs. 68 through 72 is to cause a gradual decrease in permeability with depth. This decrease would be due to decreased average pore dimension and decreased porosity. The influences of these variables on head loss (permeability) are evident in Eq. (17).

The general effect of intermixing is to provide gradual coarse to fine filtration in the direction of flow. The desirability of this coarse to fine filtration is accepted by all researchers studying filter performance. The fact that the peak hydraulic gradient of the dual-media filter is less than the peak gradient of the sand filter alone would indicate that the effectiveness of the sand layer in filtration would be somewhat diminished. However, the diminishment would be offset by the improved effectiveness of the lower coal layers where intermixing is present. The prediction of relative filter performance, in light of these observations, cannot be made at this time.

Figures 70 through 72 demonstrate excessive intermixing. Sand particles actually reached the surface of the coal layer and caused

an increase in the head loss throughout the coal layer as the coal bed permeability decreased due to the presence of the sand. The head loss increase in the coal layer was especially significant, as shown in Fig. 72. The capacity of the dual-media filter could be expected to be decreased due to the finer pore size in the surface layers of the filter. Thus, Fig. 72 gives an example of too much intermixing.

The water shutdown procedure following backwashing was also considered important to downflow hydraulic profiles and thus to filter performance. Preliminary work was done with dual media  $A_2C_2$  to determine the effect of shutdown on intermixing. Two shutdown procedures, a slow 1-min valve closure and a fast 5-sec valve closure, were tested. The bed height was 12.9 in. for all test measurements. Given high fluidizing flow rates, a large amount of intermixing was achieved before shutdown. A fast shutdown procedure allowed for a greater amount of the intermixing to be retained as the coal and sand particles settled than did a slower shutdown procedure. The slower, 1-min procedure allowed the particles of the two media to separate and stratify.

#### Expansion - Flow Rate Observations

##### Garnet Sand

The raw data collected during expansion of garnet sands in the 6-in. column were: (1) flow rate, (2) bed height, (3) manometer readings at 3-in. increments of the bed, and (4) temperature.

The following analyses of these data were made.

1. Flow meter reading was corrected by the appropriate calibration equation and changed to velocity (in gpm/sq ft and fps) based on the open cross-sectional area of the column.
2. Bed height reading was corrected by adding 1 in. The average porosity ratio of the expanded bed was calculated from the expanded height of the bed by Eq. (2) using the previously determined  $\epsilon_0$  and the observed  $l_0$ .
3. Pressure loss through the bed was calculated by subtracting a piezometer reading above the expanded bed from the piezometer reading at the bottom of the bed column.

A typical example of the data (run 1, Series A-13) is given in Table 39.

The computed values of the data for each expansion run were plotted as pressure vs flow rate, e.g., Figs. 73 and 74, and expanded bed height vs flow rate, e.g., Figures 75 through 84.

An analysis of the pressure loss vs flow rate figures leads to the following observations:

Table 39. Expansion — flow rate data of run 1, Series A-13<sup>a</sup> (-14+16 garnet sand media).

Corrected		Bed height ( $\ell$ ), in.	Average porosity ratio ( $\epsilon$ )	Pressure loss through bed, ft
Flow rate (V) gpm/sq ft	fps			
110.0	0.246	20.50	0.636	1.83
99.8	0.222	19.50	0.618	1.87
93.0	0.207	18.75	0.603	1.87
82.3	0.184	18.00	0.586	1.90
73.7	0.164	17.75	0.580	1.90
68.2	0.152	17.25	0.568	1.90
61.3	0.137	16.63	0.552	1.88
56.4	0.127	16.25	0.541	1.88
51.8	0.116	15.75	0.527	1.87
48.8	0.109	15.63	0.523	1.86
45.4	0.101	15.50	0.519	1.86
42.6	0.0950	15.25	0.511	1.85
38.6	0.0859	14.88	0.499	1.85
35.4	0.0788	14.50	0.486	1.86
32.5	0.0725	14.25	0.477	1.86
27.5	0.0613	13.80	0.460	1.73
23.6	0.0525	13.70	0.456	1.41
18.6	0.0415	13.65	0.454	1.04
12.2	0.0273	13.65	0.454	0.64

<sup>a</sup>Data for this run collected during contracting of fluidized bed only.  
Water temperature = 16.5 °C.

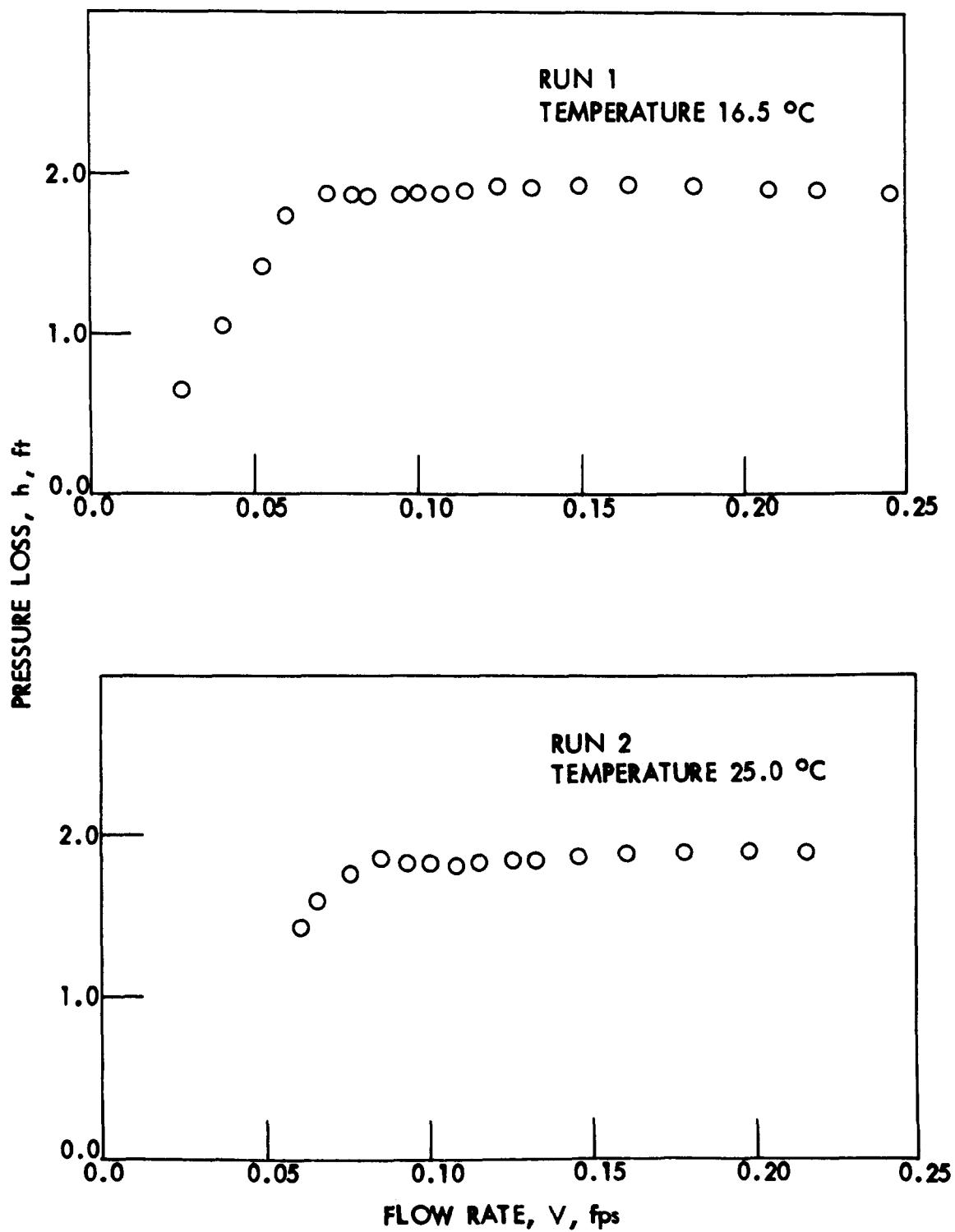


Fig. 73. Pressure loss - flow rate diagram for garnet sand media (-14+16).

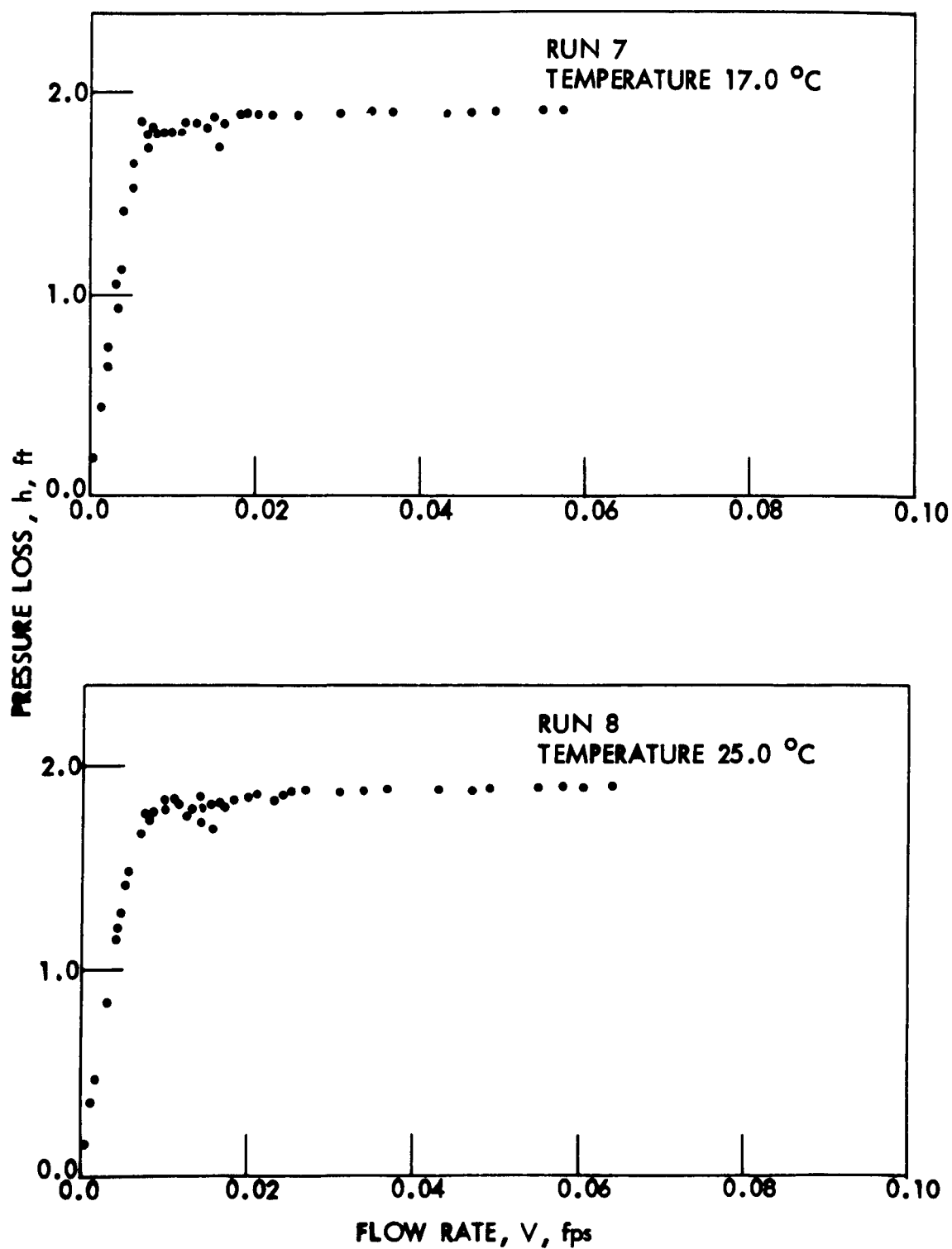


Fig. 74. Pressure loss - flow rate diagram for garnet sand media (M-60-80).

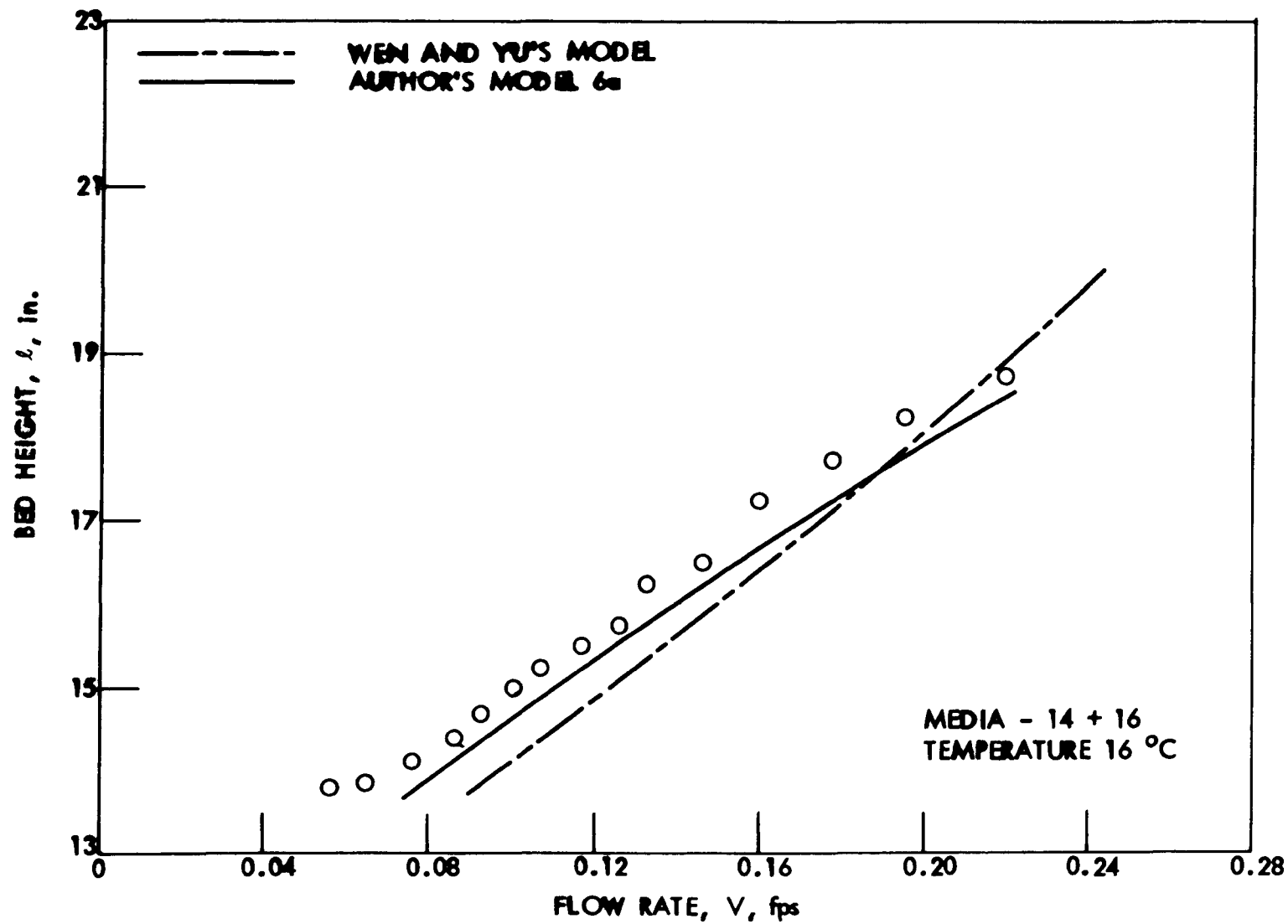


Fig. 75. Expansion - flow rate characteristics (garnet sand, run 1).

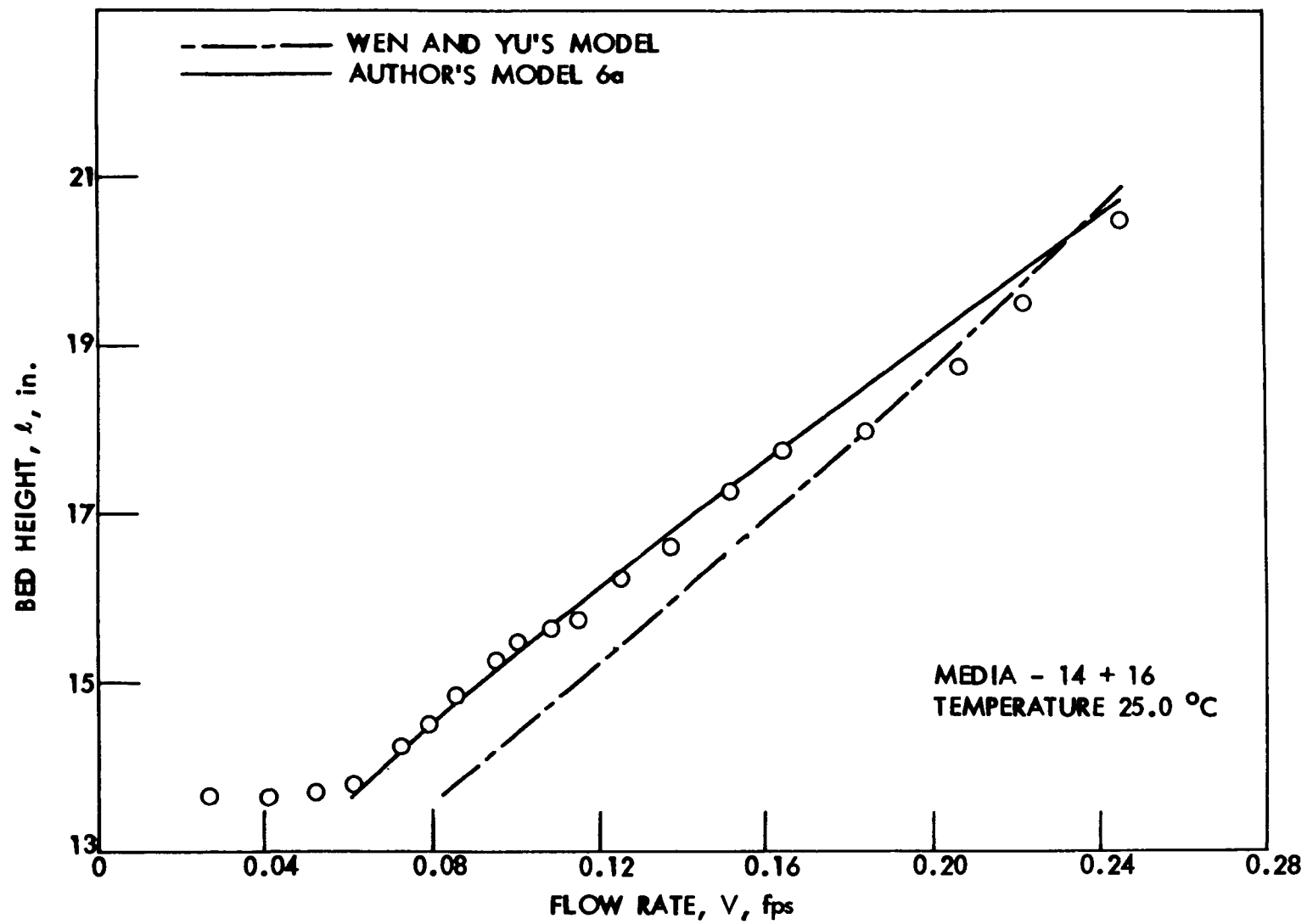


Fig. 76. Expansion - flow rate characteristics (garnet sand, run 2).

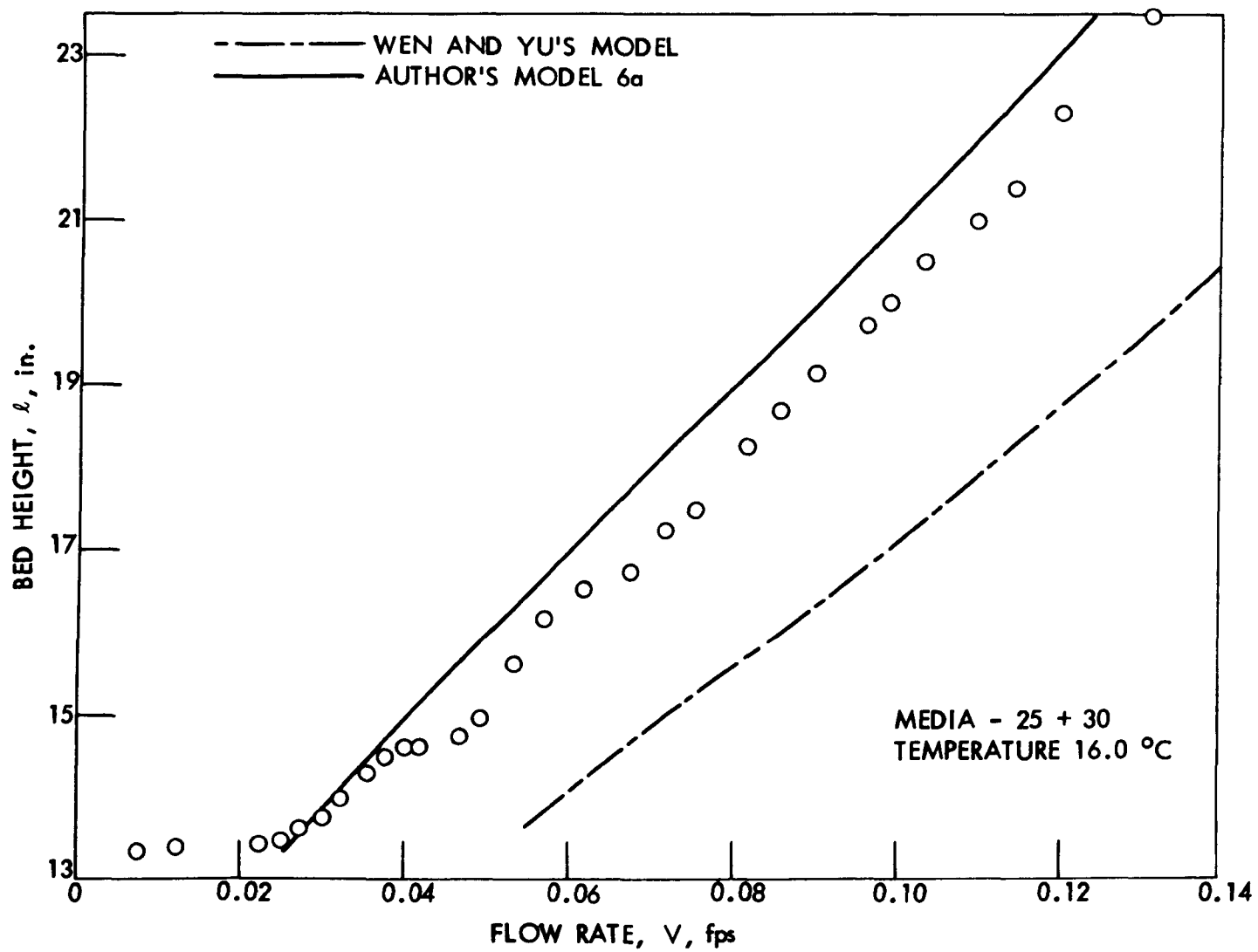


Fig. 77. Expansion - flow rate characteristics (garnet sand, run 3).

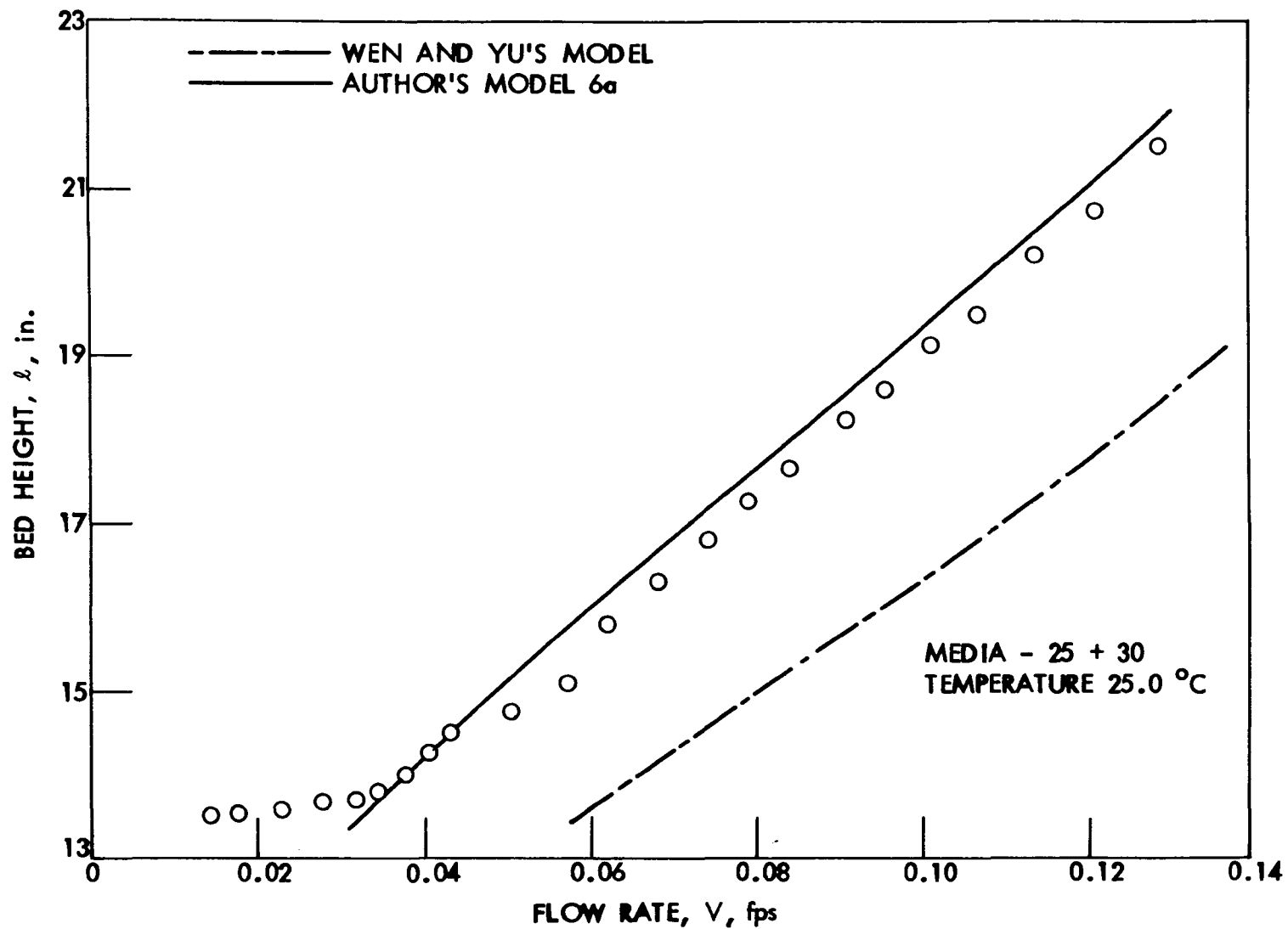


Fig. 78. Expansion - flow rate characteristics (garnet sand, run 4).

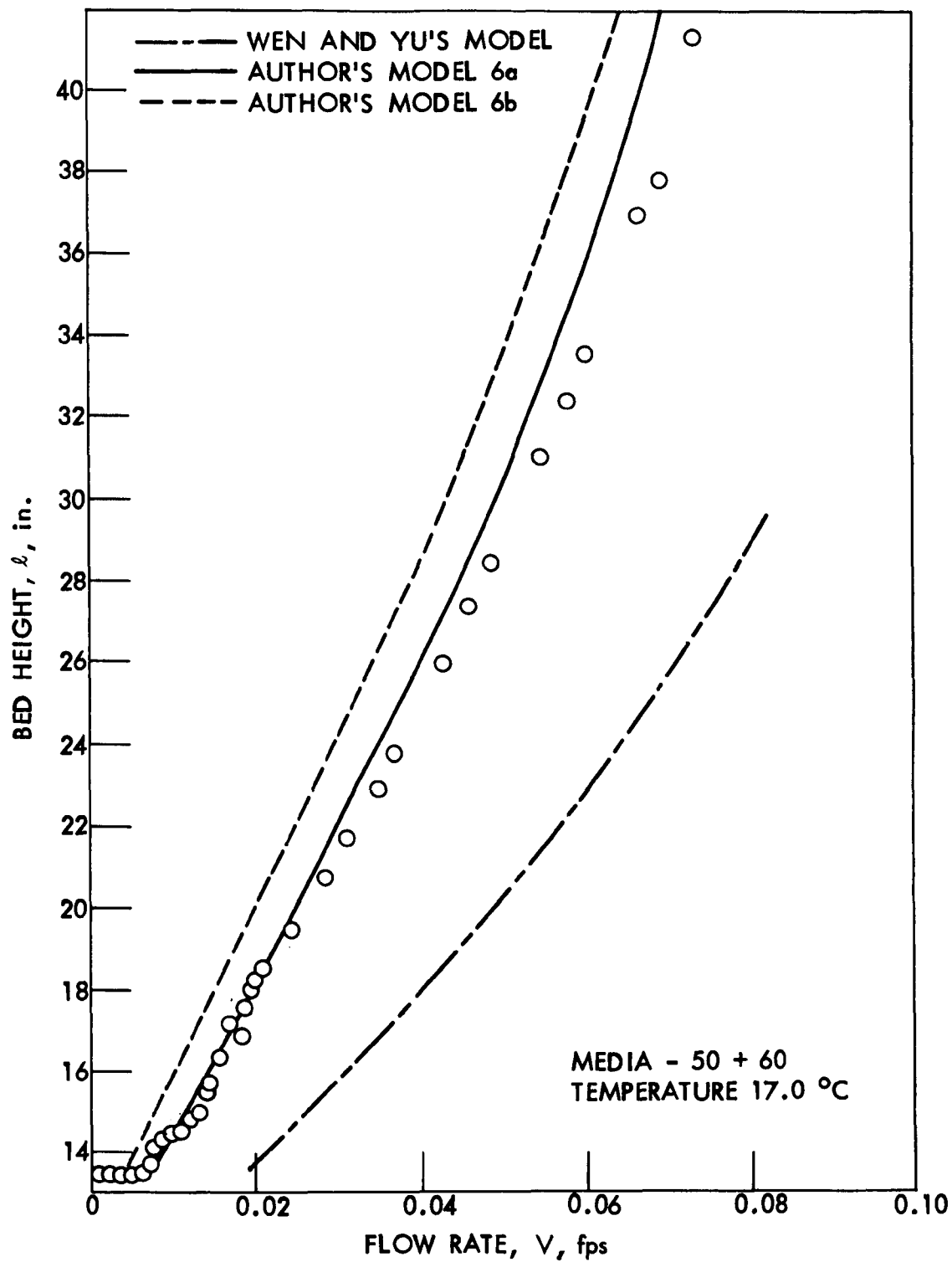


Fig. 79. Expansion - flow rate characteristics (garnet sand, run 5).

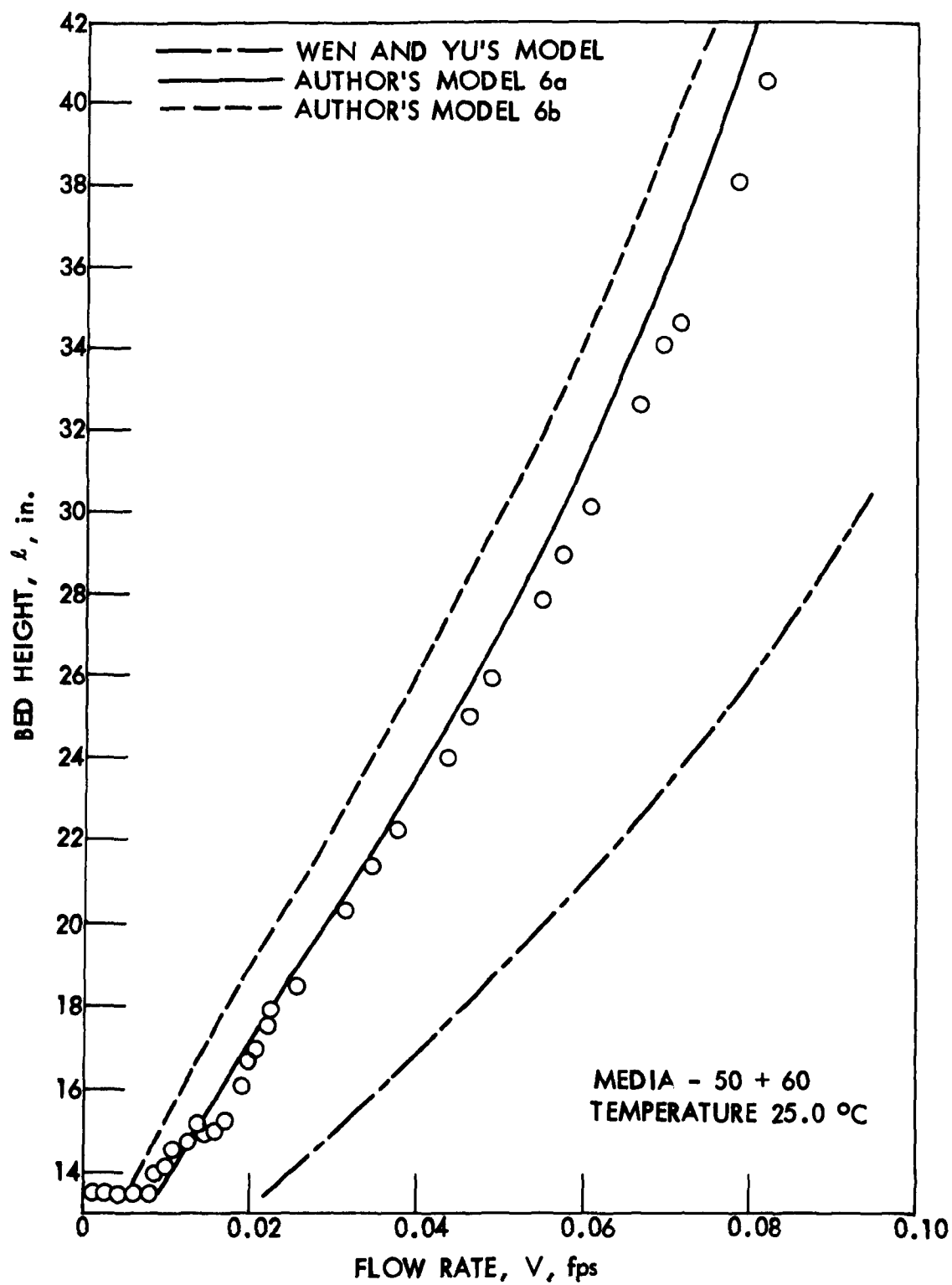


Fig. 80. Expansion - flow rate characteristics (garnet sand, run 6).

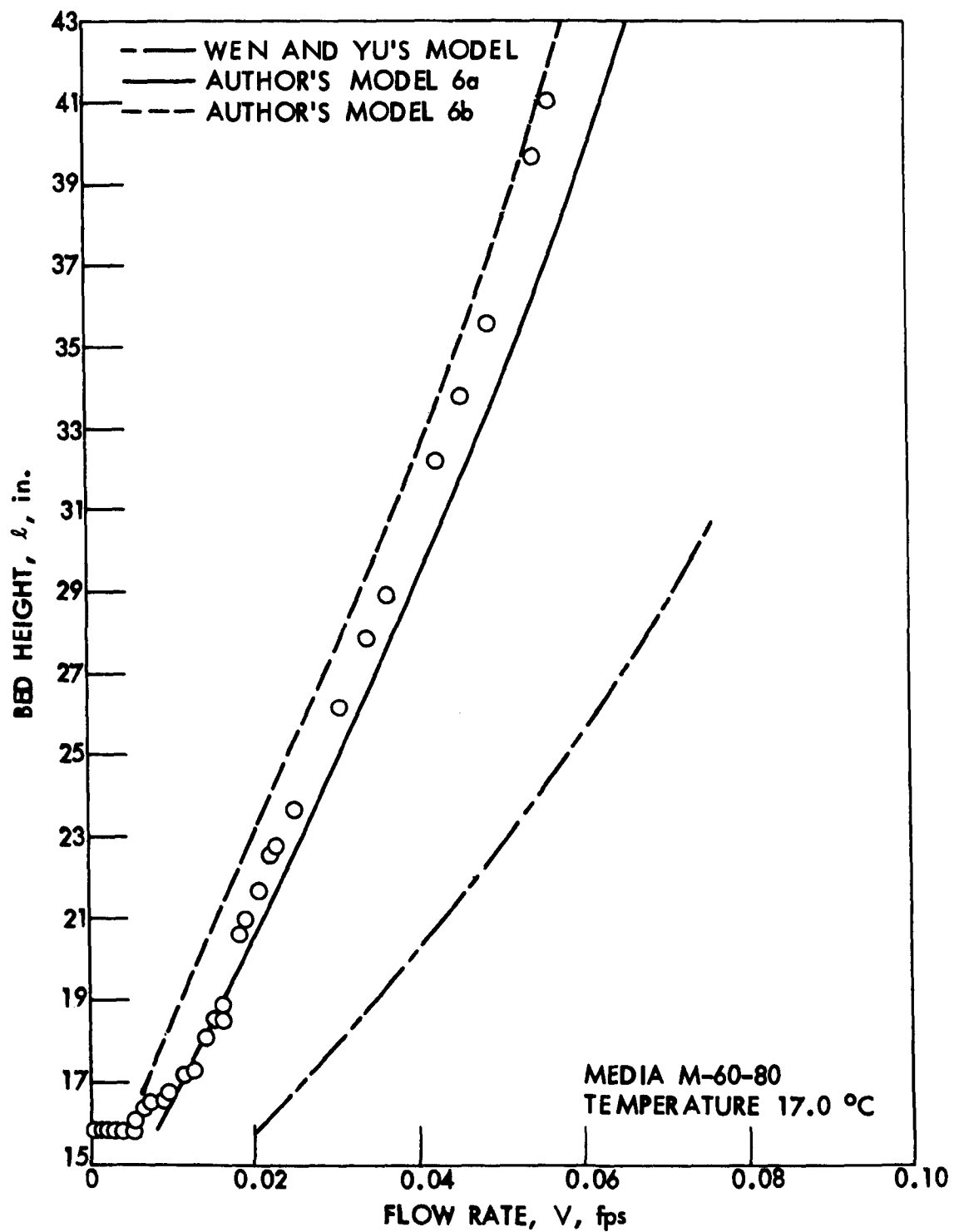


Fig. 81. Expansion - flow rate characteristics (garnet sand, run 7).

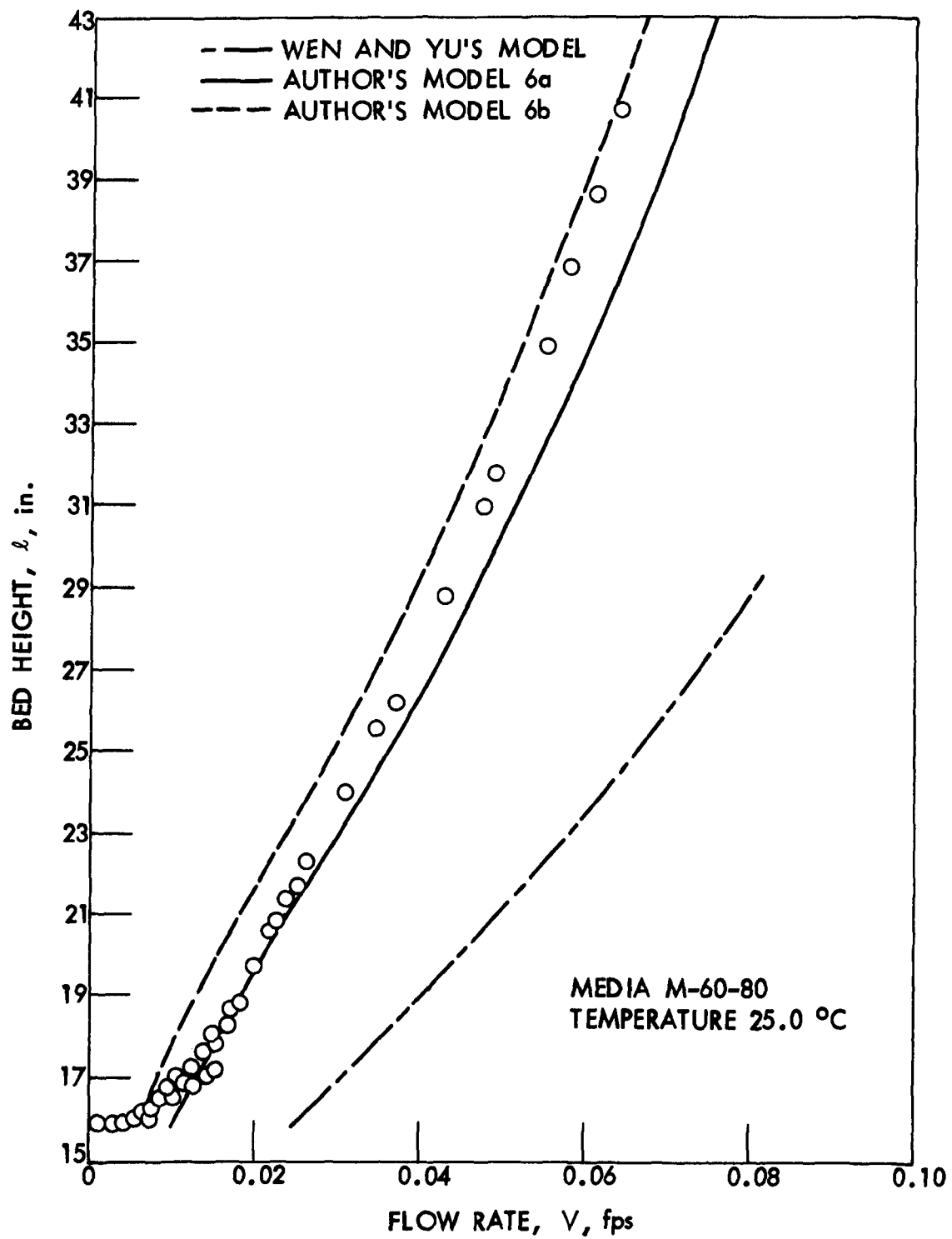


Fig. 82. Expansion - flow rate characteristics (garnet sand, run 8).

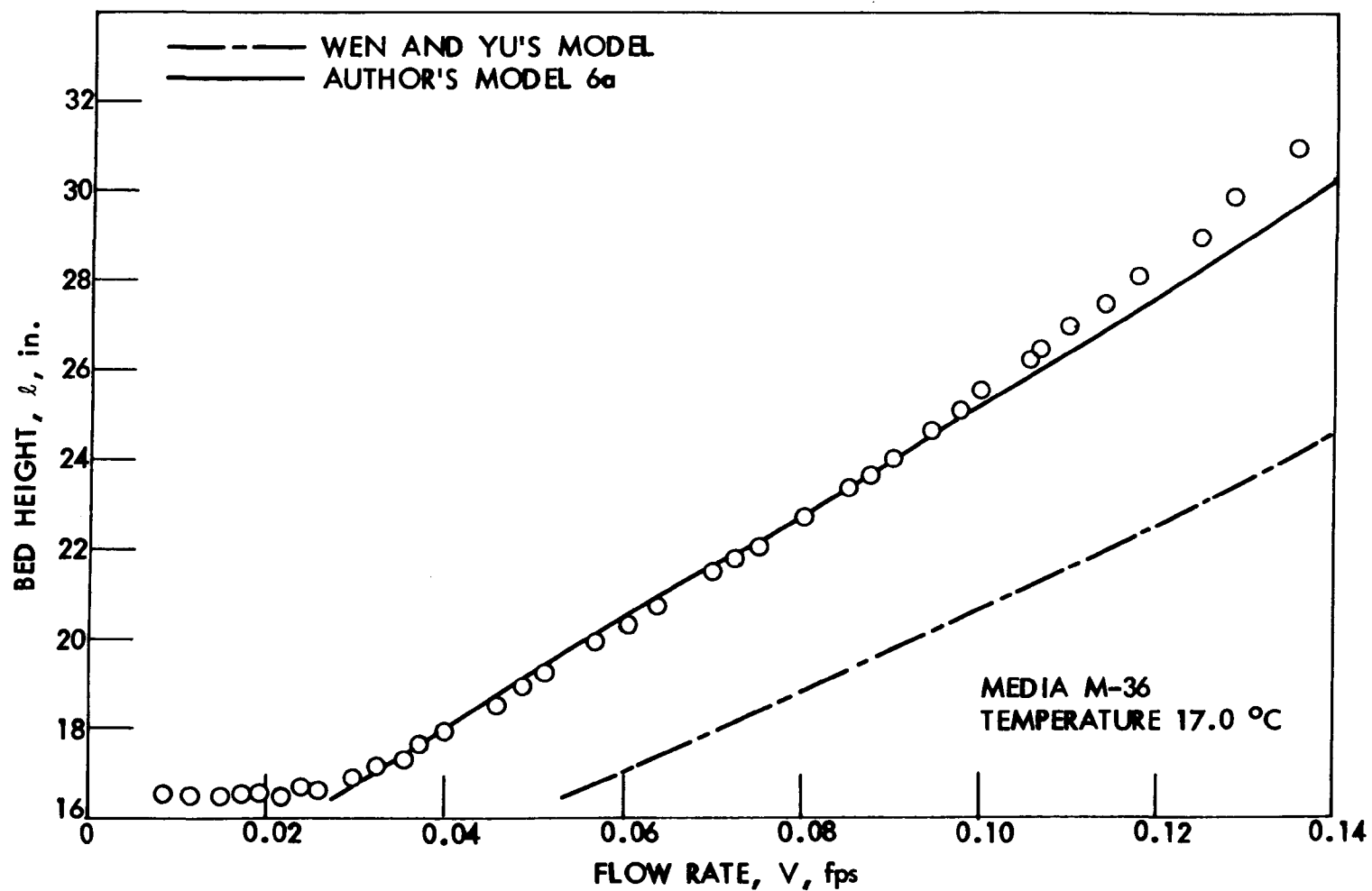


Fig. 83. Expansion - flow rate characteristics (garnet sand, run 9).

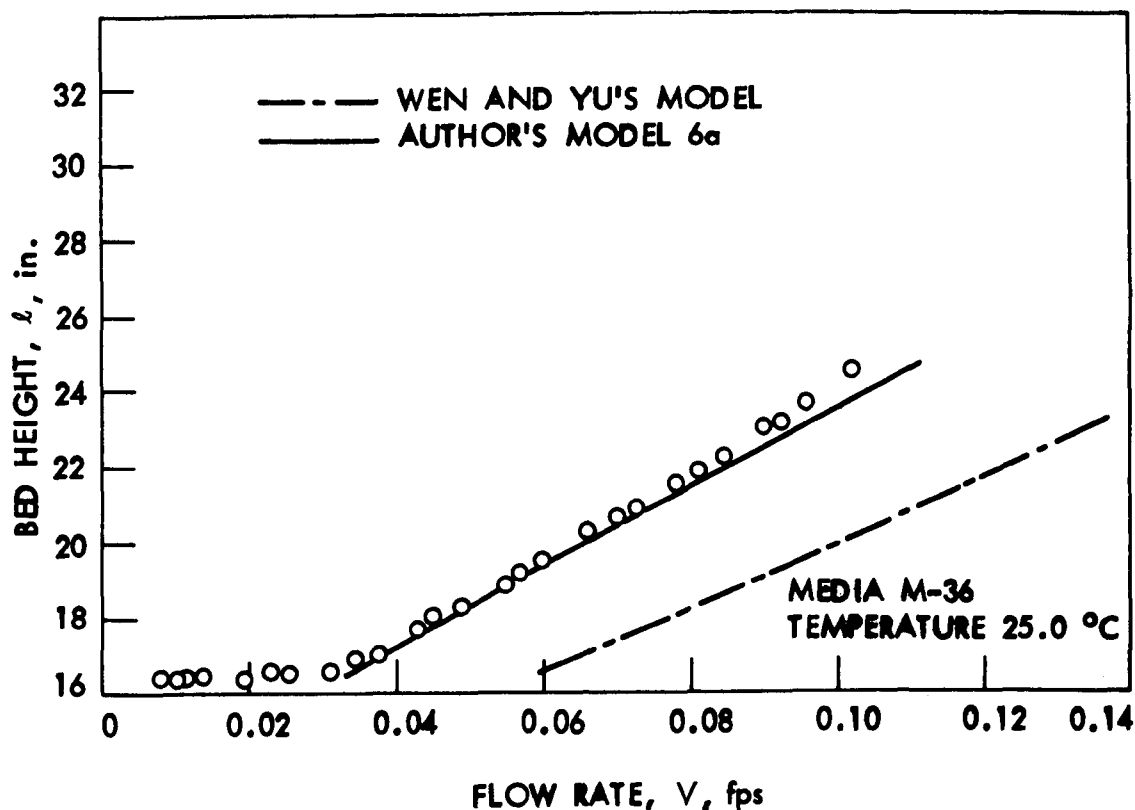


Fig. 84. Expansion - flow rate characteristics (garnet sand, run 10).

1. The apparent minimum fluidization can readily be determined as the intersection of the two linear portions of the curve. These values as well as the  $V_{mf}$  values determined from Wen and Yu's equation [Eq. (53)], Leva's equations [Eqs. (51) and (52)], and Frantz's equation [Eq. (54)] are listed in Table 40.
2. The effect of channeling is greater at about  $V_{mf}$  and decreases as expansion increases. The evidence of channeling is the lower pressure drop observed for flow values just above minimum fluidization. Channeling is especially noticeable for the finer media (Figs. 77 through 82) and was visually observed and noted during the actual fluidization. The channeling is attributed to poor flow distribution into the expansion column.

The bed height vs flow rate figures (Figs. 75 through 84) also present the results of calculated bed height for garnet sand media by various expansion models. The models and discussion will be presented later.

Table 40. Summary of minimum fluidization velocities of garnet sand media -  $V_{mf}$ .

Run	Garnet media	Minimum fluidization velocities, fps			
		From head loss vs flow rate, e.g., Figs. 73 and 74	Wen and Yu's Eq. (53)	Leva's Eqs. (51) and (52)	Frantz's Eq. (54)
1	-14+16	0.067	0.067	0.0059	0.158
2	-14+16	0.074	0.075	0.064	0.196
3	-25+30	0.027	0.021	0.024	0.040
4	-25+30	0.033	0.026	0.029	0.049
5	-50+60	0.0071	0.0040	0.0049	0.0070
6	-50+60	0.0078	0.0048	0.0058	0.0085
7	M-60-80	0.0067	0.0042	0.0051	0.0074
8	M-60-80	0.0076	0.0051	0.0061	0.0089
9	M-36	0.031	0.022	0.025	0.041
10	M-36	0.036	0.026	0.029	0.049

The analyses of the  $\log V$  vs  $\log \epsilon$  plots for the various media are the most important analyses of the expansion-flow rate experiments.

One typical plot,  $\log V$  vs  $\log \epsilon$  (run 1, Series A-13), is shown on Fig. 85. The important characteristics of this figure are the slope of the line or  $n$  slope and the velocity intercept at porosity ratio equal to one. To remove the bias of fitting a straight line to this plot, a linear regression analysis was performed. The  $V$  and  $\epsilon$  data that were used for the linear regression analysis were all of the data points above the intersection of the two straight line portions of the pressure loss vs flow rate plot, e.g., Figs. 73 and 74. The results of this analysis for all the expansion flow rate runs on garnet sand are given in Table 41. Included in this table are  $V_1$  in gpm/sq ft and fps,  $n$  slope, number of points used in the regression analysis, the correlation coefficient of the log-log line, the Reynold's number based on the arithmetic mean diameter and  $V_1$ , and Richardson and Zaki's  $n$  slope calculated from Eq. (30), neglecting  $d/D$ .

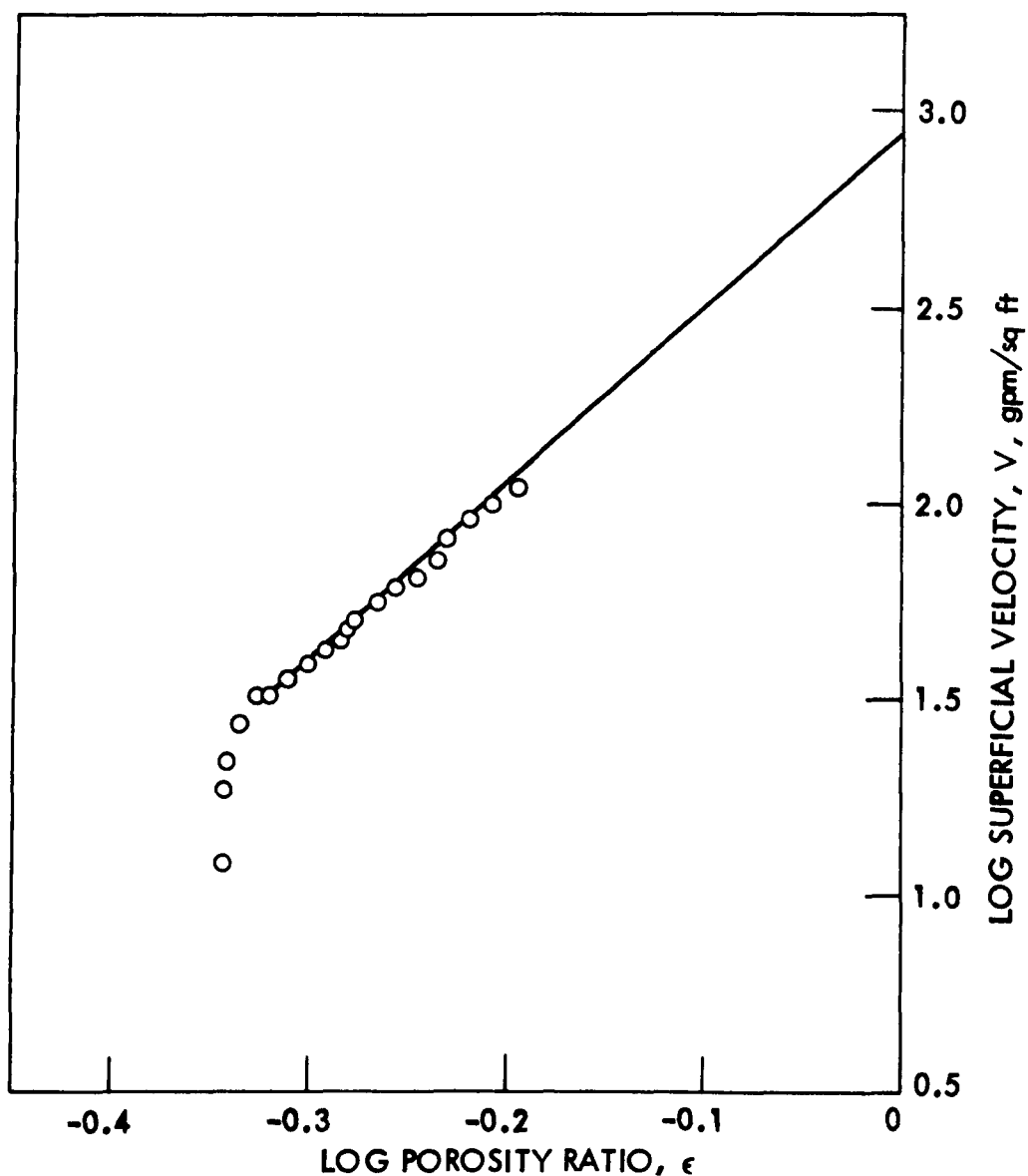


Fig. 85. Log plot of  $V$  vs  $\epsilon$  for garnet sand media (-14+16)  
(run 1, Series A-13).

The experimentally determined  $n$  slope values are higher than the  $n$  slope values from Richardson and Zaki's Eq. (30). This was expected from the literature and is attributed to the particle shape. Because the garnet sand media has a very irregular shape, no attempt will be made to correlate the  $n$  slopes for the data with the calculated  $n$  slopes by Richardson and Zaki's equations. Rather, a unique equation for the solution of  $n$  slope for garnet sand will be proposed.

Following the same approach as Richardson and Zaki,  $\log n$  vs  $\log Re_i$  was plotted (Fig. 86). The linear regression correlation equation was determined using all the 10 sets of points from column 1 and column 7 of Table 41. The resulting equation is,

$$n = 5.758 Re_i^{-0.0541} \quad (69)$$

with a coefficient of determination for the log-log line,  $r^2 = 73.32\%$ .

For the evaluation of  $n$  slope, the  $Re_i$  must be defined. The properties of the water and the linear dimensions of particle size are readily available or can be determined. The available methods for evaluating the velocity intercept, which equals the settling velocity of a discrete particle for spherical particles, are discussed in the section on prediction of settling velocities, beginning on page 229.

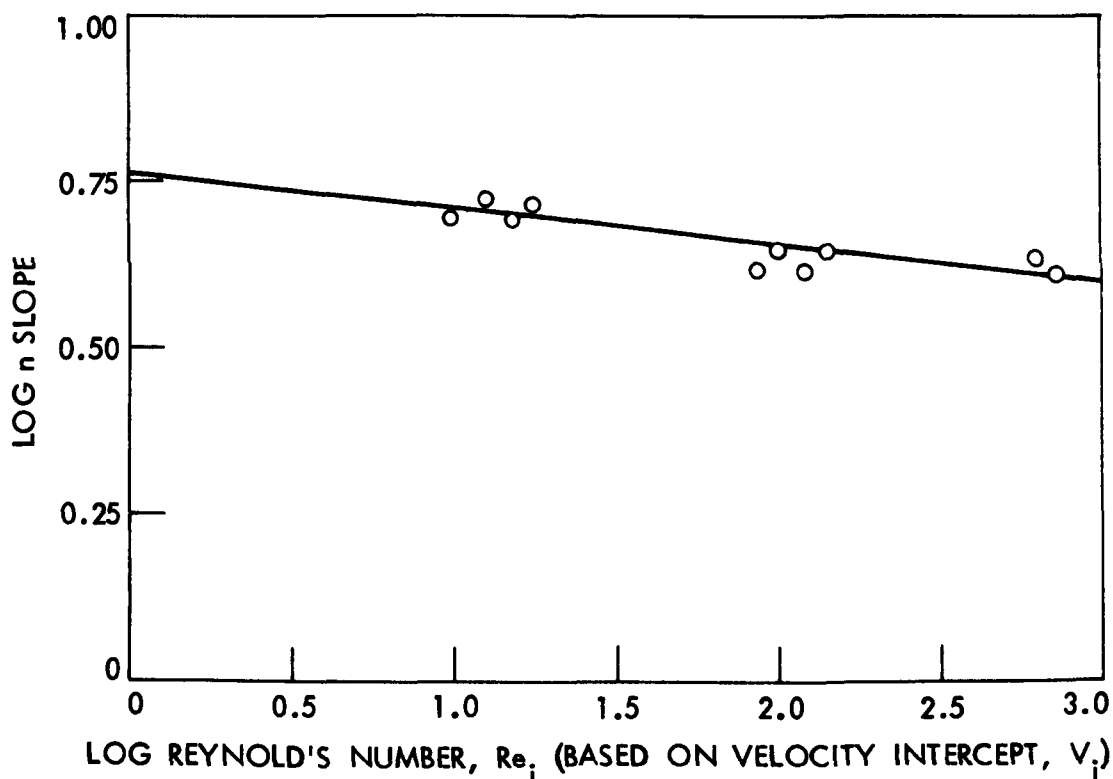


Fig. 86. Log plot of  $n$  slope vs Reynold's number -  $Re_i$  (for garnet sand media, runs 1 through 10, Series A-13 through A-17).

The weaknesses in three methods for determining settling velocity are discussed as follows:

A comparison of the experimental settling velocities of discrete particles (Table 38) with  $V_i$  (Table 41) does not show any reasonable agreement. This observation is consistent with expectations from the literature as previously described (pages 216 through 228).

Graphical correlations of the ratio of  $Re_o/Re_{mf}$  vs  $Ga$  have the inherent weakness of requiring a family of curves for varying  $\epsilon_{mf}$ , and the graphs presented did not fit the data points presented in the literature as well as would have been desired.

The graphical solution from a log-log plot of  $Re_o$  vs  $Ga$  would be a fast and simple method of determining settling velocities (pages 229-234). An attempt was made to use the correlation of  $\log Re_o$  vs  $2/3 Ga$  of Coulson and Richardson [33, p. 147]. However, values of  $V_s$  thus determined did not compare well with the experimental  $V_i$  values in Table 41. But following the same method of plotting the  $\log Re_i$  vs  $\log Ga$  (dropping the constant  $2/3$ ), the experimental values plotted closely as a straight line (Fig. 87). The linear regression equation of this line is,

$$Re_i = 0.0702 Ga^{0.823} \quad (70)$$

with a coefficient of determination for the log-log line,  $r^2 = 99.38\%$ . The values used for this determination and the resulting values from use of Eq. (70) are listed in Table 42. The agreement of the  $Re_i$  values from the above equation when compared with the experimental  $Re_i$  result in an error of - 14.7 to + 16.7%.

#### Presentation of Garnet Sand Expansion Model

The modified model for the expansion of garnet sand is proposed based on the empirical correlations presented previously [Eqs. (69) and (70)]. It is outlined in the following steps:

1. Experimentally determine arithmetic mean diameter ( $d_m$ ), the density of the particles ( $\rho_s$ ), and the fixed-bed porosity ( $\epsilon_{mf}$ ).
2. Calculate  $Ga$  from the fluid and particle properties.
3. With  $Ga$ , calculate  $Re_i$  from Eq. (70).
4. Calculate  $V_i$  from  $Re_i$  and  $n$  slope from Eq. (69).
5. The porosity at any desired flow rate can then be determined from  $V_i$ ,  $n$  slope, and Eq. (28),

Table 41. Results of the log V vs log  $\epsilon$  relationship for garnet sand media.

Run	n slope	Velocity intercept ( $V_i$ )			Number of values used	Coefficient of determination $r^2$ , %	$Re_i$ based on $V_i$ and $d_m$	n slope from Eq. (30)
		log $V_i$	gpm/sq ft	fps				
1	4.326	2.90380	801.3	1.785	16	99.56	625	2.34
2	4.089	2.87682	753.0	1.679	12	99.40	730	2.30
3	4.437	2.42580	266.6	0.594	24	98.96	104	2.80
4	4.420	2.47664	299.7	0.668	17	99.26	145	2.70
5	5.321	1.8961	78.73	0.175	32	98.62	13.1	3.45
6	5.197	1.94649	88.41	0.197	36	98.72	17.8	3.34
7	4.932	1.81071	64.67	0.144	20	97.00	11.0	3.50
8	4.926	1.87366	74.76	0.167	26	99.10	15.5	3.38
9	4.139	2.33674	217.1	0.484	27	99.82	87.5	2.85
10	4.173	2.39184	246.5	0.549	17	99.86	120	2.76

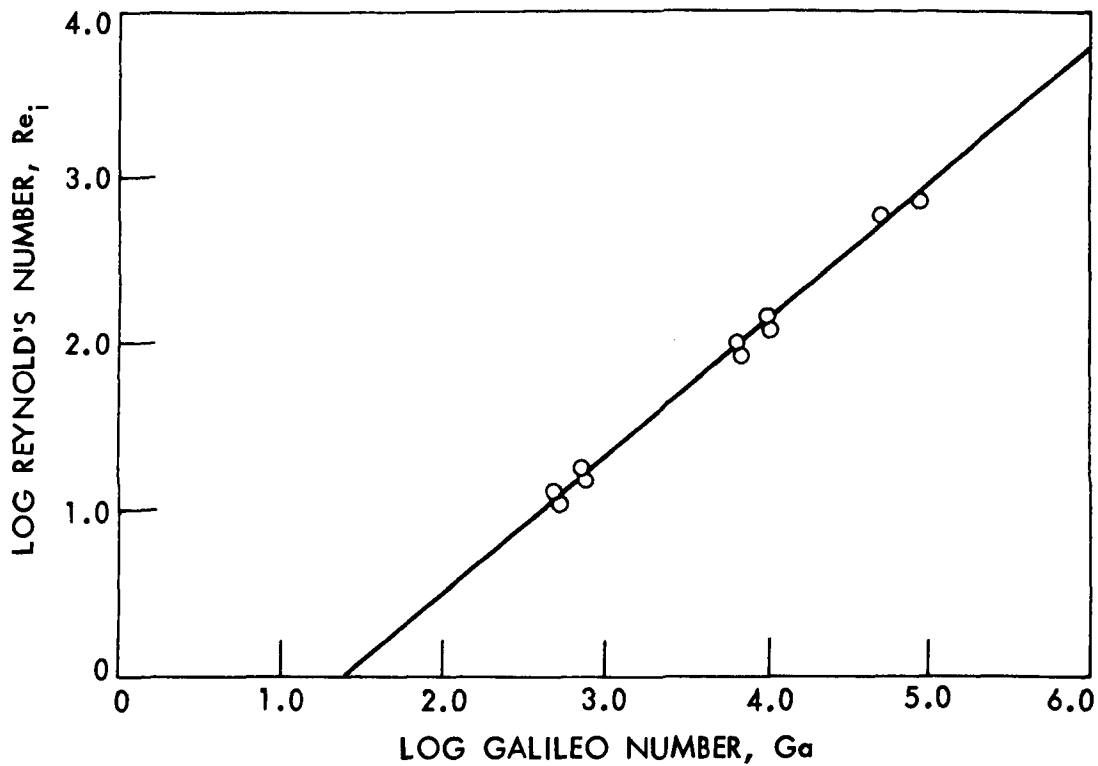


Fig. 87. Log plot of Reynold's number,  $Re_i$ , vs Galileo number,  $Ga$  (for garnet sand media, runs 1 through 10, Series A-13 through A-17).

$$\epsilon = \left( \frac{V}{V_i} \right)^{1/n}$$

- 6a. Using the experimentally determined value of  $\epsilon_{mf}$  and selecting any desired initial bed height ( $l_o$ ), the expanded height of the bed can be determined from Eq. (2),

$$l = \frac{l_o (1 - \epsilon_{mf})}{(1 - \epsilon)} .$$

- 6b. As an alternative approach, which eliminates the need to measure  $\epsilon_{mf}$  in step 1, the  $V_{mf}$  can be calculated from a minimum fluidization velocity equation. For this study, Leva's equation [Eq. (51)] with Zabrodsky's correction factor [Eq. (52)] for  $Re_{mf} > 10$  gave the most consistent results (Table 40) with the

Table 42. Values of Reynold's numbers and Galileo's number for the garnet sand media.

Run and series	Garnet media	Ga	Re <sub>i</sub> based on V <sub>i</sub> and d <sub>m</sub>	Re <sub>i</sub> from Eq. (70)	% error
1, A-13	-14+16	51,876	625	533	- 14.7
2, A-13	-14+16	80,370	730	764	4.6
3, A-14	-25+30	6,530	104	96.8	- 6.9
4, A-14	-25+30	10,117	146	139	- 4.8
5, A-15	-50+60	490	13.1	11.5	- 12.2
6, A-15	-50+60	722	17.8	15.8	- 11.2
7, A-16	M-60-80	530	11.0	12.3	11.8
8, A-16	M-60-80	780	15.5	16.9	9.0
9, A-17	M-36	6,969	87.5	102	16.6
10, A-17	M-36	10,261	120	140	16.7

V<sub>mf</sub> values determined from the intersection of the two straight line portions of the head loss vs flow rate plots. The  $\epsilon_{mf}$  is then calculated from Eq. (28),

$$\epsilon_{mf} = \left( \frac{V_{mf}}{V_i} \right)^{1/n}$$

using the V<sub>i</sub> and n slope from step 4 above. The expanded height is then calculated in the same way with Eq. (2).

The values of Re<sub>i</sub>, n, and V<sub>i</sub>, calculated from Eqs. (70) and (69) and the definition of Reynold's number, are listed in Table 43. The  $\epsilon_{mf}$  values calculated from Leva's V<sub>mf</sub> values of step 6b are also listed in Table 43.

The results of expanded bed height calculated using the above model, including step 6a (designated authors' model 6a), are presented in Figs. 75 through 84 for runs 1 through 10. Similar results for the

Table 43.  $V_i$ ,  $n$ ,  $\epsilon_{mf}$  to be used in author's expansion models.

Run	Garnet media	Ga	$Re_i$ from Eq. (70)	$n$ from Eq. (69)	$V_i$ (fps) from $Re_i$ definition	$\epsilon_{mf}^a$
1	-14+16	51,876	533	4.10	1.52	0.453
2	-14+16	80,371	764	4.02	1.77	0.443
3	-25+30	6,530	96.8	4.50	0.552	0.497
4	-25+30	10,117	139	4.41	0.637	0.496
5	-50+60	490	11.5	5.05	0.154	0.505
6	-50+60	722	15.8	4.96	0.175	0.504
7	M-60-80	530	12.3	5.03	0.160	0.505
8	M-60-80	780	16.9	4.95	0.182	0.503
9	M-36	6,969	102	4.49	0.565	0.497
10	M-36	10,260	140	4.41	0.641	0.496

<sup>a</sup>Calculated from  $\epsilon_{mf} = (V_{mf}/V_i)^{1/n}$  where  $V_{mf}$  determined by Leva's equations [Eqs. (51) and (52)] and  $V_i$  and  $n$  from this table.

model using step 6b (designated authors' model 6b) are presented for runs 5, 6, 7, and 8. The results of using step 6b for runs 1 through 4, 9, and 10 do not differ more than 1/4 in. from the results using step 6a and, therefore, are not shown in the figures.

The garnet expansion model using step 6b requires a minimum of experimental work. The average diameter from the sieve analysis and a density determination for the particles are all that is required experimentally.

For comparison purposes, the expansion equation of Wen and Yu [Eq. (36)] was also used to calculate expanded bed height, and the results are presented in Figs. 75 through 84. It is apparent that the Wen and Yu equation does not provide good predicted expansions.

#### Silica Sand and Coal

The expansion vs flow rate data for the uniform silica sands and coals were analyzed in the same manner as the garnet sands. This

was done to develop a model which could be used to predict expansion of silica sand or coal using the same general approach previously described for garnet.

The expansion vs flow rate data for the uniform media were first analyzed to determine the porosity at each flow rate. Log porosity was then plotted against log superficial velocity such as Fig. 85 presented previously. The slope of these curves  $n$  and the intercept velocity ( $V_i$ ) at  $\epsilon = 1.0$  were determined by regression analysis. The results are presented in Table 44.

The relationship between the  $n$  slope and Reynold's number based on  $V_i$  was then determined for all the sand data and separately for all

Table 44. Results of log V vs log  $\epsilon$  regression analyses for uniform sized silica sands and coals.

Media designation	$n$ slope	Velocity intercept $V_i$ , (fps)	Number of values used	Coefficient of determination $r^2$ , %	$Re_i$ based on $V_i$ and $d^a$	Galileo no.
<u>Silica Sand</u>						
A-10+12	2.573	0.557	11	99.76	347	125,296
A-12+14	2.665	0.500	13	99.95	263	74,939
A-14+16	2.900	0.492	13	99.75	217	44,054
A-16+18	2.909	0.420	14	99.82	157	26,803
A-18+20	3.153	0.383	15	99.88	119	15,662
A-20+25	3.296	0.320	16	99.37	84.7	9,553
A-25+30	3.504	0.281	14	99.47	61.9	5,539
A-30+35	3.704	0.258	13	99.54	47.9	3,327
A-35+40	4.126	0.236	14	99.47	36.9	1,958
A-40+45	4.206	0.187	11	99.55	26.1	1,404
<u>Coal</u>						
F-4+7	3.016	0.565	7	99.49	726	484,270
F-7+8	2.832	0.506	7	99.68	447	157,652
F-8+10	2.920	0.465	9	99.53	344	92,145
F-10+12	2.939	0.388	10	99.27	242	55,558
A-10+12	3.254	0.321	11	99.64	201	53,284
A-12+14	3.448	0.291	12	99.79	153	31,869
A-14+16	3.667	0.271	9	99.85	119	18,734
A-16+18	3.479	0.220	10	99.86	82.0	11,398
A-18+20	3.523	0.186	10	99.68	58.1	6,660
A-20+25	3.988	0.171	8	99.67	45.1	4,062
A-25+30	3.739	0.139	7	99.43	30.6	2,356

<sup>a</sup><sub>d</sub> = arithmetic mean of adjacent sieve sizes.

the coal data in Table 44. The results of the regression analysis yielded the following relationships:

For silica sand A, all sizes in Table 44,

$$n = 7.973 \text{ Re}_i^{-0.1947} \quad (71)$$

with coefficient of determination,  $r^2 = 98.16\%$ .

For coal F and coal A, all sizes in Table 44,

$$n = 5.517 \text{ Re}_i^{-0.1015} \quad (72)$$

with coefficient of determination,  $r^2 = 78.36\%$ .

Following the approach of the garnet sand expansion model, the relationships between  $\text{Re}_i$  and the corresponding Galileo number (Ga) were determined for the uniform silica sands and uniform coals. The values of Ga are presented in Table 44. The regression analysis of  $\log \text{Re}_i$  vs  $\log \text{Ga}$  gave the following relationships:

For silica sand A, all sizes in Table 44,

$$\text{Re}_i = 0.5321 \text{ Ga}^{0.5554} \quad (73)$$

with coefficient of determination,  $r^2 = 99.74\%$ .

For coals A and F, all sizes in Table 44,

$$\text{Re}_i = 0.2723 \text{ Ga}^{0.6133} \quad (74)$$

with coefficient of determination,  $r^2 = 99.39\%$ .

The above relationships were then tested for validity by calculating the expansion vs flow rate data for all uniform sands and coals. The procedure was exactly as described previously for garnet sand (authors' model 6a) using the appropriate  $n$  vs  $\text{Re}_i$  and  $\text{Re}_i$  vs Ga relationship for the media under analysis.

The results for the prediction of uniform sand expansions were very good as expected from the high coefficients of determination for Eqs. (71) and (73). The predicted values of  $n$  and  $V_i$  for the various sands are presented in Table 45, along with the maximum percent error in the predicted expanded bed depth up to a total expansion of 70%. It is apparent from Table 45 that the uniform sand expansions can be predicted acceptably, with errors not exceeding about 7% of actual observed values.

Table 45. Predicted values of  $n$ ,  $V_i$  with errors of prediction and maximum error of prediction of expanded bed depth for uniform sands.

Sand designation	$V_i$ from Eq. (73), fps	% error in $V_i^a$	$n$ from Eq. (71)	% error in $n^a$	Maximum % error in expansion <sup>b</sup>
A(-10+12)	0.559	- 3.64	2.533	1.52	+ 2.2
A(-12+14)	0.499	0.25	2.678	- 0.51	- 1.1
A (-14+16)	0.443	9.51	2.836	2.19	- 7.5
A(-16+18)	0.397	5.38	2.993	- 2.90	- 7.1
A(-18+20)	0.352	7.17	3.172	- 0.60	- 6.5
A(-20+25)	0.316	8.42	3.346	- 1.53	- 2.3
A(-25+30)	0.280	1.94	3.549	- 1.29	- 2.1
A(-30+35)	0.250	0.94	3.751	- 1.26	- 3.3
A(-35+40)	0.222	3.60	3.972	3.73	- 3.6
A(-40+45)	0.206	- 0.45	4.117	2.11	+ 5.9

<sup>a</sup>Compared to values in Table 44.

<sup>b</sup>[(Observed depth - predicted depth) 100/observed depth]. Maximum observed error in predicted expansion up to a total bed expansion of 70% above fixed bed depth.

On the other hand, the prediction of coal expansions were not as good as shown in Table 46. It appears that the model provides an acceptable prediction for the uniform sizes from coal A, but is unable to do as well for the uniform sizes from coal F. This may be due, in part, to different sphericity for the two coals. It may also be due to less well-defined uniform sizes due to the angularity of the crushed coals and resulting sieving difficulties. More work should be done on the crushed coals to attempt to improve the prediction accuracy.

The difficulties encountered with the coal expansion prediction emphasize one important weakness in the expansion models: they do not incorporate any direct measure of sphericity. They are empirical

Table 46. Predicted values of  $n$ ,  $V_i$  with errors of prediction and maximum error of prediction of expanded bed height for uniform coals.

Coal designation	$V_i$ from Eq. (74) fps	% error in $V_i^a$	$n$ from Eq. (72)	% error in $n^a$	Maximum % error in expansion <sup>b</sup>
F-4+7	0.629	- 11.10	2.787	7.58	13.7
F-7+8	0.459	9.20	2.989	- 5.52	- 15.0
F-8+10	0.395	15.13	3.090	- 5.85	- 26.0
F-10+12	0.343	11.69	3.189	- 8.49	- 24.8
A-10+12	0.334	- 3.96	3.197	1.74	4.7
A-12+14	0.289	0.39	3.301	4.24	5.0
A-14+16	0.249	7.85	3.413	6.94	1.9
A-16+18	0.217	1.28	3.520	- 1.16	- 1.6
A-18+20	0.187	- 0.19	3.639	- 3.30	- 3.8
A-20+25	0.163	4.73	3.753	5.89	4.1
A-25+30	0.140	- 0.62	3.883	- 3.83	- 2.7

<sup>a</sup>Compared to values in Table 44.

<sup>b</sup> $[(\text{Observed depth} - \text{predicted depth}) 100 / \text{observed depth}]$ . Maximum observed error in predicted expansion up to a total bed expansion of 70% above fixed bed depth.

models appropriate to media of about the same sphericity as that used in their development. Thus, they should be used with caution on media from other sources with potentially different sphericity. Future work should include development of simple direct measures of sphericity and collection of additional data on the effect of sphericity on the drag coefficient and on the expansion models.

Since the prediction of expansion of the uniform sands was considered acceptable, the models were used to predict the expansion of the three graded (A, A-2, and C) sands previously described in Fig. 60

and for graded sand observations reported by Amirtharajah [4]. The results of the prediction are summarized in Table 47. The procedure consisted of the following steps: (1) calculation of the average grain diameter by the inverse definition [Eq. (38)], (2) calculation of the Galileo number from the properties of the media and fluid, (3) calculation of  $Re$  from Eq. (73) and  $V_i$  from  $Re_i$ , (4) calculation of  $n$  from Eq. (71), (5) calculation of  $\epsilon$  at each superficial flow rate,  $V$  from Eq. (28) using  $V_i$  and  $n$  calculated above, and (6) calculation of expanded bed depth from Eq. (2).

It is evident from Table 47 that the predicted bed depths are all higher than observed, and the prediction is not too good. An attempt was made to determine the reasons for the consistent over-prediction. One cause is the choice of  $\epsilon_0$  used in Eq. (2). Values of  $\epsilon_0$  of 0.42 were used for the graded sands of Boss and 0.41 for those of Amirtharajah. These choices were based on porosities by the graduate cylinder technique for graded sands described previously and values reported by two investigators. If a value of 0.44 had been selected as determined by the column technique (Table 37), the prediction would have improved. The arithmetic mean diameter [Eq. (39)] consistently yields a larger diameter than the inverse diameter [Eq. (38)], as evidenced by Table 35. If the larger diameter defined by Eq. (39) had been used, the prediction would be improved. A spot check of the effect of these two factors on prediction for three graded sands in Table 47 indicates that the maximum percent errors reported would be reduced about 5% (e.g., from -15 to -10%).

From this analysis, it is evident that the prediction adequacy is sensitive to choice of  $\epsilon_0$  and mean diameter. Acceptable predictions seem possible if the column technique is used to evaluate  $\epsilon_0$  and the arithmetic mean definition [Eq. (39)] is used to calculate mean grain diameter.

The expansion of the graded sands was also calculated using the incremental approach presented in some engineering textbooks[46]. This approach calculates the expansion of increments of the media between adjacent sieves and sums the expanded depth of the increments to determine the total expanded depth. The results of the incremental approach were no better than, and in some cases worse than, those presented in Table 47.

In view of the relative inaccuracy of prediction of expansion of the uniform coals, no attempt was made at this time to test the prediction accuracy of the models for graded coals.

#### Minimum Fluidization Velocity of all Media

The minimum fluidization velocity ( $V_{mf}$ ) can be defined in a number of ways. For uniform media which fluidizes sharply at a particular flow

Table 47. Prediction of expanded bed depths for graded sands using models developed for uniform sands and average diameter based on the inverse definition [Eq. (38)].

Sand	Avg dia, mm	Water temp, °C	Ga	Re <sub>i</sub>	V <sub>i</sub> , fps	n	Maximum % error in expanded depth <sup>a</sup>
From Boss [14]							
A	0.686	17	4,383	56	0.2926	3.640	- 7.10
A-2	0.716	26	7,736	76.9	0.3092	3.424	- 6.6
C	0.947	22	14,838	110.4	0.3353	3.191	- 17.3
From Amirtharajah [4]							
A	0.612	15	2,824	43.9	0.270	3.818	- 9.5
A	0.612	13.5	2,613	42.0	0.269	3.850	- 11.5
A	0.612	30	5,773	65.3	0.281	3.534	- 14.9
A	0.612	30	5,773	65.3	0.281	3.534	- 16.2
A	0.612	30	5,773	65.3	0.281	3.534	- 16.2
B	0.919	15	9,599	86.6	0.354	3.347	- 15.8
B	0.919	15	9,599	86.6	0.354	3.347	- 17.8
B	0.919	30	19,623	129	0.370	3.096	- 15.8
B	0.919	30	19,623	129	0.370	3.096	- 16.8
C	0.688	22	5,725	65.0	0.298	3.537	- 17.4
C	0.688	35.5	10,401	90.6	0.309	3.316	- 17.7

<sup>a</sup> [(Observed depth - predicted depth) 100/observed depth], over the full range investigated, generally to an expanded depth of about 50% of fixed bed depth.

rate, it is frequently defined as the point of intersection obtained through extrapolation of the two linear sections of the envelope curve of head loss vs superficial velocity such as Figs 73 and 74. The values of  $V_{mf}$  based on this definition for garnet sands have been presented in Table 40. However, this definition is not meaningful for graded media because the coarser sizes of media comprising the bed are not fluidized at the  $V_{mf}$  defined in the above manner.

It is also difficult to define  $V_{mf}$  on the basis of first visual appearance of complete fluidization because it is subject to the observer's visual definition of complete fluidization. In view of these difficulties and the fact that all media studied were graded in size to some extent (even the uniform media), the minimum fluidization velocity was defined as that flow rate required to achieve 10% bed expansion. This expansion is close to the minimum rate at which the bed first appears fluidized. The  $V_{mf}$  values thus determined for the three media studied are presented in Fig. 88. These data are based on the expansion studies for single uniform media only in Table 33 (Series C-1 and 3 and D-1) and in Table 31 (Series A-13, 14, and 15).

This type of data is believed to be useful in determining minimum backwash rates to ensure fluidization of all media comprising the bed. If the sieve analysis of each media is available or specified, the backwash rate needed to achieve fluidization of the coarse sizes in each media should be provided. Furthermore, it would appear that media should be specified so that the coarse sizes of each media comprising the bed are fluidized at roughly the same minimum fluidization velocity. Thus, the entire bed will become fluidized simultaneously. The total bed expansion can then be determined by summing up the calculated expansions of the individual media.

Unfortunately, the experiments depicted in Fig. 88 were not conducted over a broad enough range of temperatures to present similar empirical data for other temperatures. The effect of temperature on  $V_{mf}$  can be judged from various models for  $V_{mf}$  such as Eqs. (51) through (54).

Data were collected on graded sand A and graded coal A at four different temperatures from 16 to 30 °C. To illustrate the effect of temperature on  $V_{mf}$ , the values of  $V_{mf}$  to achieve 10% expansion of these two media were determined. The results are plotted in Fig. 89. It is evident that temperature does have a distinct effect on  $V_{mf}$  as would be expected in the transitional or laminar fluid regimes. These curves could be used to select a rough temperature correction factor to be applied to the data of Fig. 88 in selecting  $V_{mf}$  for other temperatures. Inspection of Fig. 89 shows that change in  $V_{mf}$  is not a linear inverse function of viscosity as would be expected in the transitional fluid regime. Only in the laminar regime would the relation be linear.

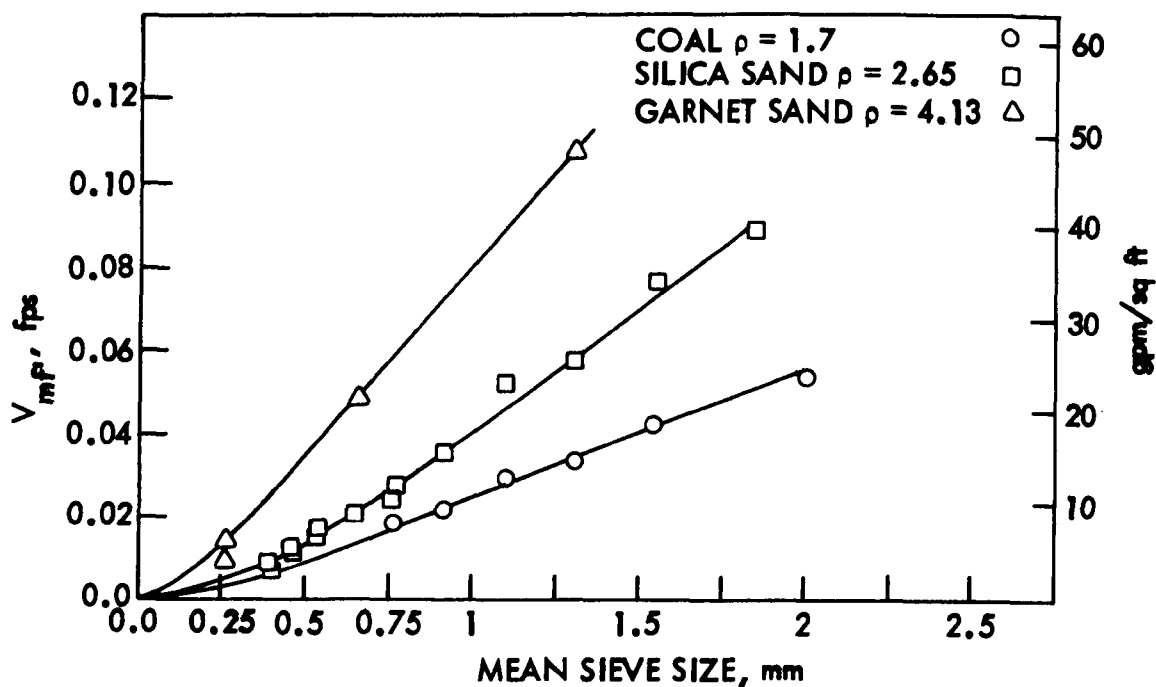


Fig. 88. Minimum fluidization velocity,  $V_{mf}$ , to achieve 10% bed expansion at 25 °C.

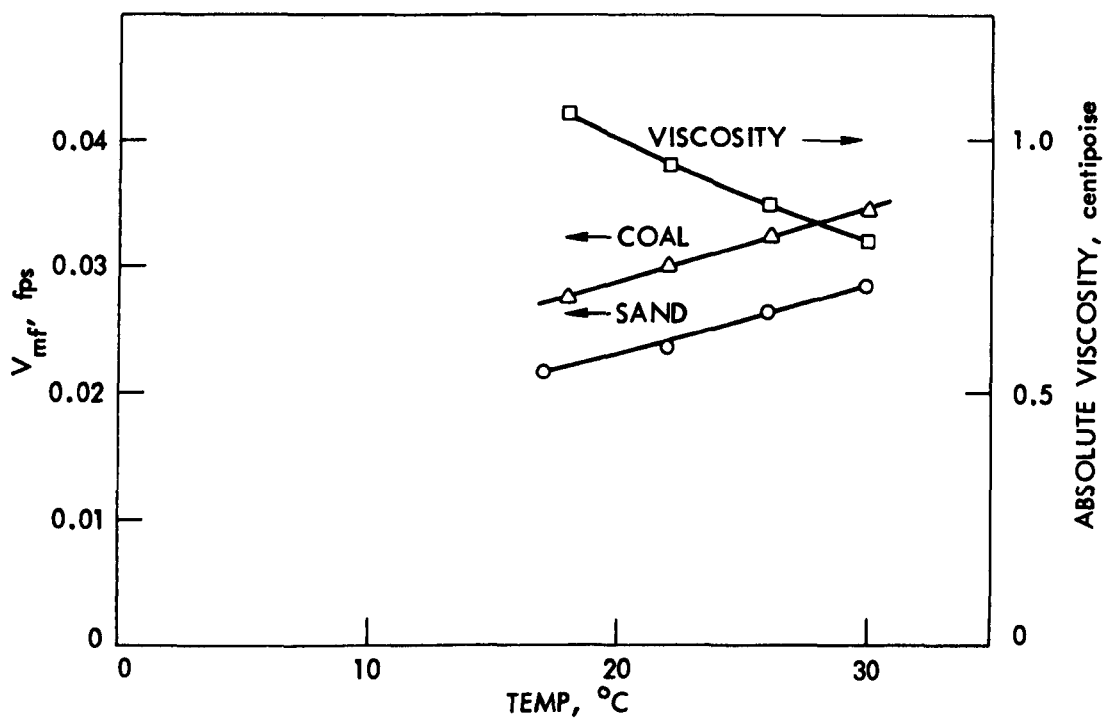


Fig. 89. Effect of temperature on  $V_{mf}$  for sand and coal and on absolute viscosity of water.

Comparison of Fig. 89 with Table 40 shows reasonable agreement with change in  $V_{mf}$  with temperature. For example, the average ratio of  $V_{mf}$  values for garnet at 25 °C and 17 °C is 1.14 in Table 40. The same ratio for sand and coal in Fig. 89 is 1.17.

It should be noted that the coarse sizes in a given media control the point of complete minimum fluidization, and skimming the fines will not alter the  $V_{mf}$ .

### Intermixing Observations

#### Garnet and Silica Sand

The objective of the intermixing experiments was to test the validity of the bulk density approach for the prediction of intermixing of the small-sized dense garnet sand and larger-sized less dense silica sand. A uniform-sized garnet sand and various uniform-sized silica sands were first fluidized individually, and then the two-component mixtures of the silica sands and garnet sands were fluidized to observe their intermixing behavior.

The data collected for the single-component fluidization experiments included flow rate and bed height. From the individual component fluidization data the following values were calculated:

1. Flow meter readings were corrected to give corrected flow rate using the appropriate calibration equation.
2. From the bed height reading, the average porosity of the bed at various flow rates was calculated from the known weight of media in the column, the column cross-sectional area, and the particle density.
3. The average bulk density was then calculated at the same flow rates from the above porosity values and the solid and fluid density by Eq. (41).

The computed values of flow rate and bulk density from single-component fluidization data for each media studied are shown in Fig. 90. An interesting and important fact can be observed on Fig. 90. The slope of the garnet sand curve is steeper than any of the silica sand curves. Thus, maximum bulk density differences (garnet - silica sand) occur at the lowest flow rates.

The data collected for the two-component fluidization experiments were the bed height, flowmeter reading, the visual observations of relative media concentrations at various depth in the bed. The results of these two-component fluidization experiments are shown in Figs. 91 through 94.

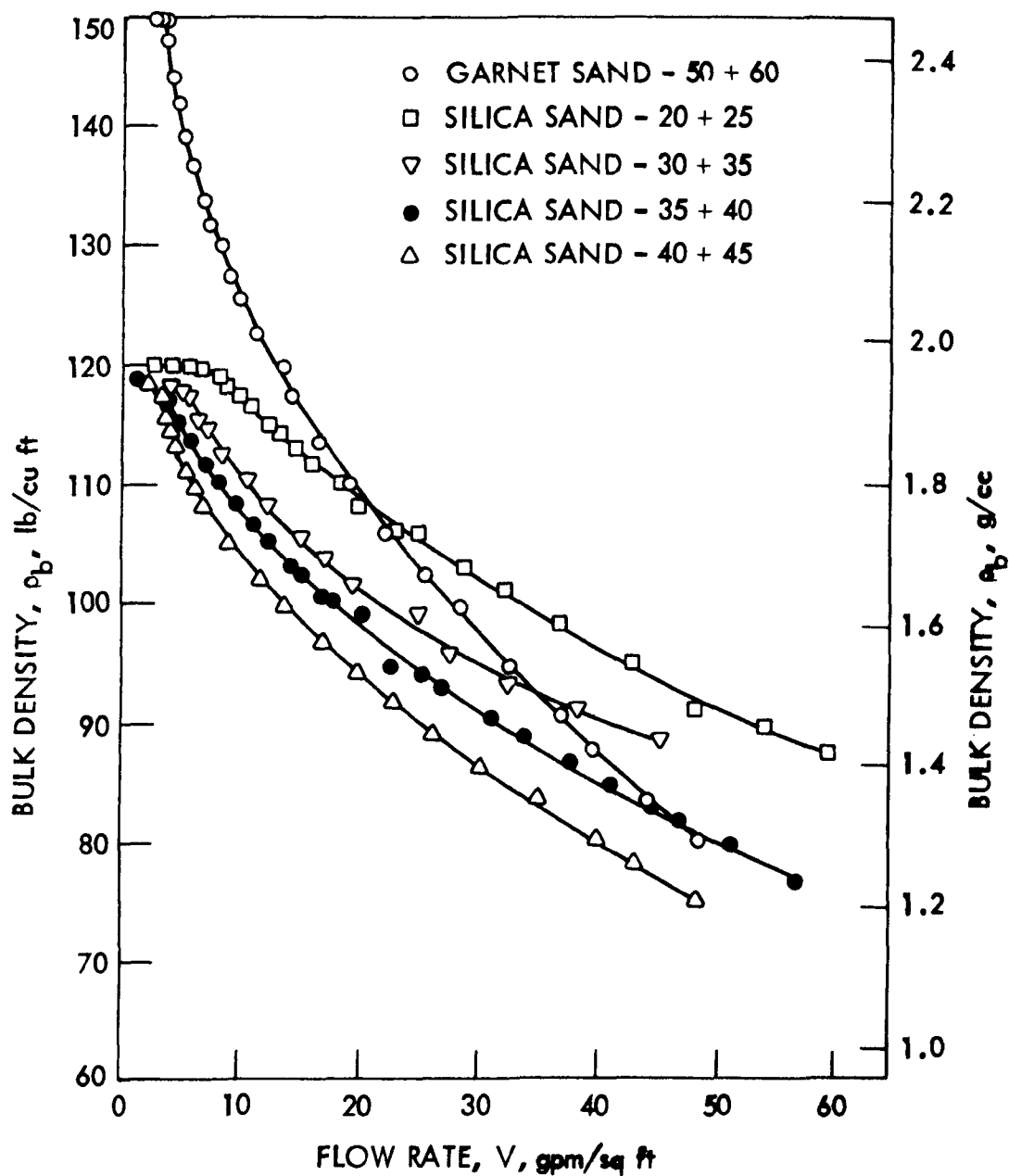


Fig. 90. Bulk density vs flow rate for garnet sand and silica sand.

Before the intermixing observations were made, the two-component mixture was fluidized and contracted to a fixed-bed state very slowly. The data presented in Figs. 91 through 94 were then collected during the expansion of the two-component mixtures. After each incremental increase in flow, sufficient time was allowed to reach equilibrium conditions before the intermixing observations were recorded. The expansion was carried up to about 200%. The major problem encountered in collecting and presenting this type of data was that it was difficult

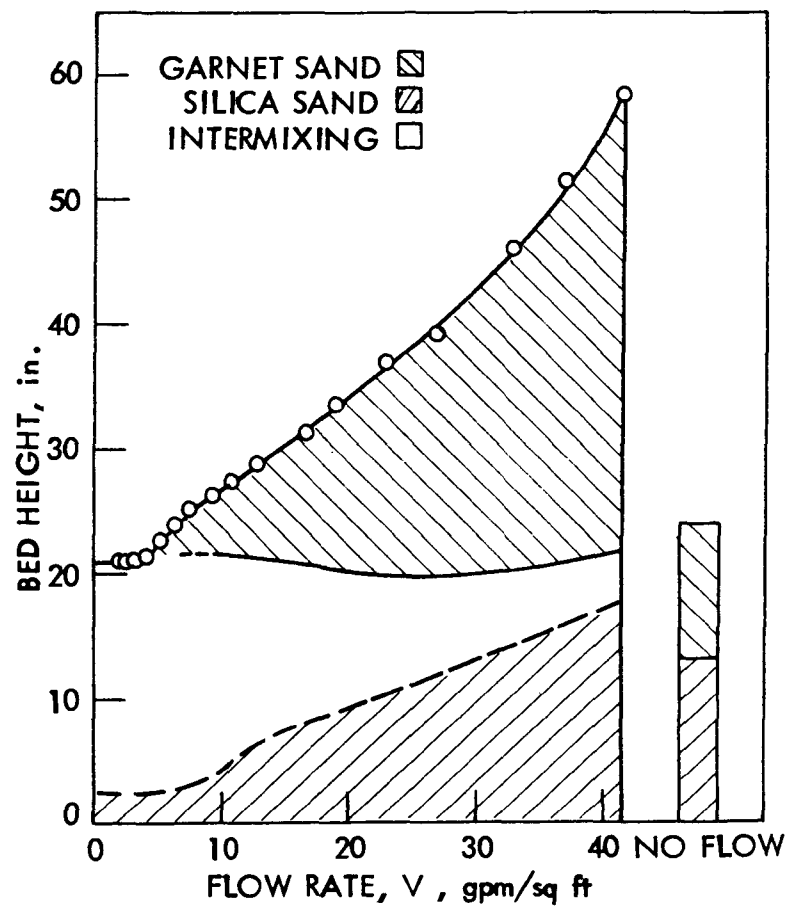


Fig. 91. Intermixing of -50+60 garnet sand and -20+25 silica sand.

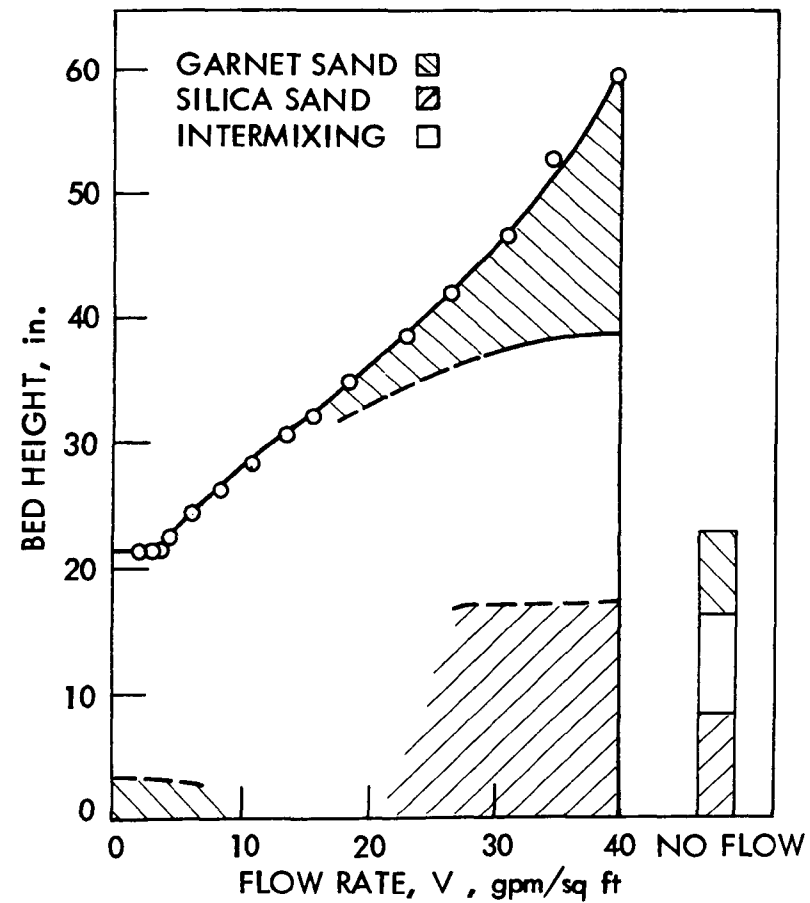


Fig. 92. Intermixing of -50+60 garnet sand and -30+35 silica sand.

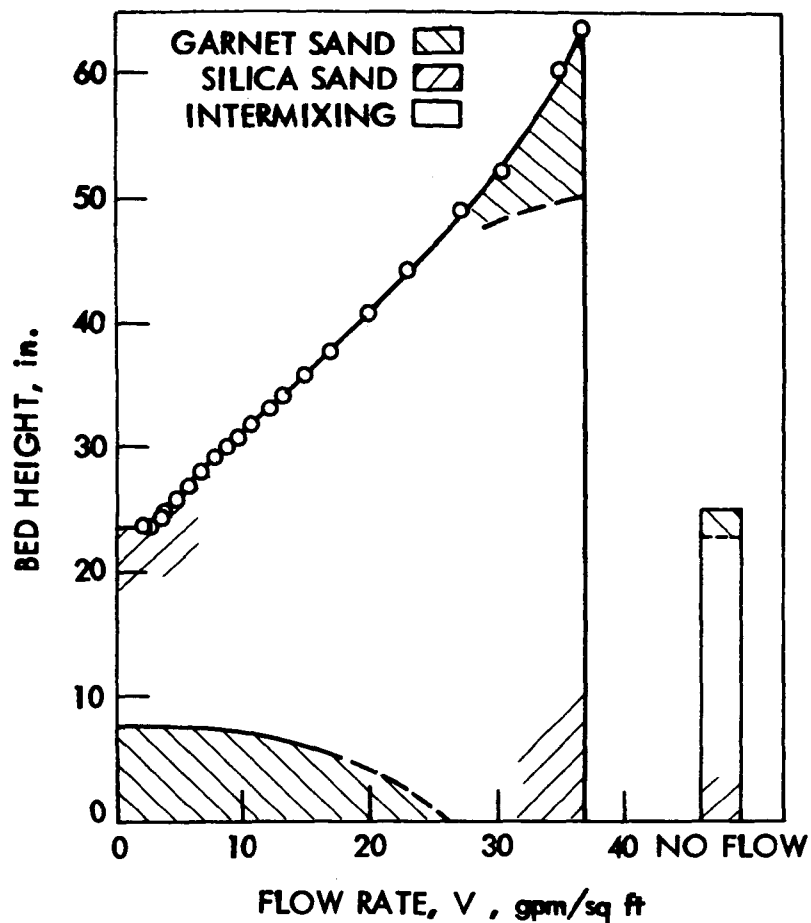


Fig. 93. Intermixing of -50+60 garnet sand and -35+40 silica sand.

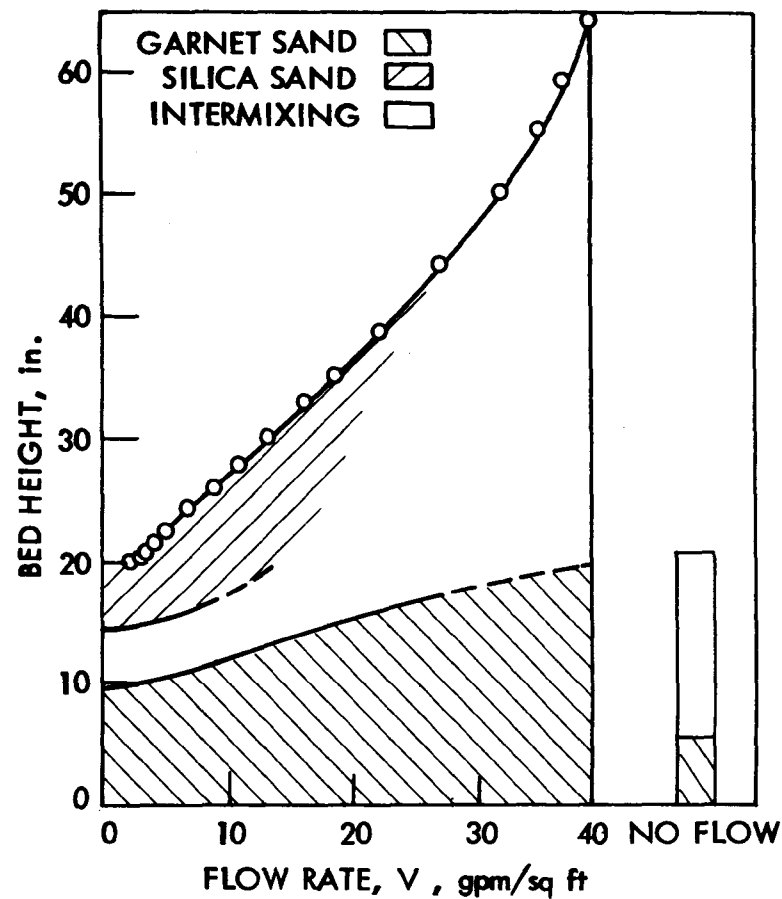


Fig. 94. Intermixing of -50+60 garnet sand and -40+45 silica sand.

at times to decide in which regions of the expanded bed one component was the sole component and in which the components were intermixed. Three regions usually existed - one region at the top and one at the bottom of the bed where the components were clearly or closely the sole component of the layer, and one between these two separate layers which was a region of intermixing. Within this region of intermixing, the concentration of each component decreased with distance away from the adjacent region where it was the major component. The interfaces between the three different regions are distinguished on the figures by a solid line which indicates a sharp interface or a dashed line representing a diffuse interface over a bed depth of 2 to 4 in.

After the two components were expanded to the maximum expanded height, the flow of water was quickly shut off, and the bed was also allowed to settle. The stratification of the bed after this settling is also included in Figs. 91 through 94.

The analysis of Figs. 91 through 94 indicates a trend for the garnet sand to occupy the lower layer of the bed at low flow rates, then as the flow rate increases, the two-component mixtures are intermixed. At still higher flow rates, the garnet sand occupies the upper portion of the bed, and the silica sand occupies the bottom of the bed. These trends would be expected from the bulk density plots of the single component data as shown in Fig. 90, because the bulk density of the garnet sand decreased more rapidly than the silica sand as the flow rate increased.

An exception to this trend was noticed in the fluidization of the -20+25 silica sand and -50+60 garnet sand mixture where the silica sand occupied the lower portion of the bed at all flow rates. This can be explained by considering the minimum fluidization velocities of the silica sand and the garnet sand. The minimum fluidization for the -50+60 garnet sand was observed to be 3.0 to 3.5 gpm/sq ft (0.007 to 0.008 fps). The silica sand minimum fluidization velocity was approximately 7.5 gpm/sq ft (0.017 fps) for the -20+25 size. Therefore, when the fluidized mixture of -20+25 silica sand and garnet sand was contracted slowly, the -20+25 silica sand reached the fixed bed state while the garnet sand was still fluidized and before the bulk density of the garnet sand was sufficiently greater than the silica sand to occupy the bottom layer of the bed. Just below minimum fluidization for the -20+25 silica sand, it was noticed that the garnet sand, which was still fluidized, displaced a small portion of the silica sand that was in a fixed state up into the intermixed layer.

The garnet sand was below the silica sand at all flow rates for the -40+45 silica sand and -50+60 garnet sand two-component mixture. The maximum flow rate of this two-component mixture was 40 gpm/sq ft (0.089 fps). At this flow rate, the garnet sand still had a higher bulk density than the -40+45 silica sand (from single-component data,

Thus, as predicted by the bulk density approach, the garnet sand should occupy the lower portion of the bed.

The sensitivity of results was hampered by the following factors.

1. The uniform sands used were not actually unisized and of consistent shape. Because of this, there would be a tendency for stratification within each individual media, and a bulk density gradient would exist in each individual media. This was supported by the observation for all of the uniform media when expanded and then contracted slowly, or when expanded and allowed to settle after the fluid flow was stopped. There was a slight but noticeable difference in particle size between the top and bottom layers.
2. Because of the physical properties of the fluid and solids, the fluidization of the components occurred in the transitional regime of flow, and mixing and circulation patterns existed in the bed during fluidization. This would tend to diminish the bulk density gradients within the individual and two-component mixtures.
3. The distribution of flow into the fluidizing column from the calming section was not perfectly uniform. However, it was quite good with short circuiting of upward flow usually limited to 2 to 3 in. above the entrance and rarely extending 6 in. up the column.

There are three major conditions of interest in the relative location of the garnet sand component:

1. stratification of the garnet sand component in the bottom of the bed with or without intermixing of garnet sand and silica sand in layers above.
2. maximum intermixing of the garnet sand with silica sand, and
3. stratification of garnet sand in the top layer with or without intermixing in layers below.

The following bulk density differences, Table 48, were obtained from Fig. 90 and the appropriate two-component intermixing figures (Figs. 91 through 94) for the three conditions. The ratio of the diameters of garnet sand to silica sand is also given below. From Table 48 or from Figs. 90 and 91 through 94, maximum intermixing of the two components (Condition 2) does not occur at zero bulk density difference as would be expected, but at a slightly positive bulk density difference, about 3 to 8 lb/cu ft. These observations are in agreement with the experimental results of Le Clair [74] who found that the velocity for a homogeneous mixture as predicted from single-component data was greater than the observed velocity where homogeneous mixing occurred.

Table 48. Bulk density difference, lb/cu ft (garnet-silica sand).

Silica sand media	Condition (1)	Condition (2)	Condition (3)	$\frac{d_m}{d_m}$ Silica sand Garnet sand
-20+25	Did not occur	8 to 3	< 12	2.84
-30+35	> 20	15 to 5	< 9	2.04
-35+40	> 10	8 to 4	< 6	1.70
-40+45	> 5	10 to $\approx 0$	Did not occur	1.47

It is evident from Table 48 that a single value of bulk density difference cannot be readily selected which could be used by the design engineer to ensure the desired degree of stratification or intermixing between garnet sand and silica sand. For example, the bulk density differences (garnet-silica sand), which ensure that Condition 1 or 3 will exist, decreased with lower diameter ratio (silica sand/garnet sand). The lower bulk density differences, indicated in the table for Condition 1 and 3, occur at higher flow rates and higher bed porosities.

Based on the data in Table 48, if one wanted to ensure that some garnet sand would always remain on the bottom regardless of the backwash rate of the filter bed, one would need to select the media so that the ratio of the bottom silica sand size to the bottom garnet sand size is not more than 1.47. The next larger ratio could be used (1.70) providing that the backwash rate was limited to 15 to 20 gpm/sq ft (0.033 to 0.045 fps) or the operator would need to allow for a slow contraction of the fluidized bed after backwashing to achieve restratification.

Attention should be drawn to the converging nature of the garnet sand and silica sand curves in Fig. 90. Because of this converging nature, excessive backwash rates result in increased tendencies to intermixing and bed inversion. This fact should be considered in selecting the media and backwash rate for dual- and multi-media filters.

In view of the apparent inadequacies, or insensitivity of the equal bulk density approach to the prediction of intermixing, an attempt was made to utilize the intermixing theory proposed by Camp et al. [26].

This theory as stated in Eq. (49) suggests that mixing will occur if the bulk density of the lower bed of smaller, more dense garnet grains is less than the density of the larger, less dense upper particles minus a drag force term for the upper grains. Figure 95 shows the results of the calculations.

Figure 95-A shows that the -20+25 mesh silica sand should intermix at all flow rates since its particle density less the drag term is still greater than the bulk density of the garnet, top or bottom layer. This intermixing was evident in Fig. 91.

Similarly, Fig. 95-B for -40+45 silica sand would predict complete intermixing if the sand grains were spherical. However, if they were cubical in shape, the drag term would be increased, and intermixing would be only partial. The sand grains used in this study are rounded in shape and would not be cubical in sphericity. Thus, intermixing should be complete. However, Fig. 94 shows that most of the garnet sand remained on the bottom of the bed at all flow rates for this sand and garnet combination.

These observations do not prove or disprove the validity of the intermixing model of Camp et al. [26]. An adequate measure of sphericity would be needed to test the model. The unavailability of such a measure is the same weakness preventing good prediction of bed expansion for nonspherical particles discussed previously. Until this weakness is resolved, the intermixing model of Camp et al. [26] is no more useful than the equal bulk density model of Le Clair [74].

#### Silica Sand and Coal

Bulk density data and intermixing observations for the silica sand and coal were collected in the same manner previously described for garnet and silica sand.

A full range of uniform media was tested in a series of tests using the 2-in. fluidization column. The uniform sizes tested ranged from -10+12 mesh to -40+45 mesh for sand and from -4+7 mesh to -25+30 mesh for coal. A known dry weight of a particular uniform filter medium was placed in the column. The expanded bed height vs flow rate was observed. Porosity at any flow rate was calculated from the known weight of the medium, particle density, and expanded bed height. Bulk density for each flow rate was calculated by Eq. (41) and then plotted in Fig. 96. Bulk density, as defined in this study, is actually the average fluid and particle composite density value within a filter bed cross section. At zero flow rate, the sand bulk density was approximately 1.9 g/cc while the coal bulk density was approximately 1.3 g/cc.

Figure 96 illustrates that, with an increasing flow rate, sand bulk densities decrease much more rapidly than the coal bulk densities. An extreme bulk density decrease of from 1.90 g/cc at zero flow rate

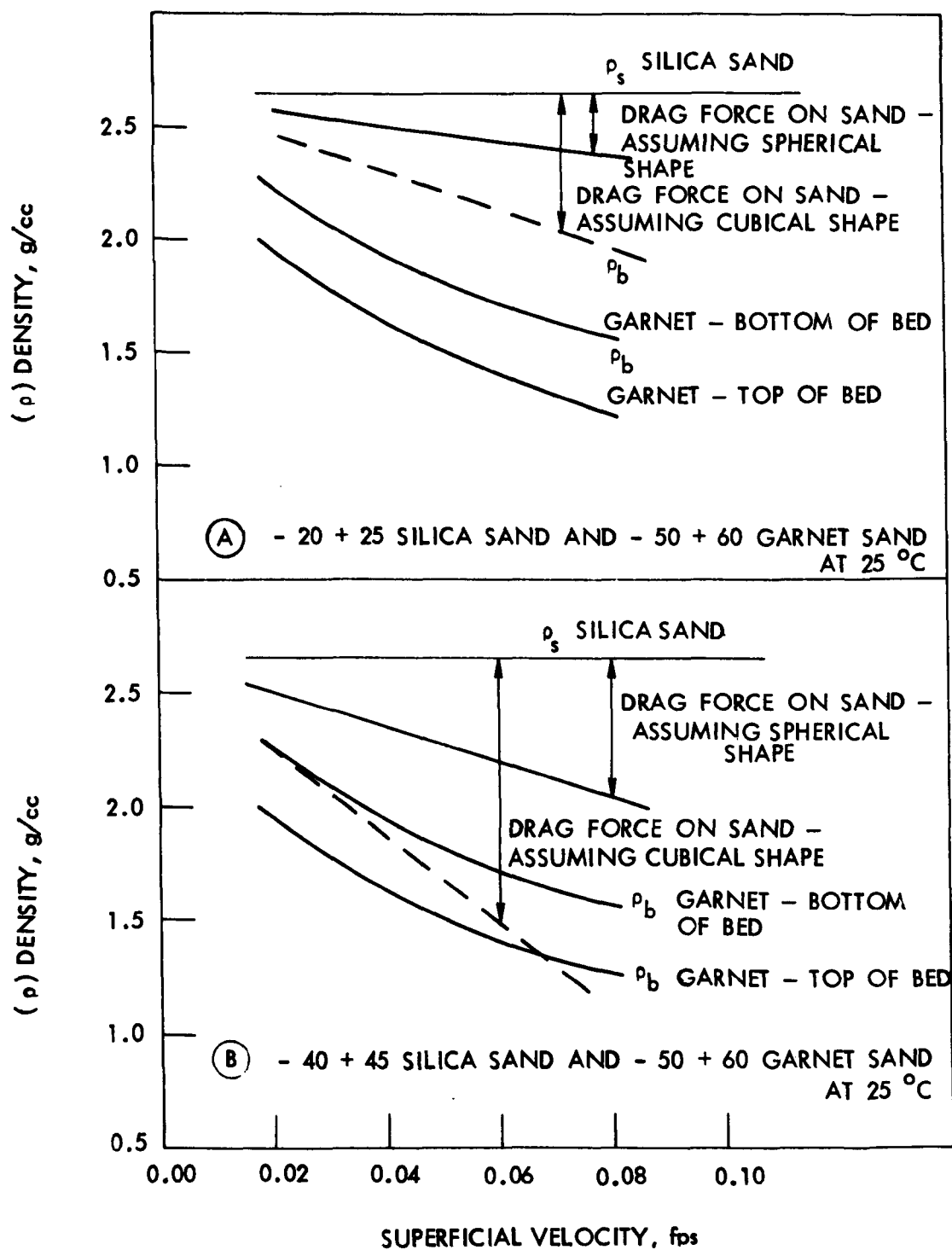


Fig. 95. Intermixing of silica sand and coal according to the model of Camp et al. [26].

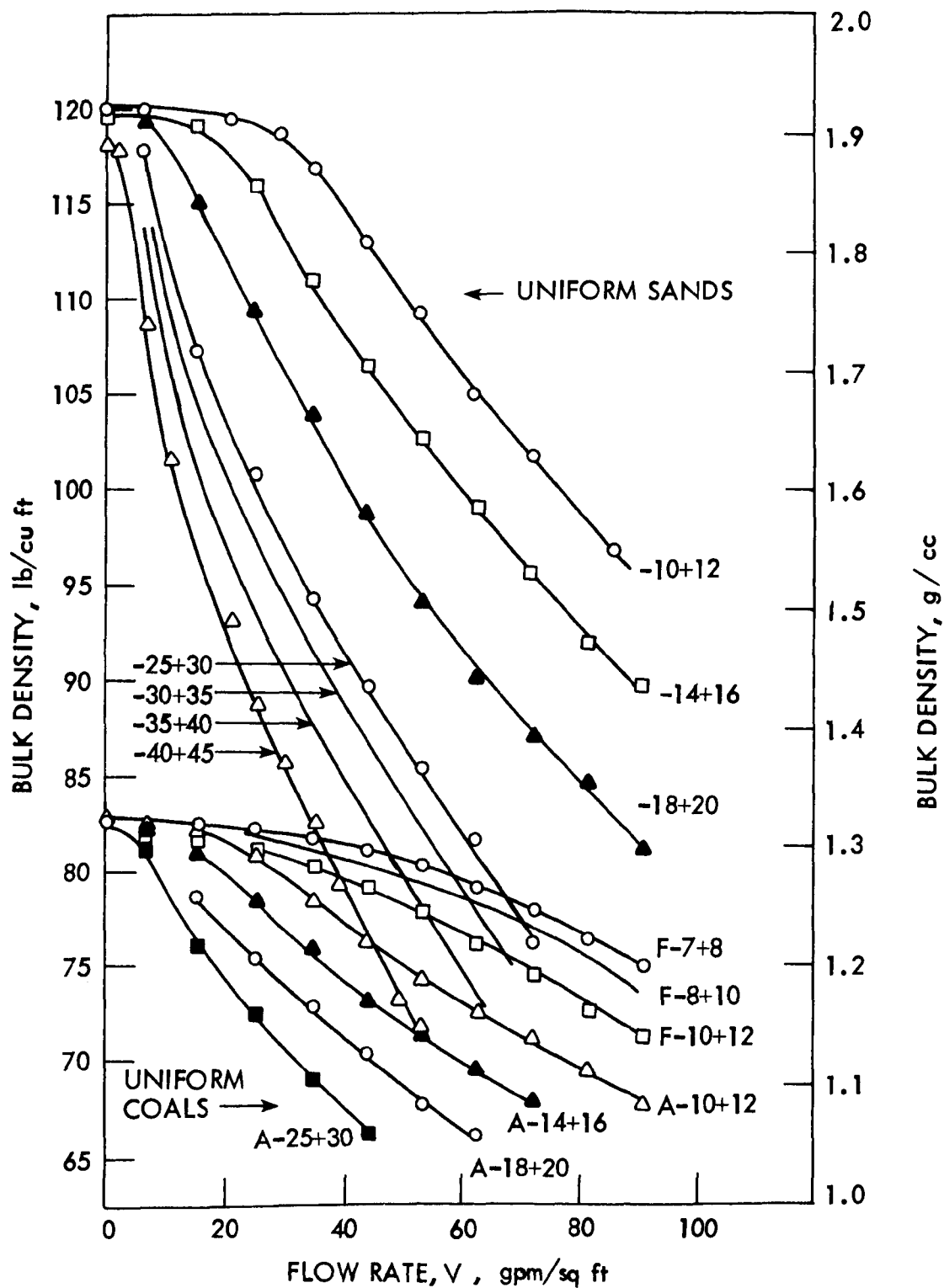


Fig. 96. Bulk density vs flow rate for coal and silica sands (data points not shown on all curves for drafting convenience).

to 1.15 g/cc at 50 gpm/sq ft was exhibited by the -40+45 mesh sand. The coal bulk densities showed less dependence on flow rate, especially coarser coals down to 12 mesh. The general pattern is similar to that for garnet and silica sand presented previously in Fig. 90.

A bulk density comparison between uniform media of the same size range but different origin (i.e., -10+12 mesh coal A and -10+12 mesh coal F) is also plotted in Fig. 96. The bulk density difference of these identically-sized uniform coals was attributed to differences in specific gravity and particle shape of the two source samples. Limited data restricted such comparisons of uniform media from different sources to the two uniform media above.

A large bulk density difference also exists between the majority of the sand and the majority of the coal media. If the back-washing flow rate is limited to 30 gpm/sq ft, only the fine -30+45 mesh sand approaches the bulk density of the coarse coal.

Intermixing observations were limited to -4+7 coal F and the various uniform sands shown in Fig. 96. Again, it was desired to test the validity and sensitivity of the equal bulk density theory of intermixing of Le Clair [74]. In retrospect, it would have been better to use several narrow, size ranges for the coal. Use of only the broad -4+7 mesh coal in the intermixing observations led to inconclusive results regarding the bulk density difference associated with partial or complete intermixing. Additional work in this area should be conducted.

#### Expansion of Graded Dual-Media Filters

This section presents some general characteristics associated with the expansion of dual-media filters.

(1) An example of the expansion plot for a graded dual-media filter bed is found in Fig. 97. The bed height ordinate shows that approximately equal 12-in. quantities of sand A and coal A were systematically expanded. The similarity shown between the expansion rate of sand A and coal A resulted, because the coal average particle size was such that the  $V_{mf}$  values were almost the same for sand A and coal A.

Figure 97 illustrates that the predicted expansion, obtained by adding bed expansion of the individual components, closely approximated the experimentally determined expansion of the dual-media filter. The results of Fig. 97 support the work of Le Clair [74], who, in restating the cell theory, suggested that in all cases each fluidized particle within a medium has a definite, surrounding cell of fluid at a particular flow rate. Introducing particles of different densities does not influence the size of the fluid cells for the particular flow rate. Therefore, the expansion of the individual components can be summed to predict dual-media filter expansion.

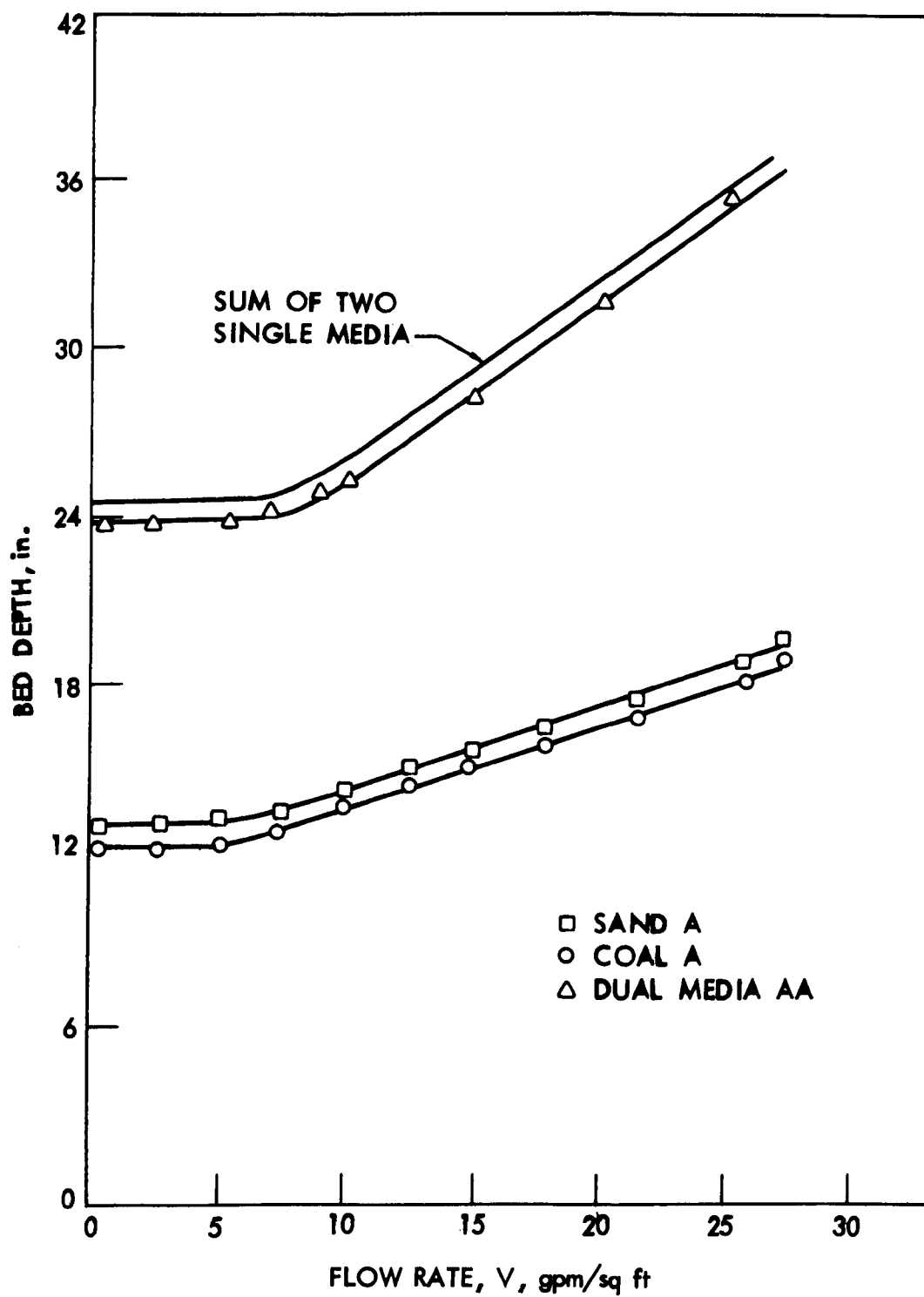


Fig. 97. Expansion vs flow rate of dual media AA and the two-component media at 22 °C.

(2) The expansion of dual media  $A_2C_2$  and the two-component media are presented in Fig. 98. Because sand  $A_2$  became fluidized first, expansion of the dual-media filter at lower flow rates was close to the amount of sand expansion. At higher flow rates, above fluidization for coal  $C_2$ , expansion of dual media  $A_2C_2$  was close to the sum of the expanded depths of the two single media.

It is apparent from Fig. 98 that sand  $A_2$  begins to expand at about 7 to 8 gpm/sq ft and reaches 10% expansion at about 12 gpm/sq ft. Coal  $C_2$  on the other hand begins expanding at about 15 to 16 gpm/sq ft and reaches 10% expansion at about 22 gpm/sq ft.

The most important fact to be concluded from Fig. 98 is that if the sand and coal of a dual-media filter are not selected to fluidize at about the same flow rate, one media may remain fixed (or nearly fixed) while the other is fluidized. The fixed bed portion may not be cleaned adequately during the backwashing. For example, if dual media  $A_2C_2$  were expanded 20%, the minimum normally required for adequate backwashing, the coal would be expanded only about 5%. At 5% expansion, the coal is essentially in a fixed-bed condition and would not clean well. Furthermore, to achieve 20% expansion of the coal in this dual media would require a flow rate of 27 gpm/sq ft, and the total bed expansion would be about 35%. Thus, observation of a total bed expansion of 20% for this dual media would not necessarily mean that both media would receive an adequate backwash.

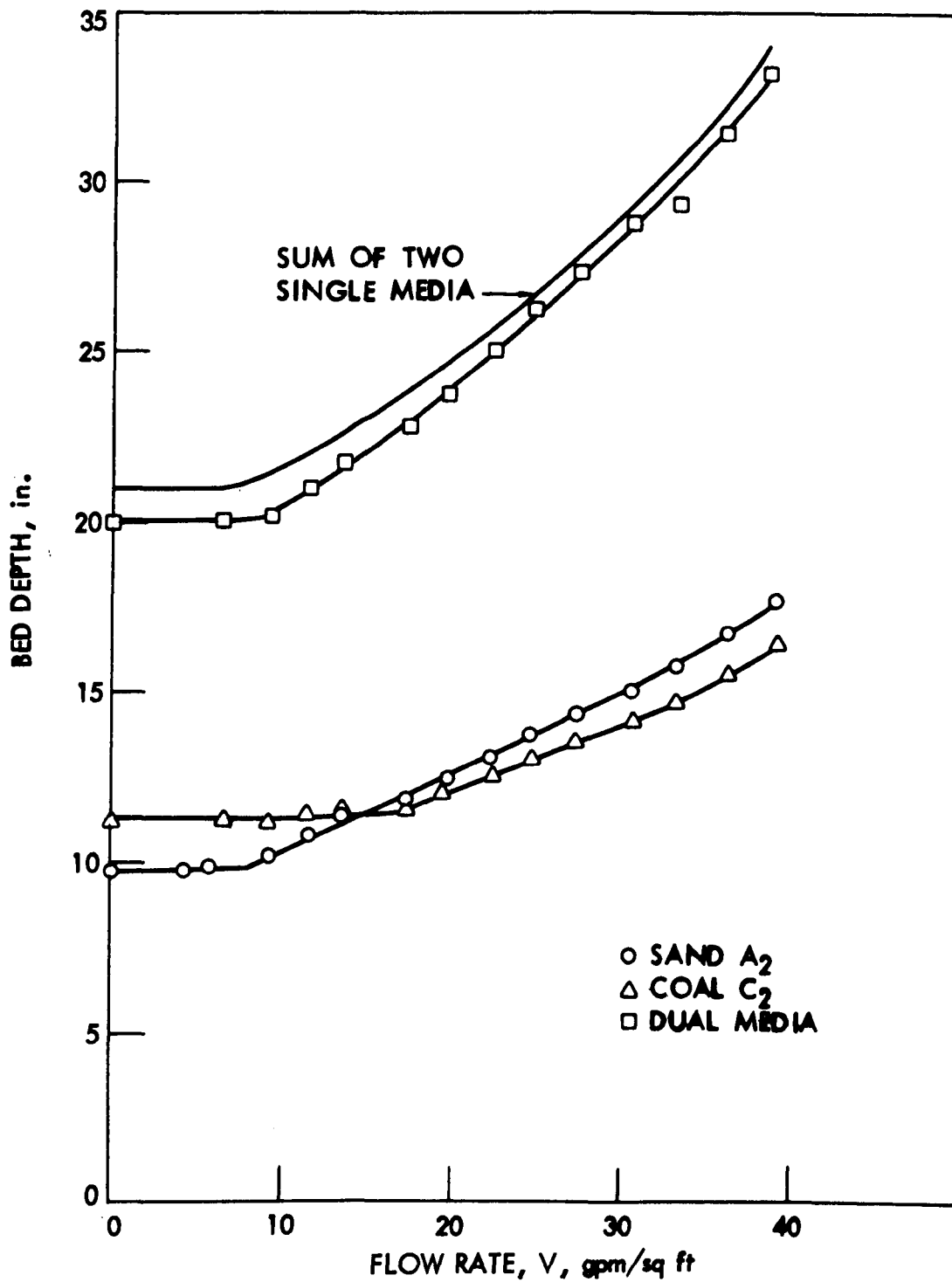


Fig. 98. Expansion vs flow rate of dual media  $A_2C_2$  and the two-component media at 22 °C.

## XI. EFFECT OF MEDIA INTERMIXING ON DUAL-MEDIA FILTRATION

### Introduction

Dual-media filters composed of anthracite coal over silica sand are widely used in water and wastewater filtration because they achieve greater water production per filter run than sand filters if other filtration conditions are the same. Furthermore, because of greater potential production per filter cycle, the percentage of filtered water used in backwashing is less for dual-media filters than for sand filters.

The coal and sand of a dual media filter will sometimes intermix at the interface, depending on the size, shape, and density of the two media at the interface, the rate of backwash, and the backwash valve closure rate. The most important parameter affecting the amount of intermixing is the relative size ratio of the sand and coal at the interface. The media may be so graded as to maintain a sharp interface (coal size to sand size ratio at the interface of about 2 to 1) or to allow a substantial zone of intermixing (coal size to sand size of about 4 to 1).

There are two conflicting ideas concerning the desirable amount of intermixing. Some researchers feel there should be no mixing at the interface, with the sand acting as a polishing filter after the coal roughing filter. Others feel that intermixing results in a more uniform decrease in grain size with depth and allows more efficient use of the storage space in the media and, thus, longer filter runs. An intermixed bed is a closer approximation of the ideal coarse to fine filter bed and thereby eliminates an impervious layer that might build up at a sharp interface.

### Objectives and Scope of This Study

Because of the differences of opinion concerning the desirability of intermixing in a dual-media filter, this study was undertaken to show what effect, if any, the intermixing has on the performance of dual-media filters. Performance differences, if they exist, will be shown by measurements of head loss development and effluent quality versus time during filtration.

It must be kept in mind that this study was not meant to be a comparison of dual-media and single-media filtration nor a study to determine the optimum amount of intermixing; rather, it is meant to show how the media intermixing or non-intermixing in dual-media filtration affects performance.

## Experimental Investigation

### Apparatus and General Approach

The system used in this study consisted of three, 4-in. inside diameter plexiglass filter columns as shown in Fig. 99. In one column, the coal and sand were placed together and allowed to mix as they might. In two other columns, operated in series, identical coal and sand were placed separately. Two gradations of coal and sand media were used, one which resulted in a mixed interface, dual-media bed and one which resulted in a sharp interface dual media.

Prior to further detailed description of the experimental investigation some terms must be defined for clarity. The term "mixed interface media" refers to the media which exhibited intermixing of the anthracite and sand at the interface when both media were placed in column 1. The term "sharp interface media" refers to the media which exhibited no intermixing of the anthracite and sand at the interface when both were placed in column 1. The term "combined media" refers to the sand and anthracite media when placed together in column 1. The term "separate media" refers to the same amount and gradation of sand and anthracite placed in separate columns. The same anthracite as in column 1 was placed by itself in column 2. The same sand as in column 1 was placed by itself in column 3.

A filter run consisted of measuring the head loss buildup and effluent quality for the combined media and the head loss buildup and effluent quality for the separate media when the separate and combined media filters were operated concurrently. Comparisons between the results obtained with mixed and with sharp interface media in subsequent filter runs were then made to evaluate the effects of intermixing on filter performance.

The filters were operated as pressure type filters with the pump applying approximately 25 psig pressure to the top of filter column 1 and column 2 (Fig. 99). The suspensions of particulates were pumped from the supply to columns 1 and 2. From the separate coal (column 2), the water flowed to column 3, containing the separate sand. The filtered water coming from column 1 and column 3 flowed through a pressure regulator, a needle valve, a rotameter, and to waste.

Constant rate filtration was achieved by use of Fisher, type 95L pressure regulators (Fisher controls Company, Marshalltown, Iowa). These regulators were used to reduce any incoming pressure to a constant exit pressure of 4 psig. This constant 4 psig pressure leaving the regulator was applied to a fixed effluent needle valve to achieve a constant flow.

This system provided a reasonably constant flow, although slight variations in flow were observable on the effluent rotameter which

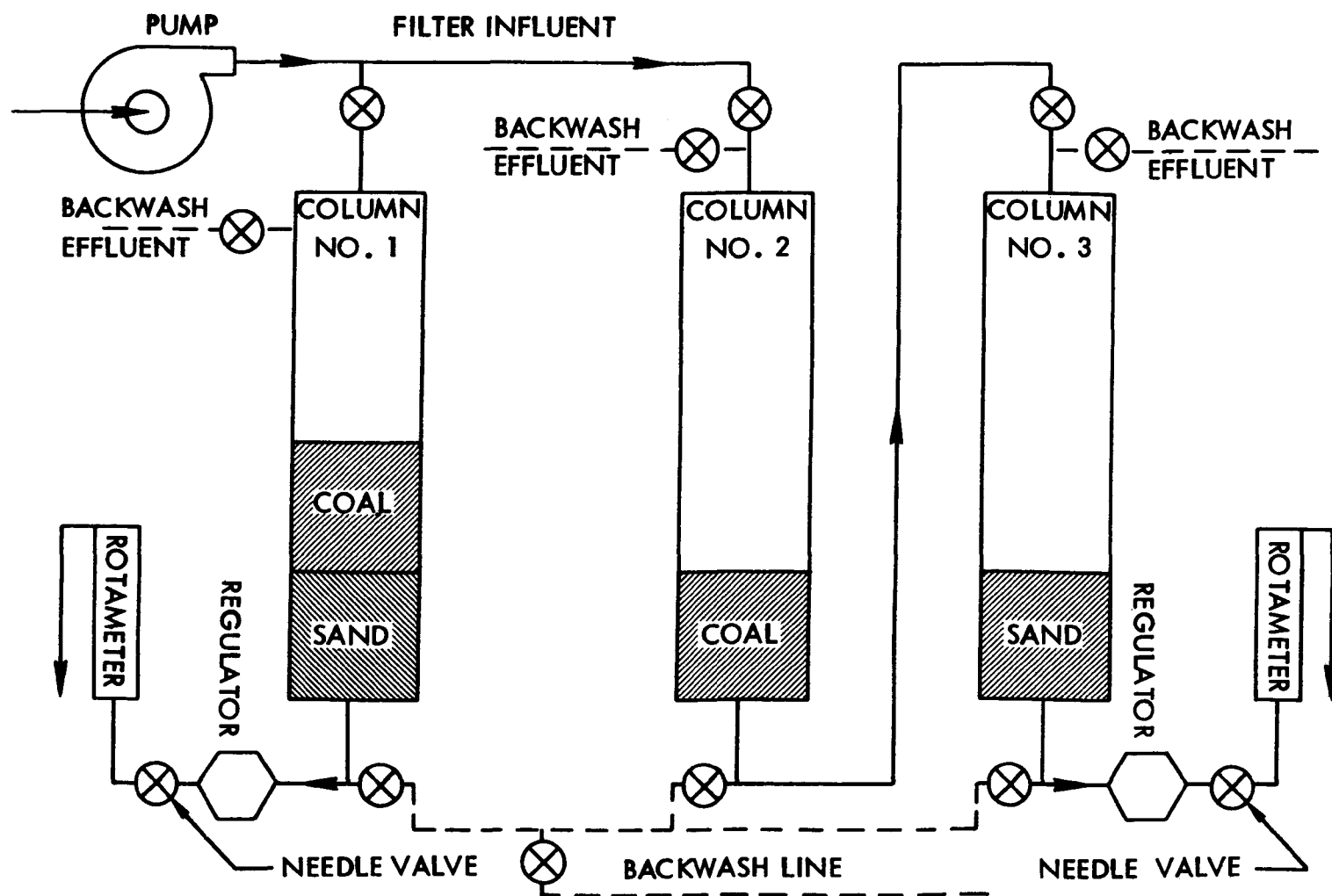


Fig. 99. Schematic diagram of apparatus.

had a full-scale capacity of 0.78 gpm. The rotameter discharged to waste.

Tap water at normal main pressure was used for backwash. The backwash system is shown in the plumbing diagram, Fig. 99.

Head loss buildup was measured using a multiple tube manometer containing four single leg manometers (Model 33KB35, Multiple Tube Manometer, Merian Instrument Division, The Scott and Fetzer Company, Cleveland, Ohio). A 1/4-in. OD copper tube was connected from the top of a filter housing to the bottom end of one manometer, while another 1/4-in. OD copper tube was connected from the bottom of a filter housing to the top end of the same manometer. The manometer operates on the principle of a U-tube with one leg of water and one leg of mercury.

Head loss buildup was observed by the differences in the readings of the mercury level at successive time intervals during a filter run. Initial head loss through each filter could not be readily measured, but head loss increase with time was readily and precisely observed.

Before and after every run, the filters were backwashed. The filters were expanded to 50% during the backwash and allowed to wash thoroughly. When a cake of solids formed on the surface of the media, air scour was sometimes used. After a thorough backwash, the backwash valve was closed rapidly. Then the bed was shocked momentarily by rapidly opening and closing the backwash valve several times in succession. This procedure was used to insure an equally dense bed for every filter run. The bed depth was recorded after every wash for each run and did not vary.

Because the patterns of head loss buildup and effluent quality were of more importance than absolute quality, the filters were operated at 7 gpm/sq ft. This high filtration rate was also selected to encourage deep penetration of some solids into the bed, hopefully through the interfacial region to allow the effects of the interface to be observed.

### Filter Media

Two different dual media were used for this study. One dual media was selected in order that intermixing would occur at the interface. The second dual media was selected in order to produce a sharp, well defined interface. The sharp interfaced dual media was intended to act as a control, to show what differences in head loss and filtrate quality could be attributed to the experimental apparatus and operation. However, the sharp interface media was not a control in the strict sense of the word, because the sharp interface media and the mixed interface media were not operated at the same time.

Any effects on head loss development and effluent quality produced by the method of operation or the equipment (presenting two surfaces to the flow, flowing through an underdrain and plumbing, etc.) had to be determined. The filtration with the sharp interface media was done to illustrate these effects. As there was no mixing of the media in column 1 (Fig. 99), there would be no effect of intermixing on the performance of the filter in column 1. There was obviously no intermixing between the coal in column 2 and the sand in column 3 and no effect due to intermixing. A comparison of the results of the combined media filtration with the separate media filtration using the sharp interface media would show what effect the operating procedure and equipment had on the results. This observation would then be useful in interpreting the data collected using the mixed interface media in subsequent filtration runs.

The dual media, selected to have a well intermixed interface, was similar to a media that is commonly specified for water treatment plant filters.

The coal was "Philterkol" from the Reading Anthracite Coal Company, Pottsville, Pennsylvania. The sand was from the Northern Gravel Company, Muscatine, Iowa. Fines from the coal and sand were skimmed from the media after hydraulic gradation of the media by backwashing. This was done because it was felt these fines might cause problems and because skimming is commonly practiced in filter plant construction.

The detailed skimming procedure was as follows. Approximately 30 in. of sand or coal was placed in the plexiglass column. The media was fluidized to approximately 50% expansion and allowed to stabilize. The backwash valve was closed rapidly, and the media was allowed to subside. The top inch or so was skimmed off by a siphon. The procedure was repeated until 10 to 20% of the finer media was removed. The media was then removed from the column and dried in an oven. A sieve analysis was run on the skimmed coal and sand. The effective sizes and uniformity coefficients of the skimmed media were as follows:

Sharp interface media	
sand	ES = 0.85 mm
	UC = 1.29
coal	ES = 0.91 mm
	UC = 1.45
Mixed interface media	
sand	ES = 0.46 mm
	UC = 1.49
coal	ES = 0.92 mm
	UC = 1.60

The size ratio at the interface is the most important factor determining the amount of intermixing of coal and sand. In this study,

the 99% finer size by weight ( $d_{99\%}$ ) was used to approximate the coarsest size coal, and the  $d_{1\%}$  size was used to approximate the finest sand. The size ratio at the mixed interface was 5.34. The size ratio at the sharp interface was 2.32. The size ratios based on the  $d_{90\%}$  for the coal and the  $d_{10\%}$  for the sand were 4.05 for the mixed interface media and 1.93 for the sharp interface media.

The specific gravity of "Philterkol" ranged from 1.65 to 1.7 on various shipments whereas the sand has consistently been 2.65.

#### Source of Suspensions

Several different suspensions of particulates commonly encountered in filtration were filtered in an attempt to ascertain what effect, if any, intermixing of the media in dual-media filtration has on filter performance. It was felt that different types of suspensions might have different transport and attachment mechanisms for the removal of solids, and the effect of intermixing for various typical filtration situations might be different.

Five different suspensions were filtered. They were an iron floc, lime-soda ash softening precipitate, aluminum sulfate coagulated and settled trickling filter effluent, activated sludge settled effluent, and trickling filter settled effluent.

Iron floc. Ferrous sulfate was mixed with Iowa State University tap water to prepare an influent suspension containing precipitated iron floc for the filtration study. A stock feed solution of 0.2 M ferrous sulfate in an acid solution of approximately 0.1 N HCL was made up in sufficient quantity to fill a 20-liter feed bottle.

To achieve a mixing tank effluent of 9 to 9.5 mg/l of iron. 17.4 ml/min of the stock ferrous sulfate solution was fed into 5.76 gpm of tap water. The iron solution was dripped from a constant head capillary feeder into a mixing tank to achieve the desired iron concentration. The iron solution was mixed by a paddle mixer in the reaction tank.

The type of precipitate formed by the addition of ferrous sulfate to water depends on the pH, alkalinity, and temperature of the water and upon the time allowed for reaction. It may consist of  $\text{Fe}(\text{OH})_3$ ,  $\text{FeCO}_3$ , or  $\text{Fe}(\text{OH})_2$ . In this research, air was not used in mixing, and the mixing time was short, about 27 min. Because of the hard alkaline nature of the tap water and the conditions of mixing, one would expect the precipitate to be mainly  $\text{FeCO}_3$ ; however, the exact nature was not determined.

Trickling filter effluent. Final effluent from the Ames Water Pollution Control Plant was filtered. The Ames sewage treatment plant consists of comminutors, pumping, aerated grit chambers, primary

settling, and standard rate trickling filters followed by final clarifiers.

Secondary effluent from the final clarifiers was pumped from the final collection chamber to the filters. Most of this filtration of trickling filter effluent was done during the month of July 1973. The raw wastewater during July averaged 130 mg/l BOD<sub>5</sub>, 161 mg/l suspended solids, and 337 mg/l COD. The secondary effluent for July averaged 16 mg/l BOD<sub>5</sub>, 20 mg/l suspended solids, and 68 mg/l COD.

Aluminum sulfate coagulated trickling filter effluent. A pilot plant was in operation at the Ames Water Pollution Control Plant that was using alum to coagulate and flocculate secondary effluent for phosphorous removal. The secondary effluent was pumped to an erdlator (upflow solids contact unit) where approximately 200 mg/l of alum were added for precipitation of the phosphorous.

Average performance for the effluent from the erdlator during the summer of 1973 was as follows [118]:

	<u>Influent</u>	<u>Effluent</u>
Average suspended solids (mg/l)	25.4	10.32
Average turbidity (units)	10.9	2.35
Average BOD <sub>5</sub> (mg/l)	38.6	10.80
Average TOC (mg/l)	14.0	7.59
Average total PO <sub>4</sub> (mg/l)	19.3	3.91
Average ortho PO <sub>4</sub> (mg/l)	18.7	2.39
Average total Kjeldahl N (mg/l)	4.9	4.93

The settled effluent described above was used as the filter influent for this study.

Activated sludge effluent. An activated sludge pilot plant was operated so as to produce an effluent to filter. The pilot plant was a Smith and Loveless "Oxigest" (Smith and Loveless Model "C" Oxigest, Smith and Loveless, Division-Union Tank Car Company, Lenexa, Kansas) unit located at the Ames Water Pollution Control Plant. The aeration tank volume is 2000 gal., and the settling tank volume is 672 gal.

The "Oxigest" unit was operated at a constant rate of 5 gpm. This gave a detention time of 6.67 hr. The influent to the unit was primary effluent from the Ames Water Pollution Control Plant. The average characteristics of influent to the "Oxigest" for the month of July 1973 were 82 mg/l of 5 day BOD, 65 mg/l suspended solids, and 204 mg/l COD. Typical characteristics of effluent from the "Oxigest" unit were 5 to 15 mg/l BOD<sub>5</sub> and 9 to 10 mg/l suspended solids. The mixed liquor suspended solids was maintained at around 2400 mg/l. Effluent from this activated sludge pilot plant was pumped from the effluent trough to the filters.

Lime-soda ash softening precipitate. The water for the City of Ames comes from ground water. This water is softened in a modified, split treatment, lime-soda ash system. The water from wells is aerated, slaked lime is added and mixed, and without intermediate settling, the split flow and soda ash are added and mixed to precipitate additional hardness. The water is then allowed to settle, and some of the sludge formed from the settling precipitants is returned to aid in the precipitation reactions in the mixing step. After settling, approximately 2 mg/l of polyphosphate is added to stabilize the water and stop the reaction of chemical precipitation so that further precipitate will not form on the filter media, piping, or in the clear wells. Chlorine and fluoride are also added.

The pilot filter plant was placed in the pipe gallery at the Ames plant, and water was taken out of the influent pipe leading to one of the city filters. The average turbidity of the influent during this study was 6.4 FTU, with a range of 4.3 to 12 FTU. The turbidity is due mostly to presence of calcium carbonate particles.

#### Sampling and Measurement

Filter performance was monitored by observing head loss development and filter influent and effluent quality. Head loss was measured, as previously discussed, by head loss buildup using mercury manometers. Quality was measured by periodically collecting a grab sample and analyzing it. The period between samples varied with the rate of head loss buildup. If head loss increased rapidly, the interval between samples was decreased. Samples were collected every 20 min for iron filtration and up to every 3 hr for softening precipitate filtration.

The quality of the influent and effluent was measured in various ways. For the iron filtration series, the total iron in the sample was measured. For the softening precipitate, trickling filter effluent, activated sludge effluent, and the alum flocculated secondary effluent, turbidity was used as one measure of quality. Since suspended solids are frequently specified as an effluent quality parameter for sewage treatment plants, grab samples were taken and composited over several time intervals for suspended solids analysis. When an adequate amount of sample had been collected, a suspended solids analysis was done. Researchers have found that, within limits, suspended solids concentrations found in treated wastewater can be roughly correlated to turbidity measurements [59,128]. Nevertheless, suspended solids analyses were also run in this study because it was felt that the turbidity measurement might not measure the larger particles in the filter influent and effluent. For each of the treated wastewaters filtered, after the suspended solids were filtered from the sample, a sample of the filtrate was taken and the turbidity determined. This result was considered to be background color or colloidal material.

Iron measurement. Iron was measured using 1,10 phenanthroline. This method is a spectrophotometric method in which the complex formed with the ferrous iron produces an orange-red color that obeys Beer's law. The method was developed so that the analysis of iron samples could be automated by using the Technicon Auto Analyzer II (Technicon Industrial Systems, A division of Technicon Instruments Corporation, Tarrytown, New York). Forty samples could be analyzed per hour. After the sample was taken, a few drops of hydrochloric acid and some hydroxylamine hydrochloride were added to reduce the ferric iron to ferrous iron and to acidify the mixture to keep the iron in solution. By doing this, the samples were preserved for later analysis on the automatic analyzer.

Turbidity measurement. Various turbidimeters were used to determine turbidity for this study. As the quality differences are based on the relative turbidity in the filter influent and filtrate, the effect of using different machines was negligible. The instruments used were all manufactured by Hach (Hach Chemical Company, Ames, Iowa) and included the Model 2100 and Model 2100A laboratory turbidimeters, the "Surface Scatter 3," and the Low Range Turbidimeter, model 7120. The latter two instruments are continuous flow and reading turbidimeters. All the turbidimeters were calibrated against prepared standards of formazin polymer, prepared by Hach. The unit of turbidity measurement was the Formazin Turbidity Unit (FTU).

The continuous flow turbidimeters were checked against the laboratory turbidimeters. Very close agreement was found. The continuous flow turbidimeters were used to measure the influent to the filters when filtering trickling filter effluent, the alum floc, and the softening precipitate. The effluent from the filters was monitored by grab samples analyzed on the laboratory turbidimeters.

Suspended solids measurement. The procedure adopted for the determination of total suspended matter was a slight modification of the procedure given in Standard Methods [117]. Whatman GF/C glass fiber filter paper was used. The filter disks were not prewashed and dried, as it was known from prior experience with this type of paper that the effect of not washing would be negligible.

## Results

### Quality and Head Loss

In this empirical study, filter performance was measured by head loss buildup and effluent quality.

The head loss buildup was measured in inches of mercury. Quality was measured by various parameters, as previously described. The effluent concentration divided by the influent concentration,  $C/C_0$ , was then calculated. Both head loss buildup and  $C/C_0$  were plotted against the total volume of filtrate. Total volume of filtrate

during a filter run was determined by taking the flow rate, multiplying it by the time, and summing to yield the total volume of filtered water. Total volume of filtrate was used to attempt to eliminate the influence of any small difference in flow rate that existed between the filters during a filter run.

As previously described, five different suspensions were filtered by two different dual media; thus there were ten series of filter runs. The series are identified in Table 49. Several filter runs were made in each series so that a consistent trend in the data was observed. Some conditioning runs were undertaken at the beginning of each series in which the suspension was filtered without close control to acclimate the filter media to the suspension.

Table 49. Identification of experimental series.

Series	Dual media used	Suspension filtered
I S	Sharp interface	Iron floc
I M	Mixed interface	Iron floc
II S	Sharp interface	Activated sludge effluent
II M	Mixed interface	Activated sludge effluent
III S	Sharp interface	Alum coagulated trickling filter eff
III M	Mixed interface	Alum coagulated trickling filter eff
IV S	Sharp interface	Trickling filter effluent
IV M	Mixed interface	Trickling filter effluent
V S	Sharp interface	Lime-soda ash softening ppt
V M	Mixed interface	Lime-soda ash softening ppt

A typical plot of head loss buildup versus volume of filtrate and  $C/C_0$  versus volume of filtrate for each series is presented in Figs. 100 through 109.

There are three different parameters presented in the graphs of head loss versus volume of filtrate. They are (1) the head loss buildup in the combined media (that media which was in column 1, Fig. 99) labeled "COMBINED TOTAL HL," (2) the head loss buildup in the separate coal (that media which was in column 2, Fig. 99) labeled "SEPARATE COAL HL," and (3) the sum of the head loss buildup in the separate coal and separate sand (that media which was in column 2

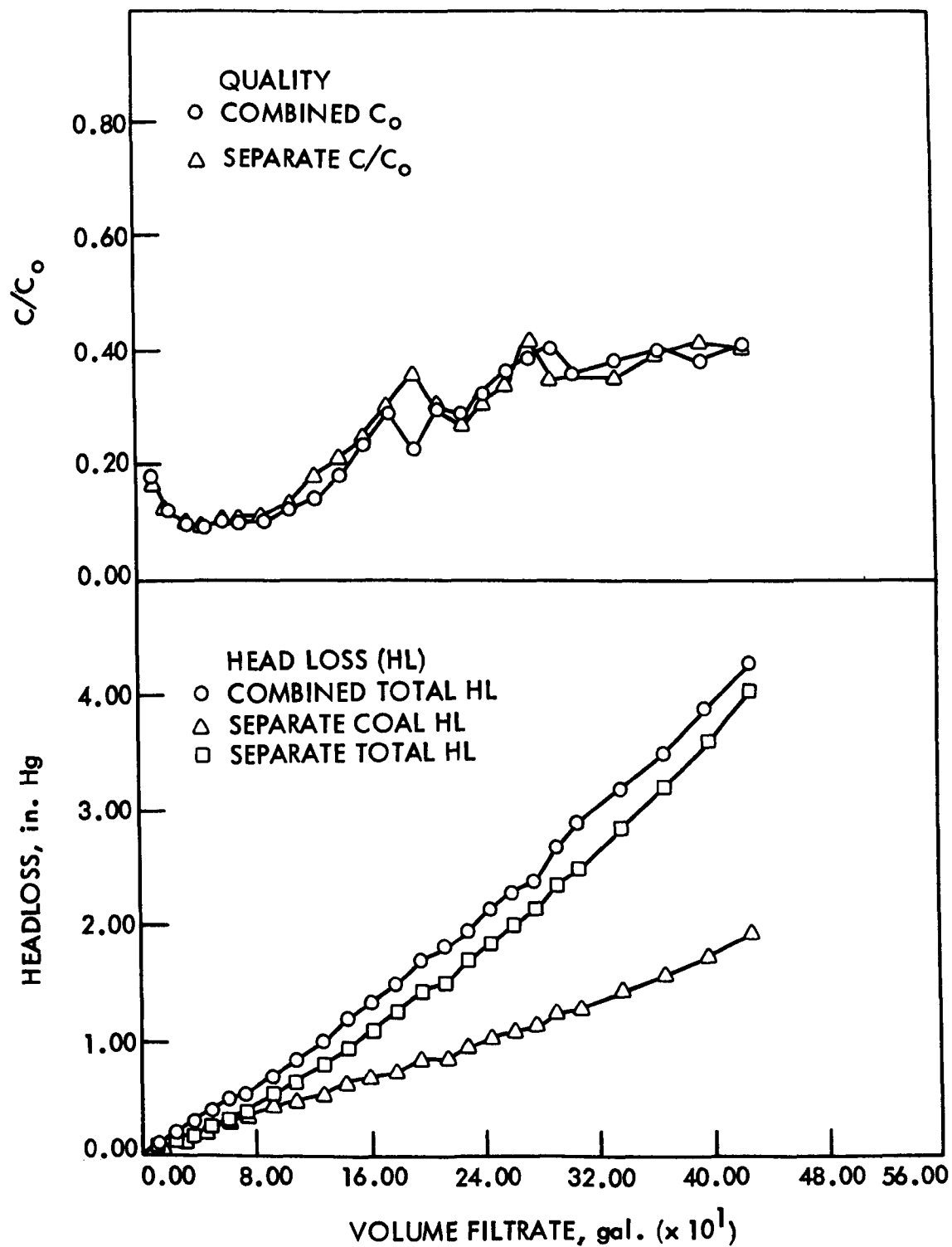


Fig. 100. Head loss and filtrate quality vs volume of filtrate, Series I S, run 2, sharp interface, filtration of iron with  $C_0 = 8.68$  to  $9.64$  mg/l Fe, Avg  $9.07$  mg/l.

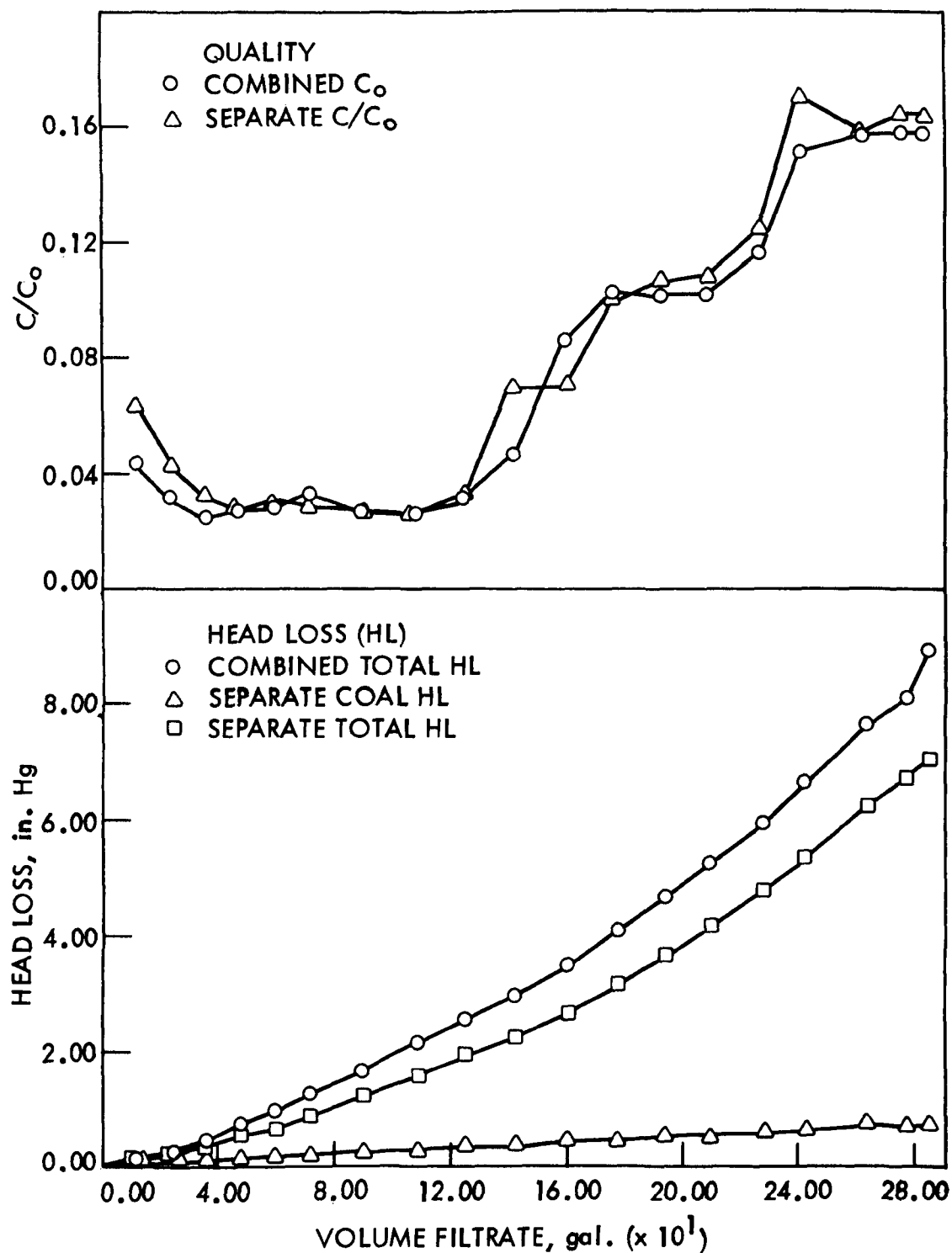


Fig. 101. Head loss and filtrate quality vs volume of filtrate, Series I M, run 11, mixed interface, filtration of iron with  $C_0 = 9.2$  to  $9.7$  mg/l Fe, Avg  $9.42$  mg/l.

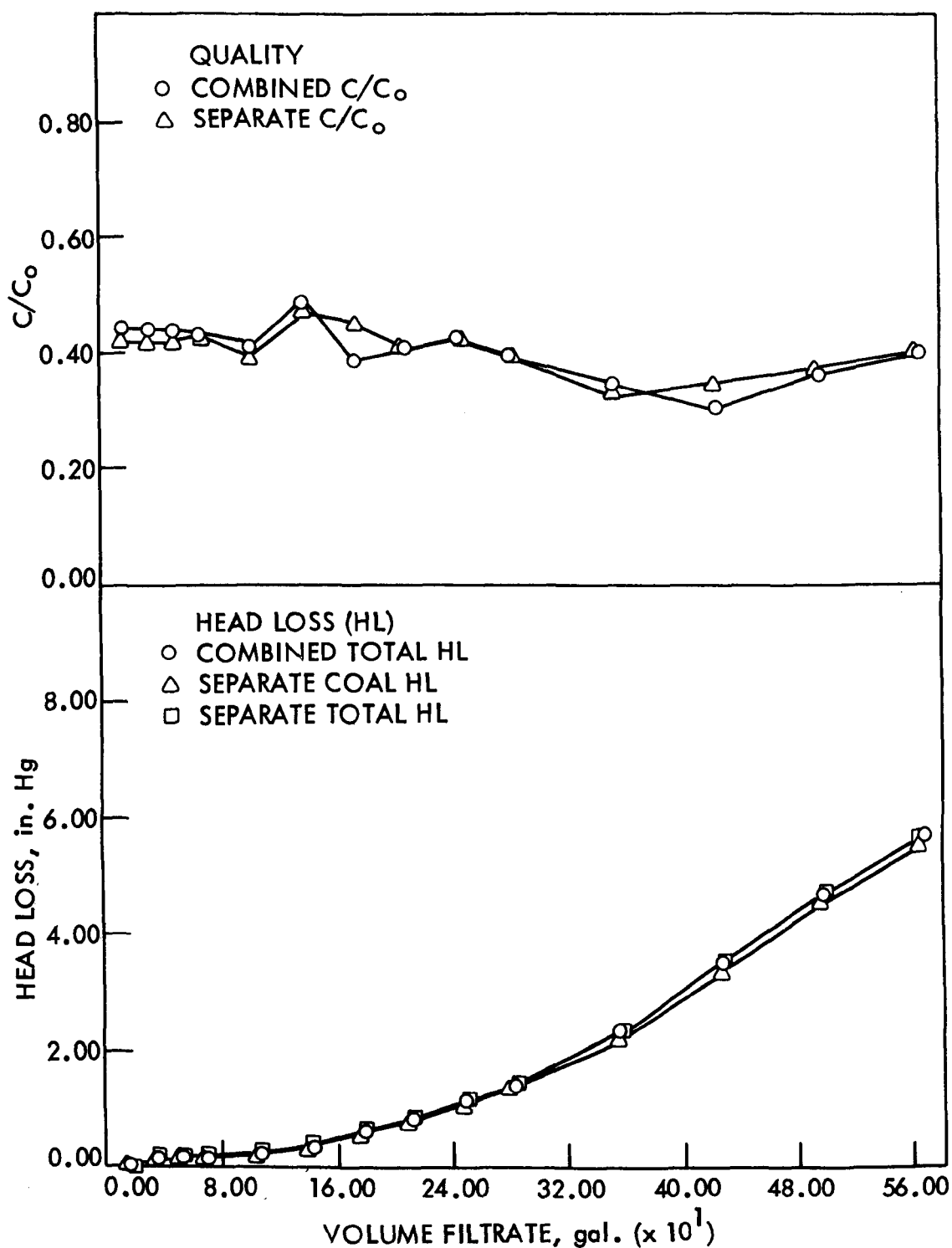


Fig. 102. Head Loss and filtrate quality vs volume of filtrate, Series II S, run 1, sharp interface, filtration of activated sludge effluent with  $C_0 = 4.5$  to  $8.5$  FTU, Avg  $6.16$  FTU.

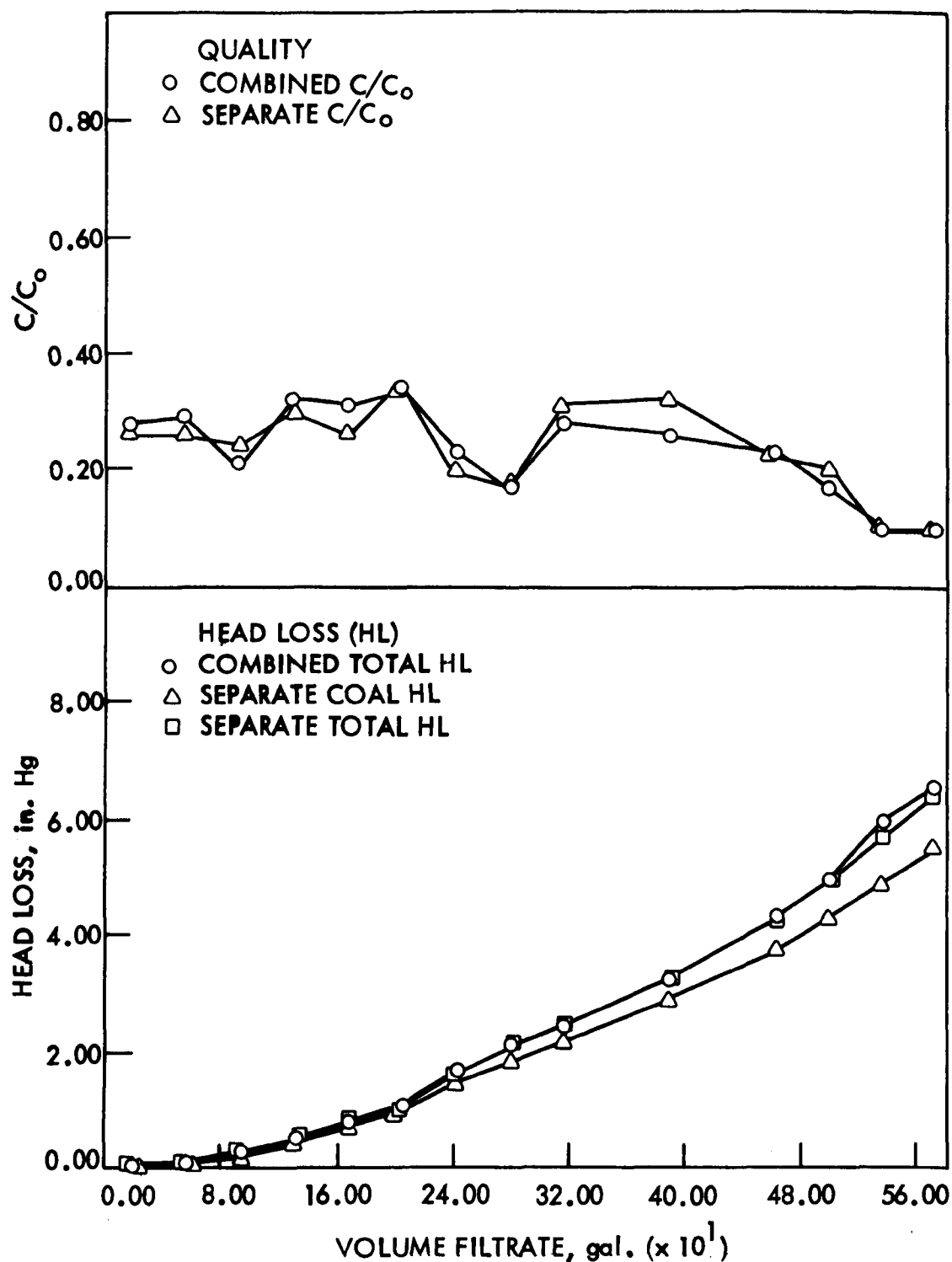


Fig. 103. Head loss and filtrate quality vs volume of filtrate, Series II M, run 1, mixed interface, filtration of activated sludge effluent with  $C_0 = 2.6$  to  $8.6$  FTU, Avg  $4.15$  FTU.

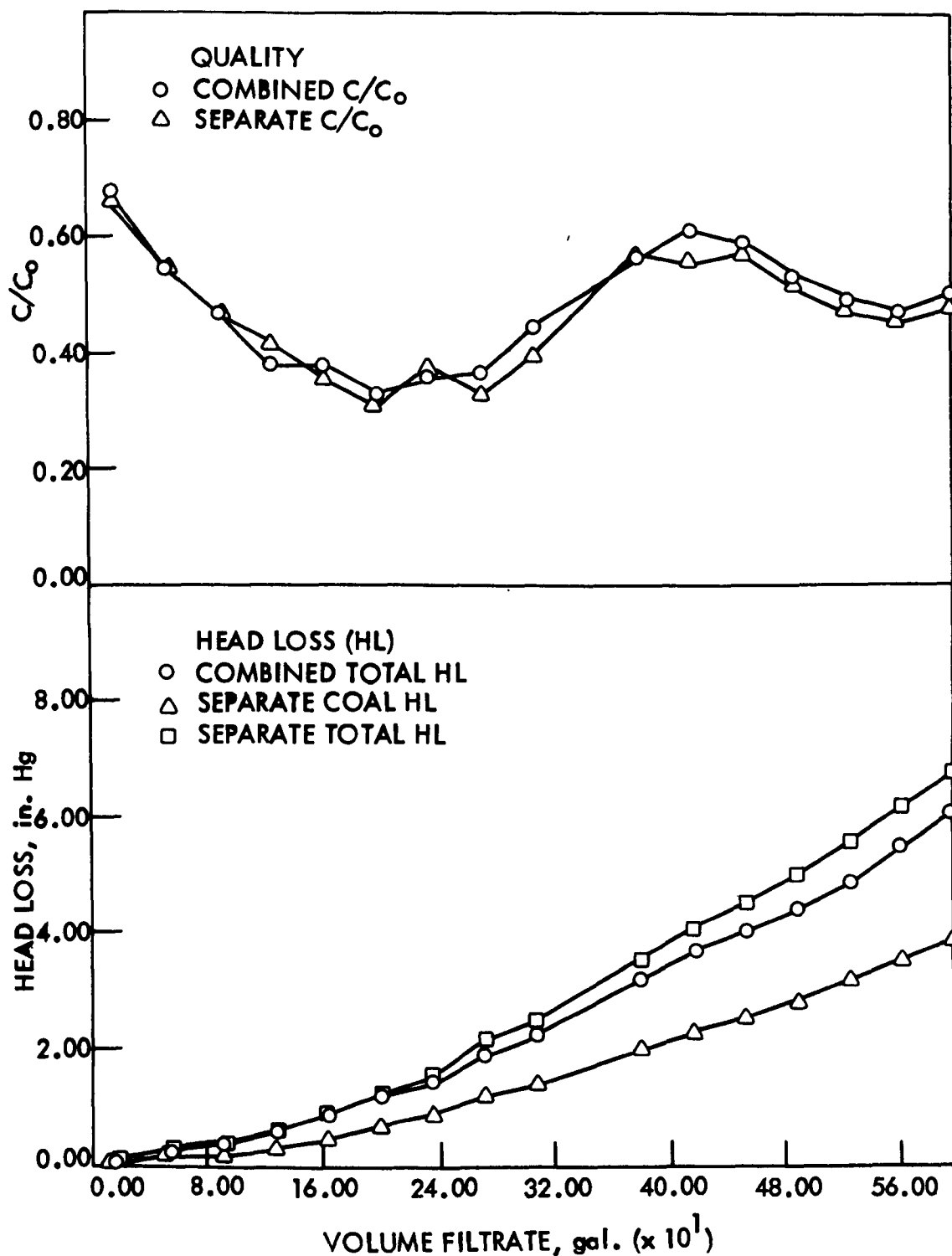


Fig. 104. Head loss and filtrate quality vs volume of filtrate, Series III S, run 3, sharp interface, filtration of alum coagulated trickling filter effluent with  $C_0 = 3.8$  to 10 FTU, Avg 5.21 FTU.

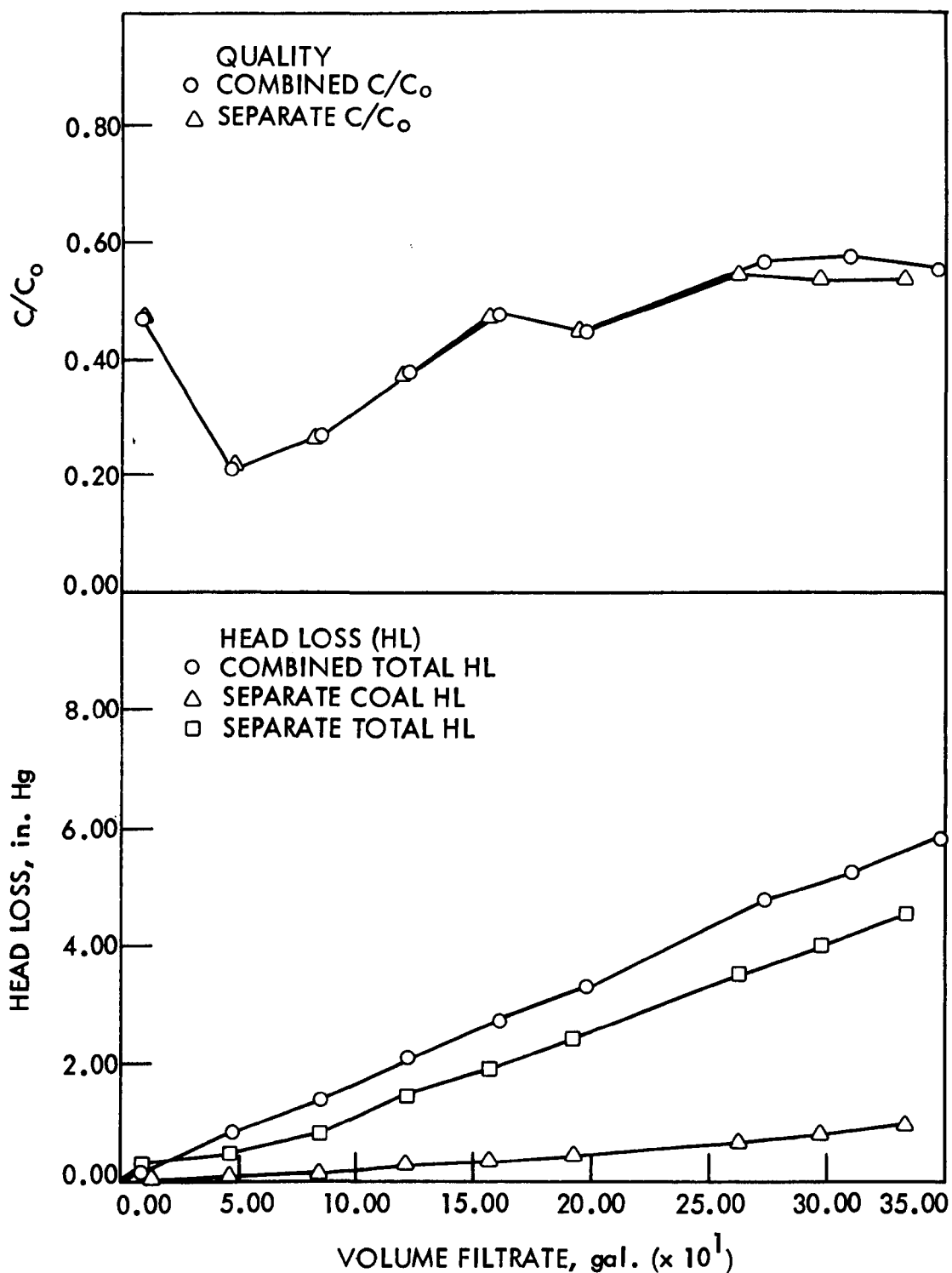


Fig. 105. Head loss and filtrate quality vs volume of filtrate, Series III M, run 5, mixed interface, filtration of alum coagulated trickling filter effluent with  $C_0 = 1.7$  to 6.2 FTU, Avg 2.95 FTU.

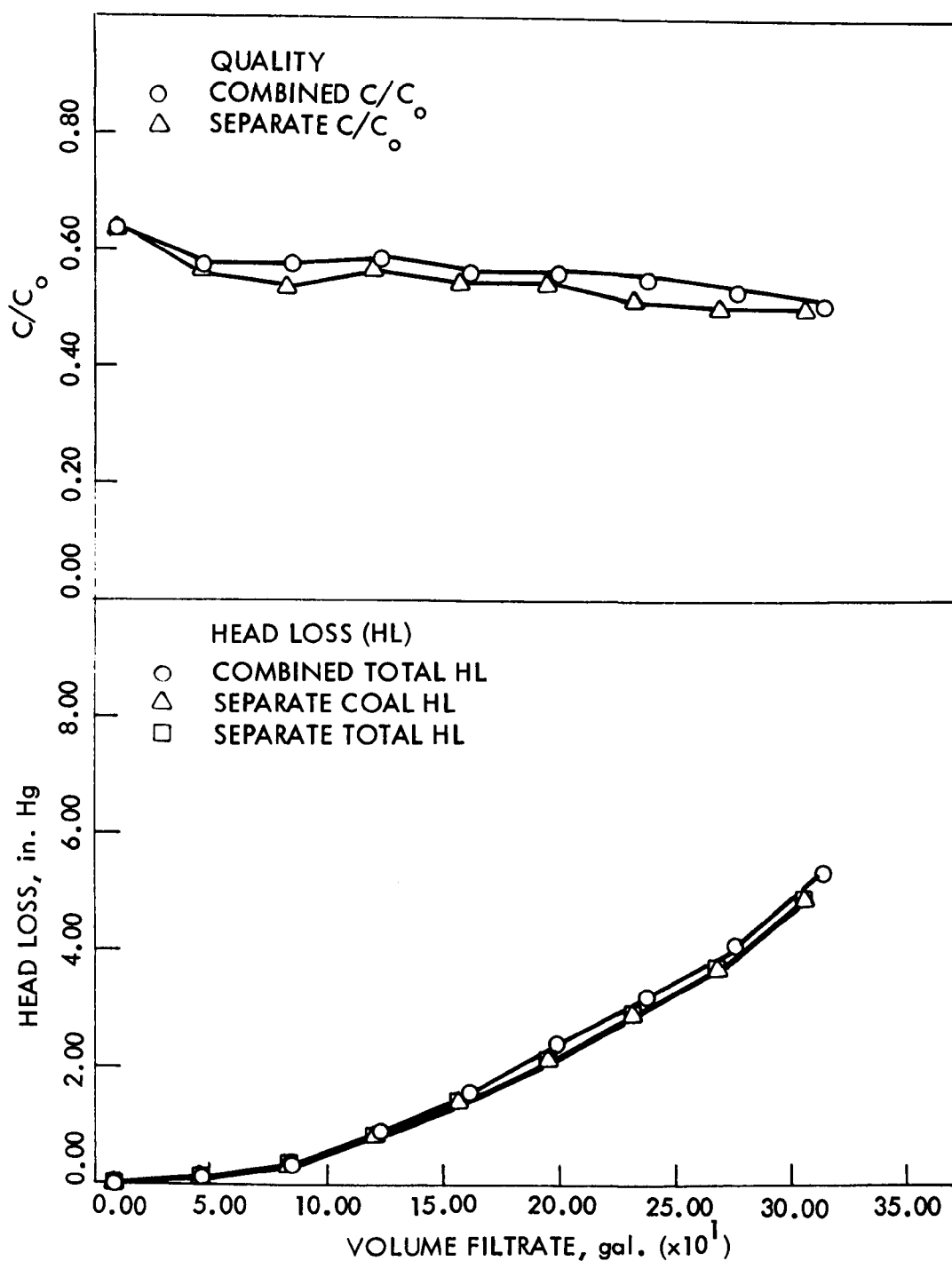


Fig. 106. Head loss and filtrate quality vs volume of filtrate, Series IV S, run 3, sharp interface, filtration of trickling filter effluent with  $C_0 = 4.7$  to 8.5 FTU, Avg 6.29 FTU.

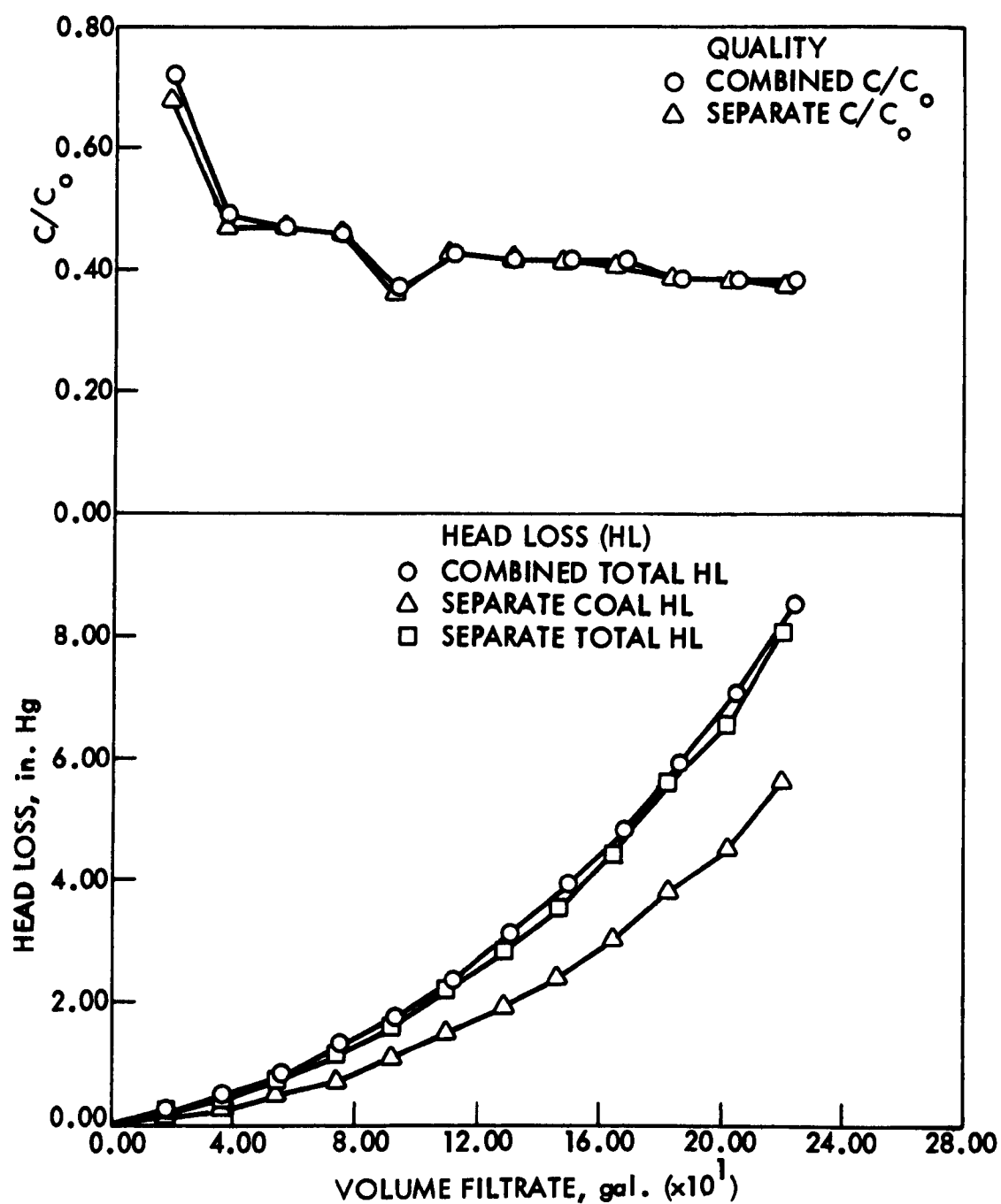


Fig. 107. Head loss and filtrate quality vs volume of filtrate, Series IV M, run 3, mixed interface, filtration of trickling filter effluent with  $C_0 = 12$  to 15 FTU, Avg 6.14 FTU.

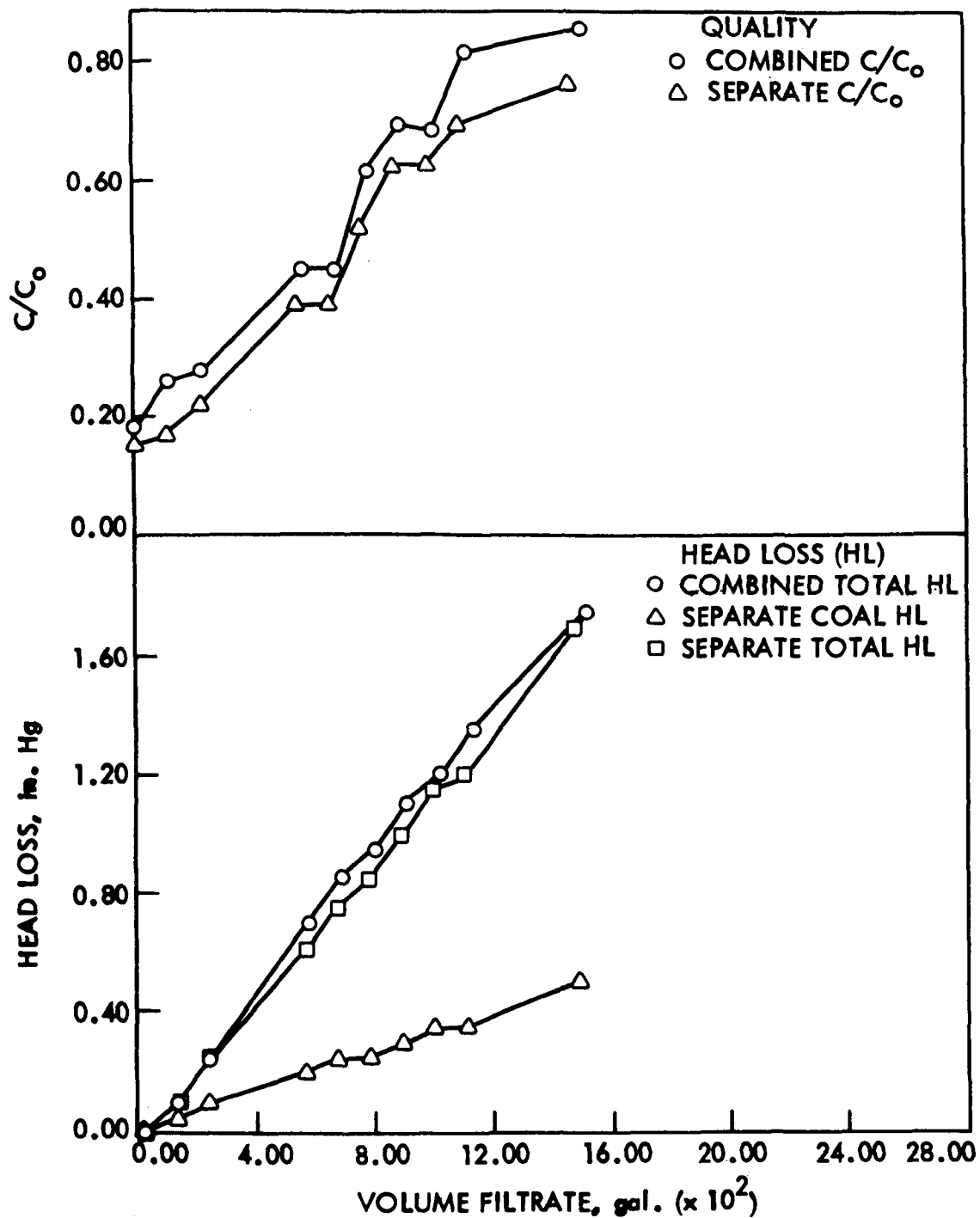


Fig. 108. Head loss and filtrate quality vs volume of filtrate, Series V S, run 4, sharp interface, filtration of lime-soda ash softening precipitate with  $C_0 = 5.6$  to  $6.5$  FTU, Avg  $6.14$  FTU.

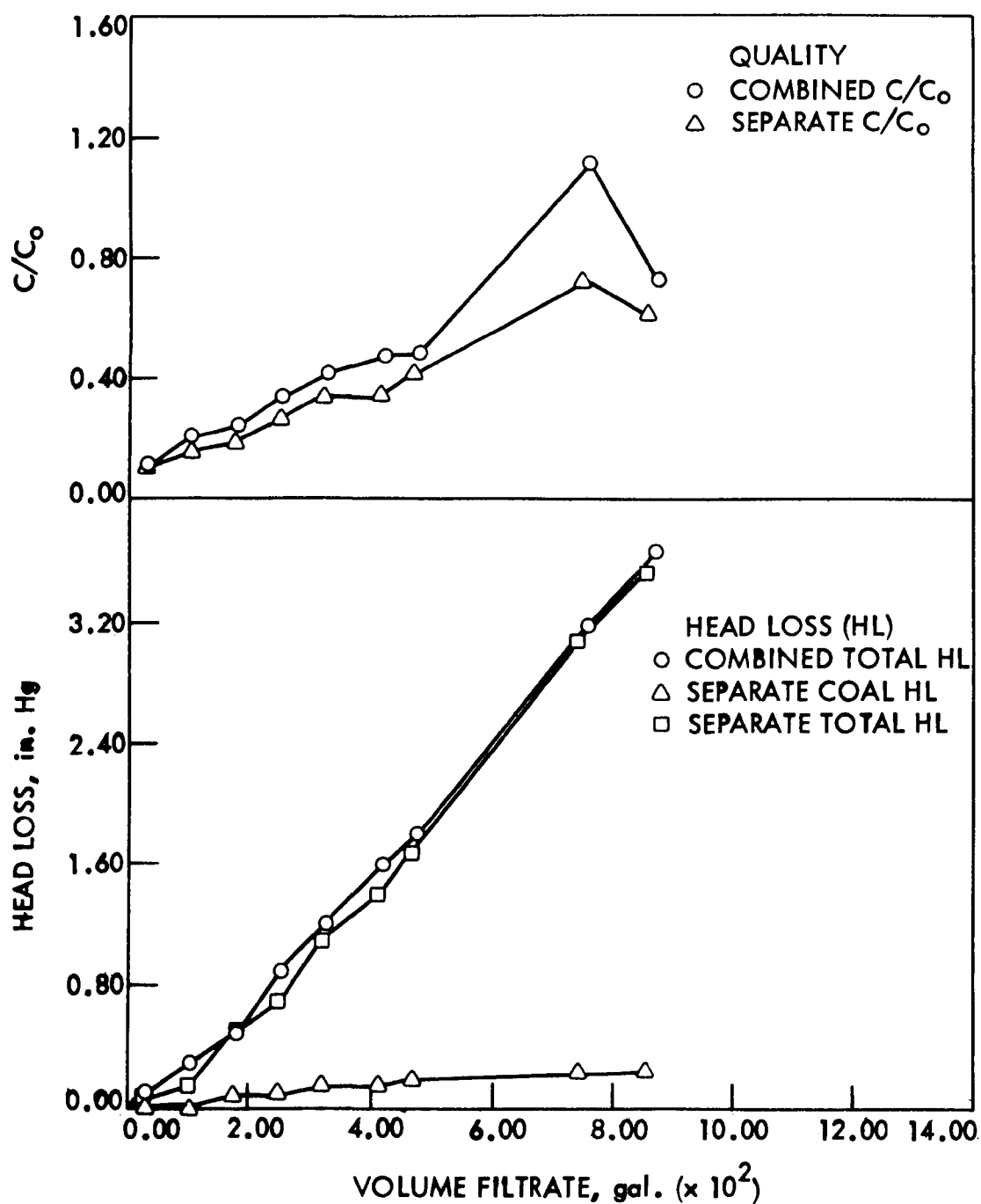


Fig. 109. Head loss and filtrate quality vs volume of filtrate, series V M, run 3, mixed interface, filtration of lime-soda ash softening precipitate with  $C_0 = 6.8$  to  $8.3$  FTU, Avg  $7.5$  FTU.

and column 3, Fig. 99, respectively) labeled "SEPARATE TOTAL HL."

The graphs of  $C/C_0$  versus volume of filtrate compare the effluent from the combined media (column 1, Fig. 99) labeled "COMBINED  $C/C_0$ " to the effluent from the separate media (the effluent from column 3, Fig. 99) labeled "SEPARATE  $C/C_0$ ."

### Suspended Solids

Suspended solids tests were run on the three treated wastewater streams, both influent to and effluent from the filters. The range of values and the average value for the influent, combined media effluent, and the separate media effluent are given in Table 50 for all suspended solids data from the indicated series.

Table 50. Influent and effluent suspended solids data, average and range, for wastewater series.

Influent suspension	Series no.		Influent, mg/l	Combined eff, mg/l	Separate eff, mg/l
Activated sludge effluent	II S	Range	4.8-8.0	0.9-2.6	0.9-2.3
		Avg	6.0	1.38	1.26
	II M	Range	3.8-14.6	0.3-1.2	0.2-1.2
		Avg	9.53	0.60	0.61
-----					
Alum coag TF effluent	III S	Range	5.0-10.2	1.0-3.9	1.0-3.2
		Avg	8.05	2.05	1.91
	III M	Range	5.6-11.2	0.5-2.9	0.4-2.8
		Avg	7.61	1.49	1.36
-----					
Trickling filter effluent	IV S	Range	10.0-30.8	3.0-9.6	3.0-9.0
		Avg	19.37	5.50	5.57
	IV M	Range	18.0-34.8	1.9-6.2	2.0-6.2
		Avg	23.30	4.48	4.13

### Background Turbidity

The background turbidity (turbidity of filtrate remaining from the suspended solids tests) of the three treated wastewater streams was determined. The average values of the background turbidity are given in Table 51. From the data presented, it can be seen that the background turbidity was affected very little by filtration (the background turbidity of the influents was approximately equal to the

Table 51. Average values of background (bg) turbidity for the treated wastewaters.

Influent suspension	Influent bg turbidity, FTU	Combined eff bg turbidity, FTU	Separate eff bg turbidity, FTU
Activated sludge	0.56	0.59	0.59
Alum coagulated TF effluent	0.53	0.59	0.58
Trickling filter effluent	1.60	1.70	1.80

background of the effluents). It may also be noted that the background turbidity was a significant percentage of each total effluent turbidity for these treated wastewater streams. Furthermore, this colloidal background matter is not measured by the suspended solids analysis.

#### Discussion

The results presented in Figs. 100 through 109 are summarized in Table 52. Where there was no difference or only a slight difference, "no difference" is indicated. Where the separate media had a better performance (i.e., lower head loss buildup or better filtered water quality), "separate better" is indicated. In the series where the combined media had a better performance, "combined better" is indicated. In Series II S and Series IV S, no comparison could be made, as will be explained later; therefore, "no comparison" is indicated.

Table 52. Summary of results comparing filter performance for sharp and mixed interface media.

Series	Filtering	Interface	Head loss	Quality
I S	Fe	Sharp	Separate better	No difference
I M	Fe	Mixed	Separate better	No difference
II S	AS	Sharp	No comparison	No comparison
II M	AS	Mixed	No difference	No difference
III S	Alum	Sharp	Combined better	No difference
III M	Alum	Mixed	Separate better	No difference
IV S	TF	Sharp	No comparison	No comparison
IV M	TF	Mixed	Separate better	No difference
V S	Soft	Sharp	No difference	Separate better
V M	Soft	Mixed	No difference	Separate better

The sharp interface media was used as a control to establish what differences in performance could be attributed to the equipment and operating procedure. Thus, if the sharp interface media presented a significant trend in one direction and the mixed interface media demonstrated the same trend in greater magnitude or the opposite trend this difference could be attributed to the mixing of the media at the interface.

Upon examination of the data and plots for the filtration of the iron floc, it can be seen that there is no difference in the quality that can be attributed to media mixing at the interface. The head loss data and plots reveal that the mixing at the interface resulted in slightly larger head loss.

No valid conclusions can be drawn from the filtration of the activated sludge effluent or the trickling filter effluent. This is because all the removal was in the coal during sharp interface filtration. Thus, the control offered by the sharp interface data was lost, and the effect of the equipment and operating procedure was not known.

The data and plots for the filtration of the alum coagulated trickling filter effluent by the sharp interface media showed the equipment and operating differences caused the combined media to have less head loss buildup than the separate media. However, the data and plots of the filtration of this suspension by the mixed interface dual media show that the separate media have less head loss buildup. Thus, the effect of the intermixing at the interface was a detrimental one because there was a greater head loss in the combined mixed interface media. This greater head loss is attributable to the intermixing. The quality data and plots could show no difference in quality attributed to intermixing.

The filtration data for the lime-soda ash softening precipitate revealed no difference in head loss buildup between the combined and separate media for both the mixed and sharp interface dual media. The quality data and plots for the sharp interface media showed that the separate media had a better effluent. This observed difference can be attributed to the equipment and operating procedure. The quality data and plots for the mixed interface media showed that the separate media also produced a better quality effluent. Since both the sharp and mixed interface media had the same trend, no difference in quality can be attributed to the mixing of the dual media at the interface. A visual observation of the upper surface of the separate sand revealed a layer of white precipitate. This blanket of precipitate on the upper surface of the separate sand in both the sharp and mixed interface media may have acted like a filter itself, thereby improving the effluent quality from the separate media.

From the results, it can be seen that the mixing of the dual media at the interface causes little or no effect on either head loss buildup or effluent quality of a dual-media filter. Some slight increase in head loss buildup may be attributed to media mixing at the interface for some suspended solids, but this is not true of all solids, and the magnitude is slight.

Filtrate quality as measured by turbidity or iron concentration showed no benefit or detriment due to intermixing. The suspended solids data in Table 50 also show no apparent effect of the media intermixing at the interface.

A point must be made concerning the effluent quality. As can be seen from the data, all of the suspended material was not completely removed ( $C/C_0$  greater than zero). Thus, some of the suspended matter must have reached the interface if some passed through the entire dual-media filter. In the case of Series II S and IV S, little of the suspended matter that reached the interface or the sand was retained due to the size of the sand.

It would be of interest to compare these observations with theoretical models of filter performance. However, it is difficult to draw firm conclusions because the models have been derived and verified only for single-media filters. Nevertheless, an attempt will be made to apply filtration theory to support the observations. Boyd and Ghosh [18] recently summarized the various models for filtrate quality. They restated the now commonly accepted idea that removal of suspended solids by a granular filter involves a transport step and an attachment step.

All of the parameters in the various models for both transport and attachment are properties of the particles in suspension or the carrying fluid except for the diameter of the filter grains. Two of the transport models, namely, interception and Brownian diffusion, indicate that removal effectiveness is an inverse function of grain diameter. Therefore, one would expect better filter efficiency with finer grain size, if all other parameters were unchanged.

Most models for prediction of head loss in granular media filtration formulate head loss to be a function of solids capture [64,84]. Thus if the solids capture is the same for the combined or separate media, the total head loss would be expected to be about the same.

The models do not deal with the effect of grain diameter in the intermixed zone on the efficiency of a dual-media filter. If the same grains are present they should yield the same removal efficiency whether they are intermixed in a dual-media bed, or operated separately in series. This idea would support the experimental results reported herein which showed no difference between the filtrate for the combined and separate media. However, it is probable that the grain diameter in the models is really important as an indirect

measure of the size and shape of the void spaces in the filter bed. When the small sand grains move up into the coarser coal layers, they tend to fill the larger voids of the coal, causing a pore size and permeability between that associated with the sand and the coal as shown previously in Chapter X. Similarly, the coal grains that subside into the upper sand layer create a pore size and permeability between the sand and coal. Intermixing resulted in a total bed depth slightly less than the sum of the depths of the two media, measured individually in this work. A similar observation had also been reported previously in Chapter X. Since the overall depth of the dual-media bed is less, it would have a lower clean bed porosity and permeability in the intermixed zone. Because of this, one would expect better filtrate quality but higher head loss from the combined media than the separate media. The higher head loss for the combined media was observed for three of the solids reported herein, but the better quality was not observed.

Substantial differences in performance were observed between the sharp and mixed interface media. These differences would be expected from the foregoing theories. The mixed interface media produced a better filtrate quality than the sharp interface media, but also generated higher head loss. Substantially the same size coal was used in the two media, but a much finer sand was used in the mixed interface media than in the sharp interface media. From the theory presented, the finer sand should result in more efficient solids removal, which in turn would generate more head loss. These media sizes were purposely selected to achieve the desired degree of interfacial intermixing or separation. The coarse sand in the sharp interface media was required to produce a sharp interface with the expectation that it would cause poorer solids capture and lower head loss.

The degree of interfacial intermixing is dependent on the size, density, and shape of adjacent media, as well as the backwash flow velocity and valve shut-off procedure as shown previously in this report in Chapter X. If a normal coal size and gradation are selected, one cannot achieve a sharp interface except by sacrificing expected filtrate quality.

The controversy as to the desirability or detriment of interfacial intermixing was started by Conley [32] and Camp [23]. Camp [23,24] stated that he felt a sharp interface acts as a safeguard against breakthrough. He discouraged intermixing. Ives [63] and Gregory [54] have also implied that one should discourage interfacial intermixing. However, other researchers and actual case studies have shown that filters perform quite adequately when intermixing occurs at the interface either by accident or by plan.

The results of this study showed substantially better filtrate quality for the mixed interface media than for the sharp interface media.

Thus the results are in opposition to the design recommendation of Camp. The better filtrate observed for the mixed interface media is due to the use of finer sand and not to the intermixing itself. However, intermixing is the inevitable result of selecting the dual media to provide substantially finer top sand size than top coal size.

None of the researchers have presented proof to back up claims that the intermixing itself is good or bad. Brosman and Malina [19] are the only ones who have attempted to measure the effect of intermixing on both head loss and effluent quality. The writers feel that their study had some experimental weaknesses [109] which led them to the false conclusions that interfacial intermixing, in and of itself, provided benefits to both filtrate quality and head loss. That conclusion is not supported by the results reported herein.

### Conclusions

The following points are concluded from this study:

1. Interfacial intermixing does not in itself affect filter performance as measured by both head loss development and effluent quality of dual-media filters.
2. The mixed interface filter media produced better filtrate quality than did the sharp interface filter media for all suspensions filtered in this study; this was due to substantially finer sand in the mixed interface media.
3. The mixed interface filter media produced higher head losses than the sharp interface filter media for all suspensions due to greater suspended solids removal.
4. Intermixing at the interface of dual-media filters is an unavoidable phenomenon which results when United States anthracite (sp. gr. about 1.7) and sand are used and the sizes are selected to achieve coarse to fine filter media in the direction of flow.

## XII. ABRASIVE LOSS OF COAL DURING AIR SCOUR

The effect of air scour on anthracite coal filter media became of concern because of the possible widespread use of air scoured filters using anthracite coal as one of the filter media. Widespread use seems probable for the following reasons: (1) the apparent benefits of air scour as an adjunct to water backwash, (2) the apparent necessity of auxiliary agitation in wastewater filtration, (3) the necessity of using dual media in wastewater filtration to achieve adequate filter run length.

The visual appearance of coal filter media when subjected to air scour was observed in plastic filter housings. The coal appears to be in rather violent motion, especially the coal near the top surface of the bed. The granules of the coal are in contact with each other and rubbing against each other, unlike those in a fluidized bed where collisions and rubbing are absent. Thus the abrasive loss of coal was of concern due to the softer nature of coal as compared to other common filter media such as silica sand and garnet sand.

An experiment was conducted to gain some view of the potential seriousness of the abrasive loss problem. The experiment consisted of subjecting a filter bed of anthracite coal to essentially continuous air scour for two weeks. Two weeks of such exposure would be comparable to about 20 years of normal filter operation assuming 24-hr filter cycles and 3 min of air scour per cycle. The filter was water backwashed twice a day to observe the visual loss of coal dust. Furthermore, changes in the depth of bed and pressure loss profile through the bed in both upflow and downflow were observed to obtain evidence of changes in the filter media.

### Experimental Procedure

The details of the experiment were as follows:

The starting coal was a standard crushed anthracite coal "Philterkol" obtained from the Reading Anthracite Coal Company, Pottsville, Pennsylvania. The suppliers specified effective size was 0.6 to 0.79 mm, the uniformity coefficient was less than 1.8, and the reported hardness was 3 on the Moh Scratch Test comparison scale.

The coal was split to obtain a representative sample, and 16 in. of coal was placed in a 6-in. ID pilot filter. The coal was backwashed with water and allowed to stratify. A total of about 2 in. of the fine coal was skimmed from the surface of the stratified bed in two increments during backwashing. The coal was then removed from the bed, air dried and oven dried, and two separate representative samples were collected for sieve analysis. A riffle type splitter was used to collect the representative sample.

The sieve analyses were performed on a nest of United States Standard sieves (12, 14, 16, 18, 20, 25, and 30 mesh) using a Tyler portable shaker for 5 min. The sample size was 356.6 and 407.9 g for the two samples.

The remainder of the coal was weighed and was placed back in the filter column, fluidized to permit stratification and the pressure loss profile was observed from the piezometer tubes located at 3-in. depth increments as shown in Fig. 4. A water temperature of 22 °C was used.

After the upflow and downflow pressure profile observations, the water level was lowered to about 6 in. above the coal surface, and the air scour was applied at a rate of 4 cfm/sq ft. The air was kept on continuously except for two short periods each day when the air was shut off and the filter was subjected to backwash with 50% bed expansion, and to upflow and downflow pressure profile observations. The amount of coal dust in the initial backwash water was observed qualitatively as one measure of abrasive loss. The downflow pressure drop between piezometer taps at 7 gpm/sq ft and 22 °C was observed to see if there was any progressive increase in pressure drop due to the formation of finer media size as a result of abrasion. The pressure drop during upflow at a rate which would provide 50% bed expansion at 22 °C was measured to see if there were any progressive changes due to abrasive loss. The upflow rate was selected to provide an expanded bed depth of 21 in. The development of a finer media would result in greater expansion at a given upflow rate and less pressure drop between the piezometer taps. The depth of the bed after each backwash was observed after carefully and slowly closing the backwash valve to ensure a consistent degree of packing of the bed. Any major loss of media or change in sphericity due to abrasion would manifest itself by a decrease in bed depth.

At the end of two weeks of the above procedure, the coal was removed from the filter, dried, weighed, and again two representative samples were taken and subjected to sieve analysis.

### Results

Some abrasive loss was evident from the color of the coal dust in the water at the end of each period of air scour. The initial backwash water was black with coal dust but cleared up in the first 2 min of backwash.

There was no substantial loss in bed depth or bed weight as shown in Table 53. Furthermore, there was no substantial change in head loss either upflow or downflow, indicating no substantial change in size of the media.

The sieve analysis before and after the two-week period of air scour is presented in Fig. 110. Each curve represents the average of two

Table 53. Changes in coal bed over a two-week period of air-scour exposure equivalent to about 20 years of normal service.

	Initial value	After two weeks
Bed depth, in.	14-1/8	13-7/8
Bed weight dry, g	5019	4775
Total downflow head loss, ft H <sub>2</sub> O	0.30	0.29
Upflow rate to achieve 21 in. bed depth, gpm	5.1	5.3
Total upflow head loss, ft H <sub>2</sub> O	0.35	0.34
Effective size of media, mm	0.80	0.78
Uniformity coefficient	1.59	1.60

sieve analyses. It is evident that the coal decreased in size slightly in this air scour exposure, about 0.02 mm in effective size, which is a negligible change.

#### Conclusions

A typical crushed anthracite coal filter media was subjected to air scour for two weeks to simulate the abrasive effects of 20 years of typical filter service. From this study, it is concluded that some abrasive loss of coal does occur, but it is a negligible amount. The total loss of media and changes in media head loss and size were less than 3%. This is considered negligible because coal filter media suppliers usually request and are granted about a 10% tolerance on the effective size of the media which they supply.

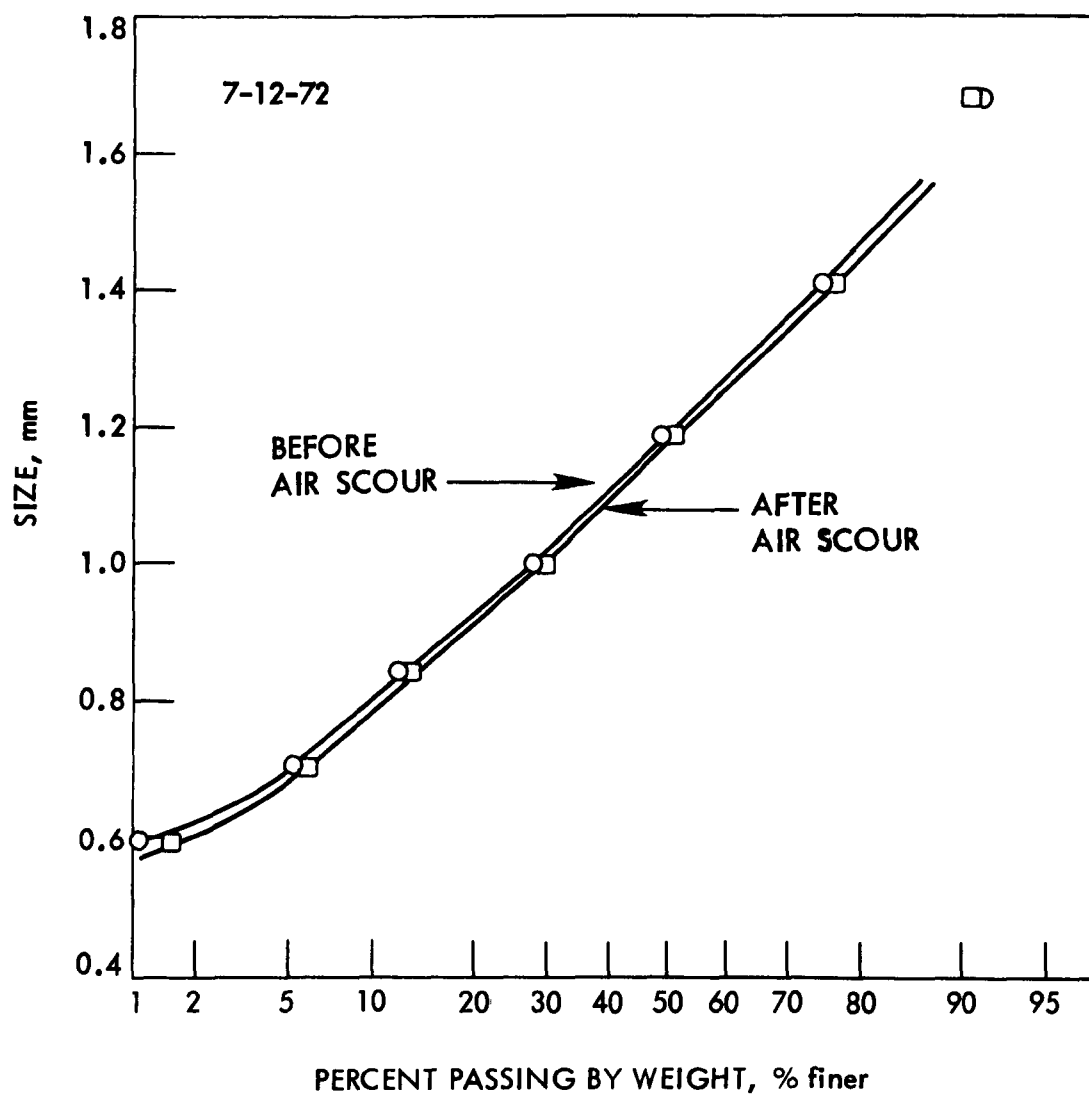


Fig. 110. Sieve analysis of coal before and after 14 days of continuous air scour.

#### XIV. REFERENCES

1. Adler, I. L., and Happel, J. The fluidization of uniform smooth spheres in liquid media. Chem. Eng. Prog., Symp. Ser., 58(38): 98-105, 1962.
2. American Society for Testing Materials. 1968 Book of ASTM Standards. Part 10. Concrete and mineral aggregates. ASTM, Philadelphia, 1972.
3. American Water Works Association, Inc. Water Quality and Treatment. New York, McGraw-Hill Book Co., Inc., 1971.
4. Amirtharajah, A. Expansion of graded sand filters during backwashing. Unpublished M.S. thesis. Ames, Iowa, Library, Iowa State University of Science and Technology, 1970.
5. Amirtharajah, A. Optimum expansion of sand filters during backwash. Unpublished Ph.D. thesis. Ames, Iowa, Library, Iowa State University of Science and Technology, 1971.
6. Amirtharajah, A. and Cleasby, J. L. Predicting expansion of filters during backwashing. J. Am. Water Works Assoc., 64:52-59, 1972.
7. Anderson, T. B., and Jackson, R. The nature of aggregative and particulate fluidization. Chem. Eng. Sci., 19:509-511, 1964.
8. Babbitt, H. E., Doland, J. J., and Cleasby, J. L. Water Supply Engineering. 6th ed. New York, McGraw-Hill Book Co., Inc., 1962.
9. Barret, A. D. Immediun filter in tertiary treatment. Process Biochem., 6(1):33-35, 1971.
10. Baylis, J. R. Nature and effects of filter backwashing. J. Am. Water Works Assoc., 51:126-156, 1959.
11. Baylis, J. R. Review of filter design and methods of washing. J. Am. Water Works Assoc., 51:1433-1454, 1959.
12. Becker, H. A. An investigation of the laws governing the spouting of coarse particles. Chem. Eng. Sci., 13:245-262, 1961.
13. Boby, W. M. T., and Alpe, G. Practical experiences using upward flow filtration. Proc. Soc. Water Treat. Exam., 16:215-229, 1967.
14. Boss, R. R. Hydraulics and intermixing of sand and coal filters. Unpublished M.S. thesis. Ames, Iowa, Library, Iowa State University of Science and Technology, 1973.
15. Botterill, J. S. M. Progress in fluidization. Br. Chem. Eng., 10:26-30, 1965.

16. Botterill, J. S. M. Progress in fluidization. Br. Chem. Eng., 13:1121-1126, 1968.
17. Bourgeois, P., and Grenier, P. The ratio of terminal velocity to minimum fluidizing velocity for spherical particles. Can. J. Chem. Eng., 46:325-328, 1968.
18. Boyd, R. H., and Ghosh, M. M. An investigation of the influences of some physiochemical variables on porous-media filtration. J. Am. Water Works Assoc., 66:94-98, 1974.
19. Brosman, D. R., and Malina, J. E. Intermixing of dual media filters and effects on performance. Technical Report EHE-72-4 CBWR-86. Center for Research in Water Resources. The University of Texas at Austin, 1972.
20. Buevich, Yu. A., and Markov, V. G. Pseudo-turbulent diffusion of particles in homogeneous suspensions. Int. Chem. Eng., 10:570-575, 1970.
21. Cairns, E. J., and Prausnitz, J. M. Longitudinal mixing in fluidization. AIChE J., 6:400-405, 1960.
22. Cairns, E. J., and Prausnitz, J. M. Macroscopic mixing in fluidization. AIChE J., 6:554-560, 1960.
23. Camp, T. R. (Discussion of) Experience with anthracite-sand filters. J. Am. Water Works Assoc., 53:1478-1483, 1961.
24. Camp, T. R. Theory of water filtration. ASCE J. Sanitary Eng. Div., 90:1-30, 1964.
25. Camp, T. R. (Discussion of) Theory of water filtration. ASCE J. Sanitary Eng. Div., 91:55-69, October 1965.
26. Camp, T. R., Graber, S. D., and Conklin, G. F. Backwashing of granular water filters. ASCE J. Sanitary Eng. Div., No. SA6, pp. 903-925, December 1971.
27. Camp, T. R., and Stein, P. C. Velocity gradients and internal work in fluid motion. J. Boston Soc. Civ. Eng., 30:219-237, 1943.
28. Carvalho, W. J. Fluidization of crushed anthracite coal. Unpublished M.S. thesis. Ames, Iowa, Library, Iowa State University of Science and Technology, 1970.
29. Clark, J. W., Viessman, W., and Hammer, M. J. Water Supply and Pollution Control. Scranton, Pennsylvania, International Textbook Company, 1971.

30. Cleasby, J. L. Iron removal, a case study. J. Am. Water Works Assoc., 67(3):147-149. March 1975.
31. Cleasby, J. L., and Baumann, E. R. Selection of sand filtration rates. J. Am. Water Works Assoc., 54(5):579-602, 1962.
32. Conley, W. R. Experience with anthracite-sand filters. J. Am. Water Works Assoc., 53:1473-1478, 1961.
33. Coulson, J. M., and Richardson, J. F. Chemical Engineering. Vol. 2, 2nd ed. New York, Pergamon Press Inc., 1968.
34. Culp, R. L., and Culp, G. L. Advanced Wastewater Treatment. New York, Van Nostrand Reinhold Company, 1971.
35. Davidson, J. F., and Harrison, D. Fluidized Particles. New York, The Syndics of the Cambridge University Press, 1963.
36. Davies, L., and Richardson, J. F. Gas interchange between bubbles and the continuous phase in a fluidized bed. Trans. Inst. Chem. Eng., 44:T293-T305, 1966.
37. Degremont, S. A. Water Treatment Handbook. 3rd English ed. Kensington, London W14, England, Hugh K. Elliot, Ltd., 1965.
38. Dvorin, R. Advances make wastewater filtration economical and effective solution. Water Sewage Works 116(9):1W/12-1W/16, 1969.
39. Efremor, G. I. and Vakhrusher, I. A. A study of the hydrodynamics of three-phase fluidized beds. Int. Chem. Eng., 10:37-41, 1970.
40. Ergun, S. Fluid flow through packed columns. Chem. Eng. Prog., 48:89-94, 1952.
41. Evans, S. C., and Roberts, F. W. Twelve months' operation of sand filtration and microstraining at Luton. Inst. Sewage Purif., J. Proc., 4:333-341, 1952.
42. Evans, S. C., and Roberts, F. W. Recent developments in sewage treatment at Luton. Inst. Sewage Purif., J. Proc., 3:225-236, 1955.
43. Evers, R. H. Tool up with mixed-media filters. Water Wastes Eng., 8(5):C14-C16, 1971.
44. Ewing, G. W. Instrumental Methods of Chemical Analysis. 3rd ed. New York, McGraw-Hill Book Co., Inc., 1969.
45. Fair, G. M., and Geyer, J. C. Water Supply and Waste Water Disposal. 8th ed. New York, John Wiley and Sons, Inc., 1958.
46. Fair, G. M., Geyer, J. C., and Okun, D. A. Water and Wastewater Engineering. Vol. 2. New York, John Wiley and Sons, Inc., 1968.

47. Fair, G. M., and Hatch, L. P. Fundamental factors governing the streamlike flow of water through sand. J. Am. Water Works Assoc., 25:1551-1565, 1933.
48. Frantz, J. F. Minimum fluidization velocities and pressure drop in fluidized beds. \* Chem. Eng., Symp. Series, 62(62):21-31, 1966.
49. Friedlander, S. K., and Topper, L. Turbulence, Classic Papers on Statistical Theory, New York, Interscience Publishers Inc., 1961.
50. Furukawa, J., and Ohmae, T. Liquidlike properties of fluidized systems. Ind. Eng. Chem., 50:821-828, 1958.
51. Galloway, T. R., and Sage, B. H. A model of the mechanism of transport in packed, distended and fluidized beds, Chem. Eng. Sci., 25:495-516, 1970.
52. Ghosh, M. M., O'Connor, J. T., and Engelbrecht, R. S. Precipitation of iron in aerated ground waters. ASCE J. Sanitary Eng. Div., 90(SA1):199-213, 1966.
53. Godard, K., and Richardson, J. F. Correlation of data for minimum fluidizing velocity and bed expansion in particulate fluidized systems. Chem. Eng. Sci., 24: 363-367, 1969.
54. Gregory, R. Media specification and backwashing - W.R.A. Paper presented at Anthracite-Sand Filtration, A Working Conference, University of Reading, England, January 3-5, 1972.
55. Handley, D., Doraiswamy, A., Butcher, K. L., and Franklin, N. L. A study of the fluid and particle mechanics in liquid-fluidized beds. Trans. Inst. Chem. Eng., 44:T260-T273, 1966.
56. Hanratty, T. J., Latinen, G. and Wilhelm, R. H. Turbulent diffusion in particulate fluidized beds of particles. AIChE J. 2:372-380, 1956.
57. Harrison, D., Davidson, J. F., and Kock, J. W. On the nature of aggregative and particulate fluidization. Trans. Inst. Chem. Eng., 39:202-211, 1961.
58. Holding, J. C. Polishing sewage effluents, Effluent Water Treat. J., 12:665-667, 669-672, 1972.
59. Huang, J. Y. C. Granular filters for tertiary wastewater treatment. Unpublished Ph.D. dissertation. Ames, Iowa, Library, Iowa State University of Science and Technology, 1972.
60. Hudson, H. E. Filter backwashing experiments at the Chicago experimental plant. J. Am. Water Works Assoc., 27:1547-1564, 1935.

61. Huisman, L. Rapid filtration, Part 1. Mimeographed book of lectures in English, Delft University of Technology, Department of Civil Engineering, 1974.
62. Hulbert, R., and Herring, F. W. Studies on the washing of rapid filters. J. Am. Water Works Assoc., 21:1445-1513, 1929.
63. Ives, K. J. Progress in filtration. J. Am. Water Works Assoc., 56(9):1225-1232, 1964.
64. Ives, K. J. Theory of filtration. Special Subject No. 7. Proc. Int. Water Supply Cong. Exhib., Vienna, 1969. London, International Water Supply Association, 1969.
65. Ives, K. J. Personal communication, September 24, 1974.
66. Jackson, R. The mechanics of fluidized beds. Part I: The stability of the state of uniform fluidization. Trans. Inst. Chem. Eng., 41:13-21, 1963.
67. Johnson, R. L., and Cleasby, J. L. Effect of backwash on filter effluent quality. ASCE J. Sanitary Eng. Div., 92:215-228, 1966.
68. Joslin, J. R., and Greene, G. Sand filter experiments at Derby. Water Pollut. Control, 69:611-622, 1970.
69. Jottrand, R. An experimental study of the mechanism of fluidization. J. Appl. Chem., 2(Supplementary Issue,1):517-526, 1952.
70. Jung, H., and Savage, E. S. Deep-bed filtration. J. Am. Water Works Assoc., 66:73-78, 1974.
71. Kada, H., and Hanratty, T. J. Effects of solids on turbulence in a fluid. AIChE J., 6:624-630. 1960.
72. Keefer, C. E. Tertiary sewage treatment. Public Works, 93(11):109-112, 1962.
73. Kramers, I. H., Westermann, M. D., de Groot, J. H., and Dupont, F. A. A. The longitudinal dispersion of liquid in a fluidized bed. Symposium on the Interaction Between Fluids and Particles. London, Institution of Chemical Engineers. pp. 114-119, 1962.
74. Le Clair, Brian P. Two component fluidization. Unpublished M.A. Sc. thesis. British Columbia, Canada, Library, University of British Columbia, 1964.
75. Lemlich, R., and Caldas, I. Heat transfer to a liquid fluidized bed. AIChE J., 4:376-380, 1958.
76. Leva, Max. Fluidization. New York, McGraw-Hill Book Co., Inc., 1959.

77. Leva, M., Grummer, M., Weintraub, M., and Pollchik, M. Introduction to fluidization. Chem. Eng. Prog., 44:511-520, 1948.
78. Leva, M., Grummer, M., Weintraub, M., and Pollchik, M. Fluidization of solid nonvesicular particles. Chem. Eng. Prog., 44:619-626, 1948.
79. Lewis, E. W., and Bowerman, Ernest W. Fluidization of solid particles in liquids. Chem. Eng. Prog., 48:603-609, 1952.
80. Malik, A. M. Air and water backwashing of granular filters. Unpublished M.S. thesis. Ames, Iowa, Library, Iowa State University of Science and Technology, 1972.
81. McCune, L. K., and Wilhelm, R. H. Mass and momentum transfer in solid-liquid system. Ind. Eng. Chem., 41:1124-1134, 1949.
82. Metcalf and Eddy, Inc. Wastewater Engineering. New York, McGraw-Hill Book Co., Inc., 1972.
83. Michaelson, A. P. Under the solids limit at Ashton-under-Lyne. Water Pollut. Control, 70(5):533-535, 1971.
84. Mohanka, S. S. Theory of multilayer filtration. ASCE J. Sanitary Eng. Div., 95:1079-1095, 1969.
85. Murray, J. D. Mathematical aspects of bubble motion in fluidized beds. Chem. Eng. Prog. Symp. Ser., 62(62):71-82, 1966.
86. Naylor, A. E., Evans, S. C., and Dunscombe, K. M. Recent developments on the rapid sand filters at Luton, Water Pollut. Control, 66(4):309-320, 1967.
87. Nicolle, N. P. Humus tank performance, microstraining and sand filtration. Inst. Sewage Purif., J. Proc., 1:19, 1955.
88. Nicolle, N. P. Operational aspects of control of rapid gravity sand filters. Inst. Sewage Purif., J. Proc., 3:273-275, 1957.
89. Ostergaard, K. The effect of particle size and bed height on the expansion of mixed phase (gas-liquid) fluidized beds. Chem. Eng. Sci., 21:413-417, 1966.
90. Ostergaard, K. On the growth of air bubbles formed at a single orifice in a waterfluidized bed. Chem. Eng. Sci., 21:470-472, 1966.
91. Othmer, D. F. Fluidization. New York, Reinhold Publishing Corporation, 1956.
92. Pettet, A. E. J., Collett, B. A., and Summers, T. H. Mechanical filtration of sewage effluents. Part 1, Removal of humus. Inst. Sewage Purif., J. Proc., 4:399-410. 1949.

93. Pettet, A. E. J., Collett, W. F., and Waddington, J. I. Mechanical filtration of sewage effluents. III. Removal of humus: Further experiments at Luton. *Inst. Sewage Purif., J. Proc.*, 4:195-202, 1951.
94. Pettet, A. E., Collett, W. F., and Waddington, J. I. Rapid filtration of sewage effluents through sand and anthracite. *Sewage Ind. Wastes*, 24(7):835-843, 1952.
95. Pinchbeck, P. H., and Popper, F. Critical and terminal velocities in fluidization. *Chem. Eng. Sci.*, 6:57-64, 1956.
96. Pruden, B. B. Particle size segregation in particulate fluidized beds. Unpublished M. A. Sc. thesis. British Columbia, Canada, Library, University of British Columbia, 1964.
97. Pruden, B. B., and Epstein, N. Stratification by size in particulate fluidization and in hindered settling. *Chem. Eng. Sci.*, 19:696-700, 1964.
98. Reuter, H. On the nature of bubbles in gas and liquid fluidized beds. *Chem. Eng. Prog., Symp. Ser.*, 62(62):92-99, 1966.
99. Rice, G. A. Direct filtration of secondary effluent, backwashing and performance. Unpublished M.S. thesis. Ames, Iowa, Library, Iowa State University of Science and Technology, 1973.
100. Richardson, J. F., and Zaki, W. N. Sedimentation and fluidization: Part I. *Trans. Inst. Chem. Eng.*, 32:35-53, 1954.
101. Rigby, G. R., Blockland, G. P. V., Park, W. H., and Capes, C. E. Properties of bubbles in three phase fluidized beds as measured by an electro-resistivity probe. *Chem. Eng. Sci.*, 25:1729-1741, 1970.
102. Ripley, P. G., and Lamb, G. L. Filtration of effluent from a biological-chemical system. *Water Sewage Works*, 120(2): 66-69, 1973.
103. Robeck, G. G., and Kreissl, J. F. Multi-media filtration: principles and pilot experiments. *Transactions of 17th Annual Conference of Sanitary Engineering. Univ. Kans. Public Bull. Eng. Arch.*, 57:10-22, 1967.
104. Romero, J. B., and Johanson, L. N. Factors affecting fluidized bed quality. *Chem. Eng. Prog., Symp. Ser.*, 58(38):28-37, 1962.
105. Rowe, P. N. Drag forces in a hydraulic model of a fluidized bed. Part II. *Trans. Inst. Chem. Eng.*, 39:175-180, 1961.
106. Rowe, P. N., and Henwood, G. A. Drag forces in a hydraulic model of a fluidized bed. Part I. *Trans. Inst. Chem. Eng.*, 39: 43-54, 1961.

107. Ruckenstein, E. Homogeneous fluidization. Ind. Eng. Chem. Fund., 3:260-268, 1964.
108. Savage, E. S., Personal communication, February 19, 1975, describing media and backwash provisions used by Pintsch Bamag (Germany) and Dravo (U.S.).
109. Sejkora, G. D. Effect of Media Intermixing on Dual Media Filtration. Unpublished M. S. thesis. Ames, Iowa, Library, Iowa State University of Science and Technology, 1974.
110. Shannon, P. T. Fluid dynamics of gas fluidized batch systems. Microfilm copy. Unpublished Ph.D. thesis. Chicago, Illinois, Library, Illinois Institute of Technology, 1961.
111. Shireman, C. Filtration boosts tertiary treatment. Water Wastes Eng., 9(4):34-37, 1972.
112. Simmonds, M. A. Public water supplies of Queensland, Australia, J. Am. Water Works Assoc., 55:1044-1080, 1963.
113. Simpson, H. C., and Rodger, B. W. The fluidization of light solids by gases under pressure and heavy solids by water. Chem. Eng., Sci., 16:153-180, 1961.
114. Singer, P. C., and Stumm, W. The solubility of ferrous iron in carbonate-bearing waters. J. Am. Water Works Assoc., 62:198-202, 1970.
115. Slis, P. L., and Willemse, T. W., and Kramers, H. The response of the level of a liquid fluidized bed to a sudden change in the fluidizing velocity, Appl. Sci. Res., 8:209-218, 1959.
116. Sosewitz, B., and Bacon, V. W. Chicago's first tertiary treatment plant. Water Wastes Eng., 5:52-55, 1968.
117. Standard Methods for the Examination of Water and Wastewater. 13th ed. New York, American Public Health Association, 1971.
118. Stangl, E. W. Air and water backwash of wastewater filters. Unpublished M.S. thesis. Ames, Iowa, Library, Iowa State University of Science and Technology, 1973.
119. Steward, P. S., and Davidson, J. F. Three-phase fluidization: Water, particles and air. Chem. Eng. Sci., 19:319-322, 1964.
120. Stookey, L. L. Ferrozine - A new spectrophotometric reagent for iron. Anal. Chem., 42:779-781, 1970.
121. Streander, B. Mechanical filtration of sewage. Water Works Sewerage, 82(7):252-257, 1935.

122. Streander, B. Sewage filtration with silica sand filters I. Water Works Sewerage, 87(8):351-357, 1940.
123. Streander, B. Sewage filtration with silica sand filters II. Water Works Sewerage, 87(9):422-429, 1940.
124. Streander, B. Sewage filtration with silica sand filters III. Water Works Sewerage, 87(10):493-495, 1940.
125. Taylor, G. I. Statistical theory of turbulence, Parts I-IV. Proc. R. Soc. London, Ser. A., 151:421-478, 1935.
126. Taylor, G. I. The spectrum of turbulence. Proc. R. Soc. London, Ser. A, 164:476-490, 1938.
127. Tchobanoglous, G. Filtration techniques in tertiary treatment. J. Water Poll. Control Fed., 42:604-623, 1970.
128. Tchobanoglous, G., and Eliassen, R. Filtration of treated sewage effluent. ASCE J. Sanitary Eng. Div., 96:243-265, 1970.
129. Tebbutt, T. H. Y. An investigation into tertiary treatment by rapid filtration. Water Res., J. Intern. Assoc. Water Pollution Research, 5:81-92, 1971.
130. Tesarik, I. (Discussion of) Theory of water filtration. ASCE J. Sanitary Eng. Div., 90:67-69, 1965.
131. Truesdale, G. A., and Birkbeck, A. E. Tertiary treatment of activated-sludge effluent. Water Pollut. Control, 67(5):483-494, 1968.
132. Ulug, S. E. The backwashing of rapid sand filters. Unpublished thesis for the Diploma of membership of Imperial College of Science and Technology. London, United Kingdom, Library, Imperial College of Science and Technology, University of London, 1967.
133. United States Environmental Protection Agency. Process Design Manual for Suspended Solids Removal. U.S. EPA Technology Transfer, 1975.
134. Van Heerden, C., Novel, A. P. P., and Van Krevelen, D. W. Studies on fluidization - The critical mass velocity. Chem. Eng. Sci., 1:37-49, 1951.
135. Volpicelli, G., Massimilla, L. and Zenz, F. A. Non-homogeneities in solid-liquid fluidization. Chem. Eng. Prog., Symp. Ser., 62(67): 42-50, 1966.
136. Vosloo, P. B. B. Some experiments on rapid sand filtration of sewage works effluents without coagulation. Inst. Sewage Purif., J. Proc., 1:204-209, 1947.

137. Walker, J. D., Aurora, Illinois. Dual media tertiary filters design parameters. Private communication with Walker Process, August 1, 1972.
138. Wen, C. Y., and Yu, Y. H. Mechanics of fluidization. Chem. Eng. Prog., Symp. Ser., 62(62):100-111, 1966.
139. Whitmore, R. L. The sedimentation of suspensions of spheres. Br. J. Appl. Phys., 6:239-245, 1955.
140. Whitmore, R. L. The relationship of the viscosity to the settling rate of slurries. J. Inst. Fuel, 30:328-342, 1957.
141. Wilhelm, R. H., and Kwauk, M. Fluidization of solid particles. Chem. Eng. Prog., 44:201-218, 1948.
142. Wood, R., Smith, W. S., and Murray, J. K. An investigation into upward flow filtration. Water Pollut. Control, 67(4):421-428, 1968.
143. Woods, C. F. Expansion and intermixing of garnet and silica sand during backwashing of granular filters. Unpublished M.S. thesis. Ames, Iowa, Library, Iowa State University of Science and Technology, 1973.
144. Zabrodsky, S. S. Hydrodynamics and Heat Transfer in Fluidized Beds. Cambridge, Massachusetts, The M.I.T. Press, 1966.
145. Zenz, F. A. and Othmer, D. F. Fluidization and Fluid Particle Systems. New York, Rheinhold Publishing Corporation, 1960.

Sieve analyses of uniform media.

Coals <sup>14</sup>			Coals <sup>14</sup> (continued)			Silica sands <sup>14</sup> (continued)		
Designation	U.S. sieve	% retained	Designation	U.S. sieve	% retained	Designation	U.S. sieve	% retained
F(-4+7)	4	3.4	A(-25+30)	25	4.9	A(-18+20)	18	4.3
	7	79.7		30	84.1		20	87.0
	Pan	16.9		Pan	11.0		Pan	8.7
F(-7+8)	7	3.3	A(-30+35)	30	3.2	A(-20+25)	20	0.6
	8	85.0		35	83.3		25	74.9
	Pan	11.7		Pan	13.5		Pan	24.5
F(-8+10)	8	4.6	A(-35+40)	35	8.8	A(-25+30)	25	2.1
	10	81.0		40	81.7		30	77.6
	Pan	14.4		Pan	9.5		Pan	20.3
F(-10+12)	10	4.8	A(-40+45)	40	4.2	A(-30+35)	30	1.3
	12	84.2		45	83.6		35	70.9
	Pan	11.0		Pan	12.2		Pan	26.8
A(-12+14)	12	4.7	Silica sands <sup>14</sup>			A(-35+40)	35	3.6
	14	80.5					40	72.6
	Pan	14.8	Pan	23.8				
A(-14+16)	14	2.2	A(-10+12)	10	0.1	A(-40+45)	40	6.2
	16	83.6		12	83.7		45	74.8
	Pan	14.2		Pan	16.2		Pan	19.0
A(-16+18)	16	7.0	A(-12+14)	12	9.2	Garnet sands <sup>143</sup>		
	18	77.8		14	80.1			
	Pan	15.2		Pan	10.7			
A(-18+20)	18	3.8	A(-14+16)	14	5.9	A(-14+16)	14	0.24
	20	77.8		16	70.1		16	87.72
	Pan	18.4		Pan	24.0		18	12.00
A(-20+25)	20	10.2	A(-16+18)	16	2.7	Pan	0.04	

Sieve analysis of uniform media (continued).

Coals <sup>14</sup>			Coals <sup>14</sup> (continued)			Silica sands <sup>14</sup> (continued)		
Designation	U.S. sieve	% retained	Designation	U.S. sieve	% retained	Designation	U.S. sieve	% retained
A(-25+30)	25	78.3	A(-20+25)	18	74.5	A(-35+40)	35	0.42
	Pan	11.5		Pan	22.8			
	25	0.11		20	0.22			
	30	88.91		25	78.40		40	85.17
	35	10.46		30	21.33		45	14.33
A(-50+60)	Pan	0.53	A(-30+35)	Pan	0.05	A(-40+45)	Pan	0.08
	50	0.14		30	0.54		40	0.70
	60	81.81		35	88.76		45	96.12
	70	16.56		40	10.58		50	3.15
	Pan	1.49		Pan	0.12		Pan	0.03

<b>TECHNICAL REPORT DATA</b> <i>(Please read Instructions on the reverse before completing)</i>		
1. REPORT NO. EPA-600/2-77-016	2.	3. RECIPIENT'S ACCESSION NO.
4. TITLE AND SUBTITLE BACKWASH OF GRANULAR FILTERS USED IN WASTEWATER FILTRATION	5. REPORT DATE April 1977 (Issuing Date)	6. PERFORMING ORGANIZATION CODE
	8. PERFORMING ORGANIZATION REPORT NO.	
7. AUTHOR(S) J. L. Cleasby and E. R. Baumann	10. PROGRAM ELEMENT NO. 1BB043, ROAP 21-ASQ, Task 13	
9. PERFORMING ORGANIZATION NAME AND ADDRESS Iowa State University Ames, Iowa 50011	11. CONTRACT/GRANT NO. R802140	
	13. TYPE OF REPORT AND PERIOD COVERED Final, 9/1/71-5/31/76	
12. SPONSORING AGENCY NAME AND ADDRESS Municipal Environmental Research Laboratory--Cin., OH Office of Research and Development U.S. Environmental Protection Agency Cincinnati, Ohio 45268	14. SPONSORING AGENCY CODE EPA/600/14	
	15. SUPPLEMENTARY NOTES	
16. ABSTRACT <p>The use of deep granular filters in waste treatment is of growing importance. The key to long-term operating success of such filters is proper bed design and adequate bed cleaning during backwashing. A number of questions related to adequate backwashing of granular filters are investigated which lead to the following conclusions:</p> <p>Cleaning granular filters by water backwash alone to fluidize the filter bed is inherently a weak cleaning method because particle collisions do not occur in a fluidized bed and thus abrasion between the filter grains is negligible.</p> <p>Due to the inherent weakness of water backwashing cited above, auxiliary means of improving filter bed cleaning are essential for wastewater filters. Three auxiliary methods were compared in a wastewater pilot filtration study. The most effective backwash was provided by air scour and water backwash simultaneously at subfluidization velocities. The other two methods, surface and subsurface wash auxiliary or air scour prior to water fluidization wash were about comparable in effectiveness.</p> <p>The performance of coarse sand, dual-, and triple-media filters was compared, and the backwashing routines appropriate for each media are discussed. A number of investigations concerning the design and backwashing of dual media filters are presented.</p>		
17. KEY WORDS AND DOCUMENT ANALYSIS		
a. DESCRIPTORS	b. IDENTIFIERS/OPEN ENDED TERMS	c. COSATI Field/Group
Filtration*, Sewage Filtration*, Sewage Treatment, Waste Treatment Water Pollution, Backwashing*, Clarification	Filter Backwash, Suspended Solids Removal, Filter Media, Filter Cleaning, Filter Design	13B
18. DISTRIBUTION STATEMENT RELEASE TO PUBLIC	19. SECURITY CLASS (This Report) UNCLASSIFIED	21. NO. OF PAGES 381
	20. SECURITY CLASS (This page) UNCLASSIFIED	22. PRICE